

FOCUS ON BIOTECHNOLOGY

Plant Tissue Culture Engineering

Edited by

S. Dutta Gupta and Yasuomi Ibaraki

Series Editors: Marcel Hofman and Jozef Anné

 Springer

PLANT TISSUE CULTURE ENGINEERING

FOCUS ON BIOTECHNOLOGY

Volume 6

Series Editors

MARCEL HOFMAN

Centre for Veterinary and Agrochemical Research, Tervuren, Belgium

JOZEF ANNÉ

Rega Institute, University of Leuven, Belgium

Volume Editors

S. DUTTA GUPTA

*Department of Agricultural and Food Engineering,
Indian Institute of Technology,
Kharagpur, India*

YASUOMI IBARAKI

*Department of Biological Science,
Yamaguchi University,
Yamaguchi, Japan*

COLOPHON

Focus on Biotechnology is an open-ended series of reference volumes produced by Springer in co-operation with the Branche Belge de la Société de Chimie Industrielle a.s.b.l.

The initiative has been taken in conjunction with the Ninth European Congress on Biotechnology. ECB9 has been supported by the Commission of the European Communities, the General Directorate for Technology, Research and Energy of the Wallonia Region, Belgium and J. Chabert, Minister for Economy of the Brussels Capital Region.

Plant Tissue Culture Engineering

Edited by

S. DUTTA GUPTA

*Department of Agricultural and Food Engineering,
Indian Institute of Technology,
Kharagpur, India*

and

YASUOMI IBARAKI

*Department of Biological Science,
Yamaguchi University,
Yamaguchi, Japan*

 Springer

A C.I.P. Catalogue record for this book is available from the Library of Congress.

ISBN 978-1-4020-3594-4 (HB)
ISBN 978-1-4020-3694-1 (e-book)

Published by Springer,
P.O. Box 17, 3300 AA Dordrecht, The Netherlands.

www.springer.com

Printed on acid-free paper

First edition 2006

Reprinted 2008

All Rights Reserved

© 2008 Springer

No part of this work may be reproduced, stored in a retrieval system, or transmitted in any form or by any means, electronic, mechanical, photocopying, microfilming, recording or otherwise, without written permission from the Publisher, with the exception of any material supplied specifically for the purpose of being entered and executed on a computer system, for exclusive use by the purchaser of the work.

FOREWORD

It is my privilege to contribute the foreword for this unique volume entitled: "Plant Tissue Culture Engineering," edited by S. Dutta Gupta and Y. Ibaraki. While there have been a number of volumes published regarding the basic methods and applications of plant tissue and cell culture technologies, and even considerable attention provided to bioreactor design, relatively little attention has been afforded to the engineering principles that have emerged as critical contributions to the commercial applications of plant biotechnologies. This volume, "Plant Tissue Culture Engineering," signals a turning point: the recognition that this specialized field of plant science must be integrated with engineering principles in order to develop efficient, cost effective, and large scale applications of these technologies.

I am most impressed with the organization of this volume, and the extensive list of chapters contributed by expert authors from around the world who are leading the emergence of this interdisciplinary enterprise. The editors are to be commended for their skilful crafting of this important volume. The first two parts provide the basic information that is relevant to the field as a whole, the following two parts elaborate on these principles, and the last part elaborates on specific technologies or applications.

Part 1 deals with machine vision, which comprises the fundamental engineering tools needed for automation and feedback controls. This section includes four chapters focusing on different applications of computerized image analysis used to monitor photosynthetic capacity of micropropagated plants, reporter gene expression, quality of micropropagated or regenerated plants and their sorting into classes, and quality of cell culture proliferation. Some readers might be surprised by the use of this topic area to lead off the volume, because many plant scientists may think of the image analysis tools as merely incidental components for the operation of the bioreactors. The editors properly focus this introductory section on the software that makes the real differences in hardware performance and which permits automation and efficiency.

As expected the larger section of the volume, Part 2 covers Bioreactor Technology- the hardware that supports the technology. This section includes eight chapters addressing various applications of bioreactors for micropropagation, bioproduction of proteins, and hairy root culture for production of medicinal compounds. Various engineering designs are discussed, along with their benefits for different applications, including airlift, thin-film, nutrient mist, temporary immersion, and wave bioreactors. These chapters include discussion of key bioprocess control points and how they are handled in various bioreactor designs, including issues of aeration, oxygen transport, nutrient transfer, shear stress, mass/energy balances, medium flow, light, etc.

Part 3 covers more specific issues related to Mechanized Micropropagation. The two chapters in this section address the economic considerations of automated micropropagation systems as related to different types of tissue proliferation, and the use of robotics to facilitate separation of propagules and reduce labour costs. Part 4, Engineering Cultural Environment, has six chapters elaborating on engineering issues related to closed systems, aeration, culture medium gel hardness, dissolved oxygen,

Foreword

photoautotrophic micropropagation and temperature distribution inside the culture vessel.

The last part (Part 5) includes four chapters that discuss specific applications in Electrophysiology, Ultrasonics, and Cryogenics. Benefits have been found in the use of both electrostimulation and ultrasonics for manipulation of plant regeneration. Electrostimulation may be a useful tool for directing signal transduction within and between cells in culture. Ultrasound has also applications in monitoring tissue quality, such as state of hyperhydricity. Finally the application of engineering principles has improved techniques and hardware used for long-term cryopreservation of plant stock materials.

Readers of this volume will find a unique collection of chapters that will focus our attention on the interface of plant biotechnologies and engineering technologies. I look forward to the stimulation this volume will bring to our colleagues and to this emerging field of research and development!

Gregory C. Phillips, Ph. D.
Dean, College of Agriculture
Arkansas State University

PREFACE

Plant tissue culture has now emerged as one of the major components of plant biotechnology. This field of experimental botany begins its journey with the concept of 'cellular totipotency' for demonstration of plant morphogenesis. Decades of research in plant tissue culture has passed through many challenges, created new dreams and resulted in landmark achievements. Considerable progress has been made with regard to the improvement of media formulations and techniques of cell, tissue, organ, and protoplast culture. Such advancement in cultural methodology led many recalcitrant plants amenable to *in vitro* regeneration and to the development of haploids, somatic hybrids and pathogen free plants. Tissue culture methods have also been employed to study the basic aspects of plant growth, metabolism, differentiation and morphogenesis and provide ideal opportunity to manipulate these processes.

Recent development of *in vitro* techniques has demonstrated its application in rapid clonal propagation, regeneration and multiplication of genetically manipulated superior clones, production of secondary metabolites and *ex-situ* conservation of valuable germplasms. This has been possible not only due to the refinements of cultural practices and applications of cutting-edge areas of molecular biology but also due to the judicious inclusion of engineering principles and methods to the system. In the present scenario, inclusion of engineering principles and methods has transformed the fundamental *in vitro* techniques into commercially viable technologies. Apart from the commercialization of plant tissue culture, engineering aspects have also made it possible to improve the regeneration of plants and techniques of cryopreservation. Strategies evolved utilize the disciplines of chemical, mechanical, electrical, cryogenics, and computer science and engineering.

In the years to come, the application of plant tissue culture for various biotechnological purposes will increasingly depend on the adoption of engineering principles and better understanding of their interacting factors with biological system. The present volume provides a cohesive presentation of the engineering principles and methods which have formed the keystones in practical applications of plant tissue culture, describes how application of engineering methods have led to major advances in commercial tissue culture as well as in understanding fundamentals of morphogenesis and cryopreservation, and focuses directions of future research, as we envisage them. We hope the volume will bridge the gap between conventional plant tissue culturists and engineers of various disciplines.

A diverse team of researchers, technologists and engineers describe in lucid manner how various engineering disciplines contribute to the improvement of plant tissue culture techniques and transform it to a technology. The volume includes twenty four chapters presenting the current status, state of the art, strength and weaknesses of the strategy applicable to the *in vitro* system covering the aspects of machine vision, bioreactor technology, mechanized micropropagation, engineering cultural environment and physical aspects of plant tissue engineering. The contributory chapters are written by international experts who are pioneers, and have made significant contributions to

Preface

this emerging interdisciplinary enterprise. We are indebted to the chapter contributors for their kind support and co-operation. Our deepest appreciation goes to Professor G.C. Phillips for sparing his valuable time for writing the Foreword. We are grateful to Professor Marcel Hofman, the series editor, 'Focus on Biotechnology' for his critical review and suggestions during the preparation of this volume.

Our thanks are also due to Dr. Rina Dutta Gupta for her efforts in checking the drafts and suggesting invaluable clarifications. We are also thankful to Mr. V.S.S. Prasad for his help during the preparation of camera ready version. Finally, many thanks to Springer for their keen interest in bringing out this volume in time with quality work.

S. Dutta Gupta
Y. Ibaraki
Kharagpur/Yamaguchi, January 2005

TABLE OF CONTENTS

FOREWORD.....	v
PREFACE.....	vii
TABLE OF CONTENTS.....	1
PART 1.....	13
MACHINE VISION.....	13
Evaluation of photosynthetic capacity in micropropagated plants by image analysis	15
Yasuomi Ibaraki	15
1. Introduction	15
2. Basics of chlorophyll fluorescence	16
3. Imaging of chlorophyll fluorescence for micropropagated plants	18
3.1. Chlorophyll fluorescence in <i>in vitro</i> cultured plants.....	18
3.2. Imaging of chlorophyll fluorescence	21
3.3. Imaging of chlorophyll fluorescence in micropropagated plants	22
4. Techniques for image-analysis-based evaluation of photosynthetic capacity	25
5. Estimation of light distribution inside culture vessels	26
5.1. Understanding light distribution in culture vessels.....	26
5.2. Estimation of light distribution within culture vessels	26
6. Concluding remarks	27
References	28
Monitoring gene expression in plant tissues	31
John J. Finer, Summer L. Beck, Marco T. Buenrostro-Nava, Yu-Tseh Chi and Peter P. Ling.....	31
1. Introduction	31
2. DNA delivery	32
2.1. Particle bombardment	32
2.2. <i>Agrobacterium</i>	33
3. Transient and stable transgene expression	33
4. Green fluorescent protein	34
4.1. GFP as a reporter gene	34
4.2. GFP image analysis.....	35
4.3. Quantification of the green fluorescence protein <i>in vivo</i>	36
5. Development of a robotic GFP image acquisition system.....	37
5.1. Overview	37
5.2. Robotics platform.....	37
5.3. Hood modifications	39
5.4. Microscope and camera.....	40
5.5. Light source and microscope optics	40
6. Automated image analysis	41
6.1. Image registration.....	41
6.2. Quantification of GFP	43

Table of Contents

7. Conclusions	43
Acknowledgements	44
References	44
Applications and potentials of artificial neural networks in plant tissue culture	47
V.S.S. Prasad and S. Dutta Gupta	47
1. Introduction	47
2. Artificial neural networks.....	48
2.1. Structure of ANN	48
2.2. Working principle and properties of ANN.....	49
2.2.1. Computational property of a node.....	49
2.2.2. Training mechanisms of ANN	51
2.3. Types of artificial neural networks	51
2.3.1. Classification and clustering models.....	51
2.3.2. Association models	52
2.3.3. Optimization models	52
2.3.4. Radial basis function networks (RBFN)	52
2.4. Basic strategy for network modelling	52
2.4.1. Database	52
2.4.2. Selection of network structure	53
2.4.2.1. Number of input nodes.....	54
2.4.2.2. Number of hidden units.....	54
2.4.2.3. Learning algorithm.....	54
2.4.3. Training and validation of the network.....	55
3. Applications of ANN in plant tissue culture systems	56
3.1. <i>In vitro</i> growth simulation of alfalfa	56
3.2. Classification of plant somatic embryos	58
3.3. Estimation of biomass of plant cell cultures	58
3.4. Simulation of temperature distribution inside a plant culture vessel.....	59
3.5. Estimation of length of <i>in vitro</i> shoots.....	61
3.6. Clustering of <i>in vitro</i> regenerated plantlets into groups.....	61
4. Conclusions and future prospects.....	65
Acknowledgement.....	66
References	66
Evaluation of plant suspension cultures by texture analysis.....	69
Yasuomi Ibaraki	69
1. Introduction	69
2. Microscopic and macroscopic image uses in plant cell suspension culture ..	69
3. Texture analysis for macroscopic images of cell suspensions.....	71
3.1. Texture features	71
3.2. Texture analysis for biological objects	72
3.3. Texture analysis for cell suspension culture	73
3.4. Considerations for application of texture analysis.....	73
4. Evaluation of embryogenic potential of cultures by texture analysis	73
4.1. Evaluation of embryogenic potential of cultures	73
4.2. Texture analysis based evaluation of embryogenic potential	74

Table of Contents

5. Concluding remarks	77
References	77
PART 2.....	81
BIOREACTOR TECHNOLOGY	81
Bioengineering aspects of bioreactor application in plant propagation	83
Shinsaku Takayama and Motomu Akita	83
1. Introduction	83
2. Advantages of the use of bioreactor in plant propagation	84
3. Agar culture vs. liquid culture.....	85
4. Transition from shake culture to bioreactor culture.....	85
5. Types of bioreactors for plant propagation	86
6. Preparation of propagules for inoculation to bioreactor	87
7. Characteristics of bioreactor for plant propagation.....	88
7.1. Fundamental configuration of bioreactor.....	88
7.2. Aeration and medium flow characteristics.....	90
7.2.1. Medium flow characteristics	90
7.2.2. Medium mixing	91
7.2.3. Oxygen demand and oxygen supply	92
7.3. Light illumination and transmittance	93
8. Examples of bioreactor application in plant propagation	95
9. Aseptic condition and control of microbial contamination.....	95
10. Scale-up to large bioreactor.....	96
10.1. Propagation of <i>Stevia</i> shoots in 500 L bioreactor	96
10.2. Safe inoculation of plant organs into bioreactor	98
11. Prospects.....	98
References	98
Agitated, thin-films of liquid media for efficient micropropagation.....	101
Jeffrey Adelberg	101
1. Introduction	101
2. Heterotrophic growth and nutrient use.....	102
2.1. Solutes in semi-solid agar	102
2.2. Solutes in stationary liquids	103
2.3. Sugar in shaker flasks and bioreactors.....	105
3. Efficiency in process	108
3.1. Shoot morphology for cutting and transfer process	108
3.2. Space utilization on culture shelf	109
3.3. Plant quality.....	109
4. Vessel and facility design.....	110
4.1. Pre-existing or custom designed vessel	110
4.2. Size and shape	111
4.3. Closures and ports	112
4.4. Biotic contaminants.....	113
4.5. Light and heat.....	113
5. Concluding remarks	115
Disclaimer	115
References	115

Table of Contents

Design, development, and applications of mist bioreactors for micropropagation and hairy root culture	119
Melissa J. Towler, Yoojeong Kim, Barbara E. Wyslouzil, Melanie J. Correll, and Pamela J. Weathers	119
1. Introduction	119
2. Mist reactor configurations	120
3. Mist reactors for micropropagation.....	122
4. Mist reactors for hairy root culture	125
5. Mist deposition modelling.....	128
6. Conclusions	130
Acknowledgements	131
References	131
Bioreactor engineering for recombinant protein production using plant cell suspension culture	135
Wei Wen Su.....	135
1. Introduction	135
2. Culture characteristics	136
2.1. Cell morphology, degree of aggregation, and culture rheology	137
2.2. Foaming and wall growth.....	140
2.3. Shear sensitivity	141
2.4. Growth rate, oxygen demand, and metabolic heat loads	145
3. Characteristics of recombinant protein expression	146
4. Bioreactor design and operation.....	148
4.1. Bioreactor operating strategies.....	148
4.2. Bioreactor configurations and impeller design	151
4.3. Advances in process monitoring	153
5. Future directions.....	154
Acknowledgements	155
References	155
Types and designs of bioreactors for hairy root culture	161
Yong-Eui Choi, Yoon-Soo Kim and Kee-Yoeup Paek.....	161
1. Introduction	161
2. Advantage of hairy root cultures	162
3. Induction of hairy roots	162
4. Large-scale culture of hairy roots	163
4.1. Stirred tank reactor	164
4.2. Airlift bioreactors	164
4.3. Bubble column reactor	165
4.4. Liquid-dispersed bioreactor	165
5. Commercial production of <i>Panax ginseng</i> roots via balloon type bioreactor	166
Acknowledgements	169
References	169
Oxygen transport in plant tissue culture systems	173
Wayne R. Curtis and Amalie L. Tuerk.....	173
1. Introduction	173

Table of Contents

2. Intrapphase transport	175
2.1. Oxygen transport in the gas phase	175
2.2. Oxygen transport in the liquid phase	176
2.3. Oxygen transport in solid (tissue) phase	177
3. Interphase transport	179
3.1. Oxygen transport across the gas-liquid interface	179
3.2. Oxygen transport across the gas-solid interface	179
3.3. Oxygen transport across the solid-liquid interface	180
4. Example: oxygen transport during seed germination in aseptic liquid culture	181
4.1. The experimental system used for aseptic germination of seeds in liquid culture	181
4.2. Experimental observation of oxygen limitation	182
4.3. Characterization of oxygen mass transfer	182
5. Conclusions	185
Acknowledgements	185
References	185
Temporary immersion bioreactor	187
F. Afreen	187
1. Introduction	187
2. Requirement of aeration in bioreactor: mass oxygen transfer	188
3. Temporary immersion bioreactor	189
3.1. Definition and historical overview	189
3.2. Design of a temporary immersion bioreactor	189
3.3. Advantages of temporary immersion bioreactor	190
3.4. Scaling up of the system: temporary root zone immersion bioreactor	191
3.5. Design of the temporary root zone immersion bioreactor	191
3.6. Case study – photoautotrophic micropropagation of coffee	193
3.7. Advantages of the system	198
4. Conclusions	199
References	200
Design and use of the wave bioreactor for plant cell culture	203
Regine Eibl and Dieter Eibl	203
1. Introduction	203
2. Background	204
2.1. Disposable bioreactor types for <i>in vitro</i> plant cultures	204
2.2. The wave: types and specification	206
3. Design and engineering aspects of the wave	209
3.1. Bag design	209
3.2. Hydrodynamic characterisation	210
3.3. Oxygen transport efficiency	217
4. Cultivation of plant cell and tissue cultures in the wave	217
4.1. General information	217
4.2. Cultivation of suspension cultures	220
4.3. Cultivation of hairy roots	222
4.4. Cultivation of embryogenic cultures	223

Table of Contents

5. Conclusions	224
Acknowledgements	224
References	224
PART 3	229
MECHANIZED MICROPROPAGATION	229
Integrating automation technologies with commercial micropropagation .	231
Carolyn J. Sluis.....	231
1. Introduction	231
2. Biological parameters.....	232
2.1. The plant's growth form affects mechanized handling.....	232
2.2. Microbial contaminants hinder scale-up	235
3. Physical parameters.....	236
3.1. Culture vessels.....	237
3.2. Physical orientation of explants for subculture or singulation.....	237
3.3. Gas phase of the culture vessel impacts automation.....	238
4. Economic parameters	238
4.1. Baseline cost models	238
4.2. Economics of operator-assist strategies	241
4.3. Organization of the approach to rooting: <i>in vitro</i> or <i>ex vitro</i>	241
4.4. Economics of new technologies.....	242
5. Business parameters	242
5.1. Volumes per cultivar	243
5.2. Seasons	244
5.3. Cost reduction targets.....	244
6. Political parameters	246
7. Conclusions	247
Acknowledgements	248
References	248
Machine vision and robotics for the separation and regeneration of plant tissue cultures.....	253
Paul H. Heinemann and Paul N. Walker.....	253
1. Introduction	253
2. Examples of automation and robotics	253
3. Robotic system component considerations	254
3.1. Plant growth systems for robotic separation	255
3.1.1. Nodes.....	255
3.1.2. Clumps	255
3.2. An experimental shoot identification system for shoot clumps.....	256
3.2.1. Shoot identification using the Arc method	257
3.2.2. Shoot identification using the Hough transform method.....	259
3.2.3. Testing the Hough transform	263
3.3. Robotic mechanisms for shoot separation	264
3.3.1. Manual separation device.....	264
3.3.2. Automated separation device	265
3.3.3. Single image versus real-time imaging for shoot separation.....	268
3.3.4. Shoot re-growth.....	269

Table of Contents

3.3.5. Cycle time	270
3.3.6. Commercial layout	270
References	271
PART 4.....	273
ENGINEERING CULTURAL ENVIRONMENT	273
Closed systems for high quality transplants using minimum resources.....	275
T. Kozai	275
1. Introduction	275
2. Why transplant production systems?	276
3. Why closed systems?	278
4. Commercialization of closed transplant production systems.....	280
5. General features of high quality transplants	280
6. Sun light vs. use of lamps as light source in transplant production.....	282
7. Closed plant production system	284
7.1. Definition	284
7.2. Main components	284
7.3. Characteristics of main components of the closed system.....	285
7.4. Equipments and facilities: a comparison	285
7.5. Features of the closed system vs. greenhouse	286
7.6. Equality in Initial investment.....	290
7.7. Reduction in costs for transportation and labour	291
7.8. Uniformity and precise control of microenvironment	292
7.9. Growth, development and uniformity of transplants	293
8. Value-added transplant production in the closed system.....	293
8.1. Tomato (<i>Lycopersicon esculentum</i> Mill.)	294
8.2. Spinach (<i>Spinacia oleracea</i>)	295
8.3. Sweet potato (<i>Ipomoea batatas</i> L. (Lam.))	295
8.4. Pansy (<i>Viola x wittrockiana</i> Gams.).....	297
8.5. Grafted transplants	297
8.6. Vegetable transplants for field cultivation	298
9. Increased productivity to that of the greenhouse	299
10. Costs for heating, cooling, ventilation and CO ₂ enrichment.....	300
10.1. Heating cost.....	300
10.2. Cooling load and electricity consumption	301
10.3. Cooling cost.....	301
10.4. Electricity consumption	303
10.5. Electricity cost is 1-5% of sales price of transplants	303
10.6. Relative humidity	304
10.7. Par utilization efficiency	304
10.8. Low ventilation cost.....	305
10.9. CO ₂ cost is negligibly small.....	305
10.10. Water requirement for irrigation	306
10.11. Disinfection of the closed system is easy.....	307
10.12. Simpler environmental control unit	307
10.13. Easier production management.....	308
10.14. The closed system is environment friendly.....	308

Table of Contents

10.15. The closed system is safer.....	309
11. Conclusion.....	310
Acknowledgement.....	311
References	311
Aeration in plant tissue culture.....	313
S.M.A. Zobayed	313
1. Introduction	313
2. Principles of aeration in tissue culture vessel	314
2.1. Aeration by bulk flow	317
2.2. Aeration by diffusion	319
2.3. Humidity-induced convection in a tissue culture vessel.....	321
2.4. Aeration by venturi-induced convection.....	325
2.5. Forced aeration by mass flow	326
3. Conclusions	326
References	327
Tissue culture gel firmness: measurement and effects on growth.....	329
Stewart I. Cameron.....	329
1. Introduction	329
2. Measurement of gel hardness.....	330
3. Gel hardness and pH	333
4. The dynamics of syneresis	334
5. Conclusion.....	335
References	336
Effects of dissolved oxygen concentration on somatic embryogenesis.....	339
Kenji Kurata and Teruaki Shimazu.....	339
1. Introduction	339
2. Relationship between DO concentration and somatic embryogenesis	341
2.1. Culture system and DO concentration variations	341
2.2. Time course of the number of somatic embryos.....	342
2.3. Relationship between somatic embryogenesis and oxygen concentration.....	346
3. Dynamic control of DO concentration to regulate torpedo-stage embryos	347
3.1. The method of dynamic DO control	347
3.2. Results of dynamic DO control.....	351
4. Conclusions	352
References	352
A commercialized photoautotrophic micropropagation system.....	355
T. Kozai and Y. Xiao.....	355
1. Introduction	355
2. Photoautotrophic micropropagation.....	356
2.1. Summary of our previous work.....	356
3. The PAM (photoautotrophic micropropagation) system and its components.....	357
3.1. System configuration.....	357
3.2. Multi-shelf unit.....	358
3.3. Culture vessel unit.....	360

Table of Contents

3.4. Forced ventilation unit for supplying CO ₂ -enriched air.....	360
3.5. Lighting unit.....	362
3.6. Sterilization	362
4. Plantlet growth, production costs and sales price	362
4.1 Calla lily plantlet growth.....	362
4.2. China fir plantlet growth	365
4.3. Percent survival during acclimatization <i>ex vitro</i>	366
4.4. Production cost of calla lily plantlets: A case study	367
4.4.1. Production cost per acclimatized plantlet	368
4.4.2. Cost, labour and electricity consumption for multiplication or rooting.....	368
4.4.3. Sales price of <i>in vitro</i> and <i>ex vitro</i> acclimatized plantlets	370
5. Conclusions	370
Acknowledgement.....	370
References	370
Intelligent inverse analysis for temperature distribution in a plant culture vessel	373
H. Murase, T. Okayama, and Suroso	373
1. Introduction	373
2. Theoretical backgrounds	375
3. Methodology	378
3.1. Finite element neural network inverse technique algorithm.....	378
3.2. Finite element formulation.....	379
3.3. Finite element model.....	380
3.4. Neural network structure	381
3.5. Neural network training	381
3.6. Optimization of temperature distribution inside the culture vessel	382
3.6.1. Genetic algorithm flowchart	382
3.6.2. Objective function	383
3.6.3. Genetic reproduction	383
3.7. Temperature distribution measurement.....	386
3.7.1. Equipment development for temperature distribution measurement.....	386
3.7.2. Temperature distribution data	388
4. Example of solution	388
4.1. Coefficient of convective heat transfer	388
4.2. Verification of the calculated coefficient of convective heat transfer .	390
4.3. Optimum values of air velocity and bottom temperature	391
References	394
PART 5.....	395
PHYSICAL ASPECTS OF PLANT TISSUE ENGINEERING.....	395
Electrical control of plant morphogenesis	397
Cogălniceanu Gina Carmen	397
1. Introduction	397
2. Endogenous electric currents as control mechanisms in plant development	397
3. Electrostimulation of <i>in vitro</i> plant development	400

Table of Contents

4. High-voltage, short-duration electric pulses interaction with <i>in vitro</i> systems.....	403
4.1. Effects of electric pulses treatment on plant protoplasts	404
4.2. Effects of electric pulses treatment on tissue fragments or entire plantlets.....	406
5. Potential applications of the electric manipulation in plant biotechnology	410
References	411
The uses of ultrasound in plant tissue culture.....	417
Victor Gaba, K. Kathiravan, S. Amutha, Sima Singer, Xia Xiaodi and G. Ananthkrishnan	417
1. Introduction	417
2. The generation of ultrasound	418
3. Mechanisms of action of ultrasound	419
4. Sonication-assisted DNA transformation.....	420
5. Sonication-assisted <i>Agrobacterium</i> -mediated transformation.....	420
6. Stimulation of regeneration by sonication	421
7. Summary of transformation and morphogenic responses to ultrasound.....	422
8. Fractionation of somatic embryos.....	423
9. Secondary product synthesis	423
10. Ultrasound and control of micro-organisms	423
11. Conclusions	424
Acknowledgements	424
References	424
Acoustic characteristics of plant leaves using ultrasonic transmission waves.....	427
Mikio Fukuhara, S. Dutta Gupta and Limi Okushima	427
1. Introduction	427
2. Theoretical considerations and system description.....	428
3. Case studies on possible ultrasonic diagnosis of plant leaves	430
3.1. Ultrasonic testing of tea leaves for plant maturity	430
3.1.1. Wave velocity and dynamic modulus for leaf tissue development	431
3.1.2. Dynamic viscosity and imaginary parts in complex waves	432
3.2. Ultrasonic diagnosis of rice leaves.....	434
3.3. Acoustic characteristics of <i>in vitro</i> regenerated leaves of gladiolus....	435
4. Conclusions	438
Acknowledgement.....	438
References	438
Physical and engineering perspectives of <i>in vitro</i> plant cryopreservation...	441
Erica E. Benson, Jason Johnston, Jayanthi Muthusamy and Keith Harding	441
1. Introduction	441
2. The properties of liquid nitrogen and cryosafety	442
3. Physics of ice.....	443
3.1. Water's liquid and ice morphologies	444
3.1.1. Making snowflakes: a multiplicity of ice families.....	445
4. Cryoprotection, cryodestruction and cryopreservation.....	447
4.1. Physical perspectives of ultra rapid and droplet freezing	448

Table of Contents

4.2. Controlled rate or slow cooling.....	450
4.3. Vitrification	451
5. Cryoengineering: technology and equipment	451
5.1. Cryoengineering for cryogenic storage.....	451
5.1.1. Controlled rate freezers	452
5.1.2. Cryogenic storage and shipment	455
5.1.3. Sample safety, security and identification	456
6. Cryomicroscopy	456
6.1. Nuclear imaging in cryogenic systems	458
7. Thermal analysis	459
7.1. Principles and applications.....	460
7.1.1. DSC and the optimisation of cryopreservation protocols	462
7.1.2. A DSC study comparing cryopreserved tropical and temperate plant germplasm	463
7.1.2.1. Using thermal analysis to optimise cryoprotective strategies....	468
8. Cryoengineering futures.....	470
Acknowledgements	473
References	474
INDEX.....	477

PART 1

MACHINE VISION

EVALUATION OF PHOTOSYNTHETIC CAPACITY IN MICROPROPAGATED PLANTS BY IMAGE ANALYSIS

YASUOMI IBARAKI

*Department of Biological Science, Yamaguchi University, Yoshida 1677-1, Yamaguchi-shi, Yamaguchi 753-8515, Japan – Fax: +81-83-933-5864
Email: ibaraki@yamaguchi-u.ac.jp*

1. Introduction

In micropropagation, *in vitro* environmental conditions (i.e., environmental conditions surrounding plantlets within culture vessels such as light conditions, temperature, and gaseous composition), have an important role in plantlet growth. Normally, *in vitro* environmental conditions cannot be controlled directly; instead, they are largely determined by regulated culture conditions outside the vessel. Therefore, culture conditions should be optimized for plantlet growth. It is necessary for optimization of culture conditions to understand relationships between culture conditions and *in vitro* plant growth, physiological state, or both. *In vitro* environmental conditions may change with plantlet growth during culture because the plantlet itself affects them. Therefore, non-destructive evaluation of the growth of micropropagated plantlets and their physiological state without disturbing the *in vitro* environmental conditions is desirable for investigating these relationships and considering their dynamics.

Recent studies revealed that *in vitro* cultured chlorophyllous plantlets had photosynthetic ability but their net photosynthetic rates were restricted by environmental conditions [1]. The photosynthetic properties of plantlets *in vitro* depend on culture conditions, including light intensity [2], the degree of air exchange between a vessel and the surrounding air [3], and the sugar content in the medium [4]. Photoautotrophic micropropagation which is micropropagation with no sugar added to the medium has many advantages, especially in plantlet quality [1]. For successful photoautotrophic micropropagation, *in vitro* environmental conditions should be properly controlled to enhance photosynthesis of the plantlets by manipulation of culture conditions. Successful photoautotrophic micropropagation also requires knowledge of when cultures should transit from photomixotrophic into photoautotrophic [1]. An understanding of changes in photosynthetic properties of cultured plantlets during the culture period is essential to optimize culture conditions for photoautotrophic culture to obtain high-quality plantlets.

It is difficult to evaluate photosynthetic properties of plantlets non-destructively. Carbon dioxide gas exchange rates of plantlets *in vitro* can be estimated *in situ* by measurements of the concentration of CO₂ inside and outside the culture vessel, the degree of air

exchange between the vessel and the surrounding air, and the head space volume in the vessel [5]. However, the estimated gas exchange rates are the rates per all plantlets within the vessel, and they should be converted to the rates per unit leaf area or unit dry weight for analysis of the photosynthetic properties. This requires estimation of leaf area or dry weight of plantlets in the vessel. In addition, it should be noted that the environmental conditions could be non-uniform in a culture vessel even under controlled culture conditions. In culture vessels, air movement is limited, and as a result, there may be gradients in humidity and/or CO₂ concentration within the vessels. In addition, vertical light intensity distribution exists in slender vessels like test tubes [6]. This might cause variations in the *in vitro* microenvironment around the cultured plants and consequently cause variations in photosynthetic capacity. This variation may affect uniformity in plantlet quality, especially when propagating by cuttings, such as for potato nodal cutting cultures. An understanding of variations in photosynthetic properties within cultured plantlets may be helpful for obtaining uniform-quality plantlets.

Chlorophyll fluorescence has been a useful tool for photosynthetic research. In recent years, the value of this tool in plant physiology has been greatly increased by the availability of suitable instrumentation and an increased understanding of the processes that regulate fluorescence yield [7]. It has enabled analysis of the photosynthetic properties of plant leaves, especially characteristics related to the photochemical efficiency of photosystem II. As chlorophyll fluorescence analysis is based on photometry, i.e., measurement of light intensity, it is a promising means of non-destructive estimation of photosynthetic capacity.

In this chapter, the methods for non-destructive evaluation of photosynthetic capacity are introduced, focusing on imaging of chlorophyll fluorescence. First, the principle of photosynthetic analysis based on chlorophyll fluorescence will be outlined, and the feasibility of imaging the chlorophyll fluorescence parameters for micropropagated plants from outside the culture vessels will be discussed. Other promising indices based on spectral reflectance for imaging the photosynthetic capacity of micropropagated plants will be also discussed. In addition, estimation methods for light intensity distribution inside culture vessels will be introduced in consideration of its influence on the photosynthetic properties of cultured plants.

2. Basics of chlorophyll fluorescence

Chlorophyll absorbs photons for use in the photochemical reaction of photosynthesis. Excited chlorophyll can re-emit a photon and return to its ground state, and this fluorescence is called chlorophyll fluorescence. Occasionally, it is also referred to as chlorophyll *a* fluorescence, since it is due to chlorophyll *a*. The analysis of chlorophyll fluorescence provides a powerful probe of the functioning of the intact photosynthetic system [8]. It especially enables us to obtain information on the functioning of photosystem II (PSII), since at room temperature chlorophyll fluorescence is predominantly derived from PSII [9]. Methods to analyze photosynthetic properties of leaves using chlorophyll fluorescence include a method using a saturating light pulse and another method based on induction kinetics (the Kautsky curve [10]). Here, the

former method, in which fluorescence is measured while varying PSII photochemical efficiency using a saturating light pulse, is more fully explained.

After dark adaptation treatment, the yield, Φ_F of fluorescence excited by very weak irradiance is expressed by the following equation:

$$\Phi_F = \frac{k_F}{k_F + k_D + k_T + k_P} \quad (1)$$

Where k_F , k_D , k_T , and k_P are rate constants for fluorescence, thermal dissipation, energy transfer to PSI and PSII photochemistry (electron transport), respectively.

As the portion of energy transfer is very small, k_T can be neglected in the above equation [7]. This fluorescence, which occurs when the primary electron acceptor, Q_A , is fully oxidized due to excitation by weak light just after dark adaptation, is referred to as F_o . Then, irradiation by a saturating light pulse (of very high intensity) leads to full reduction of Q_A (sometimes the condition is referred to as "closed"). The fluorescent yield, Φ_{Fm} , of maximum fluorescence Fm , determined under the saturating light pulse, is expressed by the following equation:

$$\Phi_{Fm} = \frac{k_F}{k_F + k_D + k_T} \quad (2)$$

From F_o and Fm , the maximum quantum yield of PSII, Fv/Fm , is estimated using the following equation:

$$\begin{aligned} Fv/Fm &= \frac{Fm - F_o}{Fm} \\ &= \left\{ \frac{k_F}{k_F + k_D + k_T} - \frac{k_F}{k_F + k_D + k_T + k_P} \right\} \left\{ \frac{k_F}{k_F + k_D + k_T} \right\} \\ &= \left\{ 1 - \frac{k_F + k_D + k_T}{k_F + k_D + k_T + k_P} \right\} \\ &= \frac{k_P}{k_F + k_D + k_T + k_P} \end{aligned} \quad (3)$$

Fv/Fm is a measure of photoinhibition and has been used for photosynthetic capacity evaluation in photosynthetic research (e.g., [11]) and cultivar screening (e.g., [12]). Under light conditions without dark adaptation (hereafter, the light is referred to as actinic light to distinguish from the light for fluorescent measurements), the actual quantum yield of PSII, Φ_{PSII} , can be also estimated using the following equation:

$$\Phi_{\text{PSII}} = \Delta F / Fm' = \frac{Fm' - F}{Fm'} \quad (4)$$

Where F is the fluorescence excited by the measuring light under the actinic light, and Fm' is the fluorescence excited by the measuring light while irradiating with the saturating light pulse (that is, when Q_A is fully closed) under the actinic light. As for the other parameters, photochemical quenching, qp , which shows the extent to which Φ_{PSII} is restricted by photochemical capacity at PSII, and indices of non-photochemical quenching, qN and NPQ , which are related to heat dissipation, can be derived by fluorescence measurement using a saturating light pulse. Also, the linear electron transport rate, ETR , can be estimated if the number of photons absorbed is known [13]. These parameters were reviewed by Maxwell and Johnson in detail [14]. The chlorophyll fluorescence parameters can be measured by a pulse amplitude modulation (PAM) fluorometer. In this fluorometer, the excitation light (pulsed light of low intensity; hereafter, measuring pulse) used to measure chlorophyll fluorescence is separately applied to the actinic light, which drives the photosynthetic light reaction [15]. Due to the selective pulse-amplification system, only fluorescence excited by the measuring pulse is recorded in the presence of the actinic light [15]. Although in some cases the parameters can be obtained non-destructively with PAM fluorometer, there are some limitations in the measurements, for example due to the short distance (10-15 mm) between the sensor probe of the fluorometer and the leaf surface.

3. Imaging of chlorophyll fluorescence for micropropagated plants

3.1. CHLOROPHYLL FLUORESCENCE IN *IN VITRO* CULTURED PLANTS

In research on micropropagation, the chlorophyll fluorescence parameter Fv/Fm has been used to evaluate photosynthetic capacity, though applications are limited to a few studies. The nutrient composition of the medium affects Fv/Fm of *in vitro* cultured *Pinus radiata* [16]. *Ex vitro* transfer for acclimatization causes a decrease in Fv/Fm of plantlets and the degree of the reduction in Fv/Fm depended on culture conditions [17,18]. In general, plants grown under low light intensity are more sensitive to photoinhibition caused by high light intensity [19]. Therefore, Fv/Fm of micropropagated plantlets may be subject to change according to culture conditions.

Evaluation of photosynthetic capacity in micropropagated plants by image analysis

Table 1. *Fv/Fm* of potato plantlets of different sucrose content treatments (Exp.1).
Reproduced from Ibaraki, Y. and Matsumura, K. (2004) [20].

	<i>Fv/Fm</i>	
	Average	CV*
30 g/L	0.795 b**	0.032 ab**
10 g/L	0.750 c	0.055 a
0 g/L	0.818 a	0.020 b

* Coefficient of variation in a single plantlet, ** Different letters within row show significant differences by Tukey multiple range test at 1% level

Table 2. *Fv/Fm* of potato plantlets of different sucrose content treatments (Exp.2).

	<i>Fv/Fm</i>	
	Average	CV*
30 g/L	0.77 a**	0.032 b**
0 g/L	0.72 b	0.115 a

* Coefficient of variation in a single plantlet, ** Different letters within row show significant differences by Tukey multiple range test at 1% level.

To investigate sensitivity of *Fv/Fm* to culture conditions, two experiments were conducted to determine *Fv/Fm* for potato plantlets cultured under various environmental conditions [20]. In one experiment, potato nodal cuttings were transplanted into glass tubes containing MS medium [21] with different contents of sucrose (30 g/L, 10 g/L, and 0 g/L). In the case of the sugar-free treatment, a hydrophobic Fluoropore[®] membrane filter (Milliseal[®], Millipore[®]) was attached to the plastic cap of the glass tube to enhance gas exchange for photoautotrophic growth. In another experiment, *Fv/Fm* values of plantlets cultured in medium with 30 g/L sucrose or in sugar-free medium were compared under conditions where gas exchange was suppressed using normal plastic caps for both treatments. At the end of culturing (35d and 40d after transplanting for experiment 1 and experiment 2, respectively), plantlets were transferred *ex vitro*, and *Fv/Fm* was measured randomly for all measurable leaves of the plantlets using a PAM fluorometer (MINI-PAM, Walz, Germany) after a 60 min dark adaptation treatment. For each treatment, 8 plantlets were tested. Average *Fv/Fm* values were affected by culture conditions (Tables 1 and 2). Without promoting gas exchange of culture vessels, *Fv/Fm* values of plantlets cultured in sugar-free medium were lower than for plantlets in 30 g/L sucrose treatment, which is a conventional medium formulation. In contrast, plantlets cultured with sugar-free medium in culture vessels promoting gas exchange showed

higher F_v/F_m than plantlets cultured in medium containing 30 g/L sucrose, indicating a higher photochemical efficiency. Combined effects of enhanced gas exchange and omission of sucrose from the medium might improve photosynthetic capacity. In comparisons between sucrose-containing treatments (experiment 1), plantlets of the 10 g/L treatment showed a lower F_v/F_m than plantlets of the 30 g/L treatment, and also suppressed growth. Variations in F_v/F_m values were observed among the plantlets and the distribution patterns in a plantlet changed slightly with sucrose content (Figures 1 and 2).

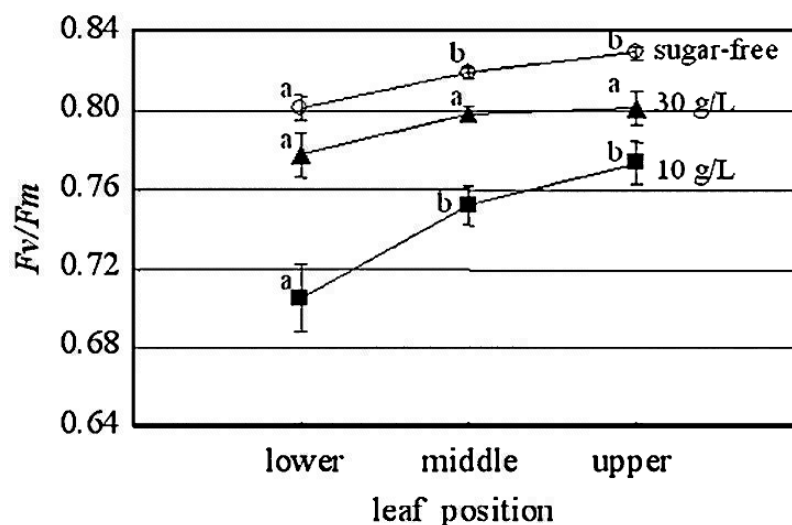


Figure 1. F_v/F_m distribution in potato plantlets cultured in MS medium contained 30 g/L, 10 g/L, or 0 g/L sucrose for 35 d (Exp. 1). Reproduced from Ibaraki, Y. and Matsumura, K. (2004) [20]. In sugar-free treatment, gas exchange was promoted by using the cap attached a hydrophobic Fluoropore (R) membrane filter. Lower 3 leaves, upper 3 leaves, and other leaves were classified into lower, upper, and middle in leaf position, respectively. Bar, SE. Different letters on graph lines show significant differences among leaf positions by Tukey multiple range test at 1% level.

These results suggest that F_v/F_m may change according to culture conditions, and that analysis of F_v/F_m for evaluation of photosynthetic capacity of cultured plantlets is effective for optimization of culture conditions.

Although F_v/F_m measurement is simple with the PAM fluorometer, there are some difficulties in measurements of plantlets within the culture vessel through the culture vessel wall. The measurement requires fixing the short distance between the sensor probe of the fluorometer and the leaf surface. This is a difficult requirement for plantlet leaves in a culture vessel. In addition, measurements for small leaves of plantlets with the fluorometer were subject to errors [20]. Non-destructive methods suited for micropropagated plants are desirable.

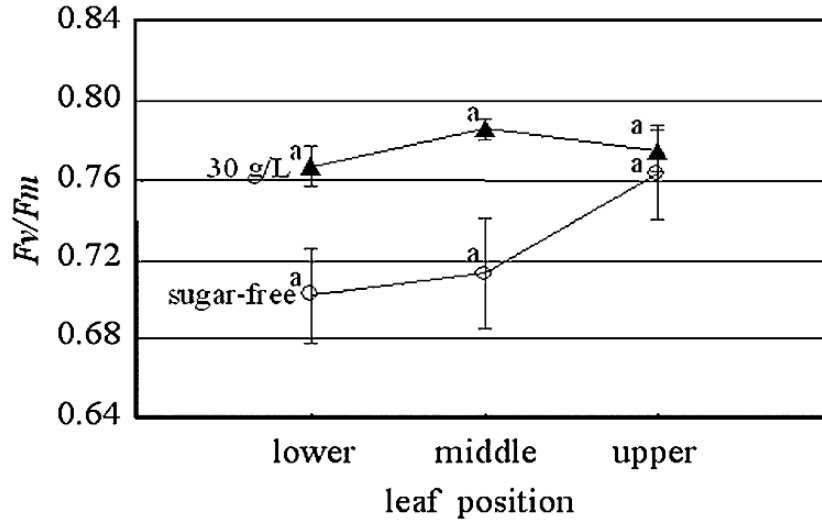


Figure 2. F_v/F_m distribution in potato plantlets cultured in MS medium contained 30 g/L or 0 g/L sucrose for 40 d (Exp. 2). Lower 3 leaves, upper 3 leaves, and other leaves were classified into lower, upper, and middle in leaf position, respectively. Bar, SE. Different letters on graph lines show significant differences among leaf positions by Tukey multiple range test at 1% level.

In a few studies, the chlorophyll fluorescence parameter $\Delta F/F_m'$, determined under actinic light by PAM fluorometer, has been used in micropropagation research. Since $\Delta F/F_m'$ depends on the level of light irradiating a leaf, and it is difficult to know the exact irradiation level, careful consideration is required to determine photosynthetic properties from values of $\Delta F/F_m'$. If the same light intensity were set for all plantlets tested, or if the light intensity distribution could be determined in culture vessels, $\Delta F/F_m'$ would offer information on plantlet photosynthetic capacity.

3.2. IMAGING OF CHLOROPHYLL FLUORESCENCE

Imaging of chlorophyll fluorescence was first reported by Omasa *et al.* [22]. In this study, the kinetics of chlorophyll fluorescence was analyzed using fluorescent images. For cultured callus and plantlets of *Daucus carota*, images of chlorophyll fluorescence induction were also used to analyze the development of photosynthetic apparatus [23]. Although several studies on chlorophyll fluorescence imaging had been reported, these primary studies required empirical calibration of the fluorescent signal using other methods, such as gas exchange, when the fluorescence images were converted to images of photosynthesis [24]. Recently, several reports showed the possibility of imaging chlorophyll fluorescence parameters based on a saturating light pulse method in order to obtain an image of photochemical efficiency over a leaf. Genty and Meyer [24] developed a method to construct the topography of the photochemical quantum yield of PSII and showed the effectiveness of the method by mapping the heterogeneous

distribution of photosynthetic activity after treatment with an herbicide, with abscisic acid, or during the course of induction of photosynthesis. Oscillations in photosynthesis initiated by a transient decrease in light intensity could be imaged over the leaf [25]. The sink-source transition of developing tobacco leaves was analyzed using images to evaluate electron transport rates [26]. Oxborough and Baker [7] proposed a method to image not only photochemical quantum yield but also non-photochemical quenching, assumed to correspond mainly to heat dissipation. In addition, Oxborough and Baker [27] developed a system to image F_o and consequently obtain an F_v/F_m image using a fluorescence microscope and a cooled charge coupled device (CCD) camera.

Chlorophyll fluorescence parameters can be imaged by considering the following points: 1) to distinguish between fluorescence and reflection by use of optical filters, and 2) to measure fluorescent quantum yield. Basic device arrangements for imaging of chlorophyll fluorescence include a light source for excitation of fluorescence, a camera, and optical filters for controlling excitation light intensity and separating reflected light and fluorescence. Normally, fluorescent intensity can be imaged as the grey level in each pixel by the camera. Therefore, it is necessary to convert fluorescent intensity into fluorescent yield to construct images mapping chlorophyll fluorescence parameters. If the irradiance distribution on a leaf were determined exactly, it would be possible to convert the fluorescent intensity to fluorescent yield. Actually, the conversion is done by controlling exposure time according to excitation light intensity [24], by imaging a fluorescent standard at the same time [25], or by imaging a reference leaf at the same time [20]. Recently, a PAM-based fluorescence imaging system (IMAGING-PAM, Walz, Germany) has been developed, which is now available. Although there have been few studies using the system to date, it is promising for non-destructive evaluation of plant photosynthetic properties.

For selection of cameras to image fluorescence, some considerations are required. In F_v/F_m measurements, F_o is not intense because it is excited by very low irradiance, so highly sensitive cameras such as expensive cooled CCD cameras are needed. Although low-cost CCD cameras with high sensitivity have become available recently, the images acquired by most have reduced numbers of distinct grey levels. It is necessary to discuss whether the number of distinct grey levels in an image is sufficient for calculations used to derive chlorophyll parameters. In addition, gamma and auto-gain features of cameras should be carefully treated because they affect the relationship between light intensity and the pixel grey level value. The relationship between light intensity and the pixel grey level value in the image should be calibrated using a fluorescent or grey standard.

3.3. IMAGING OF CHLOROPHYLL FLUORESCENCE IN MICROPROPAGATED PLANTS

A system for imaging chlorophyll fluorescence of leaves of *Solanum tuberosum* plantlet from the outside of culture vessels and for estimating the fluorescence parameter F_v/F_m was developed [20].

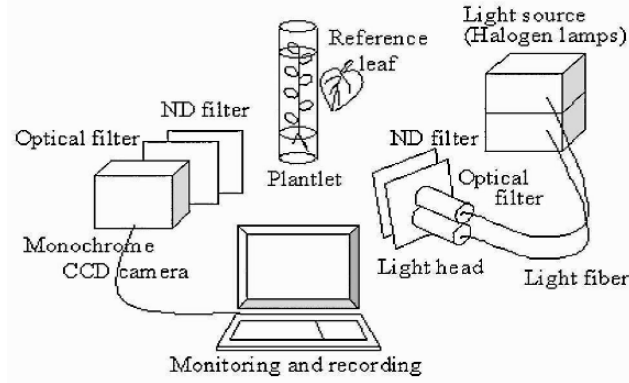


Figure 3. Schematic layout of a chlorophyll fluorescence imaging system. Reproduced from Ibaraki, Y. and Matsumura, K. (2004) [20].

Figure 3 shows the schematic layout of the system. The plantlets in glass test tubes were illuminated by a halogen lamp with a light fiber (HL-150, Hoya-Schott, Japan), and the light intensity for fluorescence excitation was controlled by neutral density filters (S-73-50-3,-13, Suruga, Japan). Fluorescence was imaged by a highly sensitive monochromatic CCD camera (WAT-120N, Watec, Japan) with long path filters. F_v/F_m was estimated from the F_o image, which was a fluorescent image acquired under low intensity illumination ($0.15 \mu\text{mol m}^{-2} \text{s}^{-1}$) after a 60 min dark adaptation treatment, and the F_m image, which was then acquired under high intensity illumination ($2500 \mu\text{mol m}^{-2} \text{s}^{-1}$). A detached *Epipremnum aureum* leaf, with a predetermined F_v/F_m , was imaged together as a reference leaf, and used to calibrate the fluorescence image. The F_v/F_m image (I_{F_v/F_m}) was constructed as a pixel-by-pixel calculation of the F_o image (I_{F_o}) and the F_m image (I_{F_m}) by the following equation:

$$I_{F_v/F_m} = \frac{(I_{F_m} - kI_{F_o})}{I_{F_m}} \quad (5)$$

Where, k is a coefficient that is used to convert fluorescent intensity into fluorescent yield and was determined so as to fit the estimated F_v/F_m of the reference leaf by equation 1 to the F_v/F_m measured before imaging by the fluorometer (MINI-PAM, Walz, Germany).

Figure 4 shows examples of chlorophyll fluorescence images, and F_v/F_m images derived from them, of potato plantlets using the system. For a few leaves of the plantlets, F_v/F_m could be imaged at the same time. Therefore, using images acquired repeatedly after dark-adaptation treatment, the F_v/F_m distribution in an individual plantlet could be determined. Changes in F_v/F_m of an individual leaf over a culture period could also be detected using the system. Figure 5 shows the changes in F_v/F_m of the 5th leaf determined by the fluorescence imaging system developed. The leaf just expanded (14 d after transplanting) showed a lower F_v/F_m (<0.8). Then, F_v/F_m increased and decreased

again after a peak at 14 d after leaf expansion. This was a reasonable pattern in F_v/F_m changes, since a decline of F_v/F_m was reported in young leaves and older leaves [28]. The system enabled gathering of information on photosynthetic capacity of cultured plantlets from the outside of culture vessels non-destructively. The system should be useful for optimizing culture conditions.

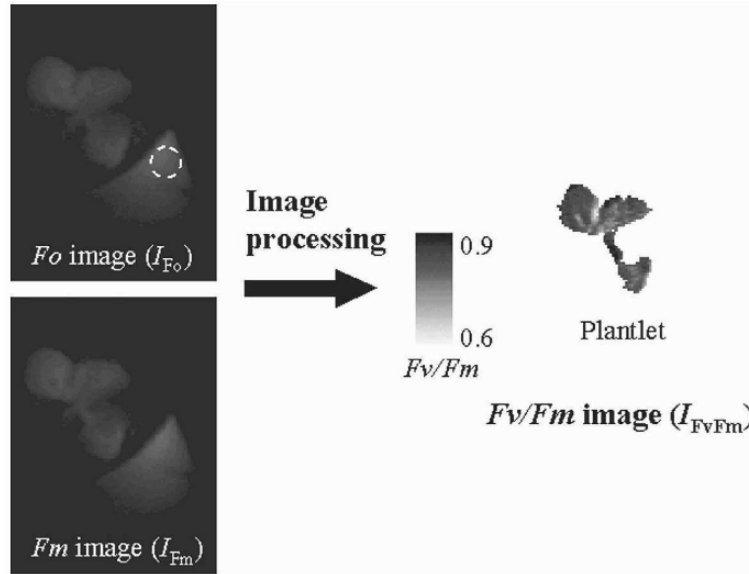


Figure 4. An example of F_v/F_m images constructed from F_o image and F_m image acquired by the chlorophyll fluorescence imaging system. Reproduced from Ibaraki, Y. and Matsumura, K. (2004)[20]. A circle in F_o image is an area to be used as the reference in the potato leaf.

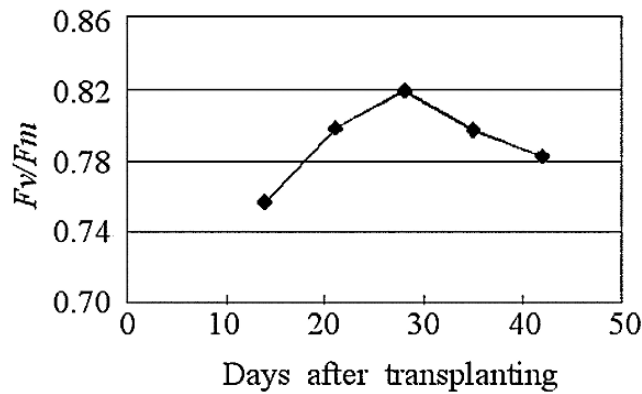


Figure 5. Changes in F_v/F_m of the 5th leaf of a potato plantlet at intervals of 7d. Reproduced from Ibaraki, Y. and Matsumura, K. (2004) [20].

4. Techniques for image-analysis-based evaluation of photosynthetic capacity

Spectral reflectance has been used to obtain plant growth information, especially in the research area of remote sensing. As spectral reflectance measurements are based on photometry, they have potential for non-destructive evaluation of plant growth and physiological state. The normalized difference vegetation index (NDVI), which can be calculated by reflectance at red and near infrared (NIR) wavelengths, has been widely used for monitoring, analyzing, and mapping temporal and spatial distributions of physiological and biophysical characteristics of vegetation [29]. It is applied not to an individual leaf, but to a plant canopy or wider area such as a forest, and is used mainly for quantification of vegetation, such as estimation of specific leaf area and evaluation of plant activity. The chlorophyll content of leaves can be estimated using the ratio of reflectance at 675 nm and 700 nm [30] or at 695 nm and 760 nm [31]. Although these indices are not a direct measure of photosynthetic capacity, they would be usable if empirical relationships between indices and photosynthetic capacity estimated by other methods could be determined.

Recently, the photochemical reflectance index (PRI) was proposed for estimation of photosynthetic radiation use efficiency [32]. This index is derived from reflectance at 531 nm and 570 nm, and is a measure of the degree of the photo-protective xanthophyll cycle pigment, zeaxanthin. The xanthophyll cycle, where the carotenoid pigment violaxanthin is converted to antheraxanthin and zeaxanthin via de-epoxidase reactions [33], is related to heat dissipation. The PRI is highly correlated with quantum yield of PSII determined by chlorophyll fluorescence for 20 species representing three functional types of plants [32]. Styliniski *et al.* [34] also reported a strong correlation of PRI to the chlorophyll fluorescence parameter $\Delta F/F_m'$ across species and seasons. As described previously, light use efficiency can vary with incident light intensity. Although several limitations still remain, the use of PRI is promising for evaluating photosynthetic capacity by a machine vision system.

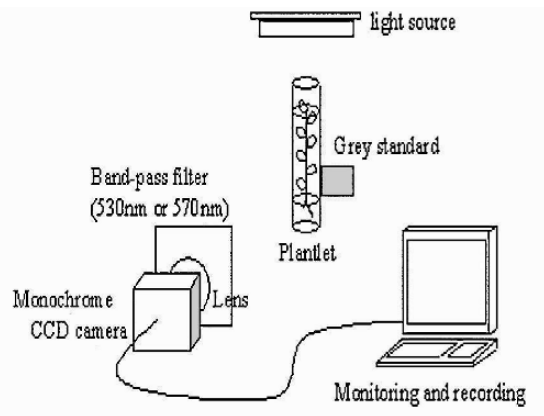


Figure 6. A concept illustration of a PRI imaging system.

Figure 6 shows a concept for a hypothetical PRI imaging system. In measurement of PRI, reflectance images should be acquired at two different wavelengths (531 and 570 nm). For this purpose, each image is taken with a grey standard by the CCD camera with a narrow-band-pass filter for the respective wavelength. The grey standard has nearly constant reflectance over the visible spectrum and is used to determine relative reflectance from light intensity. Configurations of the light source, the object (the culture vessel), and the camera should be carefully determined to collect the diffuse reflectance while reducing total internal reflection. Carter *et al.* [35] proposed a system using the same concept for reflectance imaging for early detection of plant stress.

5. Estimation of light distribution inside culture vessels

5.1. UNDERSTANDING LIGHT DISTRIBUTION IN CULTURE VESSELS

One of the most important factors for photosynthesis of cultured plantlets during micropropagation is the light environment, especially light intensity. High light intensity with sufficient CO₂ supply can enhance plantlet growth [36] and has the potential to facilitate acclimatization. From the viewpoint of photosynthesis, light intensity should be evaluated by photosynthetic photon flux density (PPFD) on the plantlet. However, since PPFD on plantlets is difficult to measure in a small culture vessel, it is usually represented by the value determined outside the vessel. PPFD on plantlets depends on the material and shape of culture vessels, the position of the vessel on the culture shelf, the position of the light sources, the optical characteristics of the shelf, etc [37]. It should be noted that PPFD in culture vessels with a closure, even with a high light transmissivity, was significantly lower than that on the empty shelf [38]. Moreover, when long culture vessels such as test tubes are used, light intensity can differ greatly between the top and bottom of the vessel. Non-uniform light distribution in a culture vessel may be responsible for differences in photosynthetic capacity and/or growth among leaves in the plantlet. As a result, this may lead to variations in plantlet quality in the case of a nodal cutting culture such as potato [6]. The estimation of light intensity distribution inside culture vessels is important for understanding the relationship between culture conditions and cultured plantlet growth properly. The use of information on light distribution in a culture vessel with information on photosynthetic capacity determined non-destructively would be helpful for optimization of culture conditions.

5.2. ESTIMATION OF LIGHT DISTRIBUTION WITHIN CULTURE VESSELS

A recently developed sensor film for measuring integrated solar radiation (Optleaf[®]), Taisei Chemical Co. Ltd., Japan) potentially offers a simple technique to estimate light intensity distribution. It has been used previously to estimate light intensity distribution in plant canopy (e.g., [39]). Here, the method [6] to estimate light intensity distribution inside a small culture vessel using the small piece of the sensor film is introduced.

This method enabled us to estimate light intensity distribution inside a culture vessel using a plantlet model whose leaves were constructed from sensor film. A plantlet

model simulating a potato plantlet consisted of 8 model leaves fabricated from sensor films (Optleaf R-2D, Taisei Chemical Co. Ltd., Japan) for measuring integrated solar radiation and a wire stem. A leaf-shaped piece of sensor film (dimensions 10 mm x 7 mm) was attached to an identically shaped piece of white paper and fixed to the wire stem at an angle of 30°. Each leaf was set at vertical intervals of 12 mm and at a horizontal angular interval of 120°. The total height of the plantlet model was 135 mm. A glass tube (25 mm x 150 mm) with a transparent plastic cap was used as the culture vessel. The sensor film was a cellulose acetate film coloured by azo dyes. Integrated radiation was estimated based on the degree of fading of the sensor film, which was quantified by measuring transmittance at 470 nm with a photometer (THS-470, Taisei Chemical Co. Ltd., Japan). Normally, measurements are performed while the film is set to a film mount (accessory of the photometer), but the model leaf was so small that the film mount could not be used. Therefore, the model leaf was set on 100% transmittance adjustment film (accessory of the photometer). The linear model determined previously could be used to correct the transmittance of model leaves. The sensor film absorbance was calculated from the sensor film transmittance and the ratio of the sensor film absorbance after exposure to that before exposure (film fading ratio) was determined. Integrated radiation was determined from the film fading ratio using a calibration curve provided by the film manufacturer (Taisei Chemical Co. Ltd., Japan).

Culture vessels with plantlet models were set on the shelf being surrounded with vessels containing potato plantlets in a temperature-controlled growth chamber at 24°C. Fluorescent tubes illuminated the growth chamber from the top (downward lighting) and the distance between the surface of fluorescent tubes and the top of vessels was 10 mm. In downward lighting condition, PPFD decreased toward the bottom of the vessel and was reduced to 50% and 30% of the maximum at the middle and the lower leaves, respectively. As compared with the PPFD measured with the photon sensor at the same position as each leaf position outside the vessel without the surrounding vessels, the steeper decline in PPFD inside the vessel could be observed. This might be due to interception of light by upper leaves and the surrounding vessels. PPFD distribution pattern inside the vessel can differ from that outside the vessel.

The results demonstrate that the use of sensor film plantlet models enables light intensity distribution inside a small culture vessel to be estimated, which was previously assumed to be too difficult to measure. This method could be applied to the determination of light intensity distribution patterns inside various types of culture vessels and under various lighting conditions, and thus would be of value in the optimization of culture conditions.

6. Concluding remarks

Non-destructive measurements of photosynthetic properties of plants in culture vessels are useful for understanding relationships between culture conditions and photosynthetic capacity, offering data on changes in physiological state of the plants during culturing without disturbing the *in vitro* microenvironment. Chlorophyll fluorescence has potential for non-destructive evaluation of leaf photosynthetic properties because the measurement can be conducted based on photometry. Parameters derived from chlorophyll fluorescence measurements relate to the functioning of PSII, including the

maximum quantum yield. Image analysis yielding these parameters is promising for non-destructive evaluation of photosynthetic capacity of micropropagated plants.

References

- [1] Kubota, C. (2001) Concepts and background of photoautotrophic micropropagation. In: Morohoshi, N. and Komamine, A. (Eds.) Molecular Breeding of Woody Plants. Elsevier Science B.V., Amsterdam; pp. 325-334.
- [2] Dubé, S.L. and Vidaver, W. (1992) Photosynthetic competence of plantlets grown *in vitro*. An automated system for measurement of photosynthesis *in vitro*. *Physiol. Plant* 84: 409-416.
- [3] Kubota, C. and Kozai, T. (1992) Growth and net photosynthetic rate of *Solanum tuberosum in vitro* under forced and natural ventilation. *Hort. Sci.* 27: 1312-1314.
- [4] Capellades, M.; Lemeur, R. and Debergh, P. (1990) Effects of sucrose on starch accumulation and rate of photosynthesis in *Rosa* cultured *in vitro*. *Plant Cell Tissue Org. Cult.* 25: 21-26.
- [5] Desjardins, Y.; Hdider, C. and de Riek, J. (1995) Carbon nutrition *in vitro* – regulation and manipulation of carbon assimilation in micropropagated systems. In: Aitken-Christie, J.; Kozai, T. And Smith, M.A.L. (Eds.) Automation and Environmental Control in Plant Tissue Cultures. Kluwer Academic Publishers, Dordrecht, The Netherlands; pp. 441-471.
- [6] Ibaraki, Y. and Nozaki, Y. (2004) Estimation of light intensity distribution in a culture vessel. *Plant Cell Tissue Org. Cult.* (in press).
- [7] Oxborough, K. and Baker, N.R. (1997) Resolving chlorophyll a fluorescence images of photosynthetic efficiency into photochemical and non-photochemical components-calculation of qp and Fv'/Fm' without measuring Fo' . *Photosynth. Res.* 54: 135-142.
- [8] Jones, H.G. (1990) Plants and microclimate. Cambridge University Press, New York.
- [9] Lichtenthaler, H.K.; Lang, M.; Sowinska, M.; Heisel, F. and Miede, J.A. (1996) Detection of vegetation stress via a new high resolution fluorescence imaging system. *J. Plant Physiol.* 148: 599-612.
- [10] Lichtenthaler, H.K.; Buschman, C.; Rinderle, U. and Schmuck, G. (1986) Application of chlorophyll fluorescence in eco-physiology. *Radiat. Environ. Biophys.* 25: 297.
- [11] Morecroft, M.D.; Stokes, V.J. and Morison, J.I.L. (2003) Seasonal changes in the photosynthetic capacity of canopy oak (*Quercus robur*) leaves: the impact of slow development on annual carbon uptake. *Int. J. Biometeorol.* 47: 221-226.
- [12] Fracheboud, Y.; Haldimann, P.; Leipner, J. and Stamp, P. (1999) Chlorophyll fluorescence as a selection tool for cold tolerance of photosynthesis in maize (*Zea mays* L.). *J. Exp. Bot.* 50: 1533-1540.
- [13] Genty, B.; Briantais, J.M. and Baker, N.R. (1989) The relationship between the quantum yield of photosynthetic electron transport and quenching of chlorophyll fluorescence. *Biochimica Biophysica Acta* 990: 87-92.
- [14] Maxwell, K. and Johnson, G.N. (2000) Chlorophyll fluorescence – a practical guide. *J. Exp. Bot.* 51: 659-668.
- [15] Lichtenthaler, H.K. and Rinderle, U. (1988) The role of chlorophyll fluorescence in the detection of stress conditions in plants. *CRC Critical Reviews in Analytical Chemistry* 19: S29-S85.
- [16] Aitken-Christie, J.; Davies, H.E.; Kubota, C. and Fujiwara, K. (1992) Effect of nutrient media composition on sugar-free growth and chlorophyll fluorescence of *Pinus radiata* shoots *in vitro*. *Acta Hort.* 319: 125-128.
- [17] Hofman, P.; Haisel, D.; Komenda, J.; Vágner, M.; Tichá, I.; Schäfer, C. and Čapková, V. (2002) Impact of *in vitro* cultivation conditions on stress responses and on changes in thylakoid membrane proteins and pigments of tobacco during *ex vitro* acclimation. *Biol. Plant.* 45: 189-195.
- [18] Serret, M.D.; Trillas, M.I. and Araus, J.L. (2001) The effect of *in vitro* culture conditions on the pattern of photoinhibition during acclimation of gardenia plantlets to *ex vitro* conditions. *Photosynthetica* 39: 67-73.
- [19] Kato, M.C.; Hikosaka, K. and Hirose, T. (2002) Leaf discs floated on water are different from intact leaves in photosynthesis and photoinhibition. *Photosynth. Res.* 72: 65-70.
- [20] Ibaraki, Y. and Matsumura, K. (2004) Non-destructive evaluation of the photosynthetic capacity of PSII in micropropagated plants. *J. Agric. Meteorol.* 60 (in press).
- [21] Murashige, T. and Skoog, F. (1962) A revised medium for rapid growth and bioassays with tobacco tissue cultures. *Physiol. Plant* 15: 473-497.

- [22] Omasa, K.; Shimazaki, K.I.; Aiga, I.; Larcher, W. and Onoe, M. (1987) Image analysis of chlorophyll fluorescence transients for diagnosing the photosynthetic system of attached leaves. *Plant Physiol.* 84: 748-752.
- [23] Omasa, K. (1996) Image diagnosis of photosynthesis in cultured tissues. *Acta Hort.* 319: 653-658.
- [24] Genty, B. and Meyer, S. (1994) Quantitative mapping of leaf photosynthesis using chlorophyll fluorescence imaging. *Aust. J. Plant Physiol.* 22: 277-284.
- [25] Siebke, K. and Weis, E. (1995) Imaging of chlorophyll-a-fluorescence in leaves: Topography of photosynthetic oscillations in leaves of *Glechoma hederacea*. *Photosynth. Res.* 45: 225-237.
- [26] Meng, Q.; Siebke, K.; Lippert, P.; Baur, B.; Mukherjee, U. and Weis, E. (2001) Sink-source transition in tobacco leaves visualized using chlorophyll fluorescence imaging. *New Phytologist* 151: 585-595.
- [27] Oxborough, K. and Baker, N.R. (1997) An instrument capable of imaging chlorophyll *a* fluorescence intact leaves at very low irradiance and at cellular and subcellular levels of organization. *Plant Cell Environ.* 20: 1473-1483.
- [28] Ibaraki, Y.; Iwabuchi, K. and Okada, M. (2004) Chlorophyll fluorescence analysis for rice leaves grown under elevated CO₂ conditions. *J. Agric. Meteorol.* 60 (in press).
- [29] Gitelson, A.A. (2004) Wide dynamic range vegetation index for remote quantification of biophysical characteristics of vegetation. *J. Plant Physiol.* 161: 165-173.
- [30] Chappelle, E.W.; Kim, M.S. and McMurtrey, J.E. (1992) Ratio analysis of reflectance spectra (RARS): an algorithm for the remote estimation of the concentrations of chlorophyll a, chlorophyll b, and carotenoids in soybean leaves. *Remote Sens. Environ.* 39: 239-247.
- [31] Carter, G.A.; Rebeck, J. and Percy, K.E. (1995) Leaf optical properties in *Liriodendron tulipifera* and *Pinus strobus* as influenced by increased atmospheric ozone and carbon dioxide. *Can. J. For. Res.* 25: 407-412.
- [32] Gamon, J.A.; Serrano, L. and Surfus, J.S. (1997) The photochemical reflectance index: an optical indicator of photosynthetic radiation use efficiency across species, functional types, and nutrient levels. *Oecologia* 112: 492-501.
- [33] Yamamoto, H.Y. (1979) Biochemistry of violaxanthin cycle in higher plant. *Pure Appl. Chem.* 51: 639-648.
- [34] Stylinski, C.D.; Gamon, J.A. and Oechel, W.C. (2002) Seasonal patterns of reflectance indices, carotenoid pigments and photosynthesis of evergreen chaparral species. *Oecologia* 131: 366-374.
- [35] Carter, G.A.; Cibula, W.G. and Miller, R.L. (1996) Narrow-band reflectance imagery compared with thermal imagery for early detection of plant stress. *J. Plant. Physiol.* 148: 515-522.
- [36] Kozai, T.; Oki, H. and Fujiwara, K. (1990) Photosynthetic characteristics of *Cymbidium* plantlet *in vitro*. *Plant Cell Tissue Org. Cult.* 22: 205-211.
- [37] Fujiwara, K. and Kozai, T. (1995) Physical microenvironment and its effects. In: Aitken-Christie, J.; Kozai, T. and Smith, M.A.L. (Eds.) *Automation and Environmental Control in Plant Tissue Cultures*. Kluwer Academic Publishers, Dordrecht, The Netherlands; pp. 319-369.
- [38] Fujiwara, K.; Kozai, T.; Nakajo, Y. and Watanabe, I. (1989) Effects of closures and vessels on light intensities in plant tissue culture vessels. *J. Agric. Meteorol.* 45: 143-149 (in Japanese with English abstract).
- [39] Watanabe, S.; Nakano, Y. and Okano, K. (2001) Simple measurement of light-interception by individual leaves in fruit vegetables by using an integrated solarimeter film. (Japanese text with English summary) *Environ. Control Biol.* 39: 121-125.

MONITORING GENE EXPRESSION IN PLANT TISSUES

Using green fluorescent protein with automated image collection and analysis

JOHN J. FINER¹, SUMMER L. BECK^{1,3}, MARCO T. BUENROSTRO-NAVA^{1,4}, YU-TSEH CHI^{2,5} AND PETER P. LING²

¹*Department of Horticulture and Crop Science, The Ohio State University, 1680 Madison Ave., Wooster, OH 44691, USA – Fax: 330-263-3887 – Email: finer.1@osu.edu*

²*Department of Food, Agricultural and Biological Engineering, OARDC/The Ohio State University, 1680 Madison Ave., Wooster, OH 44691, USA*

³*Current Address: DuPont Agriculture and Nutrition, Rt. 141 and Henry Clay Road, Wilmington, DE 19880, USA*

⁴*Current Address: IREGEP, Colegio de Postgraduados, Carretera Mexico-Texcoco Km 35.5 Montecillo, Texcoco, Mexico, C.P. 56230*

⁵*Current Address: 57 228 Lane Section 3 Yuanji Rd., Tianjhong Town, Chang-Hua 520, Taiwan*

1. Introduction

Automated systems are widely used across many discipline areas to perform tasks that may be hazardous, time consuming, or impossible to perform by humans. In the plant sciences, automated systems are being developed to execute difficult and tedious activities and reduce the exposure of workers to agricultural chemicals [1].

In the area of plant developmental biology, automated systems have been developed to gather information on how plants grow and develop under different environmental conditions. Kacira and Ling [2] describe the use of a computer-controlled motorized circular table and remote sensors to continuously monitor the health and growth of New Guinea *Impatiens* plants growing under either low or high humidity conditions. An infrared thermometer was used to collect data on the water stress index and a digital camera was used to measure the top canopy area of the plants. Using this approach, it was possible to detect the beginnings of a water deficit in the plants up to two days before detection of visible wilting.

In the area of molecular biology, automated systems have tremendously improved the capabilities of molecular biologists to perform complicated tasks with minimal efforts. One of the first automated systems to receive widespread use in the area of molecular biology is the thermocycler, which generates rapid temperature cycles,

enabling repeated synthesis of specific DNA fragments using a temperature insensitive form of DNA polymerase. The Polymerase Chain Reaction (PCR) technique [3,4] has revolutionized modern genetics by allowing efficient and accurate amplification of DNA fragments from very small amounts of starting material. DNA sequencers are also now fully automated and not only reduced the time and the labour required to obtain the sequence of a certain DNA fragment, but have also provide insight into the genome of a multitude of complex organisms. Genome sequencing is high throughput and both sequence determination and alignment is automated.

One of the most recent applications of systems automation in the area of molecular biology is the development of the microarray technology [5]. Microarrays are being successfully used to assess the expression profile of thousands of genes from biological samples [6-8]. For preparation of one type of microarray, thousands of small samples are precisely placed on a microscope slide in an area generally of 3.5 by 5.5 mm. To perform this fragile and laborious task, an automated system deposits multiple aliquots of ~0.005 μl from thousands of different samples on a single slide. After fixation, hybridization with fluorescent probe and washing, the slides are scanned with a laser fluorescent scanner, which is equipped with a computer-controlled XY stage. To detect the fluorescence, two photomultiplier tubes are used and the signal is split according to the wavelength required to detect the fluorescence from each of the probes. The data is processed and represented as an array, where each microscopic spot represents the expression profile of the gene that was fixed at that particular point [5,9].

Although the use of microarray technology to profile expression of plant genes is still relatively new, it has already become standard for high throughput analysis of gene expression. Kazan *et al.* [6] used microarrays to screen 2375 *Arabidopsis* genes (based on expressed sequence tags; ESTs), finding that 705 genes were up-regulated after the plants were inoculated with a fungal pathogen or a signal compound. Comparisons of the 705 genes with known sequences revealed that 106 of the genes had no previously known function. Although microarray technology can be used to find new genes that are up- or down-regulated under certain conditions, tissue extraction is required and precise analysis of temporal expression can be difficult. Real-time analysis of gene expression in living organisms is still useful, and visualization of transgene expression in living tissue can provide additional information, that extracted tissue cannot.

2. DNA delivery

Although a number of different methods exist for introduction of DNA into plants cells [10], particle bombardment [11] and *Agrobacterium*-mediated transformation [12] are the two methods that have proven to be the most efficient and are most commonly used by transformation laboratories for a large number of plant species.

2.1. PARTICLE BOMBARDMENT

For particle bombardment, DNAs are precipitated onto small (~1 μm) dense particles (either tungsten or gold) and accelerated towards the target plant tissue, which is placed under a partial vacuum to reduce drag on the particles. The particles are accelerated by a blast of helium, released by either a fast-acting solenoid [13] or a rupture disc [14],

manufactured to rupture at specified helium pressures. Helium is used to propel the particles as it is inert and possesses a high expansion coefficient. Once the particles enter the target cells, the DNA is released from the particles, becomes associated with the chromosomes and, if the proper conditions exist, the foreign DNA integrates into the chromosomes of the target cell.

For particle bombardment, the DNA is physically delivered into the cells which bypass any potential biological incompatibilities. But, the introduction of particles, which range in size from 0.6 - 3 μm , can be damaging to the cells, which range in size from 20 – 60 μm . To minimize damage, cells are often treated by physical or chemical drying [15], which lowers the osmotic pressure in the cells and reduces the loss of protoplasm through particle-generated holes in the cell wall.

Integrated DNA resulting from particle bombardment-mediated DNA transfer is often high copy and fragmented [16,17] but this can be regulated by modifying the introduced DNAs [18]. High copy transgenes can show variation or loss of expression due to gene silencing [19].

2.2. *AGROBACTERIUM*

For *Agrobacterium*-mediated transformation, plant tissues are cultured in the presence of *Agrobacterium*, which is a bacterium that has the unique ability to introduce part of its DNA into plants [20]. Because *Agrobacterium* is a natural plant pathogen, some biological incompatibilities exist when using certain plant species or stages of plant growth. However, most of these biological incompatibilities have been removed or at least lessened as more has been learned about the mechanism of DNA transfer [21]. With the addition of signal compounds [22] to the medium where *Agrobacterium* and the plant tissues are co-cultivated, and enhancing exposure of cells to the invading bacteria [23], the process of DNA transfer has become quite efficient for most plants.

Although antibiotics must be applied to eliminate the bacterium after DNA transfer, this method of delivery has two distinct advantages over particle bombardment. First, no instrumentation is required and the cost of performing DNA introductions is minimal. Second, the DNA transfer process, which is mediated by the bacterium, generally results in more consistent integration events. The transferred DNA (T-DNA) is usually defined by specific borders and genes of interest can simply be engineered between those borders. The resultant integrated DNA can be single copy or show somewhat more complex integration patterns [24].

3. Transient and stable transgene expression

Immediately following introduction, the fate of DNA can be inferred, based on early events and eventual outcomes. Gene expression from the introduced DNAs can be observed as early as 1.5 hours post-introduction [25] and is usually short-lived, lasting 1-3 weeks. This short-term expression is called, “transient expression” and probably results from expression of DNA as an extrachromosomal unit. In addition, many of the cells containing foreign DNA may not remain viable [26], due to the physical process of DNA introduction or the response of the cells/tissue to invading bacteria. If the cells remain viable following DNA introduction, the introduced DNA either degrades or

integrates into the DNA of the target cells. In plant cells, introduced DNAs are not maintained as extrachromosomal elements. In most cases, once the DNA becomes integrated, it becomes a stable transgenic event, resulting in “stable expression”. The introduced T-DNA from *Agrobacterium*-mediated transformation is coated with protein molecules and tagged with a protein signal peptide which assists with delivery to the nucleus and integration into the chromosome [24]. Integration patterns in transgenic plants obtained via particle bombardment-mediated DNA delivery suggests a high level of recombination, resulting in a mixing rather than an insertion of the introduced DNAs within the native plant DNA [27]. These recombination events most likely occur directly following DNA introduction, during DNA integration into the chromosome.

Although the transition from transient to stable expression is very poorly understood, it probably holds the keys to improving both transformation rates and transgene expression. Studies of transient gene expression, directly following DNA delivery along with a fine analysis of stable transgene expression are now possible using the proper transgenic reporter genes and fine tracking of gene expression using robotics and image analysis.

4. Green fluorescent protein

4.1. GFP AS A REPORTER GENE

Reporter genes have been developed and refined to “report” or visualize gene expression in a variety of tissues and organisms. Early reporter genes coded for enzymes, which required substrates which were converted into detectable or visible forms following cleavage [28]. These early reporter genes worked well but substrates were often costly and the assay itself could be toxic to the tissue, resulting in a single time point determination of transgene activity. Today, the most commonly used reporter gene is the Green Fluorescent Protein (GFP), which can be continually monitored over time and does not require the use of a substrate as the protein product itself is fluorescent. GFP has therefore become the most effective reporter gene for use in transformation and for tracking gene expression.

The Green Fluorescent Protein is a naturally occurring protein found in jellyfish (*Aequorea victoria*). The bioluminescence from this protein was first reported by Ridgway and Ashley [29] and, since that first report, the use of green fluorescent protein has expanded tremendously, impacting almost every field in the biological sciences; especially plant sciences. This reporter gene has become increasingly useful for tracking transgene expression in transformed plants.

Niedz *et al.* [30] first found that the wild-type *gfp* gene from the jellyfish could be introduced into plant cells and visualized. The *gfp* gene has since been modified and optimized to be the most effective reporter gene in plants. Wild-type GFP produces green fluorescence expression at the wavelength of 507 nm (green) upon the excitation at 395 nm (ultraviolet) or 475 nm (blue) [31]. In addition, sequence changes are usually required when genes from organisms in one kingdom are transferred to organisms in another kingdom. In plants, modifications to the *gfp* gene include the elimination of a cryptic intron, alteration in codon usage, changes in the chromophore leading to

different excitation and emission spectra, and targeting to endoplasmic reticulum [32]. It has been developed as a reporter for gene expression, a marker of subcellular protein localization, a tracer of cell lineage, and as a label to follow the development of pathogens [33]. The GFP reporter allows detection of labelled protein within cells, and monitoring of plant cells expressing GFP, directly within growing plant tissue [34]. Nagatani *et al.* [35] used digital imaging to monitor the heat shock response of transgenic rice calli using GFP as a reporter gene. Images of transgenic calli were acquired 0, 30, 60, and 120 minutes after heat treated for 10 min at 45°C. Analysis of the images showed a 2-4-fold increase in the levels of GFP expression over time compared to the control (no heat stress).

GFP has successfully been used as a reporter for evaluation of plant transformation using both *Agrobacterium* [36] and particle bombardment [25]. GFP fluoresces under blue light excitation, and it can be detected in as little as 1.5 hours following DNA introduction [25]. Since GFP detection is non-destructive, expression can be followed over extended periods of time using digital imaging [37].

Reporter genes provide an excellent way to not only examine gene expression but also to evaluate expression over time in various tissues.

4.2. GFP IMAGE ANALYSIS

In the simplest terms, image analysis is the evaluation of an object using information collected from an image. Image analysis can be totally manual or, at the highest level, fully automated. For manual image analysis, the observer simply makes visual judgments of the subject material and provides subjective qualitative ratings. At the next level (interactive image analysis), images are collected and the operator assists with, but does not complete the analysis of the images. The operator must separate the subject from its background and demarcate or segment the region of interest in the field of view. Input from the operation is therefore needed for every image, and objects or segments in the images need to be outlined before the size/colour of the targets may be determined using image analysis tools (i.e. blob analysis). Blob analysis groups pixels with the same attributes (colour) into a region, which allows subsequent quantification of other factors associated with the blob (width, length, area, etc). This interactive image analysis process, although useful for some applications, is laborious and time consuming and is not practical for high volume operations. At the highest level of image analysis, automated quantitative analyses are performed. While automated image analysis is key to high throughput monitoring of various subject materials, adaptive image analysis is paramount to the success of analyzing images of varied quality. For adaptive image analysis, the background, subject itself and regions of interest (ROI) within the subject are separated. This can be challenging when images of varied colours and contrasts are analyzed. To determine the percentage area of GFP expression in plant tissue, embryos or plants, it is necessary to precisely identify the tissue, embryo or plant within the image. In order to quantify GFP expression, it is also necessary to identify specific regions in the target and determine if these regions are associated with GFP fluorescence. Therefore, identification of the targets or blobs through “segmentation” and parts of the target via “blob analysis” are needed for quantitative and qualitative high throughput image analysis of GFP-expressing tissues. Currently, many evaluations

of gene expression and most assessments of tissue and plant quality still rely on human vision, where results can often be highly variable and very subjective.

4.3. QUANTIFICATION OF THE GREEN FLUORESCENCE PROTEIN *IN VIVO*

With the widespread use of the *gfp* gene as a reporter gene, quantitative analyses of GFP expression has been used to accurately gauge gene expression levels. Maximova *et al.* [38] applied image analysis to quantify GFP expression in *Agrobacterium*-infected leaf explants. Using the greyscale intensity of the area expressing GFP, intensity was calculated from ten random areas of the subject. In this study, samples were visually selected by the authors, which may have influenced the results. However, the potential for utilizing image analysis for evaluating *in situ* GFP expression in plant tissues was clearly demonstrated.

Hauser *et al.* [39] also used the average greyscale intensity of selected areas to quantify the strength of GFP expression. The region of interest, which contained GFP-expressing *Paramecium tetraurelia* cells was selected randomly. Vanden Wymelenberg *et al.* [33] analyzed the population of GFP-expressing *Aureobasidium pullulans* on leaf surfaces using the average fluorescence per cell vs. cell number. Threshold values were specified interactively to segment the region of interest from the background. Spear *et al.* [40] used 256 scale levels to quantify GFP expression in fungal cells and obtained intensity values using commercial image processing software. The region of interest was segmented by simple 'thresholding', while the threshold value was selected by the authors. The number of cells, individual cell areas, and total coverage area of the cells were obtained by manual image analysis.

In order to achieve precise quantification of GFP expression, other variables, which can change over time or between laboratories must be considered. Scholz *et al.* [41] used an internal rhodamine B standard to correct the intensity fluctuations of the exciting xenon arc lamp in the fluorescence spectrometer. Inoué *et al.* [42] quantified GFP expression by calculating the average pixel intensity values of a circular region of interest narrower than the samples. Since the strength of excitation light degraded with time, GFP expression was corrected by subtracting the average background intensity values of the region. The segmentation between the foreground and the background area and the selection of either region of interest or the adjoining background was done manually.

All of this research relied on manual input for image acquisition and image analysis. An automated image collection and analysis system is desirable because of the time and effort involved in collecting the and analyzing the images, which requires routine and repeated manipulations and human involvement at numerous steps. For the monitoring of a large number of targets, an automated system would insure higher efficiencies and a greater consistency of high throughput data acquisition and analysis.

5. Development of a robotic GFP image acquisition system

5.1. OVERVIEW

Over the past few years, efforts in our laboratories have focused on assembly and evaluation of an automated image acquisition for semi-continuous monitoring of GFP expression in transiently- and stably-transformed plant tissues [43,44]. The automated image acquisition system consists of a fluorescence dissecting microscope with a digital camera and a custom-designed 2-dimensional robotics platform, all under computer control (Figure 1). The total system was placed in laminar air flow hood and the hood was housed in a temperature-controlled culture room for consistent temperature control. The robotics platform was programmed to place the various samples, located in different Petri dishes, under the objective of the microscope and the camera collected the image before moving to the next target. The system presents unique problems due to the aseptic nature of the tissue culture subject material and the “movement” of the tissue due to tissue expansion and growth. Perhaps the greatest challenge was minimizing the condensation on the lids of the sealed Petri dishes, which obscured the view of the dishes’ contents and could make image analysis very inconsistent.

5.2. ROBOTICS PLATFORM

The robotics platform consisted of square piece of 5 mm thick Plexiglas measuring about 40 cm x 40 cm. The platform was mounted on a 45 x 45 cm XY belt-driven positioning table (Arrick Robotics Inc., Hurst, Texas) using 2 aluminium rails, which were 5 cm tall and 40 cm long. The Plexiglas was sufficiently rigid to hold the samples in place with no bending and the high transparency of this material minimized heat buildup from absorbing the light used to illuminate the plant tissues. This was problematic with earlier prototypes of the platform that were not transparent. Heat accumulation within or on the platform causes the temperature of the dishes’ contents to increase, leading to water condensation on the lid of the sealed Petri dishes. Condensation reduces the quality of the images and makes the process of image analysis difficult to impossible. To prevent heat accumulation on the bottom of the platform, sixteen 6 cm diameter perforations were made in the Plexiglas, directly under the eventual location of the Petri dishes. Small fans were initially mounted to the side of the platform or in the 6 cm perforations but these were found to be unnecessary and were not beneficial for elimination of condensation. But, these perforations were retained as they did increase air flow. To secure the Petri dishes to fixed locations, a mounting mechanism was incorporated into the platform design (Figure 1, inset).

The mounting mechanism was used to hold the dishes in place, suspend the dishes over the platform surface, permit mounting of a black background material below the dishes, and allow precise adjustment of the focal distances of different areas of a plate. The mounting mechanism consisted, in part, of 3 plastic positioning screws which were placed 120° apart from each other and 5 mm away from each 6 cm perforation (Figure 1, inset). One 100 x 25 mm Petri dish was placed on top of the tips of the three positioning screws. As the tissue grew, the positioning screws were adjusted to maintain focus of the subject materials. In addition, the positioning screws maintained the dishes

above the surface of the platform, permitting adequate air flow around the dish. A 7 cm diameter piece of black card stock was placed on the head of the screws, suspended 1 cm below the platform surface. The black background provided a consistent background for image analysis. To hold the Petri dishes in place, a 90° aluminium angle (2.5 cm base and 2.5 cm high) was fastened to the platform and a plastic screw was horizontally placed to press the plate against a polypropylene holder, which was cut to the same shape as a Petri dish (Figure 1).

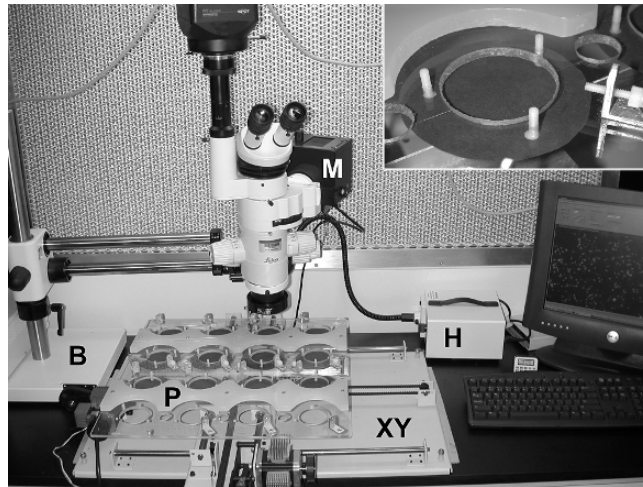


Figure 1. Automated image collection system showing the platform (P) mounted on the xy belt-driven positioning table (XY). The weighted base (B) was needed to support the weight of the microscope and camera, which were mounted on the long arm boom stand. The two different light sources for this system were a halogen bulb (H), which provided white light illumination, and a mercury bulb (M), which provided high energy blue light for GFP detection. The mounting mechanism (inset) consists of 3 positioning screws and one horizontal screw, which secured the Petri dish in place.

The platform was originally driven by two MD-2a dual stepper motors (Arrick Robotics Inc.), each motor driving the movement in the X or Y direction. The table contained two limit switches (one for each of the directions, X and Y), which were used to identify the “home” position. This position was recognized by the computer when a limit switch was activated by the platform. In order to place each sample under the microscope objective, the platform was moved a specific number of steps from the home position in the X and Y directions. The number of steps for each direction depended of the position of the object on the platform.

Ideally, the robotics platform will place the subject in exactly the same location for each image collection at each time point. Images, acquired at different times, should present the same region for analysis. Time series images, having the same region of analysis, guaranteed a precise dynamic quantification of GFP expression. Unfortunately, this level of precision was not observed with this system. Positioning error was caused by backlash of the drive belt and by the step losses from the motors. Unless the platform was returned to the home position between each sample, the error accumulated and the

target tissue could actually move out of the field of view of the CCD camera if enough points were taken prior to returning “home”. The error caused by backlash or losses of motor steps occurred along both the X and Y axes of the positioning table.

Backlash error was reduced after replacement of the original motor system with pulley reducers (PR23, Arrick Robotics, Hurst, Texas) and more powerful stepper motors (MD-2b, Arrick Robotics, Hurst, Texas). This change reduced the motor step size and increased the torque provided by the motors, improving the overall efficiency of positioning. The smaller step size reduced the error caused by backlash and larger torque reduced the possibility of step loss. This change did not eliminate backlash errors completely, but it reduced the magnitude of the error. This improvement allowed successive image collections of all of the samples within a single dish, and a return to the home position was only required between dishes. This also reduced run times as it was no longer necessary to return the platform to the home position between each sample.

After the sample was positioned under the microscope objective, a 1 second delay was used to minimize residual sample movement from the vibration caused by repositioning of the platform. After saving the image, the platform was directed to the next position within the same Petri dish or to the home position, if the next sample was located in a different Petri dish.

5.3. HOOD MODIFICATIONS

The robotics system was placed in a custom-designed laminar air flow hood. A laminar air flow hood was necessary as samples needed to be precisely placed in the dishes, after the dishes were fixed in place using the mounting mechanism on the robotics table. As a result, an aseptic environment was required. The basic hood design was an isolation table style, where the hood working surface is physically separated from the hood motors, thereby reducing or eliminating vibration from the hood motors. The table of an isolation table style hood consists of a base table with a second platform, suspended above the base table by rubber cushions. The second platform normally consists of a laminate-covered surface, which was replaced by a similar-sized piece of black epoxy lab counter top. Vibrations from the robotics system motors were reduced or partially absorbed by the “vibration-free” work surface that the hood provides. Because the image acquisition system was too tall to fit within standard hoods, the working table was lowered to allow adequate clearance for the digital camera.

As this whole system was placed within a tissue culture room with lighted shelves for growth of plant tissue cultures, light shielding was necessary. Extraneous light could interfere with image analysis, especially when fluorescence was low. In addition, lights in most laboratories are under photoperiod control and cycle on and off throughout an image collection experiment. Light screens, consisting of wood frames covered in black cloth and placed around the hood, were adequate but they were both bulky and inefficient at light screening. The use of a curtain of black fabric, suspended from the top of the hood opening was a simple and convenient solution to light leakage. The curtain length was adjusted so that open space was present at the bottom of the curtain, to allow free movement of the robotics platform. The air from the hood was able to escape through this open space and it was found that the curtain also acted as a temperature and air baffle, maintaining a more uniform temperature within the hood

space and reducing condensation on the lids of the Petri dishes even further. Condensation of the lids of the dishes has been largely eliminated from additional changes to Petri dish design (Finer, unpublished).

For long-term experiments requiring illumination, the standard fluorescent lights mounted within the hood were replaced with Gro-lux™ fluorescent bulbs used in the laboratory for growth of plant tissue cultures. These lights were placed under timer control which allowed them to cycle on and off with a regular photoperiod, or the lights could be automatically turned off during image collections.

5.4. MICROSCOPE AND CAMERA

A scientific charged-coupled device (CCD) SPOT-RT camera (Diagnostic Instruments Inc., Sterling Heights, Michigan) was mounted on a Leica MZFLIII stereomicroscope (Leica, Heerbrugg, Switzerland), which was mounted over the robotics platform using a long arm boom stand. Due to the weight of the microscope and the camera, a heavy weighted base was used with the long arm beam (Figure 1). The SPOT-RT camera was selected for the automated system due to its high sensitivity to dim signals and the flexibility to easily control basic functions such as gain, binning and exposure time. For images collected using the unfiltered halogen bulb (see below), exposure times were usually around one second. For collection of images showing GFP expression, exposure times were as long as one minute. The proper exposure time for each of the channels (red, green and blue) was predetermined for each type of image.

Digital images taken with the SPOT-RT camera could be represented in either 8 or 12 bits per pixel (bpp), which resulted in an intensity resolution of 256 or 4,096 discrete grey levels, respectively, per pixel for each channel. Although colour images, containing 12 bpp per colour channel, offer high resolution, they were seldom used because their large size makes them difficult to store and analysis is very time-consuming. To select the proper intensity resolution for the analysis of biological samples, it is important to know the conditions in which the images need to be acquired. Twelve bpp resolution images could be useful if it is difficult to distinguish objects from their background. Images obtained with the SPOT-RT camera had a 32 bpp (8 bpp per channel) resolution. The total memory size of each image was 5,760,054 bits for an image size of 1600 x 1200.

5.5. LIGHT SOURCE AND MICROSCOPE OPTICS

To detect the expression of the GFP gene, the dissecting microscope was equipped with a 100 W mercury bulb; with a "GFP-2" filter set, consisting of an excitation band pass filter of 480/40 nm and a long pass barrier filter of 510 nm. The excitation filter allowed the passage of the blue light produced by the mercury bulb, eliminating the light in the UV, red and green spectra. The barrier filter blocked the blue light used to excite the GFP and allowed observation of the green light emitted by the GFP. The barrier filter allowed the passage of any visible light above the 510 nm spectrum, which was useful in detecting fluorescence in other spectra. Green tissue, containing chlorophyll, fluoresced red upon excitation with the high intensity blue light. It was also not unusual to observe occasional yellow fluorescence in some tissues, from unknown compounds.

In addition to the mercury bulb light, the automated system also contained a 100 W halogen lamp light source that was used to illuminate the objects under the microscope with wide spectrum light. The light was transmitted from the light source to the object through a glass fiber bundle to a 66 mm FOSTEC[®] (SCHOTT-FOSTEC LLC; Auburn NY, USA) ringlight, which was attached to the objective of the microscope. This white halogen light was useful when focusing the specimen and positioning the samples in the centre of the field of view.

For experiments which did not require tracking of GFP expression, the halogen light alone was used to illuminate the subject tissues, yielding sequential image collections under white light. In this case, the filter set was not used and the halogen bulb was automatically turned on for image collection only. In contrast, for GFP image collection, the mercury bulb remained on during the whole course of the experiment, as the manufacturer recommended against continual re-starting of the bulb. With a bulb life of 200-300 hours, long-term experiments were not possible. In addition, bulb degeneration (30%) over the course of the experiment was expected, and controls were necessary to detect and compensate for this loss of illumination intensity [44]. Experimental evaluation of custom-designed blue LED illuminators, which possess much longer bulb lives, proved this light source inadequate for sufficient intensities of illumination, even when 100 narrow angle LEDs were focused within a 1 cm field.

6. Automated image analysis

To measure plant growth and development, or to evaluate changes in GFP expression accurately, the difference between two images, taken at different times, may be determined by simply subtracting one from the other, providing that the two images were taken under exactly the same conditions. Scaling, position, orientation and illumination of targets in images taken at different times should be the same with this automated image collection system.

6.1. IMAGE REGISTRATION

The automated image collection system described above provided close-to-optimal conditions for automated image analysis. Magnification was constant although sample positioning varied slightly. Positioning became more consistent with improved motors on the robotics platform and the use of pulley reducers. Errors in positioning between sequentially-collected images were corrected by an image registration operation along the x and y axes. There were no orientation shifts observed in the target due to the sample holder design.

Image registration is the process of aligning targets in an image series, using mechanical or digital signal processing techniques. Re-alignment of images requires a quantitative measurement of their similarity in order to determine the necessary adjustments. Three similarity measures [45] were evaluated using images showing transient *gfp* expression, collected using the automated image capture system. These similarity measures are shown below.

Sum of the Absolute Value of Differences (SAVD):

$$r_{m,n} = \sum_{i=b}^{W-b} \sum_{j=b}^{H-b} |X_{i,j} - Y_{i+m,j+n}| \quad (1)$$

Correlation Function (CF):

$$s_{m,n} = \sum_{i=b}^{W-b} \sum_{j=b}^{H-b} X_{i,j} \times Y_{i+m,j+n} \quad (2)$$

Correlation Coefficient (CC):

$$\rho_{m,n} = \frac{\left[4N^2 \sum_{i=\frac{W}{2}-N}^{\frac{W}{2}+N} \sum_{j=\frac{H}{2}-N}^{\frac{H}{2}+N} X_{i,j} \times Y_{i+m,j+n} - \left(\sum_{i=\frac{W}{2}-N}^{\frac{W}{2}+N} \sum_{j=\frac{H}{2}-N}^{\frac{H}{2}+N} X_{i,j} \right) \left(\sum_{i=\frac{W}{2}-N}^{\frac{W}{2}+N} \sum_{j=\frac{H}{2}-N}^{\frac{H}{2}+N} Y_{i+m,j+n} \right) \right]}{\sqrt{\left[4N^2 \sum_{i=\frac{W}{2}-N}^{\frac{W}{2}+N} \sum_{j=\frac{H}{2}-N}^{\frac{H}{2}+N} X_{i,j}^2 - \left(\sum_{i=\frac{W}{2}-N}^{\frac{W}{2}+N} \sum_{j=\frac{H}{2}-N}^{\frac{H}{2}+N} X_{i,j} \right)^2 \right] \left[4N^2 \sum_{i=\frac{W}{2}-N}^{\frac{W}{2}+N} \sum_{j=\frac{H}{2}-N}^{\frac{H}{2}+N} Y_{i+m,j+n}^2 - \left(\sum_{i=\frac{W}{2}-N}^{\frac{W}{2}+N} \sum_{j=\frac{H}{2}-N}^{\frac{H}{2}+N} Y_{i+m,j+n} \right)^2 \right]}} \quad (3)$$

where X and Y are the two images to be registered. W and H are the width and height of image X separately. m and n are the x and the y directional shift between image Y and image X . Two images overlap completely when m and n are zero. r , s and ρ are the similarity matrices between two images. The value of element (m, n) in any of the similarity matrix denotes the similarity of the two images when the shifts between the two images in x and y direction are m and n. For the elements in matrix r , a lower value means higher similarity. For the elements in matrices s and ρ , a higher value means higher similarity. The size of these similarity matrices depended on the range of m and n . The range of m and n are determined by the maximum error which could occur in the mechanical system. The range of i and j in the first 2 equations, which differ from m and n (the x and y directional shift between two images), (*region of calculation*) are from b to $W-b$ and $H-b$, where $\pm b$ is the maximum and minimum shift in x and y direction, respectively. The *region of calculation* guaranteed that every element in the similarity matrix was calculated based on the same *region of calculation*. For example, when $m = 0$ and $n = 0$, the range of i and j could be from 0 to W and 0 to H in x and y direction, which means the area of the region of calculation is $W \times H$, because two images overlap completely. When $m = 50$ and $n = 50$, the range of i and j could only be from 50 to $W-50$ and $H-50$ in x and y direction i.e. the area of the region of calculation is $(W-100) \times (H-100)$ which is different from the previous case. Different region of calculation may result in large error in finding the minimum or maximum value in those similarity matrices.

After evaluation of all three registration algorithms using artificially shifted images showing transient GFP expression, it appeared that all 3 algorithms were capable of precisely registering the images before and after the artificial shift regardless of the size of the offsets.

The computational loads, required by the three methods, however, were significantly different. Among the three algorithms evaluated, an average of 638 seconds was needed for the CC method to register two 800 x 600 images. An average of 198 seconds and 255 seconds were required to register an image pair using the SAVD and CF measures respectively. The computer used to evaluate the performance of the image registration algorithms was a Pentium 4 2.0 GHz CPU personal computer with 384MB RDRAM (Dimension 8200, Dell, Round Rock, Texas). SAVD was therefore found to be the most efficient method to register images prior to GFP expression quantification.

6.2. QUANTIFICATION OF GFP

GFP expression can be quantified and presented in a number of different ways. Analyses of transient expression have typically been presented as spot or foci counts [11], which are usually based on counting GFP-expressing foci (which represent individual GFP-expressing cells) by a human operator [25]. Foci counts are therefore quite variable, depending on the individual counting the foci and their ability to discern low intensity spots and minimize duplicate counting of foci in a crowded field. However, counting foci is simple and does provide a good estimate of successful gene introduction and an idea of the strength of the promoter used with the *gfp* gene. Using automated image analysis, foci counts can be precisely and consistently quantified and the intensity of GFP expression per focus or per sample can be easily determined.

To calculate the number of foci efficiently, blob analysis was applied to the binary images following automated image registration. The advantage of blob analysis is its computational efficiency. Blobs are areas of touching pixels that are in the same logical pixel state i.e. grey scale level. It allows identification of connected regions of pixels. The total numbers of blobs as well as the area of each blob in an image were obtained using functions in a commercial image processing library (MIL, Matrox Inc., Quebec, Canada). Fluorescence focus number per unit area was calculated using the equation below.

$$N_n = \frac{N_s}{A_i} \quad (4)$$

where N_n is the foci number per unit area, N_s is the foci number calculated by blob analysis and A_i is the area of the field of view (actual area analyzed) in mm^2 after image registration.

For quantification of GFP intensity, the average intensities in grey value of foreground and background areas in the red and green spectra were calculated. For determination of GFP expression per focus, the total grey value was divided by the number of foci obtained by blob analysis.

7. Conclusions

Although the automated image collection and analysis system described in this chapter is functional, problems exist in applying the technology to different target tissues.

For the robotics platform, samples must fit well within a Petri dish and rapidly-growing tissues are exceedingly difficult to keep within the same focal plane. Condensation on the lids of the Petri dishes has been largely controlled but the temperature in the culture room, which contains the unit, does not fluctuate very widely ($\pm 0.5^{\circ}\text{C}$). This could be more of a problem in other laboratories, where environmental control is less regimented. This system has taken 3 years to develop to the point of functionality and it is not available commercially. The original dissecting microscope, which was used to develop the system has been replaced by the manufacturer with a modified design, which allows electronic focusing and automated exchange of filter sets. Although this is very attractive, the complexity of the system would increase with additional functionality. The automated image collection system does allow for the collection of large amounts of images, which can be utilized for a number of different purposes. The limiting factor for this work is in analyses and manipulation of the large numbers of images that can be generated.

For image analysis of the collected images, semi-continual quantification of gene expression and tissue growth has been possible. Quantification of promoter strength has been shown and the potential of this system to characterize promoters and the factors that induce gene expression should be evident. Growth of GFP-expressing organisms is relatively easy to quantify [43] and the interaction of GFP-expressing organisms with other organisms should assist in the study of some interactions. Additional applications of this technology will undoubtedly arise, as it receives more widespread attention.

Individual images can be spliced together to yield time-lapse animations, which allow compression of events and visualization of processes that have not been previously observed. Time-lapse animations of tissue growth and expression of the *gfp* gene provide additional information that will contribute to a greater understanding of tissue growth and gene expression.

Acknowledgements

Salaries and research support were provided by State and Federal funds appropriated to The Ohio State University/Ohio Agricultural Research and Development Centre. Mention of trademark or proprietary products does not constitute a guarantee or warranty of the product by OSU/OARDC, and also does not imply approval to the exclusion of other products that may also be suitable.

References

- [1] Kassler, M. (2001) Agricultural automation in the new millennium. *Comput. Electron. Agric.* 30: 237-240.
- [2] Kacira, M. and Ling, P.P. (2001) Design and development of an automated and non-contact sensing system for continuous monitoring of plant health and growth. *Trans. Am. Soc. Agric. Eng.* 44: 989-996.
- [3] Saiki, R.; Scharf, S.; Faloona, F.; Mullis, K.; Horn, G.; Erlich, H. and Arnheim, N. (1985) A novel method for the parental diagnosis of sickle cell anemia. *Am. J. Hum. Gene.* 37: A172.
- [4] Lee, M.S.; Chang, K.S.; Cabanillas, F.; Freireich, E.J.; Trujillo, J.M. and Stass, S.M. (1987) Detection of minimal residual cells carrying the T-14 18 by DNA sequence amplification. *Science* 237: 175-178.

- [5] Schena, M.; Shalon, D.; Heller, R.; Chai, A.; Brown, P.O. and Davis, R.W. (1996) Parallel human genome analysis: Microarray-based expression monitoring of 1000 genes. *Proc. Natl. Acad. Sci. - USA* 93: 10614-10619.
- [6] Kazan, K.; Schenk, P.M.; Wilson, I. and Manners, J.M. (2001) DNA microarrays: New tools in the analysis of plant defense responses. *Mol. Plant Path.* 2: 177-185.
- [7] Khan, J.; Wei, J.S.; Ringner, M.; Saal, L.H.; Ladanyi, M.; Westermann, F.; Berthold, F.; Schwab, M.; Antonescu, C.R.; Peterson, C. and Meltzer, P.S. (2001) Classification and diagnostic prediction of cancers using gene expression profiling and artificial neural networks. *Nature Medicine* 7: 673-679.
- [8] Arcellana-Panlilio, M. and Robbins, S.M. (2002) Cutting-edge technology I. Global gene expression profiling using DNA microarrays. *Am. J. Physiol.* 282: G397-G402.
- [9] Eisen, M.B. and Brown, P.O. (1999) cDNA Preparation and Characterization. In: Weissman, S. (Ed.) DNA arrays for analysis of gene expression. Academic Press, New York; pp.179-205.
- [10] Finer, J.J.; Finer, K.R. and Santarem, E.R. (1996) Plant cell transformation, physical methods for. In: Meyers, R.A. (Ed.) *Encyclopedia of Molecular Biology and Molecular Medicine*. VCH Publishers, The Netherlands; pp. 458-465.
- [11] Klein, T.M.; Wolf, E.D.; Wu, R. and Sanford, J.C. (1987) High-velocity microprojectiles for delivering nucleic acids into living cells. *Nature* 327: 70-73.
- [12] Horsch, R.B.; Fry, J.E.; Hoffman, N.L.; Eicholtz, D.; Rogers, S.G. and Fraley, R.T. (1985) A simple and general method for transferring genes into plants. *Science* 227: 1229-1231.
- [13] Finer, J.J.; Vain, P.; Jones, M.W. and McMullen, M.D. (1992) Development of the Particle Inflow Gun for DNA delivery to plant cells. *Plant Cell Rep.* 11: 232-238.
- [14] Sanford, J.C.; DeVit, M.J.; Russell, J.A.; Smith, F.D.; Harpending, P.R.; Roy, M.K. and Johnston, S.A. (1991) An improved, helium-driven biolistic device. *Technique* 3: 3-16.
- [15] Vain, P.; McMullen, M.D. and Finer, J.J. (1993) Osmotic treatment enhances particle bombardment-mediated transient and stable transformation of maize. *Plant Cell Rep.* 12: 84-88.
- [16] Hadi, M.Z.; McMullen, M.D. and Finer, J.J. (1996) Transformation of 12 different plasmids into soybean via particle bombardment. *Plant Cell Rep.* 15: 500 -505.
- [17] Kohli, A.; Griffiths, S.; Palacios, N.; Twyman, R.M.; Vain, P.; Laurie, D. and Christou, P. (1999) Molecular characterization of transforming plasmid rearrangements in transgenic rice reveals a recombination hotspot in the CaMV 35S promoter and confirms the predominance of microhomology mediated recombination. *Plant J.* 17: 591-601.
- [18] Fu, X.; Duc, L.T.; Fontana, S.; Bong, B.B.; Tinjuangjun, P.; Sudhakar, D.; Twyman, R.M.; Christou, P. and Kohli, A. (2000) Linear transgene constructs lacking vector backbone sequences generate low-copy-number transgenic plants with simple integration patterns. *Trans. Res.* 9: 11-19.
- [19] Napoli, C.; Lemieux, C. and Jorgensen, R. (1990) Introduction of a chimeric chalcone synthase gene into petunia results in reversible co-suppression of homologous genes in trans. *Plant Cell* 2: 279-289.
- [20] Chilton, M.D.; Drummond, M.J.; Merlo, D.J.; Sciaky, D.; Montoya, A.L.; Gordon, M.P. and Nester, E.W. (1977) Stable incorporation of plasmid DNA into higher plant cells: the molecular basis of crown gall tumorigenesis. *Cell* 11: 263-271.
- [21] Hansen, G.; Das, A. and Chilton, M.D. (1994) Constitutive expression of the virulence genes improves the efficiency of plant transformation by *Agrobacterium*. *Proc. Natl. Acad. Sci.- USA* 91: 7603-7607.
- [22] Stachel, S.E.; Messens, E.; Van Montagu, M. and Zambryski, P. (1985) Identification of the signal molecules produced by wounded plant cells which activate the T-DNA transfer process in *Agrobacterium tumefaciens*. *Nature* 318: 624-629.
- [23] Trick, H.N. and Finer, J.J. (1997) SAAT: Sonication Assisted *Agrobacterium*-mediated Transformation. *Transgenic Res.* 6: 329-336.
- [24] Zupan, J.; Muth, T.R.; Draper, O. and Zambryski, P. (2000) The transfer of DNA from *Agrobacterium tumefaciens* into plants: a feast of fundamental insights. *Plant J.* 23: 11-28.
- [25] Ponappa, T.; Brzozowski, A.E. and Finer, J.J. (1999) Transient expression and stable transformation of soybean using the jellyfish green fluorescent protein (GFP). *Plant Cell Rep.* 19: 6-12.
- [26] Hunold, R.; Bronner, R. and Hahne, G. (1994) Early events in microprojectile bombardment: cell viability and particle location. *Plant J.* 5: 593-604.
- [27] Svitashv, S.K.; Pawlowski, W.P.; Makarevitch, I.; Plank, D.W. and Somers, D.A. (2002) Complex transgene locus structures implicate multiple mechanisms for plant transgene rearrangement. *Plant J.* 32: 433-445.
- [28] Jefferson, R.A. (1987) Assaying chimeric genes in plants: the GUS gene fusion system. *Plant Mol. Biol. Rep.* 5: 387-405.

- [29] Ridgway, E.B. and Ashley, C.C. (1967) Calcium transients in single muscle fibers. *Biochem. Biophys. Res. Commun.* 29: 229-230.
- [30] Niedz, R.P.; Sussman, M.R. and Satterlee, J.S. (1995) Green Fluorescent protein: an *in vivo* reporter of plant gene expression. *Plant Cell Rep.* 14: 403-406.
- [31] Stewart, C.N. (2001) The utility of green fluorescent protein in transgenic plants. *Plant Cell Rep.* 20: 376-382.
- [32] Haseloff, J. and Amos, B. (1995) GFP in plants. *Trends in Genetics* 8: 328-329.
- [33] Vanden Wymelenberg, A.J.; Cullen, D.; Spear, R.N.; Schoenike, B. and Andrews, J.H. (1997) Expression of green fluorescent protein in *Aureobasidium pullulans* and quantification of the fungus on leaf surfaces. *BioTechniques* 23: 686-690.
- [34] Haseloff, J. and Siemering, K.R. (1998) The uses of green fluorescent protein in plants. In: Chalfie, M. (Ed.) *Green Fluorescent Protein: Properties, Application, and Protocols*. Wiley-Liss, Inc., New York; pp. 191-219.
- [35] Nagatani, N.; Takuni, S.; Tomiyama, M.; Shimada, T. and Tamiya, E. (1997) Semi-real time imaging of the expression of a maize polyubiquitin promoter-GFP gene in transgenic rice. *Plant Sci.* 124: 49-56.
- [36] Grebenok, R.J.; Lambert, G.M. and Galbraith, D.W. (1997) Characterization of the targeted nuclear accumulation of GFP within the cells of transgenic plants. *Plant J.* 12: 685-696.
- [37] Piston, D.W.; Patterson, G.H. and Knobel, S.M. (1999) Quantitative imaging of the green fluorescent protein (GFP). In: *Methods in Cell Biology*, Nashville, Tennessee; pp. 31-48.
- [38] Maximova, S.N.; Dandekar, A.M.; and Guiltinan, M.J. (1998) Investigation of *Agrobacterium*-mediated transformation of apple using green fluorescent protein: high transient expression and low stable transformation suggest that factors other than T-DNA transfer are rate-limiting. *Plant Molec. Biol.* 37: 549 – 559.
- [39] Hauser, K.; Haynes, W.J.; Kung, C.; Plattner, H. and Kissmehl, R. (2000) Expression of the green fluorescent protein in *Paramecium tetraurelia*. *Eur. J. Cell Biol.* 79: 144-149.
- [40] Spear, R.N.; Cullen, D. and Andrews, J.H. (1999) Fluorescent labels, confocal microscopy, and quantitative image analysis in study of fungal biology. In: *Methods in Enzymology*, Vol. 307: 607-623.
- [41] Scholz, O.; Thiel, A.; Hillen, W. and Niederweis, M. (2000) Quantitative analysis of gene expression with an improved green fluorescent protein. *Eur. J. Biochem.* 267: 1565-1570.
- [42] Inoué, S.; Shimomura, O.; Goda, M.; Shribak, M. and Tran, P.T. (2002) Fluorescence polarization of green fluorescence protein. *Proc. Natl. Acad. Sci. -USA* 99: 4272-4277.
- [43] Buenrostro-Nava, M.T.; Ling, P.P. and Finer, J.J. (2003) Development of an automated image collection system for generating time-lapse animations of plant tissue growth and green fluorescent protein gene expression. In: Vasil, I.K. (Ed.) *Plant Biotechnology 2002 and Beyond*. Kluwer Academic Publishers, The Netherlands; pp. 293-295.
- [44] Buenrostro-Nava, M.T.; Ling, P.P. and Finer, J.J. (2005) Development of an automated image acquisition system for monitoring gene expression and tissue growth. *Trans. Am. Soc. Agric. Eng.* (in press).
- [45] Svedlow, M.; McGillem, C.D. and Anuta, P.E. (1978) Image registration: similarity measure and pre-processing method comparisons. *Aerospace and Electronic Systems, IEEE Trans. AES* 14: 141-149.

APPLICATIONS AND POTENTIALS OF ARTIFICIAL NEURAL NETWORKS IN PLANT TISSUE CULTURE

V.S.S. PRASAD AND S. DUTTA GUPTA

*Department of Agricultural and Food Engineering, Indian Institute of
Technology, Kharagpur 721 302, India – Fax: 91-3222-255303 –
Email: sdg@agfe.iitkgp.ernet.in*

1. Introduction

In a broad sense, intelligence is something, which deals with the ability to grasp, analyze a task and then reach for a logical conclusion upon which an action can be initiated. Over the years, many researchers have been attempting to create a non-biological entity that can match human level performance. Such attempts have manifested in the emergence of a cognitive approach termed as artificial intelligence (AI). There are many ways in which artificial intelligence can be manoeuvred to execute its function. Computers can be programmed to provide a platform for a coherent approach for executing a particular task. Complex mathematical functions can be deciphered and logical theorems can be deduced by the use of symbolic artificial intelligence. But symbolic artificial intelligence neither could decrypt a digitized image nor could deduce a signal from imperfect data, and has difficulty in adapting things to a change in a specified process. Many problems do exist which cannot be elucidated by simple stepwise algorithm or a precise formulae, particularly when the data is too complex or noisy. Such problems require a sort of connectionism or in other words a network approach. It is possible to interconnect many mathematical functions, all of which perform a dedicated task of processing the data into a desired form of meaningful output. The data can be forwarded through valued connection routes. The conduction strength of the routes, which regulates the movement of data processing can act as a sort of memory and can be very useful in adapting to process changes. Function wise, such network approach is exactly the reverse of symbolic AI. The strength of neural network analysis lies in its ability to generalize distorted and partially occluded patterns and potential for parallel processing. However, they encounter difficulty in formal reasoning and rule following. The results of applying such network technology have been found to be astounding and phenomenal with a relatively modest effort.

Biological processes are incomprehensible in terms of their behaviour with respect to time. It is a well-recognized fact that the genetic and environmental factors are the key effectors, which contribute to their functioning. These two factors have a very high degree of variability in and among themselves ultimately manifesting in a wide spectrum of biological developments that are non-deterministic and non-linear in nature. Such

developmental patterns are also characteristic to plant cells and tissues, which are cultured aseptically in controlled but stressful *in vitro* environment. *In vitro* plant culture practice is generally intended to manipulate the tissue growth and behaviour in a predefined manner either to obtain mass propagated elite plantlets within a short timeframe or to derive useful metabolites on a large scale apart from its use in transgene research. Appropriate modelling which can predict as well as simulate *in vitro* growth kinetics, thermodynamic limitations of culture conditions and energy to mass and vice versa conversions in a realistic manner are therefore considered very much essential. Conventional analytical techniques for these purposes based on mathematical models are questionable, since these methods do not conform to the non-idealities of *in vitro* culture phenomenon.

Neural network technology is an efficient alternative for reliable and objective evaluations of the biological processes. Neural network technology deals with approximation of different complex mathematical functions to process and interpret various sets of erratic data. This technology mimics the structure of the human neuron network as it incorporates information processing and decision making capabilities. With their high learning capability, they are able to identify and model complex non-linear relationships between the input and output of a bioprocess [1,2,3]. While, neural networks have shown remarkable progress in the area of on-line control of bioprocesses, their applications to complex plant tissue culture systems are comparatively recent and restricted only to a few instances.

The present chapter primarily aims to introduce the fundamental concepts of artificial neural network technology to those who own more of an authentic command in life sciences than in mathematics and allied fields. This review is intended to explain the relevance of network based evaluations in plant cell and tissue culture as compared to conventional syntactic approaches, discuss basic methodology of network modelling, describe the various applications of artificial neural networks in *in vitro* plant culture systems and provide an insight into the future perspective and potentials of network technology.

2. Artificial neural networks

2.1. STRUCTURE OF ANN

The fundamental structure of ANN is similar to that of a biological nervous system. The network architecture is a connected assembly of individual processing elements called as nodes. These nodes are arranged in the form of layers. The most common structure is a three-layered network as depicted in Figure 1. It comprises of an input layer, a hidden or interactive layer and an output layer. A three-layered network is shown as an example because it can address all the problems that a more complex network is capable of though not as efficient. The connections between nodes and the number of nodes per layer are defined by the approach, which is adopted to solve or interpret a given problem. The flow of the information through a network is governed by the direction of inter-nodal connections. In feed forward neural network, unidirectional connections exist between the neurons belonging to either same or different layers allowing the

processed data proceeds only in forward direction, whereas in Recurrent neural network (Feed-back network) connections exist in both forward and backward direction between a pair of neurons and even in some cases from a neuron to itself.

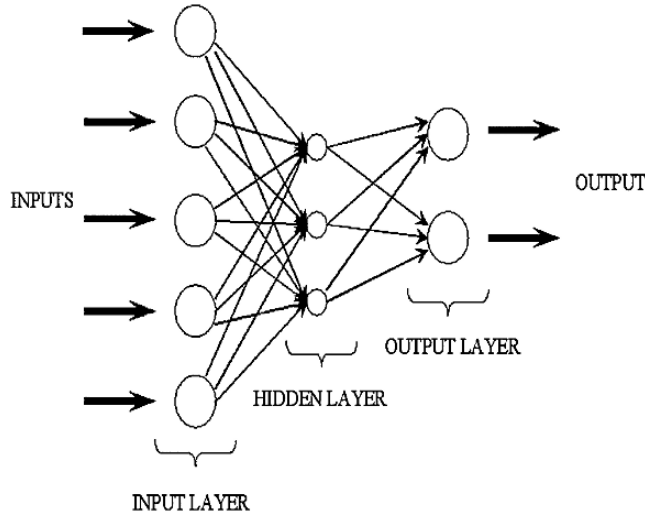


Figure 1. Three layered feed-forward network.

2.2. WORKING PRINCIPLE AND PROPERTIES OF ANN

2.2.1. Computational property of a node

The functioning of individual node in ANN is analogous to the biological neuron. Each node receives one or multiple inputs from surrounding node(s) and computes an output that is transmitted to the next node. While computing the output, the input information is weighed either positively or negatively. Assigning some threshold value to the concerned neuron simulates the output action. At the level of each node, the input values are multiplied with the weight associated with the input to give a result. The result is then adjusted by an offset variable ' θ ' according to the type of network in use. The output is then determined using the adjusted summation as the argument in a function ' f ' which is pre-defined by the algorithm (Figure 2). Function ' f ' can also be termed as either transfer function or activation function. This function can take sigmoid, linear, hyperbolic tangent or radial basis form. The selection of the activation function depends on the purpose of the network.

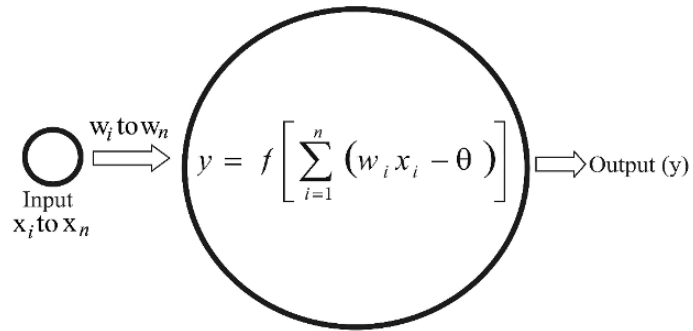


Figure 2. Basic mechanism of nodal computation $n =$ No. of inputs; $x =$ input variable; $w =$ weight of i^{th} input; $\theta =$ internal threshold value and $f =$ activation function.

The most common neuronal nonlinear activation function used in biological systems is sigmoid in nature (Figure 3).

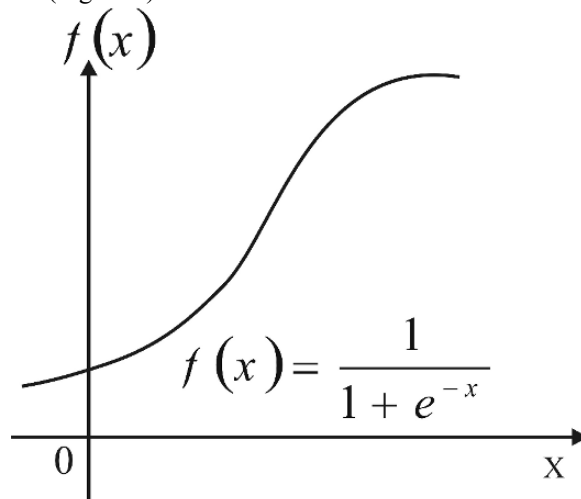


Figure 3. Sigmoid activation function.

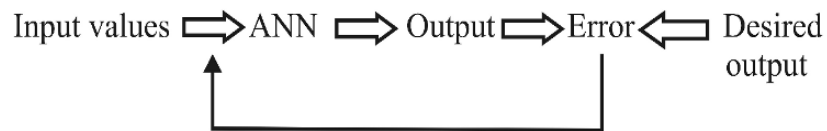


Figure 4. Steps of neural computation.

The ability of the network to memorize and process the information lies in the weights assigned to the inter-node connections, which determine their conductivity through a network. These weights are incurred during the process of training the network. The inter-nodal connections with their corresponding weights basically represent the adaptability of the network to the problem domain. When input variables are fed to the neural network, the corresponding computed outputs are compared to the desired output (as in the case of supervised training mechanism). The error thus generated is propagated back to the network for some parametric adjustments (also called as learning rule) until the network attains a good generalization of the problem domain (Figure 4).

2.2.2. Training mechanisms of ANN

One of the major properties of the neural networks is to learn and adapt to input information to produce convincing results. Many different training mechanisms have been incorporated in neural networks. Training mechanism also influences the speed with which the network converges and affects the accuracy of models, which classify unknown cases. The ANN learns either in supervised or unsupervised fashion. In supervised method, the external 'conductor' provides the desired output values that are then matched to the system output values for the purpose of correcting the network functioning. In unsupervised method, the system develops its own representation of the input stimuli. For example in pattern classification self-organizing network, the system autonomously recognizes the statistically salient features of the input patterns and categorizes them. Unlike the supervised learning paradigm, there are no pre-determined sets of categories into which the patterns are to be classified.

2.3. TYPES OF ARTIFICIAL NEURAL NETWORKS

Neural networks can be differentiated either based on the purpose for which they are devised or on their basic topology along with the associated training method. Since our interest is to describe the applicability of ANN to plant tissue culture systems, we restrict only to the types of models with respect to their applications.

2.3.1. Classification and clustering models

ANN can be used for pattern recognition, nonlinear regression and classification purpose in plant tissue culture studies. For automation in commercial mass propagation of plants, decision-making networks play a major role, which come under this category. Classification models find most common application in tissue culture. Multilayer Perceptron (MLP) [4], Backpropagation neural networks (BPNN) and ADALINE networks comprise the categorization networks with supervised learning. Unsupervised architectures rely mostly on the data for clustering the input patterns. Under this category Kohonen network, Competitive and Hebbian learning, Adaptive resonance theory (ART) can be placed. BPNN are well suited for pattern matching and trend analysis. It is just like feed-forward neural network. In order to adjust the connection weights from input to hidden nodes, the errors of the units in the hidden layers are determined by back propagating the errors of the units of the output layers in a supervised manner. This is also called as back-propagation learning rule. Such neural networks are called back propagation neural networks.

2.3.2. Association models

These are the models, which accept binary valued inputs. These neural networks associate an object by just 'seeing' a part of that object. Continuous variables in such cases can be converted to binary form to be used as input. These models endorse threshold approach. In this case, the neurons are never connected to themselves. Hopfield networks, Binary associative memory (BAM), Adaptive binary associative memory (ABAM) and Hamming networks are examples of this type.

2.3.3. Optimization models

In plant tissue culture studies, there is a need to optimize the process taking into account the factors influencing them. Optimization models find a best solution when trained with a set of constraints. The weights of these constraints are stored in the connections so that when independent variables are fed the network predicts the combination of variables that would yield optimum solution.

2.3.4. Radial basis function networks (RBFN)

These networks endorse a combination of supervised and unsupervised learning methods. They are mainly used for modelling a biological process, classification and reduction in the dimensionality of the process. In this type of architectures, the hidden layer is trained by unsupervised learning methodology like for example K-means algorithm, whereas the output nodes are modelled based on supervised learning like for example least mean square algorithm. In RBFN, centres are located among the input and output pairs. A good generalization is represented by minimum values of sum of squares of the distance between the centres to training data sets. In other words, the activation function of each node uses a distance measure as an argument. It is very much applicable to function approximation problems. RBFN are easy to work with and are very fast 'learners' and show good generalizations and classifications. They are good for image recognition. It is just like BPNN with similar kind of information flow.

2.4. BASIC STRATEGY FOR NETWORK MODELLING

The model of the neural network to be used depends largely on our purpose. The type of the network affects the required form and quality of output.

2.4.1. Database

The neural computation is largely dependent on the availability of the data sets. Neural network modelling is appropriate if the database is complete (data representing all the aspects of the subject). Network approach can also be adopted in case of incomplete database provided an expert opinion is available (as in the case of supervised learning). In network modelling the variability in the data sets is more important than its availability in large quantity. While obtaining the data the meaningful parameters must be chosen which hold significant relevance to the purpose of modelling. Some ANN accepts binary data while others accept continuous variables as inputs. In plant tissue culture studies, information can be obtained from the following data types:

- Binary data (organogenic / non-organogenic; viable / non-viable; regenerable / recalcitrant)
- Continuous (growth rate)
- Categorical (growth regulator treatment categories; poor, moderate and good response)
- Fuzzy (the degree of hyperhydricity)

While selecting an approach, relevant data must be scored in a suitable format with regard to the type of application one intends to develop. The information can be encoded into one of the data types before feeding depending on the type of output one can expect. The sensitivity of the output pattern to a particular input pattern varies not only with the value of that input, but also with the values of the other accompanying inputs. Therefore, the independent input variables should be scaled to the same range or same level of variance before they are fed to the network. Categorical variables must be ordered either in ascending or descending form. If the data is incomplete, to ensure the integrity of the information, one can enter both minimum and maximum values or enter average values taking into account its specific impact on the output quality. For online process monitoring and decision control, data can be obtained in the form of time series. In such systems, in order to avoid data overload and to accomplish real-time interpretation, proper sampling rate must be determined to keep the data points to minimum without losing crucial information. Data can also be decoded from digitized images using appropriate image software to render image information amenable for neural computation.

For optimal performance of the ANN, the size of the training data set is very important since ANN derives its information from the input data sets. The training data sets should represent full range of conditions, so that the network defines a subjected system in a comprehensive manner. The training sets should be always greater than the number of weights in ANN. A preferred size of the training set is 3 to 10 times that of the number of weights. If we train the network with small number of learning data set, initially the error in the output will be very high. But as and when the learning iterations are continued, the error in the learning set tends to decrease. The process of training is stopped when the output error does not decrease anymore but contrarily shows as increasing trend. When the network output goes perfectly through the learning samples, the error with the learning set is least. However, when test data set is fed to such trained network, the error would be very high. The average learning and test error rate is a function of the learning data set size. The learning error increases with an increasing learning set size, and the test error decreases with increasing learning set size. A reliable network performance is evaluated based on smaller test error than on the learning error. With increasing number of learning sets the error rates of learning and test sets converge to the same value at some point and at that point the learning procedure attains a good approximation.

2.4.2. Selection of network structure

Generally input and output nodes are fixed as per the necessity and one hidden layer would be sufficient for estimating any non-linear biological function. More than one interactive hidden layer can be incorporated when different layers comprising hidden

nodes have different task to perform as in the case of Hypernet algorithm. Apart from the number of layers the connectivity between the nodes affects the functioning of the network. The size of the training set and the interpretation of the output are dependent on the inter-nodal connectivity.

2.4.2.1. Number of input nodes. The number of nodes in the input layer must correspond to the number of variables that are taken into account. An expert can fix the number of nodes in input layer based on the relevancy of the corresponding variable. *ANOVA* can be performed to select statistically significant variables and nodes can be assigned to them. Threshold based selection of input nodes can also be done. That is when the weights during learning drop below a threshold level or nearly equals to zero, the nodes associated with them may be pruned accordingly. Combination of input variables that are highly correlated can also lead to justified inclusion of the input nodes.

2.4.2.2. Number of hidden units. Error criteria based upon the number of learning iterations is then taken into account to determine how many processing elements should be there in the hidden layer. When large number of hidden nodes is considered, the network fits exactly with the learning data sets. However, the function the network represents will be far wayward because of the extensive connectivity with both input and output layers. Particularly in case of learning data sets derived from biological experimentations, which contain a certain amount of noise, the network will tend to fit the noise of the learning samples instead of making a smooth and meaningful approximation. It has been shown that a large number of hidden nodes lead to a small error with the training set but not necessarily lead to a small error in the test set. Adding hidden units will always lead to a reduction of the error during learning. However, error on test sets initially gets reduced as hidden nodes are added, but then gradually increase if more than optimum hidden nodes are incorporated per layer (Figure 5). This effect is termed as the peaking effect. The architecture that gives smallest error is normally selected as the best choice.

2.4.2.3. Learning algorithm. Once the topology of the network is selected, the choice of the learning algorithm will be automatically gets defined. Learning algorithm is greatly dependent upon the type of input nodes (binary, continuous or fuzzy) and also the inter-nodal connectivity. Learning algorithm also influences the network convergence ability and its stability. Some learning algorithms may be unstable in some conditions. Therefore, certain limiting conditions must be specified. The algorithm must be appropriate for the type of input data and should be able to produce desired form of output. Algorithms that demand higher number of iterations pose problems in propagating the error.

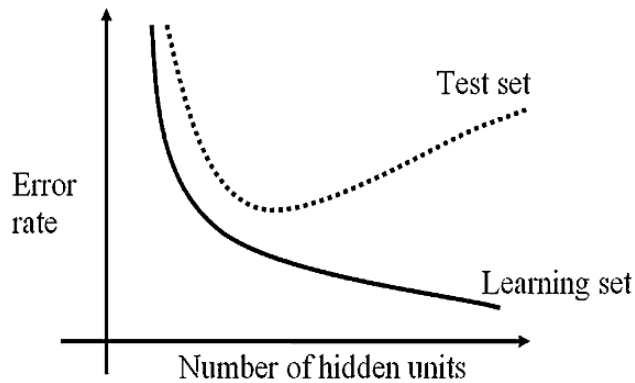


Figure 5. Effect of number of hidden nodes on output precision.

The following aspects need to be considered, while training an algorithm:

- Time required for training
- Number of iterations required
- Convergence of the algorithm
- Stability of the solutions when additional vectors are added to training set
- Stability of solution when the order of training vectors is altered.

The most common learning algorithm is backpropagation method. Here, the error that is generated due to discrepancies between the system output and the expected outcome is propagated back to facilitate readjustments of the weights assigned to the connections till the network achieves a good generalization.

2.4.3. Training and validation of the network

If there is 'N' number of experimental data representing different conditions it has to be determined whether the data should be presented to the network one set at a time (sequential) or all the data in the matrix form and then processed in parallel (parallel). Sequential training is considered best because when the network converges using a particular data set, the weights are saved and are used as initial weights for the next data set and so on which is not possible in parallel processing. Fundamental aspect of training ANN is the stop criterion, which implies the point at which the training is terminated. The error in the training set tends to decrease with training iterations when the ANN has enough degrees of freedom to represent the input/output map. After such training of the network, the validity of the network is tested. Finally a cross validation of error is obtained for different topologies comprising of different number of hidden nodes to minimize error in network response. Smaller number of nodes will cause the ANN to be insufficiently flexible to represent the experimental signal and too many nodes will allow an excess of degrees of freedom which will cause premature over-fitting and consequently, cross-validation will terminate the learning process for a higher error. An

alterative way to control it is to reduce the size of the network. Either one can set a small topology with fewer hidden nodes and add new nodes or can begin with a large network and remove the nodes to get minimum error with test set [5]. To avoid over-training or over-fitting (a condition where the ANN strongly remembers only the training patterns), the performance obtained with the validation set must be checked once in every 50 passes of the training set. The validation step should comprise at least 10% of the training steps and the data set of the validation must be distinct from the training set.

3. Applications of ANN in plant tissue culture systems

Plant tissue culture is an excellent technique for commercial mass propagation of elite plant species in a relatively short period of time overcoming the limitations posed by agro-climatic, seasonal and biotic effects on conventional plant production methodologies. Large-scale cultivation of plant cells in bioreactor has also been found effective for production of high value natural compounds. However, developmental pattern of somatic embryos, characteristics of regenerated plants and behaviour of *in vitro* cell cultures makes the conventional modelling technique ineffective for on-line monitoring. ANN can be leveraged to plant tissue cultural practices for pattern recognition of somatic embryos, photosynthetic and photometric evaluation of regenerated plants and on-line evaluation of biomass and control of secondary metabolite production. ANN based modelling approach has been found to be more flexible, effective and versatile in dealing with non-linear relationships prevalent in cell culture practices. Also the approach has distinct advantages, as it does not require any prior knowledge regarding the structure or interrelationships between input and output signals. The various applications of ANN in plant tissue culture systems are summarized in Table 1. These studies provide a comprehensive insight into the expediency of processing networks in interpreting the database derived from *in vitro* plant culture investigations.

3.1. *IN VITRO* GROWTH SIMULATION OF ALFALFA

This case study deals with the simulation of *in vitro* shoot growth of alfalfa for transplant production [6]. Combined effects of CO₂ inside the culture vessel and sucrose content of the media on *in vitro* shoot growth were studied. A growth model using Kalman filter neural network was developed for this purpose. The experimental data of growth parameters such as dry weight, leaf number and root initiation stage were correlated well with the simulated values calculated by the trained neural network.

The study demonstrates the efficacy of Kalman filter training of the neural network in simulation of *in vitro* plant growth. This pioneering work also laid a foundation towards an entirely divergent method of understanding the *in vitro* plant growth, which usually tends to behave in a non-deterministic way.

Applications and potentials of artificial neural networks in plant tissue culture

Table 1. Applications of artificial neural network in plant tissue culture studies.

Application	Network model	Associative technique employed	Database source	References
Growth simulation of alfalfa shoots as effected by CO ₂ and sucrose levels	Neural network with Kalman filter training method	Growth modelling	Dry weight, leaf number and root initiation stage	[6]
Distinguishing different embryo types from non-embryos and predicting embryo derived plantlet formation	Feed-forward	Image analysis	Area, length to width ratio, circularity and distance dispersion of plant cell cultures	[7]
Biomass estimation of cell cultures	Standard feed-forward neural network with gradient descent method of optimization and sigmoid function as neuron activation	Quick basic programming of algorithm	Sucrose, glucose and fructose level of medium	[8]
Simulation of temperature distribution in culture vessel	Three layered neural network trained with Kalman filter	Finite element formulation programmed in Visual Basic3.0	Spatial temperature distribution of culture vessel	[9]
Identification and estimation of shoot length	Fuzzy neural network with back propagation algorithm and sigmoid function of neurons	Image analysis and multiple regression modelling; algorithms programmed in VC++ language	Pixel brightness values in red blue and green colour regimes	[10]
Classification of somatic embryos	Feed-forward neural network	Image analysis and discrete and fast Fourier transformation	Radius, length, width, roundness, area and perimeter of the somatic embryo images	[11]
Clustering of regenerated plant-lets into groups	Adaptive resonance theory - 2	Image analysis; 'C' language based programming	Mean brightness values, Maximum pixel count and grey level of maximum pixel count in RBG regions	[12]

3.2. CLASSIFICATION OF PLANT SOMATIC EMBRYOS

The germination and conversion frequency of somatic embryos depend on the normalcy and the developmental stage of the normal embryo. Hands-on selection of such embryos, though accurate, is very laborious, time consuming (since the embryos take approximately eight weeks to mature) and cost intensive. Therefore, an efficient automated system is necessary to enumerate and evaluate the developmental stages of the embryos. An attempt was made to classify the celery somatic embryos from non-embryos so that an appropriate time can be decided for the transfer to next culture stage [7]. Parameters values such as area, length to width ratio, circularity and distance dispersion were derived from the images of celery cell cultures and subsequently subjected to train the ANN. After training, the network could not only classify the globular, heart and torpedo stage embryos and but also successfully predicted the number of plantlets developed from heart and torpedo shaped embryos. This is an example, where ANN could decipher relevant information even from the noisy data. This work demonstrated an efficient non-destructive approach to identify and classify the embryogenic cultures on par with human expertise. Such system of classification is essential for automation, which can economize the process in terms of time and labour.

A pattern recognition system was developed using image analysis system coupled with ANN classifiers to characterize the somatic embryos of Douglas fir [11]. Geometric features of somatic embryos and their Fourier transformations were subjected to the neural network based Hierarchical decision tree classification. Normal embryos were identified with more than 80 percent accuracy. A three layered neural network topology was used with 19 input nodes representing radius, length, width, roundness, area, perimeter and their corresponding Fourier coefficients. Hidden layer, which discriminate the normal and abnormal embryos consisted of 30 nodes, whereas 25 hidden nodes were used to differentiate the developmental stages of the normal. Back propagation learning algorithm was incorporated into the neural network system after correlation with the known features. It is apparent from the training phase that the Fourier features played a major role in distinguishing the normal and abnormal somatic embryos, whereas size dependent features were the main factor in classifying the different developmental stages. This pattern recognition system achieved about 85% accuracy for normal embryos. Thus, it could help in the optimization of developmental process of somatic embryos. Discarding abnormal embryos could also minimize the low conversion frequency in the final produce.

3.3. ESTIMATION OF BIOMASS OF PLANT CELL CULTURES

A neural network approach to estimate biomass and sugar consumption rate in cell cultures of *Daucus carota* was described by Albiol *et al.* [8]. The work demonstrated the relative efficacy of neural network in estimating plant cell mass growth over the conventional modelling tools. In order to estimate the biomass formation, feed-forward neural network architecture with bias was employed with one hidden layer. Three neurons were assigned to the hidden layer in order to achieve lower quadratic error value for biomass with minimal iterations requirement. There were eight input neurons for time, biomass, sucrose level, glucose level, fructose level and four output neurons for

the levels of biomass, sucrose, glucose and fructose. The data for feeding the network were derived from two different bioreactors with different levels of inoculum and sugar concentration. A sigmoid function is applied to the neuronal output signal for training the algorithm. Quadratic error measured from the output of the network was used as an objective function to change the weights following gradient descent method in a backward direction. Iterative process is followed for the whole set of inputs until a convergence criterion is obtained. After the training, new data sets were tested to validate the performance of the network.

A supervised training was imparted to a three-layered feed-forward network by correlating the network outputs with the experimental data. During the training phase, when the data from one bioreactor was used, the network-simulated data pertaining to both carbohydrate and biomass content correlated poorly with the experimental one. However, the network predictions were reasonably accurate when trained with two experiments representing two different culture behaviours. The first experiment was performed with Biolab reactor with an initial biomass concentration of 0.75 gm/L and the second one in Colligen bioreactor with a higher inoculum of 0.96 gm/L. Additional input in the learning process considerably improved the performance. In the validation step, changes in sugar and biomass evolutions were correctly predicted by the network output. The method successfully measures the sugar and biomass levels online of plant cell cultures. The performance of the network was compared with the Extended Kalman Filter (EKF) approach [13] based on the use of a deterministic mathematical model (Figure 6). EKF was found to be dependent on several experiments, whereas the network was able to describe the culture behaviour after training with just two experiments. Thus, the network approach offers an efficient alternative even with little experimentation and minimum available information.

3.4. SIMULATION OF TEMPERATURE DISTRIBUTION INSIDE A PLANT CULTURE VESSEL

Control of microenvironment inside the plant culture vessel is critical for plant growth [14]. Environmental control such as CO₂ concentration, ventilation rate, light intensity, air temperature inside the culture vessel affects the growth of the regenerated plants. In particular, increase in air temperature due to high light intensity inhibited the growth. Controlled cooling of culture vessel has been recommended to reduce the air temperature and it requires extensive experimentations by varying the factors like: shape and /or size of the vessel, ambient temperature, head load from light, material of the container, velocity of blowing air and bottom cooling temperature of culture vessel. An effective method to determine the forced convective heat transfer coefficient over the plant culture vessel was developed using a finite element neural network inverse technique [9] (see also the chapter of Murase *et al.* in this book).

A finite element model may predict the temperature distribution inside the culture vessel for which the constants of Nusselt number equation are required. These constant values were determined through a Kalman filter neural network route from measured temperatures of the experiments with the hidden layer comprising of 12 neurons. Four input neurons were incorporated corresponding to the node temperatures as described in the finite element model. The simulated temperature values were then fed into a three-

layered neural network in an iterative manner for adjusting the weights until a satisfactory learning level has been achieved. The four centre nodal temperatures (of gel and three air temperatures at three different heights of the culture vessel) were measured using copper-constantan thermocouples and were approximated by a system of finite elements. The temperatures at different air velocities were measured and processed through neural network to estimate the constants of Nusselt equations. Then with these coefficients, convective heat transfer over the culture vessel surface at different air velocities was calculated. The errors for air and gel temperatures between experimental and simulated values were below 5% for air velocities of 1, 2 and 4 ms^{-1} . The training data for the neural network were generated by the finite element model from random values of Nusselt equation constants. The random inputs to the network covered the entire possible combination of coefficients of convective heat transfers.

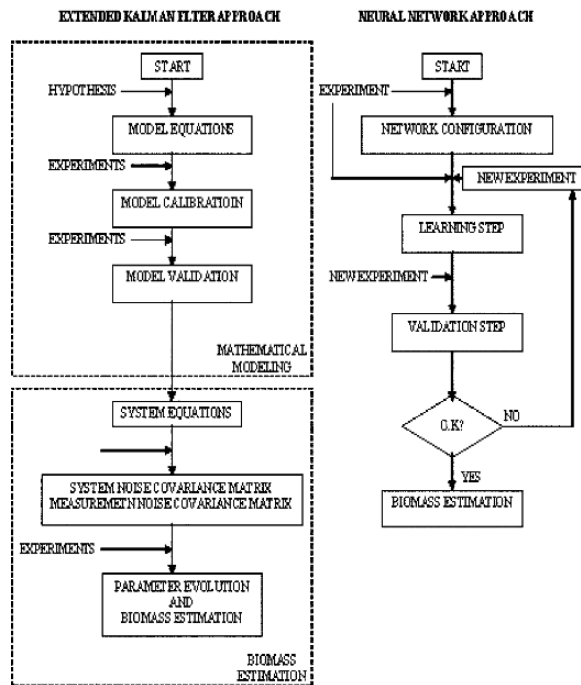


Figure 6. Stepwise procedure for estimation of plant cell culture biomass by Kalman filter approach and neural network approaches. Reprinted with permission from Prof. Manel Poch, Universitat Autònoma de Barcelona, Spain. [8].

The data is transferred through the neural network and finite element model in a circulatory fashion. Training the network, the constants of Nusselt equations were directly and accurately determined by measured temperatures from the experiments. The generalization feature of the neural network allowed the random inputs to cover the entire range of convective heat transfer coefficients pertaining to possible temperature distributions. Training of the network with finite element model outputs, made the temperature distribution estimation easy and accurate.

3.5. ESTIMATION OF LENGTH OF *IN VITRO* SHOOTS

Neural network aided estimation of shoot length of *in vitro* regenerated rice was demonstrated by Honda *et al.* [10]. Digitized images of the regenerated cultures were captured using CCD camera and fed into computer for data extraction. To assess an appropriate model for shoot region identification both multiple regression analysis (MRA) and fuzzy neural network models (FNN-A and B) were studied on comparative basis. MRA consisted of three different equations and the normalized brightness values for RGB regions were input into each equation. The outputs of these equations were positively correlated to the experimental RGB brightness values, which ascertain the identification of shoot, callus and medium regions for that particular pixel input data set.

In neural network approach, two different types of FNN were used to distinguish shoot regions. FNN-A comprised of one model with three inputs and three outputs, whereas FNN-B consisted of three independent models with three input units and one output unit per model. In this approach, numerical input values were fuzzified. The individual nodes of the fuzzy neural hold a sigmoid activation function and the networks were trained in supervised manner with back propagation algorithm. The connection weights of the trained model were entered in the colour rule table and compared with each other to derive the relevance of colour (s) in the model to distinguish the shoot, callus and medium regions. The extent of complexity in the relationship between the individual colour components was numerically derived from the connection weights of the trained neural network. Therefore, the fuzzy neural network model appears to have a higher level of accuracy in identification of shoots. Using FNN the shoot recognition was 95% accurate.

Since, FNN-B model was found to be more effective for recognizing callus region than FNN-A, a trinary image was reconstructed using the outputs of FNN-B model. This trinary image was then subjected to a two-step method of thinning and extraction of the longest path based on Hilditch's algorithm and Tanaka's algorithms respectively to separate the shoot region from the rest of the image and estimate its length. The elongated shoots of the regenerated rice calluses were measured after straightening and compared with network-simulated values. The average error of only 1.3 mm was observed between the predicted and actual lengths.

3.6. CLUSTERING OF *IN VITRO* REGENERATED PLANTLETS INTO GROUPS

One of the prime concerns of *in vitro* plant micropropagation is the poor survival of regenerated plants upon *ex vitro* transfer. The intrinsic quality of the regenerated plants is largely responsible for its survival during the period of acclimation. Variations are reflected in the physiological status and *in vitro* behavioural aspects of the plantlets viz., rooting ability, hyperhydric status and adaptability to *ex vitro* condition etc. These kinds of variation are not similar to that of well documented aspects of somaclonal variation, but deserve attention for successful *ex vitro* transfer.

Development of automatic decision making entity reflecting the variations of *in vitro* regenerated plants is necessary to ensure high rate of survival upon *ex vitro* transfer. The decision-making may be made in the form of grouping or clustering of regenerated plants based on their inherent properties. Such decision-making system

coupled with robotics can result in mechanization of commercial mass propagation. Since the physiological and behavioural variations among the regenerated plants are difficult to be resolved by human visual evaluation, machine-vision coupled neural network based clustering might be an efficient alternative.

For automated clustering of regenerated plants, reliable and contributory features need to be obtained from the plants, which would help in decision-making. Colour information based machine vision analysis (MVA) has been acclaimed as a rapid, sensitive and non-invasive method for qualitative evaluation and quantification of *in vitro* regenerated plant cultures [15]. It has been suggested that the photometric parameters could serve as reliable indicators for assessing the behaviour of regenerable cultures. Leaf spectral reflectance and brightness intensity can be captured as digitized images for compilation of input features which can further be processed with neural network algorithm to interpret and project the inherent variations. In this way, a functional activity in a biological system can be correlated to the minute machine-observed colour based information.

We test the hypothesis that whether regenerated plants can be sorted out into groups based on their photometric behaviour using image analysis system coupled with neural network algorithm. It is well understood that the successful clustering of regenerated plants gives an opportunity to identify and select plants amenable for *ex vitro* survival. A neural network based image processing method was developed for clustering of regenerated plantlets of gladiolus based on the leaf feature attributes in Red, Blue and Green colour regimes [12].

The main objective of any clustering model would be to find a valid organization of the data with respect to the inherent structure and relationship among the inputs. ART2 network, originally developed by Carpenter and Grossberg [16], is one such model which is configured to recognize invariant properties within the given problem domain. From the luminosity and trichromatic components of the leaf images, 12 attributes per individual plantlets were extracted. These 12 attributes constituted the input pattern for a single plantlet and were fed to ART2 algorithm, which was compiled by 'C' programming. Unlike ART1, ART2 model has the distinct ability to process the leaf input patterns, which are analogue-valued.

The description that follows is intended to outline the generalized ART2 network principles. ART2 network is divided into two subsystems namely attentional subsystem and orienting subsystem. The basic function of attentional subsystem is to establish valid categories based on salient features of the input patterns. The attentional subsystem forms a platform for establishing resonance conditions between activity patterns flowing in feed-forward and feed-back direction. When such bottom-up input pattern is found superposable to the top-down expectation pattern, it is regarded as a constituent of that established category. The attentional subsystem is comprised of F0, F1 and F2 layers. F0 layer comprises of 4 sub-layers namely, w_i^o x_i^o v_i^o u_i^o and F1 layer contains 6 sub-layers, namely w_i^o x_i^o v_i^o u_i^o p_i^o q_i^o . The input nodes contain a nonlinear transfer function with a threshold value (θ). The noise level in the input information dictates the nodal activation. F0 and F1 layers of the attentional subsystem function in order to enhance significant aspects of the input signals. This is particularly necessary for analogue input patterns since the difference between the possible values of a feature is much smaller than the difference that is generally described in terms of binary values.

The parametric conditions laid down for the basic ART2 clustering analysis are as follows,

$$a > 0; b > 0; d = 0 \text{ to } 1; c \text{ such that } c \times d / (1-d) \leq 1; e \ll 1; \theta \leq 1$$

'a' and 'b' are the model gain parameters. These parameters influence the stability of the network. Lower values of 'a' and 'b', allow wider range of vigilance parameter values to be used and also consequently results in the formation of increasing number of stable categories even when trained with fewer number of learning data sets. However, it must be noted that higher values of 'a' and 'b' could ultimately result in one pattern getting allocated to more than one category. The parameters 'c' and 'd' are valued as per the original ART2 model where their relationship is pre-established. The primary function of parameter 'e' is to prevent a divide by zero condition. Therefore, its value is kept relatively very small.

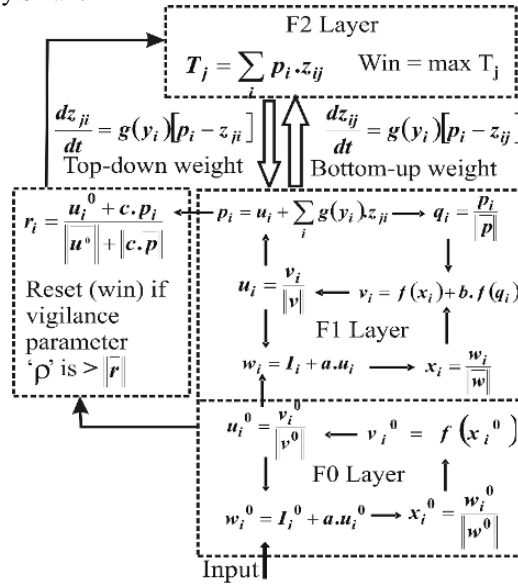


Figure 7. Block diagram of entities in ART2 network.

The values that are assigned to the network parameters in our venture are as follows:

$$a = 10; b = 10; c = 0.1; d = 0.8; e = 0.000001 \text{ and } \theta = 0.0001$$

The activities in F0 and F1 layer and the direction of the flow of signals are depicted in Figure 7. In F0 and F1 layers, the raw input values are normalised. The activity function at F0 and F1 layers is defined by the following condition,

$$f(x) = \begin{cases} x & \text{if } x \geq \theta \\ 0 & \text{otherwise} \end{cases} \quad (1)$$

Where, θ is the threshold value in non-linear function with a positive constant of less than unity. The output of F0 layer (u_i^0) forms the input to F1 layer. F2 layer sums-up processed input activity pattern (p_i) after the normalization of input pattern. The node that has maximum summation value is considered as the winning output category node. In the first cycle, since the top-down weights (Z_{ji}) are assigned as zero, a random selection determines the winning output node. During such random selection, the initial values of the bottom-up connection weight (Z_{ij}) from 'i' input node towards 'j' output node is given by,

$$z_{ij} = \frac{1}{(1-d)\sqrt{M}} \quad (2)$$

Where, d is the model parameter whose values are between 0 and 1 and M is the dimension of the supplied input patterns. When resonance condition between the bottom-up and top-down expectation pattern is insufficient to overcome the threshold set by the VP (ρ), there will be removal of winning node by a reset vector (r). Then a new parallel search cycle is carried-out until a winning node is selected that brings about resonance surpassing the threshold. When that happens, the adaptive weights associated with winning F2 node are updated accordingly. The learning equations for bottom-up and top-down adaptive weights connecting F1 and F2 layers are calculated considering the following condition,

$$g(y_i) = \begin{cases} dT_j = \max(T_j) & \& j \text{ is not reseted} \\ 0 & \text{Otherwise} \end{cases} \quad (3)$$

In the matching process, the two F1 sub-layers that take part are ' p_i ' and ' u_i '. During learning, the activity of the units on the ' p_i ' layer changes as top-down weights changes on the ' u_i ' layer. The ' u_i ' layer remains stable during training, therefore including it in the matching process prevents the occurrence of reset while learning of a new pattern is underway. The reset vector (r) situated in the orienting subsystem determines the degree of match between short term memory pattern at F1 layer and long term memory pattern at F2 layer. This reset vector is calculated after all the F1 layers have been updated to reflect the effects of feed-back from F2 layer. If reset value is higher than the VP value then the winning node is retained as an established matching category and on the contrary, if the reset value is lower than VP then the winning node is disabled accordingly.

In our study the number of generated groups increased from 1 to 2 with the VP range over 0.985. The network validity was proved when the class separability was retained with another similar set of test input patterns. Leaves having maximum similarity in terms of inherent pixel properties fall in a particular group. Hence, it has

been demonstrated that the leaf photometric property could provide a classifying feature with which the discrepancies among the regenerated plantlets can be projected. The use of flatbed scanning machine instead of CCD camera, 'C' program based compilation of the ART-algorithm in a PC with 1.6 GHz clock speed and 256 MB random access memory in lieu of professional ready made off the shelf software rendered the whole process right from the image acquisition to analysis, cost effective. The component steps of the image analysis systems are presented in Figure 8. Such an approach may provide a means of reliable and objective measurement for selecting plants amenable for *ex vitro* survival and quality control in commercial micropropagation.

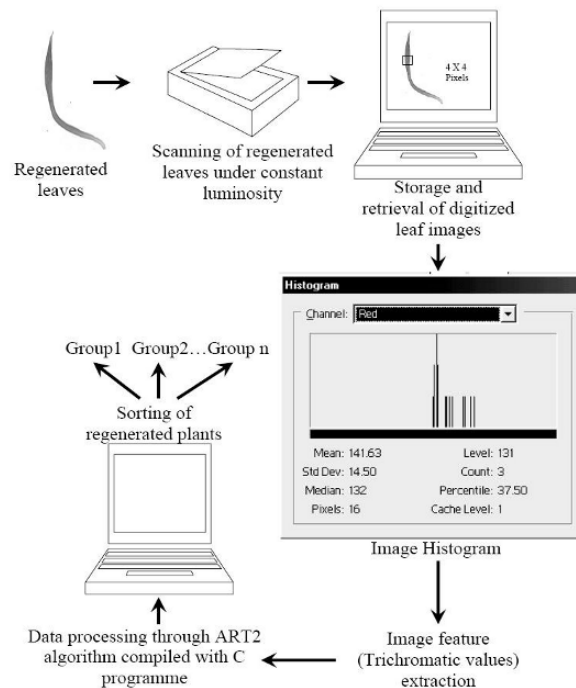


Figure 8. Component steps of machine vision analysis for sorting of *in vitro* regenerated plants into groups. Adapted from Mahendra et al. (2004) [12].

4. Conclusions and future prospects

The use of ANN is increasingly becoming most preferred methodology to model the complex biological responses. ANNs can also play central role as highly potential predictive modelling tool in *in vitro* plant culture studies. Neural computing offers reliable and realistic approach for describing *in vitro* culture of plant species even with minimal available information. The successes obtained after applying neural network technology have been phenomenal with a relatively modest experimental effort while

consuming minimum amount of time. Maximum inference has been derived from relatively simplistic experimental procedures. The ability of the ANN to accurately simulate even under altered conditions could be highly encouraging in design of cultivation systems on large scale. Various image processing methods have been developed successfully for assessing culture types, biomass production etc. but in order to bring them to a usable form, neural network solutions offer attractive incentives.

ANN can be modulated to simulate the metabolism of the *in vitro* plants under a given set of conditions. It could be useful in estimating the amount of secondary metabolites that could accumulate at a specified time period and also the time at which one can derive maximum yield. ANN based prediction of the behaviour of the *in vitro* derived plants in terms of their *ex vitro* survival rate and their rooting or organogenic ability could also be useful in large scale propagation. The outcome of the neural computations can be directed to mechanize systems to automate online processing of plant cell cultures, sub-culturing and quality based segregation of plant tissues all in aseptic fashion.

Acknowledgement

Financial assistance to VSS Prasad from CSIR, New Delhi as a SRF is acknowledged.

References

- [1] Nazmul Karim, M.; Yoshida, T.; Rivera, S. L.; Saucedo, V. M.; Eikens, B. and Oh, G. S. (1997) Global and local neural network models in biotechnology: Application to different cultivation processes. *J. Ferment. Bioengg.* 83: 1-11.
- [2] Hashimoto, Y. (1997) Applications of artificial neural networks and genetic algorithms to agricultural systems. *Comput. Electro. Agri.* 18: 71-72.
- [3] Patnaik, P. R. (1999) Applications of neural networks to recovery of biological products. *Biotechnol. Adv.* 17: 477-488.
- [4] Hudson, D. L. and Cohen, M. E. (Eds.) (2000) *Neural networks and artificial intelligence for biomedical engineering.* The Institute of Electric and Electronics Engineers Press Inc., New York.
- [5] Haykin, S. (1994) *Neural networks: A comprehensive foundation.* Macmillan College Publishing Co., New York.
- [6] Tani, A.; Murase, H.; Kiyota, M. and Honami, N (1992) Growth simulation of alfalfa cuttings *in vitro* by kalman filter neural network. *International Symposium on Transplant Production Systems. Acta. Hort.* 319.
- [7] Uozumia, N; Yoshino, T.; Shiotanib, S.; Sueharaa, K. I.; Araib, F.; Fukudab, T. and Kobayashi, T. (1993) Application of image analysis with neural network for plant somatic embryo culture. *J. Ferment. Bioengg.* 76: 505-509.
- [8] Albiol, J.; Campmajo, C.; Casas, C. and Poch, M. (1995) Biomass estimation in plant cell cultures: A neural network approach. *Biotechnol. Prog.* 11: 8-92.
- [9] Suroso; Murase, H.; Tani, A.; Hoami, N.; Takigawa, H. and Nishiura, Y. (1996) Inverse technique for analysis of convective heat transfer over the surface of plant culture vessel. *Trans. ASAE.* 39: 2277-2282.
- [10] Honda, H.; Takikawa, N.; Noguchi, H.; Hanai, T. and Kobayashi, T. (1997) Image analysis associated with fuzzy neural network and estimation of shoot length of regenerated rice callus. *J. Ferment. Bioengg.* 84: 342-347.
- [11] Zhang, C.; Timmis, R. and Shou Hu, W. (1999) A neural network based pattern recognition system for somatic embryos of Douglas fir. *Plant Cell Tissue Org. Cult.* 56: 25-35.
- [12] Mahendra; Prasad, V. S. S. and Dutta Gupta, S. (2004) Trichromatic sorting of *in vitro* regenerated plants of gladiolus using adaptive resonance theory. *Curr. Sci.* 87: 348-353.

Applications and potentials of artificial neural networks in plant tissue culture

- [13] Albiol, J.; Robuste, J.; Casas, C. and Poch, M. (1993) Biomass estimation in plant cell cultures using an extended kalman filter. *Biotechnol. Prog.* 9: 174-178.
- [14] Morohoshi, N. and Komamine, A. (Eds.) (2001) *Molecular Breeding of Woody Plants*. Elsevier Sci. B. V., The Netherlands.
- [15] Honda, H.; Ito, T.; Yamada, J.; Hanai, T.; Matsuoka, M. and Kobayashi, T. (1999) Selection of embryogenic sugarcane callus by image analysis. *J. Biosci. Bioeng.* 87: 700-702.
- [16] Carpenter, G. A. and Grossberg, S. (1987) ART2: Self organisation of stable category recognition codes for analogue input patterns. *Appl. Optics.* 26: 4919-4930.

EVALUATION OF PLANT SUSPENSION CULTURES BY TEXTURE ANALYSIS

YASUOMI IBARAKI

Department of Biological Science, Yamaguchi University, Yoshida 1677-1, Yamaguchi-shi, Yamaguchi 753-8515, Japan - Fax: 81-83-933-5864 - Email: ibaraki@yamaguchi-u.ac.jp

1. Introduction

Plant cell suspension culture has been widely used as a way for cell proliferation in research and is extending to commercial use. To make the best use of this technique, it is essential to maintain cell quality. Selection of cell suspensions having desirable properties is a routine work in plant cell suspension culture [1]. Image analysis techniques appear to be one of the promising methods for evaluation of cell suspension cultures because it can offer non-destructive monitoring of culture giving an objective index for visual information [1,2]. The macroscopic visual appearance of cell suspensions may vary with colour and size distribution of cell aggregates in the cell suspensions, depending on culture conditions, culture periods, or cell lines. Hence, the visual texture of a macroscopic image of a cell suspension may be used for evaluation of cultured cell quality [1,3].

In this chapter, the feasibility and problems of methods for the non-destructive evaluation of cell suspension cultures will be discussed, focusing on texture analysis of macroscopic images of cell suspensions. First, macroscopic images will be compared with microscopic images from the viewpoint of their use for non-destructive evaluation of cell suspension cultures, and basics of texture analysis for biological objects will be explicated. Next, as an example of application of texture analysis for macroscopic images, a research on evaluation of somatic embryogenic potential of carrot cell suspension culture will be introduced.

2. Microscopic and macroscopic image uses in plant cell suspension culture

Normally, objects in cell suspension culture are single cells or cell aggregates. Therefore, to identify cells or cell aggregates, images of cell suspensions acquired using microscopy, are necessary. As plant cells are normally several micrometers to several tens of micrometers in size, a spatial resolution of at least several micrometers per pixel is needed in microscopic images to analyze single cells or small cell aggregates. Use of microscopic images has the advantage of allowing direct observation of individual cells,

cell aggregates and differentiated cell masses. However, this microscopic image analysis has difficulties in image acquisition [1]. Generally, to acquire microscopic images, sampling of the culture is necessary. Sampling may be destructive with risks of contamination, and is labour-intensive. In addition, sampling raises questions of whether the sample population is truly representative of the cell suspension, and it may be necessary to increase the number of samples or use effective statistical methods [1]. By using an inverted microscope attached with a camera or a long working distance microscopic CCD camera, image can be acquired without sampling. However, it is difficult to obtain microscopic images of suspended cells suitable for direct observation of individual cells and cell aggregates because of cell overlapping by sedimentation or limitation in working distance. In addition, whether the populations recorded in sampled images are truly representative remains a problem.

Several microscopic imaging system in which an image of suspended cells is acquired in an imaging cell connected to a bioreactor, have been proposed. Grand d'Esnon *et al.* [4] first reported this type of system for acquiring cell microscopic images. Suspended *Ipomoea batatas* Poir. cells were passed into the imaging cell by a peristaltic pump from the bioreactor. This system was used to monitor the population dynamics of embryogenic and non-embryogenic cell aggregates in cell suspension cultures used for somatic embryo production. Smith *et al.* [5] have developed a similar system that evaluated pigment production of *Ajuga reptans* cells. Ibaraki *et al.* [6] also developed a system to acquire images of carrot somatic embryos (*Daucus carota* L.) for sorting. Harrell *et al.* [7] developed an improved system and measured cell aggregate distribution and growth rate in embryogenic cell suspension cultures of *Ipomoea batatas* Lam. In this system, to avoid cell damage the cell aggregates could not be allowed to go through the pumping unit, and a method to calculate total reactor population from the number of observed aggregates was proposed. These methods are effective for serial quality evaluation in cell suspension cultures. However, it should be noted that the population density of single cells and cell aggregates is crucial if image analysis is used to measure the properties of individual cells and cell aggregates. Low cell population density is needed to prevent cells from overlapping, and this may not be optimal for cell growth or metabolite production [1].

In contrast, macroscopic images have an advantage in imaging and have been used for quality evaluation of cell suspensions although applications are limited to a few studies. A macroscopic image of a cell culture is defined as an image viewed with normal or macro lens whose field of view contains almost a whole culture [1]. Macroscopic images can be acquired from the outside of a culture vessel without special devices if the culture vessel has transparent walls, i.e., it is perfectly non-destructive imaging. Depending on the imaging devices, these images have spatial resolutions of several hundreds of micrometers per pixel and do not allow us to identify a small cell aggregate. However, macroscopic images have often been used for quantification of cell masses on solid media [8,9,10] and in cell suspensions [11] because they included one whole culture in their fields of view. Moreover, colour /grey level analysis and/or texture analysis of macroscopic images of suspension cultures can provide us with information related to status of suspended cells and tissues. Texture analysis has the potential of characterizing individual objects in a macroscopic image, in which the individual objects were not clearly identified [12]. Experimental evaluations in plant

cell culture very frequently include visual examinations [2]. Image analysis of a macroscopic culture image may substitute for the visual examination, supporting objective decision and contributing to improvement in reproducibility in plant cell culture.

3. Texture analysis for macroscopic images of cell suspensions

3.1. TEXTURE FEATURES

As simple texture features, mean grey level, variance, range (i.e., the difference between maximum and minimum values of grey level), and other statistical features derived from grey level histogram such as skewness and kurtosis, are used for classification and segmentation of images based on texture although these texture features can not involve information on spatial distribution.

Texture analysis methods considering spatial distribution include two-dimensional frequency transformation, grey level run lengths method, spatial grey level dependence method, etc. Two-dimensional frequency transformation method has been widely used for image analysis. It can derive the power spectrum image (frequency-domain image), which expresses periodic features in the image texture. From power spectrum images, wedge-shaped features related to texture direction and ring-shaped features expressing periodic characteristics can be extracted.

In grey level run lengths method [13], features are extracted from the matrix which is a set of probabilities that a particular-length line consisting of pixels with the same grey level will occur at a distinct orientation. It is valid for analysis of band pattern texture.

Texture features extracted using spatial grey level dependence method (SGDM) developed by Haralick *et al.* [14] have been often used for texture analysis for biological objects. In SGDM, a co-occurrence matrix is determined and 14 texture features are calculated from the matrix. The co-occurrence matrix is a set of the probabilities $P(i,j)$ that a combination of a pixel at one particular grey level (i) and another pixel at a second particular grey level (j) will occur at a distinct distance (d) and orientation (θ) from each other. Of the 14 features, major features are as follows:

$$\text{Angular Second Moment} = \sum_{i=0}^{N-1} \sum_{j=0}^{N-1} P(i, j)^2 \quad (1)$$

$$\text{Contrast} = \sum_{n=0}^{N-1} n^2 \sum_{|i-j|=n} P(i, j) \quad (2)$$

$$Correlation = \frac{\sum_{i=0}^{N-1} \sum_{j=0}^{N-1} ij p(i, j) - \mu_x \mu_y}{\sigma_x \sigma_y} \quad (3)$$

$$Entropy = - \sum_{i=0}^{N-1} \sum_{j=0}^{N-1} p(i, j) \log(p(i, j)) \quad (4)$$

Where, N is the number of grey levels, and $\mu_x, \mu_y, \sigma_x, \sigma_y$ denote the mean and standard deviation of the row and column sums of the co-occurrence matrix, respectively. Briefly, “Angular Second Moment” is a measure of homogeneity, “Contrast” is a measure of local contrast, “Entropy” is a measure of the complexity or randomness of the image, and “Correlation” is a measure of grey-tone liner-dependencies. The number of grey levels, N , is often lessened for reducing calculation time and for suppressing noise effect. If the image is assumed to be isotropic, only one orientation (θ) is often tested. Moreover, recently, texture analysis using the colour co-occurrence matrix has been used [15].

A wide variety of new texture analysis methods have been proposed extensively in various research fields. Tuceryan and Jain [16] divided texture analysis methods into four categories: statistical, geometrical, model-based, and signal processing. Of these categories, histogram-derived features, grey level run lengths method, and SGDM are classified into statistical methods, and two-dimensional frequency transformation is classified into signal processing methods. Geometrical methods consider texture to be composed of texture primitives, attempting to describe the primitives and the rules governing their spatial organization [17]. Model-based methods hypothesize the underlying texture process, constructing a parametric generative model, which could have created the observed intensity distribution [17].

3.2. TEXTURE ANALYSIS FOR BIOLOGICAL OBJECTS

In remote sensing, texture analysis has been used for classification of land use or plant species identification extensively. In proximal remote-sensing for plant canopies, applications of texture analysis have been also reported. Shearer and Holmes [15] identified plant species using colour co-occurrence matrices, which were derived from image matrices for each colour attribute: intensity, hue, and saturation. Shono *et al.* [12] compared the effectiveness of several methods for texture analysis, including grey level run lengths method, SGDM, and power spectrum method, on estimation of the species composition in the pasture field.

In addition, in the filed of quality evaluation in agriculture, machine vision systems based on texture features have been used. Sayeed *et al.* [18] evaluated snack quality by neural network using textural and morphological features. Maturity in shell-stocked peanuts was detected by the histogram characteristics or the texture descriptor derived from the analysis of gradient images [19]. Texture analysis which is based on the frequency of co-occurrence of a random event and is named as Frequency Histogram of

Connected Elements was used for detection and recognition of cracks in wood boards [20]. Shono [21] analyzed leaf orientation by texture features extracted by power spectrum method. Murase *et al.* [22] quantified plant growth by analyzing texture features using neural network.

Texture analysis has been used for biological objects besides plants extensively. The applications include assessment of chromatin organization in the nucleus of the living cell [23], and medical applications for brain MR images [24], for bone radiographs [25], and for pulmonary disease images [26].

3.3. TEXTURE ANALYSIS FOR CELL SUSPENSION CULTURE

Although applications of texture analysis for plant cell suspension culture are still limited to a few studies, texture analysis has the potential of evaluating and/or selecting cell suspension cultures. The macroscopic visual appearance of cell suspensions reflects on colour and size distribution of cell aggregates, which may be indicators of cell suspension culture status. Cell aggregate size distribution patterns in cell suspension culture vary significantly between cell lines and also a consequence of culture age and culture conditions [27,28]. It has been reported that the visual appearance of suspension cultures changes with the number of subcultures [29] or with variations in embryogenic potential [3,29]. In fact, statistical texture features were effective for describing the difference in macroscopic appearances between carrot embryogenic and non-embryogenic suspensions [3]. The study will be introduced in 4.2. Texture analysis is expected to contribute to maintenance of cell quality in plant suspension culture, offering objective index for macroscopic appearance of suspension culture.

3.4. CONSIDERATIONS FOR APPLICATION OF TEXTURE ANALYSIS

It should be noted that as texture features are not the direct measures of biological properties in many cases, it is required to determine the relationships between texture features and the targeted biological properties by modelling methods such as regression analysis [3] and artificial neural network [18,20,22] to use the features for evaluation of biological properties. In addition, dependency of texture features on the experimental set-up including image acquisition, sampling, and pre-processing, should be considered [17]. All experimental results should be considered to be applicable only to the reported set-up [17]. For routine use of texture analysis of macroscopic images, simple indices for describing cell suspension culture properties without the complicated model are required. In addition, more efforts for developing the robust way to acquire a macroscopic image of a cell suspension should be made in view of dependency of texture features on image acquisition set-up.

4. Evaluation of embryogenic potential of cultures by texture analysis

4.1. EVALUATION OF EMBRYOGENIC POTENTIAL OF CULTURES

The productivity of somatic embryos depends on the quality of embryogenic cultures [3]. The embryogenic potential of cultures must be sustained in maintenance phase for

the stable production of somatic embryos. The embryogenic potential depends on genotypes. Moreover, it can change with culture period and is affected by medium composition and environmental conditions. To monitor embryogenic potential of culture would be useful to stably produce somatic embryos [30].

Using microscopic observation, a pro-embryogenic mass (PEM), which is a cell cluster to become somatic embryos under certain conditions, could be identified. In a number of systems studied to date, PEMs shared similar structural features. They consist of small and highly cytoplasmic cells which often have an accumulation of starch within the plastids [31]. On the other hand, non-embryogenic cells are large and vacuolated. Therefore, a PEM could be selected with regard to its transparency and shape under microscopy. The amount of PEMs in cell suspensions may be one direct index for determining the embryogenic potential of the culture. In a similar way, the amount in cultures of other embryogenic tissues as materials for embryo production such as embryo suspensor masses and early globular embryos can be used for evaluation of cultures.

Microscopic image analysis for suspension culture could be used to select PEMs. Grand d'Esnon *et al.* [4] monitored population dynamics of PEMs in suspension cultures of *Ipomoea batatas* for somatic embryo production using image analysis. PEMs and non-embryogenic cell aggregates were divided by using a correlation between the size and the mean transparency of the object.

Culture growth rate may be one of indices for evaluation of the embryogenic potential [1]. Differences in growth characteristics between embryogenic and non-embryogenic cultures have been reported in maize suspension culture [28], in carrot suspension culture [11,32], and in *Ipomoea batatas* callus culture [33]. Growth rates can be calculated through non-destructive cell quantification by image analysis. There have been several reports on image-analysis-based quantification of cells on gelled media [8,9,10,34]. In addition, Ibaraki and Kurata [11] quantified embryogenic suspension cultures by image analysis of macroscopic images of the suspensions. They showed the relationship between growth rate estimated by image analysis and embryogenic potential of carrot embryogenic culture.

4.2. TEXTURE ANALYSIS BASED EVALUATION OF EMBRYOGENIC POTENTIAL

Other indices to be potentially used for evaluation of suspension culture are colour, cell aggregate distribution, and consequent macroscopic texture [1]. Ibaraki *et al.* [3] reported the system for evaluation of embryogenic potential of cell suspension cultures based on texture analysis. They acquired macroscopic images of carrot cell suspensions from the bottom of a culture vessel (Erlenmeyer flask) with a video camera (GR-S95, JVC) using transmitted light. The video signal was digitized as a 24-bit RGB colour image whose size was 640 by 480 pixels. As the B component of the RGB was more sensitive to yellow carrot cells than the other two components, each image was converted into an 8-bit monochrome image based on the B value. A part of the flask bottom in the image was extracted as an elliptic region and transformed into a circle with 400-pixel diameter (Figure 1). In this condition, the spatial resolution in the image was about 0.23 mm/pixel. Texture features were extracted using SGDM. Of 14 features in SGDM, 3 features, Angular Second Moment, Contrast, and Entropy were calculated

from co-occurrence matrix and tested. Actual embryogenic potential of a cell suspension was determined by the number of PEMs in the unit volume suspension (hereafter, PEM density) or total number of embryos induced using each cell suspension.

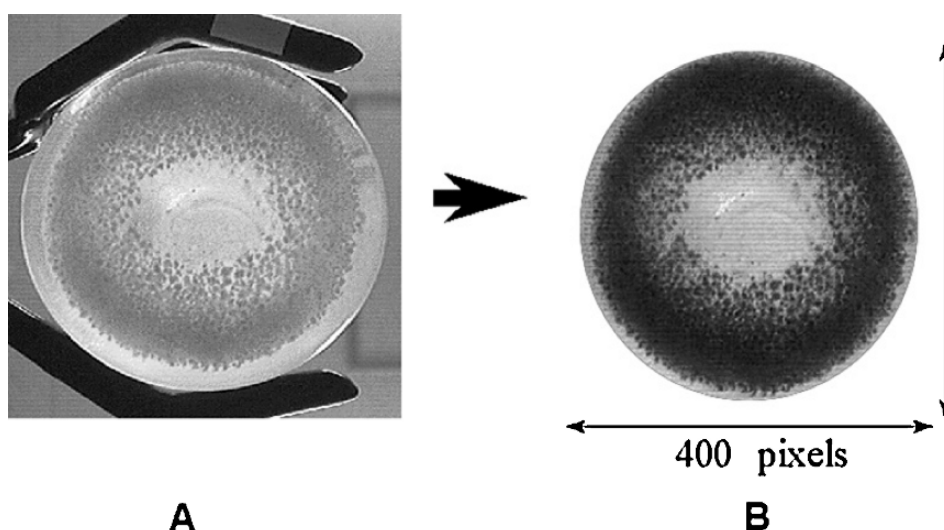


Figure 1. Macroscopic images of carrot cell suspension viewed from the bottom of culture vessel. A part of the flask bottom in the original colour image (A) was extracted after conversion into 8-bit monochrome image based on the B component value as an elliptic region and transformed into a circle with 400-pixel diameter (B).

Different carrot cell suspensions had various embryogenic potentials expressed by the PEM density. Differences in visual appearance due to differences in cell aggregate size distribution pattern between embryogenic and non-embryogenic suspensions were observed (Figure 2). Images of cell suspensions possessing high embryogenic potential had course texture, while those of non-embryogenic suspension had fine texture. In embryogenic cell suspensions, many large cell aggregates could be observed. In contrast to this, non-embryogenic suspensions had few large cell aggregates and consisted mainly of small cell aggregates. Several reports have been shown difference in cell aggregate size distribution patterns between embryogenic and non-embryogenic cultures [28,35]. The difference in textural appearance due to cell aggregate distribution patterns could be detected by texture analysis. The most useful texture feature for evaluating the embryogenic potential was Entropy, which is a measure of complexity of an image. Images of cell suspensions with higher PEM density had higher values of texture feature Entropy (Figure 3). In addition, suspensions with higher values of texture feature Entropy have the potential to produce more somatic embryos (Figure 4). These results suggested that texture analysis of a macroscopic image of a cell suspension could be used to evaluate the embryogenic potential of the suspension.

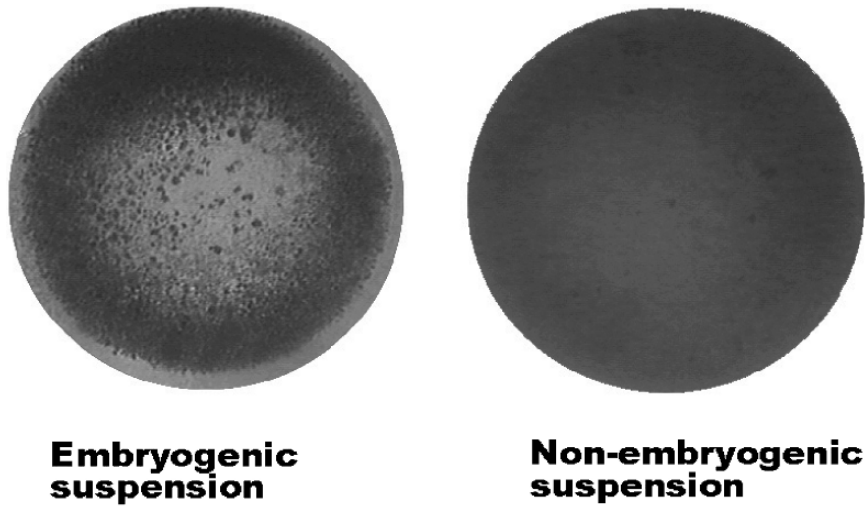


Figure 2. Images of embryonic and non-embryonic suspensions.

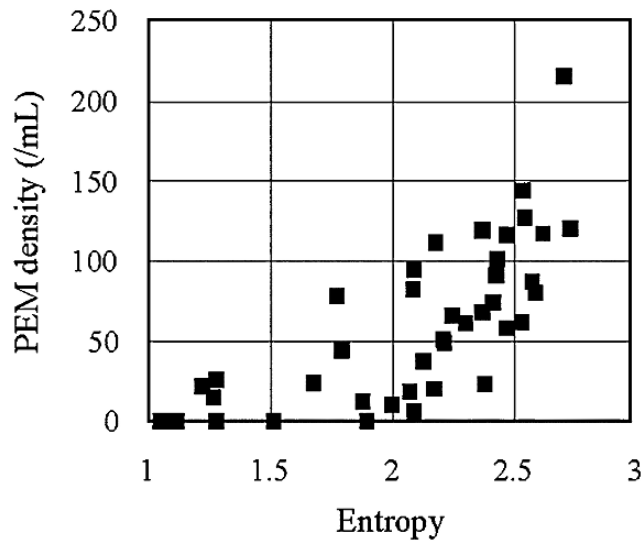


Figure 3. Relationship between texture feature entropy and PEM density when the number of grey level =8 (n=43). Reprinted from Ibaraki et al. (1998) [3].

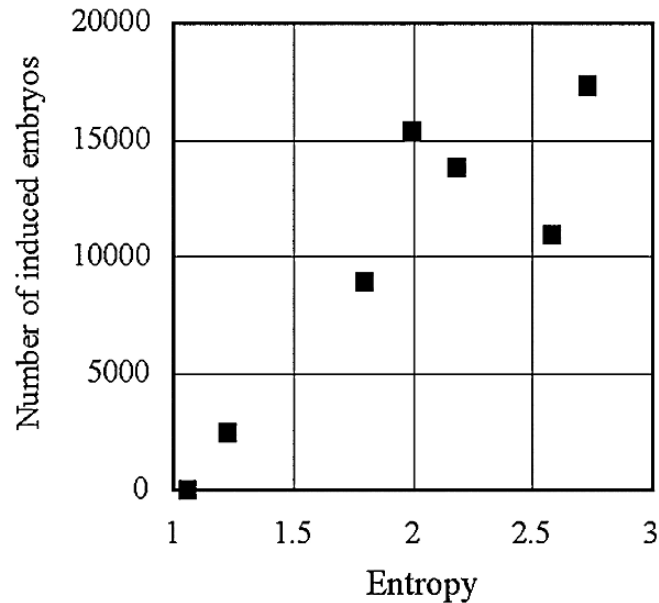


Figure 4. Relationship between texture feature entropy when the number of grey level =8 and number of induced somatic embryos. Reprinted from Ibaraki et al. (1998) [3].

5. Concluding remarks

Image analysis has potential to provide simple, non-destructive, and objective quality evaluation of cultured cells for plant cell suspension culture. As compared with microscopic images, macroscopic images are more easily acquired without sampling, showing the potential for non-destructive evaluation. The visual texture of a macroscopic image of a cell suspension can be an indicator of cultured cell quality. The texture analysis of the macroscopic image was used for evaluation of embryogenic potential in cell suspension cultures. Texture analysis techniques are expected to contribute to maintenance of cell quality in plant cell suspension culture. Texture analysis is now used extensively for biological objects in various areas and novel methods have been reported. These technologies are expected to be transferred to plant tissue culture area.

References

- [1] Ibaraki, Y. and Kurata, K. (2000) Application of image analysis to plant cell suspension cultures. *Compu. Electron. Agri.* 30:193-203.
- [2] Smith, M.A.L. (1995) Image analysis for plant tissue culture and micropropagation. In: Aitken-Christie, J.; Kozai, T. and Smith, M.A.L. (Eds.) *Automation and Environmental Control in Plant Tissue Cultures*. Kluwer Academic Publishers, Dordrecht, The Netherlands; pp. 145-163.

- [3] Ibaraki, Y.; Kaneko, Y. and Kurata, K. (1998) Evaluation of embryogenic potential of cell suspension culture by texture analysis. *Trans. ASAE* 41: 247-252.
- [4] Grand d'Esnon, A.; Chee, R.; Harrell, R.C. and Cantliffe, D. J. (1989) Qualitative and quantitative evaluation of liquid tissue cultures by artificial vision. *Biofutur* 76:S3.
- [5] Smith, M.A.L.; Reid, J.F.; Hansen, A.C.; Li, Z. and Madhavi, D.L. (1995) Non-destructive machine vision analysis of pigment-producing cell cultures. *J. Biotechnol.* 40:1-11.
- [6] Ibaraki, Y.; Fukakusa, M. and Kurata, K. (1995) SOMES2: Image-analysis-based somatic embryo sorter. *Current Plant Science and Biotechnology in Agriculture* 22: 675-680.
- [7] Harrell, R.C.; Bieniek, M. and Cantliffe, D.J. (1992) Non-invasive evaluation of somatic embryogenesis. *Biotechnol. Bioeng.* 39: texture analysis 378-383.
- [8] Smith, M.A.L. and Spomer, L.A. (1987) Direct quantification of *in vitro* cell growth through image analysis. *In Vitro Cell. Dev. Biol.-Plant* 23: 67-74.
- [9] Olofsdotter, M. (1993) Image processing: a non-destructive methods for measuring growth in cell and tissue culture. *Plant Cell Rep.* 12: 216-219.
- [10] Anthony, P.; Davey, M.R.; Power, J.B.; Washington, C. and Lowe, K.C. (1994) Image analysis assessments of perfluorocarbon- and surfactant- enhanced protoplast division. *Plant Cell Tissue Org. Cult.* 38:39-43.
- [11] Ibaraki, Y. and Kurata, K. (1997) Image analysis based quantification of cells in suspension cultures for producing somatic embryos. *Environ. Control Biol.* 35: 63-70.
- [12] Shono, H.; Okada, M. and Higuchi, S. (1994) Texture analysis of photographic images from close distance: An application to estimate species composition in a mixed pasture field (in Japanese with English abstract). *J. Agri. Meteorol.* 49: 227-235.
- [13] Galloway, M.M. (1975) Texture analysis using grey level run lengths. *Computer Graphics Image Processing* 4: 172-179.
- [14] Haralick, R. M.; Shanmugam, K. and Dinstein, I. (1973) Textural features for imaging classification. *IEEE Trans. Sys. Man Cybernet.* SMC-3: 610-621.
- [15] Shearer, S.A. and Holmes, R.G. (1990) Plant identification using colour co-occurrence matrixes. *Trans. ASAE* 38: 2037-2044.
- [16] Tuceryan, M. and Jain, A.K. (1998) Texture analysis. In: Chen, C.H.; Pau, L.F. and Wang, P.S.P. (Eds.) *The Handbook of Pattern Recognition and Computer Vision.* World Scientific Publishing Co., Hackensack, NJ; pp. 207-248.
- [17] Ojala, T. and Pietikäinen, M. Texture analysis. In: Fisher, R.B. (Ed.) *CV online: The evolving, Distributed, Non-proprietary, On-Line Compendium of Computer Vision* (http://homepages.inf.ed.ac.uk/rbf/CVonline/LOCAL_COPIES/OJALA1/texclas.htm).
- [18] Sayeed, M.S.; Whittaker, A.D. and Kehtarnavaz, N. D. (1995) Snack quality evaluation method based on image feature and neural network prediction. *Trans. ASAE* 38: 1239-1245.
- [19] Ghatge, S.R.; Evans, M.D.; Kvien, C.K. and Rucker K.S. (1993) Maturity detection in peanuts (*Arachis hypogaea* L.) using machine vision. *Trans. ASAE* 36: 1941-1947.
- [20] Guisado, M.A.P. and Gómez-Allende, D.M. (2001) Wood texture analysis by combining the connected elements histogram and artificial neural networks. In: Mira, J. and Prieto, A. (Eds.) *Bio-Inspired Applications of Connectionism-IWANN 2001.* Springer-Verlag, Heidelberg; pp.160-167.
- [21] Shono, H. (1995) A new method of image measurement of leaf tip angle based on textural feature and a study of its availability (in Japanese with English abstract). *Environ. Control Biol.* 33:1970-207.
- [22] Murase, H.; Honami, N. and Nishiura, Y. (1994) A neural network estimation technique for plant water status using textural features of pictorial data of plant canopy. *Acta Hort.* 339: 255-262.
- [23] Rousselle C.; Paillason, S.; Robert-Nicoud, M. and Ronot, X. (1999) Chromatin texture analysis in living cells. *Histochemical J.* 31:63-70.
- [24] Zhang, Y.; Zhu, H.; Ferrari, R.; Wei, X.; Eliasziw, M.; Metz, L.M. and Mitchell, R. (2003) Texture analysis of MR images of minocycline treated MS patients. In: Elli, R.E. and Peters T.M. (Eds.) *MICCAI 2003, LNCS 2878.* Springer-Verlag, Heidelberg; pp. 786-793.
- [25] Lespessailles, E.; Roux, J.P.; Benhamou, C.L.; Arlot, M.E.; Eynard, E.; Harba, R.; Padnou, C. and Meunier, P.J. (1998) Fractal analysis of bone texture on os calcis radiographs compared with trabecular microarchitecture analysed by histomorphometry. *Calcified Tissue Int.* 63: 121-125.
- [26] Sutton, R. and Hall, E.L. (1972) Texture measures for automatic classification of pulmonary disease. *IEEE Trans. Comput.* C-21: 667-676.
- [27] Kieran, P.M.; MacLoughlin, P.F. and Malone, D.M. (1997) Plant cell suspension cultures: some engineering considerations. *J. Biotechnol.* 59: 39-52.

Evaluation of plant suspension cultures by texture analysis

- [28] Stirn, S.; Hopstock, A. and Lorz, H. (1994) Bioreactor cultures of embryogenic suspensions of barley (*Hordeum vulgare* L.) and maize (*Zea mays* L.). *J. Plant Physiol.* 144: 209-214.
- [29] Molle, F.; Dupuis, J.M.; Ducos, J.P.; Anselm, A.; Crolus-Savidan, I.; Petiard, Y. and Freyssinet, G. (1993) In: Redenbaugh, K. (Ed.) *Synseeds*. CRC press, Boca Raton; pp. 257-287.
- [30] Ibaraki, Y. and Kurata, K. (2001) Automation of somatic embryo production. *Plant Cell Tissue Org. Cult.* 65: 179-199.
- [31] Yeung, E.C. (1995) Structural and developmental patterns in somatic embryogenesis. In: Thorpe, T.A. (Ed.) *In Vitro Embryogenesis in Plants*. Kluwer Academic Publishers, Dordrecht, The Netherlands; pp. 205-247.
- [32] Smith, S.M. and Street, H.E. (1974) The decline of embryogenic potential as callus and suspension cultures of carrot (*Daucus carota* L.) are serially subcultured. *Ann. Bot.* 38: 223-241.
- [33] Zheng, Q.; Dessai, A.P. and Parkash, C.S. (1996) Rapid and repetitive plant regeneration in sweet potato via somatic embryogenesis. *Plant Cell Rep.* 15: 381-385.
- [34] Hirvonen, J. and Ojamo, H. (1988) Visual sensors in tracking tissue growth. *Acta Hort.* 230: 245-251.
- [35] van Boxtel, J. and Berthouly, M. (1996) High frequency somatic embryogenesis from coffee leaves. *Plant Cell Tissue Org. Cult.* 44: 7-17.

PART 2

BIOREACTOR TECHNOLOGY

BIOENGINEERING ASPECTS OF BIOREACTOR APPLICATION IN PLANT PROPAGATION

SHINSAKU TAKAYAMA¹ AND MOTOMU AKITA²

¹*Department of Biological Science and Technology, Tokai University, 317 Nishino, Numazu, Shizuoka 410-0315, Japan. – Fax: 81-263-47-1879 – Email: takayama@wing.ncc.u-tokai.ac.jp*

²*Department of Biotechnological Science, Kinki University, 930 Nishimitani, Uchita, Naga, Wakayama 649-6493, Japan – Fax: 81-736-77-4754 – Email: akita@bio.waka.kindai.ac.jp*

1. Introduction

A large number of commercially important plants including important vegetatively propagated crops such as vegetables, flowers, ornamentals, fruit trees, woody and medicinal plants, etc., are vegetatively propagated by tissue culture. Tissue culture is carried out in most of countries in the world, and the number of plants propagated was 600 millions for one year over the world which is the best available estimates as cited in Altman and Loberant (2000) [1]. The culture technique generally used for commercial tissue culture propagation is the agar culture which requires large number of small culture vessels and labour, and results in the requirement of many laminar air flow clean benches, large autoclave(s), large culture spaces equipped with illuminated shelves, electric energy, etc. This is the major cause for both limited propagation efficiency and high production costs.

In order to overcome these problems, large-scale propagation technique with simple culture protocol with least equipments and reduced production cost should be adopted. Many attempts for establishing large-scale production of propagules with simple production facilities and techniques have been made including robotics, photoautotrophic cultures, bioreactor techniques, etc. [2]. Among them, bioreactor technique seems to be the most promising, because it is a prominent technology in reducing the labour, and providing low production cost, which will be sufficient for establishing a practical system for *in vitro* commercialization of mass propagation of plants.

The term “bioreactor” is generally used to describe a vessel carrying out a biological reaction, and to refer a reactor vessel for the culture of aerobic cells, or to columns of packed beds of immobilized cells or enzymes [3]. The bioreactors are widely used for industrial production of microbial, animal and plant metabolites. The bioreactor technique applied to plant propagation was first reported by the present author in 1981 on *Begonia* propagation using a bubble column bioreactor [4]. Since then, bioreactor

technology for plant propagation has developed and aerobic bioreactor culture techniques have been applied for large-scale production of plant propagules such as lilies, strawberry, potato, *Spathiphyllum*, *Stevia*, etc. [2,5-11]. The bioreactor technologies are also studied on their characteristics [5,12-16] and on propagation of several plant species including shoots and somatic embryos [17-29].

The use of bioreactor in micropropagation revealed its commercial applicability, and recently gained attention to commercial micropropagation process. In this chapter, the fundamental characteristics in the operation of bioreactor systems and the production of various plant propagules in bioreactors are described from the standpoint of bioengineering.

2. Advantages of the use of bioreactor in plant propagation

The use of bioreactor enhances the productivity and the efficiency of plant propagation.

Table 1. Comparison of the specifications of Spathiphyllum propagation between bioreactor and agar culture.

Items	Bioreactor	Agar culture
Equipment		
Vessel volume	20 L	500 mL
Medium volume L/vessel	16.6 L (liquid)	100 mL (agar)
Number of vessels	6	1000
Number of inocula used for subculture	96 test tubes	150 test tubes
Culture period	90 days	60 days
Culture space	0.5 m ³	36 m ³
Number of fluorescent lamps (40W)	6	30
Labour		
Operational time	200 min	2500 min
*Medium preparation (100 L)	(60 min)	(450 min)
Autoclaving	(10 min)	(140 min)
Inoculation	(45 min)	(1250 min)
Transfer to culture room	(10 min)	(60 min)
Removing cultures	(45 min)	(300 min)
Vessel washing	(30 min)	(300 min)
Transplanting	1800 min	1800 min

*The volume of culture medium was 100 L in both bioreactor culture and agar culture

Such excellent characteristics emerged from the advantages of the use of liquid medium for plant propagation in the bioreactor and are as follows:

- Large number of plantlets can easily be produced in one batch in the bioreactor and scaling up of bioreactor size and number.
- Since handling of cultures such as inoculation or harvest is easy, reducing the number of culture vessels, and the area of culture space results in the reduction of costs.
- Whole surface of cultures are always in contact with medium, uptake of nutrients are stimulated and growth rate is also increased.
- Forced aeration (oxygen supply) is performed which improves the growth rate and final biomass.
- Cultures are moving in the bioreactor, which results in the disappearance of apical dominance and stimulates the growth of numerous shoot buds into plantlets.

In spite of these advantages, there are some pitfalls such as hyperhydricity, plantlet size variation and microbial contamination [8], etc. The most important problem is the existence of recalcitrant species for bioreactor application and such species are difficult to be cultured in liquid medium even if they are possible to be propagated on agar medium.

These problems need to be rectified and warrants investigation. The efficiency of the propagation is quite high in the bioreactor compared to solid or shake culture, resulting in the saving of cost in equipments and labours as indicated in Table 1. After transplanting in soil, the efficiency of re-establishment of plants during acclimatization is almost same between the bioreactor and agar cultured plants.

3. Agar culture vs. liquid culture

The plants propagated in a bioreactor are usually submerged in liquid medium. Since most plants propagated are terrestrial, not aquatic, and under natural habitat, submerged condition is usually harmful to the plants. In tissue culture, plants can grow under submerged condition, but this does not mean that plants prefer liquid medium in tissue culture. The growth response of the plants in liquid medium varied between species or genera. For example, the growth of *Begonia* was fairly well in liquid or semi-solid agar medium (0 to 4 g/L agar) (Figure 1). On the contrary, the growth of *Fragaria* was remarkable at solid agar medium (6 to 12 g/L agar), but not in liquid or semi-solid agar medium. The growth of *Saintpaulia* revealed the intermediate response between *Fragaria* and *Begonia* (growth was stimulated at 4 to 8 g/L agar). The plants having hydrophilic nature like *Begonia* appeared to propagate easily in liquid medium in shake or bioreactor culture. In spite of the hydrophobic nature, *Fragaria* plants can grow in liquid medium in the bioreactor, but require higher aeration rate, and the growth was linear to aeration rate. In some *Clematis* species, the growth was strictly repressed in submerged conditions.

4. Transition from shake culture to bioreactor culture

The shake culture method is considered to be intermediate in establishing bioreactor techniques. As described above, the growth characteristics in liquid medium are quite

different between species or genera, so the optimization of culture condition in liquid medium is the fundamental prerequisite. Once the liquid culture condition is established in shake culture, the condition can be applied to bioreactor culture for scaling-up.

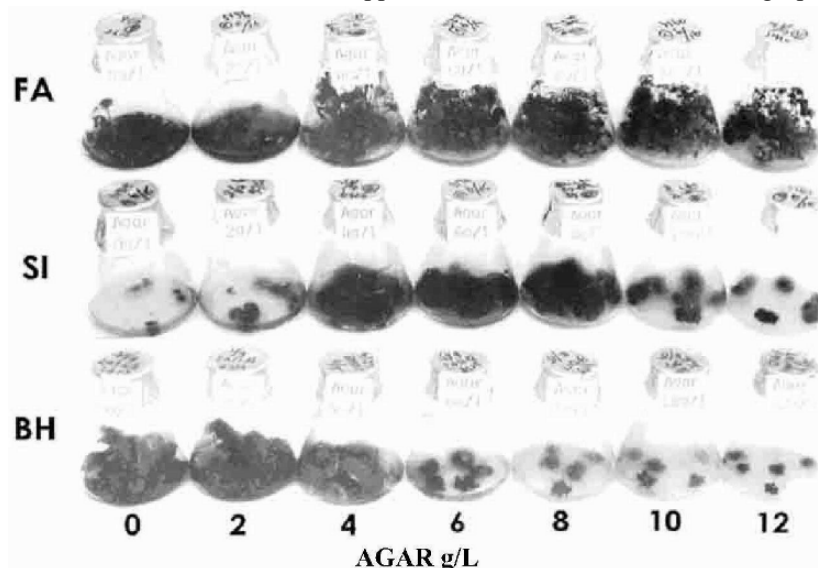


Figure 1. Effect of agar concentration on growth of *Fragaria ananassa*(FA), *Saintpaulia ionantha*(SI) and *Begonia x hiemalis*(BH).

5. Types of bioreactors for plant propagation

The bioreactors used for plant propagation are fundamentally the same as that used for secondary metabolite production by plant, microbial and animal cell cultures. Various types of bioreactors are used for this purpose which are classified by agitation methods and vessel construction into; mechanically agitated bioreactors (aeration-agitation bioreactors, rotating drum bioreactors, spin filter bioreactors), pneumatically agitated bioreactors (unstirred bubble bioreactor, bubble column bioreactor, air-lift bioreactor), and non-agitated bioreactors (gaseous phase bioreactor, oxygen permeable membrane aerator bioreactor, overlay aeration bioreactor) [7]. Mechanically agitated bioreactors (aeration-agitation bioreactor, Figures 2C, 2D, 2E), the most standardized bioreactor system in industrial processes, are applicable to plant propagation. However, pneumatically driven bioreactors such as bubble column (Figure 2A), unstirred bubble (Figures 2B, 3B) and airlift bioreactors are found to be suitable as plant bioreactors because it compensates the specific problem of mechanically agitated bioreactors such as severe shear generation. The most frequently used bioreactors having the characteristics suitable for plant organs, especially for shoot cultures are unstirred bubble bioreactors, bubble column bioreactors and airlift bioreactors.

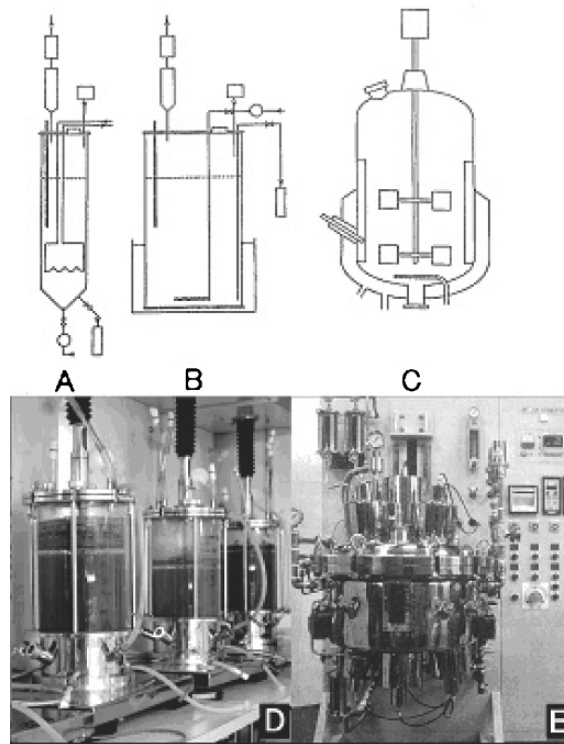


Figure 2. Various types of bioreactors. (A) Bubble column bioreactor, (B) Unstirred bubble bioreactor, (C, E) Pilot scale aeration-agitation bioreactor, (D) 10 L aeration-agitation bioreactor.

6. Preparation of propagules for inoculation to bioreactor

In practical use of bioreactor for plant propagation, large number of propagules which will be growing to plantlets should be inoculated into the bioreactor. The propagules to be used as inocula are; multiple shoot buds, regenerative tissues such as protocorm-like bodies and meristemoids, somatic embryos, and stem or shoot with numerous axillary buds. Multiple shoot buds which can be obtained by application of cytokinin to the medium, can be used as propagules for the propagation of most plant species. The reason of the use of multiple shoot buds is that these cultures are quite stable in their genetic characteristics. Small pieces of multiple shoot buds cultured in test tubes containing 10 ml agar medium were used as inocula. In case of both *Colocasia esculenta* and *Spathiphyllum* cv. Merry, multiple shoot buds collected from 8 or 16 test tubes (Figure 3A) were inoculated into 8 L or 16 L unstirred bubble bioreactors, respectively. After 2 to 3 months of bioreactor culture, a large number of shoots were fully grown in the bioreactor (Figure 3B). Morphology of inocula and their optimum inoculum size are

different between genera or species, but usually small inoculum size (1 to 5 g/L) will be sufficient as inocula in the bioreactor.



Figure 3. Preparation of inoculum in test tubes containing 10 ml of agar medium (A), and shoot growth in 20 L unstirred bubble bioreactor(B) containing 16 L medium 2 months after inoculation. The plant is *Colocasia esculenta*.

7. Characteristics of bioreactor for plant propagation

7.1. FUNDAMENTAL CONFIGURATION OF BIOREACTOR

The bioreactors usually comprise a jacketed pressure vessel which is sterilized by steam at the beginning of culture and sealed to maintain the sterile condition during cultivation. Figure 4 shows the typical aeration-agitation bioreactor vessel generally used for microbial, animal and plant cell, tissue and organ cultures. The vessel is equipped with several openings such as an inoculation port, sensor ports (pH, EC, O₂, ORP, etc.), feeding and drain pipes, air inlet and outlet, and so on. These openings should be completely closed with high quality sanitary fittings and valves. The vessel is also equipped with heating and cooling jacket which is connected to the steam and water lines and control the bioreactor temperature. A sealed agitator shaft is inserted in the bioreactor vessel. The agitator shaft is driven by agitator motor, and impeller(s) is

attached to the agitator shaft which agitates the culture medium. At the bottom of bioreactor vessel, air sparger is equipped to circulate the air into the culture medium. The baffles attached to the vessel wall ensure maximum turbulence during agitation. In case of shoot propagation, impeller and baffles are detached or mechanical agitation was stopped to avoid the damage of cultures.

The bioreactor depicted in Figure 4 is quite expensive, which is not realistic for use in the practical plant propagation. In order to reduce the costs, simplicity of structure and handling, long-term maintenance of aseptic condition, and of course, sufficient aeration and mixing are required in design the bioreactor. Practically, a quite simple bioreactor consist of a vessel with minimum openings using for inoculation, air inlet, and air outlet, is feasible. Using such a simple bioreactor in batch culture, plants produced were easily transplanted and established in soil.

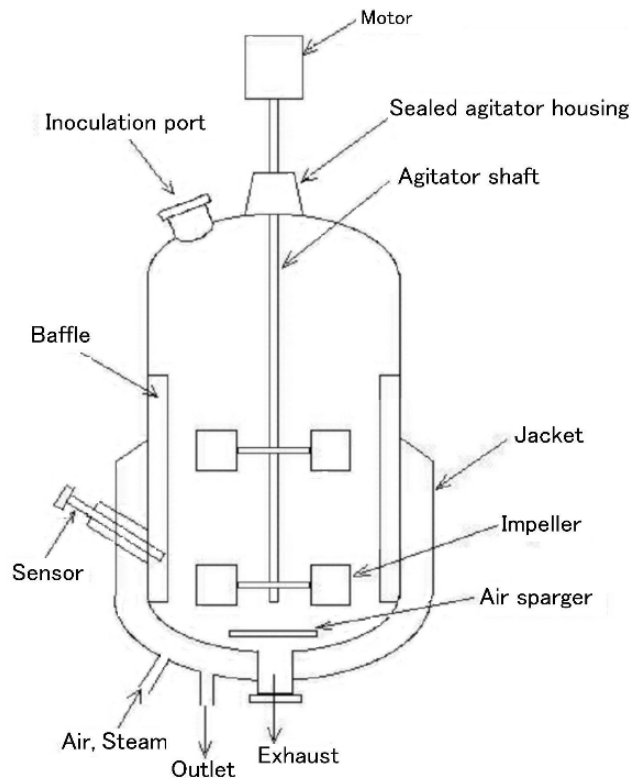


Figure 4. Diagram of the structure of typical bioreactor.

7.2. AERATION AND MEDIUM FLOW CHARACTERISTICS

The characteristics of bubble generation and their hold-up were precisely analyzed by Aiba *et al.* [30]. The size of bubbles sparged from orifice of sparger at low aeration rate was calculated by equation (1);

$$\frac{\pi}{6} \cdot d_B^3 \Delta \rho g = \pi d \sigma \quad (1)$$

Where d_B is the diameter of bubbles (mm), d is the diameter of orifice (m), $\Delta \rho$ is the difference of air and liquid density (g/m^3), g is the acceleration of gravity (m/s^2), and σ is the surface tension of liquid (dyn/cm). In equation (1), left-hand side refers to the buoyancy of bubbles, and the right-hand side is the power equivalent to the retention of bubbles. This equation was experimentally consistent when aeration rate Q (cm^3 / s) was within the limits of 0.02 to $0.5 \text{ cm}^3 / \text{sec}$, and within this limit, the diameter of bubbles d_B (mm) was correlate to $d^{1/3}$, and not depended on aeration rate Q (cm^3 / s). Above the limit of $Q = 0.5 \text{ cm}^3 / \text{sec}$, equation (1) was not consistent, and so, experimental equation (2) was used to estimate d_B

$$d_B \propto Q^{n'} \quad (2)$$

where, $n' = 0.2 \sim 1.0$

A graph on the relationship between diameter of bubbles d_B (mm) and superficial gas velocity V_B (m/s) can be split into two parts. When diameter of bubbles was 1.5 mm or less, the bubbles were mostly spherical, and superficial gas velocity correlated with the diameter of bubbles. When the ranges of diameter of bubbles were 1.5 to 6 mm, the bubble shape begins to transform, and superficial gas velocity decrease slightly. When diameter of bubbles exceeded 6 mm, the bubble shape became mushroom-like appearance, and superficial velocity correlatively increased with the diameter of bubbles in the range of 20 to 30 cm/s.

7.2.1. Medium flow characteristics

The medium flow characteristic was influenced by the types of bioreactors. The direction and velocity of the medium flow severely fluctuated in unstirred bubble bioreactor (Figure 5A) which reveals the turbulent characteristics and results in the generation of shear stress. The phenomenon was also remarkable in bubble column bioreactor. A fundamental solution is the generation of smooth laminar flow of the medium in the bioreactor. The turbulent characteristics in bubble column or unstirred bubble bioreactor was changed to smooth laminar flow characteristics when the draft tube was set in the bioreactor to form airlift bioreactor (Figure 5C). Airlift-like medium flow was easily attained in unstirred bubble bioreactor by setting the air sparger on one side at the bottom of the bioreactor (Figure 5B). Although, medium flow near sparger is turbulent, laminar medium flow is generated partly as shown in Figure 5B.

The medium flow is characterized by the shape and types of spargers. The straight bar or ring-shaped brass made sparger with several openings (0.5 to 1 mm diameter) generate rather large bubbles, and induce turbulent flow nature, but fine bubbles generated from sintered or ceramic sparger (plate or pipe) induce mild and slow medium flow. To prevent cell or shoot sedimentation in areas of poor mixing, a plate shaped sparger made of sintered material at the tapered bottom of bioreactor is effective [12]. These characteristics indicate the importance of the basic design and construction of bioreactor in scale-up.

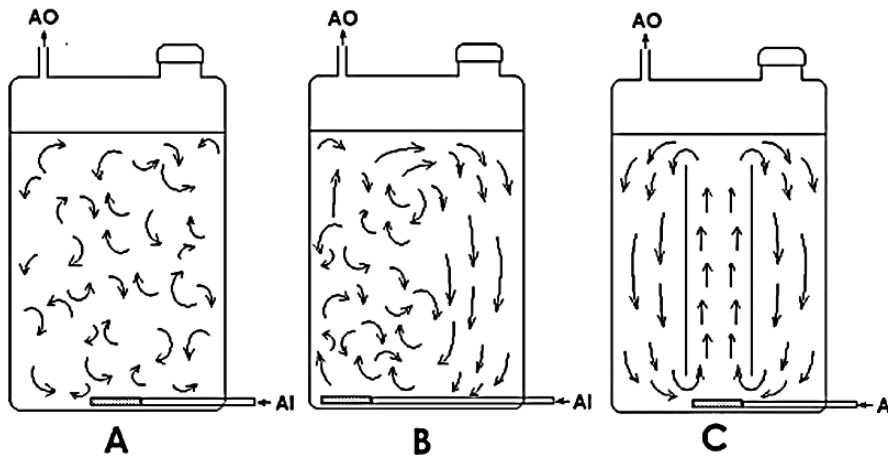


Figure 5. Medium flow characteristics in various types of bioreactors (A) Unstirred bubble bioreactor, (B) Like (A), but air sparger was set on one side at the bottom of the bioreactor, (C) Draft-tube airlift bioreactor. AI: air inlet, AO: air outlet, Shadowed region at the bottom of bioreactor reveal the air sparger.

7.2.2. Medium mixing

The mixing time in relation to shoot fresh weight was measured as shown in Figure 6. The 10 L unstirred bubble bioreactors containing 8 L medium and *Spathiphyllum* fresh shoot grown in the bioreactor, were used for the experiment. Aeration rate was 2 L/min from a ceramic sparger. Conductometric method using NH_4NO_3 as salt was used for determining mixing time.

Medium mixing time without shoot was 18 and 34 s for the unstirred bubble and the airlift bioreactor, respectively. Increase in mixing time depends on shoot fresh weight and the type of bioreactor. At the early stage of shoot growth in a bioreactor when shoot fresh weight was still low (less than 100 g/8L), mixing time was less than 60 s and the time was shorter in unstirred bubble bioreactor. When shoot fresh weight increased over 100 g/8L, the mixing time delayed exponentially depend on shoot fresh weight especially in case of unstirred bubble bioreactor. Mixing time became 2190 and 1680 s

for unstirred bubble and airlift bioreactor, respectively, at highest shoot fresh weight (2000 g/8L, equivalent to maximum shoot growth in fresh weight).

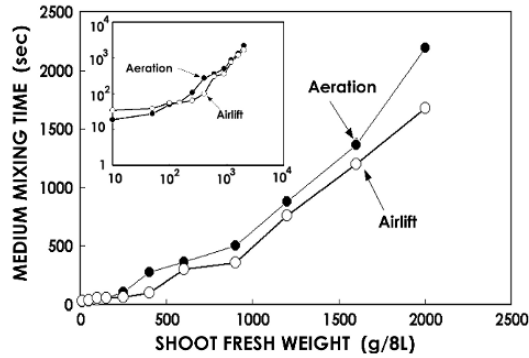


Figure 6. Relationship between shoot fresh weight in the bioreactor and medium mixing time. Small graph represent the logarithmic plot in both horizontal and vertical axis. Aeration: Unstirred bubble bioreactor, Airlift: Draft tube airlift bioreactor.

7.2.3. Oxygen demand and oxygen supply

Plants cultured aerobically require oxygen for growth. In small scale semi-solid cultures, culture vessels such as flasks or bottles are plugged using gas diffusive materials. Molecular diffusion through plugs allows oxygen to penetrate into culture flasks or bottles, and stimulate the cultures to grow. On the contrary, in case of cultures submerged in liquid medium such as shake or bioreactor culture, natural diffusion of oxygen is limited and plant growth is strictly inhibited without shaking or forced aeration. Aeration efficiency evaluated by oxygen transfer coefficient (k_La values) depends mainly on aeration rate and bubble size [12], and so the type of air sparger is important to attain higher k_La value. Bubble size generated depends on the type and size of pores of the sparger. Conventional stainless steel or brass pipe sparger (bar or ring) with pin holes about 0.5 to 1 mm in diameter is not sufficient for generation of fine bubbles, and so, to attain sufficient k_La values, aeration rate should be raised. The requirement of oxygen is different between species and genera, and in general k_La values over 10 h^{-1} is sufficient for growth in cultures of many plant species. For example, in case of tobacco cell cultures, the final biomass concentration became constant at k_La values over 10 h^{-1} [31]. But when K_La was set under 10 h^{-1} , cell yield became depended on K_La values [31]. The factors which affect K_L and a are the mixing conditions in the bulk liquid, the diffusion coefficient, the viscosity and the surface tension of the medium, air-flow rate, gas hold-up and the bubble size [32]. The specific interfacial mass transfer coefficient K_L is constant for fixed medium and temperature and is relatively insensitive to the fluid dynamics in the bioreactor [33], but the specific interfacial area a is difficult to measure, and so the two parameters are combined and referred to as the volumetric mass transfer coefficient, K_La . The difference in K_La is mainly attributed to differences in the specific interfacial area a which was affected by

aeration rate, size of bubbles, and mixing. K_La values are also affected by types of bioreactor and diameter of draft tube. In the scale up of airlift bioreactor, the long residence time of small air bubbles in tall columns may lead to the depletion of oxygen from these bubbles which resulted in the decline of K_La [34]. A need of higher K_La values was also evident in the shoot culture of strawberry in a bioreactor, where the growth of shoots correlated to k_La values and to aeration rate [35]. A problem in higher aeration is the generation of higher mechanical stress by turbulent agitation (shear stress). In order to enhance the aeration efficiency without the generation of severe shear stress, the use of ceramic or sintering steel porous sparger is effective, which generate the fine bubbles with higher K_La values (Figure 7).

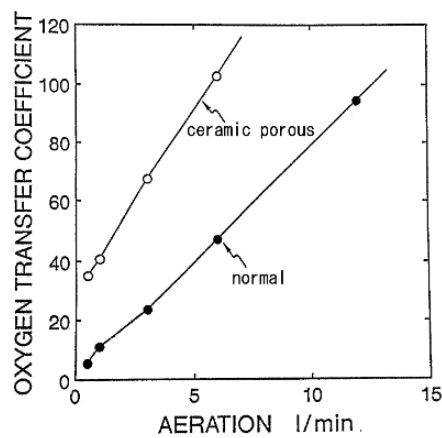


Figure 7. Effect of the types of air sparger and aeration rate on oxygen transfer coefficient in unstirred bubble bioreactor containing 6 L liquid medium. Oxygen transfer coefficient was expressed as K_La (h^{-1}).

7.3. LIGHT ILLUMINATION AND TRANSMITTANCE

Production of plants with well developed and green leaves in the bioreactor is preferable for re-establishment of the plants in soil. The production of such plants depends mainly on the intensity of illumination to the cultures. Illumination of propagules in a bioreactor is not easy because of the logarithmic reduction of light intensity passing through the plant tissues and the distance from light source. Figure 8 indicates the relationship between the distance of a source of light and its intensity. Light emitting diode (LED) is superior to other light sources because of its excellent focusing characteristics, i.e. the high energy conversion rate and reduced infrared heat radiation. Light transmittance was reduced drastically by the presence of shoot cultures in the bioreactor especially at higher fresh weight (Figure 9). When shoot cultures of *Spathiphyllum* and *Colocasia* grown in a bioreactor made of glass vessel were illuminated externally by fluorescent lamps, light transmitted to the cultures only several centimetres from the vessel surface. The leaves on illuminated shoots became green and well developed. On the other hand,

the cultures growing in the bioreactor were etiolated and leaf expansion was inhibited. The same phenomenon was also observed in shoot cultures of *Stevia* grown in large scale (500 L) bioreactor equipped with 4 lamps [36,37]. Although various illuminated bioreactors have been designed [38,39], application to commercial propagation is limited because the price becomes expensive and light introduction was not efficient. Development of new culture technology for propagation in the bioreactor with high illumination efficiency, or production of transplantable propagules in the bioreactor without or with low illumination is required.

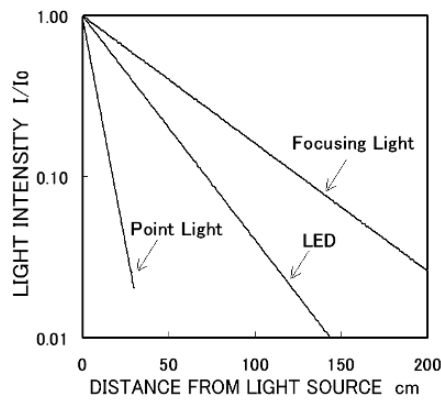


Figure 8. Relationship between the distance of a source of light and its intensity. I_0 : light intensity at the surface of light source. I : light intensity measured at certain distance.

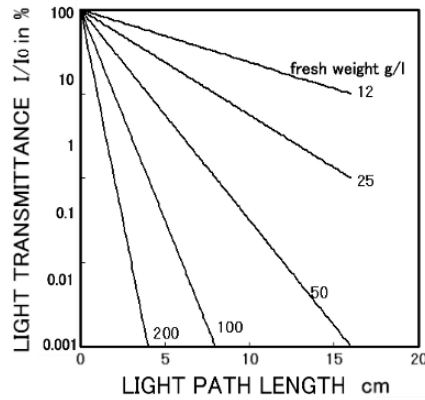


Figure 9. Relationship between light path length and light transmittance in various degree of shoot growth in cultures of *Spathiphyllum*. I_0 : light intensity at the surface of shoot cultures I : light intensity measured at certain path length.

8. Examples of bioreactor application in plant propagation

Many plant species and varieties have been cultured in the bioreactor [2,5,7,8,40]. Responses of cultures in bioreactors are quite different among species or genera and they could be also different from the responses observed under static culture conditions on semi-solid medium (see section 7.2). The cultures propagated were regenerated from inoculated cultures consists of multiple shoot buds induced by the addition of cytokinin to the medium. During cultivation in the bioreactor, various types of plant propagules such as shoots, bulbs, microtubers, corms, embryos, etc. are possible to be developed from shoot buds. The propagules produced in the bioreactor should be easily adapted to *ex vitro* conditions as possible. Storage organs such as bulbs, corms or tubers seem to be the best choice for proliferation in bioreactors. Several examples of bioreactor applications for plant propagation are listed as follows:

- Shoots: *Atropa belladonna*, *Begonia x hiemalis*, *Chrysanthemum morifolium*, *Dianthus caryophyllus*, *Fragaria ananassa*, *Nicotiana tabacum*, *Petunia hybrida*, *Primula obconica*, *Zoysia japonica*, *Scopolia japonica*, *Spathiphyllum*, *Stevia rebaudiana*, etc.
- Bulbs: *Fritillaria tunbergii*, *Hippeastrum hybridum*, *Hyacinthus orientalis*, *Lilium*, etc.
- Corms: *Caladium sp.*, *Colocasia esculenta*, *Pinellia ternate*, etc.
- Tubers: *Solanum tuberosum*
- Embryos or adventitious buds: *Atropa belladonna*

9. Aseptic condition and control of microbial contamination

The microbial contamination is frequently observed in laboratory and commercial tissue cultures, and sometimes leads to the severe damages to cultures. The cause of microbial contamination is latently expressed pathogenic or plant-associated micro-organisms and laboratory contaminants associated with the operatives and in both cases, microbes are expressed in any culture stage [41]. The microbial contamination observed in the laboratory processes is influenced by various factors but the problem is overcome by aseptic handling of vessels, equipments, and cleanliness of culture room, as well as the skilfulness of the operators. The extensive problem of microbial contamination is caused by the proliferation of mites. The mites quickly proliferate and spread around and invade the culture vessels [8]. The seed cultures of propagules used as inocula are sometimes invaded by mites, and cause the contamination after inoculation into bioreactor. To avoid these problems, periodical fumigation of culture room should be performed, and it is strongly recommended that stock cultures are maintained in test tubes with spongy silicon plugs [8].

Several factors intimately relating to microbial contamination are conceivable [42,43] especially hardware design, construction and manipulation manner. To avoid contamination, bioreactor construction should be made simple. The number of tube connectors and various openings of the culture vessel such as the inoculation port should be minimized. In addition, pre-sterilization of empty bioreactor vessel at 121°C for 30 min is usually necessary. Then bioreactor filled with the culture media should be sterilized again at 121°C for 15 min. The inoculation is the risky process because

bioreactors always exposed to external air conditions. The inoculation of the seed culture of propagules to portable sized bioreactors is performed in laminar flow clean air bench. In an open air condition, especially when the bioreactor is anchored to the floor, inoculation should be done in burning flames of alcohol or gas-burner completely covering the inoculation port. In case of large-scale bioreactor (500 L) which is anchored to the floor, Kawamura *et al.* [44] developed an apparatus to inoculate a large number of plantlets or tissue segments. The use of such equipment results in reduction of microbial contamination.

Aeration is also the cause of microbial contamination. Autoclavable heat-resistant tubes and disposable ultra-filter (pore size; 0.2 to 0.45 μm) are adopted as materials in the air line. An air outlet is sometimes equipped with glass wool filter which was wetted by the splash of culture medium and cause the invasion of aphids and microbes. A simple solution is the use of spiral tube (about one meter) with cut end, which prevents the invasion of microbes.

10. Scale-up to large bioreactor

10.1. PROPAGATION OF *STEVIA* SHOOTS IN 500 L BIOREACTOR

The advantage of the use of bioreactor for plant propagation is the easiness in scale-up. The example is the use of 500 L bioreactor for *Stevia rebaudiana* propagation (Figure 10,11) [35,36]. The cluster of shoot primordia which were propagated in the shake culture using modified MS medium (half-strength of KNO_3 , NO_4NO_3 and $\text{CaCl}_2 \cdot 2\text{H}_2\text{O}$ were used), supplemented with 0.1 mg/L NAA, 1 mg/L BA and 30 g/L sucrose, was used as inocula. The 500 L bioreactor contained 300 L MS medium supplemented with 10 g/L sucrose, sterilized at 120°C for 30 minutes by direct application of steam at 0.1 MPa. The fresh weight of shoot buds as inocula was 460 g. Cultures in a bioreactor was aerated at 15 L/minutes, illuminated at 16 h photoperiod by 4 fluorescent lamps inserted in the bioreactor, and incubated at 25°C for 1 month. During the culture period, at 3 weeks, 20 L of the medium was removed and newly prepared 50 L of the same medium containing 6,300 g sucrose was added to elevate the consumed nutrient, sucrose and water. The shoots grew actively to fill up culture vessels within one month. The total shoot weight was 64.6 kg in fresh weight, which was 140 times the inoculum weight. The growth efficiency in 500 L bioreactor was almost the same as in shake culture (100 ml medium in 300 ml flask) or in 10 L bioreactor (6 L medium in 10 L bioreactor). The shoots adjacent to fluorescent lamps were green and developed leaves, but most shoots were etiolated and leaf development was significantly suppressed because the light intensity exponentially decreased with distance under high plantlet density (Figure 10). The shoots taken out from the bioreactor had no roots, but could be easily acclimatized, and after transplant in soil, more than 90% of number of the shoots was successfully acclimatized in soil. These results indicate the practical applicability of large scale propagation using bioreactor.

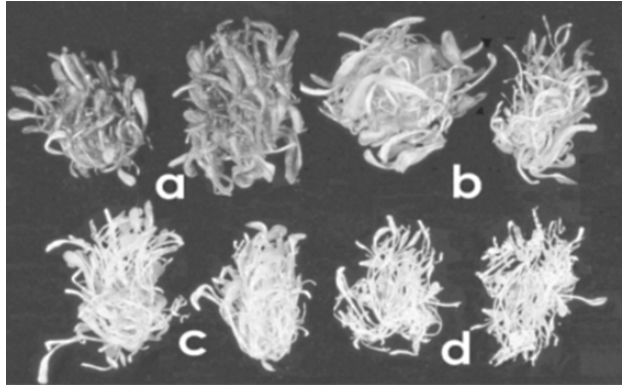


Figure 10. Propagated shoots of *Stevia* taken out from the bioreactor (a, green shoots growing around the fluorescent tube; d, completely white shoots growing remote from fluorescent tubes; b and c, intermediate location of a and d).

Other types of large bioreactors were also applicable. For example, *Stevia rebaudiana* shoots were propagated using a separated impeller-type 500 L bioreactor (Figure 11). Shoots were also well grown in this type of bioreactor and harvest of unwounded cultures was much easier than the case described above.

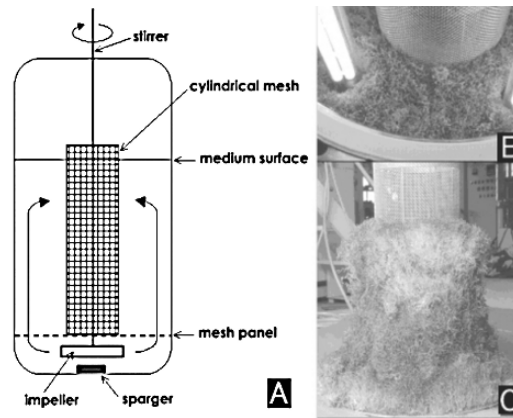


Figure 11. Large scale propagation of *Stevia rebaudiana* shoot in a separated impeller-type 500 L bioreactor. (A) Diagram of a separated impeller-type bioreactor used for mass propagation of *Stevia rebaudiana*. Shoots were cultured in a bioreactor illuminated with fluorescent lamps. Fluorescent tubes equipped within the bioreactor were abbreviated in this figure. (B) Shoot cultures in a bioreactor illuminated with fluorescent lamps, (C) Whole view of *Stevia rebaudiana* shoot cultures adhered to cylindrical mesh which was taken out from bioreactor.

10.2. SAFE INOCULATION OF PLANT ORGANS INTO BIOREACTOR

As described previously, the most risky process to microbial contamination is the inoculation of seed cultures. In general, microbial or plant cell suspension as seed (seed culture) is previously cultured in a smaller size bioreactor and transferred through inoculation tube or pipe connecting between bioreactors during an inoculation. Application of this simple method is difficult in case of plant propagation in the bioreactor because of blockage of the tube by inoculated tissue segments. The tissue segments frequently used as inocula for production of propagules are shoots, adventitious buds, axillary buds, bulb scales. These tissue segments are usually inoculated through inoculation port. The bioreactors of 1 to 20 L are settled in clean bench, and inocula are transferred into bioreactor through inoculation port using forceps. It is better to cover the inoculation port in flames using methyl alcohol or ring burner. In case of large-scale bioreactor anchored on the floor of pilot plant, use of a sanitary apparatus for inoculating a large number of plant propagules is promising.

11. Prospects

The use of liquid systems especially the bioreactor technique seems to be successfully applicable in commercial propagation, and actually a part of tissue culture nurseries already adopted this technique. However, at present, many problems still exist for wide application of this technique. The growth conditions in bioreactor are somewhat different from agar culture and it is necessary to find the optimum culture condition in the liquid medium. Skill is also required in handling and operating the bioreactors as well as in preparation of large number of aseptic seed cultures in one batch. Although it is possible to produce several types of organs in bioreactors, propagation of storage organs will be the best choice for proliferation, because the culture process is quite simple, and the produced propagules are easy to handle and suitable for acclimatization. The bioreactor technology is advantageous in their proven high efficiency and easiness of operation process, and appears to be the most promising system for industrial plant propagation.

References

- [1] Altman, A. and Loberant, B. (2000) Micropropagation of plants, principles and practices. In: Spier, R.E.; Griffiths, B. and Scragg, A.H. (Eds.) The Encyclopaedia of Cell Technology. ISBN: 0-471-16123-3, John Wiley & Sons, Inc., New York; pp.916-929.
- [2] Takayama, S. (1991) Mass propagation of plants through shake and bioreactor culture techniques. In: Bajaj, Y.P.S. (Ed.) Biotechnology in Agriculture and Forestry. Vol.17. Springer-Verlag, Berlin; pp. 495-515.
- [3] Coombs, J. (1986) MacMillan Dictionary of Biotechnology. Macmillan Press, London; pp. 1-330.
- [4] Takayama, S. and Misawa, M. (1981) Mass propagation of *Begonia hiemalis* plantlets by shake culture. Plant Cell Physiol. 22: 461-468.
- [5] Takayama, S. (2002) Practical aspects of bioreactor application in mass propagation of plants. Abst. 1st Int. Symp. Liquid Systems for *In Vitro* Mass Propagation of Plants. Norway, May 29th – June 2nd, 2002. pp. 60-62.

- [6] Takayama, S.; Arima, Y. and Akita, M. (1986) Mass propagation of plants by fermentor culture techniques. In: Abst. 6th International Congress of Plant Tissue and Cell Culture, Int. Assoc. Plant Tissue Cult. University of Minnesota. p. 449.
- [7] Takayama, S. and Akita, M. (1994) The types of bioreactors used for shoots and embryos. *Plant Cell Tissue Org. Cult.* 39:147-156.
- [8] Takayama, S. and Akita, M. (1998) Bioreactor techniques for large-scale culture of plant propagules. *Adv. Hort. Sci.* 12: 93-100.
- [9] Akita, M. and Takayama, S. (1994) Induction and development of potato tubers in a jar fermentor. *Plant Cell Tissue Org. Cult.* 36: 177-182.
- [10] Akita, M. and Takayama, S. (1994) Stimulation of potato (*Solanum tuberosum* L.) tuberization by semi-continuous liquid medium surface level control. *Plant Cell Rep.* 13: 184-187.
- [11] Akita, M. (2000) Bioreactor culture of plant organs. In: Spier, R.E.; Griffiths, B. and Scragg, A.H. (Eds.) *The Encyclopaedia of Cell Technology*. ISBN: 0-471-16123-3, John Wiley & Sons, Inc., New York; pp.129-138.
- [12] Takayama, S. (2000) Bioreactors, Airlift. In: Spier, R. E.; Griffiths, B. and Scragg, A.H. (Eds.) *The Encyclopaedia of Cell Technology*, ISBN: 0-471-16123-3, John Wiley & Sons, Inc., New York; pp. 201-218.
- [13] Archambault, J.; Williams, R.D.; Lavoie, L.; Pepin, M.F. and Chavarie, C. (1994) Production of somatic embryos in a helical ribbon impeller bioreactor. *Biotechnol. Bioeng.* 44: 930-943.
- [14] Archambault, J.; Lavoie, L.; Williams, R.D. and Chavarie, C. (1995) Nutritional aspects of *Daucus carota* somatic embryo cultures performed in bioreactors. In: Terzi, M.; Cella, R. and Falavigna, A. (Eds.) *Current Issues in Plant Molecular and Cellular Biology*. Kluwer Academic Publishers, Dordrecht, The Netherlands; pp. 681-687.
- [15] Heyerdahl, P.H.; Olsen, O.A.S. and Hvoslef-Eide, A. K. (1995) Engineering aspects of plant propagation in bioreactors. In: Aitken-Christie, J.; Kozai, T. and Smith, L.M. (Eds.) *Automation and Environmental Control in Plant Tissue Culture*. Kluwer Academic Publishers, Dordrecht, The Netherlands; pp.87-123.
- [16] Ziv, M. (2000) Bioreactor technology for plant micropropagation. *Hort. Rev.* 24:1-30.
- [17] Ammirato, P.V. and Styer, D.J. (1985) Strategies for large scale manipulation of somatic embryo in suspension culture. In: Zaitlin, M.; Day, P. and Hollander, A. (Eds.) *Biotechnology in Plant Science: Relevance to Agriculture in Eighties*. Academic Press, New York; pp. 161-178.
- [18] Harrell, R.C.; Bieniek, M.; Hood, C.F.; Munilla, A.R. and Cantliffe, D.J. (1994). Automated *in vitro* harvest of somatic embryos. *Plant Cell Tissue Org. Cult.* 39:171-183.
- [19] Jay, V.; Genestier, S. and Courduroux, J.C. 1994. Bioreactor studies of the effect of medium pH on carrot (*Daucus carota* L.) somatic embryogenesis. *Plant Cell Tissue Org. Cult.* 36:205-209.
- [20] Levin, R.; Gaba, V.; Tal, B.; Hirsch, S.; Denola, D. and Vasil, I.K. (1988) Automated plant tissue culture for mass propagation. *Bio/Technol.* 6: 1035-1040.
- [21] Preil, W.; Florek, P.; Wix, U. and Beck, A. (1988) Towards mass propagation by use of bioreactors. *Acta Hort.* 226: 99-105.
- [22] Preil, W. (1991) Application of bioreactors in plant propagation. In: Debergh, P.C.; Zimmerman, R.H. (Eds.) *Micropropagation Technology and Application*. VIII, Kluwer Academic Publishers Group, Boston, USA; pp. 425-446.
- [23] Styer, D.J (1985) Bioreactor technology for plant propagation. In: Henke, R.R.; Gher, K.W.; Constantin, J. and Hollander, A. (Eds.) *Tissue Culture in Forestry and Agriculture*. Plenum Press, New York; pp.117-130.
- [24] Taurus, T.E.; Lulsdorf, M. M.; Kikcio, S.I. and Dunstan, D.I. (1994) Nutrient utilization during bioreactor culture and maturation of somatic embryo cultures of *Picea mariana* and *Picea glauca-engelmannii*. *In Vitro Cell. Dev. Biol.- Plant* 30: 58-63.
- [25] Wheat, D.; Bondaryk, R.P. and Nystrom, J. (1986) Spin filter bioreactor technology as applied to industrial plant propagation. *Hort. Sci.* 21:819.
- [26] Ziv, M. (1990) Morphogenesis of gladiolus buds in bioreactors - Implication for scaled-up propagation of geophytes. In: Nijkamp, H.J.J.; Van Der Plas, L.H.W.; Artrijk, J. V. (Eds.) *Progress in Plant Cellular and Molecular Biology*. Kluwer Academic Publishers, Dordrecht, The Netherlands; pp. 119-124.
- [27] Ziv, M. (1995) The control of bioreactor environment for plant propagation in liquid culture. *Acta Hort.* 393: 25-38.
- [28] Ziv, M. and Shemesh, D. (1996) Propagation and tuberization of potato bud clusters from bioreactor culture. *In Vitro Cell. Dev. Biol.- Plant* 32: 31-36.
- [29] Ziv M.; Kahany, S. and Lilien-Kipnis, H. (1994) Scaled-up proliferation and regeneration of *Nerine* in liquid cultures: Part I. The induction and maintenance of proliferating meristematic clusters by paclobutrazol in bioreactors. *Plant Cell Tissue Org. Cult.* 39: 109-115.

- [30] Aiba, S.; Humphrey, A.E. and Millis, N.F. (1965) Biochemical Engineering. University of Tokyo Press; pp. 1-345.
- [31] Kato, A.; Shimizu, Y. and Noguchi, S. (1975) Effect of initial K_La on the growth of tobacco cells in batch culture. J. Ferment. Technol. 53: 744-751.
- [32] Fonseca, M.M.R.; Mavituna, F. and Brodelius, P. (1988) Engineering aspects of plant cell culture. In: Pais, M.S.S.; Mavituna, F. and Novais, J.M. (Eds.) Plant Cell Biotechnology. Springer-Verlag, Berlin; pp. 389-401.
- [33] Blenke, H. (1979) Loop reactors. Adv. Biochem. Eng. 13: 121.
- [34] Payne, G.F.; Shuler, M.L. and Brodelius, P. (1987) Large scale plant cell culture. In: Lydersen, B.J. (Ed.) Large Scale Cell Culture Technology. Carl Hanser Verlag, Munich. ISBN 3-446-14845-0; pp. 193-229.
- [35] Takayama, S.; Amo, T.; Fukano, M., and Oosawa, K. (1985) Mass propagation of strawberries by jar fermentor culture. (2) Studies on the optimum conditions in a liquid medium and the establishment of mass propagation scheme using a jar fermentor. Abst. 1985 Spring Meeting of J. Soc. Hort. Sci. Tokyo; pp. 210-221.
- [36] Akita, M.; Shigeoka, T.; Koizumi, Y. and Kawamura, M. (1994) Mass propagation of shoots of *Stevia rebaudiana* using a large scale bioreactor. Plant Cell Rep. 13: 180-183.
- [37] Akita, M.; Shigeoka, T.; Koizumi, Y. and Kawamura, M. (1994) Mass propagation of multiple shoots using a large bioreactor. J. Soc. High Technol. Agric. 6: 113-121.
- [38] Ikeda, H. (1985) Culture vessel for photoautotrophic culture, Japan Patent, Kokai. 60-237984.
- [39] Inoue, H. (1984) Culture vessel for photo-requiring organisms, Japan Patent, Kokai. 59-21682.
- [40] Takayama S.; Arima, Y. and Akita, M. (1986) Mass propagation of plants by fermentor culture techniques. Abst. 6th Int. Cong. Plant Tissue Cell Cult., Int. Assoc. Plant Tissue Cult., University of Minnesota, Minnesota, USA; p. 449.
- [41] Cassels, A.C. (1991) Control of contamination in automated plant propagation. In: Vasil, I. K. (Ed.) Cell Culture and Somatic Cell Genetics of Plants. Academic Press, New York. ISBN.0-12-715008-0. 8:197-212.
- [42] Manfredini, R.; Saporiti, L.G. and Cavallera, V. (1982) Technological approach to industrial fermentation: limiting factors and practical solutions. La Chimica e Industria. 64: 325-334.
- [43] Takayama, S. (1997) Bioreactors for plant cell tissue and organ cultures, In: Vogel, H.C. and Todaro, C.L.(Eds.), Fermentation and Biochemical Engineering Handbook. 2nd Edition, Noyes Publications, Westwood, New Jersey, USA; pp. 46-70.
- [44] Kawamura, M.; Shigeoka, T.; Akita, M. and Kobayshi, Y. (1996) Newly developed apparatus for inoculating plant organs into large-scale fermentor. J. Ferment. Bioeng. 82: 618-619.

AGITATED, THIN-FILMS OF LIQUID MEDIA FOR EFFICIENT MICROPROPAGATION

JEFFREY ADELBERG

*Department of Horticulture, Clemson University, Clemson SC, USA,
29634 - Fax: 864-656-4960 - Email: jadlbrg@clemson.edu*

1. Introduction

In vitro culture is a semi-closed system that aseptically provides oxygen, water, organic carbon source (and/or CO₂ and light), nutrients, and plant growth regulators (PGR), at a controlled temperature. A traditional view of plant tissue culture involves placing a small piece of tissue on the gelled-media surface, in a jar, plate or tube, and allows exponential growth unfettered by lack of resource in a uniform microenvironment. Many reports summarized in this volume show increased productivity (per plant, unit area or time) were achieved with larger vessels of liquid medium yielding greater numbers and / or larger plants. Liquid systems that improve distribution of dissolved nutrients, water and oxygen, in the vessel stimulate growth of plant tissues. Simplicity, cost and ergonomic factors are human constraints imposed on designs intended for commercial use.

This chapter describes a hybrid micropropagation process that invokes features of semi-solid gel and bioreactor technology. The agitated, thin-film system (or rocker) uses large, rigid rectangular vessels in a slow pitching motion to intermittently wet and aerate plantlets [1] (see Figure 1). Economy of scale was optimized for the two-dimensional growth surface area in the vessel. Gentle oxygenation of liquid media was similar to wave machines Eibl and Eibl describe for cell and tissue culture in Part 2 of this volume. Shoot surfaces, intermittently wet or dry in a large headspace, accumulate large quantities of solutes from media resulting in high shoot quality similar to temporary immersion systems. Vessel and culture room designs differ from conventional micropropagation, or the bioreactors discussed in other chapters of Part 2. The first section of this chapter discusses nutrients and heterotrophic growth in agar and liquid; the second section compares efficiency of agitated, thin-film process with agar-based media system; and third one lists design considerations for the vessel and culture shelves in the growth room during scale-up. Comparisons will be drawn to agar-gelled media in small round jars, typical of many micropropagation protocols using semi-solid media.



Figure 1. Agitated thin films are created by slowly pitching large rectangular vessels. Reproduced from Adelberg, J. (2004) [24] with permission from Society for In Vitro Biology.

2. Heterotrophic growth and nutrient use

2.1. SOLUTES IN SEMI-SOLID AGAR

Heterotrophic plant growth depends on the uptake of sugar, water, and nutrients from medium. Agar, or other organic gelling agents, are frequently used despite problems of mineral impurities, limited hydraulic conductance, limited availability of solutes to the tissue and binding of toxic exudates near the tissue interface [2,3,4]. Solute movement through gelled media and transfer to the plant is primarily by diffusion [5]. Uptake at the interface surface may proceed against concentration gradients at latter stages of the culture cycle when active uptake by roots and callus is likely to occur. The sealed culture vessel with high humidity limits transpiration, restricting mass flow of dissolved solutes through the xylem and intercellular space.

Selecting an optimal plant density is of great importance to system efficiency but creates a trade-off between productivity and plant quality. Greater plant densities per volume of medium increased the uptake of macro-nutrients, including sucrose, for four ornamental perennial crops; *Delphinium*, *Iris*, *Hemerocallis*, and *Photinia* [6,7]. Highest

plant densities had the lowest multiplication rates and the lowest rate of nutrient uptake per plant. However, the greatest yield of new plants per vessel per unit time was derived at high plant densities. Nutrient availability in high-density agar-gelled cultures was a limitation to multiplication. Nitrate, phosphate and sugar uptake of single plantlets in test tubes of static liquid media greatly exceeded what would be available to plantlets in a normal density for commercial propagation on agar with *Hemerocallis* and *Delphinium* [5].

Sucrose is the solute supplied in the largest quantity in most tissue culture media, having both nutritive and osmotic effects on plant growth. Ibaraki and Kurata [8] described the movement of sucrose in their adjacent medium model as a series of three resistance components: a) diffusion across the medium following a Fick's law equation with the diffusion coefficient specific to solute/solvent, b) boundary layer resistance at the interface surface of the plant and medium, and c) resistance in the plant tissue corresponding to the biochemical sink strength and the plant's transport properties. Diffusion in medium requires calculating the one-dimensional concentration gradients in sugar concentration with time. Sucrose moves approximately 4-times faster in stationary water than agar gel. The boundary resistance at the plant/medium interface was approximately 6000 times greater in agar than liquid media per unit surface area. It is easily envisioned that a plantlet impinged on the surface of an agar gel has a much smaller surface area for exchange at its base than a similar plantlet wet with nutrient across its entire surface. Ibaraki and Kurata [9] further developed a heterotrophic growth model that simulated fresh and dry weight based on water and sugar uptake. Dry matter accumulation was determined by the difference between sugar levels in medium and plant at the interface surface and the area of that surface. Fresh weight gain is related to the plants relative water content, the water content of the medium, and the interface surface area.

Positional non-equilibrium of sugar concentration residual in vessels of spent media (Table 1) suggests uptake by the plant may exceed replenishment across the gel. There was significantly less sugar adjacent to the plantlet compared to media in a distal position. Species and genotypes had different quantities of sugar uptake relative to sink strength and the plants' internal transport properties. Benzyladenine concentrations affected the rate of sugar uptake differently among the genotypes. Hypothetically, increasing the size of the vessel, the duration of the culture cycle, or the density of plants in the gelled media would increase the magnitude of the non-equilibrium. It is also likely that compounds less soluble than sugar would experience greater non-equilibrium at the conclusion of the culture cycle. There is a lack of experimental data published on the diffusion of common ions in agar media.

2.2. SOLUTES IN STATIONARY LIQUIDS

Stationary liquid culture (e.g. floated tissue, membrane rafts, paper bridges, foam cubes) are useful for research scale nutrient experiments, but not generally useful for large-scale propagation. Interface surface areas are roughly equivalent to what may be found with gelled media and liquid is suited to repeated sampling to develop time course data. In one such experiment, when floated leaf disks of tobacco were assayed for uptake of eight nutrient ions during 5-weeks on hormone free media, only iron uptake was significant. When shoot organogenesis was stimulated by benzyladenine, nitrate,

phosphorous, potassium and sulphur uptake became significant following a 10-day lag phase, associated with meristem initiation and shoot growth [10]. Nitrate and phosphorous residual concentrations in media approached zero near termination of the culture cycle.

Table 1. Sugar used from MS media containing two concentrations of benzyladenine, 30 g/l sucrose 0.7% agar solidified media after 5-weeks of culture. Over 300, 180-ml baby food jars containing gelled media were assayed at positions distal and adjacent to the base of the growing plantlet.

Genotype and species	Sugar used (g/l)			
	1 μ M BA		5 μ M BA	
	Distal ^a	Adjacent ^b	Distal	Adjacent
<i>Hosta</i> 'Blue Mammoth'	4.6 \pm 0.9	8.1 \pm 0.9	4.2 \pm 0.7	5.6 \pm 0.4
<i>Hosta</i> 'Francee'	8.5 \pm 1.2	11.0 \pm 0.7	4.9 \pm 0.8	7.6 \pm 0.7
<i>Hosta</i> 'Great Expectations'	6.5 \pm 1.0	8.9 \pm 1.2	3.3 \pm 1.7	2.4 \pm 1.6
<i>Hosta</i> 'Hadspen Blue'	0.2 \pm 0.9	1.1 \pm 0.9	7.4 \pm 1.0	7.6 \pm 1.3
<i>Hosta</i> 'Shade Fanfare'	1.1 \pm 1.1	-0.3 \pm .6	2.0 \pm 1.0	1.9 \pm 1.3
<i>Hosta</i> 'Inniswood'	10.5 \pm 0.8	10.6 \pm 1.3	7.5 \pm 1.6	9 \pm 1.5
<i>Hosta</i> 'Wide Brim'	15.6 \pm 1.3	15.8 \pm 1.2	16.9 \pm 1.2	17.3 \pm 1.5
<i>Colocasia antiquorum</i> 'Illustris'	8.0 \pm 3.2	12.0 \pm 2.6	13.8 \pm 1.8	14.2 \pm 1.2
<i>Zingiber miyoga</i> 'Danicing Crane'	-5.0 \pm 0.2	-4.7 \pm 0.3	-5.0 \pm 0	1.9 \pm 1.3

a. Media was sampled at harvest time with a pipette on the outer perimeter surface of media in the vessel, approximately 1 cm from the nearest plant's base.

b. Media was sampled at harvest time with pipette directly underneath the harvested plants.

Time-course studies of solutes use was conducted on membrane rafts that created a liquid interface surface area similar to that found in agar-based culture. Axillary bud proliferation of watermelon with high concentrations of benzyladenine resulted in ammonium depletion related to cessation of growth over 5-week period [11]. Lowered benzyladenine concentrations and added gibberellic acid caused shoot elongation with increased growth. Ammonium depletion was associated with cessation of growth and there was an increased uptake of nitrate, calcium and potassium, related to greater fresh weight. There was an inverse correlation between plant biomass, and residual concentrations of sugar, ammonium, nitrate, potassium, calcium, and direct correlation of biomass to water use (Table 2). Refractive index, measured in BRIX, is a rapid, inexpensive measurement with no expendable reagents and real time feedback. Decline in BRIX may be used to monitor plant growth or nutrient ion uptake in repeated batch processes. Plant cells have roughly 50% conversion efficiency of organic carbon feed to final cell dry weight [12]. Patterns of specific nutrient ion use may change dependent on developmental stage and under the influence of plant growth regulators.

Agitated, thin films of liquid media for efficient micropropagation

Table 2. Correlation coefficients of biomass (fresh and dry weight) with nutrient depletion and water use of watermelon shoot cultures in elongation medium on polypropylene membrane rafts at six sampling dates during 38-day time course experiment.

	BRIX ^a	Water ^b	Ca ^{+2 c}	K ^{+ c}	NO ₃ ^{- c}	NH ₄ ^{+ c}
Dry weight	-0.98	0.91	-0.84	-0.93	-0.98	-0.89
Fresh weight	-0.98	0.90	-0.81	-0.93	-0.98	-0.88
Dry/fresh	0.63	-0.55	0.52	0.60	0.65	0.63

a. Residual sugar in media measured with refractometer.

b. Volume of water used from media determined by volume of residual medium, adjusted for water loss from vessel by evaporation.

c. Concentration of ion in residual medium determined by ion-selective electrode by method described by Desamero *et al.* (1993).

Primarily, fresh weight gain during heterotrophic plant culture is due to the uptake of water and the dry weight gain is due mainly to the uptake of sugar and inorganic ions. Plants from agar and stationary liquid cultures had similar fresh and dry weights for Venus flytrap (*Drosera muscipula*). Relative dry matter of plants (dry weight / fresh weight) was inversely correlated to concentration of sugar in residual media at time of harvest (Figure 2). Plants grown at higher densities (5x difference from high to low) had lower residual sugar concentrations, on both agar and liquid. Also, cultures with more sucrose (5% vs. 3% w/v) used more sucrose, but had greater residual sugar concentrations. In both agar and liquid with 3% sucrose, relative dry matter was reduced from 11.5% to 9.3% by increased plant density, and in 5% sucrose medium relative dry matter was reduced from 19.6% to 13.8% in response to increased density. Water uptake depends upon the water potential difference between the plantlet and medium [9]. When sugar becomes depleted at high densities, plants continue to grow by taking on more water relative to soluble solids. Increased sugar concentrations allow higher density cultures to maintain high relative dry matter content.

2.3. SUGAR IN SHAKER FLASKS AND BIOREACTORS

In shake-flask culture, the entire plant surface is available for nutrient exchange. Turbulent media does not develop gradients and there is less resistance to solute transfer. Oxygenation of media by shaking creates shear forces that damage many plant tissues, but a few species are suited to research scale micropropagation experiments. When *Cymbidium* protocorm-like bodies (PLB's) were micropropagated in shake-flask culture with glucose concentrations in medium ranging from 0.1 -2% (w/v) fresh and dry weight increased with sugar concentration. The rate of dry weight accumulation per unit surface area remained relatively constant with PLB's having 7- 14% relative dry weight. However, the fresh weight gain per unit surface area was inversely related to relative dry weight because plants with high relative dry weights have a greater influx of water [9].

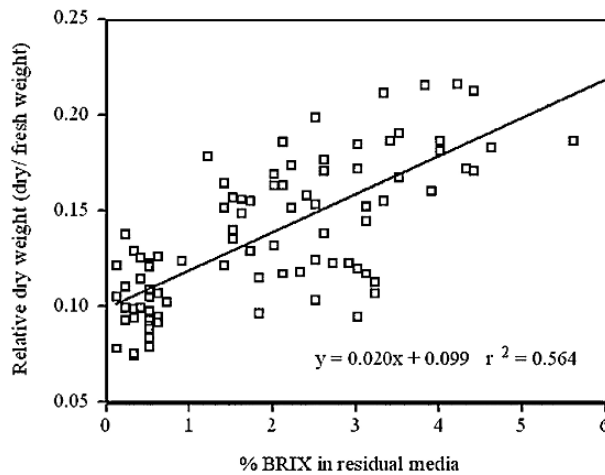


Figure 2. Correlation between residual sugar in media and relative dry weight of *Venus flytrap*, *Drosera muscipula* following five weeks in stationary culture under varied conditions. Vessels were initiated for agar and liquid medium, with 3 and 5% w/v sucrose over a range of explant densities. Each data point represents tissue sampled from one vessel.

With *Hosta* plantlets in shake-flasks, initial levels of sucrose in media from 1-7% w/v were directly related to endogenous levels of sucrose, glucose and fructose following 5-weeks of culture [13]. Shoot bud multiplication was optimal at 5% media sucrose. As sucrose was increased from 1-7% (w/v), shoot and root dry weights increased linearly in roots as did shoots in medium containing benzyladenine, but in hormone-free medium dry weight gain levelled at 5% sucrose (w/v). Media sucrose at stage II was related to greater dry weight, lowered mortality and less leaf chlorosis, following rooting, cold-storage for 7 or 14 weeks, and re-growth in greenhouse [14]. Modelling sugar uptake, translocation, storage and re-growth could be developed to maximize values of young plants for shipping and in international commerce.

Specialized storage organs of geophytes, bulbs, corms, tubers, rhizomes, are modified shoot systems with reduced stem and leaf surfaces. Bioreactor and shaker systems are well suited for large-scale micropropagation of micro-scaled storage organ in many geophytes including lily [15], garlic [16], potato [17], turmeric [18], and taro [19]. Liquid medium with high sugar concentrations (5-12% w/v) results in higher dry weights and stored carbohydrate related to better quality planting stock. Heterotrophic growth models of storage organ culture would assist in assigning value to products of bioreactor process.

With leafy shoot systems, temporary immersion (TIS), or partial immersion, with correctly timed cycles avoided hyperhydricity, limited shear force, provided adequate oxygen, and sufficient mixing of medium. Larger plants, with superior shoot quality in TIS, compared to agar are documented for many unrelated species [20] (see also Afreen, F. in this book). In one such comparison of pineapple shoots from conventional agar

and TIS, TIS shoots were larger with greater leaf area with more dry weight, due to an approximately 10-fold increase in sugar and nitrate assimilation on a fresh weight basis [21].

Table 3. Multiplication rate and number of new plants per square meter of bench space per week generated in agar containing baby food jars and large, rectangular vessels in agitated, thin film liquid system at varied initial plant densities. Equivalent ratios of explants per volume media were used for both agar and liquid media.

Initial density (plants/L)	Multiplication rate		New plants m ⁻² wk ⁻¹	
	Agar	Liquid	Agar	Liquid
<i>Hosta spp.</i> ^a				
40	2.1 ± 0.2	3.4 ± 0.2	9 ± 2	20 ± 2
80	1.7 ± 0.1	2.6 ± 0.1	12 ± 2	29 ± 3
120	1.8 ± 0.1	2.7 ± 0.2	21 ± 3	44 ± 5
200	1.7 ± 0.1	2.3 ± 0.2	29 ± 3	55 ± 7
Significant Linear Fit	L*	L***	L***	L***
<i>Alocasia macrorrhiza</i> ^b				
33	2.1 ± 0.3	3.5 ± 0.4	8 ± 2	13 ± 2
100	1.8 ± 0.2	2.3 ± 0.1	17 ± 4	21 ± 2
165	1.7 ± 0.1	2.4 ± 0.1	24 ± 5	36 ± 4
330	1.3 ± 0.1	1.9 ± 0.1	23 ± 5	45 ± 8
Significant Linear Fit	L*	L***	L* Q*	L***

a. Data were pooled for three varieties over two, 6-week culture cycles on 1 μM BA. (calculated based on data from Adelberg 2004).

b. Data were pooled for two media (1 μM BA and 3 μM BA+ 3 μM ancymidol) for a 4-week culture cycle. 33% more media per area shelf space was used in agar jars (calculated from Adelberg and Toler 2004).

In agitated thin-films, *Hosta* multiplied faster and developed into larger plants than on agar [22]. Multiplication rate was higher at low plant densities (Table 3). This phenomenon is more important in thin-film liquid, than agar. Sugar use per vessel increased with density and more sugar was used in liquid than agar at all densities tested (40 - 200 plants/L). In *Alocasia*, *Colocasia*, *Hosta*, and *Hemerocallis*, sugar use was better correlated to biomass than multiplication rate. Plantlets at harvest were in the range of 9-18% relative dry weight when sugar is ample. Higher plant densities produced greater dry matter. However with *Alocasia* and *Colocasia*, agitated-liquid high-density cultures (330 plants/L) have lower residual sugar concentration and lower relative dry weight in plants at harvest than from agar [23]. Agar cultures were not depleted of sugar in the range of 33 to 330 explants per litre, but thin-film cultures were. Supplementing high-density liquid cultures prior to harvest should allow high-density cultures to obtain higher relative dry matter content and raise soluble solids concentrations. Greater dry weights of *Alocasia*, *Colocasia* and *Hosta* in liquid are due to a greater availability of sugar compared to agar [24], as is likely for many other species.

3. Efficiency in process

3.1. SHOOT MORPHOLOGY FOR CUTTING AND TRANSFER PROCESS

Larger plants are a likely outcome of improved growth in larger vessels from TIS systems and agitated, thin-films. However, during stage II multiplication, large, wet plants are more difficult to aseptically transfer and require more space in the culture vessel. A reasonable approach is to use smaller plants to improve efficiency. Extreme size reductions of organogenic shoot systems described as meristematic nodule or bud aggregates have been used to control plant morphology for liquid bioreactor systems [25]. Growth retardants that inhibit gibberellin synthesis (ancymidol or paclobutrazol) were useful in reducing shoot size in cucumber, philodendron, and poplar [26,27,28] as well as, many of the geophytes described in the previous section. Random mechanized cutting of bud clusters and bulk inoculation of large vessels of liquid medium during stage II of micropropagation allowed cost savings of 50% to be predicted [29]. Complex downstream processing, including individual cutting, sorting and grading, was still required. A solid stationary phase, albeit on agar or liquid plug systems, was necessary to develop rooted plantlets. In highly automated attempts to mechanize micropropagation, machine vision algorithms, artificial intelligence and robotic manipulations of tissue have not justified costs.

Manual cutting and re-planting at the hood station is required for virtually all micropropagation and estimated to be 60% of labour cost [30]. In a hand-cut process for stage II multiplication with conventional agar media, approximately 7% of time is required to remove plants, 48% of time is required to cut and 45% of time was required to re-plant a new vessel [31]. Re-planting gelled media involves repetitive, careful orientation and spacing each individual bud. In agitated liquid media, bulk transfer of cut buds during re-planting allows passive spacing and orientation during growth with a concomitant reduction in technician time at the transfer station. No longer encumbered by re-planting, the technician may focus entirely on the cutting process. In a commercial beta-site operation, technicians logged six months of hood time working with a 10-L Nalgene Biosafe Box (Nalge Nunc International, Rochester, NY, USA) and a bulk transfer process. Numbers of plants harvested per vessel was the most significant factor affecting transfer rate when cuts per hour was partitioned by individual technician, plant variety, media formulation, time of day, day of week and numbers of plants harvested per vessel [22]. Cutting efficiency increased as plants harvested per vessel increased to about 100 per vessel. Transfer rate with the Biosafe was low because of excessive size and an awkward closure system.

During shoot bud division in Stage II old leaves and roots are removed prior to re-planting. Nitrogen depletion caused excessive root elongation for birch and orchid plantlets [32,33]. Preventing tangled root overgrowth by timely harvest schedules is effective in reducing cutting times. Ancymidol has been used to reduce leaf size of *Hemerocallis*, *Hosta* and ornamental taros - *Alocasia* and *Colocasia* with a greater number or smaller plants grown per vessel [24,34,35]. Ancymidol (0.32 μ M) in liquid cultures of *Hemerocallis* 'Todd Monroe' with bulk-transfer process decreased plants size by approximately 50% (FW), increased the numbers or plants per vessel from 60 to 120, and increased the number of plants cut per hour from 110 to 230 [34]. Ancymidol in

liquid media also increased sugar uptake and endogenous carbohydrate concentrations, with varied influences on plant quality in *Narcissus*, *Hemerocallis* and *Hosta* [24,35,36,37]. Ancymidol and paclobutrazol improve desiccation resistance as part of an *in vitro* hardening process for acclimatization [38]. PGR's with lasting downstream effects may benefit several aspects of a propagation system when correctly integrated.

3.2. SPACE UTILIZATION ON CULTURE SHELF

Round 'baby-food' jars are most frequently used for micropropagation due to their low cost. Dimensions vary based on market requirements in processed food industries. One typical vessel, a 180 ml cylindrical baby food-jar has 18 cm² bottom surface for plant growth. Eight of these typical vessels in a 4 x 2 arrangement create roughly the same 'footprint' on a culture room shelf as an 11 cm x 27 cm (297 cm²) rectangular vessel designed for thin-film culture. Yet, the eight jars have a combined interior growth surface of 144 cm² (144 cm² = 4 x 2 x 18 cm² per jar) that is less than half of the 297 cm² of the rectangular vessel used for thin-film vessel. Large rectangular vessels create less void space between vessels on a culture room shelf than larger numbers of smaller cylindrical jars.

Agar in jars and rectangular thin-films were compared with *Hosta* (40-200 plants/L) and *Alocasia macrorrhiza* over a wider range of densities (33-330 plants/L). As described in section 3.3., there were higher multiplication rates in liquid than agar, and the magnitude of this effect was greater at low densities. However, more new plants (per area shelf space per unit time) were initiated at higher plant densities based on the greater number plants initially in the vessel. Yields were higher in rectangular thin-film liquid vessels than round vessels agar-containing medium (Table 3). Yield of *Alocasia* in jars levelled-off between 165-330 plants/L, but increased in thin-films liquid over the entire range of densities tested. Optimization of thin-film system involves low-densities early in production cycle when rapid increase of plants is most desired. During the peak production season, high-density cultures would be favoured to obtain greatest output from a facility with least labour. The large boxes of liquid media permitted the greatest yields at the highest densities. A second ornamental taro, *Colocasia esculenta* 'Fontanesii' had similar multiplication rates in agar and liquid but highest yield of new plants in liquid system (data calculated from [23]). The greater yield of the agitated, thin-film liquid was likely a combined effect of a) increased surface area for plant growth within the vessel, and b) larger contact surface of plants and media allowing greater sugar availability.

3.3. PLANT QUALITY

Hosta from shake-flask culture had greater dry weight than plants from agar. During subsequent acclimatization, plants from liquid grew faster in greenhouse mist frame and

outdoor nursery [39]. All of the *Hosta* plants from the density experiment (described in section 2.3) were successfully acclimatized in the greenhouse. Plants derived from liquid and agar culture showed comparable vigorous growth to that of greenhouse and quality was also acceptable.

Plants of *Alocasia* and *Colocasia* from the agitated, thin-film liquid system had 2.5 times greater dry weight per plant than from agar (Table 4). Benzyladenine concentration was raised from 1 μM to 3 μM and ancymidol was added in equimolar proportion to reduce plant size and problems with tangled plants in transfer. This resulted in a 45% reduction in dry weight per plant. Plants from all treatments had greater mean dry weights from liquid than agar at all densities. Greater than 99% of plants (from 450 sampled of varied sizes) from liquid media acclimatized to greenhouse and were of acceptable quality. The agitated liquid, thin film system with bulk dump process allows managers to use higher plant densities while maintaining plant quality. When compared to agar, this system allowed more and larger plants produced in less space per unit time with reduced labour.

Table 4. Mean dry weight per plant of two species of ornamental taros after 4 weeks of culture in agar and agitated, thin film liquid system at different initial plant densities. Equivalent ratios of explants per volume media was used for both agar and liquid media.

Initial density (plants/L)	Growth medium (1 μM BA)		Multiplication medium (3 μM BA + 3 μM Ancymidol)	
	Agar	Liquid	Agar	Liquid
<i>Alocasia macrorrhiza</i> (mg dry weight per plant)				
33	109 ^a ± 22	195 ± 13	33 ± 23	119 ± 19
100	123 ± 28	187 ± 49	26 ± 9	85 ± 14
167	44 ± 28	142 ± 23	25 ± 10	75 ± 18
330	66 ± 17	93 ± 23	36 ± 5	119 ± 44
<i>Colocasia esculenta</i> 'Fontanesii' (mg dry weight per plant)				
33	14 ± 2	31 ± 21	16 ± 2	57 ± 3
100	22 ± 7	161 ± 42	21 ± 2	75 ± 18
167	11 ± 3	84 ± 26	27 ± 3	43 ± 4
330	23 ± 3	80 ± 7	25 ± 7	50 ± 8

a. Mean dry weight per plant was calculated as the product of biomass per plant and relative dry weight per vessel from data of Adelberg and Toler, 2004.

4. Vessel and facility design

4.1. PRE-EXISTING OR CUSTOM DESIGNED VESSEL

A vessel needs to be inert, inexpensive and easy to handle. Complete sterilization of all interior surfaces is essential. Single use vessels sterilized by gamma irradiation or ethylene oxide are preferred in the biomedical trade but tend to be too expensive for micropropagation. Vessels need withstand 121°C at 1.2 kg cm² pressure generated

during steam sterilization. Translucent materials are necessary to allow light transmittance into the vessel and an unobstructed view of plant material is important for quality management by visual inspection. Glass and polycarbonate are the two most commonly used materials for rigid vessels. Glass is heavy and breaks easily. Polycarbonate is expensive and becomes clouded with age. Autoclave stable, flexible film laminates are more difficult to fill with media and tissue. A single preferred material does not exist. Combining rigid multiple-use, and flexible single-use components may allow further innovations in vessel construction.

It is desirable to use the fewest parts possible in a vessel system. Each part needs to be cleaned and inspected during re-use, prior to assembly. Critical surfaces must be easily accessible and improper decisions made by workers in the dish room impede successful commercial implementation. Custom fabrication should only be considered after searching what is available, and what can be easily modified from what is already available. Work described in this Chapter was first conceived using modifications of the Nalgene Biosafe, but it was expensive, consisted of 11 parts, and required modification to allow ventilation and media sampling. It also deformed during steam sterilisation and was too large to be easily handled at the hood station. However, a mock-up commercial process with the Biosafe showed value of agitated, thin-films in micropropagation. This allowed decisions to be made on desired qualities of a custom vessel for agitated, thin-film culture.

4.2. SIZE AND SHAPE

Rigid vessels are easier to handle than flexible films. The expense of moulding a rigid vessel dictates considerations of inter-related aspects of process. Economy requires the fewest custom parts. Thermoforming techniques (injection mould, blow mould, vacuum mould, etc.) impact cost of the mould and limit choices of size, shape and the precision of critical surfaces. The mould will cost more than the materials until thousands of units have been cast. Detailed discussion of plastic fabrication is beyond the scope of this chapter.

Rectangular vessels were selected for minimal void space and maximized growth surface for the plants. A base with one longer dimension, allowed a slight pitch to create a wave capable of immersion of the entire plantlet. Pitch angles ranging from 5-30° were effective in a vessel with length of 27 cm and width of 10 cm containing 150-250 ml of medium. Length to width ratios greater than 3 are often considered awkward for handling. The 10 cm base created a large growth surface and a taper to a 6 cm upper surface made the vessel easier to grip for smaller hands. Vessels were large enough to allow at approximately 75-150 plants to be harvested per cycle for labour efficiency [22]. The height of the vessel (10 cm) was determined from other vessels common in the trade. The side-mounted closure allows greater growth surface to be accessible to a forceps with advantages in aseptic hood process explained in section 4.3.

Autoclave capacity may limit laboratory throughput. In the US, most autoclaves are circular bores, horizontally mounted, with flat tray bottoms. A well-designed vessel should fit most common autoclaves with minimal void space. If vessels are to be stacked in autoclave, a route for steam penetration within the stacks must be maintained. The Liquid Lab Vessel® (Figure 3) fits the Market Forge Sterilmatic STME Autoclave (Market Forge Industries, Everett MA, USA) in two stacks of four. The fluted top of the



Figure 3. *Liquid Lab Vessel*[®] for agitated thin film micropropagation with adhesive ventilation patches (shown in foreground).

vessel allows steam penetration to media on the bottom surface of the upper vessel layer during steam sterilization. Back to back arrangement of vessels in the upper layer accommodates the narrowed width at the top of the autoclave's bore.

Stacking of vessels during storage is facilitated by internally nested, tapered vessels or collapsed flexible film bags. This convenience was not achieved in the vessel shown.

4.3. CLOSURES AND PORTS

Closures and ports may be made of dissimilar materials from the vessel body. There must be enough elasticity to allow expansion and contraction during autoclave cycle. Rigid polycarbonate vessels with softer polypropylene closures are often combined. A snug interference fit seals by forcing the softer polypropylene cap to conform to the rigid polycarbonate vessel. For economy, vessels may be moulded to match a pre-existing closure. The seal is the most expensive part of the vessel and its length should be minimized with respect to a maximum growth area. The opening need to be large enough to allow cut buds be introduced and larger plantlets be removed (disposable vessels can be cut open at harvest and have much smaller closures). Circular closures using threaded screw-caps apply uniform pressure on the seal. Thread patterns trap condensed water and potentially provide refuge for contaminants that could be drawn to the mouth of the vessel by the screw mechanism when opening. Thread design for aseptic culture vessels involve fewer concentric rings with greater pitch than those designed for food containers. The seal should not have broad horizontal surface that allow condensation to collect.

Gas exchange between the vessel and the ambient environment is necessary to maintain adequate levels of CO₂, O₂ and water vapour [40]. A tightly sealed vessel may not allow adequate ventilation. Loose caps will ventilate the vessel but contamination

may occur with macroscopic voids. Membrane filters laminated to adhesives and structural supports may be fixed to openings designed specifically to ventilate the vessel. Microbes are excluded based on size. Ventilation patches become more cost effective when larger patches are applied to greater surface areas for growing more plants in larger vessels. Repeated aseptic sampling of liquid media during the culture cycle is possible using silicone rubber septa and syringe needles.

4.4. BIOTIC CONTAMINANTS

It is common tissue culture lore that liquid medium is more prone to contamination than agar. This misstatement is based on reasonable observations. Endogenous contaminants fastidious to the plant are easier to find suspended in turbid liquids than as cryptic 'white ghosts' hidden from sight underneath the base of the plantlet embedded in agar. Generally, bacteria and fungus will grow more quickly in agitated liquids than under agar medium. Ironically, this property of liquid culture allows a proactive manager greater lead time to take appropriate action.

Frequently liquid culture involves using larger vessels. More initial explants increase the chance of contamination as an exponential function of the fraction of plants that are contaminated. The cost of losing larger batches is higher and so a laboratory's 'base' contamination rate will dictate a reasonable scale of operation. Contaminant problems introduced in aseptic transfer process are exacerbated by work with larger vessels in the laminar flow hood. The longer the vessel remains open, the greater the size of the opening, more frequent or invasive entries, hands or tools crossing over the entry port, and blocking of laminar flow to the entry port, all increase the chance of failure with larger vessels. Also, many experiences with larger vessels involve improvised parts, ill-conceived autoclave packing and *ad hoc* cooling procedures. These failures are not due to liquid culture *per se*, but are problems of larger vessels, itinerant hardware and protocol.

A process for use of Liquid Lab Vessel[®] was developed to circumvent contamination problems. During sub-culture, vessel is placed in the hood so laminar flow is parallel to the long, linear dimension. A 25 cm forcep is used to remove a portion of plantlets with the operators' hand shielded from the growth surface by the vessels slanted, fifth side. Plants should not contact the outer rim of the vessel during removal. If the plants are too large or entangled, one may consider shorter culture period or use of ancymidol. Adequate numbers of buds for re-initiation of new vessels should be cut and stored in sterile, empty jars. Transfer of cut buds to each new vessel will be made in one motion and only the sterile jar need cross over the entry port. The size of the entry port in Figure 3 is similar to the size of petri-plate and the time the vessel remains open during inoculation has been minimized.

4.5. LIGHT AND HEAT

Large, flat transparent surfaces permit unobstructed observation of plants on the bottom and backside of the culture vessel. Cool white fluorescent light transmitted through the vessel provides both photosynthetic energy and signals that promote shoot development. Long tubes provide relatively even distribution of light flux density on the culture shelf [40]. Light fixtures are typically mounted on the underside of the shelf to provide downward lighting even though downward lighting does not always provide the

best quality growth [40]. The large, clear bottom surface of Liquid Lab Vessels[®] allowed shelves to be reduced to open support frames with light penetration coming from through the open bottom. Reflectors and canisters were removed from fluorescent tubes so light would be radially transmitted. This allowed two culture shelf-layers to be sandwiched between upper and lower lighting layers (Figure 4). Approximately 70% of the irradiance in the upper shelf came in the downward direction with the other 30% coming through the filled lower shelf.



Figure 4. Floor to ceiling arrangement of open-frame shelving in 3.7 m culture room.

Similarly, 70% of the irradiance on the lower shelf came in the upward direction through the frame (with the other 30% coming through the filled upper shelf). The sums of downward and upward irradiance were equivalent on upper and lower shelves. There was no difference for multiplication rate, sugar use or appearance of plants in comparisons between upper and lower shelves during three years of pilot scale process with thousands of vessels.

Electricity is approximately 5% of the cost of goods in a commercial lab [30]. Working with a 3.7 m shelving stack allowed 10 shelves (5 pairs of upper and lower) to utilize 7 rows of light fixtures, not 10. Lighting the culture room is about 65% of the electricity cost, and cooling those lights is another 25% of the electric cost. The 30% reduction of light fixtures is therefore significant. Theoretically, the number of lights would be reduced by 50% as the stacks get taller, but this creates man-motion and worker safety as constraints.

Removing heat trapped in tightly filled solid shelves limit how closely shelving may be arranged in a traditional vertical stack of shelves. Tilted, open frames did not appear

to trap heat, even when packed with vessels. The rocking motion dissipated any 'hot pockets' with a bellow-type motion. Tight vertical packing of shelf-pairs allows stacked planar growth surface areas to be optimized in the volume of space under environmental control.

5. Concluding remarks

Three-dimensional volumetric optimization in full immersion bioreactors is theoretically the most efficient way to grow plant cells. As the organism develops polarity, aerated shoots fixed in gaseous phase become more important to plant quality. Optimization of two dimensional growth surfaces for nutrient exchange, with an adequate aerial environment is necessary for micropropagation of shoots and plants of most species. Latter stages of somatic embryo conversion may similarly benefit from these approaches. If a system is to be readily used, it must conform to the human environment - simple, economic and robust. In this current iteration, the bioreactor has been simplified to a vessel that is placed on the shelf without mechanical linkages to pumps and motors. Unit size for plant-handling was dictated by the technician. Managers realize a scale-up factor that allows more active monitoring of process. Reasonably sized factorial experiments may rapidly determine optimization of genotype, PGR or nutrient-use scenarios. Values added to the young plant by enhanced transfer of nutrients can be delivered in the market competitively with plants produced on agar.

Disclaimer

The use of trade names does not imply product endorsement by the author, or Clemson University

References

- [1] Adelberg, J.; and Simpson, E.P. (2004) Intermittent immersion vessel apparatus and process for plant propagation. US Patent 6,753,178 B2.
- [2] Smith, M.A.L.; and Spomer, L. (1995) Vessels, gels, liquid media and support systems. In: Aitken-Christie, J.; Kozai, T. and Smith, M.A.L. (Eds.) Automation and environmental control in plant tissue culture. Kluwer Academic Publishers, Dordrecht, The Netherlands; pp. 371-405.
- [3] Williams, R.R. (1995) The chemical microenvironment. In: Aitken-Christie, J.; Kozai, T. and Smith, M.A.L. (Eds.) Automation and environmental control in plant tissue culture. Kluwer Academic Publishers, Dordrecht, The Netherlands; pp. 405-440.
- [4] Leifert, C.; Murphy, K.P. and Lumsden, P.J. (1995) Mineral and carbohydrate nutrition of plant cell and tissue cultures. CRC Crit. Rev. Plant Sci. 14: 83-109.
- [5] Williams, R.R. (1993) Mineral nutrition *in vitro* - a mechanistic approach. Austr. J. Bot. 41: 237-251.
- [6] Pryce, S.; Lumsden, P.J.; Berger, F.; Nicholas, J.R. and Leifert, C. (1994) Effects of plant density and macronutrient nutrition on Iris shoot cultures. In: Lumsden, P.J.; Nicholas, J.R. and Davies, W.J. (Eds.) Physiology, Growth and Development of Plants in Culture. Kluwer Academic Publishers, Dordrecht, The Netherlands; pp. 72-76.
- [7] Leifert, C.; Lumsden, P.J.; Pryce, S. and Murphy, K.P. (1991) Effects of mineral nutrition on the growth of tissue cultured plants. In: Goulding, K.H. (Ed.) Horticultural Exploitation of recent biological developments, Proceedings of the Institute of Horticulture, Sep. 1991; pp. 43-57.
- [8] Ibaraki, Y. and Kurata, K. (1993) Comparison of culture methods from the viewpoint of nutrient movement. ASAE paper no. 934049, Presented Spokane WA; June 1993.

- [9] Ibaraki, Y. and Kurata, K. (1998) Relationship between water content of Cymbidium protocorm-like body and growth. In L.F.M (ed.) Crop models in protected cultivation. Acta Hort. 456: 61-66.
- [10] Ramage, C.M. and Williams, R.R. (2003) Mineral uptake in tobacco leaf discs during different developmental stages of shoot organogenesis. Plant Cell Rep. 21: 1047-1053.
- [11] Desamero, N.; Adelberg, J.; Hale, A.; Young, R. and Rhodes, B. (1993) Nutrient utilization in liquid/membrane system for watermelon micropropagation. Plant Cell Tissue Org. Cult. 33: 265-271.
- [12] Curtis, W. (1999) Achieving economic feasibility for moderate value food and flavour additives: a perspective on productivity and proposal for production technology cost reduction. In: Fu, T.J.; Sing, G. and Curtis, W. (Eds.), Plant Cell and Tissue Culture for Production of Food Ingredients. Kluwer Academic/ Plenum Publ., New York; pp. 225-236.
- [13] Gollagunta, V.; Adelberg, J.; Rajapakse, N. and Rieck, J. (2004) Media composition affects carbohydrate status and quality of *Hosta tokudama* Tratt. 'Newberry Gold' micropropagules during low temperature storage. Plant Cell Tissue Org. Cult. 77: 125-131.
- [14] Gollagunta, V.; Adelberg, J.; Rajapakse, N. and Rieck, J. (2005) Sucrose in storage media and cultivar affects post-storage re-growth of *in vitro* *Hosta propagules*. Plant Cell Tissue Org. Cult. (In press).
- [15] Lian, M.; Chakrabarty, D. and Paek, K.Y. (2002) Growth and uptake of sucrose and minerals by bulblets of liliium oriental hybrid 'Casablanca' during bioreactor culture. J. Hort. Sci. Biotechnol. 77: 253-257.
- [16] Kim, E.K.; Hahn, E.J.; Murthy, H.N. and Paek, K.Y. (2003) High frequency shoot multiplication and bulbet formation of garlic in liquid cultures. Plant Cell Tissue Org. Cult. 73: 231-236.
- [17] Ziv, M. and Shemesh, D. (1996) Propagation and tuberization of potato bud clusters from bioreactor culture. In Vitro Cell. Dev. Biol.-Plant 32: 31-36.
- [18] Salvi, N.D.; George, L. and Eapen, S. (2002) Micropropagation and field evaluation of micropropagated plants of tumeric. Plant Cell Tissue and Org. Cult. 68: 143-151.
- [19] Zhou, S.; He, Y. K. and Li, S. (1999) Induction and characterization of *in vitro* corms on diploid taro. Plant Cell Tissue Org. Cult. 57:173-178.
- [20] Etienne, E. and Berthouly, M. (2002) Temporary immersion systems in plant micropropagation. Plant Cell Tissue Org. Cult. 69: 215-231.
- [21] Escalona, M.; Samson, G.; Borroto, C. and Desjardins, Y. (2003) Physiology of effects of temporary immersion bioreactors on micropropagated pineapple plantlets. In Vitro Cell. Dev. Biol.-Plant.39: 651-656.
- [22] Adelberg, J. (2004) Efficiency in thin-film liquid system for micropropagation of *Hosta*. Plant Cell Tissue Org. Cult. (In press).
- [23] Adelberg, J. and Toler, J. (2004) Comparison of agar and an agitated, thin-film liquid system for micropropagation of ornamental elephant ears. Hort. Sci. 39: 1088-1092.
- [24] Adelberg, J. (2004) Plant growth and sugar utilization in an agitated, thin film liquid system for micropropagation. In Vitro Cell. Dev. Biol.-Plant. 40: 245-250.
- [25] Ziv, M. (1999) Organogenic plant regeneration in bioreactors. In: Altman, A.; Ziv, M. and Izhar, S. (Eds.) Plant Biotechnology and In Vitro Biology in the 21st Century. Kluwer Academic Publishers, Dordrecht, The Netherlands; pp. 673-679.
- [26] Ziv, M. (1992) The use of growth retardants for the regulation and acclimatization of *in vitro* plants. In: Karsen, C.; Van Loon, L. and Vregdenhil, D. (Eds.) Progress in plant growth and regulation. Kluwer Academic Publishers, Dordrecht, The Netherlands; pp. 809-817.
- [27] Ziv, M. and Ariel, T. 1991. Bud proliferation and plant regeneration in liquid cultured *Philodendron* treated with ancymidol and paclobutrazol. Plant Growth Regul. 10: 53-57.
- [28] Vincour, B.; Carmi, T.; Altman, A. and Ziv, M. (2000) Enhanced bud regeneration in aspen (*Populus tremula* L.) roots cultured in liquid media. Plant Cell Rep.19: 1146-1154.
- [29] Gross, A. and Levin, R. (1999) Design consideration for mechanized micropropagation laboratory. In: Altman, A.; Ziv, M. and Izhar, S. (Eds.) Plant Biotechnology and In Vitro Biology in the 21st Century. Kluwer Academic Publishers, Dordrecht, The Netherlands; pp. 637-642.
- [30] Chu, I. (1995) Economic analysis of automated micropropagation. In: Aitken-Christie, J.; Kozai, T. and Smith, M.A.L. (Eds.) Automation and environmental control in plant tissue culture. Kluwer Academic Publishers, Dordrecht, Netherlands; pp. 19-28.
- [31] Alper, Y.; Young, R.; Adelberg, J. and Rhodes, B. (1994) Mass handling of watermelon microcuttings. Trans. Amer. Soc. Ag. Eng. 37: 1337-1343.
- [32] Adelberg, J.; Desamero, N.; Hale, A. and Young, R. (1997) Long-term nutrient and water use during micropropagation of *Cattleya* orchid on liquid/membrane system. Plant Cell Tissue Org. Cult. 48: 1-7.

Agitated, thin films of liquid media for efficient micropropagation

- [33] McDonald, A.J.S. (1994) Nutrient supply and plant growth. In: Lumdsen, P.J.; Nicholas, J.R. and Davies, W.J. (Eds.) *Physiology, Growth and Development of Plants in Culture*. Kluwer Academic Publishers, Dordrecht, The Netherlands; pp. 47-57.
- [34] Maki, S.; Delgado, M. and Adelberg, J. (2005) Time course study of ancymidol on micropropagated *Hosta*. *Hort. Sci.* (In press).
- [35] Adelberg, J.; Delgado, M. and Tomkins, J. (2005) Ancymidol and liquid media improved micropropagation of *Hemerocallis* cv. Todd Monroe on the 'rocker' thin-film bioreactor. *J. Hort. Biotechnol.* (In press).
- [36] Chen, J. and Ziv, M. (2001) The effect of ancymidol on hyperhydricity, regeneration, starch and antioxidant enzymatic activities in liquid-cultured *Narcissus*. *Plant Cell Rep.* 20: 22-27.
- [37] Chen, J. and Ziv, M. (2003) Carbohydrate, metabolic, and osmotic changes in scaled-up liquid cultures of *Narcissus* leaves. *In Vitro Cell. Dev. Biol-Plant* 39: 645-650.
- [38] Ziv, M. (1995) *In vitro* acclimatization. In: Aitken-Christie, J.; Kozai, T. and Smith, M.A.L. (Eds.) *Automation and environmental control in plant tissue culture*. Kluwer Academic Publishers, Dordrecht, The Netherlands; pp. 493-576.
- [39] Adelberg J.; Kroggel, M. and Toler, J. (2000) Greenhouse and nursery growth of micropropagated *Hostas* from liquid culture. *Hort. Tech.* 10: 754-757.
- [40] Fujiwara, K. and Kozai, T. (1995) Physical microenvironment and its effect. In: Aitken-Christie, J.; Kozai, T. and Smith, M.A.L. (Eds.) *Automation and environmental control in plant tissue culture*. Kluwer Academic Publisher, Dordrecht, The Netherlands; pp. 319-369.

DESIGN, DEVELOPMENT, AND APPLICATIONS OF MIST BIOREACTORS FOR MICROPROPAGATION AND HAIRY ROOT CULTURE

MELISSA J. TOWLER¹, YOOJEONG KIM², BARBARA E. WYSLOUZIL³, MELANIE J. CORRELL⁴, AND PAMELA J. WEATHERS¹

¹*Department of Biology/Biotechnology, Worcester Polytechnic Institute, Worcester, MA, 01609, USA - Fax: 508-831-5936 -Email: weathers@wpi.edu*

²*Department of Chemical Engineering, Worcester Polytechnic Institute, Worcester, MA 01609, USA*

³*Department of Chemical and Biomolecular Engineering, The Ohio State University, Ohio, USA – Fax: 614-292-3769*

⁴*Agricultural and Biological Engineering Department, University of Florida, Gainesville, FL 32611, USA-Fax: 352-392-4092*

1. Introduction

Aeroponic technology has been used extensively to study biological phenomena in plants including drought stress, symbiotic relationships, mycorrhizal associations, disease effects, mineral nutrition, overall plant morphology and physiology [1], and some work has also been completed with animal tissue culture [2]. Aeroponics offers many advantages to whole plant growth because of the enhanced gas exchange that is provided. Here we focus on the use of aeroponics (nutrient mists) for *in vitro* culture of differentiated tissue, in plant micropropagation, and in the culture of transformed (hairy) roots for secondary metabolite production.

There are two main categories of bioreactors: liquid-phase and gas-phase reactors [3]. In liquid-phase reactors, the tissue is immersed in the medium. Therefore, one of the biggest challenges in a liquid-phase culture is delivering oxygen to the submerged tissues due to low gas solubility. In gas-phase reactors (which include nutrient mist culture), the biomass is exposed to air or a gas mixture and nutrients are delivered as droplets. Droplet sizes can range from 0.01-10 μm for mists, 1-100 μm for fogs, and 10-10³ μm for sprays [4]. The mass transfer limitation, especially of oxygen, can be significantly reduced or eliminated by using a gas-phase culture system [5].

2. Mist reactor configurations

The original design of aeroponics systems dispersed nutrient medium via spray nozzles that required compressed gas and were prone to clogging by medium salts [1], while later mist reactors used submerged ultrasonic transducers. In the early mist reactors (Figures 1A and 1B), the ultrasonic transducer was in direct contact with nutrient medium salts and had to be autoclaved, considerably shortening the life of the transducer [6-8]. Buer *et al.* [8] fabricated an acoustically transparent polyurethane window to isolate the medium from the transducer (Figure 1C) but making the windows was difficult, time consuming, and the starting materials were expensive. Chatterjee *et al.* [9] replaced the custom window with an inexpensive, commercially available polypropylene container (Figure 2) and this design was successfully used for both hairy root [9] and micropropagation studies [10-12]. Similarly, Bais *et al.* [13] used a polycarbonate GA-7 vessel. The nutrient mist system currently used by Weathers *et al.* [5] (Figure 3) has an acoustic window consisting of a thin sheet that has a higher temperature tolerance than polypropylene and can also be incorporated into a reactor of almost any size or shape. The designs of the mist reactor configuration have evolved as the applications of these systems have become more varied.

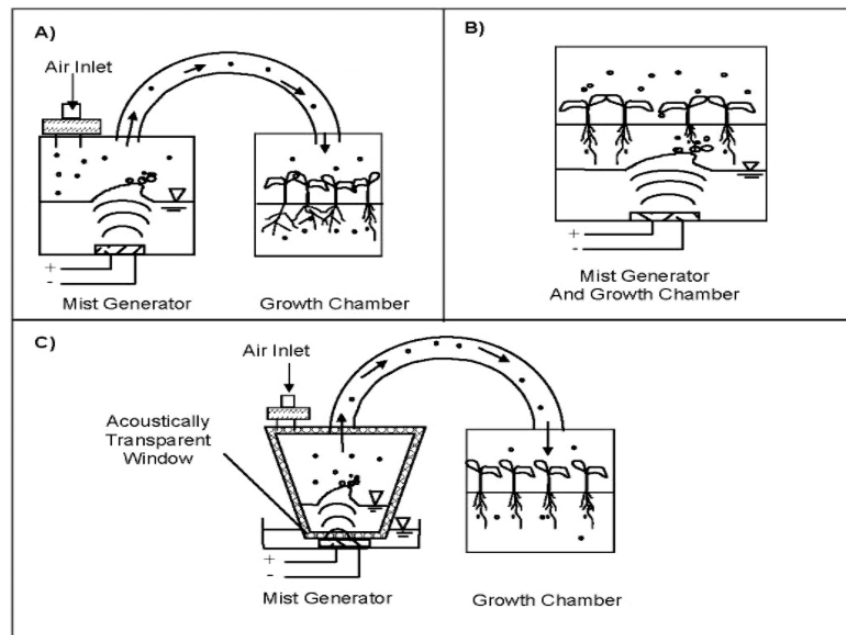


Figure 1. Three types of ultrasonic mist reactors: the mist generator and the growth chamber are in separate vessels (A) mist generator and growth chamber are in the same vessel (B) and the transducer is separated from autoclaved components by an acoustic window (C). Direction of mist movement is indicated by arrows.

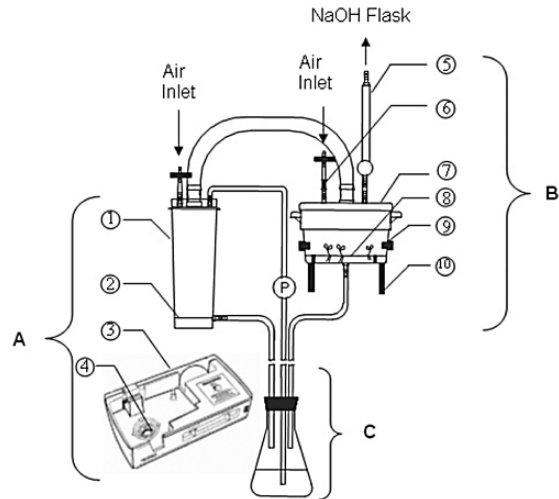


Figure 2. Acoustic window mist reactor; A, mist generator; B, micropropagation chamber; C, media reservoir; 1, polypropylene mist chamber; 2, nutrient medium level; 3, Holmes® humidifier base; 4, ultrasonic transducer; 5, coalescer; 6, one-way valve; 7, micropropagation chamber; 8, plant platform; 9, gas sampling port; 10, chamber supports; P, peristaltic pump used for pumping medium to mist chamber.

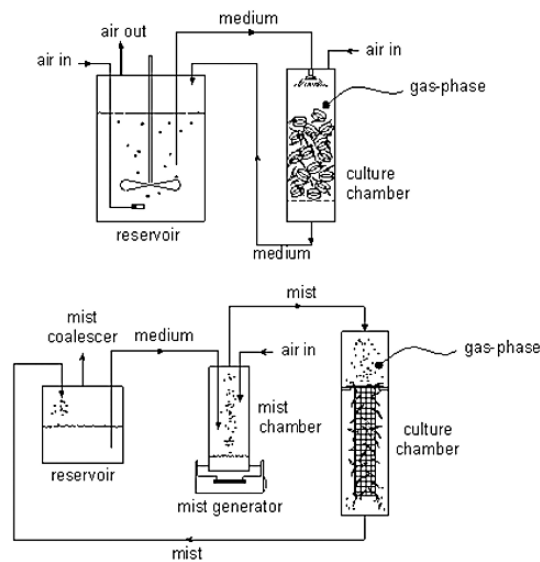


Figure 3. Two types of gas-phase bioreactors for hairy root culture. Top, trickle bed reactor. Bottom, nutrient mist reactor.

3. Mist reactors for micropropagation

Worldwide, an estimated one billion plants per year are produced by micropropagation [14]. In the micropropagation scheme (Figure 4), [15,16], stage 0 is the selection of the donor plant, and may involve genetic testing and disease indexing. In stage I, the explant (generally the shoot tip) is isolated and disinfected and sterile culture is initiated on an appropriate nourishing medium. Multiplication of the explant occurs in stage II, usually via exogenous hormonal stimulation of branching, with subcultures performed as needed. In stage III, the shoots are stimulated to produce roots by altering the hormone content of the medium. Sometimes rooting is initiated instead in conjunction with stage IV (acclimatization) to prevent damage to the fragile newly formed roots during transfer. While roots that develop *in vitro* are often considered non-functional, for some plants the presence of *in vitro* roots at the time of transplanting may have beneficial effects on the plant's water status [17]. Acclimatization (stage IV) may take weeks as the plant makes the transition to the non-sterile environment at lower relative humidity, and greater light intensity rates. The high relative humidity of the *in vitro* culture causes changes to the structure of the shoot's cuticle, wax deposits, stomata and mesophyll cells, subsequently inhibiting photosynthesis. Therefore, the plants must "learn" how to photosynthesize [18]. The final stage, stage V, involves verifying the status of the plant with respect to its genetic integrity and disease-free condition.

An important advantage of gas-phase systems such as a nutrient mist bioreactor (mist reactor) when used for micropropagation is the potential for precise control of the gas composition and relative humidity surrounding the plants because these parameters can significantly affect multiplication rates, rooting, and acclimatization [19,20]. Design and development of an effective and inexpensive mist reactor for micropropagation, however, presents engineering challenges unique to this application. A summary of studies using mist reactors for micropropagation is provided in Table 1.

Typical *in vitro* micropropagation environments have high relative humidity (95-100% RH), low light intensity (30-75 $\mu\text{mol m}^{-2}\text{s}^{-1}$), and large fluctuations in CO_2 [21]. These conditions can contribute to increased hyperhydration [22], reduced photosynthetic ability [23], or increased transpiration [24] in plants when compared to field-grown specimens. The presence of supplemental sucrose in the growth media to compensate for decreased photosynthesis can also reduce fixation of CO_2 . Further deficiencies of CO_2 result from the culture chamber, which is sealed in order to maintain the sterility of the carbon-rich media, which also leads to poor gas exchange between the tissue and the outside atmosphere.

The gaseous composition of the headspace within tissue culture vessels is a major factor influencing plant growth and development *in vitro* [25], and depending on the volume of the vessel and the extent of ventilation, is composed mainly of nitrogen, oxygen, carbon dioxide, and may contain ethylene, ethanol, acetaldehyde, and other hydrocarbons [26]. One of the main problems encountered by plants in an *in vitro* environment is hyperhydration, which is caused by the inadequate headspace conditions in the culture vessels typically used for micropropagation. Hyperhydration results in poor plant development *in vitro* and, later, *ex vitro* [26]. Plants that are hyperhydrated often do not survive outside of their protected *in vitro* environment [27]. Using a mist

reactor, Correll *et al.* [10] were able to reduce hyperhydration in *Dianthus caryophyllus* plants by altering the mist feed rate and duty cycle

Table 1. Summary of micropropagation mist reactor studies.

Species	Inoculum	Type of Mist system	Main results	Reference
<i>Artemisia</i>	Shoots	submerged ultrasonics	higher biomass and artemisinin than liquid reactors	[33]
<i>Asparagus</i>	Shoots	submerged ultrasonics	doubled root and shoot initiation and elongation	[35]
<i>Asparagus</i>	Shoots	submerged ultrasonics	higher root and shoot initiation and elongation	[36]
<i>Brassica</i>	Anthers	spray reactor	increased regeneration versus agar	[34]
<i>Capsicum</i>	cell suspension	spray reactor	fully developed plants after 10 weeks	[39]
<i>Cinchona</i>	nodal explants	spray reactor	increased shooting; 20% higher FW weight than agar	[34]
<i>Cordyline</i>	shooting tissue	submerged ultrasonics	higher shoot production versus agar	[37]
<i>Daucus</i>	Callus and shoots	spray reactor	3.5x increase in net weight compared to agar plates	[34]
<i>Daucus</i>	Shootlets	submerged ultrasonics	induction of asexual embryoids, not in liquid or agar	[6]
<i>Daucus</i>	embryogenic callus	submerged ultrasonics	more somatic embryos than agar; none in liquid controls	[6]
<i>Dianthus</i>	node cuttings	acoustic window ¹	growth comparable to test tubes; 2x less hyperhydration	[9]
<i>Dianthus</i>	node cuttings	acoustic window ¹	hyperhydration reduced by misting scheme	[10]
<i>Dianthus</i>	node cuttings	acoustic window ¹	higher ex vitro survival than GA7 culture boxes	[11]
<i>Dianthus</i>	node cuttings	acoustic window ¹	hyperhydration reduced by higher light and CO ₂	[12]
<i>Ficus</i>	callus w/shooting meristems	spray reactor	increase in shooting	[34]
<i>Lycopersicon</i>	nodal explants	spray reactor	increase in shooting	[34]
<i>Musa</i>	shooting tissue	submerged ultrasonics	higher shoot production versus agar	[37]
<i>Nephrolepis</i>	Shoots	submerged ultrasonics	increase in shooting	[37]
<i>Nephrolepis</i>	Shoots	acoustic window ²	growth comparable to submerged ultrasonics and plates	[8]
<i>Solanum</i>	nodal explants	modified Mistifier™	growth comparable to controls	[32]
<i>Solanum</i>	nodal explants	submerged ultrasonics	98% of inocula formed tubers	[38]

1, polypropylene; 2, Conap's EN6

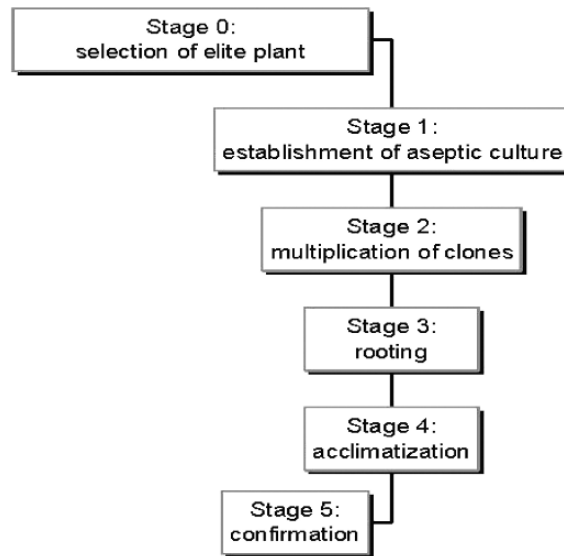


Figure 4. Stages of micropropagation.

Light intensity, CO₂, and humidity also affect hyperhydration, and the latter two conditions can be altered using mist reactors [11,12]. CO₂ enrichment has been shown to promote net photosynthesis and prepare plants for *ex vitro* acclimatization [28] and may significantly reduce the acclimatization period [29,30]. Increased CO₂ levels decreased hyperhydration in *D. caryophyllus* plants grown in the mist reactor [12], but only when used in conjunction with higher light intensity. Taken together, these studies show that hyperhydration can be reduced or eliminated using a mist reactor where gas content is regulated.

Acclimatization accounts for approximately 30% of the total production cost of micropropagation [14]. Correll and Weathers [11] used a mist reactor to grow and acclimatize carnation plants *in vitro* without using *ex vitro* acclimatization techniques, which are expensive, time-consuming, and labour-intensive [14,31]. *Ex vitro* plant survival rates were higher for plants grown in the mist reactor (91% survival) using the acclimatization protocol described in Correll and Weathers [11] versus a conventional propagation system (GA-7 culture boxes) that only had a 50% survival rate.

Multiple studies have shown that using the mist reactor in its various configurations promoted equivalent or better growth of plant inocula compared to traditional controls [8,9,32-34], increased shooting [34-37], increased formation of somatic embryos [6] and microtubers [38], and yielded higher rates of regeneration [34,39].

It should also be noted that there appears to be an unusual pattern to the spreading of contamination through the mist reactor system. While contamination is always a concern for *in vitro* systems due to the high sugar content of the medium and the fragile nature of the plant tissue, recent observations by Sharaf-Eldin and Weathers (unpublished)

suggest that areas of contamination that develop in the mist reactor growth chamber remain relatively isolated and progress more slowly than in liquid or semi-solid media. This phenomenon is presently under investigation.

Although there are many challenges that face the micropropagation industry, the most prevalent is the cost and time associated with labour. Much of the industry relies on low-wage workers from underdeveloped countries for their workforce and the economic and political instability of these countries threatens the success of this industry. The manual tasks of cutting, transplanting, and acclimatizing plant tissues are slow and increase the rates of contamination, thereby increasing loss in product and overall costs. Automation of these steps could decrease production time, lessen contamination rates, and reduce labour demands. Honda *et al.* [40] described at length an image analysis system for robotics-assisted automated selection of plant tissue in large-scale micropropagation. A mist reactor offers the potential for automating several other stages in micropropagation and combining shoot and root production with acclimatization [11].

4. Mist reactors for hairy root culture

A number of valuable pharmaceuticals, flavours, dyes, oils, and resins are plant-derived secondary metabolites. Since secondary metabolites are usually produced by specialized cells and/or at distinct developmental stages [41], plant cell suspension cultures are not usually practical sources of these chemicals. Hairy root cultures can have the same or greater biosynthetic capacity for secondary metabolite production compared to their mother plants [42,43]. Indeed, hairy roots have been considered potential production sources for important secondary metabolites [44]. A summary of studies using hairy roots in mist reactors is provided in Table 2. In nearly all cases, hairy root growth in mist reactors was as good as or better than liquid-phase cultures.

Secondary metabolism of hairy roots grown in various bioreactors has been recently reviewed by Kim *et al.* [3]. Kim *et al.* [45] noted a 3-fold increase in artemisinin accumulation in mist reactors, and subsequently, Souret *et al.* [46] provided a further analysis when they compared the expression levels of four key terpenoid biosynthetic genes in *A. annua* hairy roots grown in mist reactors versus liquid-phase systems after. Although there was notable heterogeneity in terpenoid gene expression, the differences could not be attributed directly to one single factor and were likely the result of complex interactions of multiple factors including oxygen status, presence or absence of light, culture age, and tissue location within the growth chamber of the bioreactor. Bais *et al.* [13] and Palazon *et al.* [47] likewise noted alterations in secondary metabolite content when hairy roots of *Cichorium* and *Panax*, respectively, were grown in mist reactors.

Several hairy root lines can develop mature chloroplasts capable of photosynthesis [48], and these green roots have different metabolic capabilities compared to non-green roots, although response to light is not necessarily dependent on whether the roots turn visibly green. In addition, light can have a significant effect on growth of hairy roots [49] and many enzymes in the biosynthetic pathways for secondary metabolites are regulated by light [3]. However, delivery of light into a bioreactor, especially one that is densely packed with roots, is problematic. Interestingly, the roots themselves may have light-guiding properties [50,51]. *A. annua* hairy roots were able to transmit light from a

helium-neon laser through the interior of the root (Weathers and Swartzlander, unpublished), indicating that roots may have the ability to function as leaky optical fibers.

Table 2 Summary of hairy root mist reactor studies.

Species	System	Main results	Reference
<i>Artemisia</i>	acoustic window ¹ mist reactor	growth comparable to flasks and plates	[8]
<i>Artemisia</i>	submerged ultrasonics	modified inner-loop reactor growth comparable to flasks	[69]
<i>Artemisia</i>	acoustic window ² mist reactor	no O ₂ limitation, but 50% less biomass than liquid systems	[5]
<i>Artemisia</i>	acoustic window ² mist reactor	altered branching rate versus flasks	[61]
<i>Artemisia</i>	acoustic window ² mist reactor	3 x higher artemisinin content than bubble column	[45]
<i>Artemisia</i>	acoustic window ² mist reactor	growth comparable to bubble column	[55]
<i>Artemisia</i>	acoustic window ² mist reactor	altered terpenoid gene expression versus flasks	[46]
<i>Beta</i>	submerged ultrasonic	growth comparable to flasks	[73]
<i>Carthamus</i>	submerged ultrasonics	growth comparable to flasks; 15% faster than airlift reactor	[60]
<i>Cichorium</i>	acoustic window ³ mist reactor	higher biomass and esculin content than bubble column	[13]
<i>Datura</i>	droplet reactor	1.6 x lower doubling time than submerged cultures	[74]
<i>Datura</i>	hybrid submerged/droplet reactor	successful large-scale (500 L) culture	[57]
<i>Fragaria</i>	mist reactor	biomass yield higher than droplet bioreactor	[75]
<i>Hyoscyamus</i>	spray reactor	growth comparable to shake flask	[52]
<i>Nicotiana</i>	spray reactor	50% lower doubling time than flasks	[76,77]
<i>Panax</i>	spray reactor	altered ginsenoside pattern versus native rhizome	[47]

1, Conap's EN6; 2, Teflon; 3, polycarbonate

The morphological characteristics of hairy roots demand special consideration with regards to bioreactor design. The mist reactor provides a low-shear environment for growing hairy roots and reduces gas-exchange limitations normally found in liquid-phase bioreactors. Studies by McKelvey *et al.* [52] suggested that roots are more capable of compensating for poor liquid dispersion than for poor gas dispersion within reactor systems [53]. An economically viable production scheme depends in part on the ability to attain a high biomass density. The maximum root tissue concentration that can be achieved is dependent on the delivery of oxygen and other nutrients into the dense matrix [54]. Gas-phase reactors such as the mist reactor can virtually eliminate any oxygen deficiency in dense root beds [5]. Kim *et al.* [55], however, noted that the availability of non-gaseous nutrients may be a concern; i.e. gas dispersion is improved at the expense of liquid dispersion. Furthermore, it is difficult to uniformly distribute

roots in the growth chamber of a gas-phase reactor without manual loading [3]. Several groups [44,55-57] circumvented this issue with hybrid liquid and gas-phase reactors, which were first operated as liquid-phase systems to allow the roots to circulate, distribute, and/or attach to immobilization points. Gas-phase operation could then be initiated as desired, usually when the liquid-phase reactor was no longer effective at supporting root growth due to limitations in nutrient delivery to the dense root beds. Towler and Weathers [58] have also described a method by which roots may be quickly attached to a mesh support, thereby allowing mist mode to commence shortly after inoculation.

The gas phase surrounding tissues also plays a key role in the culture and secondary metabolite productivity of hairy roots (see review by Kim *et al.* [3]). One of the major advantages of the mist reactor is the ability to alter the gas composition. Oxygen is essential for respiration and thus, the growth of roots. To assess the response of hairy roots to altered levels of oxygen in mist reactors, alcohol dehydrogenase (ADH) mRNA, an indicator of oxygen stress, was measured in *A. annua* hairy roots. Comparison of ADH mRNA expression in both shake flasks and bubble column reactors to mist reactors indicated that the mist-grown roots were not oxygen limited [5]. Roots grown in the mist reactor to a density of about 37% (v/v) had no detectable expression of ADH [59], whereas ADH mRNA was detected in roots from the bubble column at packing densities as low as 6% v/v [5]. Roots grown in the bubble column reactor, however, had higher dry mass compared to those harvested from the mist reactor. This unexpected result may be explained through modelling of mist deposition dynamics.

In addition to oxygen, carbon dioxide also affects the growth of hairy roots. CO₂-enriched nutrient mist cultures of *Carthamus tinctorius* and *Beta vulgaris* hairy roots showed increased growth versus control cultures that were fed ambient air [60]. However, a similar effect was not observed in hairy roots of *Artemisia annua*. When roots were provided mist enriched with 1% CO₂, growth was not significantly different than that of roots grown in ambient air [61], although visually the roots appeared much healthier and there was a change in the branching rate. Kim *et al.* [55] also noted similar results where the biomass accumulation was similar between root cultures grown in ambient air and those supplemented with 0.5% CO₂. It is possible that perhaps the optimum level of CO₂ enrichment for *A. annua* hairy roots was not provided to these cultures, particularly considering that the response of roots to CO₂ can vary depending on species and growth environment [1,60].

Ethylene accumulation may also be involved in regulating biomass and secondary metabolite production. Although all plant tissues can both produce and absorb the gaseous phytohormone ethylene, which has profound effects on growth, development, and even the production of secondary metabolites [62], some species of plants may produce more ethylene than others. Indeed, Biondi *et al.* [63] showed that hairy roots of *Hyoscyamus muticus* produced 3 times more ethylene than untransformed roots, and growth of *A. annua* hairy roots was significantly reduced by ethylene [64]. Sung and Huang [65] showed that hairy roots of *Stizolobium hassjoo* had lower biomass and produced lower levels of secondary metabolites when ethylene was allowed to accumulate in the headspace of the culture vessel. Recently, we also observed that ethylene, provided as ethephon, significantly inhibited both growth and artemisinin production in *A. annua* hairy roots [64]. Considering that ethylene production is

inhibited by CO₂, it is possible that the stimulation in root growth by higher levels of CO₂ is the result of inhibition of ethylene biosynthesis. Designs in reactors that scrub ethylene from the gas phase may further improve hairy root growth and promote secondary metabolite production.

5. Mist deposition modelling

Droplet transport and deposition in a bed of hairy roots may limit growth if an adequate supply of nutrients does not reach the surface of all roots. Consequently, mist deposition is a key step in the mass transfer of nutrients to the roots in a mist reactor [66]. The standard aerosol deposition model for fibrous filters was applied to mist deposition in hairy root beds by Wyslouzil *et al.* [66]. The ideal filter has evenly distributed fibres that lie perpendicular to the flow. Though root beds have regions of high and low packing density and grow in all directions, the model can still be used to study the qualitative trends of mist deposition behaviour. When the model was tested on root beds that had been manually packed to $\alpha = 0.5$ (α = volume fraction occupied by roots), it was found to correspond well to experimental data as long as the Reynolds number (Re), based on the root diameter, was <10. The Reynolds number characterizes the relative importance of inertial and viscous forces, and for filtration problems:

$$Re = \rho U_o D_R / \mu_g \quad (1)$$

where, ρ and μ_g are the density and viscosity of the carrier gas, D_R is the diameter of the root, and U_o is the gas velocity in the root bed. In terms of the number of droplets captured, the efficiency (η_B) of the root bed is a function of the particle diameter (D_p) and is equal to:

$$\eta_B = 1 - \exp [-4 L \alpha \eta_C / (\pi D_R (1-\alpha))] \quad (2)$$

where, L is the length of the root bed and:

$$\eta_C = 1 - (1 - \eta_{IMP+INT}) \times (1 - \eta_D), \quad (3)$$

the combined capture efficiency due to impaction, interception, and diffusion, respectively. Determining $\eta_{IMP+INT}$ involves solving two nonlinear equations [67], and η_D may be calculated [68]. The overall mass deposition efficiency (η_{OM}) of the root bed is the product of the root bed efficiency $\eta_B(D_{pi})$ and the mass fraction $m(D_{pi})$ of mist particles of diameter D_{pi} summed over the aerosol size distribution data:

$$\eta_{OM} = \sum_i \eta_B(D_{pi}) \times m(D_{pi}) \quad (4)$$

Typical mist particle size data were obtained experimentally by Wyslouzil *et al.* [66]. The amount of medium captured by the roots (V_{dep}) in mL per day is:

$$V_{dep} = 24 \omega \times Q_L \times \eta_{OM} \quad (5)$$

where 24 is the conversion factor from hours to days, ω is the duty cycle in minutes per hour, and Q_L is the medium flow rate in mL per minute while misting is occurring. The amount of medium required to support the growth of roots (V_{req}) depends on: the density of the roots ρ_{FW} (grams fresh weight per mL), the dry weight / fresh weight ratio (DW/FW), the specific growth rate μ (day^{-1}), the nutrient concentration in the medium C_S (g per L), the apparent biomass yield of the growth-limiting nutrient $Y_{X/S}$ (g DW biomass per g nutrient consumed), the working volume of the reactor V (L), and packing fraction α . The expression for V_{req} is:

$$V_{req} = 10^6 \rho_{FW} \times DW/FW \times \mu / C_S \times 1/Y_{X/S} \times V \times \alpha. \quad (6)$$

The growth-limiting nutrient is assumed to be sugar. Clearly, V_{dep} must be equal to or greater than V_{req} in order to maintain a desired growth rate μ .

Kim *et al.* [55] applied the model to *A. annua* hairy roots grown in the nutrient mist bioreactor, and it suggested that growth was limited by insufficient nutrient availability. This hypothesis has been tested in several ways (Towler, unpublished results). Since V_{dep} is a function of the packing fraction (α), increasing α should increase V_{dep} and thus support a higher growth rate by allowing more nutrients to be captured by the roots. To test this hypothesis, the nutrient mist bioreactor described by Weathers *et al.* [5] was modified whereby the growth chamber was replaced with a much smaller (~45 mL volume, ~30 mm diameter) cylinder into which roots were manually inoculated at an initial packing fraction of 0.29. The system was then immediately run in mist mode rather than as a hybrid liquid- and gas-phase reactor. While Kim *et al.* [55] commenced mist mode at packing fractions that were at most 0.05 and observed an average specific growth rate of 0.07 day^{-1} , the average growth rate in the modified mist reactor was 0.12 day^{-1} for a 6-day period. Due to the disparity in culture times and other operating conditions, direct comparison between these systems is difficult; however, roots grown in the modified mist reactor had higher growth rates compared to those obtained by Kim *et al.* [55], thereby supporting the hypothesis that initial inoculum density influences subsequent growth in mist reactors.

Alternatively, since V_{req} is inversely proportional to the concentration of the limiting nutrient C_S , increasing C_S should decrease V_{req} . Using the smaller modified mist reactor previously described, *A. annua* hairy roots were fed to the medium containing either 3% or 5% sucrose. After 6 days, roots grown with 5% sucrose had a significantly higher specific growth rate compared to roots grown in 3% sucrose (0.18 days^{-1} and 0.12 days^{-1} for 5% and 3% sucrose, respectively). Studies are currently underway to determine whether increasing the sucrose concentration further can further increase the growth rate.

While the model suggests that lengthening the duration of the misting cycle increases the amount of nutrients delivered to the roots and should thereby increase growth, this solution is actually more complex. For reasons as yet unknown, the misting cycle plays a significant role in the successful operation of a mist bioreactor. Liu *et al.* [69] found that a misting cycle of 3 min on / 30 min off was the optimum of those tested for transformed roots of *A. annua* grown in their nutrient mist bioreactor, though its design and operating conditions were different than those implemented by Weathers *et al.* [5]. Liu *et al.* [69] provided gas either only when mist was not being generated, or

continuously; while Weathers *et al.* [5] provided gas only when the mist was provided. Interestingly, DiIorio *et al.* [60] also observed that hairy roots seemed to have optimum mist duration for growth. Their studies with hairy roots of *Beta vulgaris* and *Carthamus tinctorius* showed that either increasing or decreasing the “off” time beyond a certain limit adversely affected root growth of those species. Chatterjee *et al.* [9] found that a mist cycle of 1 min on / 15 min off caused transformed roots of *A. annua* to darken and become necrotic after 12 d. Yet, studies with a single transformed root of *A. annua* [61] showed that a mist cycle of 1 min on / 15 min off promoted healthier-looking roots and higher fresh final biomass yields versus the other cycles tested. Studies by Towler (unpublished results) in which the misting cycle was modified so that the mass flow rate of sucrose was maintained while the sucrose concentration varied indicated that root growth could be increased by increasing the length of misting cycle while decreasing the mist off time. These results support the hypothesis that in a mist reactor, higher growth yields can be achieved with increased droplet deposition and by manipulating the on/off cycle period.

Droplet size and orientation of flow must also be considered for optimal growth and secondary metabolite production of hairy root cultures. If the droplet size is too large, the formation of a liquid layer along the root surface will impede gas transfer to the roots and the system will behave as if it were a liquid-phase reactor [62]. Similarly, when mist is provided in an upward direction, the mist can coalesce on the roots closest to the mist feed with less mist reaching the tissue in the higher layers of the growth chamber. Liu *et al.* [69] constructed an upward-fed mist reactor with three layers of stainless steel mesh to support the roots, and found that there was a greater than 50% decrease in biomass between the first (bottom) layer and the second and third layers. Likewise, necrosis was observed in hairy roots of clone YUT16 of *A. annua* using upflow mist delivery [9], but not with downflow mist delivery [61]. It is also likely that as the root bed becomes very dense, the lower sections will accumulate liquid and essentially become submerged. Mist reactors that are top fed have the advantage of co-current down-flow of gas and liquid phases along with gravity, which facilitates drainage. In contrast, top versus bottom mist feeding seems to be of less consequence in micropropagation systems and the orientation chosen is often a matter of convenience.

Another factor that may play a role in the growth of hairy roots is that of conditioned medium. Both Chatterjee *et al.* [9] and Wyslouzil *et al.* [61] used autoclaved medium with varying degrees of pre-conditioning by pre-growing roots in the medium before using it in subsequent experiments. Wyslouzil *et al.* [61] also showed that there were higher branching rates when roots were grown in conditioned medium versus fresh medium. The identity of these “conditioning factors” remains elusive, although studies have characterized some of them as oligosaccharides [70], peptides [71], and auxins [64]. For consistency, it is recommended that fresh, filter-sterilized medium be used in all experiments [72]. Work from our lab has routinely used filter-sterilized medium for experiments since 1999.

6. Conclusions

Plant tissues are highly responsive to gases in their environment, especially O₂, CO₂, and ethylene. Due to the low solubility of these gases, mass transfer of these gases to

the roots is hindered in a liquid system. Attempting to enhance gas transport by stirring, bubbling, or sparging the liquid can damage shear-sensitive plant tissues. Therefore, gas-phase reactors show many advantages over liquid-phase reactors, especially in terms of the ability to easily manipulate gas composition in micropropagation chambers and allow effective gas exchange in densely growing biomass. However, the interactions between plant tissues and the nutrient mist environment can be complex with many differing design aspects dictated by the application. For example, compare the design of the growth chamber and the misting regimens required for growing hairy roots vs. micropropagated plantlets (Figures 1 and 2). A better understanding of the biological responses of the cultured tissues must be developed in order for mist reactors to be exploited to their fullest potential. Recent results are promising and further studies are warranted.

Acknowledgements

The authors thank Sev Ritchie for assistance with reactor construction, and the following agencies for funding some of the described work: DOE P200A50010-95, NSF BES-9414858, USDA 93-38420-8804, and NIH 1R15 GM069562-01.

References

- [1] Weathers, P.J. and Zobel, R.W. (1992) Aeroponics for the cultures of organisms, tissues and cells. *Biotech. Adv.* 10: 93-115.
- [2] Friberg, J.A.; Weathers, P.J. and Gibson, D.G. (1992) Culture of amebocytes in a nutrient mist bioreactor. *In Vitro Cell. Dev. Biol.-Plant* 28A: 215-217.
- [3] Kim, Y.; Wyslouzil, B.E. and Weathers, P.J. (2002) Secondary metabolism of hairy root cultures in bioreactors. *In Vitro Cell. Dev. Biol.-Plant* 38: 1-10.
- [4] Perry, R.H. and Green, D.W. (1997) *Perry's Chemical Engineer's Handbook*, 7th ed., McGraw-Hill, New York; pp.14-82.
- [5] Weathers, P.J.; Wyslouzil, B.E.; Wobbe, K.K.; Kim, Y.J. and Yigit, E. (1999) Workshop on bioreactor technology. The biological response of hairy roots to O₂ levels in bioreactors. *In Vitro Cell. Dev. Biol.-Plant* 35: 286-289.
- [6] Tisserat, B.; Jones, D. and Galletta, P.D. (1993) Construction and use of an inexpensive *in vitro* ultrasonic misting system. *Hort. Technol.* 3: 75-78.
- [7] Woo, S.H. and Park, J.M. (1993) Multiple shoot culture of *Dianthus caryophyllus* using mist culture system. *Biotechnol. Techn.* 7: 697-702.
- [8] Buer, C.S.; Correll, M.J.; Smith, T.C.; Towler, M.J.; Weathers, P.J.; Nadler, M.; Seaman, J. and Walcerz, D. (1996) Development of a nontoxic acoustic window nutrient-mist bioreactor and relevant growth data. *In Vitro Cell. Dev. Biol.-Plant* 32: 299-304.
- [9] Chatterjee, C.; Correll, M.J.; Weathers, P.J.; Wyslouzil, B.E. and Walcerz, D.B. (1997) Simplified acoustic window mist bioreactor. *Biotechnol. Techn.* 11: 155-158.
- [10] Correll, M.J.; Wu, Y. and Weathers, P.J. (2001) Controlling hyperhydration of carnations (*Dianthus caryophyllus* L.) grown in a mist reactor. *Biotechnol. Bioeng.* 71: 307-314.
- [11] Correll, M.J. and Weathers, P.J. (2001) One-step acclimatization of plantlets using a mist reactor. *Biotechnol. Bioeng.* 73: 253-258.
- [12] Correll, M.J. and Weathers, P.J. (2001) Effects of light, CO₂ and humidity on carnation growth, hyperhydration and cuticular wax development in a mist reactor. *In Vitro Cell. Dev. Biol.- Plant* 37: 405-413.
- [13] Bais, H.P.; Suresh, B.; Raghavarao, K.S.M.S. and Ravishankar, G.A. (2002) Performance of hairy root cultures of *Cichorium intybus* L. in bioreactors of different configurations. *In Vitro Cell. Dev. Biol.-Plant* 38: 573-580.

- [14] Ilan, A. and Khayat, E. (1997) An overview of commercial and technological limitations to marketing of micropropagated plants. *Acta Hort.* 447: 642-648.
- [15] DeBergh, P.C. and Maene L.J. (1981) A scheme for commercial micropropagation of ornamental plants by tissue culture. *Sci. Hort.* 14: 336-345.
- [16] Cassells, A.C. (1997) Pathogen and microbial contamination management in micropropagation - an overview. In: Cassells, A.C. (Ed.) *Pathogen and Microbial Contamination Management in Micropropagation*. Kluwer Academic Publishers, Dordrecht, The Netherlands; pp. 1-14.
- [17] Sutter, E.G.; Shackel, K. and Diaz, J.C. (1992) Acclimatization of tissue cultured plants. *Acta Hort.* 314: 115-119.
- [18] Hempel, M. (1993) From micropropagation to "microponics". *Practical Hydroponics International*, November/December: 21-23.
- [19] Zobel, R.W. (1987) Gaseous compounds of soybean tissue culture: carbon dioxide and ethylene evolution. *Environ. Exp. Bot.* 27: 223-226.
- [20] Lee, C.W.T. and Shuler, M.L. (1991) Different shake flask closures alter gas phase composition and ajmalicine production in *Catharanthus roseus* cell suspensions. *Biotechnol. Techn.* 5: 173-178.
- [21] Kozai, T. (1991) Photoautotrophic micropropagation. In *Vitro Cell. Dev. Biol.- Plant* 27: 47-51.
- [22] Ziv, M. (1991) Vitrification: morphological and physiological disorders of *in vitro* plants. In: DeBerge, P.C. and Zimmerman, R.H. (Eds.) *Micropropagation*. Kluwer Academic Publishers, Dordrecht, The Netherlands; pp. 45-69.
- [23] Kirdmanee, C.; Kitaya, Y. and Kozai, T. (1995) Effects of CO₂ enrichment and supporting material *in vitro* on photoautotrophic growth of Eucalyptus plantlets *in vitro* and *ex vitro*. In *Vitro Cell. Dev. Biol.- Plant* 31: 144-149.
- [24] Diaz-Perez J.C.; Shackel K.A. and Sutter E.G. (1995) Effects of *in vitro*-formed roots and acclimatization on water status and gas exchange of tissue cultured apple shoots. *J. Am. Soc. Hort. Sci.* 120: 435-440.
- [25] Lowe, K.C.; Anthony, P.; Power, J.B. and Davey, M.R. (2003) Invited review: novel approaches for regulating gas supply to plant systems *in vitro*: application and benefits of artificial gas carriers. In *Vitro Cell. Dev. Biol.- Plant* 39: 557-566.
- [26] Ziv, M. (2000) Bioreactor technology for plant micropropagation. In: Janick, J. (Ed.) *Horticultural Reviews*. John Wiley and Sons, New York; pp.1-30.
- [27] Nairn, B.J.; Furneaux, R.H. and Stevenson, T.T. (1995) Identification of an agar constituent responsible for hydric control in micropropagation of radiata pine. *Plant Cell Tissue Org. Cult.* 43: 1-11.
- [28] Kanechi, M.; Ochi, M.; Abe, M.; Inagaki, N. and Mackawa, S. (1998) The effects of carbon dioxide enrichment, natural ventilation, and light intensity on growth, photosynthesis, and transpiration of cauliflower plantlets cultured *in vitro* photoautotrophically and photomixotrophically. *J. Am. Soc. Hort. Sci.* 123: 176-181.
- [29] Solarova, J. and Pospisilova, J. (1997) Effects of carbon dioxide enrichment during *in vitro* cultivation and acclimation to *ex vitro* conditions. *Biol. Plant.* 39: 23-30.
- [30] Pospisilova, J.; Ticha, I.; Kadlec, P.; Haisel, D. and Plzakova, S. (1999) Acclimatization of micropropagated plants to *ex vitro* conditions. *Biol. Plant.* 42: 481-497.
- [31] Fila, G.; Ghashghaie, J.; Hoarau, J. and Cornic, G. (1998) Photosynthesis, leaf conductance, and water relations of *in vitro* cultured grapevine rootstock in relation to acclimatization. *Physiol. Plant.* 102: 411-418.
- [32] Kurata, K.; Ibaraki, Y. and Goto, E. (1991) System for micropropagation by nutrient mist supply. *Am. Soc. Agricult. Engineers* 34: 621-624.
- [33] Liu, C.Z.; Guo, C.; Wang, Y.C. and Ouyang, F. (2002) Comparison of various bioreactors on growth and artemisinin biosynthesis of *Artemisia annua* L. shoot cultures. *Process Biochem.* 39: 45-49.
- [34] Weathers, P.J. and Giles, K.L. (1988) Regeneration of plants using nutrient mist culture. In *Vitro Cell. Dev. Biol.- Plant.* 24: 727-732.
- [35] Cheetham, R.D.; Weathers, P.; DiLorio, A.; Glubiak, M. and Mikloiche, C. (1990) *In vitro* growth of a recalcitrant male asparagus cultivar. Abstracts VII Intl. Congress on Plant Tissue and Cell Culture. Amsterdam, The Netherlands, 24-29 June, 94.
- [36] Cheetham, R.D.; Mikloiche, C.; Glubiak, M. and Weathers, P. (1992) Micropropagation of a recalcitrant male asparagus clone (MD 22-8). *Plant Cell Tissue Org. Cult.* 31: 15-19.
- [37] Weathers, P.J.; Cheetham, R.D. and Giles, K.L. (1988) Dramatic increases in shoot number and lengths for *Musa*, *Cordyline*, and *Nephrolepis* using nutrient mists. *Acta Hort.* 230: 39-44.

- [38] Hao, Z.; Ouyang, F.; Geng, Y.; Deng, X.; Hu, Z. and Chen, Z. (1998) Propagation of potato tubers in a nutrient mist bioreactor. *Biotechnol. Techn.* 12: 641-644.
- [39] Mavituna, F. and Park, J.M. (1986) Improvements relating to biotransformation reactions. International Patent Application # PCT/GB85/00508.
- [40] Honda, H.; Liu, C. and Kobayashi, T. (2001) Large-scale plant micropropagation. *Adv. Biochem. Eng. Biotechnol.* 72: 157-182.
- [41] Balandrin, M.F.; Klocke, J.A.; Wurtele, E.S. and Bollinger, W.H. (1985) Natural plant chemicals: sources of industrial and medicinal materials. *Science* 228: 1154-1160.
- [42] Banerjee, S.; Rahman, L.; Uniyal, G.C. and Ahuja, P.S. (1998) Enhanced production of valepotriates by *Agrobacterium rhizogenes* induced hairy root cultures of *Valeriana wallichii* DC. *Plant Sci.* 131: 203-208.
- [43] Kittipongpatana, N.; Hock, R.S. and Porter, J.R. (1998) Production of solasodine by hairy root, callus, and cell suspension cultures of *Solanum aviculare*. *Forst. Plant Cell Tissue Org. Cult.* 52: 133-143.
- [44] Flores, H.E. and Curtis, W.R. (1992) Approaches to understanding and manipulating the biosynthetic potential of plant roots. *Ann. NY Acad. Sci.* 665: 188-209.
- [45] Kim, Y.; Wyslouzil, B.E. and Weathers, P.J. (2001) A comparative study of mist and bubble column reactors in the *in vitro* production of artemisinin. *Plant Cell Rep.* 20: 451-455.
- [46] Souret, F.F.; Kim, Y.J.; Wyslouzil, B.E.; Wobbe, K.K. and Weathers, P.J. (2003) Scale-up of *Artemisia annua* L. hairy roots cultures produces complex patterns of terpenoid gene expression. *Biotechnol. Bioeng.* 83: 653-667.
- [47] Palazon, J.; Mallol, A.; Eibl, R.; Lettenbauer, C.; Cusido, R.M. and Pinol, M.T. (2003) Growth and ginsenoside production in hairy root cultures of *Panax ginseng* using a novel bioreactor. *Planta Medica* 69: 344-349.
- [48] Flores, H.E.; Yao-Rem, D.; Cuello, J.L.; Maldonado-Mendoza, I.E. and Loyola-Vargas, V.M. (1993) Green roots: photosynthesis and photoautotrophy in an underground plant organ. *Plant Physiol.* 101: 363-371.
- [49] Taya, M.; Sato, H.; Masahiro, K. and Tone, S. (1994) Characteristics of pak-bung green hairy roots cultivated under light irradiation. *J. Ferment. Bioeng.* 78: 42-48.
- [50] Mandoli, D.F. and Briggs, W.R. (1982) Optical properties of etiolated plant tissues. *Proc. Natl. Acad. Sci.* 79: 2902-2906.
- [51] Mandoli, D.F. and Briggs, W.R. (1983) Physiology and optics of plant tissues. *What's New in Plant Physiology* 14: 13-16.
- [52] McKelvey, S.A.; Gehrig, J.A.; Holar, K.A. and Curtis, W.R. (1993) Growth of plant root cultures in liquid- and gas-dispersed reactor environments. *Biotechnol. Prog.* 9: 317-322.
- [53] Curtis, W.R. (1993) Cultivation of roots in bioreactors. *Curr. Opin. Biotechnol.* 4: 205-210.
- [54] Curtis, W.R. (2000) Hairy roots, bioreactor growth. In: Spier, R.E. (Ed.) *Encyclopedia of Cell Biotechnology*. John Wiley and Sons, New York; pp. 827-841.
- [55] Kim, Y.J.; Weathers, P.J. and Wyslouzil, B.E. (2002a) Growth of *Artemisia annua* hairy roots in liquid- and gas-phase reactors. *Biotechnol. Bioeng.* 80: 454-464.
- [56] Ramakrishnan, D.; Salim, J. and Curtis, W.R. (1994) Inoculation and tissue distribution in pilot-scale plant root culture bioreactors. *Biotechnol. Techn.* 8: 639-644.
- [57] Wilson, D.G. (1997) The pilot-scale cultivation of transformed roots. In: Doran, P.M. (Ed.) *Hairy Roots: culture and applications*. Gordon and Breach / Harwood Academic, UK; pp. 179-190.
- [58] Towler, M.J. and Weathers, P.J. (2003) Adhesion of plant roots to poly-L-lysine coated polypropylene substrates. *J. Biotechnol.* 101:147-155.
- [59] Kim, Y.J. (2001) Assessment of bioreactors for transformed root cultures. Ph.D thesis, Worcester Polytechnic Institute, Worcester, MA.
- [60] DiIorio, A.A.; Cheetham, R.D. and Weathers, P.J. (1992) Growth of transformed roots in a nutrient mist bioreactor: reactor performance and evaluation. *Appl. Microbiol. Biotechnol.* 37: 457-462.
- [61] Wyslouzil, B.E.; Waterbury, R.G. and Weathers, P.J. (2000) The growth of single roots of *Artemisia annua* in nutrient mist bioreactors. *Biotechnol. Bioeng.* 70:143-150.
- [62] Weathers, P.J. and Wyslouzil, B.E. (2000) Bioreactors, mist. In: Spier, R.E. (Ed.) *Encyclopedia of Cell Technology*. John Wiley and Sons, New York; pp. 224-230.
- [63] Biondi, S.; Lenzi, C.; Baraldi, R. and Bagni, N. (1997) Hormonal effects on growth and morphology of normal and hairy roots of *Hyoscyamus muticus*. *J. Plant Growth Regul.* 16: 159-167.
- [64] Weathers, P.J.; Bunk, G. and McCoy, M. (2005) The effect of phytohormones on growth and artemisinin production in *Artemisia annua* hairy roots. *In Vitro Cell. Dev. Biol.- Plant*, accepted for publication.

- [65] Sung, L.S. and Huang, S.Y. (2000) Headspace ethylene accumulation in *Stizolobium hassjoo* hairy root culture producing L-3,4-dihydroxyphenylalanine. *Biotechnol. Lett.* 22: 875-878.
- [66] Wyslouzil, B.E.; Whipple, M.; Chatterjee, C.; Walcerz, D.B.; Weathers, P.J. and Hart, D.P. (1997) Mist deposition onto hairy root cultures: aerosol modeling and experiments. *Biotechnol. Prog.* 13: 185-194.
- [67] Crawford, M. (1976) *Air Pollution Control Theory*. McGraw-Hill, New York; pp.424-433.
- [68] Friedlander, S.K. (1977) In: *Smoke, Dust and Haze: Fundamentals of Aerosol Behavior*. Wiley, New York.
- [69] Liu, C.Z.; Wang, Y.C.; Zhao, B.; Guo, C.; Ouyang, F.; Ye, H.C. and Li, G.F. (1999) Development of a nutrient mist bioreactor for growth of hairy roots. *In Vitro Cell. Dev. Biol.- Plant* 35: 271-274.
- [70] Schroder, R.; Gertner, F.; Steinbrenner, B.; Knoop, B. and Beiderbeck, R. (1989) Viability factors in plant suspension cultures – some properties. *J. Plant Physiol.* 135: 422-427.
- [71] Matsubayashi, Y. and Sakagami, Y. (1996) Phytosulfokine, sulfated peptides that induce the proliferation of single mesophyll cells of *Asparagus officinalis* L. *Proc. Natl. Acad. Sci. USA* 93: 7623-7627.
- [72] Weathers, P.J.; DeJesus-Gonzalez, L.; Kim, Y.J.; Souret, F.F. and Towler, M. (2004) Alteration of biomass and artemisinin production in *A. annua* hairy roots by media sterilization method and sugars. *Plant Cell Rep.* DOI: 10.1007/s00299-004-0837-4.
- [73] Weathers, P.J.; DiLorio, A.A. and Cheetham, R.D. (1989) A bioreactor for differentiated plant tissues. In: *Proceedings of the Biotech USA Conference*, San Francisco, CA, 247-256.
- [74] Wilson, P.D.G.; Hilton, M.G.; Meehan, P.T.H.; Waspe, C.R. and Rhodes, M.J.C. (1990) The cultivation of transformed roots from laboratory to pilot plant. In: Nijkamp, H.J.J.; van der Plas, L.H.W. and van Aartrijk, J. (Eds.) *Progress in Plant Cellular and Molecular Biology*. Kluwer Academic Publishers, Dordrecht, The Netherlands; pp. 700-705.
- [75] Nuutila, A.M.; Lindqvist, A.S. and Kauppinen, V. (1997) Growth of hairy root cultures of strawberry (*Fragaria x. ananassa* Duch.) in three different types of bioreactors. *Biotechnol. Techn.* 11: 363-366.
- [76] Whitney, P.J. (1990) Novel bio-reactors for plant root organ cultures. *Abstracts VII Intl. Cong. Plant Tissue Cell Cult.*, Amsterdam, The Netherlands; Abstract C4-19, 342.
- [77] Whitney, P. (1992) Novel bioreactors for the growth of roots transformed by *Agrobacterium rhizogenes*. *Enz. Microbiol. Technol.* 14: 13-17.

BIOREACTOR ENGINEERING FOR RECOMBINANT PROTEIN PRODUCTION USING PLANT CELL SUSPENSION CULTURE

WEI WEN SU

Department of Molecular Biosciences and Bioengineering, University of Hawaii, Honolulu, Hawaii 96822, USA – Fax: 1-808-956-3542 – Email: wsu@hawaii.edu

1. Introduction

Plant cell culture has long been considered as a potential system for large-scale production of secondary metabolites. In recent years, with the advances in plant molecular biology, plant cell culture has also attracted considerable interests as an expression platform for large-scale production of high-value recombinant proteins. Many plant species can now be genetically transformed. Callus cells derived from the transgenic plants can be grown in simple, chemically defined liquid media to establish transgenic cell suspension cultures for recombinant protein production. For certain plant species, such as tobacco, it is also possible to establish transgenic suspension cell cultures by directly transforming wild-type cultured cells. There are several notable benefits of using plant suspension cultures for recombinant protein production. Plant cells, unlike prokaryotic hosts, are capable of performing complex post-translational processing, such as propeptide processing, signal peptide cleavage, protein folding, disulfide bond formation and glycosylation, which are required for active biological functions of the expressed heterologous proteins [1]. Plant cells are also easier and less expensive to cultivate in liquid media than their mammalian or insect cell counterparts. The potential human pathogen contamination problem associated with mammalian cell culture does not exist in plant cell culture since simple, chemically defined media are used [2]. When compared with transgenic plants, cultured plant cells also possess a number of advantages. Cultured plant cells have a much shorter growth cycle than that of transgenic plants grown in the field. Plant cell cultures are grown in a confined environment (*i.e.* enclosed bioreactor) and hence devoid the GMO release problem. Furthermore, cell suspension cultures consist of dedifferentiated callus cells lacking fully functional plasmodesmata and hence there is minimum cell-to-cell communication. This may reduce systemic post-transcriptional gene silencing (PTGS) which is believed to be transmitted *via* plasmodesmata and the vascular system [3,4]. On the down side, plant cells generally have a longer doubling time than bacterial or yeast cells. Genetic instability associated with de-differentiated callus cells due to somaclonal variation is another potential drawback in using cultured plant cells for recombinant protein production. Due in part to their more evolved and more tightly controlled gene/protein

regulation machinery, it is more difficult to manipulate protein expression in plant cells, rendering a generally lower protein expression level, normally between 0.1-1 mg L⁻¹ of culture [2], although product level as high as 129 mg L⁻¹ has also been reported in the case of recombinant human granulocyte-macrophage colony stimulating factor (hGM-CSF) production in transgenic rice cell suspension culture [5].

Plant cell cultures have been used for producing a variety of recombinant proteins. Several research groups have reported expression of antibodies or antibody fragments in plant cell suspension cultures. Some notable examples are the expression of a secretory anti-phytochrome single-chain Fv (scFv) antibody [6], a TMV-specific recombinant full-size antibody [7], a mouse IgG1 recognizing a cell-surface protein of *Streptococcus* mutants [8], and a mouse scFv [7,9], all using tobacco suspension culture. A number of therapeutic proteins have also been expressed in plant cell cultures, including Hepatitis B surface antigen (HBsAg) [10], human cytokines such as Interleukin IL-2, IL-4 [11], IL-12 [12], and GM-CSF [5,13], ribosome-inactivating protein [14], and human α_1 -antitrypsin [15,16]. Readers are also referred to other comprehensive reviews on the subject of recombinant protein expression in plant tissue cultures [2,4,17].

Plant cell culture processes for recombinant protein production resemble conventional recombinant fermentation processes in that they also encompass upstream and downstream processing. However, there are distinctive properties associated with plant cells that call for unique approaches in designing and operating plant cell bioprocesses. The emphasis of this review will be on the upstream processing; specifically, on the engineering considerations associated with the design and operation of bioreactors for recombinant protein production using plant cell suspension cultures. While much of the knowledge derived from the development of plant cell bioreactors for secondary metabolite production are still relevant, issues unique to recombinant protein production will be emphasized in this chapter. New findings since the publications of other recent reviews of plant cell bioreactor [18,19] will be highlighted. Effective bioreactor design and operation assures high productivity which is key to successful bioprocess development. This chapter will begin with an overview of the unique properties of plant cell cultures relevant to bioreactor design. Next, characteristics of recombinant protein expression in plant cell culture are reviewed. This is followed by discussions on a number of key topics relevant to bioreactor engineering, including plant cell bioreactor operating strategies, bioreactor configurations and impeller design, and innovative process sensing, as pertinent to recombinant protein production.

2. Culture characteristics

Plant cell suspension cultures are derived from callus cells. These are unorganized, generally undifferentiated cells [20]. When suspended in liquid media, cells are sloughed off friable calli to form a culture suspension. An effective plant cell suspension culture system for recombinant protein production is expected to possess certain desirable features, including fast growth rate, ease of genetic transformation, high protein expression capacity, low endogenous proteolytic activity, low content of phenolics (which may form complexes with proteins and complicates protein purification) and other phytochemicals (such as oxalic acid) that may interfere with downstream processing, superior post-translational processing capability, and good

culture stability (*i.e.* with low degrees of somaclonal variation and transgene silencing). The most widely reported host species for developing plant suspension cultures to produce recombinant proteins is tobacco (*Nicotiana tabacum*), followed by rice (*Oryza sativa*). Other plant species such as tomato [21] and ginseng [22] have also been used. Tobacco suspension culture is most widely used owing to its desirable growth characteristics and ease of genetic transformation. However, it has been reported that recombinant hGM-CSF is subject to more severe proteolytic degradation in the tobacco cell culture medium than in the rice culture medium [5]. Therefore, while tobacco is a convenient host, plant host species remains a factor to be considered in optimizing recombinant protein production in plant suspension cultures. As far as bioreactor development is concerned, the most relevant culture characteristics for recombinant-protein production include:

- Cell morphology, degree of aggregation, and culture rheology
- Foaming and wall growth
- Shear sensitivity
- Growth rate, oxygen demand, and metabolic heat evolution.

2.1. CELL MORPHOLOGY, DEGREE OF AGGREGATION, AND CULTURE RHEOLOGY

Plant cells in suspension cultures display a range of shapes, with the largely spherical and the rod (sausage-like) shapes being the most common. Size of single plant cells is typically in the range of 50-100 μm . Suspension cultures normally exhibit various degrees of cell aggregation with the aggregate sizes varying dependent on the plant species, growth stage, and culture conditions. While some plant cells form fine suspensions with few large aggregates (with the largest aggregates smaller than 1 mm), such as *N. tabacum* [5,23] and *Anchusa officinalis* [24], others form huge aggregates as large as 2 cm in diameter, as in the case of *Panax ginseng* suspension culture used in the Nitto Denko ginseng process [25] (cited in [18]). Formation of cell aggregates is mainly due to the tendency of the cells to not separate after division. Cell adhesion due to the presence of cell wall extra-cellular polysaccharides may enhance cell clumping especially in the later stages of growth [26] (and references cited within). Cell aggregates may consist of a mixture of highly mitotic and less mitotic cells (the latter usually have greater potential for cellular differentiation into adventitious tissues or organs). Cell aggregation promotes cellular organization and differentiation which is generally believed to benefit secondary metabolite production, although in some cases secondary metabolite production was found to be independent of aggregate sizes, such as ajmalicine production in *Catharanthus roseus* culture [27] (cited in [18]). It appears what is important for secondary metabolite production may not be the size of the aggregates, but the state of organization and cellular differentiation within the cell aggregates, which may not be entirely dependent on the aggregate size. For recombinant protein production, cellular organization and differentiation potential is not as important, and thus cell aggregation is generally viewed as undesirable since such feature complicates the bioreactor operation. To this end, presence of oxygen/nutrient gradients in complex cell clumps and sedimentation of large cell clumps are two apparent problems. Formation of large cell clumps also complicates fluid pumping of the culture

broth for downstream processing. Separating and dispersing the cells from the aggregates by mechanical means in a bioreactor (*e.g.* by increasing bioreactor agitation) is usually not very effective and may lead to cell damage, or even larger aggregates [18]. Addition of pectinase and cellulase, higher cytokinin concentration, or lower calcium concentration in the media may help to reduce the aggregate size [28]. However, the high cost associated with adding the hydrolytic enzymes at large scale prevents the use of such strategy in industrial bioprocesses. It has been shown that over-expression of bacterial secretory cellulases leads to improved plant biomass conversion [29]. It is plausible, therefore, to engineer plant cells to over-express cell wall bound or secreted pectinase and/or cellulase as a means to control aggregate size in the suspension culture; although its feasibility is yet to be tested.

Similar to the degree of cell aggregation, cultured cell morphology also depends on the plant species, growth stage, and culture conditions. Suspension tobacco cell cultures are often used for the expression of recombinant proteins. Under usual batch culture conditions (*e.g.* in commonly used MS or B5 medium supplemented with auxin 2,4 -D and 2-3% sucrose or glucose), the majority of suspension tobacco cells typically form un-branched chains consisting of multiple sausage-shaped cells. Plant cell elongation occurs after cell division ceases [30], it is tightly regulated (*e.g.* controlled by expansin [30] and is believed to involve polar auxin transport [31]. Arrest of cell cycle by over-expressing cell-cycle inhibitor, while stops cell division, may also lead to cell elongation [32]. Curtis and Emery [33] reported that when carrot cultures maintained on a 7-day subculture interval were switched to a 14-day subculture interval, the cells changed from spherical to elongated morphology. It is plausible, in the culture with a longer subculture interval, cell division was slowed down due to nutrient limitation and cell elongation was switched on. Cell elongation characteristics thus might be altered by adjusting the nutrient regime and/or the types and concentrations of auxin (*e.g.* NAA is known to promote cell elongation [31]) or by genetic manipulations (*e.g.* by altering the expansin expression or by arresting the cell cycle). Note that elongated, filamentous cells tend to entangle together to form a cellular network, resulting in higher packed cell volume (PCV) for a given number of cells per reactor volume (than spherical cells), and hence higher apparent viscosity. Curtis and Emery [33] reported the highly viscous and power-law type rheological properties associated with batch-cultured tobacco suspension cells were resulting from elongated cell morphology. The bioprocess implication is significant in that less biomass can be attained with cultures of elongated cells as opposed to spherical-shaped cells. When cultured in similar high-density perfusion bioreactors, and under comparable growth conditions, tobacco cell culture reached only 10 g/L dry weight (with PCV exceeding 60%), whereas *A. officinalis* cell culture (which consists of mostly spherical cells and forms fine suspension with few large aggregates) can reach cell dry weight over 35 g/L with PCV over 60% [34]. It may be possible to use molecular approaches to reduce/block auxin efflux or to manipulate cellulose biosynthesis (and hence cell wall composition and structure) to alter the morphology of the cells.

Culture rheological property significantly affects bioreactor mixing, oxygen, and heat transfer. It also affects how high cell concentrations can reach. In addition to cell size, morphology and degree of aggregation, rheological property of suspension plant cell culture is affected by cell concentration (especially in terms of biotic phase volume,

as opposed to cell numbers or cell dry weight) and cellular water content. Plant cell suspension cultures are usually considered highly viscous. This view comes from the fact that typically plant cell cultures reach a very high culture biotic phase volume fraction (PCV over 50%) even in batch cultures. The culture spent media however usually is not viscous and behaves as Newtonian fluid. Power-law models including Bingham plastics, pseudoplastics, and Casson fluids have been applied to describe the rheological properties of high-density plant cell suspension cultures [28,35]. In power-law rheological models,

$$\tau = \tau_o + K\dot{\gamma}^n \quad (1)$$

where τ is shear stress, $\dot{\gamma}$ is shear rate, K is consistency index, τ_o is yield stress, and n is the flow behaviour index. For pseudoplastic fluids, $n < 1$ and $\tau_o = 0$; for Bingham plastics, $n = 1$, and $\tau_o \neq 0$. As stated earlier, cell morphology can have a considerable influence on the culture rheological characteristics. Cultures consist of mainly large non-friable cell aggregates form very heterogeneous particulate suspensions. At low cell concentrations, these cultures typically behave more like a Newtonian fluid [33]. At high cell concentrations, the presence of a large number of large, discrete cell aggregates renders an unambiguous determination of the culture rheological properties more difficult [28]. Cultures that consist of mainly large aggregates are generally shown to be less viscous than those consists of elongated cells entangled into a filamentous cellular network [33]. Most viscous high-density plant suspension cultures exhibit shear-thinning, pseudoplastics characteristics [35,36]. In this case, the apparent culture viscosity (μ_a) is related to the shear rate as:

$$\mu_a = K\dot{\gamma}^{n-1} \quad (2)$$

implying that apparent viscosity is lower under higher shear. As such, mixing and bubble dispersion should be more efficient in the impeller region where high shear exists, whereas the region away from the impeller may experience a higher apparent viscosity and may lead to poor mixing and mass transfer. Another unique phenomenon was noted recently during high density cultures of tobacco cells (PCV over 60%; Su, unpublished) in a 3-L stirred-tank bioreactor, where cells became immobilized on standard six-blade Rushton disc turbine impellers (*i.e.* impeller became completely covered by a thick layer of plant cell biomass) to an extent that the impeller became shaping like an elliptical object. Mixing and mass transfer efficiency dropped as a result. This perhaps was triggered by an initial accumulation of entangled filamentous tobacco cell clumps in the gas-filled cavities behind the impeller blades. Since this phenomenon can cause considerable reduction in impeller performance, it warrants further investigation. In some culture systems, yield stress has been reported (*i.e.* behaving as Bingham fluids). The existence of a yield stress may impact aeration efficiency in a way that small bubbles may experience a much longer residence time and become depleted in oxygen [36]. Therefore, oxygen transfer in the bioreactor may not be efficient despite a high gas hold-up. Manipulating culture medium osmotic pressure has been shown to

reduce apparent culture viscosity in some studies [28,37]. However, increasing medium osmotic pressure generally causes plasmolysis (shrinkage of cytoplasm within the cell) but may not significantly reduce the overall cell size due to the presence of the rigid cell wall. As such, its effect on reducing culture viscosity may not result from reducing the cell size.

2.2. FOAMING AND WALL GROWTH

Plant cells are commonly cultured in bioreactors with bubble aeration, which produces foaming at the culture broth surface. A number of factors are believed to attribute to foam formation. These include presence of extra-cellular polysaccharides, proteinacious substances, fatty acids (secreted or released by lysed cells), and high sugar concentration during the early stage of cultivation [28,37]. Extent of foaming is affected by aeration rate, medium composition, culture viscosity, biomass level, and the bioreactor configuration [38]. As summarized in Abdullah *et al.* [37], common measurement techniques and parameters for characterizing culture foaming include the ratio of foam volume to gas flow rate, volume of liquid held in the foam, volumetric rate of foam overflow, and decrease of foam volume with time. As a result of culture foaming, a large amount of cells become entrapped in the foam layer, rendering reduced volumetric biomass concentration in the broth. These foam-entrapped cells develop a thick crust adhering to the reactor vessel and the probes. The accumulated cell crusts may become necrotic and secrete inhibitory substances such as proteases or superannuated cell organelles. Under severe foaming, foam overflow can clog the air vent filter and make the culture susceptible to contamination. Wall growth is also known to affect the scale up and dynamic operating characteristics of chemostats and bioreactor cultures with substrate inhibition [39]. Several strategies have been employed to combat the foaming/wall growth problem, including addition of silicone-based and polypropylene glycol antifoam agents, mechanical foam disruption, reduced bubble aeration rate, intermittent bubble aeration, bubble-free surface or membrane aeration, reduced calcium concentration in the medium, coating of reactor vessel wall with Teflon or silicone, and use of mechanical/magnetic scrapper units to push the wall-growth cell crusts back into the culture broth. Since plant cells entrapped in the foam layer have the tendency to stick to the antifoam sensor, it is difficult to use the conductive-type sensor commonly applied in microbial fermentors for monitoring foam formation and effectively control the foam by accurately triggering the automatic dosing of antifoam agents. Once the meringue-like cell crust layer is built up above the broth, addition of antifoam agents becomes less effective in suppressing further wall-growth development. Furthermore, overdosing of antifoam agents may reduce oxygen transfer since antifoam reduces surface tension, lowering the mobility of the gas/liquid interface and causing interfacial breakage [40]. Abdullah *et al.* [37] examined various strategies to overcome foaming and wall growth in the culture of *Morinda elliptica* cell suspension culture and concluded that bubble-free aeration using thin-walled silicone membrane tubing was the only strategy capable of completely eliminating wall-growth. Bubble-free membrane aeration however is not suited for large-scale bioreactors due to reduced membrane surface to volume ratio and hence reduced oxygen transfer upon scale-up. We found that at least in smaller bench-scale bioreactors, silicone-based antifoam addition and use of a magnetic scrapper (consists of two small but strong magnets, one placed on the interior reactor wall and

the other on the exterior wall to form a magnetic pair) can at least reduce the extent of wall growth of transgenic tobacco cells cultured in a sparged stirred-tank bioreactor. Under these circumstances, however, a significant foam layer still built up around the rotating shaft and the probes, leads to biomass loss. We found that by using an impeller installed above the culture broth to serve as a mechanical foam breaker was not effective in breaking up foams. On the contrary, since the rotating speed of the impeller is not sufficiently high, the cells entrapped in the foam layer actually formed a thick crust on the foam-breaker impeller. As mentioned earlier, this phenomenon was also noted even for the impellers that were immersed in the culture broth. Since none of the aforementioned strategies offer a practical solution to effectively eliminate foaming and wall growth, it remains a challenge to overcome such problem in plant cell bioreactor design. Fortunately, as the reactor is geometrically scaled up, the reactor cross-section per volume ratio drops, and the wall growth problem is expected to reduce.

2.3. SHEAR SENSITIVITY

Cultured plant cells embrace vacuoles up to 95% of cell volume and their primary cell wall is made of parallel cellulose micro fibrils embedded in a polysaccharide matrix. Therefore, plant cells are generally considered shear sensitive. However, shear sensitivity varies greatly among plant species and may be affected by the culture age. Over the past two decades several studies have been conducted to investigate how cultured plant cells respond to various shear environments. Major studies published prior to 1993 had been summarized in a review by Meijer *et al.* [41]. More recently, Kieran *et al.* [42] conducted a comprehensive review of the same subject. A number of studies in this topical area have been published by Erick Dunlop's group [43-45] and by Kieran and co workers [42,46]. Studies of the sensitivity of cultured cells to hydrodynamic forces are complicated by the difficulties to establish a defined hydrodynamic environment mimics that of the bioreactors. Shear studies have been conducted under well-defined laminar or turbulent flow conditions using capillary, jet, and Couette flows [42]. One common shortcoming in these studies is that the flow conditions in these model systems are not entirely representative of the complex turbulent flow conditions in typical bioreactors. For shear studies conducted directly in bioreactors, however, it is necessary to correlate cellular shear responses to some quantifiable bioreactor parameters, owing to the poorly defined hydrodynamic environment in the bioreactors. To this end, a number of physiological parameters have been used as indicator of cellular shear response; these include loss of viability, membrane integrity, respiratory (mitochondrial) activity, release of intracellular components, and morphological variations [41,42]. Cellular response to hydrodynamic shear is affected by the intensity as well as the exposure duration of the cells to shear stress. In this context, the cumulative energy dissipation has been suggested as a useful basis for correlating data from shear studies involving a wide range of plant species, hydrodynamic conditions, and physiological indicators [19,42,43]. The cumulative energy dissipation imposed on the cells per unit reactor working volume (E_c) can be calculated using the following equation [19,43]:

$$E_c = \int \frac{P\phi}{V_R} dt = \int \frac{\frac{P_g}{P_o} (\rho N_p N_i^3 D_i^5) \phi}{V_R} dt \quad (3)$$

where P is power input, V_R is the reactor working volume, ϕ is the biotic phase volume fraction in the culture, t is time, P_g is gassed power input, P_o is ungassed power input, ρ is broth density, N_p is the impeller power number, N_i is the impeller speed, and D_i is the impeller diameter. Figure 1 (reproduced from reference [18]) shows various shear response indices obtained under a variety of flow conditions, as a function of E_c in three different cell cultures. Each shear response index appears to be associated with a threshold level of cumulative energy dissipation, beyond which extensive reduction in cellular activity is noted. For instance, membrane integrity of *Morinda citrifolia* cells was severely damaged at a critical cumulative dissipated energy level exceeding 10^8 Jm^{-3} (Figure 1, curve d). Doran [19] compared the performance of various impeller designs for plant cell bioreactors using a threshold E_c level of 10^7 Jm^{-3} . Cumulative energy dissipation serves as a convenient index for estimating hydrodynamic shear damage. However, as indicated by Doran [19] and by Kieran [18], the application of this index also has its limitations. Effect of hydrodynamic shear on the plant cells in an aerated/stirred-tank bioreactor does not result entirely from the impeller power input; under the same impeller power input, shear damage on the cells is also anticipated to vary depending on the impeller geometry. Note that E_c is a global (average) hydrodynamic property, and hence it does not reflect how the energy dissipation rates are distributed within the reactor. The highest specific rates of energy dissipation occur near the impellers, and impellers having different sweep volumes and trailing vortex structures are expected to inflict different local shear conditions in the vicinity of the impellers [19,44]. Doran [19] and Sowana *et al.* [44] also pointed out that for impellers that produce more rapid broth circulation, cells are transported to the high-shear impeller region more frequently and hence more shear damage is expected. Another point to consider is that under gassing conditions, the impeller power input is reduced, and hence the cumulative energy dissipation is expected to decrease according to equation (3). While shear damage resulting from the hydrodynamic forces associated with bubble rupture is believed to be insignificant in plant cell cultures [18,43], there is no evidence indicating shear damage is reduced with increasing bubble aeration rates at a fixed stirrer speed. The suitability of E_c as a common basis to quantify the agitation-based shear forces under different bubble aeration rates apparently warrants further investigations.

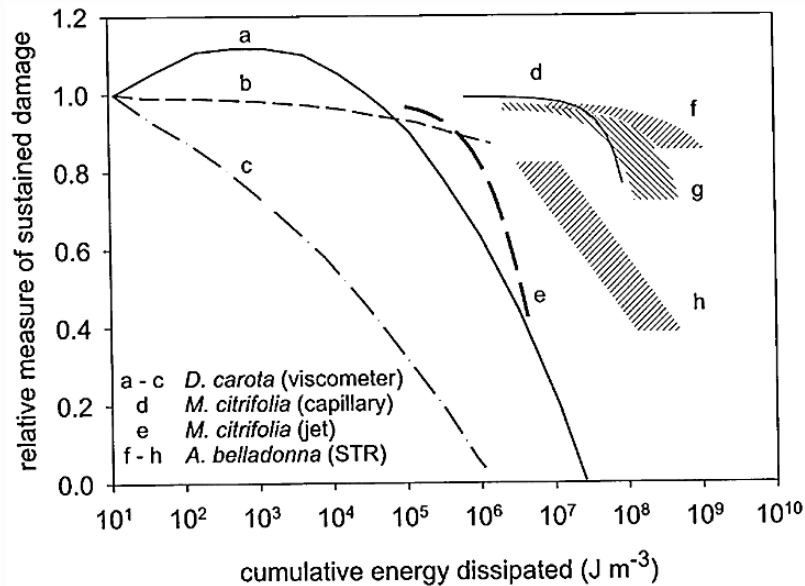


Figure 1. Cellular shear responses as a function of E_c for *Daucus carota* [43], *Morinda citrifolia* [46], and *Atropa belladonna* [38]. Shear response indicators: (a) aggregate size, (b) cell lysis, (c) mitochondrial activity, (d) – (f) membrane integrity, (g) protein release, and (h) cake permeability/aggregate size. Reproduced from Kieran, P. M. (2001) [18], with permission from Taylor and Francis.

The biological basis for cell response to hydrodynamic shear is not well understood. It has been hypothesized that calcium ion flux, osmotic regulation, cell–cell contact/aggregation, and stress protein expression might be the key processes involved in perception and responses to hydrodynamic shear [47]. In recent years, more experimental evidence has emerged indicating oxidative burst as a potentially important step in the signal transduction cascade that triggers the plant defence mechanism in response to hydrodynamic shear. Shortly after pathogenic attack, plant cells usually produce and release active oxygen species (AOS) at the cell membrane surface; these include the superoxide radicals, the hydroxyl radicals, and hydrogen peroxide [18,48]. This is known as the oxidative burst. Yahraus *et al.* [49] were among the first to present evidence for mechanically induced oxidative bursts in plant suspension cultures. Recently, Han and Yuan [48] investigated the oxidative bursts in suspension culture of *Taxus cuspidate* induced by short-term laminar shear under Couette flow condition. They found that NAD(P)H oxidase is the key enzyme responsible for oxidative bursts under shear, and the superoxide radical burst may cause changes in the membrane permeability, while hydrogen peroxide burst plays an important role in activating phenylalanine ammonia lyase and phenolic accumulation. Han and Yuan [48] further postulated that G-protein, calcium channel, and phospholipase C may be involved in the

signal transduction pathway of oxidative bursts induced by hydrodynamic shear, as depicted in the model shown in Figure 2.

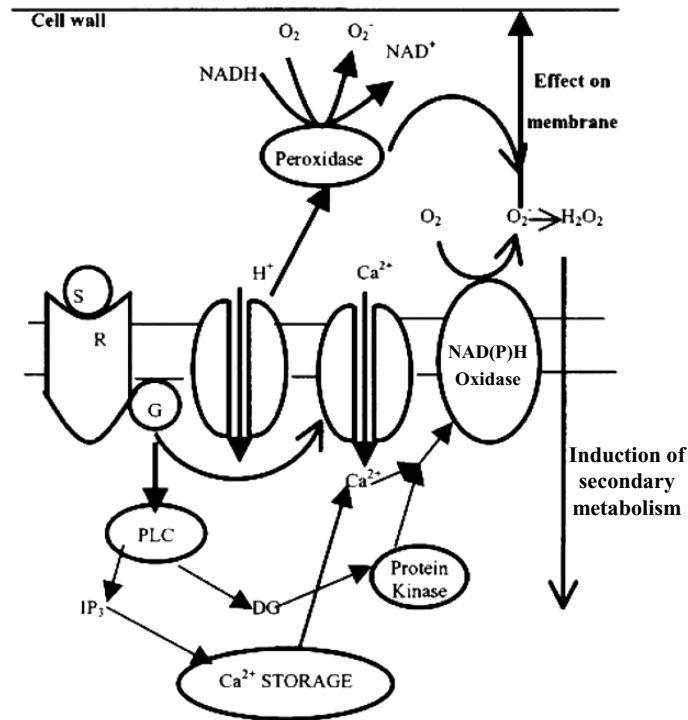


Figure 2. Hypothetical model proposed by Han and Yuan [48] for oxidative burst in cultured plant cells induced by hydrodynamic shear. (S) shear stress; (G) G-protein; (R) shear signal receptor in the cell membrane; (IP₃) inositol phosphates; (DG) diacylglycerol; (PLC) phospholipase C. Adapted from Han, R. and Yuan, Y. (2004) [48], with permission from the American Chemical Society.

According to such model, it might be possible to engineer plant cell lines that are less susceptible to shear damage by disrupting the signal pathway that leads to oxidative bursts. Alternatively, shear induced genes might be identified using DNA microarray and/or proteomics tools to further elucidate the biological basis of shear sensitivity. Thus far, two notable approaches have been demonstrated to improve plant cell tolerance to shear damage. One involves the selection of shear-tolerant strains [35] and the other the application of a non-ionic surfactant, Pluronic® F-68. Sowana *et al.* [45] reported beneficial effect of Pluronic® F-68, which has been demonstrated as an efficient protection agent of mammalian and insect cells from shear damage, on protecting cultured plant cells from hydrodynamic damage, and suggested that the protection

mechanism is likely to result from cell membrane manipulation (perhaps by reduction of plasma membrane fluidity, leading to an increase in cellular resistance to shear).

2.4. GROWTH RATE, OXYGEN DEMAND, AND METABOLIC HEAT LOADS

For recombinant protein production, plant species that generate fast-growing cell cultures are often preferred. Top the list are tobacco and rice cell cultures. Tobacco BY-2 cells are particularly appealing because of their remarkably fast growth rate, as well as the ease for *Agrobacterium*-mediated transformation and cell cycle synchronization. Doubling time as short as 11 hours has been reported for the tobacco BY-2 cells [50]. Koroleva *et al.* [51] recently demonstrated that the growth rate of BY-2 cells can be transiently increased by expressing a putative G1 cyclin gene, *Antma;CycD1;1*, from *Antirrhinum majus*; this cyclin gene is known to be expressed throughout the cell cycle in the meristem and other actively proliferating cells. Expression of *cycD2* was also shown to increase tobacco plant growth [52]. Effect of over-expressing *cycD* genes in tobacco cell cultures on cell proliferation and recombinant protein production is currently being investigated in our laboratory. Tobacco cell cultures derived from other tobacco varieties, *e.g.* *Xanthi*, do not grow as fast as the BY-2 cells, but still has a relatively short doubling time about 1.5-2 days. Gao and Lee [53] reported a doubling time of about one day for tobacco NT-1 cells (which is similar to the BY-2 cells) expressing β -glucuronidase (GUS). For rice cell culture, Trexler *et al.* [16] reported doubling time of 1.5 ~ 1.7 days for a transgenic rice cell culture expressing human α_1 -antitrypsin. Terashima *et al.* [15], on the other hand, reported a very long doubling time of 6-7 days in their transgenic rice cell cultures expressing human α_1 -antitrypsin. Maximum specific oxygen uptake rate was 0.78 ~ 0.84 mmol O₂/(gdw h) in the transgenic rice cell culture reported by Trexler *et al.* [16]; 0.4 ~ 0.5 mmol O₂/(gdw h) for the transgenic tobacco NT-1 cells expressing GUS [53]. Kieran [18] reported that specific oxygen consumption rate for plant cell cultures is generally of the order of 10⁻⁶ g O₂/(gdw s) (*i.e.* 0.11 mmol O₂/(gdw h)). Gao and Lee [53] observed improved cell growth, increased oxygen consumption rate, and GUS production with higher oxygen supply [53]. In general, if expression of the recombinant protein is driven by a constitutive promoter, expression is usually growth associated and hence factors that promote cell growth (such as improved oxygen supply) are expected to promote protein expression. Unlike plasmid-based expression in bacterial cells that lead to huge amount of over-expression, the metabolic burden resulting from foreign protein expression in plant cells is generally not high enough to substantially impact the cell growth or oxygen demand, except if the foreign gene product is toxic or able to interact with the plant metabolism to cause altered growth characteristics.

In cell cultures there generally exists a critical dissolved oxygen level, below which linear (in lieu of exponential) growth is seen as a result of oxygen limitation. The critical dissolved oxygen level in plant cell cultures is typically at 15 ~ 20% air saturation [36]. Based on the specific oxygen consumption rate, one can estimate the metabolic heat evolution since the heat of reaction for aerobic metabolism is approximately -460 J per mmol of oxygen consumed [54]. As cited in reference [18], metabolic heat evolution rate of 138 J/(g dw h) was reported by Hashimoto and Azechi [55] in a large-scale (6,340 litres of working volume) tobacco chemostat culture with an average cell density

of 17 g/L. Therefore an oxygen demand of about 0.3 mmol O₂/(gdw h) is estimated, which is in good agreement with that reported by Gao and Lee [53]. Assuming comparable heat transfer characteristics between high-density plant cell culture and viscous fungal fermentation, Kieran [18] suggests that efficient heat removal in plant cell bioreactors can be easily achieved even with moderate mixing.

Tolerance to low-oxygen stress by cultured plant cells is expected to be species dependent. While physiological responses of bioreactor-cultured plant cells/hairy roots to extended hypoxic stress (at the molecular level) is not well documented, it is generally believed that engineering plant cells for improved hypoxic stress tolerance is desirable, or even necessary, to complement the bioreactor design to combat the oxygen supply problem in large-scale plant cell bioreactor, especially for high-density cultures. Two notable approaches have been taken to engineer cultured plant cells and/or hairy roots for improved tolerance to hypoxic stress. In one approach, it involves over-expression of bacterial or plant haemoglobin genes [56,57]. In another approach, Doran and co-workers [58] found that hairy roots over-expressing either *Arabidopsis* pyruvate decarboxylase or alcohol dehydrogenase, the two major enzymes in the fermentation pathway, showed improved growth over control roots under microaerobic conditions.

3. Characteristics of recombinant protein expression

In bioreactor design, it is useful to relate the pattern of product synthesis to cell growth. The production occurs either predominantly during active cell growth (*i.e.* growth associated) or after active cell growth is ceased (*i.e.* non-growth associated). In recombinant protein production, the production pattern is strongly affected by the type of promoter used. When a constitutive promoter, such as the widely popular cauliflower mosaic virus (CaMV) 35S promoter, is used to drive the transgene expression, the recombinant protein production is considered largely growth associated. Cells may continue to produce the recombinant protein upon initial entering into the stationary phase of the growth cycle, but this is usually accompanied with increased proteolytic activities, and hence the recombinant protein level tends to descend during the stationary phase when the 35S promoter is used. If an inducible promoter is used, generally the transgene is induced after the culture reaches a high biomass concentration in the late/post exponential growth phase [59]. In this case, recombinant protein production is decoupled from the active cell growth. A number of inducible promoters have been used for expressing recombinant proteins in plant suspension cultures. The rice α -amylase (RAmy3D) promoter which is induced by sugar starvation was used in rice cell cultures to express recombinant α_1 -antitrypsin [15,16] and recombinant hGM-CSF [5]; the *Arabidopsis thaliana* heat-shock (HSP18.2) promoter [60], the tomato light inducible *rbcS* promoter [61], the methyl jasmonate inducible potato cathepsin D inhibitor (CDI) promoter [59], the glucocorticoid-inducible GVG promoter [62], the sweet potato oxidative stress-inducible peroxidase (POD) promoter [63], and the abscisic acid, tetracycline, and copper inducible promoters [64], have all been examined in tobacco cell cultures for recombinant protein production. In order to optimize the efficiency of an inducible gene expression system, it is necessary to examine the inducer concentration and timing of inducer addition. Depending on the nature of the inducer, repeated inducer feeding may be desirable, and hence optimization of inducer feeding

would be necessary. Published data in this area for plant cell culture is scarce. Suehara *et al.* [59] investigated optimal induction strategies for the expression of a GUS reporter driven by the CDI promoter. Since the addition of the inducer, methyl jasmonate, led to metabolic by-products that reduced cell growth, Suehara *et al.* [59] had to replace the spent media with fresh ones to remove the potential inhibitory substances, and to devise an inducer feeding strategy by keeping the inducer concentration within a narrow range. Trexler *et al.* [16] postulated that expression systems based on the rice α -amylase promoter could be further improved by optimizing the timing of medium exchange using suitable physiological indicators, and by exposing the culture to consecutive growth and sugar-starvation phases. Atsuhiko Shinmyo's group [50,65] isolated several growth-phase dependent strong promoters from tobacco BY-2 cells, based on the principle that genes with low copy number in the genome, but with abundant transcripts are likely controlled by a strong promoter. Among these, promoter fragments of two genes that encode putative alcohol dehydrogenase and pectin esterase, respectively, were found to strongly express during the stationary phase. Strong promoters active in the stationary phase are good candidates for driving recombinant protein production in high-density stationary-phase cultures (*e.g.* in high-density perfusion cultures) or immobilized cell cultures [50].

In addition to the knowledge on how protein production pattern is related to the cell growth pattern, it is useful to know whether the protein products are secreted into the media. Recombinant proteins might be targeted to the ER-Golgi secretion pathway using a proper signal peptide. It is highly desirable to enable effective secretion of the protein product to simplify downstream protein purification. The secretory pathway also provides a better cellular environment for protein folding and assembly than the cytosol, since the endoplasmic reticulum contains a large number of molecular chaperones and is a relatively oxidizing environment with low proteolytic activities, rendering generally higher accumulation of the recombinant proteins [66]. However, there are exceptions to the rule, suggesting the overall protein yield may also be affected by the intrinsic properties of each protein product. Furthermore, it should be cautious that the extra-cellular compartment is not loaded with proteolytic activities that can degrade the proteins of interests. Shin *et al.* [5] observed higher proteolytic activities in the tobacco cell culture than in the rice cell culture. Addition of stabilization agents such as gelatin, polyvinyl pyrrolidone (PVP), and bovine serum albumin (BSA) have met with various degrees of success among the proteins tested for stabilization [2]. Comparing to these common protein stabilizing agents, the peptide antibiotic bacitracin may be more effective towards stabilizing a broader range of proteins; although at high concentrations (1 mg/ml) bacitracin becomes toxic to plant cells [67]. Another strategy to stabilize secreted recombinant proteins in plant suspension cultures is *via in-situ* adsorption. James *et al.* [68] coupled an immobilized protein G and a metal affinity column to a culture flask to recover secreted heavy-chain mouse monoclonal antibody and histidine-tagged hGM-CSF, respectively, by recirculating the culture filtrates through these columns. Increased product yields for both proteins were noted, resulting from reduced protein degradation.

A variety of molecular strategies exist for improvement of gene expression and heterologous protein accumulation in plants and plant cells [69]. General points of consideration include the use of appropriate promoters, enhancers, and leader sequences

[70]; optimization of codon usage; control of transgene copy number; sub-cellular targeting of gene products (*e.g.*, by using an ER-targeting signal peptide or ER-retention HDEL or KDEL signal); the position in the plant genome at which the genes are integrated [71]; and the removal of mRNA-destabilizing sequences [72]. In some cases, nuclear matrix attachment regions (MARs) have been found to increase transgene expression [73]. Viral genes that suppress PTGS, such as the potyvirus hc protease genes, can be used to prevent transgene PTGS [74]. As plants expressing these genes may have greatly increased virus susceptibility, this approach may not be practical for field plants but could work well in suspension cells. Additional ways to increase expression levels include the use of different plant species, integration-independent expression, and enhancing correct protein folding by co-expressing disulfide isomerases or chaperone proteins [69].

4. Bioreactor design and operation

The culture and production characteristics described in the preceding sections provide the basis for effective bioreactor design and operation to produce recombinant proteins from transgenic plant cell suspension cultures. In addition, it is important to incorporate cellular stoichiometry, mass and energy balances, reaction kinetics, heat and mass transfer, hydrodynamics and mixing, shear, and process monitoring and control, in bioreactor design for transgenic plant cell cultures. General discussions on the topic of plant cell bioreactors can be found in a number of comprehensive reviews. Two of the more recent ones are from Doran [19] and Kieran [18]. Here we will focus on plant cell bioreactor operating strategies, bioreactor configurations and impeller design, and innovative process sensing, as pertinent to recombinant protein production.

4.1. BIOREACTOR OPERATING STRATEGIES

While it is most common to culture plant cells in the single-stage batch mode, two-stage batch [15], fed-batch [23,59], chemostat [75], and perfusion modes [34,76] have also been explored for protein production from cultured plant cells [4]. As discussed in the previous section, choice of bioreactor operation mode is largely governed by the pattern of product formation and the way the product is translocated following its synthesis. For growth-associated, intracellular protein products (*e.g.* when a constitutive promoter and an ER-retention signal are used), protein productivity could be improved by increasing the cell growth rate and prolonging the active cell-growth phase in a single-stage batch or fed-batch bioreactor. To increase biomass output, chemostat cultures generate a constant stream of biomass, from which intracellular recombinant proteins can be harvested. However, it is difficult to run a true chemostat at high biomass concentration with plant cell suspensions, due to cell aggregation, slow growth, surface adhesion and high viscosity at high biomass densities [28]. Semi-continuous cultivation, in which a portion of the cell suspension is periodically removed and then replenished with fresh medium, can be applied as an alternative to chemostat cultures. Biomass (and recombinant protein) productivities may be further improved using perfusion culture with a bleed stream. A much higher cell density can often be obtained in perfusion cultures compared to continuous and semi-continuous cultures, because cells are

retained within the reactor via a cell retention device. With a bleed stream, the perfusion reactor can be operated under a (quasi-) steady state at a very high cell concentration. It is well known that for a culture system that follows simple Monod kinetics, the maximum biomass output rate in a perfusion reactor with a bleed stream is higher than that in a chemostat by a factor of $1/\psi$, where ψ is the bleed ratio (the ratio between flow rates of the bleed stream and the feed stream). In a perfusion reactor, the specific growth rate can be manipulated by adjusting the bleed stream. Another advantage of perfusion operation is that inhibitory by-products in the spent medium can be removed efficiently, since very high perfusion rates can be used without cell washout.

For growth-associated, extra-cellular protein products, one also needs to consider increasing cell growth rate, prolonging active cell growth, and raising biomass output, as for the growth-associated intracellular products; but since the product is secreted into the media, one may also consider coupling a suitable protein recovery unit (such as an affinity column) to the reactor by re-circulating the culture spent media through the recovery unit to harvest the product [68]. If operated at the perfusion mode, a high perfusion rate should be used with the bleed stream adjusted to give a high specific growth rate.

For non-growth associated, intracellular protein products (*e.g.* when an inducible promoter or a stationary-phase specific promoter is used along with an ER-retention signal), two-stage batch cultures should be advantageous. Two-stage culture can be conducted in one physical bioreactor unit or in two separate reactors. For the latter, if the culture cycle in the growth stage is shorter than the production stage, one growth stage reactor may be used to feed multiple production stage reactors [77]. The production-stage operation strongly depends on the gene induction system used. For instance, when a stationary-phase specific promoter [65] is used, it would be desirable to prolong the stationary phase (*i.e.* the production stage) to increase the protein production yield. One apparent challenge would be to provide a suitable culture regime and cellular microenvironment that enable essentially zero net growth while avoids or at least minimizes culture degradation (*e.g.* programmed cell death or elevated proteolytic activity). In plant cell cultures, the net cell growth usually ceases when the packed cell volume approaches *ca.* 60-70%. Under such high biomass volume fraction, the cellular mitotic index generally is very low and the culture usually is not able to sustain a high metabolic activity for very long. This problem can be alleviated, in part, by perfusing the culture with fresh media [34]. Further improvements are expected to derive from deeper understanding of the cellular responses to the biotic stress caused by the extremely high biomass volume fraction. Sugar-starvation inducible α -amylase promoter has been used to express hGM-CSF at a level as high as 129 mg/L [5]. When a sugar-starvation inducible promoter is used, it is necessary to remove sugar from the media to induce transgene expression. In such case, one needs to conduct a media exchange into a sugar-free nutrient solution [15] or solution containing an alternative carbon source [78], or to supplement macro- and micro-nutrients into the sugar-depleted media at the end of the growth stage, in a single reactor unit, or to concentrate the cells from the growth-stage reactor and inoculate the cells into a second reactor to induce the protein expression. If a single reactor unit is employed, medium exchange can be achieved by filtration or sedimentation. If a chemical inducer is used to induce transgene expression, the inducer may be fed into the culture at late growth stages and repeated inducer feeding may

prolong and increase transgene expression. However, optimization of inducer dosage and feeding strategy is dependent on the nature of the inducer (considering its toxicity and chemical stability) and how the inducer activates the promoter. In principle, two-stage chemostats may also be considered. Here the first stage chemostat is used to provide the cells for the second stage chemostat, which is manipulated to enhance product synthesis. A low dilution rate should be used in the second-stage chemostat to reduce the cell growth rate. This could be done by increasing the reactor volume of the second stage chemostat. One major drawback of this operation is that the low dilution rate also reduces the biomass output rate and hence decreases the intracellular recombinant protein productivity.

For non-growth associated, extra-cellular protein products, it would be advantageous to employ fed-batch or perfusion bioreactors. These reactors can potentially be operated at high cell density without rapid cell division for a prolonged period, with constant supply of fresh nutrient. The secreted product can be continuously harvested from the spent medium. For cultures limited by accumulation of extra-cellular growth inhibitors, perfusion culture is preferred. Perfusion cultures of *A. officinalis* plant cells have been conducted in uniquely designed air-lift [76] and stirred-tank [34] bioreactors for secreted protein production (Figure 3). A stirred-tank perfusion bioreactor similar to that described in Su and Arias [34] has been used recently to culture transgenic tobacco cells for the production of a constitutively expressed secretory green fluorescent protein (GFP) (Su, W. and Liu, B. unpublished).

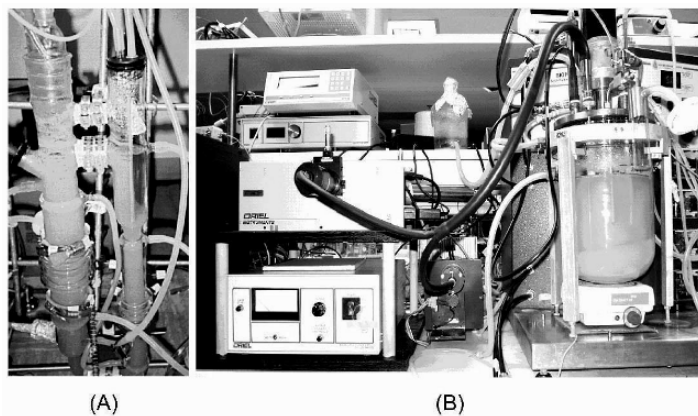


Figure 3. (A) An external-loop air-lift perfusion bioreactor (note the cell-free zone in the upper portion of the downcomer); (B) A stirred-tank perfusion bioreactor with a cylindrical skirt baffle; shown with the optical sensor setup for on-line monitoring of culture fluorescence (note the cell sediment in the bottom of the bioreactor).

Perfusion bioreactors may also be operated under the fed-batch mode, with constant recirculation of the spent medium from the cell-free zone of the reactor through a protein recovery unit to harvest the secreted protein product (Figure 4). More

information on perfusion bioreactor design for plant cell cultures can be found elsewhere [79].

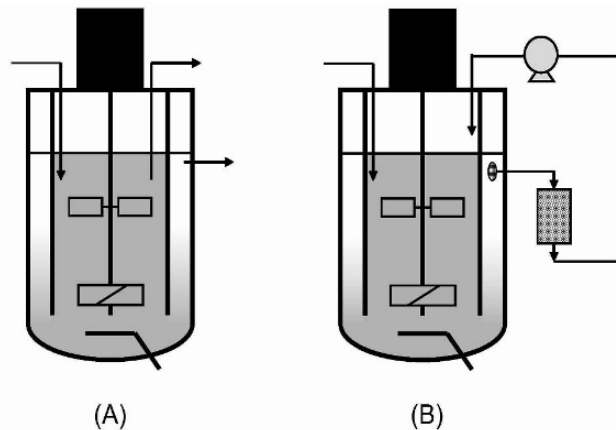


Figure 4. A stirred-tank perfusion bioreactor (equipped with a skirt baffle) operated under (A) perfusion mode with medium feeding, culture bleeding, and cell-free spent medium removal; and (B) fed-batch mode with nutrient feeding and constant recirculation of the spent medium through an external protein recovery unit for continuous or periodic harvesting of the secreted protein product.

4.2. BIOREACTOR CONFIGURATIONS AND IMPELLER DESIGN

Air-lift, bubble column, and stirred-tank bioreactors have all been tested for culturing transgenic plant cells for recombinant protein production [53], but stirred tanks are most widely used. On the basis of time-constant/regime analysis, Doran [36] concluded that for high-density plant cell cultures (over 30 gdw/L), mixing becomes a limiting factor in airlift bioreactors, leading to poor oxygen transfer and heterogeneous biomass distribution in the reactor. Another serious problem associated with pneumatically agitated plant cell bioreactors such as the airlift and bubble columns is foaming. Airlift/bubble columns however should work well at low to moderate biomass concentrations. With their less complicated mechanical design, these reactors are good candidates for low-cost bioreactors, such as the plastic-lined bubble column proposed by Curtis and co-workers [80]. To increase reactor volumetric productivity, generally it is preferred to operate the reactor at high cell densities, and hence stirred-tanks remain the reactor of choice. An intricate part of designing stirred tank reactors for culturing plant cells entails how to set the appropriate operating conditions (aeration rates, agitation speeds, cooling/heating, *etc.*) so that cellular oxygen demand can be met without causing excess foaming and shear damage to the cells. For stirred tank reactors, impeller system is one of the most crucial elements. Doran [19] has conducted a detailed theoretical engineering analysis of Rushton turbine (RT) and pitched blade turbines (PBT) for a hypothetical 10 m³ stirred-tank plant cell bioreactor of standard configuration, by concurrently considering gas dispersion, solid suspension, oxygen transfer, and shear

damage. The analysis results were presented in flow-regime maps, which indicate that for the RT, the minimum speed that enables complete solids and gas dispersion for sufficient oxygen transfer is likely to cause shear damage. On the other hand, PBT operating at the upward-pumping mode was shown in the analysis to be superior in gas handling and solids suspension, under power input setting constrained by shear damage considerations. Since the publication of Doran's analysis in 1999, more studies have been published on the hydrodynamics of upward-pumping axial-flow impellers in two or three-phase systems, but there is no report on using such impeller in plant cell cultures. These more recent hydrodynamics studies do support the notion that the axial-flow impellers operating at an upward pumping mode is insensitive to aeration (*i.e.* exhibiting low power drop upon gassing and thus not prone to impeller flooding), and is efficient in solids suspension (*i.e.* minimum stirrer speed required for particle suspension is low). However, as pointed out by Kieran [18], there are also data indicating unfavourable mass transfer performance of upward-pumping axial-flow impellers in viscous fermentation broths. For instance, Junker *et al.* [81] reported insufficient oxygen transfer using Lightnin[®] A315 impeller in the up-pumping mode in viscous *Streptomyces* fermentations; while the same impeller operated at the down-pumping mode gave better oxygen transfer under increased broth viscosities. Nienow and Bujalski [82] indicated that wide-blade, axial flow hydrofoils such as the A315 operated at the up-pumping mode should be considered when just physical suspension is required or when solid-liquid reactions are rate limiting. Although not analyzed by Doran in her work [19], due to limited hydrodynamic data available at the time, low-power number radial flow concave blade disc impellers such as the Chemineer[®] CD-6 impeller have been shown to provide improved oxygen transfer (over Rushton turbines) in *Streptomyces* fermentations [83]. Recently, an improved version of CD-6, called BT-6, has been developed [84]. Unlike the CD-6 which has 6 symmetric concave blades, BT-6 has six vertically asymmetric blades with the upper section of the blades longer than the lower section (Figure 5). The BT-6 impellers exhibit very little power drop upon gassing, even at very high flow numbers, compared with other commonly used impeller systems, such as Rushton turbines or high solidity ratio hydrofoils. Therefore, BT-6 is believed to be well suited for dispersing gas in reactors and fermentors where a wide range of gas rates is required [84]. According to Chemineer[®] (Dayton, Ohio) [85], the mass transfer capability of BT-6 is higher than the CD-6, on the order of 10%, and the BT-6 is also claimed to be relatively insensitive to viscosity. These new impeller designs (Figure 5) may indeed help improving mixing and oxygen transfer in viscous, shear-sensitive high-density plant cell cultures, although this promise will need to be experimentally verified first.

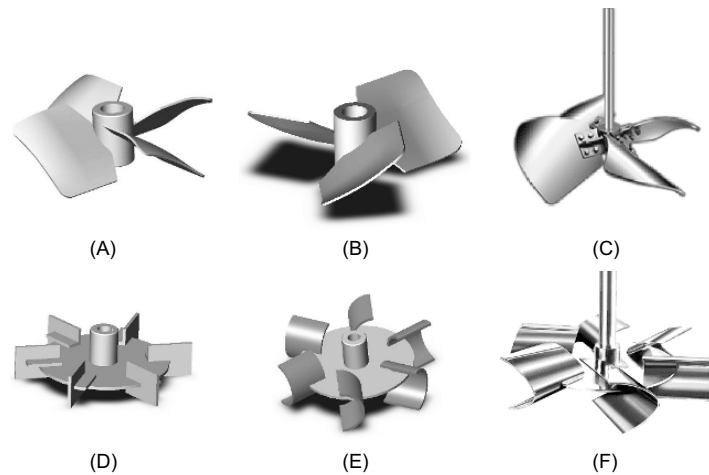


Figure 5. (A) Lightnin[®] A315 axial-flow impeller; (B) Lightnin[®] A340 up-pumping axial-flow impeller; (C) Chemineer[®] Maxflow W axial-flow impeller; (D) Rushton disc turbine; (E) Chemineer[®] CD-6 radial-flow impeller; (F) Chemineer[®] BT-6 radial-flow impeller. Photograph provided courtesy of Post-Mixing.com (A, B, D, and E) [86] and Chemineer[®] (C and F) [85].

4.3. ADVANCES IN PROCESS MONITORING

Research on monitoring of plant cell culture processes has largely emphasized on detecting cell growth and related physiological parameters such as oxygen uptake rate (OUR), carbon dioxide evolution rate (CER), and respiratory quotient (RQ). To this end, Dalton [87] was among the first to apply off-gas analysis coupled with on-line mass balancing to estimate the growth rate of cultured plant cells. Off-gas analysis using gas analyzers or mass spectroscopy has also been applied by several other groups to detect metabolic changes in plant cell cultures on-line [88-90]. Several methodologies have been reported to directly or indirectly monitor cell concentration in plant cell suspension culture, based on medium conductivity, osmolarity, culture turbidity (using a laser turbidity probe), or dielectric properties (see references cited in [91]). Komaraiah *et al.* [92] recently developed a multisensor array (an electronic nose) that consisted of nineteen different metal oxide semiconductor sensors and one carbon dioxide sensor to continuously monitor the off-gas from batch plant cell suspension cultures. Using two pattern recognition methods, principal component analysis and artificial neural networks, Komaraiah *et al.* [92] were able to analyze the multiarray responses to predict the culture biomass concentration and formation of a secondary metabolite, antraquinone. Availability of cell growth, OUR and CER information from on-line measurement during bioreactor culture is useful in guiding the development of effective substrate/inducer feeding in plant cell cultures for recombinant protein expression. On-line monitoring of culture fluorescence from intrinsic fluorophores such as NAD(P)H,

or recombinant fluorescent reporters such as GFP, can provide valuable information of the culture metabolic states, allowing development of improved process control strategies to increase protein production. Asali *et al.* [93] used NAD(P)H fluorescence to monitor the response of starved *Catharanthus roseus* cells to metabolic perturbations. Choi *et al.* [94] used a fibre-optic probe for on-line sensing of NAD(P)H culture fluorescence of tobacco suspension culture and correlated the fluorescence signal to biomass concentration. Recombinant protein product can be genetically fused with GFP or GFP variants in a number of ways [95], allowing on-line monitoring of the recombinant protein production by simply measuring the culture GFP fluorescence. In addition, non-invasive detection of GFP-based sensor proteins in real time is also highly valuable for studying the dynamics of cellular processes in plant cells that are relevant to recombinant protein product formation. For instance, FRET (fluorescence resonance energy transfer)-based GFP nanosensors have been developed to monitor signal transduction and sugar transport in mammalian cells *in vivo* [96,97]. In the batch culture of transgenic tobacco cells with constitutive expression of an ER-retained GFP, Liu *et al.* [23] showed that culture GFP fluorescence followed closely with cell growth. A medium feeding strategy based on culture GFP fluorescence measured off line was then developed that resulted in improved biomass as well as GFP production in a fed-batch culture [23]. Su *et al.* [95] recently demonstrated on-line monitoring of secretory GFP production in a transgenic tobacco cell culture bioreactor using an optical light-rod sensor. GFP culture fluorescence is a composite signal that can be influenced by factors such as culture autofluorescence, inner filter effect (IFE), and fluorescence quenching. These factors complicate accurate estimation of GFP concentrations from culture fluorescence. IFE is especially problematic when using GFP in monitoring transgenic plant cell suspension cultures, due to the aggregated nature of the cells and the high biomass concentration in these culture systems. Reported approaches for online compensation of IFE in monitoring culture NAD(P)H fluorescence or bioluminescence require online measurement of biomass density or culture turbidity/optical density, in addition to fluorescence measurement. Su *et al.* [98] recently developed a model-based state observer, using the extended Kalman filter (EKF) and on-line measurement of GFP culture fluorescence, to accurately estimate GFP concentration and other important bioreactor states on line, while rectifying the influences of IFE and culture autofluorescence without needing an additional biomass sensor. Software sensors, including the use of EKF [99] and artificial neural network [100] have also been used for monitoring biomass concentration in plant cell cultures. Zhang and Su [101] succeeded in applying EKF coupled with simple on-line OUR measurement for estimating the intracellular phosphate content during batch cultures of *A. officinalis*. The combination of GFP-based sensing and software sensors forms a powerful tool that can greatly advance process monitoring in transgenic plant cell cultures, allowing development of more productive bioprocesses.

5. Future directions

In order to establish plant cell culture as a competitive host system for large-scale commercial production of high-value recombinant proteins, the production cost has to come down significantly. The technological/engineering advances reviewed in this

chapter point to many opportunities for improving recombinant protein productivity. While further increase in productivity is expected to rely considerably on further advances in plant molecular biology, innovative engineering solutions are equally important to complement the molecular approaches to enhance and sustain high productivity, as well as reducing capital and operating costs.

Acknowledgements

The author is grateful to the funding supports from the National Science Foundation (BES97-12916 and BES01-26191), the United States Department of Agriculture (USDA) Tropical & Subtropical Agriculture Research (TSTAR) Program (01-34135-11295), and the USDA Scientific Cooperative Research Program (58-3148-9-080).

References

- [1] Gomord, V. and Faye, L. (2004) Posttranslational modification of therapeutic proteins in plants. *Curr. Opin. Plant Biol.* 7: 171-181.
- [2] James, E. and Lee, J.M. (2001) The production of foreign proteins from genetically modified plant cells. *Adv. Biochem. Eng. Biotechnol.* 72: 127-156.
- [3] Crawford, K.M. and Zambryski, P.C. (1999) Plasmodesmata signaling: many roles, sophisticated statuses. *Curr. Opin. Plant Biol.* 2: 382-387.
- [4] Doran, P.M. (2000) Foreign protein production in plant tissue cultures. *Curr. Opin. Biotechnol.* 11:199-204.
- [5] Shin, Y.J.; Hong, S.Y.; Kwon, T.H.; Jang, Y.S. and Yang, M.S. (2003) High level of expression of recombinant human granulocyte-macrophage colony stimulating factor in transgenic rice cell suspension culture. *Biotechnol. Bioeng.* 82: 778-783.
- [6] Firek, S.; Draper, J.; Owen, M.R.; Gandecha, A.; Cockburn, B. and Whitelam, G.C. (1993) Secretion of a functional single-chain Fv protein in transgenic tobacco plants and cell suspension cultures. *Plant Mol. Biol.* 23: 861-870.
- [7] Fischer, R.; Liao, Y.C. and Drossard, J. (1999) Affinity-purification of a TMV-specific recombinant full-size antibody from a transgenic tobacco suspension culture. *J. Immunol. Methods* 226: 1-10.
- [8] Sharp, J.M. and Doran, P.M. (2001) Characterization of monoclonal antibody fragments produced by plant cells. *Biotechnol. Bioeng.* 73: 338-346.
- [9] Xu, H.; Montoya, F.U.; Wang, Z.; Lee, J.M.; Reeves, R.; Linthicum, D.S. and Magnuson, N.S. (2002) Combined use of regulatory elements within the cDNA to increase the production of a soluble mouse single-chain antibody, scFv, from tobacco cell suspension cultures. *Protein Expr. Purif.* 24: 384-394.
- [10] Smith, M.L.; Mason, H.S. and Shuler, M.L. (2002) Hepatitis B surface antigen (HBsAg) expression in plant cell culture: Kinetics of antigen accumulation in batch culture and its intracellular form. *Biotechnol. Bioeng.* 80: 812-822.
- [11] Magnuson, N.S.; Linzmaier, P.M.; Reeves, R.; An, G.; HayGlass, K. and Lee, J.M. (1998) Secretion of biologically active human interleukin-2 and interleukin-4 from genetically modified tobacco cells in suspension culture. *Protein Expr. Purif.* 13: 45-52.
- [12] Kwon, T.H.; Seo, J.E.; Kim, J.; Lee, J.H.; Jang, Y.S. and Yang, M.S. (2003) Expression and secretion of the heterodimeric protein interleukin-12 in plant cell suspension culture. *Biotechnol. Bioeng.* 81: 870-875.
- [13] James, E.A.; Wang, C.; Wang, Z.; Reeves, R.; Shin, J.H.; Magnuson, N.S. and Lee, J.M. (2000) Production and characterization of biologically active human GM-CSF secreted by genetically modified plant cells. *Protein Expr. Purif.* 19: 131-138.
- [14] Francisco, J.A.; Gawlak, S.L.; Miller, M.; Bathe, J.; Russell, D.; Chace, D.; Mixan, B.; Zhao, L.; Fell, H.P. and Siegall, C.B. (1997) Expression and characterization of bryodin 1 and a bryodin 1-based single-chain immunotoxin from tobacco cell culture. *Bioconjug. Chem.* 8: 708-713.

- [15] Terashima, M.; Murai, Y.; Kawamura, M.; Nakanishi, S.; Stoltz, T.; Chen, L.; Drohan, W.; Rodriguez, R.L. and Katoh, S. (1999) Production of functional human alpha 1-antitrypsin by plant cell culture. *Appl. Microbiol. Biotechnol.* 52: 516-523.
- [16] Trexler, M.M.; McDonald, K.A. and Jackman, A.P. (2002) Bioreactor production of human alpha(1)-antitrypsin using metabolically regulated plant cell cultures. *Biotechnol. Prog.* 18: 501-508.
- [17] Fischer, R.; Emans, N.; Schuster, F.; Hellwig, S. and Drossard, J. (1999) Towards molecular farming in the future: using plant-cell-suspension cultures as bioreactors. *Biotechnol. Appl. Biochem.* 30 (Pt 2): 109-112.
- [18] Kieran, P.M. (2001) Bioreactor design for plant cell suspension cultures. In: Cabral, J.; Mota, M. and Tramper, J. (Eds.) *Multiphase bioreactor design*. Taylor and Francis, London; pp. 391-426.
- [19] Doran, P.M. (1999) Design of mixing systems for plant cell suspensions in stirred reactors. *Biotechnol. Prog.* 15: 319-335.
- [20] Wetzstein, H. and He, Y. (2000) Anatomy of plant cells. In: Spier, R. (Ed.), *Encyclopedia of cell technology*. Wiley, New York; pp. 24-31.
- [21] Kwon, T.; Kim, Y.; Lee, J. and Yang, M. (2003) Production and secretion of biologically active human granulocyte-macrophage colony stimulating factor in transgenic tomato suspension cultures. *Biotechnol. Letters* 25: 1571-1574.
- [22] Kwon, S.; Jo, S.; Lee, O.; Choi, S.; Kwak, S. and Lee, H. (2003) Transgenic ginseng cell lines that produce high levels of a human lactoferrin. *Planta Medica* 69: 1005-1008.
- [23] Liu, S.; Bugos, R.C.; Dharmasiri, N. and Su, W.W. (2001) Green fluorescent protein as a secretory reporter and a tool for process optimization in transgenic plant cell cultures. *J. Biotechnol.* 87: 1-16.
- [24] Su, W.; Lei, F. and Su, L. (1993) Perfusion strategy for rosmarinic acid production by *Anchusa officinalis*. *Biotechnol. Bioeng.* 42: 884-890.
- [25] Hibino, K. and Ushiyama, K. (1999) Commercial production of ginseng by plant tissue culture technology. In: Far, T.; Singh, G. and Curtis, W. (Eds.) *Plant Cell and Tissue Culture for the Production of Food Ingredients*. Kluwer Academic Publisher, New York; pp. 215-224.
- [26] Chattopadhyay, S.; Farkya, S.; Srivastava, A. and Bisaria, V. (2002) Bioprocess considerations for production of secondary metabolites by plant cell suspension cultures. *Biotechnol. Bioproc. Eng.* 7: 138-149.
- [27] Keßler, M.; ten Hoopen, H. and Furusaki, S. (1999) The effect of aggregate size on the production of ajmalicine and tryptamine in *Catharanthus roseus* suspension culture. *Enz. Microbiol. Technol.* 24: 308-315.
- [28] Su, W. (1995) Bioprocessing technology for plant cell suspension cultures. *Appl. Biochem. Biotechnol.* 50: 189-230.
- [29] Danna, K. (2001) Production of cellulases in plants for biomass conversion. *Recent Adv. in Phytochemistry* 35: 205-231.
- [30] Cosgrove, D.J. (1997) Relaxation in a high-stress environment: the molecular bases of extensible cell walls and cell enlargement. *Plant Cell* 9: 1031-1041.
- [31] Vissenberg, K.; Feijo, J.A.; Weisenseel, M.H. and Verbelen, J.P. (2001) Ion fluxes, auxin and the induction of elongation growth in *Nicotiana tabacum* cells. *J. Exp. Bot.* 52: 2161-2167.
- [32] Joubes, J.; De Schutter, K.; Verkest, A.; Inze, D. and De Veylder, L. (2004) Conditional, recombinase-mediated expression of genes in plant cell cultures. *Plant J.* 37: 889-896.
- [33] Curtis, W. and Emery, A. (1993) Plant cell suspension culture rheology. *Biotechnol. Bioeng.* 42: 520-526.
- [34] Su, W. and Arias, R. (2003) Continuous perfusion plant cell culture: Bioreactor characterization and secreted enzyme production. *J. Biosci. Bioeng.* 95: 13-20.
- [35] Kieran, P.M.; MacLoughlin, P.F. and Malone, D.M. (1997) Plant cell suspension cultures: some engineering considerations. *J. Biotechnol.* 59: 39-52.
- [36] Doran, P. (1993) Design of reactors for plant cells and organs. *Adv. Biochem. Eng. Biotechnol.* 48:115-168.
- [37] Abdullah, M.; Ariff, A.; Marziah, M.; Ali, A. and Lajis, N. (2000) Strategies to overcome foaming and wall growth during the cultivation of *Morinda elliptica* cell suspension culture in a stirred-tank bioreactor. *Plant Cell Tissue Org. Cult.* 60: 205-212.
- [38] Wongsamuth, R. and Doran, P. (1997) The filtration properties of *Atropa belladonna* plant cell suspensions; effect of hydrodynamic shear and elevated carbon dioxide levels on culture and filtration properties. *J. Chem. Technol. Biotechnol.* 69: 15-26.

- [39] Howell, J.; Chi, C. and Pawlowsky, U. (1972) Effect of wall growth on scale-up problems and dynamic operating characteristics of the biological reactor. *Biotechnol. Bioeng.* 14: 253-265.
- [40] Kawase, Y. and Moo-Young, M. (1990) The effect of antifoam agents on mass transfer in bioreactors. *Bioprocess Eng.* 5: 169-173.
- [41] Meijer, J.; ten Hoopen, H.; Luyben, K. and Libbenga, K. (1993) Effects of hydrodynamic stress on cultured plant cells: A literature survey. *Enz. Microbial Technol.* 15: 234-238.
- [42] Kieran, P.M.; Malone, D.M. and MacLoughlin, P.F. (2000) Effects of hydrodynamic and interfacial forces on plant cell suspension systems. *Adv. Biochem. Eng. Biotechnol.* 67: 139-177.
- [43] Dunlop, E.; Namdev, P. and Rosenberg, M. (1994) Effect of fluid shear forces on plant cell suspensions. *Chemical Eng. Sci.* 49: 2263-2276.
- [44] Sowana, D.; Williams, D.; Dunlop, E.; Dally, B.; O'Neill, B. and Fletcher, D. (2001) Turbulent shear stress effects on plant cell suspension cultures. *Trans. Chem.E* 79: 867-875.
- [45] Sowana, D.; Williams, D.; O'Neill, B. and Dunlop, E. (2002) Studies of the shear protective effects of Pluronic F-68 on wild carrot cell cultures. *Biochemical Eng. J.* 12: 165-173.
- [46] MacLoughlin, P.F.; Malone, D.M.; Murtagh, J.T. and Kieran, P.M. (1998) The effects of turbulent jet flows on plant cell suspension cultures. *Biotechnol. Bioeng.* 58: 595-604.
- [47] Namdev, P.K. and Dunlop, E.H. (1995) Shear sensitivity of plant cells in suspension. *Appl. Biochem. Biotechnol.* 54: 109-131.
- [48] Han, R. and Yuan, Y. (2004) Oxidative burst in suspension culture of *Taxus cuspidata* induced by a laminar shear stress in short-term. *Biotechnol. Progress* 20: 507-513.
- [49] Yahraus, T.; Chandra, S.; Legendre, L. and Low, P.S. (1995) Evidence for a mechanically induced oxidative burst. *Plant Physiol.* 109: 1259-1266.
- [50] Shinmyo, A.; Shoji, T.; Bando, E.; Nagaya, S.; Nakai, Y.; Kato, K.; Sekine, M. and Yoshida, K. (1998) Metabolic engineering of cultured tobacco cells. *Biotechnol. Bioeng.* 58: 329-332.
- [51] Koroleva, O.A.; Tomlinson, M.; Parinyapong, P.; Sakvarelidze, L.; Leader, D.; Shaw, P. and Doonan, J.H. (2004) CycD1, a Putative G1 Cyclin from *Antirrhinum majus*, accelerates the cell cycle in cultured tobacco BY-2 Cells by enhancing both G1/S entry and progression through S and G2 phases. *Plant Cell* 16: 2364-2379.
- [52] Cockcroft, C.E.; den Boer, B.G.; Healy, J.M. and Murray, J.A. (2000) Cyclin D control of growth rate in plants. *Nature* 405: 575-579.
- [53] Gao, J. and Lee, J. (1992) Effect of oxygen supply on the suspension culture of genetically modified tobacco cells. *Biotechnol. Progress* 8: 285-290.
- [54] Cooney, C.; Wang, D. and Mateles, R. (1969) Measurement of heat evolution and correlation with oxygen consumption during microbial growth. *Biotechnol. Bioeng.* 11: 269-281.
- [55] Hashimoto, T. and Azechi, S. (1988) Bioreactors for large-scale culture of plant cells. In: Bajaj, Y.P.S. (Ed.), *Biotechnology in Agriculture and Forestry*. Springer, Berlin; pp. 104-122.
- [56] Farres, J. and Kallio, P.T. (2002) Improved cell growth in tobacco suspension cultures expressing *Vitreoscilla* hemoglobin. *Biotechnol. Progress* 18: 229-233.
- [57] Igamberdiev, A.U.; Seregelyes, C.; Manac'h, N. and Hill, R.D. (2004) NADH-dependent metabolism of nitric oxide in alfalfa root cultures expressing barley hemoglobin. *Planta* 219: 95-102.
- [58] Shiao, T.L.; Ellis, M.H.; Dolferus, R.; Dennis, E.S. and Doran, P.M. (2002) Overexpression of alcohol dehydrogenase or pyruvate decarboxylase improves growth of hairy roots at reduced oxygen concentrations. *Biotechnol. Bioeng.* 77: 455-461.
- [59] Suehara, K.; Takao, A.; Nakamura, K.; Uozumi, N. and Kobayashi, T. (1996) Optimal expression of GUS gene from methyl jasmonate-inducible promoter in high density culture of transformed tobacco cell line BY-2. *J. Ferment. Bioeng.* 82: 51-55.
- [60] Yoshida, K.; Kasai, T.; Garcia, M.R.; Sawada, S.; Shoji, T.; Shimizu, S.; Yamazaki, K.; Komeda, Y. and Shinmyo, A. (1995) Heat-inducible expression system for a foreign gene in cultured tobacco cells using the HSP18.2 promoter of *Arabidopsis thaliana*. *Appl. Microbiol. Biotechnol.* 44: 466-472.
- [61] Uozumi, N.; Inoue, Y.; Yamazaki, K. and Kobayashi, T. (1994) Light activation of expression associated with the tomato rbcS promoter in transformed tobacco cell line BY-2. *J. Biotechnol.* 36: 55-62.
- [62] Nara, Y.; Kurata, H.; Seki, M. and Taira, K. (2000) Glucocorticoid-induced expression of a foreign gene by the GVG system in transformed tobacco BY-2 cells. *Biochemical Eng. J.* 6: 185-191.
- [63] Kim, K.Y.; Kwon, S.Y.; Lee, H.S.; Hur, Y.; Bang, J.W. and Kwak, S.S. (2003) A novel oxidative stress-inducible peroxidase promoter from sweet potato: molecular cloning and characterization in transgenic tobacco plants and cultured cells. *Plant Mol. Biol.* 51: 831-838.

- [64] Boetti, H.; Chevalier, L.; Denmat, L.A.; Thomas, D. and Thomasset, B. (1999) Efficiency of physical (light) or chemical (ABA, tetracycline, CuSO₄ or 2-CBSU)-stimulus-dependent gas gene expression in tobacco cell suspensions. *Biotechnol. Bioeng.* 64: 1-13.
- [65] Nagaya, S.; Nakai, Y.; Kato, K.; Sekine, M.; Yoshida, K. and Shinmyo, A. (2000) Isolation of growth-phase-specific promoters from cultured tobacco cells. *J. Biosci. Bioeng.* 89: 231-235.
- [66] Fischer, R.; Stoger, E.; Schillberg, S.; Christou, P. and Twyman, R.M. (2004) Plant-based production of biopharmaceuticals. *Curr. Opin. Plant Biol.* 7: 152-158.
- [67] Bateman, K.; Congiu, M.; Tregear, G.; Clarke, A. and Anderson, M. (1997) Bacitracin significantly reduces degradation of peptides in plant cell cultures. *Biotechnol. Bioeng.* 53: 226-231.
- [68] James, E.; Mills, D. and Lee, J. (2002) Increased production and recovery of secreted foreign proteins from plant cell cultures using an affinity chromatography bioreactor. *Biochemical Eng. J.* 12: 205-213.
- [69] Goddijn, O. and Pen, J. (1995) Plants as bioreactors. *TIBTECH* 13: 379-387.
- [70] Gallie, D. and Walbot, V. (1992) Identification of the motifs within the tobacco mosaic virus 5'-leader responsible for enhancing translation. *Nucleic Acids Res.* 20: 4631-4638.
- [71] Day, C.; Lee, E.; Kobayashi, J.; Holappa, L.; Albert, H. and Ow, D. (2000) Transgene integration into the same chromosome location can produce alleles that express at a predictable level, or alleles that are differentially silenced. *Genes Dev.* 14: 2869-2880.
- [72] Hilleren, P. and Parker, R. (1999) Mechanisms of mRNA surveillance in eukaryotes. *Ann. Rev. Genet.* 33: 229-260.
- [73] Spiker, S. and William, F. (1996) Nuclear matrix attachment regions and transgene expression in plants. *Plant Physiol.* 110: 15-21.
- [74] Voinnet, O.; Pinto, Y. and Baulcombe, D. (1999) Suppression of gene silencing: A general strategy used by diverse DNA and RNA viruses of plants. *Proc. Natl. Acad. Sci. USA* 96: 14147-14152.
- [75] Verdelhan des Molles, D.; Gomord, V.; Bastin, M.; Faye, L. and Courtois, D. (1999) Expression of a carrot invertase gene in tobacco suspension cells cultivated in batch and continuous culture conditions. *J. Biosci. Bioeng.* 87: 302-306.
- [76] Su, W.; He, B.; Liang, H. and Sun, S. (1996) A perfusion air-lift bioreactor for high density plant cell cultivation and secreted protein production. *J. Biotechnol.* 50: 225-233.
- [77] Drapeau, D.; Blanch, H.W. and Wilke, C.R. (1987) Economic assessment of plant cell culture for the production of ajmalicine. *Biotechnol. Bioeng.* 30: 946-953.
- [78] Terashima, M.; Ejiri, Y.; Hashikawa, N. and Yoshida, H. (2001) Utilization of an alternative carbon source for efficient production of human alpha(1)-antitrypsin by genetically engineered rice cell culture. *Biotechnol. Prog.* 17: 403-406.
- [79] Su, W. (2000) Perfusion bioreactors. In: Spier, R. (Ed.), *Encyclopedia of Cell Technology*. Wiley, New York; pp. 230-242.
- [80] Hsiao, T.Y.; Bacani, F.T.; Carvalho, E.B. and Curtis, W.R. (1999) Development of a low capital investment reactor system: application for plant cell suspension culture. *Biotechnol. Prog.* 15: 114-122.
- [81] Junker, B.; Stanik, M.; Barna, C.; Salmon, P. and Buckland, B. (1998) Influence of impeller type on mass transfer in fermentation vessels. *Bioproc. Eng.* 19: 403-413.
- [82] Nienow, A.W. and Bujalski, W. (2002) Recent studies on agitated three-phase (gas-solid-liquid) systems in the turbulent regime. *Chemical Eng. Res. Design* 80: 832-838.
- [83] Junker, B.H.; Mann, Z. and Hunt, G. (2000) Retrofit of CD-6 (Smith) impeller in fermentation vessels. *Appl. Biochem. Biotechnol.* 89: 67-83.
- [84] Pinelli, D.; Bakker, A.; Myers, K.J.; Reeder, M.F.; Fasano, J. and Magelli, F. (2003) Some features of a novel gas dispersion impeller in a dual-impeller configuration. *Chemical Eng. Res. Design* 81: 448-454.
- [85] Anon. (2002) <http://www.chemineer.com/impellers.php>.
- [86] Csiszar, P. (2004) <http://www.postmixing.com/>.
- [87] Dalton, C. (1985) Application of gas analysis to continuous culture. In: Neumann, K.; Barz, W. and Reinhard, E. (Eds.) *Primary and secondary metabolism of plant cell cultures*. Springer, Berlin; pp. 58-65.
- [88] Bond, P.; Fowler, M. and Scragg, A. (1988) Growth of *Catharanthus roseus* cell suspensions in bioreactors: on-line analysis of oxygen and carbon dioxide levels in inlet and outlet gas streams. *Biotechnol. Lett* 10: 713-718.
- [89] Nikolova, P.; Moo-Young, M. and Legge, R. (1991) Application of process mass spectroscopy to the detection of metabolic changes in plant tissue culture. *Plant Cell Tissue Org. Cult.* 25: 219-224.
- [90] Zhong, J.; Konstantinov, K. and Yoshida, T. (1994) Computer-aided on-line monitoring of physiological variables in suspended cell cultures of *Perilla frutescens* in a bioreactor. *J. Ferment. Bioeng.* 77: 445-447.

- [91] Zhong, J. (2001) Biochemical engineering of the production of plant-specific secondary metabolites by cell suspension cultures. *Adv. Biochemical Eng. Biotechnol.* 72: 1-26.
- [92] Komaraiah, P.; Navratil, M.; Carlsson, M.; Jeffers, P.; Brodelius, M.; Brodelius, P.E.; Kieran, P.M. and Mandenius, C.F. (2004) Growth behaviour in plant cell cultures based on emissions detected by a multisensor array. *Biotechnol. Prog.* 20: 1245-1250.
- [93] Asali, E.C.; Mutlmma, R. and Humphrey, A.E. (1992) Use of NAD(P)H-fluorescence for monitoring the response of starved cells of *Catharanthus roseus* in suspension to metabolic perturbations. *J. Biotechnol.* 23: 83-94.
- [94] Choi, J.; Park, Y.; shin, C.; Kim, D. and Lee, W. (1995) Analysis of culture fluorescence by a fiber-optic sensor in *Nicotiana tabacum* plant cell culture. *Korean J. Chemical Eng.* 12: 528-534.
- [95] Su, W.W.; Guan, P. and Bugos, R.C. (2004) High-level secretion of functional green fluorescent protein from transgenic tobacco cell cultures: characterization and sensing. *Biotechnol. Bioeng.* 85: 610-619.
- [96] Miyawaki, A.; Liopis, J.; Heim, R.; McCaffery, J.M.; Adams, J.A.; Ikura, M. and Tsien, R.Y. (1997) Fluorescent indicators for Ca²⁺ based on green fluorescent proteins and calmodulin. *Nature* 388: 882-887.
- [97] Fehr, M.; Frommer, W.B. and Lalonde, S. (2002) Visualization of maltose uptake in living yeast cells by fluorescent nanosensors. *Proc. Natl. Acad. Sci. USA* 99: 9846-9851.
- [98] Su, W.; Liu, B.; Lu, W.; Xu, N.; Du, G. and Tan, J. (2004) Observer-based online compensation of inner filter effect in monitoring fluorescence of GFP-expressing plant cell cultures. (under publication).
- [99] Albiol, J.; Robuste, J.; Casas, C. and Poch, M. (1993) Biomass estimation in plant cell cultures using extended Kalman filter. *Biotechnol. Progress* 9: 174-178.
- [100] Albiol, J.; Campmajo, C.; Casas, C. and Poch, M. (1995) Biomass estimation in plant cell cultures: a neural network approach. *Biotechnol. Progress* 11: 88-92.
- [101] Zhang, J. and Su, W. (2002) Estimation of intracellular phosphate content in plant cell cultures using an extended Kalman filter. *J. Biosci. Bioeng.* 94: 8-14.

TYPES AND DESIGNS OF BIOREACTORS FOR HAIRY ROOT CULTURE

YONG-EUI CHOI¹, YOON-SOO KIM² AND KEE-YOEUP PAEK³

¹*Department of Forestry, College of Forest Sciences, Kangwon National University, Chunchon 200-701, Kangwon-do, Korea – Fax: 82-33-252-8310 – Email: yechoi@kangwon.ac.kr*

²*Korea Ginseng Institute, Chung-Ang University, Ansung-shi, Kyunggi-do, Korea – Fax: 82-31-676-6544 – Email: yoosony@hanmail.net*

³*Research Centre for the Development of Advanced Horticultural Technology, Chungbuk National University, Cheongju 361-763, Korea- Fax: 82-43-272-5369 – Email: paecky@chungbuk.ac.kr*

1. Introduction

Plants synthesize a wide range of secondary metabolites such as alkaloids, anthocyanins, flavonoids, quinins, lignans, steroids, and terpenoids, which play a major role in the adaptation of plants to their environment. The secondary metabolites have been used as food additives, drugs, dyes, flavours, fragrances, and insecticides. Such chemicals are extracted and purified from naturally grown plants. However, production of secondary metabolites from plants is not always satisfactory. It is often restricted to a limited species or genus, and geographically to a specific region. Many important medicinal plants were endangered by overexploitation. Some plants are difficult to cultivate and grow very slowly or are endangered in their natural habitats. The biotechnological approach by utilizing plant cell and organ culture system can offer an opportunity to produce the secondary metabolites. Plant materials via *in vitro* culture are produced with high uniformity regardless of geographical and seasonal limitations and environmental factors. However, there are many problems in the production of metabolites by plant cell and organ culture technology due to the high cost to natural counterparts, and the low yield of metabolites in cultured plant cells. Although there are many efforts for establishing the cell and organ culture systems, application in the commercial production of pharmaceuticals is limited to a few examples only. Production of shikonin from the cell culture of *Lithospermum erythrorhizon* [1,2], taxol from *Taxus baccata* [3] and berberine from *Coptis japonica* [4] was reached for the application for industrialization. The main problem using cell suspension culture is a low product yield and instability of the cell lines [5].

The secondary metabolites can be produced by developed organ and plantlets [6,7]. An alternative method for the production of plant materials for secondary metabolite production is the culture of shoots, roots, or whole plants. However, the organ culture tends to grow slowly and renders the difficulty of the large-scale cultivation compared

to cell culture. *Agrobacterium rhizogenes*-transformed hairy roots synthesize the same component as does the roots of the intact plants and have a fast growth property in hormone-free medium. Many efforts have been made to commercialize the plant metabolites via a bioreactor culture of hairy roots. The bioreactor for microorganism fermentation (stirred tank bioreactor) is unsuitable for the mass production of hairy roots because of strong shear stress. Therefore, various types of bioreactor systems were designed and evolved to enhance the productivity and the bioprocess. Among them, airlift, bubble column, and liquid-dispersed bioreactor are largely adopted for the hairy root culture because of the low shear stress and the simplicity of their design and construction. Significant progress has been made in biotechnology and bioprocess for the large-scale culture of hairy roots. In this chapter, we focus on the recent technology covering the bioreactor culture systems, such as the shape of bioreactor, aeration condition, and introduce the large-scale production of ginseng hairy-like roots for commercialization.

2. Advantage of hairy root cultures

Normally, adventitious root cultures need an exogenous phytohormone supply and grow very slowly. Hairy roots can be produced by transformation with the soil bacterium *Agrobacterium rhizogenes*, resulting in the so-called hairy roots disease [8]. Long-term genetic and biosynthetic stability was noted from this type of culture [9,10]. In addition, they produce similar secondary metabolites to the normal roots and much higher levels than do cell cultures [6,11,12]. Therefore, hairy roots can offer a valuable source of root-derived secondary metabolites that are useful as pharmaceuticals, cosmetics, and food additives. Transformed roots of many plant species have been widely studied for the *in vitro* production of secondary metabolites [13,14].

Another interesting strategy of hairy root cultures is the genetic engineering of secondary metabolism by introducing useful genes. Enhanced production of alkaloid nicotine by the introduction of ornithine decarboxylase into *Nicotiana rustica* was reported [15]. The hairy roots of *Atropa belladonna* overexpressing hyoscyamine 6-beta-hydroxylase (H6H) gene isolated from *Hyoscyamus niger* produced high amounts of scopolamine [16]. In *Hyoscyamus niger* hairy root cultures, overexpression of genes encoding both putrescine N-methyltransferase (PMT) and the downstream enzyme hyoscyamine-6-beta-hydroxylase (H6H) resulted in the enhanced scopolamine biosynthesis [17]. Hairy root cultures of *Datura metel* overexpressing the SAM N-methyltransferase (PMT) gene encodes for putrescine, which accumulated higher amounts of tropane alkaloids (hyoscyamine and scopolamine) than do the control hairy roots [18]. The transgenic hairy roots by introducing the genes regulating secondary metabolism will provide an effective approach for efficient and large-scale commercial production of secondary metabolite production.

3. Induction of hairy roots

Hairy roots are induced from the transfer and integration of the genes of Ri plasmid of *Agrobacterium rhizogenes* [8]. Integration of a DNA segment (T-DNA) of Ri-plasmid

into the host plant genome results in the active proliferation of hairy roots [8]. The Ri plasmids are grouped into two main classes: agropine and mannopine type strains [19]. The agropine type strains contain both the TL (about 15-20 kb) and TR (about 8-20 kb) region in their Ri plasmid are more virulent than mannopine strains, and are therefore more often used for the establishment of hairy root cultures [20]. *Agrobacterium rhizogenes* A4 type (A4, ATCC, 15834, 1855, TR105, etc) can synthesize both agropine and mannopine. *Agrobacterium rhizogenes* 8196 type (TR7, TR101, etc.) synthesize the mannopine only.

The *vir* region comprises about 35 kb in the Ri plasmid, and encodes six transcriptional loci: *vir* A, B, C, D, E, and G, which have important functions in gene transfer. Transcription of the *vir* region is induced by various phenolic compounds such as acetosyringone [21]. Acetosyringone or related compounds have been reported to increase the frequency of *Agrobacterium* mediated transformations in a number of plant species [22], especially for recalcitrant monocotyledonous plant species [23]. Various sugars also act synergistically with acetosyringone to induce a high level of *vir* gene expression [24,25].

In the agropine Ri plasmid T-DNA is referred to as left T-DNA (T_L -DNA) and right T-DNA (T_R -DNA) [26]. Genes involved in agropine and auxin syntheses are located in the T_R DNA region. Genes of Ri T_L -DNA such as *rolA*, *rolB*, *rolC* and *rolD* stimulate hairy root differentiations under the influence of endogenous auxin synthesis [27]. T-DNA analysis in hairy roots reveals that TL and TR-DNAs exist in random manners either as distinct inserts, or as a single and continuous insert including the region between TL and TR on pRi 15834 [28]. Sequencing of genomic DNA/T-DNA junctions in hairy roots reveals that genomic DNA at the cleavage sites are usually intact, whereas donor T-DNA ends are often resected, as are found in random T-DNA inserts. Batra *et al.* [29] reported that growth and terpenoid indole alkaloid production in *Catharanthus roseus* hairy root clones is related to left and right-termini-linked Ri T-DNA gene integration. Therefore, each hairy root line shows different morphology and growth pattern together with different biosynthetic capability of secondary metabolites.

4. Large-scale culture of hairy roots

Generally, the hairy root culture in bioreactors is focused on both secondary metabolites production via the biomass growth of root tissues. Growth of hairy roots and production of secondary metabolites is controlled by the genetic characteristics of plant species, and they are strongly influenced by physical and chemical culture conditions such as the types of culture vessels, composition and concentration of macro and micro-element, concentration of carbon sources, pH, light, and temperature etc. In hairy root culture systems, biomass growth is achieved due to a series of two characteristic growths: the lateral root primordium formation on parent root segments and their elongation [30]. In comparison to a cell suspension culture, the growth of hairy roots in liquid medium results in the packed root mass playing an inhibitory role in fluid flow and limiting oxygen availability [31]. In addition, the roots hairs play a detrimental role for the growth in a liquid environment because they induce the stagnation of fluid flow and limit the availability of oxygen [31]. Therefore, the morphological character of hairy roots and oxygen supply are primary factors for designing and optimizing the culture

condition of hairy roots [32,33]. To achieve successfully a scale-up, reactor types and assessments of reactor performance must be considered to minimize the problems, which will be encountered during the scale-up. In the case of the Erlenmeyer flask culture, it is very difficult to modify the culture environment within flasks and is used for only small-scale culture due to the limited air supply. A bioreactor fitted with controllers for air supply, pH, temperature etc. is mainly utilized for the large-scale culture of hairy roots. Various configurations of hairy root bioreactors such as the stirred tank, airlift, bubble column, liquid-dispersed bioreactor have been designed for hairy root cultures [14,34]. Therefore, we introduce the cultures of well-known bioreactors for the production of hairy roots and recent advances on the bioreactor culture technology for large-scale production of hairy roots.

4.1. STIRRED TANK REACTOR

In this type of bioreactor, mortar-derived impeller or turbine blades regulate aeration and medium currency. This reactor is widely adopted for microorganism, fermentation and plant cell culture. Temperature, pH, amount of dissolved oxygen, and nutrient concentration can be better controlled within this reactor than in other type of reactors. In general, the impellers used in this reactor produce a high-shear stress compared to other types [35-37]. For hairy roots culture, the impeller must be operated with restricted power input and speed to minimize the shear stress. Ways of improving impeller performance by modifying internal reactor geometry have been designed [38-40]. In the hairy root culture of *Catharanthus trichophyllus*, hairy root line cultures in stirred bioreactor showed a similar alkaloid composition to normal root [41]. The cultivation of *Swertia chirata* hairy roots in a 2-L stirred-tank bioreactor was successful only with a stainless-steel mesh fitted inside the culture vessel for immobilization of the roots [42]. In the *Panax ginseng* hairy root culture, the growth of roots in a stirred bioreactor in which stainless-steel mesh fitted in culture vessel was about three times as high as in the flask cultivation [43].

4.2. AIRLIFT BIOREACTORS

In the airlift bioreactor, both liquid currency and aeration are driven by externally supplied air. This reactor is advantageous for the culture of plant cells and organs those are sensitive to shear stress. However, this reactor is not suitable for high-density culture because of insufficient mixing process inside the reactor. In 2.5-L hairy root culture of *Pueraria phaseoloides*, puerarin accumulation is 200 times as much as in a 250 ml shake flask culture [44]. In the hairy root culture of *Astragalus membranaceus*, both the dry weight of hairy roots and astragaloside IV from a 30-L airlift bioreactor were higher than the yields from a 10-L bioreactor [45]. In the *Panax ginseng* hairy root culture, the growth of roots in both the bubble column and the stirred bioreactor was about three times as high as in the flask cultivation [46]. Hairy roots growth was about 55-fold of inoculums after 39 d in a 5-L airlift bioreactor and about 38-fold of inoculums after 40 d in a 19-L airlift bioreactor [43].

4.3. BUBBLE COLUMN REACTOR

The bubble column reactor is one of simplest types of reactors and is easy to scale-up. Its disadvantage is the undefined flow pattern inside the reactor resulting into non-uniform mixing. Like an airlift bioreactor, the bubbles in a bubble column create less shear stress compared to other stirred types, so that it is useful for organized structures such as hairy roots. In this case, the bubbling rate needs to be gradually increased with the growth of hairy roots. However, at a high tissue density level, the bubble column has been observed to reduce growth performance [47]. In hairy root culture of *Solanum tuberosum* in a 15-L bubble column, stagnation and channelling of gas through the bed of growing roots exists, however, the gas-liquid interface is not the dominant resistance factor to oxygen mass transfer, and the oxygen uptake of growing tips increase with the oxygen tension of the medium [48]. The growth and production of hyoscyamine and scopolamine in the culture of hairy roots of *Datura metel* was enhanced by the treatment of permeabilizing agent Tween 20 in an airlift bioreactor with root anchorage [49]. In hairy root cultures of *Hyoscyamus muticus* accumulated tissue mass in submerged air-sparged reactors was 31% of gyratory shake-flask controls [50]. They reported that impaired oxygen transfer due to channelling and stagnation of the liquid phase are the apparent causes of poor growth [50]. Inclusion of polyurethane foam in the vessel of air-sparged bioreactor reduces the entrapping of gas by hairy roots, which improve biomass and alkaloid production [51]. In *Artemisia annua* hairy root culture, the bubble column reactor was superior to mist reactors for the biomass concentration [52,53]. Souret *et al.* [53] examined the difference between the two types of bioreactors, a mist reactor and a bubble column reactor. Mist reactors produce significantly more artemisinin, while bubble column reactors produce greater biomass. The roots grown in shake flasks contain a negligible amount of artemisinin. The high-density culture of red beet hairy roots was obtained by a radial flow reactor, which consists of a cylindrical vessel with a radial flow of medium [54].

4.4. LIQUID-DISPERSED BIOREACTOR

The reactors used for hairy root culture can be classified as either liquid-phase or gas-phase. Liquid-dispersed reactor is advantageous both for sufficient oxygen supply to roots and for a low shear stress environment compared with reactors in which the roots remained submerged in a liquid medium [50]. In liquid-dispersed reactors, roots are exposed to ambient air, or gas mixture, and the nutrient liquid, which is dispersed as spray or mist onto the top of the root bed [52,55]. The sprayed liquid and mist are drained from the bottom of the bioreactor to a reservoir and is re-circulated. The degree of distribution of liquid varies according to the mechanism of liquid delivery at the top of the reactor chamber. Various types of liquid-dispersed reactors are developed for the hairy root culture. Mist or nutrient mist [56-59], droplet [52,59], trickle-bed or tricking film [57,60], and drip-tube [61] are reported. In these bioreactors, certain types of configurations to internal support of roots such as glass beads, rasching rings, steel wire scaffolding, polyurethane foam, horizontal mesh trays, and cylindrical stainless steel mesh are invented [52,57,59-61]. *Cichorium intybus* hairy roots grown in an acoustic mist bioreactor produce nearly twice as much aesculin as compared to roots grown in bubble column and nutrient sprinkle bioreactors [62]. *Artemisia annua* hairy roots

grown in nutrient mist reactors produce nearly three times as much artemisinin as roots grown in bubble column reactors [63], and the authors suggest that higher levels of artemisinin in roots grown in the mist reactors are due to a response to the increased osmotic strength of the medium within the mist reactor, the medium becomes concentrated due to water evaporation [63]. In contrast to artemisinin accumulation in *Artemisia annua* hairy roots, the mist reactor accumulates lower biomass than does the bubble column reactor due to insufficient nutrient availability [52].

5. Commercial production of *Panax ginseng* roots via balloon type bioreactor

Panax ginseng has been used for important Oriental medicine since ancient time, owing to its tonic properties. The ginseng root contains terpenoid saponins, referred to as ginsenosides. Cultivation of ginseng requires at least more than four years under shade condition and also requires the careful control of disease. Cell and organ culture technology have been developed for the alternative production of ginseng raw materials and secondary metabolites. The ginseng cell culture has been applied to the production of useful secondary metabolites [64,65]. Hormone-independent embryogenic cells are induced and cultivated via a bioreactor [66,67]. The cell suspensions produced from pilot scale culture have been commercialized into various ginseng tea and tonic beverages by Nitto Denko Co., Japan. [68].

Hairy roots provide an efficient way of biomass production due to fast growth and displays high biosynthetic capabilities that are comparable to those of natural roots [6, 11,12]. There are many publications on the hairy root culture of ginseng [43,69]. However, hairy roots are still not well utilized for the production of health food and need further analysis for the safety of proteins and compounds expressed by introduced genes of T-DNA. Recently, hairy-like adventitious roots culture without transformation with *Agrobacterium rhizogenes* was reported [70,71]. Induction and growth of hairy-like adventitious roots is achieved from initial root explants by exogenous auxin supply, which is direct motive for the mass production of ginseng roots for commercial scale. Son *et al.* [71] designed a balloon-type bubble bioreactor (BTBB) (Figures 1, 2A), which is superior for biomass growth than the bubble column bioreactor, and stirred tank bioreactor in cell culture of *Taxus cuspidata* [72], *Beta vulgaris* hairy roots [73], ginseng hairy root [74] and adventitious root culture [75]. The fresh weight of ginseng hairy-like adventitious root culture in 20-L BTBB was three-times higher than that of the stirred tank bioreactor [71]. The maximum biomass production of 2.2 kg fresh weight in 20-L bioreactor was obtained after 42 days after inoculation of 240 g [76]. In mountain ginseng cell line maintained by CBN Biotech Co., Korea, biomass growth of ginseng roots is reached to 30-fold of inoculums after 42 days of culture (Table 1).

Types and designs of bioreactors for hairy root culture

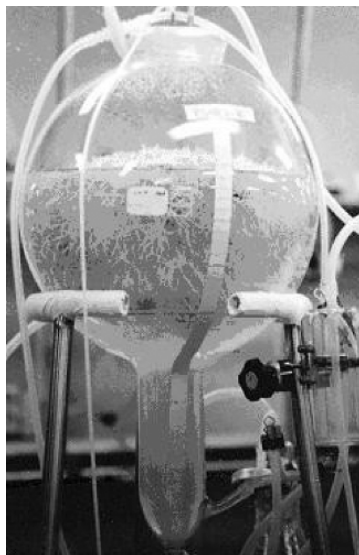


Figure 1. Actively growing ginseng hairy roots in 20-L balloon-type bubble bioreactor after 42 days of culture. Photograph provided by Son SH of VitroSys Co., Korea.

Table 1. Growth and saponin accumulation of adventitious ginseng roots after 42 days of culture in 5, 20, 500 and 1,000-L balloon-type bubble bioreactors.

Working volume (L)	Inoculums (g)	Fresh Wt. (g)	Dry Wt. (g)	Saponin content (mg/g ⁻¹ Dry Wt.)
4	20	520	48	5.6
18	90	2,294	212	5.8
500	2,500	58,500	5,800	6.0
1000	50,000	108,000	120,000	33.5*

* Methyl-jasmonate (100 μ M) treatment 7 days before harvest.

The pilot-scale 500 and 1000-L stainless bioreactor was designed according to the BTBB type (Figure 2B). This reactor is comprised of a main body, air bubbling device, steam generator for sterilization, air inlet, air vent system, and various control systems for checking the temperature, oxygen, pH, and pipeline systems for transferring steam, air, medium, and root masses (Figure 3). Additional equipments such as a distilled water reservoir, medium mixer, medium sterilizer, and inoculation bioreactor are necessary.



Figure 2. Scale-up of hairy-like adventitious roots of *Panax ginseng*. (A) 20-L balloon-type bubble bioreactors. (B) 500 and 1000-L pilot-scale balloon-type bubble bioreactors. (C) 10,000-L pilot-scale balloon-type bubble bioreactors for the commercial production of ginseng roots. (D) Harvested ginseng roots from a 10,000-L pilot-scale balloon-type bubble bioreactor. Photograph provided by Paek KY of CBN Biotech Co., Korea.

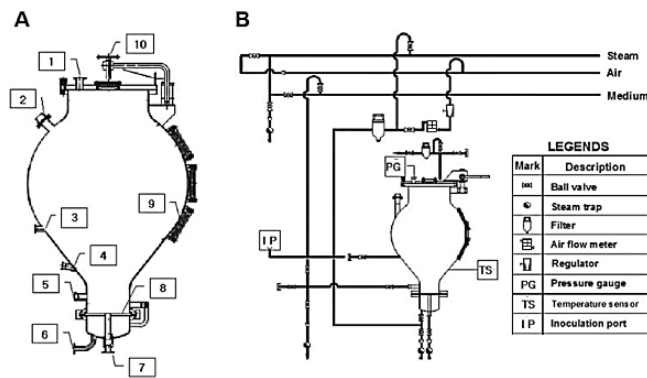


Figure 3. Schematic diagram of a balloon type bioreactor (A) and steam, air, and medium flow (B) in pilot scale culture (1,000 L). 1, ventilation port; 2, light glass; 3, dissolved oxygen probe port; 4, pH probe port; 5, inoculation port; 6, air inlet; 7, medium drain port; 8, stainless sparger; 9, sight glass; 10, screwed lid opener.

Before transfer to large-scale tanks, root tissues are homogenized into approximately one cm length size and are moved via an air compressor through the inter-connector between the inoculation reactor and the main tanks. The increase of the fresh weight of ginseng roots was more than 30-fold after 40 days of culture in both bioreactors. The

biomass increase in this bioreactor was similar to the ginseng hairy root culture [43,69]. There is no serious problem with the stagnation of fluid flow and limit oxygen due to the actively growing root mass. Based on the pilot-scale balloon-type bioreactor, production of ginseng roots via 10,000-L bioreactor was practically attempted for the commercial production (Figure 2C). In Korea, three companies produce the ginseng roots commercially using pilot-scale bioreactor (10,000 to 20,000-L) and the basic design follows the balloon-type bubble bioreactor. The root materials are processed into various types of health foods and food ingredients (Figure 2D).

Acknowledgements

This work was funded in part by the Korea Research Foundation (F010608) and Biogreen 21 of Rural Development Administration, Republic of Korea.

References

- [1] Fujita, Y. (1988) Industrial production of shikonin and berberine. In: Applications of Plant Cell and Tissue Culture, Ciba Foundation Symposium 137, Wiley, Chichester; pp. 228–238.
- [2] Shimomura, K.; Sudo, H.; Saga, H. and Kamada, H. (1991) Shikonin production and secretion by hairy root cultures of *Lithospermum erythrorhizon*. Plant Cell Rep. 10: 282–285.
- [3] Srinivansan, V.; Pestchankar, L.; Moser, S.; Hirasuna, T.J.; Taticek, R.A. and Shuler, M.L. (1995) Taxol-production in bioreactors: kinetics of biomass accumulation, nutrient uptake, and taxol production by cell suspensions of *Taxus baccata*. Biotechnol. Bioeng. 47: 666-676.
- [4] Kobayashi, Y.; Fukui, H. and Tabata, M. (1988) Berberine production by batch and semi-continuous cultures of immobilized *Thalictrum* cells in an improved bioreactor. Plant Cell Rep. 7: 249-253.
- [5] DiCosmo, F. and Misawa, M. (1995) Plant cell tissue culture: alternatives for metabolite production. Biotechnol. Adv. 13: 425-453.
- [6] Flores, H.E.; Hoy, M.W. and Puckard, J.J. (1987) Secondary metabolites from root cultures. Trends Biotechnol. 5: 64-69.
- [7] Ramachandra Rao, S. and Ravishankar, G.A. (2002) Plant cell cultures: Chemical factories of secondary metabolites. Biotechnol. Adv. 20: 101-153.
- [8] Chilton, M.D.; Tepfer, D.; Petit, A.; David, C.; Casse-Delbart, F. and Tempé, J. (1982) *Agrobacterium rhizogenes* inserts T-DNA into the genomes of host plant root cells. Nature 295: 432–434.
- [9] Lipp Joao, K.H.L. and Brown, T.A. (1994) Long-term stability of root cultures of tomato transformed with *Agrobacterium rhizogenes* R1601. J. Exp. Bot. 45: 641-647.
- [10] Baiza, A.M.; Quiroz-Moreno, A.; Ruiz, J.A. and Loyola-Vargas, V.M. (1999) Genetic stability of hairy root cultures of *Datura stramonium*. Plant Cell Tissue Org. Cult. 59: 9-17.
- [11] Flores, H.E. and Filner, P. (1985) Metabolic relationships of putrescine, GABA and alkaloids in cell and root cultures of Solanaceae. In: Neumann, K.H.; Barz, W. and Reinhart, E.J. (Eds.) Primary and Secondary Metabolism of Plant Cell Cultures. Springer-Verlag, New York; pp. 568–578.
- [12] Kamada, H.; Okamura, N.; Satake, M.; Hirada, H. and Shimomura, K. (1986) Alkaloid production by hairy root cultures in *Atropa belladonna*. Plant Cell Rep. 5: 239-242.
- [13] Shanks, J.V. and Morgan, J. (1999) Plant ‘hairy root’ culture. Curr. Opin. Biotechnol. 10: 151-155.
- [14] Giri, A. and Narasu, M.L. (2000) Transgenic hairy roots: recent trends and applications. Biotechnol. Adv. 18: 1-22.
- [15] Hamill, J.D.; Robins, R.J.; Parr, A.J.; Evans, D.M.; Furze, J.M. and Rhodes, M.J. (1990) Over-expressing a yeast ornithine decarboxylase gene in transgenic roots of *Nicotiana rustica* can lead to enhanced nicotine accumulation. Plant Mol. Biol. 15: 27-38.
- [16] Hashimoto, T.; Yun, D.Z. and Yamada, Y. (1993) Production of tropane alkaloids in genetically engineered root cultures. Phytochem. 2: 713-718.

- [17] Zhang, L.; Ding, R.; Chai, Y.; Bonfill, M.; Moyano, E.; Oksman-Caldentey, K.M.; Xu, T.; Pi, Y.; Wang, Z.; Zhang, H.; Kai, G.; Liao, Z.; Sun, X. and Tang, K. (2004) Engineering tropane biosynthetic pathway in *Hyoscyamus niger* hairy root cultures. Proc. Natl. Acad. Sci. USA 101: 6786-6791.
- [18] Moyano, E.; Jouhikainen, K.; Tammela, P.; Palazon, J.; Cusido, R.M.; Pinol, M.T.; Teeri, T.H. and Oksman-Caldentey, K.M. (2003) Effect of pmt gene overexpression on tropane alkaloid production in transformed root cultures of *Datura metel* and *Hyoscyamus muticus*. J. Exp. Bot. 54: 203-211.
- [19] White, F.F. and Sinkar, V.P. (1987) Molecular analysis of root induction by *Agrobacterium rhizogenes*. In: Hohn, T. and Schell, J. (Eds.) Plant DNA infectious agents. Springer-Verlag, New York; pp. 149-177.
- [20] Jung, G. and Tepfer, D. (1987) Use of genetic transformation by the Ri T-DNA of *Agrobacterium rhizogenes* to stimulate biomass and tropane alkaloid production in *Atropa belladonna* and *Calystegia sepium* roots grown *in vitro*. Plant Sci. 50: 145-151.
- [21] Vernade, D.; Herrera-Estrella, A.; Wang, K. and Van Montagu, M. (1988) Glycine betaine allows enhanced induction of the *Agrobacterium tumefaciens* vir genes by acetosyringone at low pH. J. Bacteriol. 170: 5822-5829.
- [22] Stachel, S.E.; Messens, E.; Van Montagu, M. and Zambryski, P. (1985) Identification of the signal molecules produced by wounded plant cells that activate T-DNA transfer in *Agrobacterium tumefaciens*. Nature 318: 624-629.
- [23] Manickavasagam, M.; Ganapathi, A.; Anbazhagan, V.R.; Sudhakar, B.; Selvaraj, N., Vasudevan, A. and Kasthuriengan, S. (2004) *Agrobacterium*-mediated genetic transformation and development of herbicide-resistant sugarcane (*Saccharum* species hybrids) using axillary buds. Plant Cell Rep. 23:134-43.
- [24] Shimoda, N.; Toyoda-Yamamoto, A.; Nagamine, J.; Usami, S.; Katayama, M.; Sakagami, Y. and Machida, Y. (1990) Control of expression of *Agrobacterium* vir genes by synergistic actions of phenolic signal molecules and monosaccharides. Proc. Natl. Acad. Sci. USA 87: 6684-6688.
- [25] Cangelosi, G.A.; Ankenbauer, R.G. and Nester, E.W. (1990) Sugars induce the *Agrobacterium* virulence genes through a periplasmic binding protein and a transmembrane signal protein. Proc. Natl. Acad. Sci. USA. 87: 6708-6712.
- [26] White, F.F.; Taylor, B.H.; Huffman, G.A.; Gordon, M.P. and Nester, E.W. (1985) Molecular and genetic analysis of the transferred DNA regions of the root-inducing plasmid of *Agrobacterium rhizogenes*. J. Bacteriol. 164: 33-44.
- [27] Taylor, B.H.; Amasino, R.M.; White, F.F.; Nester, E.W. and Gordon, M.P. (1985) T-DNA analysis of plants regenerated from hairy root tumor. Mol. Gen. Genet. 201: 554-557.
- [28] Brillianceau, M.H.; David, C. and Tempe, J. (1989) Genetic transformation of *Catharanthus roseus* G. Don by *Agrobacterium rhizogenes*. Plant Cell Rep. 8: 63-66.
- [29] Batra, J.; Dutta, A.; Singh, D.; Kumar, S. and Sen, J. (2004) Growth and terpenoid indole alkaloid production in *Catharanthus roseus* hairy root clones in relation to left- and right-termini-linked Ri T-DNA gene integration. Plant Cell Rep. 23: 148-154.
- [30] Han, B.; Linden, J.C.; Gujarathi, N.P. and Wickramasinghe, S.R. (2004) Population balance approach to modelling hairy root growth. Biotechnol. Prog. 20: 872-879.
- [31] Bordonaro, J.L. and Curtis, W.R. (2000) Inhibitory role of root hairs on transport within root culture bioreactors. Biotechnol. Bioeng. 70: 176-86.
- [32] Shiao, T.L. and Doran, P.M. (2000) Root hairiness: effect on fluid flow and oxygen transfer in hairy root cultures. J. Biotechnol. 83: 199-210.
- [33] Weathers, P.J.; Wyslouzil, B.E.; Wobbe, K.K.; Kim, Y.J. and Yigit, E. (1999) The biological response of hairy roots to O₂ levels in bioreactors. In Vitro Cell. Dev. Biol.-Plant 35: 286-289.
- [34] Doran, P.M. (1997) Hairy roots: Culture and Application. Harwood Academic Publishers.
- [35] Hilton, M.G. and Rhodes, M.J. (1990) Growth and hyoscyamine production of 'hairy root' cultures of *Datura stramonium* in a modified stirred tank reactor. Appl. Microbiol. Biotechnol. 33: 132-138.
- [36] Kim, Y.H. and Yoo, Y.J. (1993) Development of a bioreactor for high density culture of hairy roots. Biotechnol. Lett. 7: 859-862.
- [37] Nuutila, A. M.; Lindqvist, A. S. and Kauppinen, V. (1994) Growth of hairy root cultures of strawberry (*Fragaria x ananassa* Duch.) in three different types of bioreactors. Biotechnol. Techn. 11: 363-366.
- [38] Kondo, O.; Honda, H.; Taya, M. and Kobayashi, T. (1989) Comparison of growth properties of carrot hairy root in various bioreactors. Appl. Microbiol. Biotechnol. 32: 291-294.
- [39] Uozumi, N.; Kohketsu, K. and Kobayashi, T. (1993) Growth and kinetic parameters of *Ajuga* hairy roots in fed-batch culture on monosaccharide medium. J. Chem. Tech. Biotechnol. 57: 155-161.
- [40] Doran, P.M. (1999) Design of mixing systems for plant cell suspensions in stirred reactors. Biotechnol. Prog. 15: 319-335.

- [41] Davioud, E.; Kan, C.; Hamon, J.; Tempé, J. and Husson, H-P. (1989) Production of indole alkaloids by *in vitro* root cultures from *Catharanthus trichophyllus*. *Phytochem.* 28: 2675-2680.
- [42] Keil, M.; Hartle, B.; Guillaume, A. and Psiorz, M. (2000) Production of amarogentin in root cultures of *Swertia chirata*. *Planta Med.* 66: 452-457.
- [43] Jeong, G.T.; Park, D.H.; Hwang, B. and Woo, J.C. (2003) Comparison of growth characteristics of *Panax ginseng* hairy roots in various bioreactors. *Appl. Biochem. Biotechnol.* 107: 493-503.
- [44] Kintzios, S.; Makri, O.; Pistola, E.; Matakias, T.; Ping, Shi H. and Economou, A. (2004) Scale-up production of puerarin from hairy roots of *Pueraria phaseoloides* in an airlift bioreactor. *Biotechnol. Lett.* 26: 1057-1059.
- [45] Du, M.; Wu, X.J.; Ding, J.; Hu, Z.B.; White, K.N. and Branford-White, C.J. (2003) Astragaloside IV and polysaccharide production by hairy roots of *Astragalus membranaceus* in bioreactors. *Biotechnol. Lett.* 25: 1853-1856.
- [46] Jeong, G.T.; Park, D.H.; Hwang, B.; Park, K.; Kim, S.W. and Woo, J.C. (2002) Studies on mass production of transformed *Panax ginseng* hairy roots in bioreactor. *Appl. Biochem. Biotechnol.* 98: 1115-1127.
- [47] Kwok, K.H. and Doran, P.M. (1995) Kinetic and stoichiometric analysis of hairy roots in a segmented bubble column reactor. *Biotechnol. Prog.* 11: 429-435.
- [48] Tescione, L.D.; Ramakrishnan, D. and Curtis, W.R. (1997) The role of liquid mixing and gas-phase dispersion in a submerged, sparged root reactor. *Enzyme Microb. Technol.* 20: 207-13.
- [49] Cusido, R.M.; Palazon, J.; Pinol, M.T.; Bonfill, M. and Morales, C. (1999) *Datura metel*: *in vitro* production of tropane alkaloids. *Planta Med.* 65: 144-148.
- [50] McKelvey, S.A.; Gehrig, J.A.; Hollar, K.A. and Curtis, W.R. (1993) Growth of plant root cultures in liquid- and gas-dispersed reactor environments. *Biotechnol. Prog.* 9: 317-322.
- [51] Muranaka, T.; Kazuoka, T.; Ohkawa, H. and Yamada, Y. (1993) Characteristics of scopolamine-releasing hairy roots clones of *Duboisia leichhardtii*. *Biosci. Biotech. Biochem.* 57: 1398-13
- [52] Kim, Y.J.; Weathers, P.J. and Wyslouzil, B.E. (2002) Growth of *Artemisia annua* hairy roots in liquid- and gas-phase reactors. *Biotechnol. Bioeng.* 80: 454-464.
- [53] Sourret, F.F.; Kim, Y.; Wyslouzil, B.E.; Wobbe, K.K. and Weathers, P.J. (2003) Scale-up of *Artemisia annua* L. hairy root cultures produces complex patterns of terpenoid gene expression. *Biotechnol. Bioeng.* 83: 653-667.
- [54] Kino-Oka, M.; Hitaka, Y.; Taya, M. and Tone, S. (1999) High-density culture of red beet hairy roots by considering medium flow condition in a bioreactor. *Chem. Eng. Sci.* 54: 3179-3186.
- [55] Williams, G.R. and Doran, P.M. (2000) Hairy root culture in a liquid-dispersed bioreactor: characterization of spatial heterogeneity. *Biotechnol. Prog.* 16: 391-401.
- [56] Dilorio, A. A.; Cheetam, R. D. and Weathers, P. J. (1992) Growth of transformed roots in a nutrient mist bioreactor: Reactor performance and evaluation. *Appl. Microbiol. Biotechnol.* 37: 457-462.
- [57] Whitney, P. J. (1992) Novel bioreactors for the growth of roots transformed by *Agrobacterium rhizogenes*. *Enzyme Microbiol. Technol.* 14: 13-17.
- [58] Buer, C.S.; Correll, M.J.; Smith, T.C.; Towler, M.J.; Weathers, P.J.; Nadler, M.; Seaman, J. and Walcerz, D. (1996) Development of a nontoxic acoustic window nutrient-mist bioreactor and relevant growth data. *In Vitro Cell. Dev. Biol.-Plant* 32: 299-304.
- [59] Wilson, P.D.G. (1997) The pilot-scale cultivation of transformed roots. In: Doran, P.M. (Ed.) *Hairy roots: culture and application*. Harwood Academic, Amsterdam; pp. 179-190.
- [60] Taya, M.; Yoyama, A.; Kondo, O. and Kobayashi, T. (1989) Growth characteristics of plant hairy roots and their cultures in bioreactors. *J. Chem. Eng. Japan* 22: 84-89.
- [61] Holmes, P.; Li, S-L.; Green, K.D.; Ford-Lloyd, B.V. and Thomas, N.H. (1997) Drip-tube technology for continuous culture of hairy roots with integrated alkaloid extraction. In: Doran, P.M. (Ed.) *Hairy Roots: Culture and Application*; Harwood Academic, Amsterdam; pp. 201-208.
- [62] Bais, H.P.; Suresh, B.; Raghavarao, K.S.M.S. and Ravishankar, G.A. (2002) Performance of hairy root cultures of *Cichorium intybus* L. in bioreactors of different configurations. *In Vitro Cell. Dev. Biol.-Plant* 38: 573-580.
- [63] Kim, Y.; Wyslouzil, B.E. and Weathers, P.J. (2001) A comparative study of mist and bubble column reactors in the *in vitro* production of artemisinin. *Plant Cell Rep.* 20: 451-455.
- [64] Furuya, T.; Yoshikawa, T.; Orihara, Y. and Oda, H. (1994) Studies of the culture conditions for *Panax ginseng* cells in jar fermentors. *J. Natural Products* 47: 70-75.
- [65] Wu, J.Y. and Zhong, J.J. (1999) Production of ginseng and its bioactive components in plant cell culture: current technological and applied aspects. *J. Biotechnol.* 68: 89-99.

- [66] Asaka, I.; Li, I.; Hirotsu, M.; Asada, Y. and Furuya, T. (1993) Production of ginsenoside saponins by culturing ginseng (*Panax ginseng*) embryogenic tissues in bioreactors. *Biotech. Lett.* 15: 1259-1264.
- [67] Choi, Y.E.; Jeong, J.H. and Shin, C.K. (2003) Hormone-independent embryogenic callus production from ginseng cotyledons using high concentrations of NH_4NO_3 and progress towards bioreactor production. *Plant Cell Tissue Org. Cult.* 72: 229-235.
- [68] Hibino, K. and Ushiyama, K. (1998) Commercial production of ginseng by plant cell culture technology, In: Fu, T.J.; Singh, W.R. and Curtis, W. (Eds.) *Plant Cell Culture for the Production of Food Ingredients*, Proc ACS Symp, San Francisco, CA, USA, Plenum Press, New York; pp. 13-17.
- [69] Yoshikawa, T. and Furuya, T. (1987) Saponin production by cultures of *Panax ginseng* transformed with *Agrobacterium rhizogenes*. *Plant Cell Rep.* 6: 449-453.
- [70] Kevers, C.; Jacques, Ph.; Thonart, Ph. and Gaspar, Th. (1999) *In vitro* root culture of *Panax ginseng* and *P. quinquefolium*. *Plant Growth Regul.* 27: 173-178.
- [71] Son, S.H.; Choi, S.M.; Soo, J.H.; Yun, S.R.; Choi, M.S.; Shin, E.M. and Hong, Y.P. (1999) Induction and cultures of mountain ginseng adventitious roots and AFLP analysis for identifying mountain ginseng. *Biotechnol. Bioproc. Eng.* 4: 119-23.
- [72] Son, S.H.; Choi, S.M.; Lee, Y.H.; Choi, K.B.; Yun, S.R.; Kim, J.K.; Park, H.J.; Kwon, O.W.; Noh, E.W.; Seon, J.H. and Park, Y.G. (2000) Large-scale growth and taxane production in cell cultures of *Taxus cuspidata* (Japanese yew) using a novel bioreactor. *Plant Cell Rep.* 19: 628-633.
- [73] Shin, K.S.; Murthy, H.N.; Ko, J.Y. and Paek, K.Y. (2002) Growth and betacyanin production by hairy roots of *Beta vulgaris* in airlift bioreactor. *Biotechnol. Lett.* 24: 2067-2069.
- [74] Yu, K.W.; Gao, W.Y.; Son, S.H. and Paek, K.Y. (2000) Improvement of ginsenoside production by jasmonic acid and some other elicitors in hairy root culture of Ginseng (*Panax ginseng* C.A. Meyer). In *Vitro Cell. Dev. Biol. -Plant* 36: 424-428.
- [75] Yu, K.Y.; Gao, W.; Hahn, E.J. and Paek, K.Y. (2002) Jasmonic acid improves ginsenoside accumulation in adventitious root culture of *Panax ginseng* C.A. Meyer. *Biochem. Eng. J.* 11: 211-215.
- [76] Choi, S. M.; Son, S. H.; Yun, S. R.; Kwon, O. W.; Seon, J. H.; and Paek, K. Y. (2000) Pilot-scale culture of adventitious roots of ginseng in a bioreactor system. *Plant Cell Tissue Org. Cult.* 62: 187-193.

OXYGEN TRANSPORT IN PLANT TISSUE CULTURE SYSTEMS

Oxygen transport limitations

WAYNE R. CURTIS¹ AND AMALIE L. TUERK²

¹108 Fenske Laboratory, The Pennsylvania State University, University Park PA-16802, USA - Fax: 1-814- 865-7846 - Email: wrc2@psu.edu

²Department of Chemical Engineering, The Pennsylvania State University, University Park, PA 16802

1. Introduction

The typical approach for teaching transport phenomena is from ‘first principles’ where the physical model is simplified to point where it can be mathematically characterized. The strength of this approach is that the mathematical description is rigorous – even though the physical model may not be realistic. Often the rigorousness of the mathematical description continues to be a sufficient means of characterizing the system, even when the assumptions associated with the model are no longer valid. The most common characterization of oxygen transport in gas-liquid systems is the lumped parameter, $k_L a$. The physical model for this situation is shown in Figure 1.

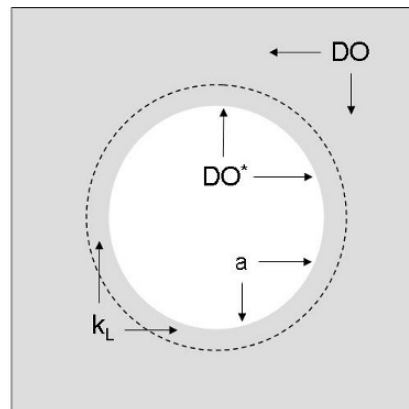


Figure 1. Simplified physical model of oxygen transfer based on well-mixed gas and liquid phases. The resulting description of oxygen transfer rate $OTR = k_L a (DO^ - DO)$ is widely used to describe oxygen transfer in bioreactors.*

The liquid and gas phases within the bioreactor are lumped as effectively well-mixed gas and liquid phases that are interconnected by the ‘limiting’ transport resistance associated with the interfacial area per unit volume (a). The mathematical description associated with this model is typical of mass transfer where the measure of conductance ($k_L a$) provides for transport in proportion to the concentration difference (“driving force”), which is the deviation of the system from equilibrium.

$$\text{OTR} = kLa (\text{DO}^* - \text{DO}) \tag{1}$$

In Equation 1, DO^* is the equilibrium dissolved oxygen concentration in the medium, which for aqueous systems at 25°C is roughly 258 μM or 8.24 ppm (exact values for media depend on medium composition and atmospheric pressure [1]). DO is the bulk liquid dissolved oxygen concentration. This simple equation has proven very useful for characterizing oxygen transfer in a wide variety of bioreactors, including diffused air systems where the assumptions of well mixed phases are clearly not valid. While this limits the physical meaning of kLa (and prevents extrapolation to altered conditions), the resulting logarithmic uptake of oxygen into a depleted liquid phase is behaviourally valid for nearly any bioreactor configuration.

This paper presents an alternative approach for examining oxygen transport. The starting point is the more realistic model of the bioreactor as a multiphase heterogeneous system. The aim is not to develop rigorous mathematical descriptions, but to understand the utility and limitations of commonly used mass transfer relationships. This framework should provide a means of understanding oxygen transport under conditions that cannot be readily characterized with mathematics. Understanding what factors can be limitations to mass transfer is far more useful than attempting to pragmatically guess at what should be the limiting factors for mass transfer.

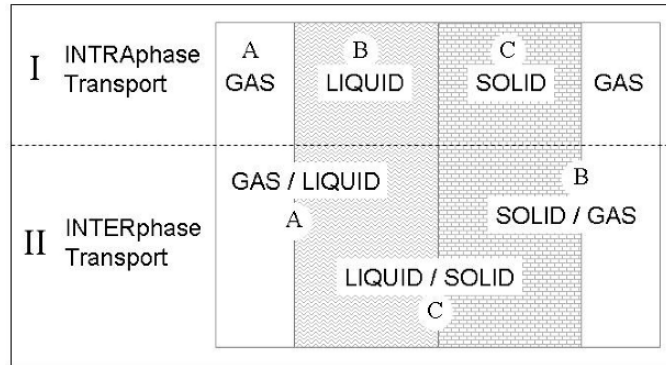


Figure 2. Schematic presentation of the different physical transport considerations for oxygen transfer in a three-phase system. Transport is described in terms of transport within a phase (INTRApHase) transport as well as between phases (INTERpHase) transport. The numerals and numbers correspond to the sections in which they are discussed. (e.g. II.A is the section that examines gas-liquid interface mass transfer).

The framework for presenting oxygen transport is organized according to the physical situations encountered in a multi-phase bioreactor system (Figure 2). Interphase oxygen transfer refers to the transport of oxygen within a given phase, which includes the fundamental mechanisms of diffusion and convection, as well as the less well-defined concept of mixing. Interphase oxygen mass transfer refers to passing of oxygen from one phase to another.

2. Intrapphase transport

Oxygen transport within a phase should not be overlooked in bioreactor systems since it is clearly the dominant form of transport. Nearly all of the oxygen that enters a bioreactor, leaves the bioreactor in the gas phase without ever being transported to the medium or tissue. In addition, while it is typical to focus on the gas and liquid phase, oxygen consumption takes place within the plant tissue. The movement of oxygen from the liquid in contact with the gas to liquid in contact with the tissue is of critical importance. The transport of oxygen within these phases takes place by very different mechanisms. Each of the three phases of gas, liquid and solid (tissue) are discussed below.

2.1. OXYGEN TRANSPORT IN THE GAS PHASE

In most bioreactors, gas is the dispersed phase which is sparged into the system as gas bubbles. While local mixing within a gas bubble is relatively rapid due to diffusion (and small bubble size relative to mean free path), neither radial nor axial mixing of gas within the reactor is assured. Since the general flow of gas is upward in a three-phase system, axial mixing will only occur if there is sufficient axial liquid mixing to exceed the rise velocity of the bubbles. For the low power levels used in agitation of plant cell suspension culture [2], there will be minimal axial mixing. Radial mixing of a sparged gas will occur to some extent as a result of rise-induced circulation cells. However, the issue of dispersion of the gas bubbles does not really address the issue of mixing of the gas phase. For mixing to occur, the bubbles must coalesce and breakup as they pass through the vessel. Otherwise, each bubble acts as its own compartmentalized 'batch' of gas, and only the residence time distribution of the gas will determine the extent of gas transfer from the bubble. Measurements of gas-phase residence time distribution are rather difficult and require techniques such as gas tracers and mass spectrometry [3]. "Fortunately", the efficiency of oxygen transfer is so poor, that these issues of dispersion and mixing within the gas phase are not typically very important because there is not a large change in the gas phase composition as it passes through the reactor. Even at extremely low gas flow rates, the composition of the gas exiting a vessel is nearly the same as entering. While microbial reactors can be operated at sparge rates of 0.1-1 VVM (volumes of gas per volume of liquid per minute), a plant tissue culture bioreactor can be operated at an order of lower magnitude gas flow rates and still have minimal change in gas composition as a result of lower total respiration rates.

The gas phase can be the continuous phase within a bioreactor. This is true for a root culture trickle-bed [4] or nutrient mist [5] bioreactors. In these systems, the gas flows as a continuous stream from entrance to exit, and the liquid is dispersed (e.g. sprayed) and

passes through the reactor. Much like gas dispersed systems; the small change in gas phase composition greatly simplifies the analysis. More importantly, the performance of the bioreactor will not be dependent upon mixing with the bioreactor gas phase, and assuming a constant well-mixed gas phase is a reasonable assumption. In the situation of passive gas exchange in a plant tissue culture vessel (e.g. sponge plugs, plastic closures or caps) the assumption of a uniform gas phase may be achieved; however, the composition of the gas phase can be variable and unknown. We have measured accumulation of carbon dioxide as much as 5% in a culture flask headspace – indicating a significantly impaired exchange with ambient air (which is 0.03% CO₂). Insufficient gas exchange will reduce oxygen availability.

2.2. OXYGEN TRANSPORT IN THE LIQUID PHASE

Mixing in the liquid phase is highly dependent on bioreactor geometry and operational conditions. For cell or tissue cultures that require more gentle conditions, the reduced intensity of energy input will reduce liquid mixing. However, the time scale for growth of plant tissues is very long relative to mixing times that would be encountered in most liquid plant culture systems. It only takes a few seconds to completely mix a fluorescent tracer in a shake flask culture [6]. However, mixing in a 15 L root culture took several hours [3]. It is important to recognize the difference between mixing and circulation. Both represent mechanisms of transporting oxygen throughout the bioreactor. Liquid circulation is a measure of how fast a fluid element gets from one side of the bioreactor to the other. Whereas, mixing is a measure of how quickly a fluid element can be dispersed throughout the entire bioreactor. Achieving good liquid circulation can be important to assure suspension of plant cell tissues. Liquid circulation can be greatly affected by bioreactor geometry [7]. Note, however, that achieving greater bulk flow throughout the reactor, does not necessarily imply better mixing. For example, low shear paddle impellers which have proven effective in pilot scale plant cell suspension culture, create flow, but lack the intense mixing of radial flow (Rushton) impellers [2]. Reduced mixing should rarely be an issue for plant tissues because of their long culture times.

The bioreactor configurations used in plant tissue culture systems, are very varied as compared to traditional fermentation. For example, fill and drain bioreactor configurations (used in plantlet propagation) achieve liquid mixing as the media flows in and out of the bioreactor [8]. In root cultures, the root matrix represents a tremendous resistance to the flow and mixing of fluid [9]. In a gas-sparged (or air-lift) bioreactor, liquid circulation and mixing results from flows induced by the differences in density caused by the presence of the gas bubbles in the bioreactor. No matter what the specific configuration, oxygen transfer to the plant tissues requires both mixing and circulation. Mixing is required to disperse the oxygenated liquid in contact with gas to areas with less oxygenation. Circulation is needed to move the oxygenated liquid to regions where gas-liquid transport may not be as effective.

The extent, to which the liquid is mixed, has a fundamental impact on oxygen mass transfer in larger vessels because the hydrostatic pressure (P) of the liquid in the tank will increase oxygen transfer in the deeper parts of the tank. This is apparent from Henry's law, which describes the equilibrium oxygen solubility (C_L^*):

$$C_L^* = \frac{y_{O_2} P}{H} \quad (2)$$

Developing equations which account for either the depth within the tank and the degree of mixing within the liquid phase quickly becomes quite complex. Analytical solutions are available for the limiting cases of complete axial mixing versus complete axial segregation of the liquid phase [10]. Qualitatively the results can be understood in terms of the impact of elevated oxygen transfer rates at the bottom of the bioreactor, and the extent to which that liquid is circulated to other regions of the bioreactor.

Equation 2 is extremely important towards understanding various strategies of enhancing oxygen transport in bioreactors. Most obvious is increasing the gas phase oxygen mole fraction (y_{O_2}) through oxygen supplementation of the gas phase. The effects of temperature are captured in the Henry's law coefficient (H) where H increases with temperature and the oxygen solubility is reduced. In this respect, the tendency to grow plant tissues at 20-25°C is an advantage over *E. coli* or mammalian cell cultures that have optimal growth rates at body temperature (37°C). By combining Equations 1 and 2, the complexity in rigorous description of oxygen mass transfer quickly becomes apparent. The driving force for oxygen transfer throughout the reactor changes depending on both depth and the composition of the gas phase. As mentioned in the previous section, the analysis is simplified because the gas phase tends to remain relatively constant within the vessel as a result of low rates of mass transfer relative to the typical rates of gas introduction into the reactor.

A final condition worth noting for oxygen transport within the liquid phase is when the culture medium has been solidified with agar or other gel matrix. Although the medium is no longer a fluid, the gelled media is still 99% water and the rates of diffusion of oxygen (and other nutrients) are indistinguishable from predictions based on liquid diffusivities (unpublished data). For oxygen diffusion in water at 25°C, the diffusion coefficient (D_{O_2}) is $2.26 \times 10^{-5} \text{ cm}^2/\text{s}$ [11]. As will be discussed further below, the diffusion rate of oxygen in stagnant water is also typically used to characterize oxygen transfer rates within tissues.

2.3. OXYGEN TRANSPORT IN SOLID (TISSUE) PHASE

An organized tissue or cell aggregate can be oxygen deprived deep within the tissue even if the surface is exposed to oxygen saturated medium. Cultured plants and plant tissue present very large structures which must have considerable oxygen transport within the tissue to maintain aerobic respiration. As the oxygen moves into the tissues, it is consumed by respiration. The transport rate through the outermost tissues must be sufficient to supply the oxygen to all tissues that are deeper within. A general (Cartesian coordinate) mass balance for oxygen consumption within the tissue becomes:

$$\frac{\partial C_{O_2}}{\partial t} = \frac{\partial}{\partial x} (N_{O_2}) - r_{O_2} \quad (3)$$

The flux of oxygen (N_{O_2}) is described by Fick's Law [e.g. $N_{O_2}=D_{eff}(\partial C_{O_2}/\partial x)$], and r_{O_2} is the biological oxygen demand (BOD) and associated conversion factors to obtain consistent units (see Table 1). If the rate of oxygen consumption is dependent on the tissue oxygen concentration, then solution of 3 is difficult. However, if the BOD is assumed to be constant, the concentration profiles within the tissue are readily derived from the steady state mass balance ($\partial C_{O_2}/\partial t=0$) based on the surface oxygen concentration (C_s). Table 1 presents these equations for various geometries that are often used as approximation of tissues (plate, cylinder and sphere). The integration of these equations assumes that there is no exhaustion of the oxygen within the tissue. The assumption of 'zero order' oxygen use kinetics (BOD=constant) can be rationalized in part because the tissues will invariably utilize any available oxygen before they would resort to anaerobic respiration.

Table 1. Mass balance and oxygen concentration gradients within tissue that result from diffusional mass transfer limitations.

	Mass balance	Concentration profile within tissue	
Plate	$\frac{\partial C}{\partial t} = D_{eff} \frac{\partial^2 C}{\partial x^2} - BOD \cdot \rho_{tissue}$	$C = C_s - \frac{1}{2} \left(\frac{BOD \cdot \rho_{tissue}}{D_{eff}} \right) (L^2 - x^2)$	[4]
Cylinder	$\frac{\partial C}{\partial t} = D_{eff} \left(\frac{1}{r} \right) \frac{\partial}{\partial r} \left(r \frac{\partial C}{\partial r} \right) - BOD \cdot \rho_{tissue}$	$C = C_s - \frac{1}{4} \left(\frac{BOD \cdot \rho_{tissue}}{D_{eff}} \right) (R^2 - r^2)$	[5]
Sphere	$\frac{\partial C}{\partial t} = D_{eff} \left(\frac{1}{r^2} \right) \frac{\partial}{\partial r} \left(r^2 \frac{\partial C}{\partial r} \right) - BOD \cdot \rho_{tissue}$	$C = C_s - \frac{1}{6} \left(\frac{BOD \cdot \rho_{tissue}}{D_{eff}} \right) (R^2 - r^2)$	[6]

The diffusion of oxygen within the tissue phase is often assumed to be equivalent to water ($D_{eff}=D_{O_2,H_2O}$). The success of this approach is somewhat surprising given the structural aspects of cells and convection associated with cytoplasmic streaming. It is logical that an organism will transport oxygen throughout the tissue phase in such a way that the net diffusion rate matches the oxygen transfer rate of the surrounding aqueous system. Thus, the observation that the diffusion coefficient of oxygen in water is comparable to the effective diffusion coefficient within a tissue (D_{eff}) may reflect a logical adaptation of the tissue physiology rather than a validation of diffusion as the true transport mechanism. An example is provided on the use of these equations to characterize oxygen transport in plant tissue culture in Section 4.

There are gas spaces within plant tissues-most notably within leaves. However, gas spaces can develop in other tissues such as roots (aerenchyma) under conditions where they become oxygen deprived [12]. We have also observed hollow plant cell aggregates that suggests the mechanism of tissue death to create these gas spaces is active even in undifferentiated plant cells [2]. Although such structures clearly enhanced oxygen transport, simple descriptions such as presented in Table 1 will not be useful. There are also more complicated mechanisms of transport within differentiated plants in tissue culture (e.g. Knudsen pore diffusion). The high humidity of a tissue culture vessel will

invariably limit transpirational convective flow and supply of sugar in the medium (rather than synthesis in the leaves) will also alter 'natural' plant phloem transport. The diversity of structures and tissues that are observed in plant tissue culture makes generalizations difficult. An equally important determinant of transport gradients is the rate of oxygen consumption. The impact of elevated BOD at tissue meristems is discussed at the end of Section 3.

3. Interphase transport

3.1. OXYGEN TRANSPORT ACROSS THE GAS-LIQUID INTERFACE

The transport of oxygen across the gas-liquid interface is described in detail in all biochemical engineering texts. Since gas phase diffusion is comparatively rapid, the dominant resistance is in the liquid boundary layer. The subscript 'L' in $k_L a$ reflects this observation, and a refined version of Equation 1 can be written to specify transport that is taking place through the gas-liquid interface.

$$\text{OTR}_{g-L} = k_L a (C_L^* - C_L) \quad (7)$$

The parameter 'a' is the interfacial area per unit volume. Because 'a' is not typically a measurable quantity, the two parameters ' k_L ' and 'a' are lumped together as a single parameter. The equilibrium dissolved oxygen level (C_L^*) is available for a wide variety of conditions due to the fundamental importance for oxygen transport. There are correlations for $k_L a$ that have been developed for a wide variety of bioreactor conditions (e.g. agitator speed, gas sparge rate, reactor geometry); however, because the interfacial area of a gas dispersion can be affected by so many operating conditions, application of design equations to make predictions of OTR can be problematic. The example problem in section 4 includes experimental determination of $k_L a$ and application to characterized oxygen transport rates at the gas-liquid interface.

3.2. OXYGEN TRANSPORT ACROSS THE GAS-SOLID INTERFACE

Oxygen transfer at the gas-solid interface is rarely discussed in the context of biological reactors. Similar to the situation of mass transfer from the gas to liquid, there is minimal resistance to transport in the gas phase. As a result, oxygen delivery is limited by transport within the tissue and the surface concentration (C_S) will be determined by the equilibrium relationship of Equation 2.

$$C_{S,g-s} = C_L^* = \frac{y_{O_2} P}{H} \quad (8)$$

In contrast to microbial or other tissue culture systems, direct tissue-gas contact is common in plant tissue culture. The ability of plant tissues to transport water and resist desiccation, permits this type of growth for aseptic plants, callus and root culture. In addition, intermittent liquid contacting [8] and even trickle-bed reactors [4] have

substantial tissue surface area that is exposed directly to gas. When a tissue is in contact with gas, the characterization of oxygen transport is 'simplified' since the tissue surface concentrations associated with internal oxygen transport is known and not calculated iteratively with boundary layer mass transfer as is required for a solid-liquid interface (Section 3.3).

3.3. OXYGEN TRANSPORT ACROSS THE SOLID-LIQUID INTERFACE

Mass transfer at a solid liquid interface is similar to the gas-liquid interface, only the area of transport is more defined. As a result, the area is no longer lumped with the mass transfer coefficient (k_S) and the resulting equation is

$$\text{OTR}_{L-S} = k_S (A_{\text{tissue}} / V)(C_L - C_S) \quad (9)$$

To obtain OTR per unit volume, the tissue surface area (A_{tissue}) must be divided by the culture volume (V). In this case, the 'driving force' for mass transfer is the difference between the bulk dissolved oxygen level (C_L) and the dissolved oxygen at the surface of the tissue (C_S). The mass transfer coefficient at a liquid-solid interface (k_S) is dependent on the extent of convection near the surface. There are hundreds of correlations that can be used to estimate k_S because they are generally used to describe mass and heat transfer [13,14].

The scenario of a reaction being limited by transport at the fluid interface is a rather challenging problem that is faced very frequently in non-biological and biochemical reactors. As a result, there are many descriptions and approaches to solving this problem in all reaction engineering texts and biochemical engineering texts. The general solution to this problem is iterative: The net reaction depends upon the surface concentration and the oxygen concentration profile that results from consumption and internal diffusion (Equation 3). However, the net reaction also determines the required oxygen transfer rate at the solid-liquid surface (Equation 9). The balance of boundary layer transport and internal oxygen consumption can be found by choosing a surface concentration (C_S) then determining total internal oxygen consumption by integrating the internal concentration profile (e.g. Table 1) and comparing oxygen transport at the surface until it matches the boundary layer transport. If BOD can be considered independent of the tissue oxygen level, then this approach is greatly simplified. Net reaction is calculated directly from BOD, and the surface concentration is then fixed by the required boundary layer transport rate. While the details of these approaches are not within the scope of this chapter, these concepts are utilized in the analysis of example 4.3.

It is important to recognize that experimental measurements of tissue BOD are unavoidably influenced by internal and external transport rates. As a result, the measured oxygen consumption rates can actually be a combined measure of both tissue oxygen consumption and solid-liquid mass transfer limitations. Correcting observed BOD for the actual surface concentration was carried out in a recent evaluation of respiration at the tips of hairy roots [15]. The key to carrying out assessments of oxygen transport at the tissue-media interface is identifying an appropriate correlation for mass transfer. These mass transfer correlations usually have the generalized form:

$$\frac{k_S \cdot d_p}{D_{O_2}} = N_{Sh} = f \left(N_{Re} = \frac{\rho_{media} \cdot v_o \cdot d_p}{\mu_{media}}, N_{Sc} = \frac{\mu_{media}}{\rho_{media} \cdot D_{O_2}} \right) \quad (10)$$

where the equation is developed in terms of dimensionless groups: N_{Sh} is the Sherwood number, N_{Re} is the Reynolds number, and N_{Sc} is the Schmidt number. The major determinant of the mass transfer coefficient is the extent of convection near the liquid-solid surface which is correlated within these equations as a bulk or superficial liquid velocity (v_o). Proper use of these correlations involves carefully matching units and definitions used in the regression of the correlated experimental data.

A final important characteristic of plant tissues that affects liquid-solid transport rates is growth from meristems. The high metabolic activity in a meristem results in elevated meristematic BOD as compared to the bulk oxygen demand associated with the majority of the tissue. Respiration in root culture meristems were measured as 10-times greater than in the bulk [16]. A localized oxygen demand proportionately increases the required mass transfer coefficients needed to avoid oxygen transport limitation. Convection around this tissue must be much more intense than would be expected based on assuming uniform distribution of total tissue BOD was assumed. When localized meristematic oxygen demand is present, it must be accounted for by treating the high BOD tissues separately from the bulk respiring tissue [4]. While the mathematical treatment of localized meristem oxygen demand is rather involved, the important qualitative implication of localized oxygen demand is that it greatly increases the likelihood that the tissue respiration will be oxygen limited.

4. Example: oxygen transport during seed germination in aseptic liquid culture

The following section is presented to provide a specific application of the principles of oxygen transfer. It also provides some experimental details on how this information can be obtained and analyzed. Finally, the data presented should also clarify why oxygen transport limitations are so common in cultured plant tissues, despite their apparent low oxygen demand.

4.1. THE EXPERIMENTAL SYSTEM USED FOR ASEPTIC GERMINATION OF SEEDS IN LIQUID CULTURE

The following experimental system provided a clear example of oxygen transport limitation in plant tissue culture. The system was not created for this purpose; therefore, the experimental system will only be described briefly with details being presented elsewhere. Transgenic plants of *Nicotiana benthamiana* were created with a viral replicase (REP) of bean-yellow dwarf geminivirus [17] expressed under the control of the *Aspergillus nidulans* ethanol-inducible promoter [18]. Replicase gene insertion was verified by PCR [(+)REP] and homozygous plants were generated by successive 'selfing' with selection based on the dominant kanamycin resistance gene. Seeds were germinated in 50 mL of culture medium after surface sterilizing with 10% Clorox. Germination took place in a Gamborg's (B₅) liquid medium [19] on a gyratory shaker with 1.52 cm stroke at 150 rpm in a 25°C environmental incubator. Humidified air or

oxygen-enriched air were introduced into the shaker flask headspace at a flow rate of ~ 15 mL/min after passing the gas through a 0.2 μm gas sterilization filter.

4.2. EXPERIMENTAL OBSERVATION OF OXYGEN LIMITATION

Transgenic (+)REP seedlings germinated under ambient air conditions displayed severely stunted hypocotyls (Figure 3).

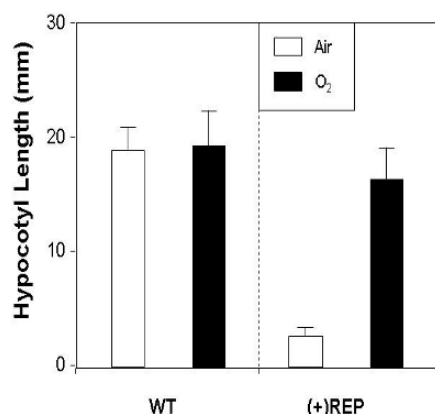


Figure 3. Germination of transgenic *N. benthamiana* seeds that contain a viral replicase (REP) under the control of an alcohol inducible promoter. WT = wild-type non-transgenic seeds. (+)REP = homozygous plants. Inhibition of hypocotyl elongation results from induction of REP as a result of alcohol formation during insufficient oxygen provided by ambient oxygen (air). Error bars are standard deviation of ~30 seedlings.

Germination under 37% and 100% oxygen displayed a germination phenotype that was indistinguishable from wild type plants. The lengths of hypocotyl segments were measured by scanning the seedlings on a flat-bed scanner with a reference scale, then digitizing length using the “NIH Image J image” analysis program. These results suggest that under ambient air conditions, the germinating seeds experience sufficiently anaerobic respiration to produce ethanol which induces the *AlcA* promoter and produce the inhibitory replicase protein. Hypocotyl length for wild-type and (+)REP *N. benthamiana* plants.

4.3. CHARACTERIZATION OF OXYGEN MASS TRANSFER

To provide a comparison of oxygen demand relative to oxygen transfer rates, the mass transfer coefficient ($k_L a$) was measured in shake flasks by adapting a sodium sulfite oxidation test method [20]. The initial amount of Na_2SO_3 added to the flask corresponded to the amount needed to react with an initially saturated water at 25°C (9.3 mg O_2/L) plus a sufficient amount to react with 50% of iodine reaction indicator. The method is based on the unreacted sulfite in a 10 mL sample reacting with 1mL of 0.025 N iodine under acidic conditions (0.5 mL glacial acetic acid). Then the unreacted iodine is titrated with a 0.0025 N sodium thiosulfate solution (containing 1 g Sodium furoate for stabilization) in conjunction with a saturated starch solution. $K_L a$ measurement was

carried out as replicated 2-point reaction rates (between 1 and 8 minutes) where the reaction was initiated with 60 mL (50 mL water containing 6 µg CoCl₂ as the reaction catalyst plus 10 mL containing 9.1 mg Na₂SO₃). The k_La measured for these experimental conditions was 4.83 hr⁻¹.

Carrying out measurements of oxygen uptake rate of germinating seeds as a function of age is not within the scope of this report. Instead, it is known that respiration will vary from essentially zero to values that are characteristic of meristematic tissue. Meristematic tissues have considerably higher respiration rates [15,16]. The two basic techniques used for BOD measurements are a submerged micro-dissolved oxygen cell, and a Warburg respirometer [21]. In a dissolved oxygen cell, the BOD is calculated based on the consumption of oxygen from the liquid phase: $\frac{dC}{dt} = BOD \cdot \rho_{tissue}$. The rate of oxygen usage is measured with a dissolved oxygen probe. The Warburg respirometer measures the volume change in the gas phase as the carbon dioxide evolved from respiration is absorbed into a basic solution [22]. It should be kept in mind that both these techniques can only measure the rate of oxygen transport for the experimental condition of the apparatus. As a result, the BOD values measured in this way are directly impacted by mass transfer limitations such as the intra-tissue transport and boundary layer transport described above. Correcting such observed values to intrinsic BOD values is very involved [15]. For the purpose of this analysis, we have chosen to use a range of BOD values of 0–100 µmole/g fresh weight/hr based on experience and reported literature values [1].

Mass transfer at the seed surface is estimated based on the rate of sedimentation of the seeds. Although liquid mixing may be considerably faster than the seed sedimentation rate, the seeds tend to move with the bulk flow; therefore, the sedimentation rate provides a reasonable estimate of mass transfer at the surface. Seed sedimentation velocities of 1.29 ± 0.059 cm/s (n=30) were measured in a glass tube. Seed diameter estimated was 0.053 cm. The correlation for mass transfer coefficient around a sphere is available as:

$$k_s = \frac{D_{O_2}}{d_p} \left[2.0 + 0.6 \left(\frac{\rho_{media} \cdot v_s \cdot d_p}{\mu_{media}} \right)^{\frac{1}{2}} \left(\frac{\mu_{media}}{\rho_{media} \cdot D_{O_2}} \right)^{\frac{1}{3}} \right] \quad (11)$$

Viscosity of water at 25°C is 0.89 cP. These conditions provide a seed surface mass transfer coefficient of 0.00605 cm/s. The preceding analysis provides parameters needed to examine oxygen transport for the seedling germination study. For the 40 seeds germinating in each flask, the total oxygen demand of the system would be 0.468 µmoles per hour at a BOD of 100 µmole / g FW /hr. If the BOD is considered a constant, the minimum surface concentration of 216 µM can be calculated when the center of the seed reaches a zero oxygen concentration from Equation 6:

$$C_s = \frac{BOD \cdot \rho_{tissue} \cdot R^2}{6 \cdot D_{eff}} \quad (12)$$

This shows that the dissolved oxygen level at the seed surface must approach the ambient equilibrium dissolved oxygen ($C_L^* = 250 \mu\text{M}$) to avoid mass transfer limitation. If the mass transfer limitation was only at the gas-liquid interface (Equation. 7, $C_L=C_S$), the total oxygen transfer capacity through the gas-liquid interface ($V \cdot \text{OTR}_{g-L}$) would be $8.33 \mu\text{moles per hour}$ which is 18-times greater than the seed oxygen demand. For the mass transfer limitations at the solid-liquid interface, the total oxygen transfer to the 40 seeds can be calculated as $40(\text{OTR}_{L-S} \cdot V) = k_S(40 \cdot A_{\text{seed}})(C_L^* - C_S)$. This provides a total transport rate at the media-seed interface of $0.265 \mu\text{moles of oxygen per hour}$, which is about half as much oxygen as the seeds require. These calculations indicate that although the gas-liquid interface is not limiting oxygen transport, the oxygen flux at the media-seed interface is insufficient to meet the oxygen demand.

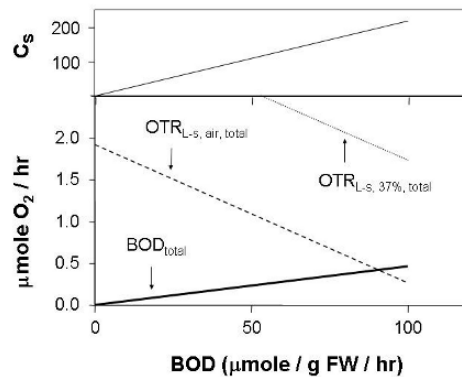


Figure 4. Application of the oxygen transport equations to the example case study of seed germination in a gyratory shake flask. Surface concentration of the seed (C_S) is calculated by Equation 12. Total biological oxygen demand (BOD) is compared to the total oxygen that can be transported across the media-seed interface.

A more comprehensive analysis is presented in Figure 4. In this figure, the surface concentration of the seed is calculated for the full range of BOD using Equation 6. The remaining driving force ($C_L^* - C_S$) is then used to calculate the transport at the seed-media interface. [Note that to be totally rigorous, the bulk liquid concentration (C_L) would have to be corrected for the required gas-liquid transport; however, since that rate is more than an order of magnitude higher than the solid-liquid interface, the correction is very small for this example].

In this graph, oxygen deprivation is predicted within the germinating seed if the total transfer rate for the seed-media interface is less than the total oxygen demand. As shown in this figure, these calculations predict an oxygen limitation for germination under ambient conditions. It should be kept in mind that the intention of these calculations is not intended to be exact. It is very likely that the diffusion of oxygen within the compact tissues of a seed will be considerably less than water. None-the-less, the calculations are consistent with the observation of induction of the viral replicase as a result of anaerobic metabolism. In addition, the calculations also predict that oxygen deprivation can be prevented using an elevated oxygen partial pressure which is consistent with the experimental observation of a wild-type phenotype for germinating transgenic seeds at 37 and 100% oxygen.

5. Conclusions

The principles of oxygen mass transfer are presented to provide a qualitative understanding of the culture conditions where oxygen transport limitations can be observed. The context of the discussion is the applications of these principles to plant tissue culture propagation vessels and bioreactors. An experimental system which effectively uses an inhibitory protein driven by alcohol-inducible promoter is used as a qualitative probe of oxygen deprivation in the germinating seeds. Oxygen limitation is correctly predicted in this system even when the consumption rates of the seeds are extremely small as compared to the gas-liquid oxygen transfer rates. It is shown that the solid-liquid boundary layer is far more constraining for the delivery of oxygen. Use of oxygen enrichment of the gas phase overcomes this mass transfer limitation by increasing the driving force for transport in the bulk liquid phase. These principles of oxygen mass transfer can be adapted (both qualitatively and quantitatively) to many other aspects of oxygen-limited growth of plant tissues in culture.

Acknowledgements

Viral replicase construct with alcohol-inducible promoter was obtained from Hugh Mason (Dept. Plant Biology, Arizona State University). Generation of the transgenic plants was carried out through efforts of Jennifer Campbell, Jennifer Stick, Gregory Thurber, Jason Collens, and Kelly Tender. Measurements of k_La were carried out with the assistance of Randhir Shetty. Lauren Andrews carried out seed sedimentation studies. Tobacco seeds were obtained from the <<http://www.ars-grin.gov>> USDA National Plant germplasm system. Finally, we acknowledge financial support of the National Science Foundation (REU supplement to Grant # BCS-0003926 & GOALI program and) for A.L.T. and a Research Experience for Undergraduate site program (Grant # EEC-0353569) for L.A.

References

- [1] Curtis, W.R. (2005) Application of bioreactor design principles to plant micropropagation. Invited contribution, 1st Int. Symp. on Liquid Systems for *In Vitro* Mass Propagation of Plants. Kluwer Academic Publishers, The Netherlands; (in press).
- [2] Singh, G. and Curtis, W.R. (1994) Reactor design for plant cell suspension culture. In: Shargool, P.D. and Ngo, T.T. (Eds.) *Biotechnological Applications of Plant Culture*. CRC Press, Boca Raton, FL; pp.153-184.
- [3] Tescione, L., Ramakrishnan, D. and Curtis, W.R. (1997) The role of liquid mixing and gas-phase dispersion in a submerged, sparged root reactor. *Enz. Microbial Technol.* 20: 207-213.
- [4] Ramakrishnan, D. and Curtis, W.R. (2004) Trickle-bed root culture bioreactor design and scale-up: Growth, fluid-dynamics, and oxygen mass transfer. *Biotechnol. Bioeng.* 88(2): 248-260.
- [5] Kim, Y.J.; Weathers, P.J. and Wyslouzil, B.E. (2002) Growth of *Artemisia annua* hairy roots in liquid- and gas-phase reactors. *Biotechnol. Bioeng.* 80(4): 454-464.
- [6] Bordonaro, J.L. and Curtis, W.R. (1997) Development of a fluorescent tracer technique to evaluate mixing in plant root culture. *Biotechnol. Techniques* 11(8): 597-600.
- [7] Hsiao, T.Y.; Bacani, F.T.; Carvalho, E.B. and Curtis, W.R. (1999) Development of a low capital investment reactor system: Application for plant cell suspension culture. *Biotechnol. Prog.* 15(1): 114-122.

- [8] Buwalda, F.; Frenck, R.; Lobker, B.; Berg-De Vos, B. and Kim, K.S. (1995) EBB and flow cultivation of *Chrysanthemum* cuttings in different growing media. *Acta Hort.* 401:193-200.
- [9] Carvalho, E. and Curtis, W.R. (1998) Characterization of fluid-flow resistance in root cultures with a convective flow tubular bioreactor. *Biotechnol. Bioeng.* 60(3): 375-384.
- [10] Tescione, L.; Asplund P. and Curtis, W.R. (1999) Reactor design for root culture: Oxygen mass transfer limitation. In: Fu, T.J.; Singh, G. and Curtis, W.R. (Eds.) *Plant Cell and Tissue Culture for the Production of Food Ingredients*. Kluwer Academic/Plenum Publishers, New York; pp. 139-156.
- [11] Wilke, C.R. and Chang, P. (1955) Correlation of diffusion coefficients in dilute solutions. *AIChE J.* 1(2): 264-270.
- [12] Ramakrishnan, D. and Curtis, W.R. (1994) Fluid dynamic studies on plant root cultures for application to bioreactor design. In: Furusaki, S. and Ryu, D.D.Y (Eds.) *Studies in Plant Science, 4: Advances in Plant Biotechnology*. Elsevier, Amsterdam; pp. 281-305.
- [13] Cussler, E.L. (1997) *Diffusion: Mass transfer in fluid systems*. 2nd Edition, Cambridge University Press.
- [14] Bennett, C.O. and Myers, J.E. *Momentum Heat and Mass Transfer*. 3rd Ed., McGraw Hill, 1982.
- [15] Asplund, T.A. and Curtis, W.R. (2001) Intrinsic oxygen use kinetics of transformed root culture. *Biotechnol. Prog.* 17: 481-489.
- [16] Ramakrishnan, D. and Curtis, W.R. (1995) Elevated meristematic respiration in plant root cultures: implications to reactor design. *J. Chem. Eng. Japan* 28(4): 491-493.
- [17] Mor, T.S.; Moon, Y.S.; Palmer, K.E. and Mason, H.S. (2003) Gemini-virus vectors for high-level expression of foreign proteins in plant cells. *Biotechnol. Bioeng.* 81(4): 430-437.
- [18] Felenbok, B. (1991) The ethanol utilization regulon of *Aspergillus nidulans*: the alcA-alcR system as a tool for the expression of recombinant proteins. *J. Biotechnol.* 17:11-18.
- [19] Gamborg, O.L.; Miller, R.A. and Ojima, K. (1968) Nutrient requirements of suspension of soybean root cells. *Exp. Cell Res.* 50: 148-151.
- [20] Ruchti, G.; Dunn, I.J.; Bourne, J.R. and Von Stockar, U. (1985) Practical guidelines for the determination of oxygen transfer coefficients (K_La) with the sulfite oxidation method. *Chem. Eng. J.* 30(1): 29-38.
- [21] Carvalho, E.B. and Curtis, W.R. (2002) Effect of elicitation on growth, respiration and nutrient uptake of root and cell suspension cultures of *Hyoscyamus muticus*. *Biotechnol. Progress* 18: 282-289.
- [22] Umbreit, W.H.; Burris, R.H. and Stauffer, J.F. (1972) *Manometric and biochemical methods applicable to the study of tissue metabolism*. Burgess Publishing Company, Minneapolis, MN.

TEMPORARY IMMERSION BIOREACTOR

Engineering considerations and applications in plant micropropagation

F. AFREEN

*Department of Bioproduction Science, Chiba University, Matsudo, Chiba
271-8510, Japan-Fax: 81-47-308-8841-Email:afreen@restaff.chiba-up.jp*

1. Introduction

Commercial laboratories need to produce a large number of high quality plants at the lowest possible costs of production which mainly includes labour cost, general overhead cost and the cost per unit space in the growth room. Large-scale plant propagation by using tissue culture technique is often criticized because of the intensive labour requirement for the multiplication process; thus, scaling-up of the production systems and automation of unit operations are necessary to cut down the production costs [1,2]. In order to achieve efficient and automated production in plant tissue culture, plant production systems have evolved from a small research scale to a large volume and high-yield culture system, and liquid media are preferably used to facilitate handling [3]. The use of bioreactors with liquid media for micropropagation is becoming more popular due to the ease of scaling-up [4] and the low production costs [5]. Bioreactor is a self-contained, sterile environment which capitalizes on liquid nutrient or liquid/air inflow and outflow systems, and is mainly designed for intensive culture. The basic function of a bioreactor is to provide optimum growth conditions by regulating various chemical and/or physical factors. More specifically, it affords the maximal opportunity to monitor and control over micro-environmental conditions such as agitation, aeration, temperature and pH of the liquid medium. Several types of bioreactors are currently available such as air lift-bioreactor, stirred tank bioreactor, rotating drum bioreactor, column bioreactor etc. In these bioreactors, the plantlets or explants are cultured under complete submerged condition in the liquid medium which may limit the gas exchange of the plant materials and consequently result in vitrification or hyperhydricity of plant tissues [6]. Vitrification is a severe physiological disorder involving apoplastic water accumulation, due to the extended contact between the explants [7,8]. Symptoms of vitrification include chlorophyll deficiency, cell hyperhydricity, hypolignification, reduced deposition of epicuticular waxes and changes in enzymatic activity and protein synthesis [7,8]. To avoid the problems associated with liquid culture in bioreactor, different systems have been developed, such as membrane raft system, nutrient mist bioreactor, temporary immersion bioreactor etc. [9]. Among those, temporary immersion

bioreactor has gained popularity mainly due to its simplicity and high production rate with minimum physiological disorders. In the current chapter the definition, brief historical description, designing, benefits and related problems of the system will be provided with special reference to the development of a new scaled-up system.

2. Requirement of aeration in bioreactor: mass oxygen transfer

Generally for normal plant cell metabolism, oxygen is required and only the dissolved oxygen can be utilized by plants growing in an aqueous culture medium. Therefore, in a bioreactor where oxygen transport limitations can usually be observed, aeration is required to promote the mass transfer of oxygen from the gaseous phase to the liquid phase. To meet the demand of the actively respiring plant tissues, forced-diffusion of oxygen in the liquid nutrient medium is required and this can be achieved by aeration of the liquid medium, agitation of the system, continuous shaking of the container etc. Gas-liquid oxygen transfer can be explained by using the equation of Leathers *et al.* [3]:

$$OTR = K_L a (C_x - C_L) \quad (1)$$

Where, OTR is the volumetric oxygen transfer rate ($\text{mmol l}^{-1} \text{h}^{-1}$), K_L is the mass transfer coefficient (m h^{-1}), a is the specific gas-liquid interfacial area. The terms K_L and a are generally considered together and thus $K_L a$ in the current equation can be termed as oxygen mass transfer coefficient (h^{-1}). C_x is the dissolved oxygen concentration at equilibrium with the gas phase (mmol l^{-1}) and C_L is the actual dissolved oxygen concentration (mmol l^{-1}) in the culture medium. $K_L a$ is frequently used to measure the efficiency of oxygen transfer in a bioreactor. Oxygen solubility increases with decreasing temperature; the dissolved oxygen concentration for 100% air saturated water at sea level is $8.6 \text{ mg O}_2 / \text{L}$ at 25°C . The oxygen mass transfer coefficient is strongly affected by agitation speed, air flow rate and design of a bioreactor. In general,

$$K_L a = k \left(\frac{P_2}{V_R} \right)^{0.4} * (V_s)^{0.5} * (N_s)^{0.5} \quad (2)$$

Where, P_2 is the power required to aerate the bioreactor, V_R is the volume of the bioreactor, V_s is the air flow rate, N is the agitation speed. Note that the mass transfer coefficient increases with agitation speed and/or air flow rate. Most of the bioreactors designed are capable to agitate (mixing) and aerate the medium simultaneously. In some cases, such as in airlift bioreactor [10] to increase the dissolve oxygen concentration, only aeration is used. In such case, N can be counted as zero. Many bioreactors have been designed with liquid medium circulation system with the aim to improve the oxygen transport. There are usually two different mechanisms of transporting oxygen throughout the bioreactor, one is mixing and the other one is circulation. [see Curtis and Tuerk in this volume]. As described by Curtis and Tuerk, liquid circulation is a measure of how fast a fluid element gets from one side of the bioreactor to the other. Whereas, mixing means, how quickly a fluid element can be dispersed throughout the

entire bioreactor. However, achieving greater circulation throughout the bioreactor does not necessarily result in better mixing. A detailed description of oxygen transport in liquid culture system such as in bioreactor has already been described in this volume [see Curtis and Tuerk]. In order to fulfil the oxygen demand of the cultured plants in the bioreactor, a completely different approach has been taken, where, the plant materials are exposed only temporarily to the liquid nutrient medium. Such a bioreactor does not require any aeration or agitation and is termed as temporary immersion bioreactor.

3. Temporary immersion bioreactor

3.1. DEFINITION AND HISTORICAL OVERVIEW

The method of temporarily wetting the entire culture or plant tissue with nutrient solution followed by the draining away of the excess nutrient solution under gravity so that the plant tissue has access to air is defined as temporary immersion system. This system usually involves a wetting and drying cycle which occurs periodically in a given period of time and hence it can also be termed as periodic, temporary immersion. Heller in 1965 [11], first mentioned that a mere up-and-down motion of the nutrient medium, without renewal showed the same effect as a true renewal in suspension culture; this is probably the first concept of the temporary immersion system. In 1985, Tisserat and Vandercook [12], probably, first applied the idea of temporary immersion system in plant tissue culture; they designed a system consisting of a large elevated culture chamber that was drained and then refilled with fresh medium at certain intervals. Aitken-Christie *et al.* in 1988 [13], developed a semi-automated culture system where plant materials were cultured in a large container with automatic addition and removal of liquid medium on a periodical base. After that, Simonton *et al.* [14] developed a programmable micropropagation apparatus with cycled liquid medium; in this system the liquid medium was intermittently applied to the cultured plants according to a selected schedule. In order to overcome the physiological and technical limitations encountered in bioreactors in the year 1993, a new temporary immersion system known as RITA bioreactor was developed at CIRAD [15] This new technique has been used for the improvement of plant propagation such as: banana [15], coffee [16], *Hevea* [17], *Citrus deliciosa* [18] and many other plant species.

3.2. DESIGN OF A TEMPORARY IMMERSION BIOREACTOR

The principal components of a temporary immersion bioreactor are the same as those in airlift or bubble column-type bioreactors, except, a fixed or floating raft support system inside the culture vessel is required to support the explants. Liquid medium is pumped into the culture vessel from a storage tank usually located underneath the vessel (Figure 1) or from a separate bottle in case of a twin bottle system.

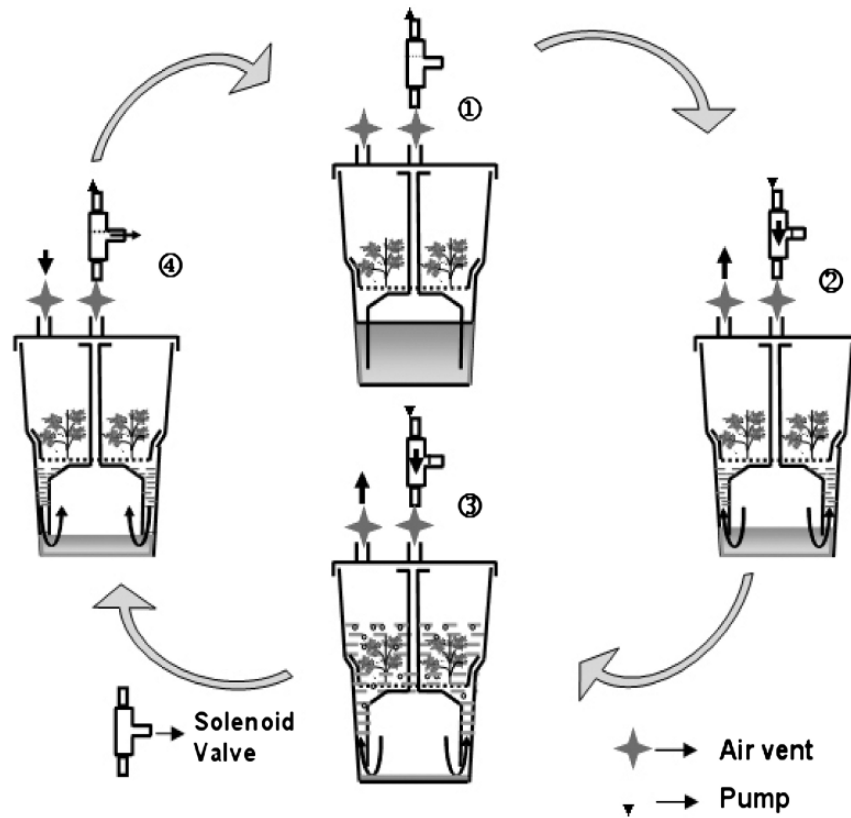


Figure 1. Design and operation procedure of a temporary immersion bioreactor.

The medium remains in the vessel for few minutes, after which it drains back to the storage tank for reuse. The entire process is controlled by a solenoid valve and the interval period varies from three to six hours depending on the plant species or requirement of the explants.

3.3. ADVANTAGES OF TEMPORARY IMMERSION BIOREACTOR

Temporary immersion bioreactors provide an excellent way of using liquid medium at the same time controlling the gaseous environment. Moreover, it can provide the possible automation of the production system which facilitates low production costs. In other words, increasing the rate of growth and multiplication by using bioreactors more plants per unit area of the growth room are produced, which reduces the cost per plant per unit space of growth room. Liquid culture bioreactors are mainly suitable for the large-scale production of small size somatic embryos, growth of bulb, corms, microtubers, compact shoot cultures etc.

Major features of a temporary immersion bioreactor are:

- Reduction of hyperhydricity, compared with that of permanent immersion, is the major achievement of a temporary immersion system. As plants are immersed in the liquid medium only for 5-10 min. in every 3 or 6 h, the physiological disorders are reduced and the plants become healthier.
- Plant growth and development can be controlled by manipulating the frequency and duration of immersion in liquid medium.
- Plant growth is improved because during every immersion the plant is in direct contact with the medium and a thin film of liquid covers the plant throughout the interval period.
- Air vents attached to the vessel prevent the cultures from contamination.
- Due to the lack of agitation or aeration, the mechanical stress on plant tissues are generally low compared with the other bioreactor systems.

3.4. SCALING UP OF THE SYSTEM: TEMPORARY ROOT ZONE IMMERSION BIOREACTOR

The major problem imposed by liquid media in bioreactors even temporary immersion bioreactor is the phenomenon of hyperhydricity, morphogenic shoot and leaf malformation, due to the continuous immersion of the tissues in the medium [19]. The malformations are manifested in glossy hyperhydrous leaves, distorted root and shoot anatomy. Another important issue is the expression of contamination because sugar-containing liquid medium in general encourages contamination. Exogenous contamination can often be controlled by good sterile technique; however, endogenous contamination cannot easily be controlled in repeated subcultures. To deal with these problems, Afreen *et al.* [20] developed a scaled-up bioreactor known as temporary root zone immersion bioreactor. The system is basically based on photoautotrophic (sugar-free medium) micropropagation and thus can reduce the chance of microbial contamination. Moreover, the system can enhance the growth as well as improve the quality of plants.

3.5. DESIGN OF THE TEMPORARY ROOT ZONE IMMERSION BIOREACTOR

The temporary root zone immersion bioreactor consisted mainly of two chambers (Figure 2); the lower chamber was used as a reservoir for the nutrient solution and the upper one for culturing embryos. A narrow air distribution chamber was located between these two chambers. Two air-inlet tubes (internal diameter 5 mm; length 10 mm) opened into the air distribution chamber and were directly connected to an air pump (Non noise S200, Artem Co. Ltd., Japan) via a filter disc (pore diameter 0.45 μm ; diameter 45 mm; Nippon Millipore Co. Ltd., Yonezawa, Japan) to prevent microbes entering the culture vessel.

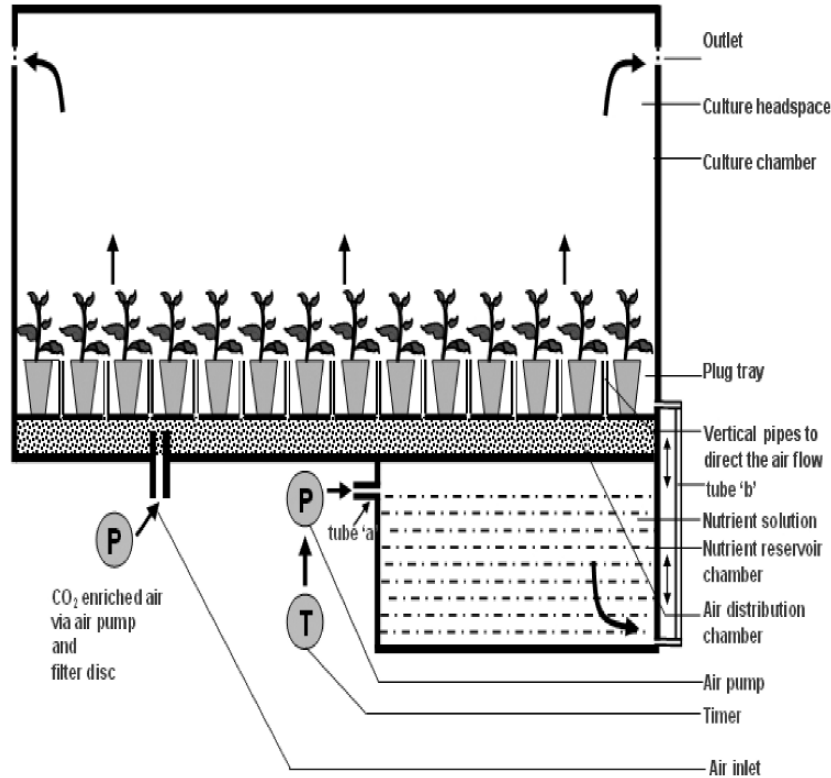


Figure 2. Schematic diagram of the temporary root zone immersion (TRI-bioreactor) bioreactor with forced ventilation system. Reproduced from Afreen et al. (2002) [20]).

The top of the air distribution chamber had several narrow tubes which were fitted vertically in between the rows of the cell tray and opened in the culture chamber headspace. The CO₂ enriched air entered the culture chamber from the air distribution chamber by means of these vertical tubes. Outflow was through four Millipore membranes (pore diameter 0.45 µm; Nippon Millipore Co. Ltd., Yonezawa, Japan) attached covering the outlet holes (10 mm diameter) on the sidewalls of the bioreactor. The culture chamber contained a 6 cell by 9 cell autoclavable cell tray (Minoru Sangyo Co. Ltd, Japan) for culturing the explants.

The nutrient reservoir chamber had an air inlet tube (a), which connected an air pump to the headspace of the nutrient reservoir; an electric timer operated the pump. A second tube (b) ran from close to the base of the reservoir to the culture chamber. To supply nutrient solution to the culture chamber the air pump was switched on, thereby raising the pressure in the headspace of the reservoir and forcing the nutrient solution from the reservoir into the culture chamber. The nutrient solution immersed the root zone temporarily for a total of 15 min every 6 h. After 15 min the air pump was switched off and the excess nutrient solution flowed back into the reservoir under gravitation.

3.6. CASE STUDY – PHOTOAUTOTROPHIC MICROPROPAGATION OF COFFEE

Coffee plays a major role in the economy of many African, American and Asian countries. The coffee plant is an evergreen, woody perennial that belongs to the Rubiaceae family. The commercially important two species, *Coffea arabica* and *Coffea canephora* were combined in a new species named *Coffea arabusta* [21]. The *in vitro* growth of *C. arabusta* microcuttings is very slow [22] and therefore for the mass clonal multiplication somatic embryogenesis is considered to be an effective, alternative method.

In the multi-stage somatic embryogenesis of *C. arabusta*, cotyledonary stage is the earliest stage embryo, capable of photosynthesizing [23]. However, the extent of plantlet heterotrophy, photomixotrophy or photoautotrophy is dependent not only on photosynthetic ability of the plant material but also on medium composition, volume of culture vessels, aeration of the vessel etc. Therefore, Afreen *et al.* [20] cultured cotyledonary stage coffee somatic embryos under photoautotrophic conditions in different culture systems with the aim of developing an optimized protocol for large-scale embryo-to-plantlet conversion and culture system.

The establishment and high PPF pre-treatment of somatic embryos have been described by Afreen *et al.* [23]. Pre-treated cotyledonary stage embryos were selected and then cultured under photoautotrophic conditions (in sugar-free medium with CO₂ enrichment in the culture headspace and high PPF) in three different types of culture systems as followed:

- Magenta vessel
- Modified RITA-bioreactor with temporary immersion system (Figure 1) and
- Temporary root zone immersion system bioreactor (TRI-bioreactor; Figure 2).

A mixture of vermiculite and paper pulp (as described by Afreen *et al.* [24]) was used as supporting medium in the Magenta vessels and in TRI-bioreactors. For modified RITA-bioreactors, MS liquid nutrient solution was used and the immersion frequency was 5 min/6 h by connecting an air pump through an electric timer. The planting density for all the treatments was 2.4 X 10³ plantlets/m² area of culture tray.

To provide natural ventilation in the Magenta vessels, two gas-permeable Millipore filter membranes (pore diameter 0.45 µm) were attached on the hole (10 mm diameter) of the lid of the vessels. RITA-bioreactors were modified by attaching three gas-permeable filter membranes with 0.45 µm pore diameter and covering the hole (10 mm diameter) of the lid of each of these vessels. The number of air exchanges was 2.6 h⁻¹ in both Magenta vessels and modified RITA-bioreactors throughout the experiment (measured according to Kozai *et al.* [25]).

In TRI-bioreactor, forced ventilation was introduced by using an air pump connected to the headspace of the air distribution chamber (Figure 2); the flow rates were initially 50 ml min⁻¹ (number of air exchanges was 1.6 h⁻¹) and were gradually increased every 2 or 3 days to maintain the CO₂ concentration in the culture headspace in a range *ca.* 1000 µmol mol⁻¹, the maximum flow rate was 200 ml min⁻¹ on day 45 (number of air exchanges was 5.8 h⁻¹).

For all the treatments, hormone free MS medium was used as a basal medium; sucrose, vitamins and amino acids were subtracted from the formulation to ensure the photoautotrophic conditions. Vessels were placed in a growth chamber with an enriched

CO₂ concentration (1000-1100 $\mu\text{mol mol}^{-1}$) and with a PPF of 100 $\mu\text{mol m}^{-2} \text{s}^{-1}$ during the 16 h photoperiod; ambient relative humidity was 80-85% and the air temperature was 23°C.

Experiments were conducted for 45 days and the harvesting included recording of plantlet conversion percentage, fresh and dry mass of the plantlets and percentage of rooting. For the chlorophyll fluorescence, chlorophyll contents and stomatal studies ten replicates were taken from each treatment. CO₂ concentration in the culture headspace was measured throughout the culture period and the net photosynthetic rate was calculated according to the method of Fujiwara *et al.* [26]. Plantlets were transplanted in the greenhouse (average temperature 29±2°C; RH 60-70%) and on Day 7 the survival percentage was recorded. After 30 days of transplanting, plants were harvested and fresh and dry mass of the survived plants were recorded.

In terms of plantlet conversion percentage the difference was very distinct among the treatments; in TRI-bioreactor almost 84% of the cotyledonary stage embryos produced plantlets, whereas in Magenta vessel and in modified RITA-bioreactor the conversion percentages were 53 and 20% respectively [24]. Taking into account of all the parameters of growth and development within the three different types of culture vessels, it is evident that embryos grown in the TRI-bioreactor produced more vigorous shoots and normal roots than those grown in Magenta vessel. The growth of the plantlets attained in modified RITA-bioreactor was intermediate between that of plantlets grown in the TRI-bioreactor and Magenta vessel (Figure 3).

The leaf fresh and dry mass of the plantlets from TRI-bioreactor were significantly higher than those of the plantlets grown in modified RITA-bioreactor and Magenta vessel. The most noticeable difference was observed in case of root growth. In TRI-bioreactor, 90% of plantlets developed roots, 3 and 1.6 times more than plantlets grown in modified RITA-bioreactor and Magenta vessel, respectively. It should be mentioned here that even the roots which developed in a few plantlets in modified RITA-bioreactor remained very small and stunted. Plantlets cultured in Magenta vessel exhibited an intermediate root growth pattern between those of TRI-bioreactor and modified RITA-bioreactor.

In TRI-bioreactor, as the plantlets grew in the course of time, the CO₂ concentration in the culture headspace was controlled by increasing the air inflow rate and thus the number of air exchanges [24]. Thus, despite the increase in biomass, CO₂ concentrations were nearly the same throughout the experimental period (approx. 1280 $\mu\text{mol mol}^{-1}$).

Temporary immersion bioreactor

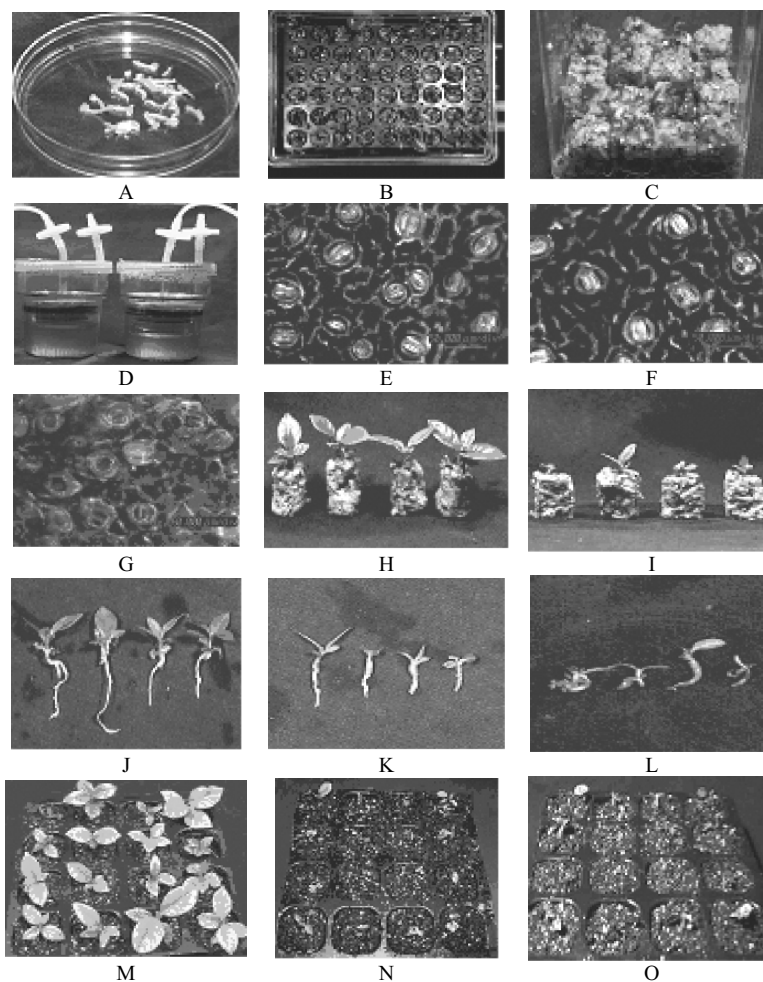


Figure 3. A. Coffee somatic embryos regenerated from leaf discs after 14 weeks of culture under low light ($30 \mu\text{mol m}^{-2} \text{s}^{-1}$) followed by 2 weeks under high light ($100 \mu\text{mol m}^{-2} \text{s}^{-1}$) ($\times 0.5$). B–D, 45-d-old plantlets developed from cotyledonary stage embryos under photoautotrophic conditions in a temporary root zone immersion (TRI) bioreactor (B, $\times 0.2$), a Magenta vessel (C, $\times 0.7$) and a modified RITA-bioreactor (D, $\times 0.2$). E–G, Stomata from the abaxial (lower) surface of the first true leaves of plantlets developed photoautotrophically in TRI-bioreactor (E), Magenta vessel (F) and modified RITA-bioreactor (G). H and I, Individual plantlets immediately before transplanting *ex vitro* grown in a TRI-bioreactor (H) and a Magenta vessel (I). J–L, Root development of plantlets grown in a TRI-bioreactor (J), a Magenta vessel (K) and a modified RITA-bioreactor (L). M–O, On day 30 after transplanting, plantlets previously grown in a TRI-bioreactor (M), a Magenta vessel (N) and a modified RITA-bioreactor (O). Reproduced from Afreen et al. (2002) [20].

In contrast, in Magenta vessels and in the modified RITA-bioreactor, the number of air exchanges could not be controlled, and were thus 3.3 h^{-1} throughout the experimental

period (under natural ventilation). In the modified RITA-bioreactor, the CO₂ concentration in the headspace fell from 1278 μmol mol⁻¹ on day 7 to 1266 μmol mol⁻¹ on day 42 despite the low air exchange rate; possible reasons for this low consumption of CO₂ by plantlets include:

- due to the small size of chlorophyllous plant materials, total CO₂ consumption is low;
- total chlorophyll contents of the plantlets are lower than those of plantlets in other treatments; and most importantly,
- as the chlorophyllous plant material remained moist almost all the time due to complete immersion of plantlets and the high humidity in the culture headspace, these plantlets were probably virtually unable to fix any CO₂ from the atmosphere for *in vitro* metabolism.

The highest net photosynthetic rate was observed in plantlets grown in the TRI-bioreactor [20]. In general, chlorophyll *a* and *b* contents (606 and 241 μg g⁻¹ fresh mass, respectively) based on the fresh mass of leaves was highest in plantlets grown in the TRI-bioreactor, which were, 2 and 1.6 times, respectively those of leaves of plantlets grown in the modified RITA-bioreactor. In the case of Magenta vessels, chlorophyll *a* and *b* contents of leaves were intermediate between those of plantlets grown in TRI- and modified RITA-bioreactors.

The potential activity of PSII (ϕ_p^{MAX}), as estimated in the dark, was nearly the same in leaves of plantlets grown in the TRI-bioreactor ($\phi_p^{\text{MAX}} = 0.89$) and in Magenta vessels ($\phi_p^{\text{MAX}} = 0.83$) in contrast, ϕ_p^{MAX} was low in leaves of plantlets grown in the modified RITA-bioreactor (0.76). Similarly, in case of actual photochemical efficiency of PSII (ϕ_p) an increase in the quantum yield for electron transport was noted in leaves of plantlets grown in both the TRI-bioreactor (ϕ_p reaching 0.35) and in Magenta vessel ($\phi_p = 0.32$), whereas the value was comparatively lower ($\phi_p = 0.25$) in plantlets of modified RITA-bioreactor than those of plantlets in the other two treatments [20].

Microscopy highlighted that stomatal density was highest in the leaves of plantlets grown in the TRI-bioreactor (8.3 mm⁻² leaf area) followed by those of plantlets from the modified RITA-bioreactor (7.5 mm⁻² leaf area) and lowest in leaves of plantlets grown in Magenta vessels (5.9 mm⁻² leaf area). The most noticeable feature was that in the leaves of plantlets from modified RITA-bioreactor some stomata were open wide while others were distorted or still morphologically immature. It is possible that these stomata may not function properly [20].

The survival percentage *ex vitro* of the plants, which was recorded on Day 7 followed a similar pattern and was highest (98%) in the plantlets grown in TRI-bioreactor followed by 61% and 30% survival of the plants from modified RITA-bioreactor and Magenta vessels, respectively.

The research [20] provides clear evidence that, for the embryo-to-plantlet development under photoautotrophic conditions, the use of Magenta vessels and modified RITA-bioreactor is less effective at promoting shoot and root growth both *in* and *ex vitro* compared with the TRI-bioreactor. Moreover, for large-scale production the use of small vessel has many disadvantages. On the other hand, RITA bioreactor is claimed to be suitable for embryo-to-plantlet development without handling the plant material [20]; however at the end of each phase the culture medium needs to be changed. In case of RITA-bioreactor, density of plant material is also a limiting factor.

Temporary immersion bioreactor

In general, RITA bioreactors are used for the development of plantlets from embryogenic cell suspension cultures using sugar-containing medium. Therefore when modified RITA-bioreactor was used for embryo-to-plantlet development under photoautotrophic conditions, the growth was substantially reduced compared to the growth obtained in TRI-bioreactor. This is most likely to be because in the modified RITA-bioreactor after every immersion of the plant material with nutrient solution, the entire plant becomes wet and, the plants remain covered by a film of nutrient medium by capillary attraction during the interval period (Figure 4a).

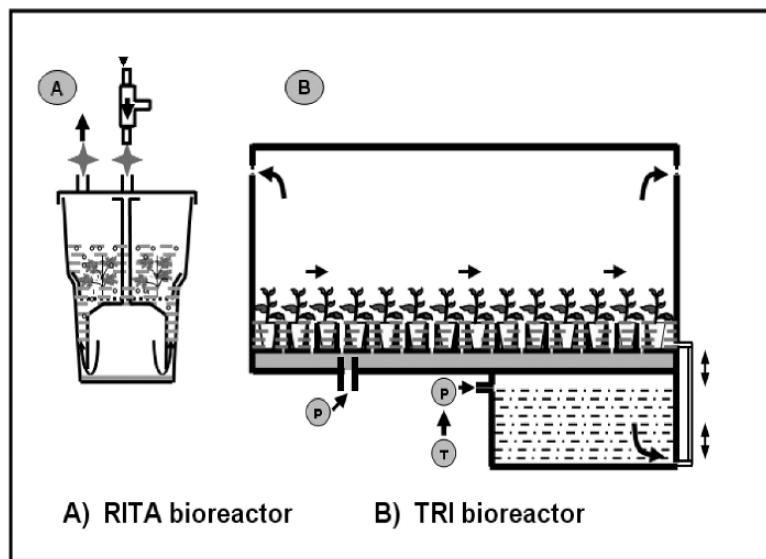


Figure 4. Comparison between the Operation procedures of a) modified RITA-bioreactor [16] and b) TRI-bioreactor [20].

In addition to this, because the relative humidity inside the vessel is normally high (95-99%), the plant material either is never completely dried out or it takes a long period to dry out. Thus, a thin layer of nutrient medium surrounding the plant material acts as a liquid boundary layer, which impedes the exchange of gases between the plant and the surrounding environment and possibly prevents the CO_2 fixation in the chlorophyll-containing zones - clearly a key factor for the photoautotrophic growth of embryos. In case of conventional photomixotrophic systems, the media contain sugar and therefore the lack of air exchanges may not be as serious a consequence as it is for the plantlets, which completely depend on CO_2 in the atmosphere for their photoautotrophic growth. Again, it is emphasized that the RITA-bioreactor system has not been developed for culturing plantlets under photoautotrophic conditions. Moreover, in this study, the RITA-bioreactor was modified by attaching three gas permeable filter membranes on the lid, as was done for Magenta vessels. Thus, a completely different result can be expected if the original RITA-bioreactor with sugar-containing nutrient solution was to be used.

In contrast, in case of TRI-bioreactor only the root zone is immersed and the plant remains undisturbed (Figure 4b). Therefore the exchange of gases between the plant and the surrounding environment is unimpeded because there is no liquid boundary layer resistance. In this situation, the plant can easily photosynthesize and produce its own carbohydrate. Therefore, the TRI-bioreactor grown plantlets, not only exhibited the best growth, but they were physiologically normal, survived well and grew faster *ex vitro*.

As discussed by Gupta *et al.* [27], in the conventional system, for embryo-to-plantlet development following steps are necessary:

- Embryo selection and transfer on the germination medium.
- Germinated and rooted plantlet selection and transfer to soil.
- Acclimatization.

Generally, in each of the above phases, cotyledonary, late cotyledonary or germinated somatic embryos are selected individually, in most cases by hand under the stereo microscope. The invention of machine vision [28] and image analysis [29] systems offer great potential for classifying and sorting embryos but the use is still limited. These selected embryos are then transferred onto gelled medium for germination.

After 6-10 weeks of germination, plantlets with epicotyl are selected by hand, transferred to soil and incubated in a greenhouse with frequent misting for acclimatization and growth. In somatic embryogenesis procedures aimed at mass production, these methods are still very time consuming and involve high labour costing. However, in case of TRI-bioreactor system, cotyledonary stage embryo selection is necessary which is done by hand, but once the embryos are transferred to the bioreactor, germination, root development and acclimatization take place in the same bioreactor and without handling the plant material or changing the culture medium. Another advantage of the new system is that by increasing the number of cells in the culture cell tray the density limitations can be overcome.

3.7. ADVANTAGES OF THE SYSTEM

- Healthy, quality transplants or plantlets can be produced and the problem of hyperhydricity can be reduced.
- Microbial contamination is a major challenge to use liquid medium in bioreactor system; by growing the plants in photoautotrophic conditions (sugar-free medium) in TRI-bioreactor, this can be overcome very easily.
- Most importantly it is ideally suitable for growing a variety of sizes of plantlets starting from cotyledonary stage somatic embryos (0.6-1 cm) to 6-7 cm height plantlets, which is not possible in other temporary immersion systems.
- Unlike other bioreactors including temporary immersion bioreactor, the shoot part remains undisturbed and thus the plant growth is not hampered.
- After every immersion, the draining off of the excess nutrient reduces the risk of nutrient stagnant condition.
- Planting density limitations encountered in other systems can be overcome by increasing the number of cells in the culture cell tray.
- Planting density per self area can be increased significantly without reducing the dry mass.

- Handling is simple; once the bioreactor is filled and underway, the plants do not require any attention other than assuring that the nutrient solution supply system is operating properly.
- If necessary, the pH, nutrient composition etc. can be easily measured and controlled even during the production period.
- Labour cost can be reduced at least 50% as large culture vessel are used in this system.

4. Conclusions

For the large scale plant propagation purposes, bioreactors with liquid culture medium can offer the most useful technique with many advantages over the other systems with solid medium. Most importantly, the system can be automated and thus labor cost can be reduced significantly. However, the occurrence of hyperhydricity of the propagules hinders the commercialization of the system. The scaled-up system (TRI-bioreactor) described in this chapter can overcome this problem successfully. The vigorous growth and the higher survival percentage observed in plants from the TRI-bioreactor are the cumulative results of many environmental and physiological factors during the *in vitro* culture period: for example, the relative humidity in TRI-bioreactor under forced ventilation was lower (85-90%) than that in the modified RITA-bioreactor (95-99%) or in Magenta vessels ($\leq 95\%$). The advantages of growing plants in an environment with reduced relative humidity are manifold such as development of functional stomata, increased wax deposition all of which can, in turn, prevent water loss when transferred *ex vitro* and thus increase the chance of survival and subsequent growth. Furthermore, in TRI-bioreactor the environmental parameters are maintained in such a way that the difference between the *in* and *ex vitro* conditions is minimum, as a consequence when the plants are transferred *ex vitro* they are capable to photosynthesize normally and thus can easily overcome the transition stress during the first week of *ex vitro* condition. Another important aspect is the supply of CO₂ enriched air; the enhanced growth of plants could have been largely due to the greater carbohydrate production of the plants due to the supply of CO₂.

We hope that the photoautotrophic culture system discussed here might also provide the basis of a useful model for the *in vitro* propagation by somatic embryogenesis and organogenesis of other important plant species. Future prospects of using TRI-bioreactor are enormous. By using TRI-bioreactor it will be possible to reduce production costs to a level lower than conventional propagation methods, making the products commercially feasible. Recently this bioreactor has been used for propagation and increment of medicinal concentrations of various medicinally important plants such as St. Johns wort, *Scutellaria baicalensis*, Chinese licorice etc. Optimized environmental parameters of the bioreactor can significantly influence secondary metabolite production and may contribute to the development of an optimized and large-scale phytochemical production system in bioreactor.

References

- [1] Aitken-Christie, J. (1991) Automation. In: Debergh, P. C. and Zimmerman, R. H. (Eds.) Micropropagation. Kluwer Academic Publishers, Dordrecht, The Netherlands; pp. 342-354.
- [2] Vasil, I. K. (1991) Rationale for the scale-up and automation of plant propagation. In: Vasil, I. K. (Ed.) Scale-Up and Automation in Plant Propagation. Cell culture and Somatic Cell Genetics of Plants, Vol. 8. Academic Press, San Diego; pp. 1-12.
- [3] Leathers, R. R.; Smith, M. A. L. and Aitken-Christie, J. (1995) Automation of the bioreactor process for mass propagation and secondary metabolism. In: Aitken-Christie, J.; Kozai, T. and Smith, M. A. L. (Eds.) Automation and Environmental Control in Plant Tissue Culture. Kluwer Academic Publishers, Dordrecht, The Netherlands; pp. 187-214.
- [4] Preil, W. (1991) Application of bioreactors in plant propagation. In: Debergh, P. C. and Zimmerman, R. H., (Eds.) Micropropagation. Kluwer Academic Publishers, Dordrecht, The Netherlands; pp. 425-445.
- [5] Paek, K. Y.; Hahn, E. J. and On, S. H. (2001) Application of bioreactors for large-scale micropropagation system of plants. *In Vitro Cell. Dev. Biol.- Plant*. 37: 149-157.
- [6] Debergh, P. and Maene, L. (1984) Pathological and physiological problems related to the *in vitro* culture of plants. *Parasitica* 40: 69-75.
- [7] Ziv, M. (1991) Quality of micropropagated plants - vitrification. *In Vitro Cell. Dev. Biol.- Plant* 27: 64-69.
- [8] Ziv, M. (1991) Vitrification: morphological and physiological disorders of *in vitro* plants. In: Debergh, P.C. and Zimmerman, R.H. Micropropagation. Kluwer Academic Publishers, Dordrecht, The Netherlands; pp. 45-69.
- [9] Akita, M. and Takayama, S. (1994) Stimulation of potato (*Solanum tuberosum* L.) tuberization by semicontinuous liquid medium surface level control. *Plant Cell Rep.* 13: 184-187.
- [10] Zobayed, S. M. A.; Murch, S. J.; Rupasinghe, H. P. V.; de Boer J. G.; Glickman, B. W.; and Saxena, P. K. (2004) Optimized system for biomass production, chemical characterization and evaluation of chemopreventive properties of *Scutellaria baicalensis* Georgi. *Plant Sci.* 167: 439-446.
- [11] Heller, R. (1965) Some aspects of the inorganic Nutrition of plant tissue cultures. In: White, P.R. and Grove, A.R. (Eds). Proceedings of an International Conference on Plant Tissue Culture. England. pp. 1-8.
- [12] Tisserat, B. and Vandercook, C. E. (1985) Development of an automated plant culture system. *Plant Cell Tissue Org. Cult.* 5: 107-117.
- [13] Aitken-Christie, J.; Singh, A. P. and Davies, H. (1988) Multiplication of meristematic tissue: a new tissue culture system for radiata pine. In: Hanover, J.W. and Keathley, D.E. (Eds.) Genetic Manipulation of Woody Plants. Plenum Press, New York; pp. 413-432.
- [14] Simonton, W.; Robacker C. and Krueger S. (1991) A programmable micropropagation apparatus using cycled liquid medium. *Plant Cell Tissue Org. Cult.* 27: 211-218.
- [15] Alvard, D.; Cote, F. and C. Teisson (1993) Comparison of methods of liquid medium culture for banana propagation. Effects of temporary immersion of explants. *Plant Cell Tissue Org. Cult.* 32: 55-60.
- [16] Berthouly, M.; Dufour, M.; Alvaro, D.; Carasco, C.; Alemanno, L. and Teisson, C. (1995) Coffee micropropagation in liquid medium using temporary immersion technique'. In: *16ème Colloque*, Paris, 2, pp. 514-519.
- [17] Etienne, H.; Lartaud, M.; Michaux-Ferrière, N.; Carron, M. P.; Berthouly, M. and Teisson, C. (1997) Improvement of somatic embryogenesis in *Hevea brasiliensis* (Mull. Arg.) using the temporary immersion technique. *In Vitro Cell. Dev. Biol.-Plant* 33: 81-87.
- [18] Cabasson, C.; Ollitrault, P.; Coate, F.; Michaux-Ferrière, N.; Dambier, D.; Dalnic, R. and Teisson, C. (1995) Characteristics of citrus cell cultures during undifferentiated growth on sucrose and somatic embryogenesis on galactose. *Physiol. Plant.* 93: 464-470.
- [19] Ziv, M. (2002) Simple bioreactors for mass propagation of plants. 1st Int. Symp. Liquid Systems for *In Vitro* Mass Propagation of Plants, Ås, Norway, May 29th – June 2nd.
- [20] Afreen, F.; Zobayed, S. M. A. and Kozai, T. (2002) Photoautotrophic culture of *Coffea arabusta* somatic embryos: Development of a bioreactor for the large-scale plantlet conversion from cotyledonary embryos. *Ann. Bot.* 9: 20-29.
- [21] Capot J. (1972) L'amélioration du caféier en Côte d'Ivoire - Les hybrides 'Arabusta' Café Cacao The, 16: 3-17.
- [22] Dublin, P. (1980) Multiplication végétative *in vitro* de l'Arabusta. Café-Cacao-The. Vol. WWIV, 4: 281-290.
- [23] Afreen, F.; Zobayed, S. M. A. and Kozai, T. (2002) Photoautotrophic culture of *Coffea arabusta* somatic embryos: Photosynthetic ability and growth of different stage embryos. *Ann. Bot.* 9: 11-19.

Temporary immersion bioreactor

- [24] Afreen, F.; Zobayed, S. M. A.; Kubota, C.; Kozai, T. and Hasegawa, O. (2000) A combination of vermiculite and paper pulp supporting material for the photoautotrophic micropropagation of sweet potato. *Plant Sci.* 157: 225-231.
- [25] Kozai, T.; Koyama, Y. and Watanabe, I. (1998) Multiplication of potato plantlets *in vitro* with sugar free medium under high photosynthesis photon flux. *Acta Hort.* 230: 121-127.
- [26] Fujiwara, K.; Kozai, T. and Watanabe, I. (1987) Fundamental studies on environments in plant tissue culture vessels. (3) Measurement of carbon dioxide gas concentration in closed vessels containing tissue cultured plantlets and estimates of net photosynthetic rates of plantlets. *J. Agric. Meteorol.* 43: 21-30.
- [27] Gupta, P. K.; Timmis R. and Carlson, W. C. (1993) In: Soh, W.Y.; Liu, J.R. and Komamine, A (Eds.) *Advances in Development Biology and Biotechnology of Higher Plants*. The Korean Society of Plant Tissue Culture, Korea; pp. 18-37.
- [28] Harrell, R. C. and Cantliffe, D. J. (1991) In: Vasil, I.K. (Ed.) *Scale-up and Automation in Plant Propagation*. Academic Press, New York; pp. 179-195.
- [29] Cazzulino, D.; Pederson, H. and Chin, C. K. (1990) In: Vasil, I.K. (Ed.) *Bioreactors and Image Analysis for Scale-Up and Plant Propagation*. Academic Press, New York; pp. 147-175.

DESIGN AND USE OF THE WAVE BIOREACTOR FOR PLANT CELL CULTURE

REGINE EIBL AND DIETER EIBL

*Department of Biotechnology, University of Applied Sciences Wädenswil,
P.O Box 335, CH-8820 Wädenswil, Switzerland - Fax: 41-1-78850 -
Email: r.eibl@hsw.ch*

1. Introduction

Typical bioreactors for plant cell and tissue cultures have been made of glass or stainless steel for more than 40 years. In this area, stirred reactors, rotating drum reactors, airlift reactors, bubble columns, fluidised bed reactors, packed bed reactors and trickle bed reactors with culture volumes up to 75 m³ as well as their modifications are the most commonly used bioreactor types in research and commercial production processes.

Disposable bioreactors represent modern alternatives to such traditional cultivation systems. These bioreactors consist of a sterile plastic chamber that is partially filled with media (10% to 50%), inoculated with cells and discarded after harvest. The single-use chamber eliminating any need for cleaning or sterilisation is made of FDA-approved biocompatible plastics such as polyethylene, polystyrene and polypropylene. Usually, the disposable bioreactors are low cost, simple to operate and guarantee high process security. It is suggested that their use could improve process efficiency and results by reducing the time-to-market of new products.

The aim of this chapter is to critically outline the potential of the disposable Wave Bioreactor (hereafter referred to as Wave) based on wave-induced agitation for secondary metabolite production from suspension cultures, hairy roots and embryogenic cultures. With respect to the types of disposable bioreactor reported in the literature, their classification, application and characterisation, here we describe the features of Wave as well as summarise the results of hydrodynamic studies (characterisation of fluid flow, estimation of mixing time, distribution time, energy input) and investigations of oxygen transport efficiency. This allows a comparison of the Wave to other commonly used bioreactors in plant cell based biomass as well as secondary metabolite production.

2. Background

2.1. DISPOSABLE BIOREACTOR TYPES FOR *IN VITRO* PLANT CULTURES

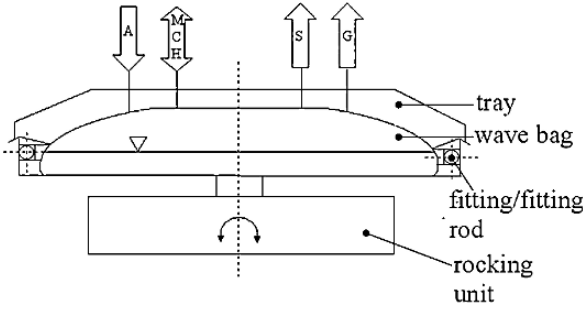
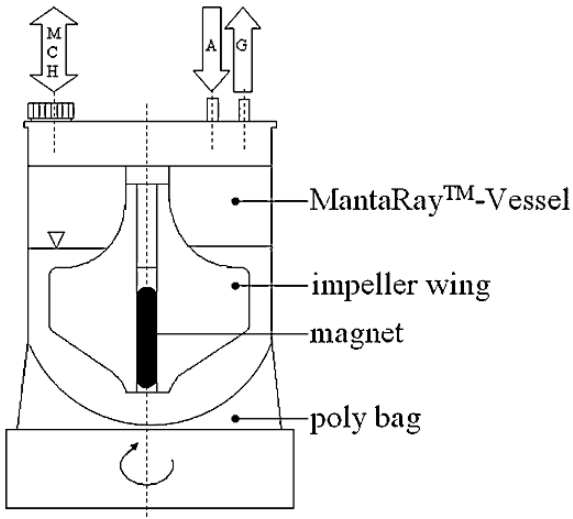
Table 1 gives an overview of the most frequently cited disposable bioreactors and disposable bioreactor facilities for plant cell and tissue cultures, their schematic diagram, manufacturers and described application.

Table 1. Disposable bioreactors (DB) and disposable bioreactor facilities (DBF) for plant cell and tissue cultures

Mechanically driven membrane bioreactor	
miniPerm® (DB)	
Max. culture volume: 15 mL	
Culture type: Embryogenic cultures	
Application: Biomass production	
Manufacturer: Sartorius AG http://www.sartorius.com	
Pneumatically driven bag bioreactor	
LifeReactor® (DBP) Ebb and Flow BioReactor (DBF)	
Max. culture volume: 5 L	
Culture type: Organogenic cultures (bud or merismatic clusters), embryogenic cultures	
Application: Micropropagation, production of secondary metabolites	
Manufacturer: Osmotek LTD http://www.osmotek.com	
Mechanically driven bag reactor	
MantaRay® (DB)	
Max. culture volume: 1 L	
Culture type: Plant cell cultures	
Application: No references	
Manufacturer: Wheaton Science Products INC http://www.wheatonsci.com	

Design and use of the wave bioreactor for plant cell culture

Table 1. Disposable bioreactors (DB) and disposable bioreactor facilities (DBF) for plant cell and tissue cultures. (continued)

Mechanically driven bag reactor	
Optima and OrbiCell (DBF)	
Max. culture volume: 10 L	
Culture type: Plant cell cultures	
Application: No references	
Manufacturer: Metabios INC http://www.metabios.com	
Wave (DB and DBF)	
Max. culture volume: 500 L	
Culture type : Callus cultures, suspension cultures, embryogenic cultures, hairy roots	
Application: Mass propagation, production of secondary metabolites	
Manufacturer: Wave Biotech AG (Switzerland) http://www.wavebiotech.ch http://www.wavebiotech.net Wave Biotech LLC (USA) http://www.wavebiotech.com	

A air inlet, C - cells, E - gas exchange, G - gas exhaust, H - harvest, M – medium

In contrast to disposable bioreactor facilities (self-contained systems), disposable bioreactors require external equipment such as incubators to provide the proper physical as well as the necessary chemical environment for cells (e.g. temperature, aeration, pH etc.) and to ensure monitoring and control of key process parameters. As indicated in Table 1, there are generally two main types of disposable bioreactors (bioreactor facilities), the choice of which depends on methods employed for supply of air and mechanical energy of mixing: membrane reactors (mechanically driven) and bag reactors (pneumatically and mechanically driven) [1-12].

Membrane bioreactors have been developed for the production of small product volumes since the middle of the 80 s. Today their manufacturers offer specified production chambers or modules, which can be chosen to suit the cells and product. Müller-Uri and Dietrich [8] successfully applied the mechanically driven bioreactor miniPerm[®] (Sartorius AG, Germany) equipped with a dialysis membrane for mass propagation of proembryogenic suspension culture of *Digitalis lanata*. The main disadvantage of membrane reactors consisting of a cultivation or production chamber and a medium storage chamber (nutrient module) is their small culture volume. Therefore, either the application of multiple units is required or the use of this reactor type is restricted to research and production of high value compounds.

Larger culture volumes are offered by bag reactors. Bag reactors include bioreactors in which the cultivation chamber is manufactured from plastic film and is designed as a bag. For pneumatically driven bag reactors, the bag with the internal equipment such as air sparger is fixed by a clamp arrangement, brought to a specified range of temperature and aerated. The first disposable bioreactor for plant cell and tissue cultures cited in the literature is a pneumatically driven bag reactor, namely a plastic bubble column. This so-called LifeReactor[®] (Osmotek LTD, Israel) has a volume capacity of 2 L and 5 L and is suitable for plant micropropagation (organogenic cultures of potato, banana, pineapple, fern and orchid etc.) as well as cultivation of somatic embryos [9-12]. In addition, two LifeReactors[®] based on temporary immersion technique and named Ebb and Flow BioReactor[®] were constructed by Osmotek LTD (Rehovot, Israel). As illustrated in Figure 1, the energy input of the Wave (Wave Biotech AG, Switzerland and Wave Biotech LLC, USA) is caused by rocking the platform which induces a wave (wave induced motion) in the bag with the cells in the medium. In this way, oxygenation and mixing with minimal shear forces result. The surface of the medium is continuously renewed and bubble-free surface aeration takes place. Optima[®] and OrbiCell[®] reactors (Metabios INC, Canada) are based on a similar working principle.

2.2. THE WAVE: TYPES AND SPECIFICATION

Table 2 shows frequently used Wave Bioreactors for process scale-up (R & D, laboratory scale, GMP manufacturing) and their technical specification. All the systems facilitate measurement and regulation of rocking angle, rocking rate, temperature, aeration rate as well as CO₂ rate. Optional monitoring and control of pH, dissolved oxygen as well as weight and flow rates in perfusion mode are possible. These are typical process parameters [3,13-15] for the cultivation of plant cell and tissue cultures. With only a few exceptions [16,17], addition of CO₂ is necessary because of its positive influence on biomass growth and secondary metabolite production, as in the case of in vitro production of taxanes. However, the equipment of the Wave with an integral or

external aeration pump for plant cell cultivation usually achieves similar results without the addition of CO₂.

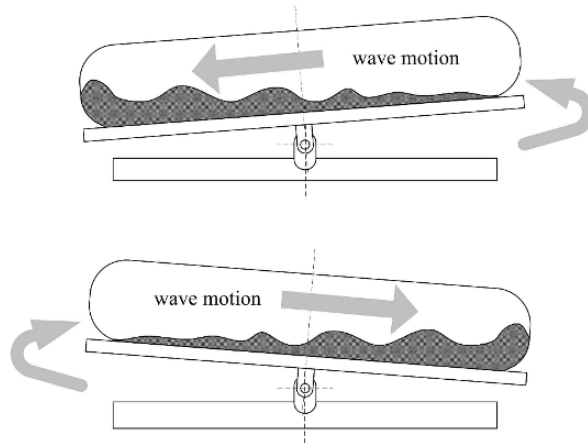





Figure 1. Working principle of the Wave.

Combining the laboratory Wave with an appropriate on-line analysing technique such as ANTRIS, developed by Sensorix AG (Switzerland) and shown in Figure 2 on the right, enables improved process control and allows realization of feeding strategies [18].



Figure 2. BioWave[®] 20 SPS with ANTRIS for on-line measurement of metabolites.

Table 2. Wave Bioreactors and their specifications.

	BioWave® 2 SPS	BioWave® 20 SPS	BioWave® 200 SPS
			
Dimension	433 x 330 x 210 mm	720 x 580 x 400 mm	1900 x 1100 x 1100 mm
Performance	2 x Wave Bag 1 L ¹ 2 x Wave Bag 2 L ¹ 1 x Wave Bag 10 L ¹	2 x Wave Bag 2 L ¹ 2 x Wave Bag 10 L ¹ 1 x Wave Bag 20 L ¹	2 x Wave Bag 100 L ¹ 1 x Wave Bag 200 L ¹
Scale (maximum culture volume)	R&D (1 L)	Laboratory scale (10 L)	GMP manufacturing (100 L)
Agitation	Rocking rate from 6 to 42 rpm Angle from 5 to 10°	Rocking rate from 6 to 42 rpm Angle from 5 to 10°	Rocking rate from 5 to 25 rpm Angle from 4 to 12°
Temperature	Integral heater or place in incubator	Integral heater or place in incubator	Integral heater
Aeration	Separate aeration unit and flow meter	Integral aeration pump	Integral aeration pump, flow meter and load cell
Standard instrumentation	Temperature ^{2,3} ; agitation speed ^{2,3} ; air flow rate ^{2,3} ; angle ²	Temperature ^{2,3} ; agitation speed ^{2,3} ; air flow rate ^{2,3} ; angle ²	Temperature ^{2,3} ; agitation speed ² ; air flow rate ^{2,3}
Optional instrumentation	O ₂ ^{2,3} ; CO ₂ ^{2,3} ; pH ^{2,3} ; weight ^{2,3,4}	Temperature ^{2,3} ; O ₂ ^{2,3} ; CO ₂ ^{2,3} ; pH ^{2,3} ; weight ^{2,3,4}	Agitation speed ^{2,3} ; O ₂ ^{2,3} ; CO ₂ ^{2,3} ; pH ^{2,3} ; weight ^{2,3,4}

¹working volume or culture volume (filling level) of 50%, ² measurement, ³ control, ⁴ perfusion module with load cell

3. Design and engineering aspects of the wave

3.1. BAG DESIGN

Bioreactor, which forms the external cell environment, greatly influences plant cell line growth and product formation. Existing bioreactor design concepts are based on observations that the biosynthetic potential of a cell culture is closely linked to the physical characteristics of cultivated cells and varies with cell line as well as culture type. Thus, bioreactor design has to consider the morphology of cells including differences between suspension and more differentiated organ cultures like hairy roots for optimal cultivation. The biosynthetic capabilities of these cultures are not greatly affected by their growth environment as long as the organised nature of the culture morphology is maintained [1,19-22]. In the case of the Wave, this means that specially designed cultivation bags are advantageous for different cell culture types (Figure 3).

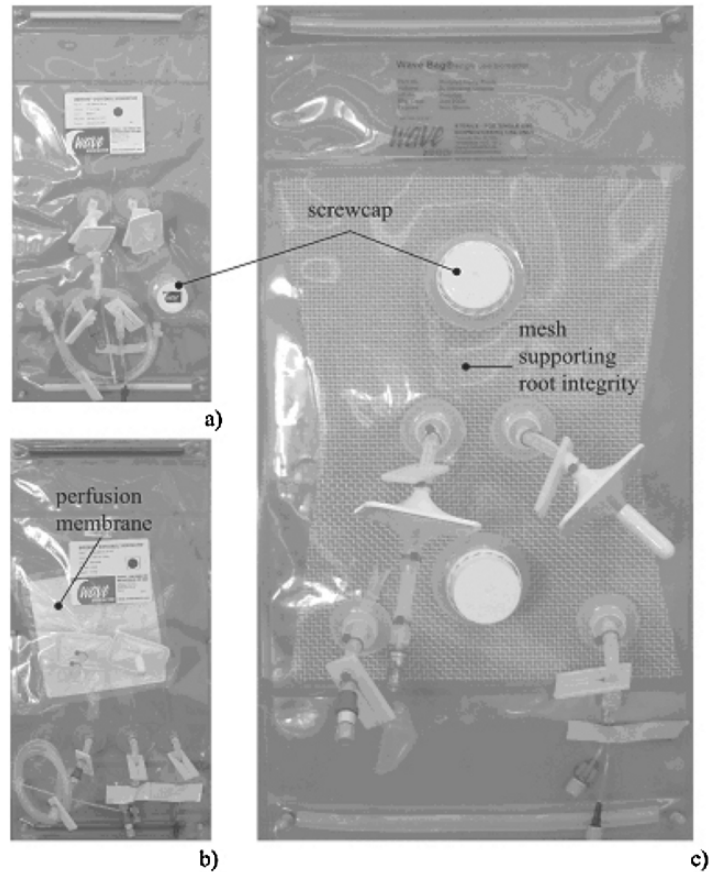


Figure 3. Specially designed Wave Bags for different plant cell and tissue cultures.

The standard Wave Bag has an inoculation and sampling port, an inlet air as well as an exhaust air filters, on-line probe insertion ports for pH, dissolved oxygen etc. and is suitable for suspension cultures allowing inoculation via standard ports. If the cells grow in aggregates and high biomass amounts are formed, a Wave Bag (Figure 3a) with enlarged port to prevent the port quickly becoming clogged and screw cap for inoculation and sampling is to be preferred. The Wave Bag shown in Figure 3b contains a floating membrane of polyethylene, ensuring a perfusion mode in which suspension cells can be continuously cultivated over a number of weeks. For hairy root cultivations, a wasted nylon mesh is integrated into the bag (Figure 3c). The mesh acts as an immobilisation matrix in order to prevent firstly the collection of free-floating roots at one or two points in the cultivation chamber and secondly highly localised biomass with a core of material which has lost its root morphology as well as productivity.

For plant cell and tissue cultures which do not release their products into the culture medium, the biomass harvest before downstream processing of the product is necessary. Under these circumstances, the formed biomass is removed by gloved hands after opening the bag, which also allows lyophilisation. The different Wave Bag types available in sizes from 2 L up to 100 L total volume have varying bag geometries, which result in changing mass and energy transfer situations.

3.2. HYDRODYNAMIC CHARACTERISATION

As already proved, fluid dynamics (in particular fluid flow and fluid mixing) encountered in a bioreactor are important factors for cell growth and production of secondary metabolites based on plant cells (suspension cultures, hairy roots, embryogenic cultures) [23-29]. A number of hydrodynamic studies have been carried out for stirred and column reactors [26,30-32], but studies relating to the Wave, which is still a relatively new cultivation system, are limited [33-36].

However, recent studies allow the comparison of the Wave to other commonly used bioreactors. Consequently, one aspect of the work we have carried out is the hydrodynamic characterization of the Wave. Our investigations were focused on fluid flow, mixing time, distribution time, energy input and identification of interactions between these features. All experiments were performed with standard Wave Bags and water.

A modified Reynolds number (Re_{mod}) can be used to describe the fluid flow in the Wave. The Reynolds number, which is the ratio of inertial force to internal friction, is generally governed by Eq. (1) where w is the fluid velocity, l is the characteristic length of the system (bag), and ν is the kinematic viscosity of the culture medium.

$$Re = \frac{w * l}{\nu} \quad (1)$$

In order to determine Re_{mod} , the characteristic length can be assumed to be a rectangular cross-section calculated from liquid level (h) and width of the Wave Bag (B) preconditioned steady state (Figure 4a). The liquid level of the bag is a function of working volume (culture volume) and the bag geometry (i) is given by ratio of (L) to (B). It is possible to correct deviations of the bag shape from a rectangular cross-section

by experimental determination (CAD) of true length (U) under liquid surface (A_0). The fluid velocity (w) is defined as the ratio of medium flow rate (volumetric flow rate) to the hydraulic cross-section (A_q); the volumetric flow rate (\dot{V}) depends on the bag, the working volume, the rocking angle (φ) as well as the rocking rate (k) of the Wave. Depending on the combination of these four parameters, the volumetric flow rate varies and as a result different amounts of substances are exchanged over the rotation point (Figure 4b). The influence of the bag and rocking angle on volumetric flow rate can be determined by experimental observations and calculated by introducing a correction factor (C) obtained with the aid of regression analysis. Correction factors (C) for Wave Bag 20 L are listed in Table 3.

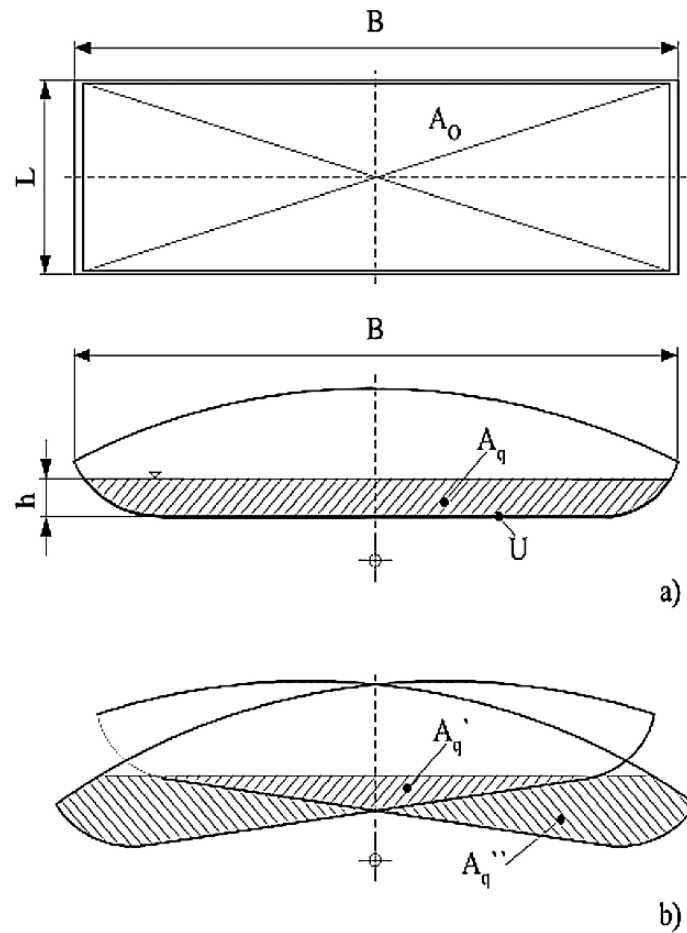


Figure 4. Assumptions used to estimate Re_{mod} in the Wave. a) Initial position: $\varphi=0$, b) Final position: $\varphi=\text{maximum}$.

Table 3. Correction factor (C) for Wave Bag 20 L. Reproduced from Lisica, S. (2004) with permission [37].

Rocking angle [°]	Working volume [L]				
	2	4	6	8	10
2	0.5354	0.2892	0.2025	0.1602	0.1323
4	0.819	0.5612	0.4083	0.3138	0.2583
6	0.9882	0.7628	0.5797	0.4554	0.3747
8	1.000	0.894	0.7167	0.585	0.4815
10	1.000	0.9548	0.8193	0.7026	0.5787

A correction factor (D), which depends on the bag type (Table 4), describes the correlation of the Wave's Re_{mod} and Re_{mod} occurring in stirred bioreactors.

Table 4. Correction factor (D) for Wave Bag. Reproduced from Lisica, S. (2004) with permission [37].

Wave Bag	Correction factor (D)
Wave Bag 2 L	0.0565
Wave Bag 10 L	0.0398
Wave Bag 20 L	0.312
Wave Bag 100 L	0.015
Wave Bag 200 L	0.0489

Applying the correction factors (C) and (D), Re_{mod} for the Wave can be calculated as:

$$Re_{mod} = \frac{V * k * C * D}{15 * \nu * (2 * h + B)} \quad (2)$$

Re_{mod} for Wave Bag 2 L, 20 L, 100 L and 200 L working with a constant rocking rate of 18 rpm and a rocking angle of 8° are illustrated in Figure 5a. It can be seen that Re_{mod} decreases with increased filling level in Wave Bags working with higher volume. Increased filling level results in reduced headspace volume as demonstrated in Figure 5b, so that, the linear development of the wave movement is no longer possible after a certain point. When using bags with large headspace, these phenomena did not occur. Figure 5c shows Re_{mod} of Wave Bag 2 L working with 50% culture volume in dependency on rocking rate and rocking angle. Re_{mod} increases according to the increase

of rocking rate and rocking angle. For different Wave Bags we were able to determine the zone of $Re_{mod\ crit}$ and established that $Re_{mod\ crit}$ values range between 200 and 1000 (Figure 5d)).

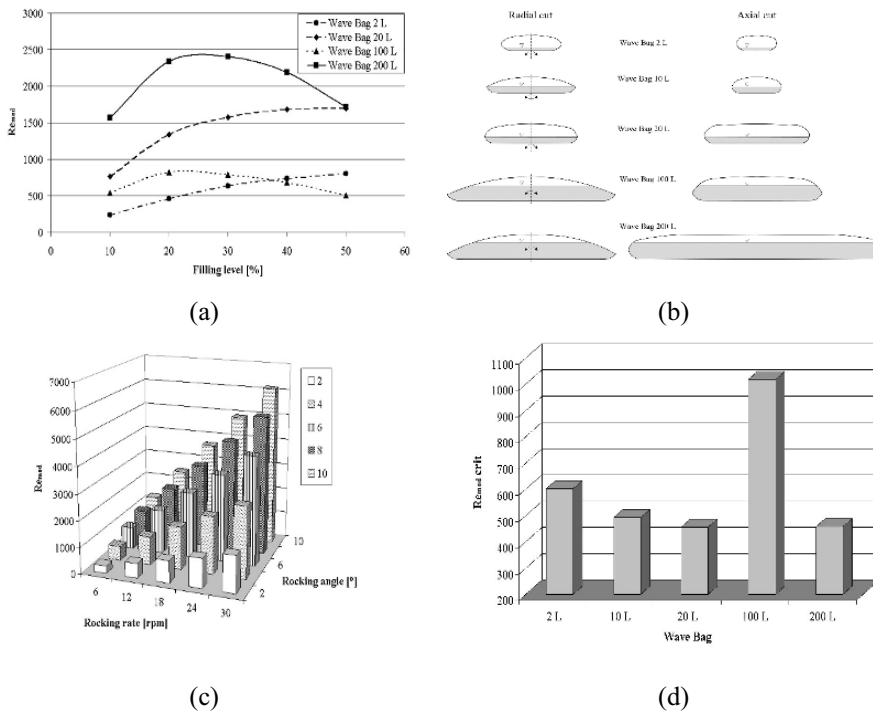


Figure 5. Determination of Re_{mod} values for different wave bags.

Mixing time θ_{95} (time required to achieve 95% homogeneity) is measured by injecting a tracer. It directly depends on the rocking rate and indirectly depends on the rocking angle in the Wave [33,37]. The relationship between mixing time, rocking rate, rocking angle and filling level for Wave Bag 200 L is shown in Figure 6. With the smallest possible energy input (low rocking angle and rocking rate) and assuming identical process parameters, the filling level of the Wave Bag significantly influences mixing time, resulting in mixing time differences of over 100%. For higher rocking rates as well as rocking angles, filling level has no significant effect on mixing time. Mixing times based on 40% and 50% filling level lie between 10 s and 1400 s [36,38] for Newtonian fluids (Table 5) and reach satisfactory values for cell culture bioreactors.

Even when there are specific production conditions (low rocking rate, low rocking angle and filling level or medium to maximum rocking rate, rocking angle as well as maximum filling level), mixing times generated in the Wave are comparable to commonly used stirred reactors. Clearly, the most ineffective mixing (high mixing times) takes place at the smallest possible rocking rate, rocking angle and maximum filling level. Mixing time can be reduced by increasing the rocking rate and/or the

rocking angle, which results in a more intensive wave movement, rapid as well as effective mixing.

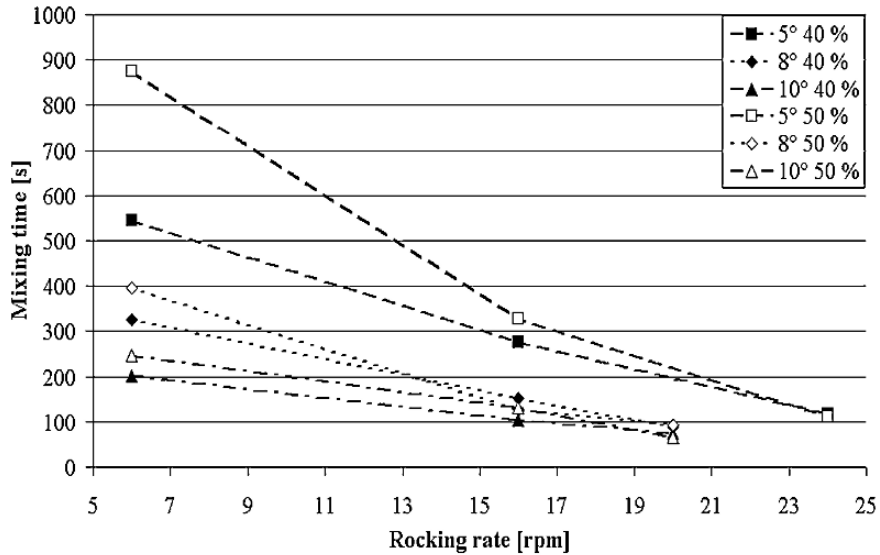


Figure 6. Mixing times in BioWave® 200 SPS working with wave bag 200 L (40% and 50% filling level).

Table 5. Mixing times of different Wave Bags working with 40% and 50% filling level.

Wave Bag	Mixing time [s]
2 L	9 - 264
20 L	40 - 1402
100 L	22 - 837
200 L	65 - 874

The mixing time is a function of Re_{mod} and depends on the type of Wave Bag as well as the filling level (Figure 7). The increase in Re_{mod} over values between 1000 and 2000 does not further reduce the mixing time. From Table 5, it becomes clear that the most ineffective mixing of all bags investigated is shown by Wave Bag 20 L, which attains mixing times lower than 100 s with considerably higher turbulences ($Re_{mod} > 1500$) than other bag types. The most effective mixing is obtained with Wave Bag 2 L.

Design and use of the wave bioreactor for plant cell culture

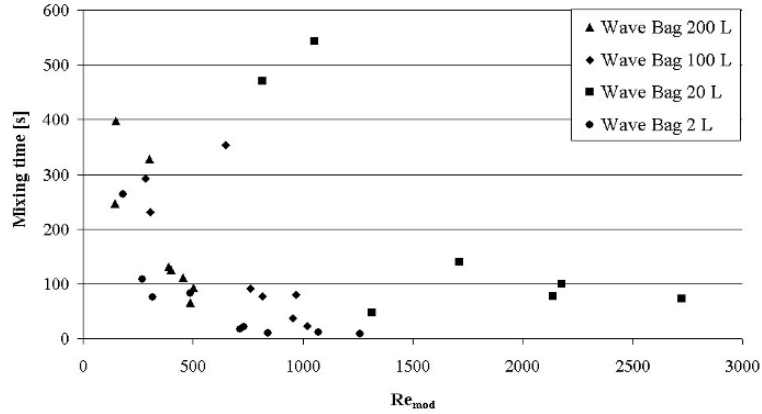


Figure 7. Mixing time as a function of Re_{mod} in different wave bags using 50% filling level.

Investigations focused on residence time distribution [39] have demonstrated that a continuously operating Wave can be described by the ideally mixed stirred tank model. In these experiments, the displacement technique was employed using BioWave® 20 SPS. Figure 8 compares the measured response in the Wave and the calculated residence time distribution in an ideally mixed stirred tank. Both curves are congruent.

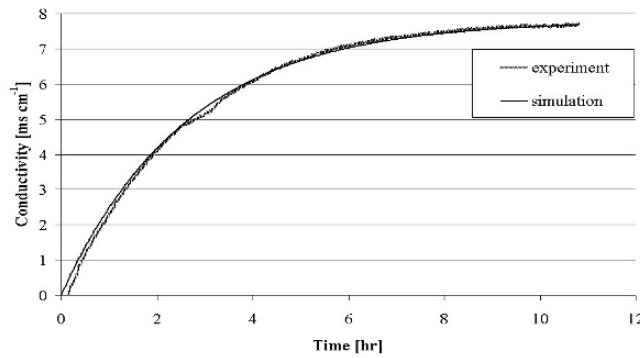


Figure 8. Comparison of measured residence time distribution in BioWave® 20 SPS. ($\tau=2.6$ h, filling level=50%, rocking rate=6 rpm, rocking angle=5.1°) and theoretical residence time distribution in an ideally mixed stirred tank.

In order to consider engineering aspects of a bioreactor system extensively, the hydrodynamic characterization must also include energy input. In the case of the Wave, the mechanical energy produced by the rocking platform facilitates mixing and improves mass as well as heat transfer. First energy input modelling approaches [37,40] have generated three static models, an inertia model, a momentum transport model, a model

for transformation into thermal energy and a model for electric power. Currently, static model 3 is the most exact if we assume real flow behaviour in the bag. It is based on films taken to calculate the momentums. The film sequences (30 per second) analysed by CAD software show the actual distribution of fluid during wave movement. Static model 3 is also valid for turbulent flow. In general, the static models presuppose a static behaviour of the fluid in the bag. This assumption imposes the condition of equilibrium for the sum of all acting momentums. Observing a cross-section of a bag at different angles and in final positions presents the scenario in which the fluid movement is finished. It can be seen that, the fluid is distributed according to the angles on the other side of the rotation point. By analytical as well as graphical determination of the point of gravity of the bag and the liquid surface, the resulting momentums can be calculated. The energy input of the Wave is analogous to the work required for the movement between the angles $-\phi_{\max}$ and $+\phi_{\max}$.

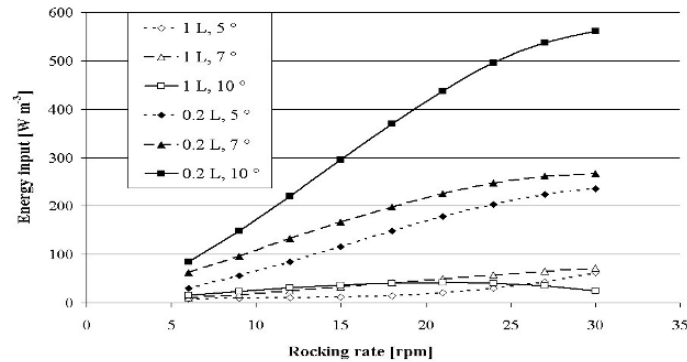


Figure 9. Courses of specific energy input as a function of rocking rate, rocking angle, maximum and minimum filling level for wave bag 2 L.

Figure 9 shows the courses of specific energy input as function of the rocking rate, rocking angle and maximum as well as minimum filling level for Wave Bag 2 L. Minimum filling level, maximum rocking angle and rate cause the maximum possible energy input, which is one decimal power higher than operation with maximum filling level. Up to rocking rates of 20 rpm, the specific energy input of all the systems is directly proportional to the rocking rate. By increasing the rocking rate, the energy input increases and reaches a stationary value limited by the technical specification of the rocking unit. As a consequence of increased filling level, rocking rate and rocking angle, a phase shift of the wave towards rocking movement occurs. Thus, the energy input is slightly reduced at maximum filling level, with rocking angle and rocking rates greater than 20 rpm. The energy input values of Wave Bag 2 L range from 8 to 561 W m^{-3} .

Some authors have determined the specific power input P/V or dissipation rate, in particular cumulative energy dissipation, as a product of the energy dissipation rate and the exposure time in an attempt to quantify the shear effects in stirred bioreactors working with plant cells. Unfortunately, the obtained critical values based on significant cell damage of 20% can vary considerably depending on cell line, cell age and culture

maintenance conditions. A critical value of energy dissipation of 10^7 J m^{-3} (10^4 J kg^{-1}) has often been reported [26,41-44]. This value corresponds to a specific power input of about 111 W m^{-3} for stirred reactors. For more sensitive mammalian cells, Henzler [30] proposes an optimal range between 30 and 50 W m^{-3} .

3.3. OXYGEN TRANSPORT EFFICIENCY

Surface aeration is used to supply the medium containing the cells with oxygen in Wave bioreactors. Experiments to determine the volumetric oxygen transfer coefficient ($k_L \cdot a$) within the Wave (dynamic gassing-in method) using model media provide results identical with published values of other bioreactors suitable for cell cultures [38].

The maximum value of $k_L \cdot a$ measured was around 4 hr^{-1} at aeration rates of 0.002 vvm and 0.004 vvm in the Wave, whereas the maximum volumetric oxygen transfer coefficient arising at 0.25 vvm was 9.8 hr^{-1} . We finally obtained a value of $k_L \cdot a$ reaching 11.2 hr^{-1} at an aeration rate of 0.5 vvm . Under comparable cultivation conditions, the values reported above are similar to those achieved in 1 L Biostat stirred reactor with membrane aeration (4.5 hr^{-1} to 6.4 hr^{-1}) from Sartorius BBI Systems GmbH, Germany [45], 1.5 L stirred reactors with surface aeration (1.01 hr^{-1} to 3.1 hr^{-1}) [46], 8 L reactor with eccentric motion stirrer from Chema Balcke Dürr Verfahrenstechnik GmbH, Germany, (maximum 13 hr^{-1}) [47] and 15 L jar fermentor with stirrer and aeration tube (Model MSJ-15, Marubishi Lab. Equip. Co. Ltd., Japan) (about 10 hr^{-1}) [48]. Volumetric oxygen transfer coefficients obtained by Knevelman et al. [33] for Wave bioreactors are a decimal power higher than the values reported by Rhiel and Eibl [34], Singh [35] and Eibl *et al.* [38]. However, they confirm the direct relation to rocking rate and rocking angle.

Higher oxygen transfer efficiency results from increased energy input which caused by increased rocking rate, rocking angle and aeration rate. A decreased filling level increases $k_L \cdot a$ at constant parameters. Oxygen transfer coefficients exceeding 11 hr^{-1} are theoretically achievable in Wave bioreactors operated at high rocking rates and rocking angles as well as aeration rates over 0.5 vvm , with direct dissipation of air into the medium or application of pure oxygen. However, Wave Bag modifications would be required to achieve such results. In the closed Wave Bag, oxygen transfer is limited. Depending on bag size and filling level, oxygen saturation reaches 35% to 50% . Higher saturation requires additional aeration.

4. Cultivation of plant cell and tissue cultures in the wave

4.1. GENERAL INFORMATION

Because of the sensitivity of plant cells to hydrodynamic shear stress, it is essential to minimize the shear forces which occur during mixing and aeration generally. Exposure of plant cells to high shear forces can reduce cell viability, change morphology and/or aggregation pattern, impair growth and alter the concentration as well as the profile of secondary metabolites significantly [26,29,43,44,49-52]. Based on results presented in section 3, it can be deduced that the Wave guarantees optimal hydrodynamic conditions

for a large number of cell lines through adjustment of bag size, filling level, rocking angle and rocking rate. Further reduction of hydrodynamic shear stress can be achieved by use of viscous additive-supplemented media [53], addition of Pluronic® F-68 [26] and cell immobilisation [1,54-56]. Shear stress and cell damage resulting from bubble rising and bubble bursting does not occur in Wave systems (see 3.3, surface aeration).

The major physical cultivation conditions summarised in Table 6 have to be maintained. A temperature between 25 and 27°C is one important parameter measured and controlled in Wave systems. The pH is measurable and controllable by CO₂ should the necessity arise. The oxygen requirements and resulting aeration rates for most plant cell and tissue culture cell types are low [3,57]. Where growth and product formation are enhanced by the introduction of light, periodic illumination of cultures is possible with external tubes installed around the Wave.

There is also a need for long-term sterility as a practical consequence of plant cell and tissue cultures with relatively low growth rates (0.24 d⁻¹ to 1.1 d⁻¹ or doubling times of 0.6d to 5d). Our experience shows that sterile Wave Bags can be used in plant cell culture cultivation processes for up to 4 months. Contaminations by the bioreactor itself are highly unlikely (less than 1%).

Table 6. Major physical cultivation conditions for plant cell and tissue cultures.

Parameter	Range
Temperature	25 - 27°C
pH	5.2 - 5.8
Aeration	0.1 - 0.3 vvm
Light	0 - 3000 Lux, often periodic light conditions (16 hr on, 8 hr off)

In the case of long-term cultivation processes with middle and high culture volumes, the application of filter heaters to prevent moisture build-up on exhaust air filters or the periodic exchange of exhaust air filters is required. Table 7 shows the results of selected batch and fed batch cultivations carried out in BioWave® 20 SPS with Wave Bag 2 L.

Design and use of the wave bioreactor for plant cell culture

Table 7. Results of cultivations in BioWave® 20 SPS.

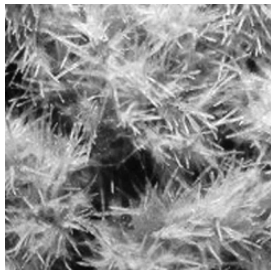
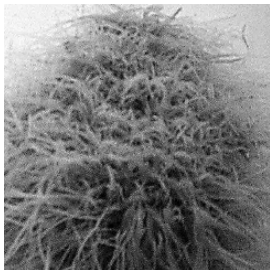
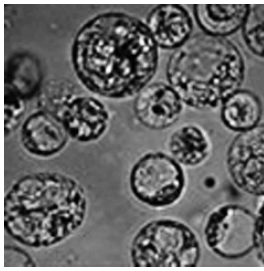
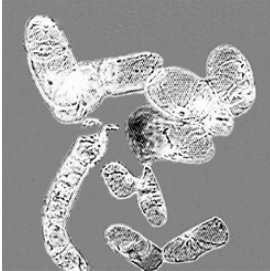
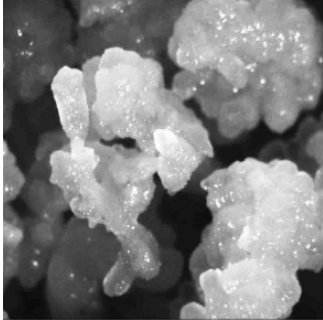
Culture type / Species	<i>Hyoscyamus muticus</i> *		<i>Panax ginseng</i> **	
Hairy roots				
Reactor mode	Fed batch (feeding)	Fed batch (feeding and exchange)	Fed batch (feeding)	Fed batch (feeding and exchange)
Biomass productivity	21 g L ⁻¹ d ⁻¹ fresh weight	20.3 g L ⁻¹ d ⁻¹ fresh weight	2.3 g L ⁻¹ d ⁻¹ fresh weight	5.1 g L ⁻¹ d ⁻¹ fresh weight
Secondary metabolite content (max.)	5.2 mg g ⁻¹ dry weight hyoscyamine	5 mg g ⁻¹ dry weight hyoscyamine	28 mg L ⁻¹ dry weight ginsenosides	146 mg L ⁻¹ dry weight ginsenosides
Culture type / Species	<i>Taxus baccata</i> ***		<i>Nicotiana tabacum</i>	
Suspension culture				
Reactor mode	Fed batch (feeding), free cells	Fed batch (feeding), immobilised cells	Batch	
Biomass productivity	not determined		12 g L ⁻¹ d ⁻¹ fresh weight	22 g L ⁻¹ d ⁻¹ fresh weight
Secondary metabolite content (max.)	10 mg L ⁻¹ dry weight paclitaxel 5 mg L ⁻¹ dry weight baccatin III	20.8 mg L ⁻¹ dry weight paclitaxel 7.8 mg L ⁻¹ dry weight baccatin III	none	

Table 7. Results of cultivations in BioWave® 20 SPS. (continued)

Culture type / Species	<i>Allium sativum</i>
Embryogenic culture	
Reactor mode	Fed batch (exchange)
Biomass productivity	2.8 g L ⁻¹ d ⁻¹ fresh weight
Secondary metabolite content (max.)	0.124 mg g ⁻¹ dry weight alliin

*Clone KB5 from Kirsi Oksman-Caldentey, Helsinki, Finland; **Clone T12 from Anna Mallol, Barcelona, Spain; ***from Salima Bentebibel, Barcelona, Spain

In the following sections, we describe these experiments and our observations as well as discuss the results in term of engineering and design aspects. The statements directed to energy input based on static model 3 [37] (Figure 9). The theoretical predictions are quite good in explaining the observed data and visual effects.

4.2. CULTIVATION OF SUSPENSION CULTURES

In the Wave working with 1L culture volume (bag with screw cap, Figure 3a), a tobacco cell line was cultivated to evaluate the optimal parameters for biomass growth and investigate the influence of increased energy input. The suspension culture (*Nicotiana tabacum*) used was established and maintained in shake flasks at 25°C and 100 rpm in a shaker-incubator as described by Rothe [7].

The batch cultivations of tobacco cells in MS medium were carried out in shake flask with inoculum (30 and 50 g L⁻¹ fresh weight) in logarithmic growth phase for 17 and 21 days. At a constant rocking angle of 6° or 10°, the rocking rates ranged from 17 to 25 rpm. Based on existing standard operation procedures in our group, the sampling of the illuminated suspension cells was realised every second day to estimate the biomass increases in terms of fresh weight and dry weight, the conductivity, the cell viability, the pH as well as the sucrose consumption. Total biomasses between 290 and

432 g L⁻¹ fresh weight were harvested under flow conditions in transition zone and turbulent flow (Figure 10).

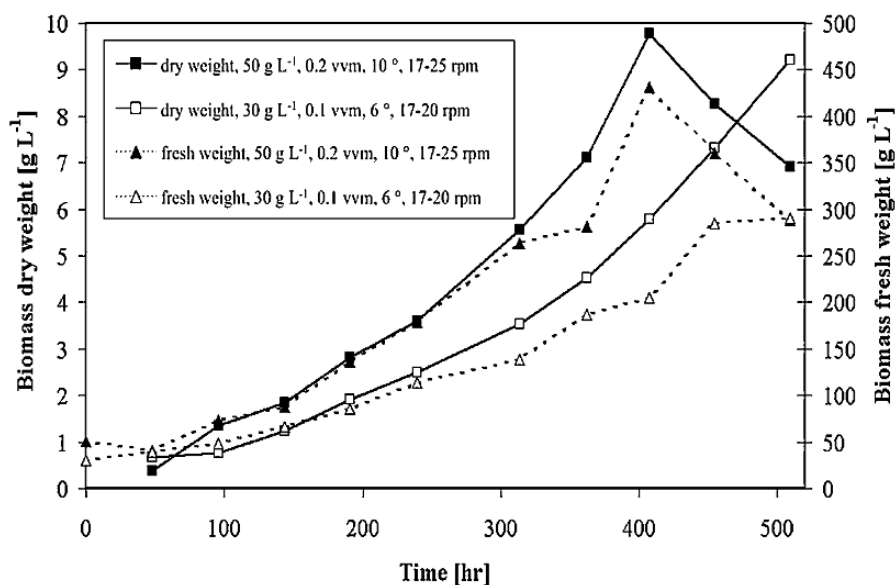


Figure 10. Influence of energy input on time course of biomass fresh weight and dry weight for tobacco in the wave (1 L culture volume).

As illustrated in Table 7 and Figure 10, we achieved the highest biomass productivities using 50 g L⁻¹ inoculum, 0.2 vvm and about 1.4 times higher energy inputs at rocking rates between 17 and 25 rpm as well as the highest possible rocking angle. This can be explained by the improved mass transfer as a result of increasing culture broth viscosity during biomass growth. However, the increase in the rocking rate does not favour energy input in the Wave operating at a rocking angle of 10° with the maximum filling level of bag 2 L, because the energy input is constant for rocking rates between 17 and 20 rpm (45W m⁻³). At a rocking rate of 25 rpm, energy input drops (35W m⁻³). In other words, a further increase in rocking rate does not damage the cells, but increases the oxygen transfer efficiency. To deliver higher energy inputs, it would be necessary to decrease the rocking angle or filling level (see Figure 9). We have made similar observations in Wave experiments working with suspension cultures of *Vitis vinifera*.

Bentebibel [1] describes the successful cultivation of free and immobilised (Ca²⁺ alginate beads) cells of *Taxus baccata* growing in modified Gamborg's B₅ medium. Here, the process gain was the production of paclitaxel as well as baccatin III in Wave Bags (equipped with screw cap) with 0.4 L working volume. The cultivations running in fed batch mode for 24 days represent two-stage processes with a growth and a production phase. The production phase was introduced using production medium included elicitors. The initial culture volume was 0.25 L inoculated with 40 g fresh weight of cell suspension in the growth phase. The experiments were carried out at

0.3 vvm, a constant rocking angle of 6°. An increase in the rocking rate from 20 to 40 rpm was made step by step as fresh culture medium was fed in. This strategy resulted in a constant energy input of about 190W m⁻³ and flow in transition zone from laminar to turbulent during the whole cultivation. It was found that immobilised suspension cells of *Taxus baccata* produce 2-fold and 1.5-fold greater amounts of paclitaxel and baccatin III than free suspension cells cultivated under comparable conditions in BioWave® 20 SPS (Table 7). The obtained values of paclitaxel (10 to 20.8 mg dry weight L⁻¹) lie in the range of highest paclitaxel values reported earlier [16,59-62].

4.3. CULTIVATION OF HAIRY ROOTS

Studies with two transformed root lines also demonstrate the suitability of the Wave (bags with screw cap) for hairy root cultivations under laminar fluid flow conditions. The transformed root line of *Hyoscyamus muticus* (clone KB5, light-culture), supplied by Dr. Kirsi Marja-Oksman, VTT, Espoo, Finland, produces intracellular tropane alkaloids such as scopolamine and hyoscyamine in Gamborg's B₅ medium without phytohormones [63,64]. Palazón *et al.* [6] discuss the procedures to cultivate ginsenosides producing root line of *Panax ginseng* (clone T12, dark-culture) in SH medium using different types of laboratory reactors.

Biomass growth and secondary metabolite production with the hairy root clones used were promoted in the Wave (Wave Bag 2 L) by energy input values between 30 and 50W m⁻³. These values are comparables to those we applied for the cultivation of tobacco cells. It is also important to note that parts of the roots should grow alternately in submerged and emerged conditions by changing the position of the rocker unit. Therefore, it is recommended to start cultivation with a minimum filling volume of 200 mL and energy input values of about 50W m⁻³ (6°, 6 rpm). The feeding is coupled with a decrease in energy input (Figure 9), which maintains root integrity. An increase in rocking rate in accordance with the medium feeding was characterised by changes in morphology of both hairy root clones. We observed the formation of ball-like structures which show poor growth and changes in branching, colour and root hair development. In cultivations with increased energy input without feeding, a wound-response (production of callus-type tissue) and the loss of biosynthetic capacity was noticed. It is presumed that increases in energy input induce shear rates which represent stressful conditions for the growing roots, although not sufficient enough to disrupt them.

The data in Figure 11 for the *Hyoscyamus muticus* hairy roots indicate significant increase in biomass using the BioWave® 20 SPS with the optimal culture conditions [3,5]. Independent of bioreactor mode, the growth of root biomass containing tropane alkaloids (5 mg g⁻¹ dry weight hyoscyamine) was about 120-fold after 28 days (Table 7). This is the highest biomass productivity of the laboratory cultivation systems investigated. The biomass produced maintained their typical morphology.

Under optimum conditions, as described above, it has been reported [6] that Wave cultured ginsenosides producing hairy roots can enhance root fresh weight more than 5-fold compared to 3.7-fold in an emerged spray reactor. From periodic medium exchanges and doubling the cultivation time, 28-fold higher biomass increases in the Wave and 12.1-fold higher biomass increases in the spray reactor result. While the maximum ginsenoside productivity has been reached 2.6 mg L⁻¹ d⁻¹ in the Wave, the maximum ginsenoside productivity in the spray reactor was 0.7 mg L⁻¹ d⁻¹. The first run

of Wave Bag 20 L (maximum 5 L culture volume) provided 423.6 g ginsenosides biomass (total 214 mg L⁻¹ ginsenosides) in 52 days. Through the use of the special hairy root bag with integrated mesh, the highly localised root mass loses its typical root morphology and should be avoided at higher culture volumes of 0.5 L.

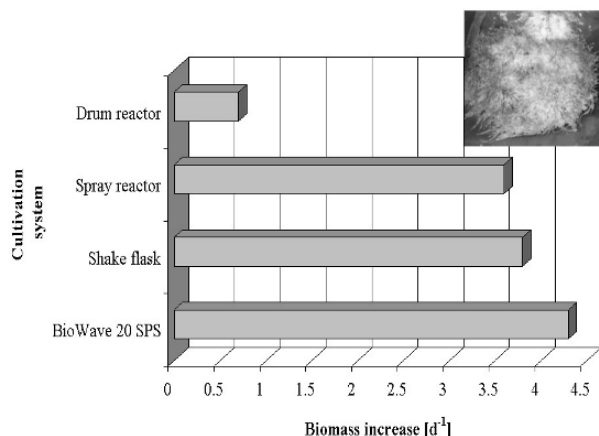


Figure 11. Biomass increase of hyoscyamine producing hairy roots (*Hyoscyamus muticus*, clone KB5) for different cultivation systems.

Follow-up tests indicated the possibility of direct inoculation with hairy roots from plates for both hairy root clones. No differences in hairy root morphology, biomass growth and secondary metabolite production were detected in experiments with inoculum from plates and shake flasks. The shake flask mass propagation procedure for inoculum production can therefore be omitted. This results in reduced time and process costs.

4.4. CULTIVATION OF EMBRYOGENIC CULTURES

Embryogenic culture of *Allium sativum* was established to produce alliin in laboratory stirred reactors, column reactors and the Wave [57]. The cells were grown in modified MS medium in shake flasks (100 rpm, dark). Provided with an inoculum of 30 g L⁻¹ fresh weight, the cells were cultured in fed batch (medium exchange in production phase) liquid suspension with light (25°C, 0.2 vvm). The Wave cultivations were performed in Wave Bags 2 L with screw cap at a constant energy input of 70W m⁻³ corresponding to 0.5 L culture medium, 6° angle and 11 rpm for 28 days. In the Wave, 20% higher biomass production was achieved under fluid flow in the transition zone from laminar to turbulent. The maximum biomass productivity was approximately 2.8 g L⁻¹ d⁻¹ fresh weight, yielding 0.124 mg g⁻¹ dry weight alliin (Table 7).

5. Conclusions

For plant cell and tissue cultures, disposable bioreactors such as the Wave provide an efficient alternative to standard glass or steel bioreactors. Its application in process development as well as in small and middle volume commercial production processes can increase process safety and reduce time as well as process costs. For example, time-intensive cleaning and sterilisation procedures as well as intermediate steps for inoculum production can be omitted. Biomass as well as secondary metabolite production in Wave bioreactors is comparable or even higher than in traditional laboratory reactors. This is a consequence of optimum hydrodynamic characteristics for hairy roots, suspension cultures and embryogenic cultures. High shear stress can be countered by high filling volume, minimum rocking rates and angles. Because of these characteristics and, in addition, its scale-up capability, the Wave has enormous potential for efficient commercial production processes based on plant cells. We expect this potential to be verified in the near future.

Acknowledgements

The authors' research was partly supported by the Commission of Technology and Innovation in Switzerland (CTI).

References

- [1] Bentebibel, S. (2003) Estudio de la producción de taxanos por cultivos de células en suspensión e inmovilizadas de *Taxus baccata*. Ph D Thesis, University of Barcelona, Barcelona.
- [2] Eibl, R. (2002) Fermentative Herstellung bioaktiver Wirkstoffe mit dem Wave. BioWorld 6: Sonderdruck BiotechNet.
- [3] Eibl, R. and Eibl, D (2002) Bioreactors for plant cell and tissue cultures. In: Oksman-Caldentey, K.M. and Barz, W. (Eds.) Plant Biotechnology and Transgenic Plants. Marcel Decker, Inc., New York; ISBN 0-8247-0794-X; pp. 163-199.
- [4] Eibl R (2003) Pflanzliche Zell- und Gewebekulturen-Wirkstoffproduzenten mit Zukunftspotential. Drogenreport 30: 17-19.
- [5] Lettenbauer, C. and Eibl, R. (2001) Application of the wave bioreactor 20 for hairy root cultures. In: Wildi, E. and Wink, M. (Eds.) Trends in Medicinal Plant Research: Screening, Biotechnology and Rational Phytotherapy. Romneya-Verlag, Dosenheim; ISBN 3934502024; pp. 139-141.
- [6] Palazón, J.; Mallol, A.; Eibl, R.; Lettenbauer, C.; Cusidó, R.M. and Piñol, M.T. (2003) Growth and ginsenoside production in hairy root cultures of *Panax ginseng* using a novel bioreactor. Planta Med. 69: 344-349.
- [7] Rothe, S. (2004) *In vitro* Produktion kosmetischer Wirkstoffe mit Pflanzenzell- und Gewebekulturen. Diploma Thesis; University of Applied Sciences Giessen Friedberg, Giessen.
- [8] Müller-Urri, F. and Dietrich, B. (1999) Kultivierung proembryogener Massen von *Digitalis lanata* im MiniPerm Bioreaktor. In Vitro News 3: 4.
- [9] Harrell, R.C.; Bieniek, M.; Hood, C.F.; Munilla, R. and Cantliffe, D.J. (1994) Automated *in vitro* harvest of somatic embryos. Plant Cell Tissue Org. Cult. 39: 171-183.
- [10] Fukui, H. and Tanaka, M. (1995) An envelope-shaped film culture vessel for plant suspension cultures and metabolite production without agitation. Plant Cell Tissue Org. Cult. 41: 17-21.
- [11] Ziv, M.; Ronen, G. and Raviv, M. (1998) Proliferation of meristematic clusters in disposable presterilized plastic bioreactors for large-scale micropropagation of plants. In Vitro Cell Dev. Biol.-Plant 34: 152-158.

- [12] Escalona, M.; Lorenzo, J.C.; Gonzalez, B.L.; Daquinta, M.; Gonzalez, J.L.; Desjardine, Y. and Borroto, C.G. (1999) Pineapple (*Ananas comosus* L. Merr) micropropagation in temporary immersion systems. *Plant Cell Rep.* 18: 743-748.
- [13] Curtis, W.R. (1999) Achieving economic feasibility for moderate-value food and flavour additives: A perspective on productivity and proposal for production technology cost reduction. In: Fu, D.J.; Singh, G. and Curtis, W.R. (Eds.) *Plant Cell and Tissue Culture for the Production of Food Ingredients*. Kluwer Academic Press, New York; ISBN 0-306-46100-5; pp. 225-236.
- [14] Endress, R. (1994) *Plant Cell Biotechnology*. 1st Edition. Springer Verlag, Heidelberg; ISBN 3-540-56947-2; pp. 46-83.
- [15] Lee, B.H. (1996) *Fundamentals of Food Biotechnology*. 1st Edition, VCH Publishers, Inc., New York; ISBN 1-56081-694-5; pp. 355-370.
- [16] Mirjalili, N. and Linden, J.C. (1995) Gas phase composition effects on suspension cultures of *Taxus cuspidata*. *Biotechnol. Bioeng.* 48: 123-132.
- [17] Linden, J.C.; Haigh, J.R.; Mirjalili, N. and Phisaphalong, M. (2001) Gas concentration effects on secondary metabolite production by plant cell cultures. *Adv. Biochem. Eng. Biotechnol.* 72: 28-62.
- [18] Pechmann, G.; Ducommun, C.; Lisica, L.; Lisica, S.; Blum, P.; Eibl, R.; Eibl, D.; Schär, M.; Wolfram, L.; Rhiel, M.; Emmerling, M.; Röhl, M.; Lettenbauer, C.; Rothmaier, M. and Flükiger, M. (2004) Production of pharmaceutical compounds with Wave 20 SPS. In: *Conference proceedings, BioPerspectives*, Wiesbaden (FRG), May 4-6 2004; pp. 338.
- [19] Flores, H.E.; Hoy, M.W. and Pickard J.J. (1987) Secondary metabolites from root cultures. *Trends Biotechnol.* 5: 64-69.
- [20] Wilson, P.D.G. (1997) The pilot-scale cultivation of transformed roots. In: Doran, P.M. (Ed) *Hairy Roots: Culture and Applications*. Harwood Academic Publishers, The Netherlands; ISBN 90-5702-117-X; pp. 179-190.
- [21] Kim, Y.H. and Yoo, Y.J. (1993) Development of a bioreactor for high density culture of hairy roots. *Biotechnol. Lett.* 7: 859-862.
- [22] Nuutila, A.M.; Toivonen, L. and Kauppinen, V. (1994) Bioreactor studies of *Catharanthus roseus*: comparison of three bioreactor types. *Biotechnol. Lett.* 8: 61-66.
- [23] Hitaka, Y.; Kino-oka, M.; Taya, M. and Tone, S. (1999) Effect of liquid flow on pigment formation of red beet hairy roots. *J. Chem. Eng. Jpn.* 32: 370-373.
- [24] Honda, H.; Liu, C. and Kobayashi, T. (2001) Large-scale plant micropropagation. *Adv. Biochem. Eng. Biotechnol.* 72: 157-182.
- [25] Hu, W.W. and Zong J.J. (2001) Effect of a bottom clearance on performance of airlift bioreactor in high-density culture of *Panax notoginseng* cells. *J. Biosci. Bioeng.* 92: 389-392.
- [26] Kieran, P.M.; Malone, D.M.; MacLoughlin, P.F. (2000) Effects of hydrodynamic and interfacial forces on plant cell suspension systems. In: Scheper, T.; Schügerl, K. and Kretzmer, G. (Eds.) *Advances in Biochemical Engineering Biotechnology; Vol 67, Influence of Stress on Cell Growth and Product Formation*. Springer Verlag, Berlin Heidelberg; ISBN 3-540-66687-7; pp. 141-177.
- [27] Tescione, L.D.; Ramakrishnan, D. and Curtis, W.R. (1997) The role of liquid mixing and gas-phase dispersion in a submerged, sparged root reactor. *Enz. Microb. Technol.* 20: 207-213.
- [28] Williams, G.R.C. and Doran, P.M. (2000) Hairy root culture in a liquid-dispersed bioreactor: Characterization of spatial heterogeneity. *Biotechnol. Prog.* 16: 391-401.
- [29] Zhong, J.J.; Pan, Z.W.; Wu, J.; Chen, F.; Takagi, M. and Toshiomi, Y. (2002) Effect of mixing time on taxoid production using suspension cultures of *Taxus chinensis* in a centrifugal impeller bioreactor. *J. Biosci. Bioeng.* 94: 244-250.
- [30] Henzler, H.J. (2000) Particle stress in bioreactors. In: Scheper, T.; Schügerl, K. and Kretzmer, G. (Eds.) *Advances in Biochemical Engineering Biotechnology; Vol 67, Influence of Stress on Cell Growth and Product Formation*; Springer Verlag, Berlin Heidelberg; ISBN 3-540-66687-7; pp. 38-82.
- [31] Lübbert, A. (2000) Bubble column bioreactors. In: Schügerl, K. and Bellgardt, K.H. (Eds.) *Bioreaction Engineering: Modelling and Control*. Springer-Verlag, Berlin Heidelberg; ISBN 3-540-66906-X; pp. 247-273.
- [32] Reuss, M.; Schmalzriedt, S. and Jenne, M. (2000) Application of computational fluid dynamics (CFD) to modelling stirred tank bioreactors. In: Schügerl, K. and Bellgardt, K.H. (Eds.) *Bioreaction Engineering: Modelling and Control*. Springer-Verlag, Berlin Heidelberg, ISBN 3-540-66906-X; pp. 208-246.
- [33] Knevelman, C.; Hearle, D.C.; Osman, J.J.; Khan, M.; Dean, M.; Smith, M.; Aiyedebinu, A. and Cheung, K. (2002) Characterisation and operation of a disposable bioreactor as a replacement for conventional steam in place inoculum bioreactors for mammalian cell culture processes. ACS Poster, Lonza Biologics, SL1 4DY (UK).

- [34] Rhiel, M. and Eibl, R. (2004) Der Wave als System zur Prozessentwicklung für Proteinexpressionen In: Conference proceedings, Biotech 2004, Wädenswil (CH), May 11-12 2004; pp. 20.
- [35] Singh, V. (2004) Overview of the Wave Bioreactor system. <http://www.wavebiotech.com> (accessed 17 July 2004).
- [36] Singh, V. (1999) Disposable bioreactor for cell culture using wave-induced agitations. *Cytotechnol.* 30: 149-158.
- [37] Lisica, S. (2004) Energieeintrag in Wave-Bioreaktoren. Modelling approaches. University of Applied Sciences Wädenswil, Wädenswil.
- [38] Eibl, R.; Eibl, D.; Pechmann, G.; Ducommun, C.; Lisica, L.; Lisica, S.; Blum, P.; Schär, M.; Wolfram, L.; Rhiel, M.; Emmerling, M.; Röhl, M.; Lettenbauer, C.; Rothmaier, M. and Flükiger, M. (2003) Produktion pharmazeutischer Wirkstoffe in disposable Systemen bis zum 100 L Massstab, Teil 1, KTI-Projekt 5844.2 FHS. Final Report; University of Applied Sciences Wädenswil, Wädenswil.
- [39] Pechmann, G. G. (2002) Disposable Wirkstoffproduktion im Wave-Reaktor mit minimalen Suspensionszellen. Diploma Thesis, University of Applied Sciences Anhalt, Köthen.
- [40] Kallapurackal, J. (2004) Beitrag zur Beschreibung des Energieeintrages im Wave-System. Semester Thesis; University of Applied Sciences, Wädenswil, Wädenswil.
- [41] Sowana, D.D.; Williams, D.R.G.; Dunlop, E.H.; Dally, B.B.; O'Neill, B.K. and Fletcher, D.F. (2001) Turbulent shear stress effects on plant cell suspension cultures. *Trans. I.Chem.E.* 79: 867-875.
- [42] Tanaka, H. (1981) Technological problems in cultivation of plant cells at high density. *Biotechnol. Bioeng.* 23: 1203-1218.
- [43] Dunlop, E.H.; Namdev, P.K. and Rosenberg, M.Z. (1994) Effect of fluid shear forces on plant cell suspensions. *Chem. Eng. Sci.* 49: 2263-2276.
- [44] Chen, S.Y. and Huang, S.Y. (2000) Shear stress effects on cell growth and L-DOPA production by suspension culture of *Stizolobium hassjoo* cells in an agitated bioreactor. *Bioprocess Eng.* 22: 5-12.
- [45] Präve, P.; Faust, U.; Sittig, W.; Sukatsch, D.A. (1994) *Handbuch der Biotechnologie*. 4. Auflage, R. Oldenbourg Verlag, München Wien; ISBN 3-486-26223-8; pp. 189.
- [46] Griffiths, J.B. (1999) Mammalian cell culture reactors. In: Flickinger, S.W. and Drew, S.W. (Eds) *Encyclopaedia of Bioprocess Technology*, Vol 3, Fermentation Biocatalysis and Bioseparation. John Wiley & Sons, Inc., New York; ISBN 0-471-13822-3; pp. 1594-1607.
- [47] Eibl, R.; Hans, D.; Lettenbauer, C. and Eibl, D. (1999) Einsatz eines Taumelreaktorsystems mit interner Beleuchtung. *BioWorld 2*: 10-12.
- [48] Kato, A.; Shimizu, Y. and Nagai, S. (1975) Effect of initial $k_L a$ on the growth of tobacco cells in batch culture. *J. Ferment. Technol.* 53: 744-751.
- [49] Meijer, J.J.; ten Hoopen, H.J.G.; Luyben, K.C.A.M. and Libbenga, K.R. (1993) Effects of hydrodynamic stress on cultured plant cells: A literature survey. *Enz. Microbiol. Technol.* 15: 234-238.
- [50] Wheathers, P.J.; Wyslouzil, B.E. and Whipple M. (1997) Laboratory-scale studies of nutrient mist reactors for culturing hairy roots. In: Doran, P.M. (Ed.) *Hairy Roots: Culture and Applications*. Harwood Academic Publishers, The Netherlands; ISBN 90-5702-117-X; pp. 191-199.
- [51] Yoshikawa, T. (1997) Production of ginsenosides in ginseng hairy root cultures. In: Doran, P.M. (Ed.) *Hairy Roots: Culture and Applications*. Harwood Academic Publishers, The Netherlands; ISBN 90-5702-117-X; pp. 73-79.
- [52] Kato, Y.; Honda, H.; Hiraoka, S.; Tada, Y.; Kobayashi, T.; Sato, K.; Saito, T.; Nomura, T. and Ohishi, T. (1997) Performance of a shaking vessel-type bioreactor with a current pole. *J. Ferment. Bioeng.* 84: 65-69.
- [53] Honda, H.; Hiraoka, K.; Nagamori, E.; Omote, M.; Kato, Y.; Hiraoka, S. and Kobayashi, T. (2002) Enhanced anthocyanin production from grape callus in an air-lift type bioreactor using a viscous additive-supplemented medium. *J. Biosci. Bioeng.* 94: 135-139.
- [54] Kim, D.J. and Chang, H.N. (1990) Enhanced shikonin production from *Lithospermum erythrorhizon* by *in situ* extraction and calcium alginate immobilization. *Biotechnol. Bioeng.* 36: 460-466.
- [55] Brodelius, P. (1985) The potential role of immobilisation in plant cell biotechnology. *Trends Biotechnol.* 3: 280-285.
- [56] Dörnenburg, H. and Knorr, D. (1995) Strategies for the improvement of secondary metabolite production in plant cell cultures. *Enz. Microbiol. Technol.* 17: 674-684.
- [57] Kieran, P.M.; MacLoughlin, P.F. and Malone D.M. (1997) Plant cell suspension cultures: some engineering considerations. *J. Biotechnol.* 59: 39-52.
- [58] Warlies, S.; Reinhardt, K. and Eibl, R. (1999) Optimierung der Synthese von Alliin/Allicin mit pflanzlichen Zellkulturen *in vitro* und im Bioreaktor. Report; University of Applied Sciences Wädenswil, Wädenswil.

Design and use of the wave bioreactor for plant cell culture

- [59] Hirasuna, T.J.; Pestchanker, L.J.; Srinivasan V. and Shuler, M.L. (1996) Taxol production in suspension cultures of *Taxus baccata*. *Plant Cell Tissue Org. Cult.* 44: 95-102.
- [60] Ketchum, R.E.B. and Gibson, D.M. (1996) Paclitaxel production in cell suspension cultures of *Taxus*. *Plant Cell Tissue Org. Cult.* 46: 9-16.
- [61] Navia-Osorio A.; Garden, H.; Cusidó, R.M.; Alfermann, A.W. and Piñol, M.T. (2002) Taxol[®] and baccatin III production in suspension cultures of *Taxus baccata* and *Taxus wallichiana* in an airlift bioreactor. *J. Plant Physiol.* 159: 97-102.
- [62] Cusidó, R.M.; Palazón, J.; Bonfill, M.; Navia-Osorio, A.; Morales, C. and Piñol, M.T. (2002) Improved paclitaxel and baccatin III production in suspension cultures of *Taxus media*. *Biotechnol. Prog.* 18: 418-423.
- [63] Oksman-Caldentey, K.M.; Vuorela, H.; Strauss, A. and Hiltunen, R. (1987) Variation in the tropane alkaloid content of *Hyoscyamus muticus* plants and culture clones. *Planta Med.* 53: 349-354.
- [64] Ouhikainen, K.; Lindgren, L.; Jokelainen, T.; Hiltunen, R.; Teeri, T.M. and Oksman-Caldentey, K.M. (1999) Enhancement of scopolamine production in *Hyoscyamus muticus* L. hairy root cultures by genetic engineering. *Planta Med.* 208: 545-551.

PART 3

MECHANIZED MICROPROPAGATION

INTEGRATING AUTOMATION TECHNOLOGIES WITH COMMERCIAL MICROPROPAGATION

An economic perspective

CAROLYN J. SLUIS

*Tissue-Grown Corporation, 6500 Donlon Road (PO 702), Somis,
California 93066, USA - Fax: 805-386-8227-
Email: carolynsluis@tissuegrown.com*

1. Introduction

Replacement of the people who do micropropagation work in laminar flow hoods, with equipment of any kind, is neither technologically simple nor readily economically achievable. The fundamental fact remains that the human eye-hand-brain combination is both highly sophisticated, technologically, and incredibly inexpensive, certainly when considered on a global scale. Consequently, commercial micropropagation companies in both Europe and North America have followed the path of lower costs to those countries for which the infrastructure, such as reliable power supplies, and logistics, such as political stability and transportation issues, are favourable.

Cost accounting needs to take into consideration many factors which are not always obvious at the onset of a project; in the case of micropropagation these include risk assessments, refinement of protocols, and employee training. Aseptic culture systems are vulnerable to bacterial, fungal and even insect contaminants which can destroy the plantlets, as well as to genetic and epigenetic shifts, which can seriously impair their quality. The transfer of the operation from human to mechanical means can differentially affect each of these factors. The costs of maintaining a high level of genetic purity and the risk of contamination must be factored into the long-term costs of mechanized systems. The history of micropropagation has created a legacy of sudden, disastrous plantlet losses, the magnitude of which have cooled the ardor of all but the hardiest researchers. Likewise, the financing and funding of various companies and projects has been erratic, often resulting in a lack of continuity and instability; as evidenced by ventures such as Plant Genetics, of the United States, based on scale-up of somatic embryogenesis [1], ForBio, of Australia, focussed on elite tree micropropagation using robotics [2] and Osmotek, of Israel, a supplier of plastics for biofermentation and liquid culture systems.

2. Biological parameters

2.1. THE PLANT'S GROWTH FORM AFFECTS MECHANIZED HANDLING

The list of plants which can be grown *in vitro* is broad and covers many genera [3,4]; nonetheless, the vast majority of plant species are not able to be economically micropropagated, due either to technical difficulties in tissue culture or to their expense relative to standard propagation by seed, cuttings, tubers or bulbs. The growth form of a plant can be significantly modified *in vitro* by the use of plant growth regulators and environmental controls, so that a plant which normally grows as a linear vine, such as a potato, can become either a linear, straight-stemmed plantlet, such as is commonly seen in test tubes, or a dense compact cluster of buds, such as is possible in liquid culture using ancymidol, or even a linear microtuber, as can occur under certain environmental conditions. Other genera naturally grow as rosettes, and inducement of axillary bud growth results in dense masses of tiny shoots (see the *Limonium* plantlets in Figures 1 and 2). For example, in the case of potato and carnation, the preferred growth form for robotic access and separation has been linear; the plantlets can be grown upright, then laid flat for cutting (see Figure 3) or they can be grown in shallow plastic boxes with domed tops and repeatedly "hedged," as was described by Aitken-Christie and Jones for pine [5]. Both of these methods are effective in increasing access for mechanical handling of the plantlets. Potatoes can be grown in liquid culture as nodes [6-8] as bud clusters [9-11] or made into microtubers [6,8,12,13] or even somatic embryos [14]. However, none of these methods have been scaled up to millions of plantlets due to two barriers:

- Economics: the potato industry is based on tuber seed pieces costing less than a penny a piece
- Size issues: in North America, field conditions dictate that the tuber seed piece will not be replaced by anything smaller than a greenhouse minituber for many years to come.



Figure 1. Axillary branching in *statice* using liquid medium additions.

Historically, commercial micropropagation was based on enhanced axillary bud break; overcoming the natural apical dominance with cytokinins and other factors to encourage lateral buds to grow out into shoots; this increases the number of shoots per culture per month, the multiplication rate. However, if strategies with lower multiplication rates, for example, straight stemmed, unbranched shoots, give significant advantages to mechanization, then branching options may be to be reexamined within the new framework. Multiplication rates of greater than 10-fold per month can be achieved in tissue culture (see Figures 1 and 2); however, these may not contribute significantly to reduce the end-product cost if the labour for singulation/rooting is increased (see Table 1) and/or the quality of the plantlets decreased.



Figure 2. Subculture of explants (shown in Figure 1) for rooting.



Figure 3. Cassette style (square Petri dish) of potato cultures at 2 week for robotic access.

Somatic embryogenesis continues to be a highly attractive biological strategy for large-scale production research, despite the difficulties, although full automation still appears to be years away. The largest ongoing operations based on this technology appear to be in the forestry sectors, where manual handling of the output embryos is still the norm, dramatically raising final costs [15]. Even if the embryos cost next to nothing apiece and can be made in the hundreds of thousands, a single manual handling step, such as singulation or planting, can make the system economically prohibitive [16]. The genetic component within species regarding the ability to form somatic embryos can be significant [14] as is the potential for loss of genetic fidelity in the pre-embryoid tissues. Genetic testing technologies are assisting vegetable breeding companies in confirming the true-to-type characteristics critical for seed parents (Rijk Zwaan, personal communication) and the existing automation of PCR testing of cotyledon discs could enable future monitoring of somatic embryo-derived plugs; however, the automated somatic seed concept still appears many years off [17,18].

On an international scale, another biological method for micropropagation, known as bud clusters, has gained widespread acceptance both for its potential application to many species, as well as its obvious physical compatibility with mechanical handling [19]. One method developed by the late Levin [20] and Ziv [11,21,22], combines the bud cluster growth form, either in liquid culture or on agar, with a simple fixed-blade mechanical cutting device, such as a grid of blades, allowing the clusters to be mechanically subdivided into up to 100 pieces with one operation; this has been shown to work in potato, lilies and several other crops.

The most common media typically used for induction of bud cluster growth patterns involve the use of liquid culture, a gibberellin inhibitor, such as ancymidol, and an axillary bud growth promoting agent, such as the cytokinin benzylaminopurine. The bud cluster induction treatment needs to be repeated serially for several subcultures to establish the formation of true clusters. It is difficult to scale up to commercial levels in liquid culture systems, due to hyperhydricity [21] and bacterial contamination problems. While this avenue of production research has great potential for long-term production in high volumes of quality plantlets, the difficulties remain problematic and the limitations, especially for commercial laboratories, remain significant. Several major genera of plants already in mass propagation via tissue culture are quite amenable to the liquid bud cluster construct, as they readily form a densely compact mass of basal proliferation and are tolerant of high humidities, liquid environments and mechanical damage. These will probably be propagated in increasing numbers over time using biofermentation approaches.

Researchers in several crops and from several countries are scaling up the bud cluster system [11,19,21-24]. Basically, cluster culture involves the reduction of the tissue culture plantlet to a compact mass of leafless, highly branched, short masses of buds; there is little or no callus proliferation or adventitious bud formation. These organized bud clusters are then maintained in a multiplication mode as long as necessary for production of sufficient numbers to meet the goals of the project. When it is time for finishing the plantlets, the pressure of the cytokinin/growth retardant combination is removed and the shoots grow out into their normal morphology.

Currently the most advanced commercial biofermentation systems in application are based on the incubation of cultures in a redesigned biofermentation vessel consisting of a five or ten liter autoclavable plastic bag, similar to a medical medium or serum bag, complete with input and output ports. Implementation of this technology is being intensely pursued by at least two major high volume laboratories in North America. Rather than being an automated system, biofermentation of bud clusters is actually still an operator-assist method, the subcultures are still carried out by hood operators; the vessels combined with bud clusters greatly increases the productivity of the operator and hence significantly reduces the cost per plantlet, while still benefiting from human decision-making. Attempts to automate these systems further have not yet been realized, but are nearing. The bag fermentors, equipment and supplies facilitating the production of plantlets, bud clusters, somatic embryos and other propagules in liquid fermentation was commercially available prior to 2004, but the withdrawal of the manufacturer currently makes the development of liquid bud cluster systems less accessible to smaller operations.

Liquid culture systems are, in general, more difficult to stabilize, maintain and commercialize than simple agar-based standards. Humidity must be carefully managed for maintenance of consistent medium volumes and component concentrations. In smaller vessels, the variability between vessels can be dramatic. When propagation is transferred from agar-based to liquid many factors in the medium itself will need to be adjusted. In some cases this can amount to starting from scratch, never an attractive option for the tissue culture propagation laboratory.

Many plants do not take easily to being submerged in liquid. To overcome problems such as hyperhydration, deformed growth, insufficient cuticles and other side effects of oxygen depletion and underwater growth, enhanced oxygenation of the solution, and timed, temporary immersion rather than full-time exposure to the liquid environment can improve the quality of plantlets substantially [25,26]. However, intermittent flooding, while clearly of benefit to many species, is cumbersome and even more prone to difficulties with contamination, so challenges remain [21].

2.2. MICROBIAL CONTAMINANTS HINDER SCALE-UP

Microbes present much more of a threat to the mass propagation of plants *in vitro* than they do in greenhouses. Normally harmless, airborne organisms, such as molds, yeasts and otherwise unheard of bacteria [27-31], become lethal to plantlets in the micropropagation environment, simply by overwhelming the cultures. Internal bacteria, some of which can be quite significant, can be carried at extremely low populations for years without detection [32].

Plant tissue culture originated in tightly capped, glass culture vessels using very small tissues, such as meristems, which had no capacity to produce sufficient photosynthate for growth and development. Consequently, sugars were required in the medium, and sugars are used in nearly all of today's commercial laboratories, including our own. Plants do not normally require extraneous sugar for growth and development; the artificial conditions of restricted gas exchange, low light levels and high humidity, incur the need for sugar in tissue culture media. While true meristems, embryos, protoplasts and other tissues certainly require carbohydrate sustenance; micropropagated

plantlets are fully capable of supporting themselves. The micropropagation industry has paid heavily for its reliance on sugar, both from the severe restrictions on automation and mechanization research resulting from the extreme requirements for sterility in any process involving sugar-based production, and from the plantlet losses during transitioning due to weaknesses in the epidermal tissues and root systems [33-38]. Photoautotrophy has clearly been demonstrated to produce healthy and vigorous plants, but it has not been fully incorporated into production laboratories.

Photoautotrophy, which clearly reduces the bloom of microorganisms and which equally clearly promotes healthy plantlet growth, has not been an easy goal to attain at the commercial level, in part due to the reluctance to aerate the culture vessels, thereby risking contamination, which can be a very real problem, and in part due to reluctance to spend significant funds on facilities and culture vessel modifications. The requirements for environmental controls and modified vessels are somewhat stringent in order to achieve true parity on a production scale. Cutting corners, while still permitting improvements in plant performance, do not help with bacterial control in automation research, as even a little sugar in the medium will support very vigorous microbial populations. Although green plantlets conduct photosynthesis while in tissue culture, the rates are often low and reliance on sugar is high, even in the greenest plantlets. Still, it is logical that photoautotrophy or at least enhanced photomixotrophy [25,38] will become standard for standard types of commercial propagation *in vitro*.

Culture indexing, whereby plantlets or tissues are assayed for the presence of internal, or non-obvious, bacteria is commonly practiced using several standard media which encourage bacterial growth, such as nutrient broth and potato dextrose agar. While culture indexing is important in agar-based systems, it is critical for liquid-based systems, where contamination can overtake the cultures within a matter of days, or even hours.

Sterility is critical to maximum batch size, as a greater percentage of the plantlets produced are at risk when more explants are in a single vessel. Obviously, if plantlets are subcultured in test tubes, and 1% of the explants are contaminated, then 1% of the plantlets are lost; however, if 50 plantlets are subcultured into each culture vessel, a 1% contamination rate quickly adds up to many more plantlets being lost.

Antibiotics and bactericides, such as hydrogen peroxide and sodium hypochloride, have been added to culture media to kill bacteria, or at least inhibit their growth [30]. Other strategies, such as refrigeration, filtration or ozonation of the recirculation medium, have been implemented to a lesser degree [39,40].

3. Physical parameters

Several physical parameters can be re-examined for potential modifications or options which may favour new automation or mechanization technologies. Physical constraints which have been accepted as fixed for standard parameters may need to be modified in order to make new systems feasible. For example, the benefits of automation on final cost-per-unit may ultimately outweigh the subsidiary input costs of using more expensive culture vessels. The benefits of photoautotrophy may outweigh the outlay of expenses for culture room modifications.

3.1. CULTURE VESSELS

The physical parameters of the micropropagation system begin with the choice of culture vessel. The culture vessel either permits ready access or hinders it; it allows varying degrees of gas exchange and clarity, and it has an impact on plantlet growth and quality. Many factors come into play when choosing a vessel for commercial propagation. Inexpensive culture vessels which impede operators are, in fact, far more costly than slightly more expensive culture vessels which streamline labour. From a materials-handling perspective, glass is heavy, awkward and requires washing, an added expense. From an access perspective, test tubes are seriously limiting, and operators can rarely handle more than 800 per day; but test tubes retain their usefulness in many applications, including culture initiations and germplasm maintenance. Culture vessels may be designed specifically with an automation device in mind, as is the case with most robotic applications [41,42].

The choice of culture vessel is also important to controlling contamination losses: the larger the vessel, the greater the number of plantlets which are lost with each introduced contaminant. Consequently, the use of larger vessels typically requires ultra-clean laboratories, incurring additional facilities costs [43]. In addition to the higher multiplication rates attainable in 10 L liquid culture bags, these vessels have good accessibility throughout the subculture cycle, and daily operator productivity, can be increased substantially as a result.

3.2. PHYSICAL ORIENTATION OF EXPLANTS FOR SUBCULTURE OR SINGULATION

Over the past 20 years, many different concepts for the mechanization or automation of micropropagation have been envisioned; originally, mechanical approaches were based on either robotics with computer imaging, for cutting of straight stemmed cultures (potatoes, trees, sugarcane, carnations) [41,42], or adventitious regeneration approaches, which are combined a 'blender' approach to cutting of tissues, with species such as ferns. Subsequently, researchers studied the semi-automated production of artificial seeds using somatic embryos [2,7,18].

Each of these systems had its drawbacks and limitations. For mass regeneration systems, the phenotypic and genotypic changes of somatic embryos were problematic in crops which required a high degree of uniformity [17]. For robotic cutting systems, there were few suitable crops needed in the volumes required to amortize the high costs of the initial production line and its maintenance, and there were ongoing issues of low speed relative to the human operator. In the case of somatic seed, commercial efforts still had a heavy reliance on operators at the final stages of singulation and sorting.

Bud clusters are physically compatible with random, or spatial, mechanical cutting equipment in the multiplication stages, as there are so many buds in various stages of development that damage to a certain percentage of them is bearable. Once true bud clusters have been created, subdividing the clusters by means of mechanical, fixed blade cutting devices becomes feasible [9,22,24]. For potatoes, even operator-assist devices, such as grid blades (similar to French fry cutters) can greatly increase efficiency, as essentially 25-36 sub-divisions can take place with one cut. Resterilization of the grid

blades over the course of the day is not any more cumbersome than resterilization of forceps and scalpels, but the cost of multiple tools and handling the cutting devices is slightly more expensive and awkward.

3.3. GAS PHASE OF THE CULTURE VESSEL IMPACTS AUTOMATION

Plantlets grown under conditions of reduced humidity, reduced ethylene, adequate carbon dioxide and adequate oxygen perform better during the transitioning period, which is instrumental to elimination of the tissue culture rooting stage. The choice of vessel influences the amount of gas exchange possible between the sterile interior and ambient, or external air. Currently, biofermentation using temporary immersion or nutrient film delivery techniques, rather than full submersion, can provide environments that are highly favourable to the plantlet in terms of both photosynthetic activity and epidermal function.

Innovations in photoautotrophy are accompanied with greater understandings of the effects of light spectra and intensity on the quality of plantlets [44-46]. Research into “chopper light” may allow significant savings in cooling costs, as well as decrease electrical costs for lighting.

Greenhouse operations have been adding carbon dioxide to the plant environment for years. Increased carbon dioxide in the growth room (at 2-4 x ambient levels) can enhance the performance of plantlets even on sugar-based media, especially when culture vessels are well vented. Advances in porous filters and tapes (i.e. 3M Micropore™ tape) have enabled the venting of many previously sealed containers.

4. Economic parameters

For any new technology, such as automation of micropropagation, the primary indicator of its commercial potential is its projected impact on the cost of the plantlet. While true cost accounting is a complex and multifaceted task that is required for ongoing operations and fine decision making [47], it can be simplified for the purposes of preliminary evaluations. For this purpose Table 1 was designed to permit comparison of various factors, such as labour daily costs and multiplication factors; it is a model only, each major crop group within each commercial laboratory requires its own analysis for accurate cost accounting.

4.1. BASELINE COST MODELS

The total payroll of micropropagation laboratories is typically over 65% of the monthly budget; however, this does not give an accurate picture of the pyramid of costs linked to each hood operator hour. Costs need to take into account all aspects of the operation, so one simplistic approach, used by several laboratories including ours, is to take the total monthly outlays and divide them by the parameter being evaluated, for example hood operator hours per month (excluding medium preparation, dishwashing and other non-hood activities), for an average cost per hour of the hood work.

Integrating automation technologies with commercial micropropagation

Table 1a. Model of cost per plantlet, as influenced by various factors.

Multiplication							
Rate (xx)	Daily hood operator rates						
TC Systems:	600/day	900	1200	1500	1800	2100	2400
Standard^b							
	Cost fixed at \$35/hr fully loaded ^a						
2x	\$0.933	\$0.622	\$0.467	\$0.373	\$0.311	\$0.267	\$0.233
3x	\$0.700	\$0.467	\$0.350	\$0.280	\$0.233	\$0.200	\$0.175
4x	\$0.622	\$0.415	\$0.311	\$0.249	\$0.207	\$0.178	\$0.156
5x	\$0.583	\$0.389	\$0.292	\$0.233	\$0.194	\$0.167	\$0.146
6x	\$0.560	\$0.373	\$0.280	\$0.224	\$0.187	\$0.160	\$0.140
7x	\$0.544	\$0.363	\$0.272	\$0.218	\$0.181	\$0.156	\$0.136
8x	\$0.533	\$0.356	\$0.267	\$0.213	\$0.178	\$0.152	\$0.133
9x	\$0.525	\$0.350	\$0.263	\$0.210	\$0.175	\$0.150	\$0.131
Advanced^c							
10x	\$0.519	\$0.346	\$0.259	\$0.207	\$0.173	\$0.148	\$0.130
20x	\$0.491	\$0.327	\$0.246	\$0.196	\$0.164	\$0.140	\$0.123
30x	\$0.483	\$0.322	\$0.241	\$0.193	\$0.161	\$0.138	\$0.121
40x	\$0.479	\$0.319	\$0.239	\$0.191	\$0.160	\$0.137	\$0.120
50x	\$0.476	\$0.317	\$0.238	\$0.190	\$0.159	\$0.136	\$0.119
60x	\$0.475	\$0.316	\$0.237	\$0.190	\$0.158	\$0.136	\$0.119
70x	\$0.473	\$0.316	\$0.237	\$0.189	\$0.158	\$0.135	\$0.118

^aFully loaded cost per hour includes both direct and indirect costs: facilities, utilities, materials, freight

^bStandard tissue culture (TC) includes: axillary branching, nodal culture

^cAdvanced tissue culture (TC) includes: somatic embryos, adventitious bud cultures, hedge, biofermentation

Table 1b. Variation in plantlet cost with global labour costs.

Loaded cost per hour (US\$)	Daily hood operator rates						
	600/day	900	1200	1500	1800	2100	2400
TC Systems:							
Standard (5x fixed)							
\$35/hr ^a	\$0.583	\$0.389	\$0.292	\$0.233	\$0.194	\$0.167	\$0.146
\$25/hr	\$0.417	\$0.278	\$0.208	\$0.167	\$0.139	\$0.119	\$0.104
\$15/hr	\$0.250	\$0.167	\$0.125	\$0.100	\$0.083	\$0.071	\$0.063
\$ 5/hr	\$0.083	\$0.056	\$0.042	\$0.033	\$0.028	\$0.020	\$0.021
\$ 2/hr	\$0.033	\$0.022	\$0.017	\$0.013	\$0.011	\$0.010	\$0.008
Advanced (30x fixed)							
\$35/hr	\$0.483	\$0.322	\$0.241	\$0.193	\$0.161	\$0.138	\$0.121
\$25/hr	\$0.345	\$0.230	\$0.172	\$0.138	\$0.115	\$0.099	\$0.086
\$15/hr	\$0.207	\$0.138	\$0.103	\$0.083	\$0.069	\$0.059	\$0.052
\$ 5/hr	\$0.069	\$0.046	\$0.034	\$0.028	\$0.023	\$0.020	\$0.017
\$ 2/hr	\$0.028	\$0.018	\$0.014	\$0.011	\$0.009	\$0.008	\$0.007

^a \$ 1-2 = lesser developed nations (China), \$ 5-15 = developing nations, \$ 25-35 = industrialized nations (US, Europe)

Although this is overly simplistic, it is useful for evaluating the impact of various systems. For standard agar-based systems, the fully loaded hood operator rate is ranging between \$ 27 and \$ 42 per hour, which is actually 20-25% of the total monthly expenses. This figure can then be divided by the average annual plantlet output per hour for a very rough general cost per plantlet. The average annual plantlet sales per hood operator are on the order of 200,000 plantlets for laboratories producing steady volumes of a spectrum of standard ornamentals; this number converts to approximately 100 saleable plantlets per hour per operator over the course of a typical 2,000 hour year. Using this average number, with the average hourly cost of \$ 35 per hour, gives an average plantlet cost of US\$ 0.35 apiece, a figure which will then require a sales price of

US\$ 0.45 or above per plantlet rooted *in vitro* (Stage IIIb). In fact, very few plantlets in the United States or Europe are sold for much less.

Given these high costs, and correlating high prices, it is easy to see why micropropagation is increasingly taking place in India, Singapore, South Africa, China and Eastern Europe, where direct wages can be as low as US\$ 0.40-50 per hood operator hour; less than US\$ 2.00 per fully loaded hood operator hour, giving an estimated final plantlet cost of US\$ 0.03 (see Table 1).

4.2. ECONOMICS OF OPERATOR-ASSIST STRATEGIES

While automation research is extensive and ongoing at university and government levels [16,21,48-52], some work is actually accessible to commercial laboratories. A person can perform a typical cut-and-place operation, without any additional steps, in 3 seconds, which translates into a theoretical maximum of 9000 per operator day (7.5 working hours). This simple calculation reveals that the hood operator is seriously under-optimized, from the standpoint of the inherent skills in the human complex of hand-eye-brain, which are essential to the tasks of:

- explant analysis for selection of the cuts
- making the cuts with minimal damage, and,
- sorting and placing the explants in new media.

We have seen one operator can reach 8000 potato node cuttings in a single day when supplied with ideal plantlets grown in 25x150 (mm) petri dishes at 20 nodes per dish; in this case, plantlets were hedged, i.e., cut in place, they were not removed from the agar in order to be cut. The workstation was expanded to a full eight foot hood, or 24 square feet of workspace, sufficient for the entire load of inputs and outputs. We have also seen daily rates with potatoes of 8000 with 2-person teams using electric knife hedging systems (one operator shears 2 cm. long microcuttings onto a paper towel roll while a second operator selects and places the cuttings into fresh medium, with the assistance of a foot-pedal operated conveyor). Realistically, it is difficult to maintain operator rates over 3000 for many weeks on end, as people prefer to work at a lesser level of concentration for the pay scale typical of micropropagation jobs. Subsequently, on a sustainable monthly basis, operator performance rates for average tissue culture laboratories stabilize at around 1200 per day. This is similar to equivalent tasks, such as hand grafting of vegetable transplants (J. Boskermolen, JOBU plastics, personal communication) and transplanting of 288 cell seedling flats to 4 inch (10 cm) pots on conveyor lines (L. Oki, UCD personal communication).

It seems probable that sustainable operator rates of 2400 plantlets per day are attainable with operator-assist strategies at slightly elevated pay rates. However, some degree of alleviation of the cut-and-place operations is usually necessary for most operators to sustain performance over long periods of time.

4.3. ORGANIZATION OF THE APPROACH TO ROOTING: *IN VITRO* OR *EX VITRO*

Table 1 is based on a single one-to-one handling step by a person; a single step can be costly, but if more than one direct step is needed, costs can dramatically increase. If the

single one-to-one manual step takes place in the greenhouse, under non-sterile conditions, costs are less than if the handling occurs under sterile conditions. Research aimed at elimination of the final rooting stage *in vitro* has an immediate impact on costs, which, while not as dramatic as automation, is still very worthwhile. The combination of semi-automated sterile fermentor production with plantlets that can be separated and planted in the greenhouse has many advantages for the commercial laboratory. Bud masses can be shipped from foreign laboratories more readily than plantlets can, and certainly more readily than once they are in soil. Mechanization of the greenhouse planting of tissue cultured plantlets is clearly already functioning on a commercial scale. Final refinements in technologies which singulate, or unitize, plantable explants from fermentation vessels will bring micropropagation to the next level of commercialization.

4.4. ECONOMICS OF NEW TECHNOLOGIES

The general consensus of the micropropagation industry regarding new technologies is that the growth of cultures in liquid temporary immersion systems can drive the price down by 50%, after a somewhat significant learning curve, and, in the hands of skilled personnel can drop the price by as much as 67%. However, there is a significant increase in the degree of precision and sterility required throughout the production process and sudden losses, due to slight variations in medium, environment or other parameters, can still be costly and disruptive.

Overlays [53,54] and hedging [5] are still very viable ways of bringing costs down while maintaining quality and true-to-type characteristics of non-callus based propagation systems [17]. These have the added advantage of being adaptable to many species and compatible with both high volume and low volume applications.

Operator assist mechanisms, such as mechanical grafting equipment, are not always commercially successful. Vegetable transplants in the Netherlands are grafted, or stunted, by hand despite the existence of mechanized equipment. The vegetable seedlings are selected on a wide variety of criterion, then matched, scion to rootstock, cut and clipped; the grafts are slightly more successful with trained personnel, working with the clips manually, than they are with existing machinery, and there is insufficient financial incentive to stay with the mechanized grafting equipment. In micropropagation work, a similar degree of refinement exists in decision-making at the operator level; consequently, it seems logical that the very last step to be mechanized will be the singulation of difficult species.

5. Business parameters

In addition to the biological, physical and economic parameters, there are business parameters to be considered in determining if new technology can be applied commercially. Every business evaluates its production options for the products it sells; importation and outsourcing, either via establishment of foreign operations or importation of multiplied clusters or clumps of shoots, or even importation of entire plantlets, is on the rise in industrialized nations and can be expected to increase substantially over time. Automation, mechanization and other strategies for cost controls

will be employed by foreign operations as well and can be expected to benefit the global industry as larger markets open up.

In the case of potato, the United States produces less than 7% of the world's crop [55], even so, literally billions of seedpieces are planted annually in the United States [56], and the cost of each commercial grade seedpiece, which consists of a minimum of 50 grams of tuber with 2-3 eyes, is less than \$ 0.01 apiece (US\$ 7.50/cwt÷800 seedpieces). An average potato seedpiece is more than 50 times the size of an average microtuber. The entire commercial crop in the United States technically requires less than 400 first field generation acres, or 8 million minitubers, which are produced from approximately two million plantlets, on a highly seasonal basis in specialized greenhouses. The numbers of plantlets required for production of elite minitubers, which are the starting point for the North American potato industry, are orders of magnitude less than is required for justification of automation in the laboratory. A closely monitored, multi-year certification process is in place to minimize the reintroduction of potato diseases, and this is used to bring down the high cost of each minituber derived from laboratory plantlets. Frito-Lay, the major purchaser and manufacturer of potato minitubers in North America, established a state-of-the-art modified hydroponic warehouse for production of 'Technitubers[®]', a hybrid between sterile microtubers and ultrasmall (1.5 gm) minitubers, using a system enabling harvest of an average of 100 tiny tubers per plant. Even this operation, which produced 15 million tubers in one year, required only 150,000 plantlets from the laboratory, easily producible by hand. Unfortunately, Technitubers[®] proved too expensive and too small for acceptable field performance in the United States, and production ceased in 2003. Similar facilities in regions of the world where field seed cannot be kept free of diseases for more than a few years, such as India and China, may be able to justify microtubers, or ultrasmall tubers. Even in these countries, the few hundred thousand potato plantlets required to make these tubers are easily produced manually.

Perhaps that the future role of micropropagation-oriented laboratories in the industrialized nations will be to expand their expertise into creation of improved tissue culture systems and interface between foreign operations and in country greenhouse plant and plug operations with quality, biological systems development, germplasm isolation and maintenance and disease management functions.

5.1. VOLUMES PER CULTIVAR

Significant reasons for micropropagation include:

- propagation when other methods are too slow or too expensive,
- to increase new cultivars rapidly,
- to modify the growth form, for example to increase branching and fullness, and
- to maintain and distribute elite stock plants for propagation [57].

For any crop to be considered a candidate for micropropagation, the value-added benefits need to economically offset their higher costs relative to the alternative propagation methods. One of the primary advantages of tissue culture over other methods of vegetative propagation, such as cuttings, is that the cleanliness of the starting culture, in terms of bacteria, viruses, fungi and insects, can be ascertained, and, once

indexing and eradication procedures have been completed, large populations of elite stock can be produced without significant risk of recontamination. Consequently, micropropagation is also used for germplasm maintenance and early stock build up of vegetatively propagated crops such as lilies and potatoes, where many additional generations of field increase are used to bring the costs down to the requisite levels of only pennies apiece.

Generally speaking, crops with a single primary cultivar saleable year-round in numbers of totalling over 10 million units per year are excellent candidates for robotic automation, as it exists today. The advantages of robotic or fully automated tasks in micropropagation hinge on high volume, year-round and nonstop operation.

5.2. SEASONS

The second most significant factor in economic assessment of a new production technique, mechanical or otherwise, is the practicality, or adaptability, of the system to the crops and situations encountered in actual production cycles, product mixes and annual seasons of the commercial laboratory. Very few laboratories in any country are built around a season-less production of a single crop. There remain a few examples where a nearly steady production of over 5 million plantlets per year of a single cultivar, or its closely related derivatives, are in demand in the United States; these industry standards include: *Spathiphyllum* 'Petite', *Syngonium* 'White Butterfly,' and *Nephrolepis* 'Boston' ferns.

5.3. COST REDUCTION TARGETS

Robotic plantlet production will have a major impact on the industry when costs can be driven down to 25% of the current pricing for manually equivalent operations and when new markets become accessible which are currently out of reach. Examples of such markets include: more advanced generations of elite stock programs, high cost seed transplants, elite tree cultivars, and specialty fruits and vegetables. Each and every application meets competition in the marketplace, so pricing is of the essence in bringing robotics to the micropropagation industry. The hardware for robotic applications is in existence, and has been for many years. What is really needed is readily modifiable software to enable the industry to adapt the functions of the cut and place style robots to various needs over the course of the year and over the course of shifts in the marketplace. Pick and place robots themselves are basically hands; the technical difficulty lies in the presentation of the tissues and in 'seeing' and programming the control of the operations. The second issue for robotics/software remains cost; the cost per microcutting handled needs to drop to at least 25% of the cost of a human handling operation in order to drive the shift away from people and towards mechanized handling.

For example, in elite stock programs, each step in cost reduction increases the volumes approximately ten-fold. Each generation of potatoes is roughly fifteen times the acreage of its predecessor [55] with a price per planting unit dropping nearly 50% in the first field year. To assert a market acceptance at ten-fold volumes, minitubers or field plantable equivalents, must perform equally to the larger field-grown seedpieces for 1/3

of the price. A micropropagated verbena plantlet selling for US\$ 1.00 is needed in only small quantities; the same product at US\$ 0.15 would have a ten-fold increase in market size. However, in both of these examples, the market exists for literally only a few months of the year. From a business perspective, profitability does not increase if the market size increase is offset by reduced sales price, i.e., the net profitability of selling 1 million plantlets at US\$ 0.60 may not be much different from the profitability of selling 10 million plantlets at US\$ 0.06. For many segments of the elite stock plant market, there may be no great volume increases for intermediate price reductions. At the end of the fiscal year, from the business perspective, all of the additional work of bringing such a change to fruition may not have resulted in greater financial gains.

Automation and mechanization will most logically enter the micropropagation arena from the greenhouse transplanting end [58-60]. The final cost of the greenhouse plant sold is impacted directly by one-on-one handling steps: the two most obvious steps are the final tissue culture singulation step and the planting of singulated units into soil. Looking at the greenhouse industry it is clear that robotics have made significant inroads in elite plant plug production.

An illustrated web site with a virtual tour depicting an automated tissue culture planting and growing facility can be found at www.pothosplant.nl (under Company: Product Routing) for the company Pothos Plants, B.V. in the Netherlands. Robots as large as fork lifts move 2m x 5m benches of mechanically sorted plantlets in soil plugs from the planting station, through the hardening facilities (large multileveled, artificially lit, computer controlled rooms) to the greenhouses, where automated watering, feeding and spraying ensure that very few people ever need to enter. Smaller robots have additional, specialized tasks. Vision screening systems assist in grading the plantlets and transitioned plugs, ensuring that entire benches of homogeneously sized plants are produced. Plug trays are mechanically filled and transported. Empty benches are mechanically moved to sterilization areas. The facility, operational since 2001, brings in plantlets from tissue culture facilities around the world and then plants, hardens, grows, and ships nearly 80,000 plants per day, using a production crew of only 25 people, an efficiency at least five times that seen in non-automated greenhouses. This style of thinking will clearly produce the types of laboratory systems that will bring tissue culture micropropagation to its next level of productivity. This company, although it is closely linked to a micropropagation lab in the Netherlands, VitroCom, still makes use of all its options in tissue culture plantlet procurement, including significant importation and foreign liaisons, and sees no immediate prospects for automation in the laboratory (P. Olsthoorn, personal communication).

For some species, the singulation, rooting and planting steps can be combined, for example, when unrooted shoot clumps are separated into individual units at the time of planting. While this slows down the planting, it still is much less expensive than singulation under sterile conditions in the laboratory. Production is also advanced with systems where plantlets are singulated, or separated from the parent plantlet, under sterile conditions, but not rooted *in vitro*. Hedging, or the multiple harvest, of nodes or shoots from a base that is maintained in one container for many passages, can be used for hardy species in production of unrooted microcuttings that proceed directly to greenhouse planting [34]. Another, highly productive technique in this category is

overlaying of the multiplying cultures with a rooting medium [53,54]. In this case, explants are subcultured onto multiplication medium and, after numerous shoots have been induced, overlaid with a rooting medium (or an elongation medium, depending on the species). The stative shoot clusters in Figure 1 were produced with an overlay of multiplication medium, resulting in a 50-fold multiplication factor after 10 weeks, as shown in Figure 2. Since the medium overlay is very quick and easy, the labour for increasing the culture base is decreased.

Cultivars required year-round in volumes of at less than one million per year make better candidates for mechanization than automation, and this is where the greatest opportunities currently exist for less glamorous, but perhaps more practically useful, and more economically viable, operator-assisted systems. The price of entry, or start-up costs, is significantly lower and the flexibility is significantly greater for many of these systems.

In both the United States and Europe, labour costs have risen, without commensurate horticultural pricing increases, driving greenhouse plant growers and laboratories to foreign operations and importation. Commercial laboratories in the high-cost labour areas of the world are internally shifting towards production of lower volumes of higher priced disease-elite plantlets, while setting up foreign divisions, in countries with lower labour costs, for production of the high volume, standard varieties. In both North America and Europe, many laboratories are currently involved in production of literally hundreds of varieties or cultivars and many different genera of plants in relatively low numbers per variety.

The original assumptions of automation engineers, with regard to the ultimate pricing of the end products targeted, sometimes have overlooked their essential competition: laboratories in low labour-cost countries. Consequently, automation systems designed to produce plantlets at a cost of US\$ 0.15 apiece in the industrial countries of Europe and North America have been made obsolete by importation.

Even in countries with lower labour wages, cost of plantlets are still higher than seedlings or vegetative cuttings, and therefore, operator assisted mechanization is as attractive in those countries as elsewhere. The largest example of robotic production was set in the Monsanto/ForBio joint venture: Monfiori Nusantara, in Indonesia, for the production of elite tree cultivars. Propagation targets were for tens of millions of tree plantlets within a few key genera: notably Eucalyptus and teak. With the 2001 liquidation of ForBio in Australia, the Indonesian venture, as well as the Singapore facility and other locations internationally where the equipment had been set up, stopped using the robotic units and nothing appears to remain of these robots in production. The fact that these robotic stations are sitting in warehouses around the globe, with no current financial encumbrances beyond supplies and software updates, attests to the difficulty of establishing viable production systems at the technical level using simple robotics.

6. Political parameters

Even in micropropagation, international politics play a role. Governments determine trade priorities and fund, either directly via grants, or indirectly, via favourable taxation

and trade agreements, various sectors of their economies. The European Union has established a favourable position on micropropagation: Thus, for a sustainable and competitive agriculture and forestry in Europe, *in vitro* culture is essential: it is a prerequisite for the successful application of plant breeding by biotechnological methods, for the rapid introduction of improved plants in the market and it offers unique possibilities for the production of plants of superior quality.

The high costs of labour in the EU, needed for the skilled manual labour inherent in the current processes of micropropagation, present a major economic obstacle if *in vitro* culture is to be fully exploited. Currently, labour accounts for 60-70% of the costs of a plant produced *in vitro*. Thus, in the EU the competitiveness of the plant-based industries is compromised. Furthermore, the benefits that may be achieved through tissue culture are being applied successfully only to a limited number of crops, because many crops are unresponsive to tissue culture.

The action focuses on two strategies to increase competitiveness of the European *in vitro* plant production industry:

- the development of high-tech micropropagation methods which reduce labour input
- the production of plants of superior quality compared with the plants that are usually produced in tissue culture [61].

7. Conclusions

Micropropagation is still an industry in its infancy; costs are too high to compete in the marketplace effectively and consequently, the volumes necessary to make full use of advanced automation technologies are often lacking. If automation can be developed which decreases the direct cost per plantlet, by 50%, i.e., from US\$ 0.35 to US\$ 0.17, then certain markets will open up and volumes of plantlets sold will increase. Likewise, if flexibility and software advances permit users to modify robotic production lines in house, then greater numbers of varieties and species can be run through a single line, allowing more compatibility with the existing framework of micropropagation laboratories and their product mixes and annual fluctuations.

Photoautotrophic culture systems offer significant hope for the future. As production volumes from biofermentation and other large scale handling systems become increasingly reliable, the industry will gain a higher degree of credibility in the eyes of large volume plant producers and additional inroads into markets with stringent requirements for delivery times and volumes can be made.

Historical emphasis of micropropagation research has been on multiplication rates; however, these are not, in fact, the primary cost controlling factors. Once a minimum increase of 3.5-4 fold per subculture has been established, operator daily productivity contributes far more to the final cost; consequently, optimization of the operator throughput rates can yield significant benefits.

Full automation and mechanization research needs to focus on dropping the price by nearly an order of magnitude, while establishing reliability and throughput quality, in order to drive the micropropagation industry to its next level.

Acknowledgements

The author wishes to acknowledge the long term support and years of stimulating exchange of both extremely creative and extremely practical ideas with three key individuals: the late Dr. Robert Levin, who was instrumental in the development of many of the technologies outlined in this chapter and a champion of commercial micropropagation, Rodney Kahn and Donald Griffey who contributed similarly creative inputs without the ability to publish due to commercial restraints.

References

- [1] Redenbaugh K.; Fuji, J.; Slade, D.; Viss, P. and Kossler, M. (1991) Artificial seeds encapsulated somatic embryos. In: Bajaj, Y.P.S (Ed.) *Biotechnology in Agriculture and Forestry v. 17. High-Tech and Micropropagation*. Springer-Verlag: Berlin; pp. 395-416.
- [2] Herman, E. (2000). Automated micropropagation systems. In: *Regeneration and Micropropagation: Techniques, Systems and Media 1997-1999. Recent Advances in Plant Tissue Culture, v 6*. Agritech Publications/Agricell Report: Shrub Oak, NY.
- [3] George, E.F. and Sherrington, P.D. (1994) *Plant Propagation by Tissue Culture*. Exegetics Ltd.: Basingstoke, U.K.; pp. 704.
- [4] Pierik, R.L.M. (1985) *Plantenteelt in kweekbuizen*. Ponsen en Looijen: Wageningen, the Netherlands; pp. 202.
- [5] Aitken-Christie J. and Jones, C. (1987) Towards automation: Radiata pine shoot *in vitro*. *Plant Cell Tissue Org. Cult.* 8: 185-196.
- [6] Akita, M. and Takayama, S. (1988) Mass propagation of potato tubers using jar fermentor techniques. *Acta Hort.* 230: 55-61.
- [7] Kim, S.J., Hahn, E.J., Paek, K.Y. and Murthy, H.N. (2003) Application of bioreactor culture for large scale production of *Chrysanthemum* transplants. *Acta Hort.* 625: 187-191.
- [8] Oka, I. and Sluis, C. (1995) Methods for producing potato microtubers. US Patent 5498541.
- [9] Watad, A.A.; Sluis, C.; Nachmias, A. and Levin, R. (2001). Rapid propagation of virus-tested potatoes. In: Loebenstein, G.; Berger, P. H.; Brunt, A. A. and Lawson, R.H. (Eds.). *Virus and Virus-like Diseases of Potato and Production of Seed-Potatoes*. Kluwer Academic Publishers: Dordrecht, The Netherlands; pp. 391-406.
- [10] Ziv, M. and Shemesh, D. (1996) Propagation and tuberization of potato bud clusters from bioreactor culture. *In Vitro Cell. Dev. Biol - Plant* 32: 26-31.
- [11] Ziv, M. (1999) Bioreactor technology for plant micropropagation. In: Janick, J. (Ed.). *Horticultural Reviews*. John Wiley and Sons, New York; pp. 1-30.
- [12] Estrada, R.; Tovar, P. and Dodds, J.H. (1986) Induction of *in vitro* tubers in a broad range of potato genotypes. *Plant Cell Tissue Org. Cult.* 7: 3-10.
- [13] Hussey, G. and Stacey, N.J. (1984) Factors affecting the formation of *in vitro* tubers of potato *Solanum tuberosum* L. *Ann. Bot.* 53: 565-578.
- [14] Seabrook, J.E.A. and Douglass, L. (2001) Somatic embryogenesis on various potato tissues from a range of genotypes and ploidy levels. *Plant Cell Rep.* 20: 175-182.
- [15] Mann, C.C. and Plummer, M.L. (2002) Forest biotech edges out of the lab. *Science* 295: 1626-1629.
- [16] Paek, K-Y.; Hahn, E-J. and Son, S-H. (2001) Application of bioreactors for large-scale micropropagation systems of plants. *In Vitro Cell. Dev. Biol.- Plant* 37 (2): 284-292.
- [17] Gielis, J. and Oprins, J. (2002) Micropropagation of temperate and tropical woody bamboos-from biotechnological dream to commercial reality. [www. bamboonetwork. org/ publications/ gielis/ GIELIS03.PDF](http://www.bamboonetwork.org/publications/gielis/GIELIS03.PDF). Accessed 9/12/04.
- [18] Ibaraki, Y.; Kurata, K. (2001) Automation of somatic embryo production. *Plant Cell Tissue Org. Cult.* 65(3): 179-199.

- [19] McCown, B.H.; Zeidin, E.L. and Pinkalla, A.H. (1988) Nodule culture: a developmental pathway with high potential for regeneration, automated micropropagation and plant metabolite production from woody plants. In: Hanover, J.W. and Keathly, E.D. (Eds). Genetic Manipulation of Woody Plants. Plenum Publishing Corp., New York; pp. 49-166.
- [20] Levin, R. and Vasil, I.K. (1989) Progress in reducing the cost of micropropagation. Newsletter, IAPTC. 59: 2-12.
- [21] Ziv, M.; Chen, J. and Vishnevetsky, J. (2003) Propagation of plants in bioreactors: prospects and limitations. Acta Hort. 616: 85-93.
- [22] Ziv, M.; Ronin, G. and Raviv, M. (1998) Proliferation of meristematic clusters in disposable presterilized plastic bioreactors for the large-scale micropropagation of plants. In Vitro Cell. Dev. Biol.-Plant 34 (2): 152-158.
- [23] Hale, A.; Young, R.; Adelberg, J.; Keese, R. and Camper, D. (1992) Bioreactor development for continual-flow, liquid plant tissue culture. Acta Hort. 319: 107-112.
- [24] Konstas, J. and Kintzios, S. (2003) Developing a scale-up system for the micropropagation of cucumber (*Cucumis sativus* L.): the effect of growth retardants, liquid culture and vessel size. Plant Cell Rep. 21 (6): 538-548.
- [25] Escalona, M.; Samson, G.; Borroto, C. and Desjardins, Y. (2003) Physiology of effects of temporary immersion bioreactors on micropropagated pineapple plantlets. In Vitro Cell. Dev. Biol.-Plant 39(6): 651-656.
- [26] Santamaria, J.M.; Murphy, K.P.; Leifert, C. and Lumsden, P.J. (2000) Ventilation of culture vessels. II. Increased water movement rather than reduced concentrations of ethylene and CO₂ is responsible for improved growth and development of *Delphinium in vitro*. J. Hortsci. Biotech. 75 (3): 320-327.
- [27] Brunner, I.; Echegary, A. and Rubluo, A. (1995) Isolation and characterization of bacterial contaminants from *Dieffenbachia amoena* Bull, *Anthurium andreanum* Linden and *Spathiphyllum* sp. Shoot cultured *in vitro*. Scientia Horticulturae 62: 103-111.
- [28] Buckley, P.M.; DeWilde, T.N. and Reed, B.M. (1995) Characterization and identification of bacteria isolated from micropropagated mint plants. In Vitro Cell. Dev. Biol.-Plant 31: 58-64.
- [29] Cassells, A.C. and Tahmatsidou, V. (1996). The influence of local plant growth conditions on non-fastidious bacterial contamination of meristem-tips of *Hydrangea* cultured *in vitro*. Plant Cell Tissue Org. Cult. 47: 15-26.
- [30] Leifert, C.; Camotta, H.; Wright, S.M.; Waites, B.; Cheyne, V.A. and Waites, W.W. (1991) Elimination of *Lactobacillus plantarum*, *Corynebacterium* spp., *Staphylococcus saprophyticus* and *Pseudomonas paucimobilis* from micropropagated *Hemerocallis*, *Choisya* and *Delphinium* cultures using antibiotics. J. Appl. Bacteriol. 71: 307-330.
- [31] Leifert, C. and Waites, W.M. (1992) Bacterial growth in plant tissue culture media. J. Appl. Bacteriol. 72: 460-466.
- [32] Isenegger, D.A.; Taylor, P.W.; Mullins, K.; McGregor, G.R.; Barlass, M. and Hutchinson, J.F. (2003) Molecular detection of a bacterial contaminant *Bacillus pumilus* in symptom less potato plant tissue cultures. Plant Cell Rep. 21: 814-820.
- [33] Adelberg, J.; Fujiwara, K.; Kirdmanee, C. and Kozai, T. (1999) Photoautotrophic shoot and root development for triploid melon. Plant Cell Tissue Org. Cult. 57: 95-104.
- [34] Hazarika, B.N. (2003) Acclimatization of tissue-cultured plants. Curr. Sci. 85(12): 1704-1712.
- [35] Kozai, T. (1988) High technology in protected cultivation, horticulture in a new era. International Symposium on High Technology in Protected Cultivation. Tokyo; pp. 1-49.
- [36] Xiao, Y.; Lok, Y.H. and Kozai, T. (2003) Photoautotrophic growth of sugarcane plantlets *in vitro* as affected by photosynthetic flux and vessel air exchanges. In Vitro Cell. Dev. Biol.-Plant 39 (2): 186-192.
- [37] Ziv, M.; Meir, G. and Halevy, A.H. (1983) Factors influencing the production of hardened glaucous carnation plants *in vitro*. Plant Cell Tissue Org. Cult. 2: 55-56.
- [38] Zobayed, S.M.A.; Afreen-Zobayed, F.; Kubota, C. and T. Kozai. (1999) Stomatal characteristics and leaf anatomy of potato plantlets cultured *in vitro* under photoautotrophic and photomixotrophic conditions. In Vitro Cell. Dev. Biol.-Plant 35 (3): 183-188.
- [39] Levin, R.; Stav, R.; Alper, Y. and Watad, A.A. (1996) *In vitro* multiplication in liquid culture of *Syngonium* contaminated with *Bacillus* spp. and *Rathayibacter tritici*. Plant Cell Tissue Org. Cult. 45: 277-280.

- [40] Levin, R.; Stav, R.; Alper, Y. and Watad, A.A. (1997) A technique for repeated non-axenic subculture of plant tissues in a bioreactor on liquid medium containing sucrose. *Plant Tissue Cult. Biotechnol.* 3 (1): 41-44.
- [41] Kaizu, Y.; Okamoto, T. and Imou, K. (2002) Shape recognition and growth measurement of micropropagated sugarcane shoots. *Ag. Eng. Intl. CIGR J. Sci. Res. & Dev.* IV no 18 (IT 02 003). www.cigr.org e-journal accessed 8/1/04.
- [42] Otte, C.; Schwanke, J. and Jensch, P. (1996) Automatic micropropagation of plants. In: Menesatti, P. (Ed.) *Measurement accuracy of stereovision systems based on CCD video-photographic equipment in application to agricultural and environmental surveys. Proceedings of SPIE.* V. 2907. pp 80-87.
- [43] Gross, A. and Levin, R. (1999) Design considerations for a mechanized micropropagation laboratory. In: Altman, A.; Ziv, M. and Izhar, S. (Eds.) *Plant Biotechnology and In Vitro Biology in the 21st Century*, Vol 36. Kluwer Academic Publishers, The Netherlands; pp. 637-642.
- [44] Adelberg, J.; Bishop, D.; Bostick, M. and Pollock, R. (2000) Photoautotrophic micropropagation in natural light. In: Kubota, C. and Chun, C. (Eds.) *Transplant Technology for the 21st Century*. Kluwer Academic Publisher, Dordrecht, The Netherlands; pp. 153-158.
- [45] Ciolkosz, D.E.; Walker, P.N.; Heinemann, P.H. and Mistrick, R.G. (1997) Design issues for micropropagation lighting systems. *Trans. Am. Soc. Agric. Engineers.* 40 (4): 1201-1206.
- [46] Seabrook, J.E.A. and Douglass, L. (1998) Prevention of stem growth inhibition and alleviation of intumescence formation in potato plantlets *in vitro* by yellow filters. *Am. J. Potato Res.* 75: 219-224.
- [47] Landsburg, S.E. (1992) *Price Theory and Applications*. The Dryden Press, New York; pp. 761.
- [48] Aitken-Christie, J.; Kozai, T. and Takayama, S. (1995) Automation in plant tissue culture. General introduction and overview. In: Aitken-Christie, J.; Kozai, T. and Lila Smith, M.A. (Eds.) *Automation and Environment Control in Plant Tissue Culture*. Kluwer Academic Publishers, Dordrecht, The Netherlands; pp. 1-18.
- [49] Damiano, C; Gentile, A; La Starza, S.R.; Frattarelli, A. and Monticelli, S. (2003) Automation in micropropagation through temporary immersion techniques. In: *International Symposium on Acclimatization and Establishment of Micropropagated Plants. Acta Hort.* 616: 359-364.
- [50] Hvoslef-Eide, A.K.; Heyendahl, P.H. and Olsen, O.A.S. (2003) Challenges in scaling-up and automation in micropropagation. In: *International Symposium on Acclimatization and Establishment of Micropropagated Plants. Acta Hort.* 616: 77-84.
- [51] Kozai, T. (1994) Some robotic micropropagation systems recently developed in Japan. In: Aitken-Christie, J.; Kozai, T. and Lila Smith, M.A. (Eds.) *Automation and Environmental Control in Plant Tissue Cultures*. Kluwer Academic Publishers, Dordrecht, The Netherlands; pp.
- [52] Brown, F.R. and Billington, W.P. (1995) Method and apparatus for use in micropropagation. US Patent No. 05382268.
- [53] Maene, L. and Debergh, P.C. (1985) Liquid medium additions to established tissue cultures to improve elongation and rooting *in vivo*. *Plant Cell Tissue Org. Cult.* 5: 23-33.
- [54] Vanderschaeghe, A.M. and Debergh, P.C. (1988) Automation of tissue culture manipulations in the final stages. In: *International Symposium on Vegetative Propagation of Woody Species. Acta Hort.* 227: 399-401.
- [55] Anon. (2004) *Potato Area 2003. FAOSTAT Database 2004.* <http://apps1.fao.org/faostat>. Accessed: 31 August 2004.
- [56] Anon. (2004) *Potatoes Pot 6 (04) - 2003 Summary.* United States Department of Agriculture, National Agricultural Statistics Service. <http://usda.mannlib.cornell.edu/reports/nassr/field/ppo-bbp/pots0904.txt>. Accessed: 31 August 2004.
- [57] Kurtz, S.L.; Hartman; R.D. and Chu, I.Y.E. (1991) Current method of commercial micropropagation. *Cell Culture and Somatic Cell Genetics of Plants* 8: 7-34.
- [58] Honami, N.; Taira, T.; Murase, H.; Nishiura, Y. and Yasukuri, Y. (1992) Robotization in the production of grafted seedlings. In: *International Symposium on Transplant Production Systems. Acta Hort.* 319: 579-584.
- [59] Ji, Q. and Singh, S. (1996) Automated visual grading of vegetative cuttings. In: Meyer, G.E. and DeShazer, J.A. (Eds.) *Optics in Agriculture, Forestry, and Biological Processing II. Proc. SPIE.* 2907: 88-99.
- [60] Kondo, N. and Ting, K.C. (1998) Robotics for plant production. *Artificial Intelligence Rev.* 12 (1-3): 227-243.

Integrating automation technologies with commercial micropropagation

- [61] Anon. (2000) Quality enhancement of plant production through tissue culture. European Co-operation in the Field of Scientific and Technical Research (COST) <http://www.cost843.org> (accessed 1 September 2004).

MACHINE VISION AND ROBOTICS FOR THE SEPARATION AND REGENERATION OF PLANT TISSUE CULTURES

PAUL H. HEINEMANN AND PAUL N. WALKER

*Department of Agricultural and Biological Engineering, Pennsylvania State University, University Park, PA 16809-1909, Fax: 814-863-1031-
Email: hzh@enr.psu.edu*

1. Introduction

Plant propagation through tissue culturing is widely used for multiplication to produce genetically identical plants. However, the process is labour-intensive, and efforts to introduce automation have been pursued worldwide. Perhaps the most challenging aspect of automation is the cutting or separation and replanting of micropropagated shoots and plantlets. Because of the variability of plant growth, finding the location where a plantlet should be cut or pulled apart requires human thought processes, or an approach that mimics human recognition and thinking. Therefore, to automate the identification of proper cutting or separation points of plant clusters, stems, and nodes, machine vision systems are used, and to perform the cutting or separation process, robotics are used. This chapter covers the utilization of machine vision and robotics for the automation of plant tissue culture separation and transplant.

2. Examples of automation and robotics

Several investigations have shown the feasibility of automating steps in the tissue culturing process. Some of these have been implemented in commercial systems. Automation refers to the change from a process performed manually to the process being performed through mechanization. Labour cost and availability are the driving factors in the desire to automate commercial micropropagation operations.

Robotic mechanisms are commonly used in many industries, particularly those that manufacture components and systems in an assembly-line manner. Investigations have been made on robotic mechanisms for picking and transplanting plant parts or whole plants. In the mid 1980's through the early 1990's, several investigations were reported related to automated regeneration of micropropagated plants. However, there was a reduction in the research activity in the late 1990's and the first years of the 21st century. Several of these investigations are summarized here.

Zandvoort and Holdgate [1] give a brief overview of mechanization of all aspects of commercial plant tissue culture, including media preparation, cutting and transferring of

plantlets, movement of containers, and final transplanting to field condition. Steps in cutting and transfer of cultures are described, although Zandvoort and Holdgate point out the problems associated with maintaining sterile conditions in automated systems.

A robotic case study for *geranium* propagation was described by Simonton [2]. The robotic unit grasped geranium cuttings from a tray, then removed leaves, trimmed the stems, measured stem bends, and inserted cuttings into plugs for further growth. The system was evaluated for damage to the plant, proper grasping locations, and success in transplanting. Overall the system was successful on 94% of cuttings. The losses were from improper insertion into the plugs. Propagation of *Chrysanthemum* by another robotic unit was investigated by Brown [3]. The experimental work cell contained the robotic unit for dissecting and replanting the plant pieces, a container handling unit to position containers in front of a video camera for plant location and identification, a laser for opening of the plant containers, a container handling unit for placing of new plantlets, and computer for system control.

Miwa *et al.* [4] describe different examples of robotic mechanisms used for plant tissue culture. They investigated the use of robotic mechanisms for lily bulblet and *Chrysanthemum* multiplication. Kurata [5] and Kurata [6] give several examples of components and systems for automated micropropagation. Examples include cutting mechanisms for shoot clumps and nodal plantlets, laser beam cutting, feeder mechanisms, and complete experimental system designs for cutting and transplanting micropropagated plants.

Kaizu *et al.* [7] used machine vision to identify stem axis angle, position, and degree of growth for potential robotic separation of sugarcane plantlets. They used an Olympus C3030 colour digital camera connected to a Hitachi IP-5000 colour digitizing board. The board was mounted in a PC, which utilized a 450 MHz Intel II processor. The digitizing board came with a library of image processing routines so that customized applications could easily be developed utilizing the C++ language. The camera was mounted on a stand equipped with 500 W daylight bulbs. The camera faced down towards a table top covered with black velvet used as a contrast background. Images of sugar cane plantlets were captured at 512 by 384 pixel resolution. The algorithm used the Hough transform and boundary extraction information to distinguish leaves from stems.

3. Robotic system component considerations

The variable nature of plant growth makes the identification of proper separation or cutting sites a challenge. In manual separation and transplant processes, humans use eyesight and judgment to determine the proper location. An automated separation or cutting system can not depend upon the cutting or separation points being in the same location for each plant. Therefore, machine vision is used to simulate human eyesight for identification of these points.

Critical considerations for the robotic transplant of plant parts need to be made. These include:

- Presentation of the plant part to a machine vision system
- Proper contrast between plant part and background for image analysis
- Algorithms for identifying location of separation or cutting points

- Separation and cutting mechanisms that precisely move to and operate at the locations identified by the identification algorithms
- Gripping mechanisms that hold plants securely yet minimize pressure and resulting damage to plant parts during separation or cutting and transplanting
- Cost balance between precision of computer-based vision system, software for identification algorithm, and hardware mechanisms.

Machine vision systems that have been used in plantlet separation or cutting are relatively standard. The components consist of a digital CCD or similar camera, frame digitizing board, and computer. An image of the plantlet is captured by the camera and stored on the digitizing board. In some applications, grey scale images are sufficient because the contrast between plant material and a solid background (such as black) is strong. Complex algorithms have been developed to extract information from the images to identify the plant parts and furthermore, determine the locations for cutting or separation.

3.1. PLANT GROWTH SYSTEMS FOR ROBOTIC SEPARATION

Micropropagated plantlets grow in different forms. Two common growth patterns are elongated stems, where identifiable nodes help to determine cutting points, and clumps, where the separable shoots grow from a single point. These growth patterns will greatly affect the design of the machine vision and robotic mechanisms used to make the transplants.

3.1.1. Nodes

Many plants exhibit growth behaviour that consists of an elongated stem. When these plants are reproduced through micropropagation, they are cut along the stem ensuring that a leaf node is present in each piece. Each piece will then re-grow into a new plant. An example of prototype robotic unit for cutting and replanting of nodal plants is described by Fujita and Kinase [8]. A six-degree of freedom robotic unit was used to pick out a plant from a tray and hold the plant while a separate unit sensed the correct position of the nodes and cut the plant. A laser was used to detect the position of the plant.

A grasping device and a scissor-like cutter were both mounted on a second-generation robotic unit. The position of nodes was identified by determining the stem boundary from the base of the plant to the top. The stem diameter was then assumed from the average width of the stem boundary. Areas that exceeded this assumed width were determined to be nodes, and the unit would then cut the plant apart ensuring that a node was included with each piece. The cycle time (time required to complete recognition, cutting, and transplanting) was 15 seconds.

3.1.2. Clumps

Sugarcane is a good example of a micropropagated plant that grows from a clump. These clumps take on a three-dimensional structure when grown in conventional tissue culture vessels. However, three-dimensional structure can present problems when the clump is presented to a machine vision system that is responsible for identifying shoots to be separated and transplanted. Depth of field causes blurring within the image, and

viable shoots can be hidden from the view. One solution to this problem is to develop a method that decreases the three-dimensional structure of the clump and forces the shoots to grow in a two-dimensional plane.

A two-dimensional "parallel plate" growth structure system was developed by Schaufler and Walker [9] and Escribens [10]. The approach utilized the standard Hawaiian Sugar Planters Association procedures for micropropagated sugarcane using Magenta GA7 vessels. These vessels are made of clear polycarbonate and are 60 by 60 mm wide and 110 mm tall. A tightly fitting polypropylene top helps to keep the vessels from being contaminated. The parallel plates were placed at the bottom of the vessels and nutrient media could flow around the plates (Figure 1).

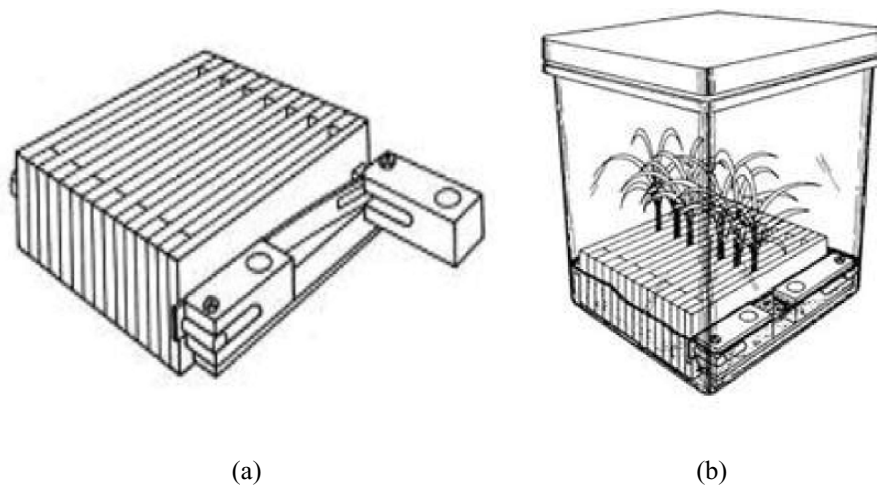


Figure 1. Design of parallel plate system for two-dimensional growth of sugarcane shoots: a) parallel plate detail; b) plates within Magenta 7 vessel. Reprinted from Schaufler, D.H. and Walker, P.N. (1994) [9].

The presence of parallel plates was used to reduce the number of viable shoots compared to vessels without parallel plates. However, placing the vessels on a shaker and allowing five extra days of growth allowed the two-dimensional shoot clumps to develop shoot numbers and dry weights that were not significantly different from the shoots grown in vessels without parallel plates.

3.2. AN EXPERIMENTAL SHOOT IDENTIFICATION SYSTEM FOR SHOOT CLUMPS

Sugarcane presents a challenging problem for robotic separation because the shoots grow from a clump rather than the stem and node structure found in other plants. Each shoot needs to be identified separately, and several different algorithms have been developed to maximize the correct identification of shoots and minimize missed shoots or incorrect identifications of shoots. The following sections provide examples of shoot identification algorithm development.

3.2.1. Shoot identification using the Arc method

Schafler and Walker [11] developed a shoot identification algorithm to extract separation locations for the automated micropropagation of sugarcane. The prototype system utilized a lighting chamber in which a sugarcane clump was placed on a black felt cloth background. Two 20 W General Electric "Gro & Sho" fluorescent lamps supplied the illumination. A data translation quickcapture monochrome digitizing board mounted on a Macintosh computer captured images at a 640 by 480 pixel resolution. The NIH (National Institute of Health) Image software was used to drive the image capture procedure, and the ANSI C language routines were developed to analyze the image by calling functions from the catenary systems vector image processing library.

The digitized images of shoot clumps revealed that the stems had a lower reflectance than the leaves, which made distinction between leaves and stems easier (Figure 2).

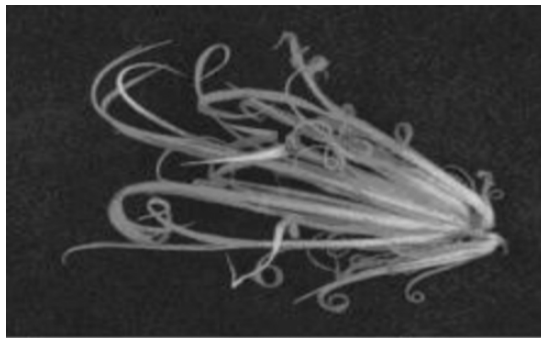


Figure 2. Digitized image of sugarcane shoot clump grown in parallel plate system.

The goal was to separate the plantlets at the intersection of the stems. Orientation of the shoot clump is a concern because the shoot identification algorithms will make assumptions as to the location of the base of the clump. Any separation mechanism developed will need to consider orientation in the presentation of the clump to the camera. In this case, the shoot clump was oriented with the base to the lower right side of the image, though not in a precise location or orientation.

The shoot identification algorithm included three steps: a) locating clump base, b) defining lines or arcs to determine location of shoots, and c) locating shoots along the line or arc. A 3 by 3 pixel filter was first used to identify and remove regions that had changes in grey level values but were too small to be the shoot clump base. Following the image filtering, vertical sweeps, starting on the upper right of the image, searched for a change in the grey level intensity. When the intensity changed substantially, the algorithm assumed that the shoot clump base had been identified. Two algorithmic approaches were used for identifying the shoots. One set vertical lines at 15 pixel spacing, the other drew 180° arcs from the base of the clump at 15 pixel spacing. In each case, the algorithm searched a line or arc for increases and then decreases in the pixel intensity, which would indicate the presence of a shoot. When this occurred, the middle range between the apparent edges was set as a shoot location.

Different intensity thresholds were used to distinguish a shoot from the background. There were three classifications of results: correct find, when an actual shoot is

identified as a shoot; incorrect find, when a leaf is identified as a shoot or more than one point is found on a single shoot; and missed shoot, when a shoot exists but was not located.

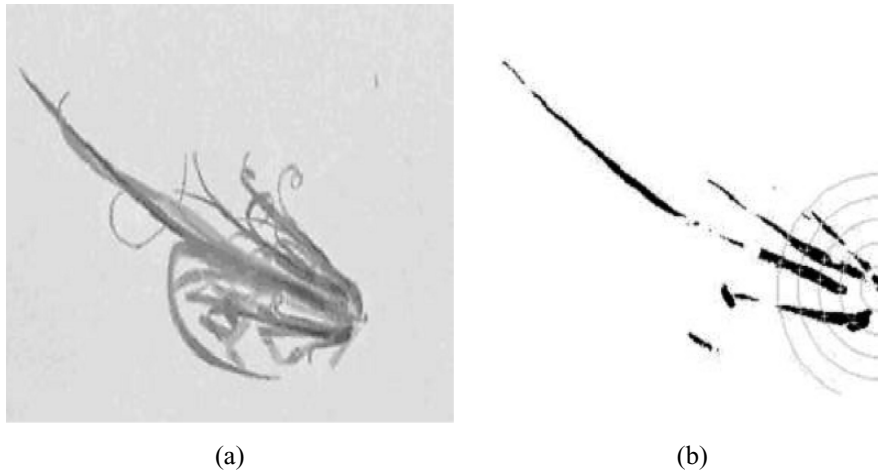


Figure 3. Sugarcane shoot a) original digitized image; b) image after binary operation and grasping locations (+) found using the arc method. In this example all shoots were correctly identified when arc radius 4 was used.

As the threshold value was increased (i.e. from darker to lighter), the number of good finds increased, but so did the number of incorrect finds, as the algorithm would tend to identify leaves as stems. An example result for the arc method identification process is shown in Figure 3. For the arc method, a threshold of 120 and arc number 4 (from the centre of the clump base) provided the best result of 74 good finds and 12 bad finds out of 99 total shoots. For the line method, a threshold of 120 and line number 5 provided the best result of 68 good finds and six bad finds out of 99 total shoot clumps.

A second set of 26 clump images was analyzed with the threshold set to 120 and use of arc 4 only. This set of clumps had a total of 71 actual shoots. Application of the arc method resulted in 58 good finds (82%) and 8 bad finds (11%). The same set of clump images was analyzed using a threshold of 120 and line 5. The line method resulted in 46 good finds (65%) and 8 bad finds (11%).

A third set of shoot clump images was analyzed using the arc method. Twenty-five shoot clumps containing 109 actual shoots were imaged. In this case, the positioning of a set of clamps and forceps were simulated based on the shoot locations identified by the algorithm. It was determined that 75% of the shoots would be separated correctly based on visual examination. This work showed the feasibility of identifying shoots from clumps, which can present a complicated image to be analysed. The actual separation mechanism may not be the critical component, rather proper image analysis and algorithm development is crucial for automation of the separation process. The research was encouraging because it showed that natural variability of plant growth, and the

resulting complications in automated separation, can be handled with relatively inexpensive computers, algorithms, and mechanical devices.

Although 75-80% successful separation and replanting is good, there are economic consequences to the 20-25% incorrect or missed identifications. Separation of a leaf that was misidentified, as a shoot would result in a transplant that would not grow properly or may not grow at all. Missed shoots would most likely result in two viable shoots being transplanted as one, reducing the number of subsequent planting. Correct shoot identification should be maximized to the extent possible.

3.2.2. Shoot identification using the Hough transform method

Wang *et al.* [12,13] continued the work began by Schaufler and Walker, with an effort to improve the successful identification of the shoots and also to automate the separation device. Use of the Hough transform [14] to identify shoots from a digitized image was introduced. The Hough transform attempts to determine if points in an image are lying on one or more lines. In this case, lines would potentially represent individual shoots. A black and white video camera connected to a Data Translation DT55-60 monochrome digitizing board was used in this project. The board was mounted in a 33 MHz 486 personal computer and images were captured at a 640 by 480 pixel resolution. Based on work by Kondo [15] and Kondo *et al.* [16], reflectance differences between stems and leaves were found to be stronger in the longer wavelengths (towards the infrared region). Therefore, two standard 60 W incandescent lights were chosen for illumination of the sugar cane plantlets, instead of the fluorescent lamps used in the Schaufler and Walker experiments. The plantlets were placed on a black background for high contrast.

Prior to the line identification process using the Hough transform, pre-processing the clump image is necessary so that individual shoots are reduced to single lines. The images are first processed utilizing a sharpening algorithm. A 3 by 3 pixel filter is passed over the image (Figure 4).

-1	-1	-1
-1	9	-1
-1	-1	-1

Figure 4. 3 by 3 pixel sharpening filter. Reprinted from Wang, Z. (1997)[12].

The coefficients shown in the filter are multiplied by the corresponding pixel intensity, so that the centre pixel value is multiplied by 9 and the surrounding eight pixels are multiplied by -1 . These nine results are then summed, and the sum is used as the centre value. This essentially highlights the transition between separate shoots; particularly those that lie next to each other and may appear as one in an unsharpened image (Figure 5).

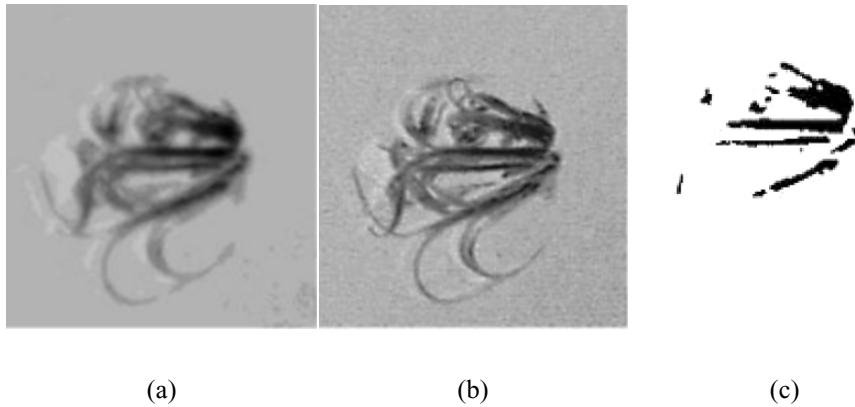


Figure 5. Results of sharpening filter a) before sharpening; b) after, c) binary image after sharpening. Reprinted from Wang et al. (1998)[13].

The next step is to utilize a thinning technique to reduce the shoots to single lines in the image [12]. A fast thinning approach [17, 18] was used for the sugarcane shoots. Using an intensity threshold, a binary image is created as shown in Figure 5c. Again, a 3 by 3 pixel filter is used (Figure 6). The P values refer to the pixel intensity, which are either 0 (no intensity present) or 1 (intensity present), and the indices i and j refer to the pixel coordinates relative to the centre of the filter. The goal of the filter is two-fold: to eliminate the southeast boundary points and northwest corner points, and to eliminate the northwest boundary points and southeast corner points. First, if the contour point P_1 satisfies all of the following conditions, it is eliminated:

- (a) $3 \leq B(P_1) \leq 6$
- (b) $A(P_1) = 1$
- (c) $P_2 \times P_4 \times P_6 = 0$
- (d) $P_4 \times P_6 \times P_8 = 0$

$A(P_1)$ is equal to number of 0-1 patterns in the neighbouring pixels as the pattern is observed in order from P_2 through P_9 , and $B(P_1)$ is equal to the number of nonzero neighbouring pixels, i.e. $B(P_1) = P_2 + P_3 + P_4 + \dots + P_9$. If any of the conditions are not met, the value of $A(P_1)$ is set to 2 and the filter is incremented by a pixel. The value of 2 for $A(P_1)$ prevents the point from being eliminated after the next pixel iteration.

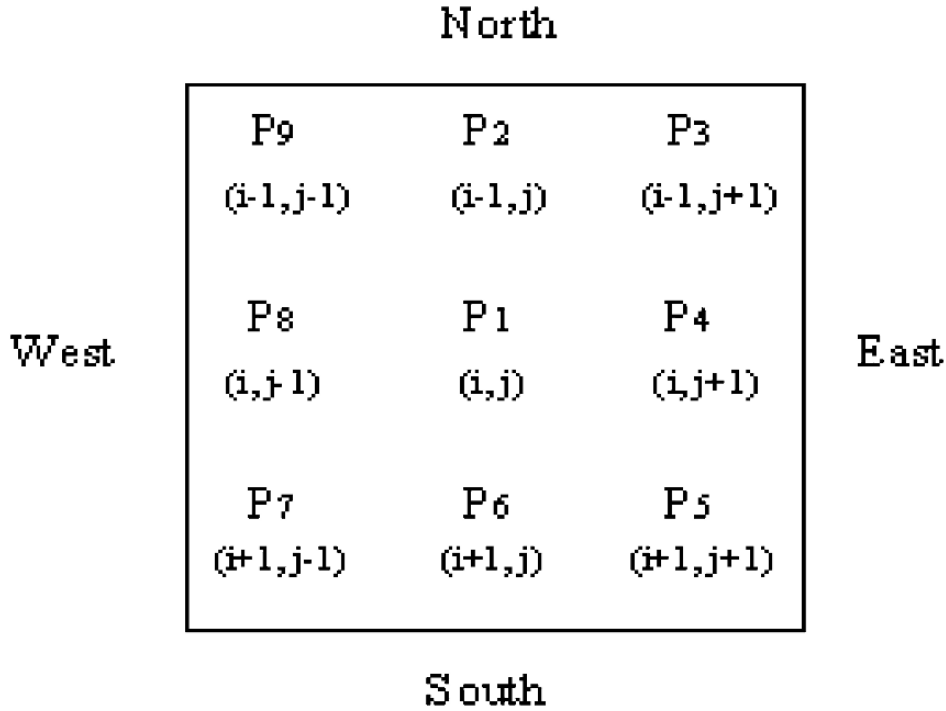


Figure 6. 3 by 3 pixel thinning filter. Reprinted from Wang, Z. (1997)[12].

An example is shown in Figure 7. In this example, moving clockwise from the P₂ location in the top centre, condition (a) is met (the sum of the neighbouring pixels is 3), and cases (c) and (d) are met (both products = 0). However, case (b) is not met (two 01 patterns can be found). Therefore, the P₁ pixel will be assigned a value of 2. Three iterations of the thinning filter were determined to be the optimal number to turn the shoot image into a single pixel line.

The final step in the shoot identification process is to apply the Hough transform. A point can be represented in Cartesian space as (x_i, y_i), where 'i' represents the Cartesian coordinates (or, in the case of a digital image, it would represent the pixel location). A line can be represented in Cartesian space as

$$y_i = ax_i + b \tag{1}$$

with "a" representing the slope and "b" representing the intercept. The possibility exists that as lines become more vertical, the slope approaches infinity. Because of this, the line is often represented in the form of polar coordinates

$$r = x_i \cos \Theta + y_i \sin \Theta \quad (2)$$

where, Θ is the angle made by a normal to the line with the x axis and r is the length of the normal (Figure 8). Because an infinite number of lines can pass through a point (x_i, y_i) in Cartesian space, equation 2 represents a continuous sinusoidal curve. Similar to the slope/intercept concept in (x, y) space, the intercept points (r', Θ') in Figure 8 will provide the Θ and r values for the original line in (x, y) space.

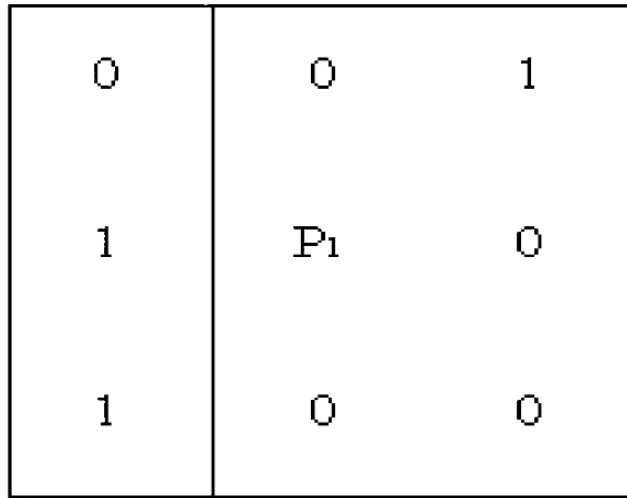


Figure 7. Example of thinning filter applied to an image with pixels of positive and no intensity, Reprinted from Wang, Z. (1997)[12].

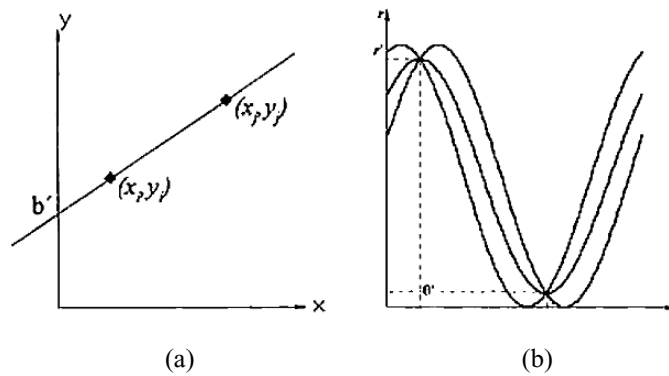


Figure 8. Lines represented in a) Cartesian coordinates; b) polar coordinates. Reprinted from Wang, Z. (1997)[12].

The pixel values contained in a digital image can be visualized as bar type graphs, with pixel intensity values on the x-axis and the quantity of each of these values on the y-axis. This arrangement is referred to as a histogram, and the pixel values are often called "bins". In a 256-level grey scale digital image, the x-axis of the histogram may contain bins, or pixel values, from 0 to 255. The (r, Θ) space is divided into an array of finite cells. The increment of r and Θ , Δr and $\Delta \Theta$, is determined based on the desired tolerance of identification. For each point in (x, y) space that a line contains, there is a predetermined set of bins in the (r, Θ) space. When a series of collinear points are examined, a histogram is created, and the bin with the highest number of points corresponds to a straight line.

3.2.3. Testing the Hough transform

To test the effect of changing the lighting, images were acquired for 50 shoot clumps grown in vessels containing parallel plates. Twenty-five of the images included the gripper mechanism that would separate the shoots from the clump, and 25 images did not include the grippers. The inclusion of the grippers was based on the possibility that their presence in a robotic system may interfere with the shoot identification procedure success rate. For comparison, the original arc method described by Schaufler and Walker was used. With the grippers absent, 84% of 105 actual shoots were correctly identified, and 8% were incorrectly identified. With the grippers present, 82% of 101 actual shoots were correctly identified and 7% were incorrectly identified.

The Hough transform approach was then tried on the 25 images without grippers and a threshold test was performed. With a low threshold (intensity of 155), the correct rate (actual shoots identified as shoots) was 89%, the missed rate (actual shoots not found) was 11%, and the incorrect rate (shoots identified that were not actual shoots) was 0%. As the threshold was increased, the correct rate increased up to 98% and the missed rate decreased to 2%; however, the incorrect rate also rose to 14%. This means that the robotic unit guided by this image analysis would attempt to transplant 14% of non-existing shoots, which would leave open spaces in the transplant vessels. A threshold of 175 was used as a balance between high correct and low incorrect identification rates.

The Hough transform approach was then compared to the arc method on 25 shoots clumps that included the grippers in the image and a second set of 25 that did not include the grippers. For the images without grippers, the Hough transform method correctly identified 95% of 103 actual shoots, missed 5% of the shoots, and identified 7% of shoots that were not actually shoots. The arc method correctly identified 87% of the 103 actual shoots, missed 13%, and incorrectly identified 3% of shoots that were not actually shoots. With grippers present, the Hough transform method identified 93% of the actual shoots, missed 7%, and incorrectly identified 6%. The arc method correctly identified 82%, missed 18%, and incorrectly identified 7%. It was evident that the Hough transform method did better than the arc method, particularly when grippers were present.

3.3. ROBOTIC MECHANISMS FOR SHOOT SEPARATION

As mentioned previously, an effective and accurate shoot identification algorithm is critical to the feasibility of any robotic separation and transplanting mechanism. Essentially, missed shoots or the identification of non-shoots as shoots results in reduced numbers of replicated plants and hence an economic reduction. The next important consideration in the development of an automated separation or cutting and transplanting device is a mechanism that will properly perform these tasks. The mechanism must be able to precisely move to the points identified by the location algorithm, perform the separation or cutting task with accuracy and with minimal or no plant tissue damage, and successfully move the separated or cut shoots to the re-growth vessel.

3.3.1. Manual separation device

A separation device was fabricated by Schaufler and Walker [11] to physically test the separation algorithm (Figure 9). The device utilized fine-tolerance threaded rods to manipulate a clamp and forceps in an x-y plane. The clamp held the shoot clump in place and the forceps grabbed a shoot and pulled it from the clump. The clamp and forceps were guided manually based on the locations found by the locator algorithm. The operator of the device was prevented from observing the actual shoot clump, so that the manipulation of the mechanism was based solely on the locations found by the arc method algorithm.

Ten shoot clumps were imaged, with a total of 40 actual shoots, to test the device. The manual separation mechanism was used for each shoot clump. Of the 40 possible actual shoots, the algorithm identified 36. Of these 36 identifications, one was a leaf incorrectly identified as a shoot. Five shoots were not identified. The clumps were imaged only one time, prior to any separations. Once the separations began, no further image analysis was performed. The mechanism successfully separated 35 of the 36 identified shoots.

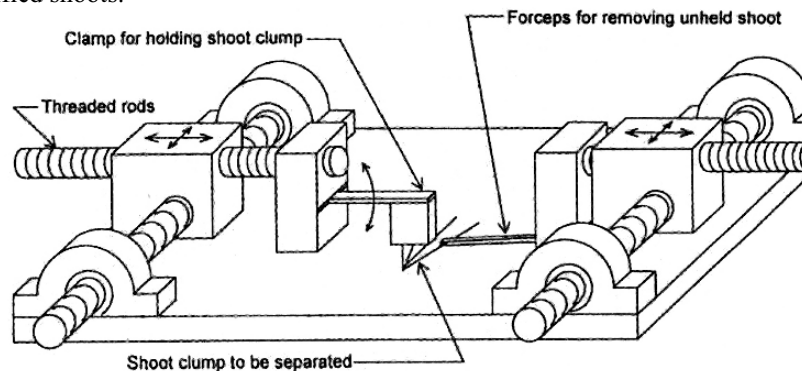


Figure 9. Manual sugarcane shoot separation device, Reprinted from Schaufler, D.H. and Walker, P.N. (1995)[11].

3.3.2. Automated separation device

Wang, *et al.* [19] describes a mechanism developed to separate and replant sugarcane plantlets from shoot clumps (Figure 10). The system utilized the machine vision system described in the previous section. The Hough transform method was utilized to identify the location of shoots to separate from the clump. Two separate screw-driven milling tables were used to position grippers for separation. These milling tables were modified to be automatically controlled by four stepper motors that had a step angle of 1.8° . The stepper motor control allowed the computer to position the grippers based on the locations found by the identification algorithm. Stainless steel forceps were attached to pneumatic grippers to perform the separation operation. The air pressure required to operate these grippers ranged from 206 kPa to 689 kPa.

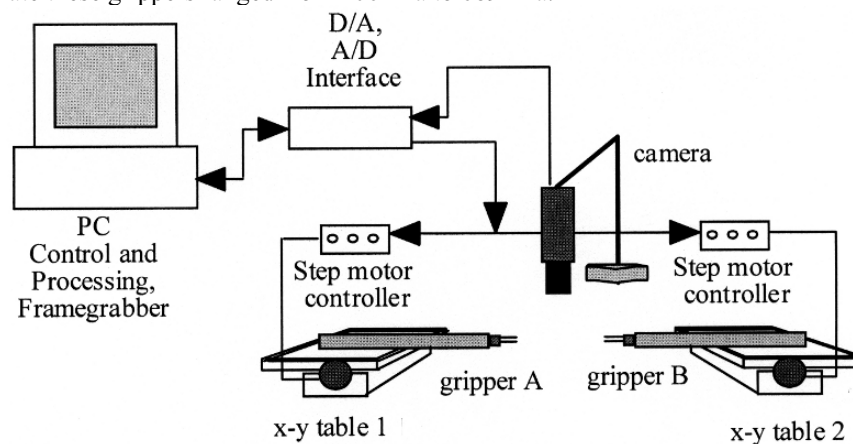


Figure 10. Diagram of experimental sugarcane shoot separation mechanism described by Wang *et al.* [19].

Opening and closing of the gripper device was controlled by a pneumatic circuit, which included two flow control valves. The valves allowed the gripper closing speed to be controlled so that damage to the plant tissue would be minimized. Rapid closing of the forceps onto the shoot or clump would result in possible crushing of the stem or clump. The forceps were 30 mm long, with a tip width of 3 mm. It was determined that using a pressure of 345 kPa provided 1.76 N of force which was sufficient to grasp the clump or shoot firmly but with little or no damage to the plant tissue. A diagram of the pneumatic circuit used in this system is shown in Figure 11.

The vision system must be calibrated to the coordinates of the separation mechanism. The video camera lens can cause distortions in the field of view, which may misalign the image with the position of the separation mechanism. Depth of image can also cause distortion problems when working with three-dimensional objects. In most cases, the closer the plant is to the centre of the field of view, the less distortion will occur. In this particular example, the shoot clump is essentially two-dimensional and a small working area (100 mm X 100 mm) was utilized, so distortion was minimized. A least-squares method was used to calibrate the vision system with the

actual mechanism coordinates (referred to as the "world coordinates"). Paper with a grid drawn on it was placed under the camera where an image of the grid was captured and digitized.

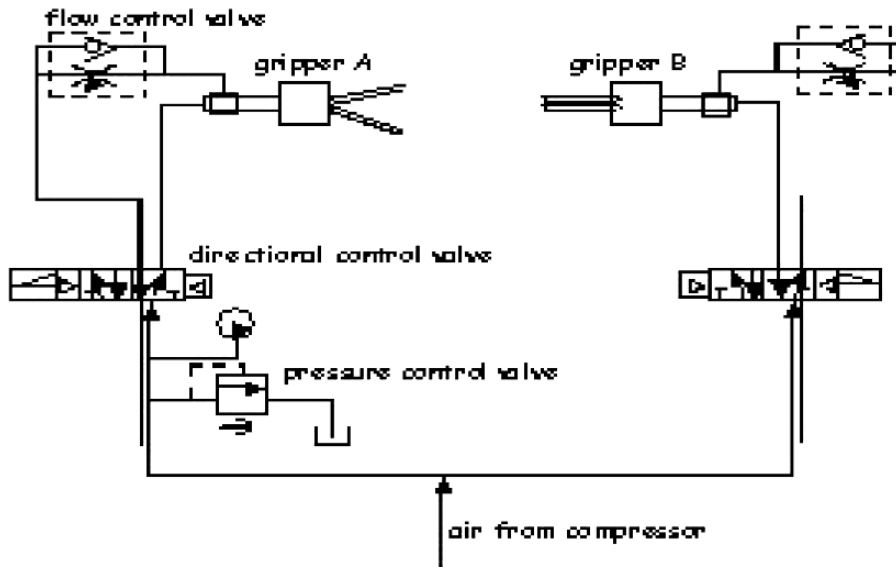


Figure 11. Pneumatic circuit diagram for shoot separation mechanism. Reprinted from Wang, Z. (1997)[12].

Linear mapping coefficients were determined by using an algorithm to search the image grid points and their respective image coordinates. Since the world coordinates of these points were known, the mapping coefficients could be calculated by comparing the vision and world coordinates for the grid points. The coefficients were stored and used each time a new set of clump images was taken.

The manual process of separating a shoot from a clump is performed by holding the clump in place and grasping one shoot, then pulling gently on the shoot until it separates from the clump. The shoot is then placed in a separate re-growth vessel. A human performing this task utilizes visual recognition and easily manipulates the forceps for the grasping and pulling steps. When the process is automated, it becomes a multi-step process. Two methods were compared to determine the more efficient way to separate and transplant the shoots.

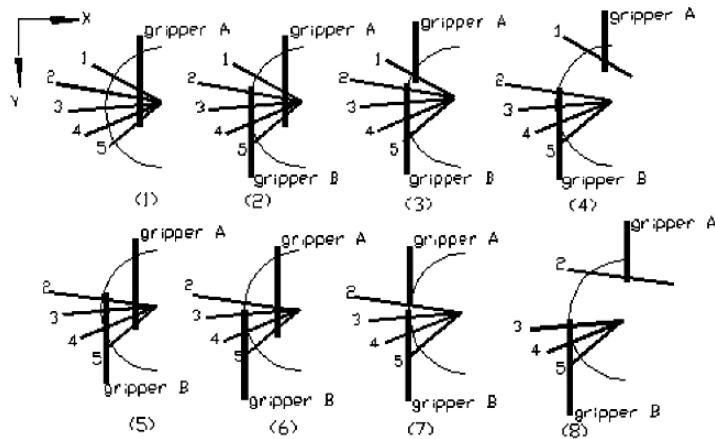


Figure 12. Separation of shoots following steps of method 1. Reprinted from Wang et al. (1999)[19].

For separation method 1, one gripper (gripper A) always held the shoot clump while the other gripper (gripper B) would pull off the individual shoots. The procedure is outlined as follows (Figure 12):

- Place shoot clump to separation station using gripper A to grasp shoot clump base
- Take image of shoot clump
- Run algorithm to identify grasping points
- Move gripper B to grasp all shoots except shoot 1
- Open gripper A and position it to grasp shoot 1 at identified grasping point
- Move gripper A backwards away from the clump to separate shoots 1
- Transplant shoot 1, then move gripper A back to grasp the entire shoot clump
- Open gripper B and move it backwards, then grasp on all remaining shoot except shoot 2
- Grasp shoot 2 with gripper A at the identified grasping point
- Go to step 5 and continue for shoot 2
- Continue process until all shoots are separated, except that the last shoot is merely handed from gripper B to gripper A for transplanting.

The gripper-pulling angle must be adjusted to ensure that the shoot is completely pulled apart from the clump. Although the shoots are connected to the clump in the lower left area, a shoot at the top of the clump (as viewed in Figure 12) needs to be pulled at a different angle than shoot 5. Gripper A was set to pull at a 45° degree angle along the negative y-axis if the shoot was found in the upper left area and a 0° angle if the shoot was found in the lower left area. Gripper A would pull the shoot in the designated direction for a distance of 25 mm, which was determined to be the maximum needed to completely separate the shoot from the clump.

The second method (separation method 2) was similar to separation method 1, but in this case the grippers alternated pulling shoots (Figure 13). As with method 1, gripper A

grasps the base of the shoot clump, and gripper B is positioned to grasp all shoots except shoot 1. Gripper A moves to the grasping point of shoot 1 identified by the location algorithm, grasps shoot 1, and then pulls back at a 45° angle for 25 mm, which separates the shoot. Gripper A then moves and grasps all of the shoots except shoot 5, and gripper B retracts to the grasping position on shoot 5 as determined by the location algorithm. Gripper B pulls the shoot at a 45° angle for 25 mm, which separates the shoot from the clump. After a shoot is removed, the mechanism moves and drops it into a replant vessel. This pattern continues until all shoots are separated.

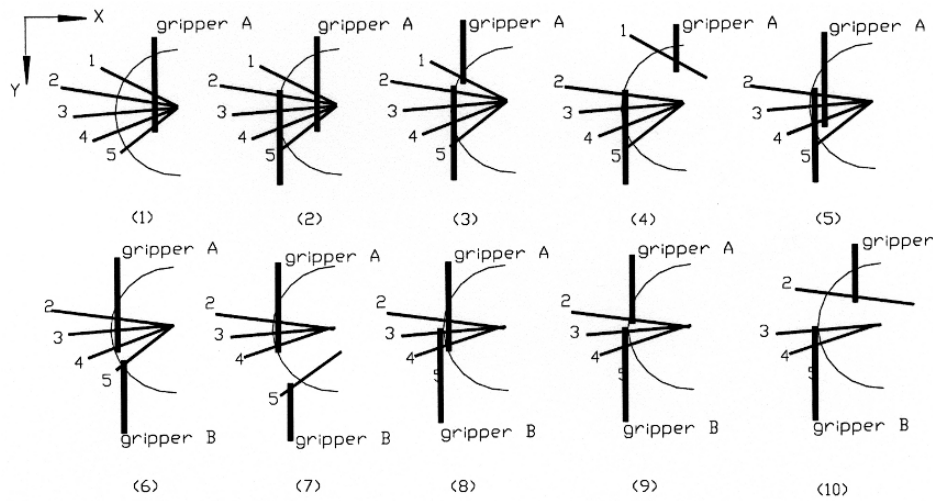


Figure 13. Separation of shoots following steps of method 2. Reprinted from Wang et al. (1999)[19].

3.3.3. Single image versus real-time imaging for shoot separation

Image processing speed is an important consideration for the transition from experimental system design to a commercial separation and transplanting system design. If the image analysis takes too long to identify separation-grasping points, mechanization would not be commercially feasible. But there needs to be a balance between accuracy of identification and speed. One concern that arises in this process is the movement of the shoot clump during separation. Cutting mechanisms may be able to slice or snip a shoot cleanly without moving the stem from its current location. However, grasping and pulling a shoot away from a clump causes some of the other shoots to move in the direction of the pull. Although it was observed that the shoots tend to return to their general original location, they may not return to the exact location that was captured by the vision system. If a shoot was identified but not separated, the control algorithm would send the gripper to the next shoot location, which results in two shoots being transplanted as a single shoot. If the gripper accidentally pulled two shoots instead of one, the gripper would then go to the location where the second shoot was previously, and would attempt to separate it from the clump and transplant it, resulting

in a blank space in the re-growth vessel. Because of these possibilities, two methods were tried by Wang *et al.* [19] to determine if one image capture is sufficient or if an image should be taken after each separation.

The first approach captured a single image of the full clump and separation was performed based on the original locations of the shoots. The second approach took a repeated (new) image before each shoot was separated. Although in theory this approach should prove to be more accurate, it also requires more image processing time.

To test the automated separation system, three sets of experiments were performed.

- Single image capture using the Hough transform identification method.
- Repeated image capture using the Hough transform identification method and comparison to single image capture.
- Re-growth of shoots after mechanized separation.

Shoots were grown in 10 Magenta vessels for experiment 1. Five of the vessels contained clumps that were used for separation method 1, and five were used for separation method 2. For separation method 1, 99 of 122 (85%) shoots were identified, and 84 of those 99 (69% of total) were separated. For separation method 2, 102 of 126 (74%) actual shoots were identified and 75 of those 102 (60% of total) were successfully separated. Gripper interference was primarily responsible for the relatively low successful identification and separation rate.

Separation method 1 was used for the testing of the Hough transform in shoot separation. Although separation method 2 was slightly faster, results from the previous experiment showed that method 1 was more reliable. In this experiment, a single image approach was compared to repeated imaging. A total of 115 actual shoots were used in the single image experiment. Of those 115 shoots, 103 (88%) were correctly identified, and 91 of the 103 (79% of total) identified shoots were successfully separated. For the repeated imaging experiment, 104 total shoots were used. Of these 104 shoots, the Hough transform approach identified 94 (90%), and 88 (85% of total) were successfully separated. Although the shoots held by the grippers tended to return to their original location after a shoot was separated, grasping points on those that shifted could be better located when a new image was taken. This approach showed the best overall separation result.

3.3.4. Shoot re-growth

Plant tissue can be soft and the force exerted by the grippers can potentially damage tissue, which may negatively affect re-growth after transplanting. In addition, if the grippers close too rapidly, damage can occur from the resulting impact force on the tissue. Although the flow control valves are used to minimize damage, it is important to assess the potential damage caused by the mechanism. Sufficient damage and subsequent loss of re-growth may make the use of a robotic mechanism economically unfeasible.

Sugarcane shoots were grown in seven vessels containing the parallel plates [9]. A total of 34 shoot clumps were obtained from these seven vessels, yielding 120 shoots that were separated by the automated separation system. Sixty of the shoots were then placed into seven containers without parallel plates, and 60 were placed into eight containers with parallel plates. A separate set of shoots were separated by hand from shoot clumps and cultured in eight vessels with parallel plates and eight vessels without

parallel plates. Two measurements were taken on the re-grown shoots, multiplication (number of new shoots) and dry weight. For plantlets grown without parallel plates, the automated system yielded 76% of the shoots surviving vs. 83% from manual separation. The average multiplication was 21 shoots for the automated system vs. 25 for manual separation. The dry weight averaged 0.1820 g/vessel for the automated system vs. 0.2062 g/vessel for manual separation. Although these values were not significantly different at a 95% confidence level, the manual separation did show slightly higher average yields and dry weights.

For plantlets grown in parallel plates, the automated system had 65% of the transplanted shoots survive vs. 77% for the manual separation. The average multiplication per vessel was 16.8 for the automated system vs. 19.6 for the manual system. The dry weights were 0.1607 g/vessel for the automated system vs. 0.1782 for the manual separation. Again, these values were not significantly different at the 95% confidence level, but the manual separation approach did show slightly higher average values.

3.3.5. Cycle time

Speed of identification, separation, and transplanting of the shoots is critical to a successful automated system. The cycle time is defined as the time it takes to start the identification process by capturing an image, move the grippers to the correct location, separate the shoot, move the shoot to the transplant vessel, and begins the next image capture. The total cycle time for the system described above [19] was 25 s. Of this time, 5 s was for image processing and 20 s was for mechanism movement. At the time this system was first tested, a 486 processor was used. A test of a faster processor (133 MHz) reduced the processing time to 1 second. Personal computer processors on the market today are 20 times or more faster than that, so image processing time is not the constraining factor with regard to speed. To reduce the mechanism movement time, larger, faster step motors could be used to control the mechanisms. Units built specifically for this purpose could also reduce the cycle time. The x-y tables could be replaced with multi-dimensional robotics units that have much more freedom of movement as well as speed.

3.3.6. Commercial layout

Although the experimental automated shoot separation mechanism presented by Wang *et al.* [19] was successful in identifying the shoot separation locations and performing the separation task, the experimental layout would not be practical in a commercial operation. The vessels that grow the shoots to be separated must be conveniently located for the separation mechanisms to pull the clump out of the vessel and present it to the vision system. A layout for a commercial operation utilizing the separation approach is proposed here (Figure 14).

In the proposed design, the separation mechanism resides in a vertical x-z plane. This allows the vessels to approach the separation mechanism on conveyors, and the mechanism can reach into the vessel and pick out the clump. Original growth vessels, containing clumps grown between parallel plates, travel on conveyor 1. The separation mechanism reaches into the vessel and selects the first clump, then presents the clump to the machine vision system camera in the x-z plane against a dark background.

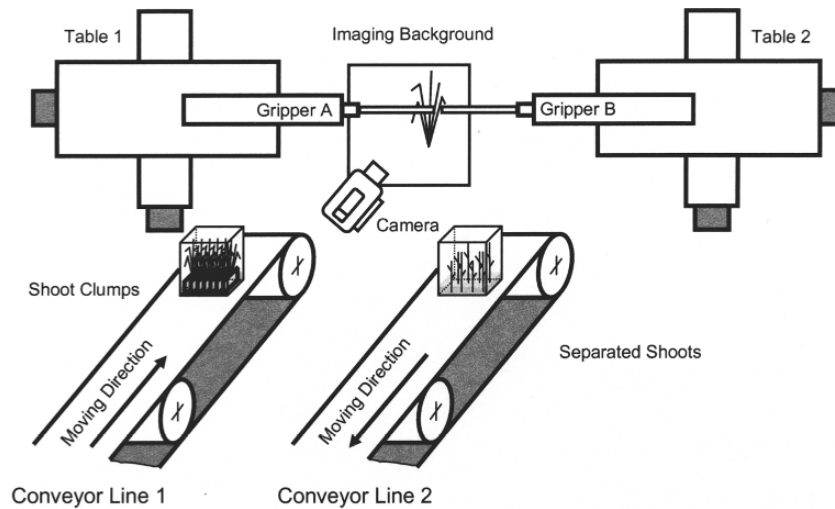


Figure 14. Proposed commercial shoot separation layout design.

Gripper A holds the clump while gripper B separates the shoots and place them within the re-growth vessel located on conveyor line 2. When appropriate number of separated shoots has filled the re-growth vessels, a new vessel is moved to the site for more separated shoots. As mentioned previously, the x-y table mechanisms could be replaced by robotic mechanisms with three dimensional movement capabilities to increase the speed and efficiency of the operation.

References

- [1] Zandvoort, E.A. and Holdgate, D.P. (1991) Mechanisation in tissue culture systems. *Acta Hort.* 289: 203-212.
- [2] Simonton, W. (1992) Issues in robotic system design for transplant production systems. In: Kurata, K. and Kozai, T. (Eds.) *Transplant Production Systems*. Kluwer Academic Publishers, Dordrecht, The Netherlands; pp. 103-116.
- [3] Brown, F.R. (1992) Robotics and image analysis applied to micropropagation. In: Kurata, K. and Kozai, T. (Eds.) *Transplant Production Systems*. Kluwer Academic Publishers, Dordrecht, The Netherlands; pp. 283-296.
- [4] Miwa Y.; Kushihashi, Y. and Kozai, T. (1995) Mechanical engineering approaches to plant biotechnology. In: Aitken-Christie, J.; Kozai, T. and Smith, M.A.L. (Eds.) *Automation and Environmental Control in Plant Tissue Culture*. Kluwer Academic Publishers, Dordrecht, The Netherlands; pp. 125-143.
- [5] Kurata, K. (1992) Transplant production robots in Japan. In: Kurata, K. and Kozai, T. (Eds.) *Transplant Production Systems*. Kluwer Academic Publishers, Dordrecht, The Netherlands; pp. 313-329.
- [6] Kurata, K. (1995) Automated systems for organogenesis. In: Aitken-Christie J.; Kozai, T. and Smith, M.A.L., *Automation and Environmental Control in Plant Tissue Culture*. Kluwer Academic Publishers, Dordrecht, The Netherlands; pp. 257-272.

- [7] Kaizu, Y.; Okamoto, T. and Imou, K. (2002) Shape recognition and growth measurement of micropropagated sugarcane shoots. *Agricultural Engineering International: the CIGR Journal of Scientific Research and Development*. Manuscript IT 02 003. Vol. IV.
- [8] Fujita N. and Kinase, A. (1991). The use of robotics in automated plant propagation. In: Vasil, I.K. (Ed.) *Scale-up and Automation in Plant Propagation*. Academic Press, Inc. San Diego; pp. 231-244.
- [9] Schaufler, D.H. and Walker, P.N. (1994) Micropropagation of sugarcane between parallel plates. *Trans. ASAE*. 37(4): 1224-1240.
- [10] Escribens, J.I. (1996). Micropropagation of sugarcane between parallel plates in a bubble column reactor. MS Thesis, The Pennsylvania State University, University Park, PA.
- [11] Schaufler, D.H. and Walker, P.N. (1995) Micropropagated sugarcane shoot identification using machine vision. *Trans. ASAE*. 38(6): 1919-1925.
- [12] Wang, Z. (1997) Vision-guided separation of micropropagated sugarcane shoots. PhD Thesis, The Pennsylvania State University, University Park.
- [13] Wang, Z.; Heinemann, P.H.; Sommer, H.J. III; Walker, P.N.; Morrow, C.T. and Heuser, C.E. (1998) Identification and separation of micropropagated sugarcane shoots based on the Hough Transform. *Trans. ASAE*. 41(5): 1535-1541.
- [14] Fu, K.S. (1987) *Robotics, Control, Sensing, Vision, and Intelligence*. McGraw-Hill, New York; McGraw Hill; pp. 365-369.
- [15] Kondo, N. (1988) Selection of suitable wavelength bands for discrimination between parts of plant body using their spectral reflectance. *Environ. Control Biol.* 26(4): 60-65.
- [16] Kondo, N.; Nakamura, H.; Monta, M; Shibano, Y.; Mohri, K. and Arima, S. (1994) Visual sensor for cucumber harvesting robot. In: *Proc. of the Food Processing Automation Conf. III*, ASAE: St. Joseph, MI. 461-470.
- [17] Zhang, T.Y. and C.Y. Suen (1984) A fast parallel algorithm for thinning digital patterns. *Commun. Assoc. Comp. Mach.* 27(3): 236-239.
- [18] Lu, H.E. and Wang, P.S.P. (1986) A comment on "A fast parallel algorithm for thinning digital patterns". *Commun. Assoc. Comp. Mach.* 29(3): 239-242.
- [19] Wang, Z.; Heinemann, P.H.; Walker, P.N. and Heuser, C.E. (1999) Automated separation of micropropagated sugarcane shoots. *Trans. ASAE*. 42(1): 247-254.

PART 4

ENGINEERING CULTURAL ENVIRONMENT

CLOSED SYSTEMS FOR HIGH QUALITY TRANSPLANTS USING MINIMUM RESOURCES

T. KOZAI

*Faculty of Horticulture, Chiba University, Matsudo, Chiba 271-8510,
Japan-Fax: 81-47-308-8841-Email: kozai@faculty.chiba-u.jp*

1. Introduction

Micropropagation is a method to propagate plants vegetatively under aseptic conditions in a culture vessel mostly under artificial light to produce a number of disease-free transplants. "Photoautotrophic" micropropagation is a method of micropropagation to grow plants photosynthetically under aseptic conditions on the sugar-free culture medium using leafy or chlorophyllous explants in a ventilated culture vessel (See also Kozai and Xiao in this book). Photoautotrophic micropropagation differs from conventional vegetative propagation in size of explants (or cuttings) and the degree of asepsis of culture medium and/or plants. In addition, conventional vegetative propagation is conducted mostly under natural light in a greenhouse or a nursery.

Micropropagated plants *in vitro* grown on sugar-containing or sugar-free medium are basically aseptic, but conventionally propagated plants using cuttings are not. Strictly speaking, the purpose of micropropagation is not to produce aseptic plants, but to produce pathogen- or disease-free and physiologically healthy plants, which are tolerant to various kinds of environmental stress. Aseptic plants are pathogen free, but pathogen free plants are not necessarily aseptic, because microorganisms are not necessarily pathogens.

A closed transplant production system using artificial light described in this chapter is a system for producing disease-free transplants (but not aseptic transplants) at low costs with minimum use of resources. The system can be used both for plantlet and seedling production (Plantlets mean small plants vegetatively propagated and seedlings mean small plants grown from seeds.) In this sense, a closed transplant production system is one type of plant propagation and/or transplant production systems. In the closed transplant production system, however, more attention is paid with respect to resource saving and environmental conservation than in the photoautotrophic micropropagation system.

In this chapter, the definition, concept, theoretical backgrounds, methods, materials, applications, and advantages of the closed system for transplant production using lamps over a greenhouse using sunlight are described from biological, engineering and economic points of view.

2. Why transplant production systems?

The world population in the year 2004 is about 6.4 billions and has been predicted to reach 9 billions by the middle of the 21st Century. Recent annual rate of population increase is nearly 3% in Asian, African and South American countries. In those countries, the environmental pollution and the shortages of food, feed, phytomass (plant biomass) and natural resources including fossil fuels and usable fresh water will become more and more serious on a larger scale in the forthcoming decades.

The difficulty with solving these global issues on food, energy, phytomass and environmental pollution is that we need to solve these issues concurrently based upon one common and innovative concept and methodology created from broad and long-term viewpoints, and to develop a new industry, which is strongly related to agriculture, horticulture, forestry and aquaculture and also to other manufacturing industries, but is not the same as any of those industries [1,2].

The reason why we need to solve those issues concurrently is that solving only one issue separately from the other two often makes the situations of the other two even worse. For example, the worldwide spread of advanced agricultural technology for increasing crop yield may often make the environmental pollution worse, increase the atmospheric CO₂ concentration, and cause shortages of fossil fuels and other natural resources. This is because the modern agricultural technology is heavily dependent upon the oil-derived products such as chemical fertilizers, chemical pesticides, plastics, and fuels for machines.

Increase in phytomass in Asian, African and South American countries is also essential to stabilize their climates and to conserve their ecosystems or environments, while the forest area in tropical countries has recently been decreasing at an annual rate of 0.7% with a yearly net decrease in area of about 13 million hectares for years 1990 to 1995. For reforestation of this area, 25-40 billions of transplants (2,000-3,000 transplants per hectare) are required annually. In addition, the decrease in phytomass due to desertification in arid regions is considerable (World desertification area is 5-8 million ha every year). Such local and global decreases of the vegetation areas, and consequently the decrease in phytomass, are possible factors causing recent meteorological changes on different geographical scales.

In order to solve these global issues in the 21st Century, we are requested to develop a concept, a methodology and an industry to produce billions of plants every year not only for food, feed and environmental conservation, but also for alternative raw materials to produce bio-energy, bio-degradable plastics and many other industrial products (Figure 1). By using plant-derived products, we can minimize the environmental pollution and the use of fossil fuels and atomic power. It has been predicted that, in the forthcoming decades, demands for transplants for use in afforestation and re-afforestation will rise sharply in the pulp, paper, timber, energy, plantation, horticulture and furniture industries, and in the desert rehabilitation for environment conservation [3,4].

Use of phytomass in those industries is essential to reduce the consumption of fossil fuels and to lower the atmospheric CO₂ concentration, and to stabilize local and global climates. A large number of high quality transplants, woody and herbaceous horticultural plants, are also needed every year for people living in cities to improve their quality of life or green amenities (Figure 2). The same is true for medicinal plants.

By use of high quality transplants, we can save resources such as labour, pesticides, insecticide and fuel for agricultural machines to be used in the open fields or in the greenhouse (Figure 3).

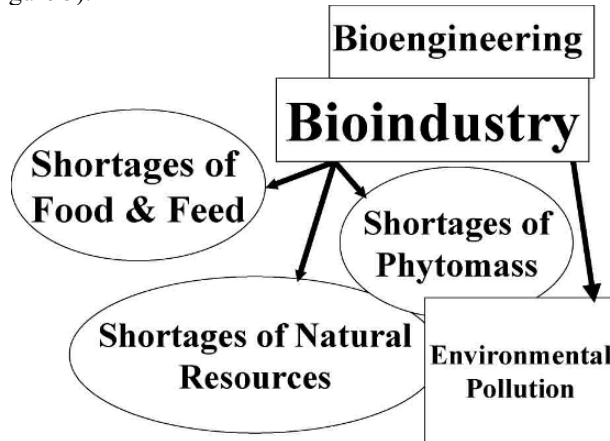


Figure 1. A diagram showing the importance of high quality transplants to solve global issues on shortages of food and feed, shortages of natural resources such as fossil fuel and water, and environmental pollution.

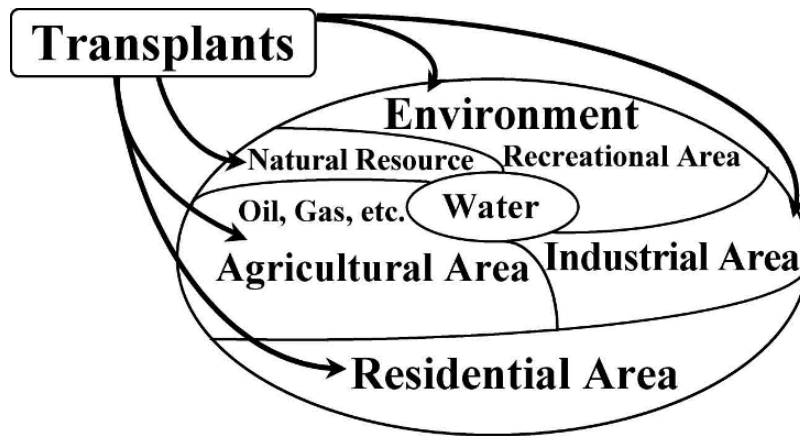


Figure 2. A diagram showing that an increasing number of high quality transplants is needed in various aspects for solving the global issues.

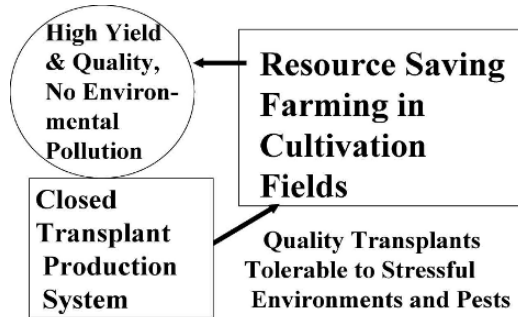


Figure 3. A diagram showing that we can save resources for high yield and quality in the open fields or in the greenhouse by use of high quality transplants.

Quality of transplants is determined by their genetic, physiological, and morphological characteristics. High quality transplants with superior physiological and morphological characteristics can be produced only under carefully controlled environments. “Closed transplant production systems”, discussed in this paper, are expected to be useful concepts and methods to produce a large number of high quality transplants at a low cost with use of minimum resources. These ideas were originated from our research backgrounds as environmental control engineers and environmental physiologists specializing in greenhouse, plant growth chamber and plant factory. This chapter is an extended version of our previous work [5].

3. Why closed systems?

A production system releasing a significant amount of pollutants is called an open production system or a one-way production system (Figure 4). In the following description, greenhouses with ventilators are open and/or which release wastewater is considered as typical open production systems. On the other hand, a production system, which releases no, or a negligible amount of pollutants, is called a closed production system (Figure 4). In a closed production system, all primary by-products are converted within the closed system into secondary products that have some economic value. A closed production system releasing no pollutants is called a zero emission production system.

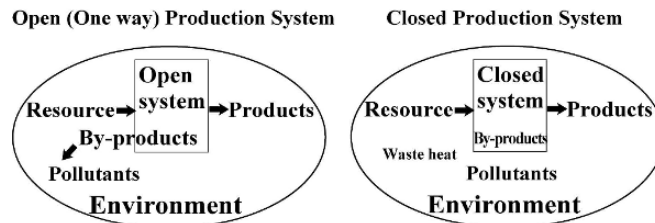


Figure 4. Schematic diagrams of open (or one way) system (left) and closed system (right).

All the resources are converted into products in a closed system, so that amount of resourced can be minimized, resulting in no waste or pollutants, although the closed system produces a certain amount of waste heat. The role of closed production system will become increasingly important in the 21st century for resource saving and environmental conservation. It would be ideal if we could produce high quality transplants using the closed production system.

Conventionally, transplants are produced in a greenhouse or a nursery, which is a typical open production system. A greenhouse with the ridge height of 6-8 m, as shown in Figure 5, is often used to produce transplants with the height of about 10 cm only. In order to use solar light, which is considered to be free of charge, for growing transplants, a considerable amount of fossil or electric energy is consumed for heating, shading, ventilation, etc. Can we really save resource and conserve environments more by using a greenhouse with solar light than by using a closed system with artificial light? Can we produce a higher quality transplant in a greenhouse than in a closed system? In this chapter, the author shows that we can produce a higher quality and disease-free transplant using less water, fertilizer, pesticide, labour, time and space in a closed system than in a greenhouse, and that initial investment and a sum of oil and electricity energy costs for environmental control in the closed system is more or less the same as that in the greenhouse.



Figure 5. A conventional greenhouse covered with glass sheets. In order to use solar light that is free of charge, many kinds of environmental control equipment often need to be installed for ventilation, heating, heat conservation (thermal screen), shading, watering, etc. Much fuel or other kinds of energy are also necessary. In order to lessen the rapid changes with time in air temperature and relative humidity, a tall greenhouse (6-10 m high) with large air mass is needed for growing short transplants with only about 0.1-0.2 m high, which is space inefficient and costly.

4. Commercialization of closed transplant production systems

A 'closed plant production system' or simply a 'closed system' has been commercialized in Japan since 2002, largely based upon the research at Chiba University, for production of tomato, cucumber, eggplant, lettuce and spinach transplants from seeds. Commercial productions of herbs, leafy vegetables, bedding plants such as pansy, medicinal plants, and orchid plants are now under trial in Japan. The closed system is defined as a warehouse-like structure covered with opaque thermal insulators, in which ventilation is kept at a minimum, and lamps are used as the sole light source for plant growth.

Advantages of the closed system over a greenhouse for producing high quality transplants include: a) rapid and efficient growth of transplants mainly resulting from a considerably higher light utilization efficiency (2-3 times) of transplants due to optimized growth conditions, b) the significantly higher quality transplants produced under uniformly controlled environments in the protected area free from pest insects/pathogens and the disturbance of outside weather, c) the higher (about 10 times) productivity per floor area per year, mainly due to the use of multi-layered shelves (e.g. 4-5 shelves) with the ratio of planting area to floor area of 1.2-1.5, a high planting density per tray area (1500 transplants/m²), a high percentage of saleable transplants (>90%), 10-20% higher sales price due to their higher quality and uniformity of transplants, and 30-70% shorter production period, d) the drastically higher utilization efficiencies of water, CO₂, (about 15 times for water and 2 times for CO₂) and fertilizers mainly due to the minimized ventilation and recycling use of dehumidified water by air conditioners, resulting in little waste water to the outside, e) virtually no requirement of heating cost even in the winter because of its thermally insulated structure, f) the lower labour cost (50% or less) due to the smaller floor area, the worker-friendly shelves, comfortable working environments, and g) the easier control of plant developments such as stem elongation, flower bud initiation, bolting, root formation [6-11].

High electricity cost and initial investment are often mentioned as a disadvantage of the closed system. However, the electricity cost for lighting and cooling per transplant was found to be roughly 0.5 to 1.0 US cent, which accounts for 1-5% of the sales prices of tomato, eggplant, pansy, and sweet potato transplants in Japan. Electricity cost for transplant production could be reduced considerably by using thermally insulated walls and multi-shelves and advanced lighting and air conditioning systems.

Since only about 10% of greenhouse floor area is required to produce the same amount of transplants, initial cost per annual plant production in closed systems is lower than that in greenhouses. By using a closed system with a floor area of 150 m² with 60 shelves having 960 plug trays in total, about 10 million transplants can be produced annually.

5. General features of high quality transplants

General features of high quality transplants are listed below:

- Genetically superior and uniform.
- Physiologically and morphologically normal and uniform with a compact plant form without elongated shoots, and with normal colour.

Closed systems for high quality transplants

- Developmental stages of flower buds, leaves and roots are uniform and as planned.
- Tolerant to high and low temperatures, strong wind, variable solar radiation, and dry and wet soil and air conditions.
- Tolerant to and uninfected by pathogens and insect pests, requiring less agrochemicals during cultivation.
- Low labour and other costs for handling, transportation and transplanting, leading to low production costs.
- Little or no physical damages of aerial and root parts at transplanting.
- High ability of rapid growth after transplanting, leading to high quality and high yields at harvest when cultivated under variable cultivation conditions.

However, it is often difficult for us to produce transplants having such features in the greenhouse under variable weather conditions and limited resources. Problems often encountered in transplant production using the greenhouse are:

- Non-uniform transplant growth due to the non-uniform environmental conditions.
- Season, weather and human-skill dependent growth rate due to the sensitiveness of growth rate to environmental conditions.
- Difficult to standardize the details of production technology. High-level expertise and labour-intensive work needed for high quality transplant production.
- A greenhouse with large air volume (high ridge) and equipped with an environmental control system needed for precise environmental control under variable solar radiation, wind speed and temperatures outside the greenhouse.
- High initial investment and operation costs for a greenhouse with large air volume (high ridge) and equipped with an environmental control system.
- Possible damages of crops by insect pests, fungi and bacteria throughout the year. Difficult to reduce the costs for preventing these damages.
- Difficult to avoid the stable employment of workers and a low operation rate of the greenhouse due to the varying demands of transplants with season.
- To meet the high demand of transplants in early fall (September), the transplant production needs to be started under hot climate (August), when the air temperature in the greenhouse is still too high to produce high quality transplants.
- A possible mismatch of supply and demand due to the unstable transplant productivity under variable weather and unpredictable demands, which results in high production costs.

To produce high quality transplants and to avoid problems, we need intensive labour and a greenhouse heavily equipped with a variety of environmental control units, both of which are costly. An alternative approach is the adoption of closed plant production system which not only be applicable for *in vivo* grown transplants but also for growing the *in vitro* raised plants.

6. Sun light vs. use of lamps as light source in transplant production

Most people think that use of solar radiation or natural sun light is more economical than artificial light from lamps for plant production, because solar radiation is free of charge. This is generally true. However, this free solar radiation is often disadvantageous over artificial light in transplant production using the greenhouse because we have to invest a lot for controlling the greenhouse environment to use the solar radiation efficiently. Disadvantages of the use of solar radiation in transplant production are:

- Only about 50% of solar radiation energy (waveband: 300-3000 nm) is photosynthetically active (waveband: 400-700 nm). Radiation with a wavelength longer than 800 nm has a thermal effect only. Thus, air and leaf temperatures tend to be high under solar radiation due to the heating action of thermal radiation.
- Difficult to control the light intensity within a range suitable for transplant production. The light intensity is too low in the morning and evening or on cloudy and rainy days, while it is often too high around noon on clear days.
- Seasonal changes of daylength often affect photomorphogenesis, development and growth of transplants.
- Seasonal and diurnal changes of light quality (red/far-red ratio, blue/red ratio, etc.) caused mainly by the changes in solar altitude and atmospheric transmittance affect flower bud development, shoot elongation, germination, rooting, photosynthesis, transpiration, etc.
- Difficult to control the light quality independent of light intensity.
- Light intensity at plant level is often reduced by surrounding and greenhouse structures. Direction and orientation of direct solar light beam is determined by the solar position.
- Rapid changes in light intensity with time cause rapid changes in temperature and relative humidity in the greenhouse, which is unfavourable for high quality transplant production. To lessen the rapid changes in air temperature and relative humidity, a tall greenhouse (6-10 m high) with large air mass is needed for growing short transplants with about 0.2 m high (Figure 6).

On the other hand, use of artificial light is sometimes advantageous over natural light in transplant production, and it is worthy to compare the advantages of artificial light with the disadvantages of natural light. Rationale and advantages of use of lamps as light source in transplant production are listed below:

- Optimum light intensity is relatively low (photosynthetic photon flux of 150-300 $\mu\text{mol m}^{-2} \text{s}^{-1}$), which can be obtained by 5 or 6 fluorescent tubes (40W each) installed about 40 cm above the shelf.
- Optimum light intensity, which depends on growth stage, planting density and plant species, can easily be provided.
- Light and dark periods can be controlled precisely. Lighting cycle (light period plus dark period) need not to be 24 hours.
- Lamps which emit photosynthetically active radiation (400–700 nm) or phytochrome sensitive active radiation (e.g. 700–800 nm) only can be used.

Closed systems for high quality transplants

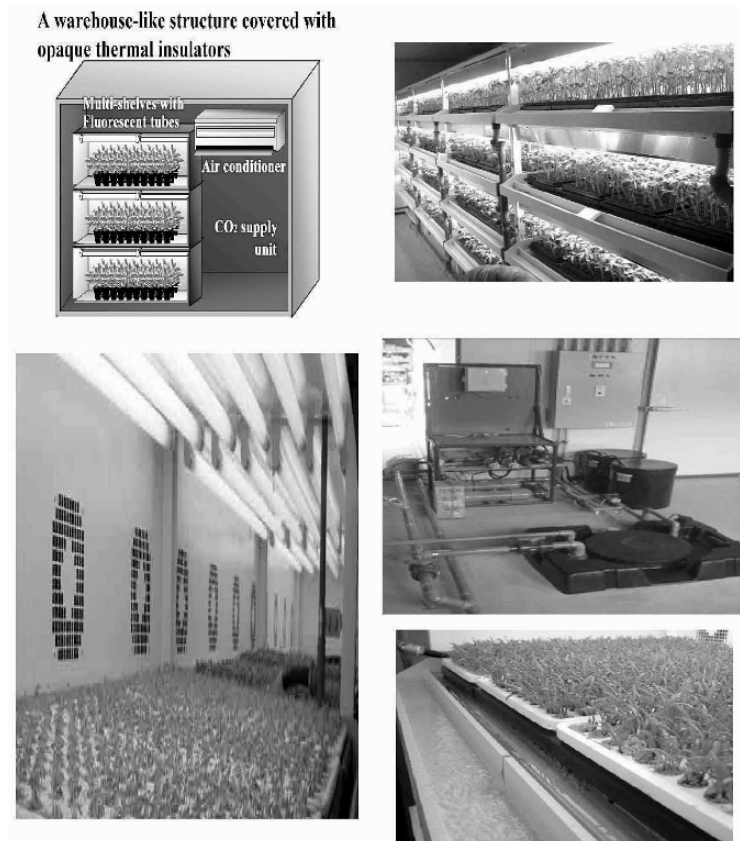


Figure 6. Schematic diagram showing four components of the closed transplant production system (upper left) and the inside view of a closed system commercially used in Japan (upper right). Fans for internal circulation of air, usually installed at the back-wall of each shelf and fluorescent lamps (lower left). Nutrient solution supply unit (Lower right). A commercially-sold closed system has a floor area of 22 m² (6.3 m long, 3.6 m wide), 7 sets of four 4-layered shelves (4 shelves at one side and 3 shelves in the other side). Each shelf with six 40W fluorescent tubes is 0.7 m wide and 1.5 m long. Then, one closed system holds 112 (= 7x 4 x 4) cell trays (30 cm wide x 60 cm long). Since 200 tomato transplants are grown in one tray, 22,400 transplants can be produced in one batch, totalling 400,000 transplants per year (one cycle is 20 days, 18 batches per year).

- Intensity and light period for photomorphogenesis can be set independently of those for photosynthesis.
- Planting density of transplants is relatively high (1000-3000 m⁻²) and production period of transplants is relatively short (2-4 weeks). Electricity cost per transplant is relatively low (0.3–1.0 US cent per transplant) because it is proportional to a product of light intensity and production period, divided by the planting density.

- Sales price of transplants is relatively high, especially in case of fruit vegetables (20-100 US cents), and the electricity cost accounts for 5% or less of the production cost.

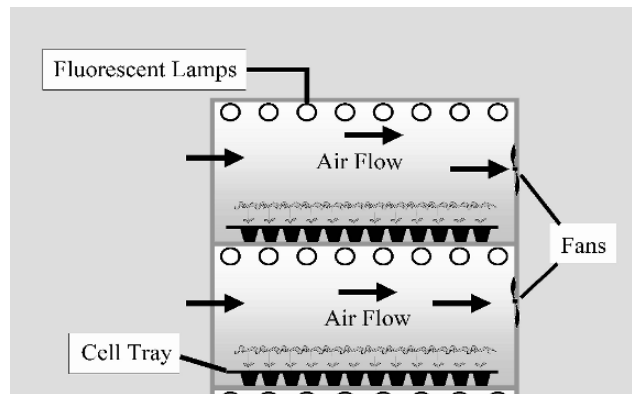


Figure 7. Cross section of multi-shelves (two shelves only are shown) showing the direction of air flow and positions of micro fans. This air flow guarantees the uniformity of microenvironments over the trays and within the transplant canopy.

7. Closed plant production system

7.1. DEFINITION

A ‘closed plant production system’ or simply called ‘closed system’ in this chapter is defined as a warehouse-like structure, a) covered with opaque thermal insulators b) in which ventilation is minimized, c) which uses lamps as the sole light source for plant growth and development, and d) which uses heat pump (or an air conditioner) instead of a ventilation fan even when the set point of room air temperature is higher than the outside air temperature. In addition, multi-layered shelves each with lamps are used to increase the production capacity per floor area. On the other hand, a greenhouse can be called an ‘open plant production system’ or simply ‘open system’, in the sense that: it is covered with transparent materials such as glass sheets for use of sunlight, and it requires ventilation especially in summer, and thus heat energy, radiation energy, CO₂ and water exchanges between inside and outside the greenhouse are considerable and are not well controlled.

7.2. MAIN COMPONENTS

Main components of a typical closed transplant production system (Figure 6) are:

- a warehouse-like structure covered with opaque thermal insulators,

- air conditioners for home use, which are mostly used for cooling and dehumidification, and sometimes for heating,
- fans for internal circulation of air (Figure 7),
- a CO₂ supply unit for promoting plant photosynthesis, e) multi-shelves usually with fluorescent lamps installed in the warehouse-like structure, and
- an environmental control unit.

7.3. CHARACTERISTICS OF MAIN COMPONENTS OF THE CLOSED SYSTEM

All the main components of the closed system are mass-produced for home use or for industrial use, except for a CO₂ supply unit. Advantages of use of mass-produced electric or industrial products as main components of the closed system are as follows:

- Cost performance of the product has been improved every year due to severe competitions among the manufacturers.
- Recycling and reuse systems for the products such as fluorescent tubes, air conditioners and thermal insulators have been established socially, and found to be environment friendly.
- In case of malfunction or a decrease in performance, the part(s) or the product itself can be replaced by a newly released part or a product with a higher cost performance.
- Easy access to the parts of the products at a low price.
- A considerable discount (60-80%) is possible for bulk purchase.
- Virtually maintenance free or easy maintenance. Free repair and replacement are guaranteed for one year or so in case of malfunction of the products.

The main components of the closed system can be used without any modification for constructing the closed system. And each component has a rich variety of types, sizes, capacities etc. Therefore, we are able to construct various types of closed systems. These characteristics significantly reduce the investments for research and development of the closed system. When the room air temperature is higher than its set point, air conditioners are operated for cooling and air is not ventilated.

Reasons for use of air conditioners (heat pump) instead of ventilation fans even when outside air temperature is lower than the set point of room air temperature can be summarized as below:

- Evapotranspired water is lost to the outside by ventilation (More than 95% of irrigated water is evapotranspired).
- Respired CO₂ by plants and enriched CO₂ are lost to the outside by ventilation.
- Dusts, pathogens, and insects can enter to the closed system by ventilation.
- Relative humidity and air temperature in the closed system are affected by the relative humidity and air temperature outside the system, if ventilated. Then, the accuracy of environment control is decreased.
- Electricity cost for cooling accounts only for 15% or less of that for lighting.

7.4. EQUIPMENTS AND FACILITIES: A COMPARISON

Components which are unnecessary in the closed system, but are often or definitely necessary in the greenhouse are:

- thermal screens
- shading screens
- roof and side ventilators or fan ventilators
- oil or gas heaters
- benches, beds or bags containing substrate
- transparent covering materials such as glass sheets and plastic films, and, in some areas, and
- an evaporative cooling system and/or a supplemental lighting system using high pressure sodium and/or metal halide lamps (Table 1).

Table 1. Equipment and facilities necessary in the closed system and the greenhouse respectively, for transplant production.

Item	Closed system	Greenhouse (Open system)
Basic structure	A warehouse like structure covered with opaque thermal insulators with 1/10 th of greenhouse floor area.	A greenhouse structure covered with transparent glass sheets or plastic film.
Basic facility	Multi-layered shelves with fluorescent Lamps	Bench or beds
Basic environmental control equipment	Air conditioners (or heat pumps), air mixing fans for internal circulation of air, CO ₂ enrichment system, nutrient solution supply system, and timer clock	Heating system, thermal screen system, shading screen system, natural or forced ventilation system, and timer clock
Optional environmental control equipment	None	CO ₂ enrichment system, evaporative cooling system, nutrient solution supply system, mesh screen for preventing insects from entering, air mixing fans, computerized environmental control system, and alarm system for strong wind, snow, rain and human invasion.

Most of these components have been developed and used only for the greenhouse industry, except for transparent glass sheets. Thus, investment for research and development of the greenhouse components are costly and limited.

Components common to both closed system and greenhouse for transplant production are cell trays, an irrigation unit and an environmental control unit. However, control algorithms of these units for the closed system are much simpler than those for the greenhouse. On the other hand, a CO₂ supply unit is indispensable for the closed system, but dispensable for the greenhouse.

7.5. FEATURES OF THE CLOSED SYSTEM VS. GREENHOUSE

The features of the closed system in comparison with the greenhouse are summarized as follows from the viewpoints of transplant production:

Closed systems for high quality transplants

- Annual productivity of transplants is about 10-fold. Transplants are produced as scheduled. A risk of physical damage of transplants is minimized because they are produced in a warehouse like structure.
- Production period is shortened by about 30% and high quality transplant is almost always produced due to the optimized environment regardless of the weather and season.
- Operation rate of the system and, thus, annual production capacity are high, because of the shortened production period regardless of the weather and season.
- Favourable environments, which cannot be achieved in nature or in the greenhouse, can easily be realized (e.g. horizontal air current speed within the transplant canopy of 50 cm s^{-1} , relative humidity of 60% during dark period, etc.).
- The system is of resource saving, environmentally friendly, space-saving, and labour-saving (Consumptions are 1/20 for irrigation water, 1/2 for CO₂ enrichment, 2/3 for fertilizer, 1/10 for pesticide, and 1/10 for floor area. Labour hour is halved and there is no nutrient-containing water wasted to the outside.
- High cost performance and easy recycling of main components of the system (air conditioners, fluorescent tubes, air mixing fans, thermal insulating boards, multi-layered shelves, CO₂ controller, etc.). No pollutants are released to the outside.
- High discount percentages of the main components by bulk purchase.
- Cost for cooling accounts only for about 15% of electricity cost even in summer. Electricity cost for lighting and cooling per transplant is 0.5-1.0 US cent and accounts for less than 5% of production cost.
- Low initial investment cost per transplant.
- Low operation cost per transplant. No or little heating cost even in winter at high latitudes. Relative humidity during the photoperiod is naturally kept at 60-70%.
- Comfortable working environments.
- Mental stress is lightened and environmental management work is reduced because no attention is necessary for the effect of outside weather on the transplant growth.
- Suited for production of scions and stocks for (robotic) grafting because seedlings grow uniformly.
- Suited for nursing and acclimatization of grafted transplants.
- No sudden rise/drop of room air temperature at noon/night in summer/winter in case of electricity failure due to the thermally insulated structure of the system.
- Light utilization efficiency in the closed system is over 2 times that in the greenhouse because of the optimized environment.
- Cost for CO₂ enrichment per transplant is negligibly small because of the air tightness of the closed system.
- An environmental controller is simple in algorithm and less expensive because considerations on weather are unnecessary.
- Disinfection of the closed system is relatively easy.

However, from the viewpoints of resource saving and environmental conservation, the closed transplant production system has the following attributes (Table 2).

Reasons for labour saving characteristics of the closed system in comparison with the greenhouse are claimed as:

- Floor area and thus working area of the closed system is 1/10th of that of the greenhouse.
- Easy irrigation and fertilization, because of no influence of the outside weather on the growth of transplants in the closed system.
- A low risk of invasion of insect pests to the closed system, and much less application of pesticide.
- No need to pay attention to the outside weather to control the environment in the system.
- Comfortable working environment throughout the year.
- Raising of plug transplants to the pot transplants are unnecessary in most cases.

Listed are some examples of environmental control, which is easy to realize technically at a low cost in case of the closed system but is difficult to achieve in the greenhouse.

- Provide 24 hour light period and change the set points of light intensity and air temperature every day.
- Change light and dark periods each time independently each other.
- Control flower bud growth, shoot and hypocotyls elongation, bolting, photosynthetic activity by modifying the light quality of lamps.
- Maintain the horizontal air current speed within the transplant canopy at 30 cm s⁻¹ or higher.
- Maintain the relative humidity within the densely populated transplant canopy at 85% or lower during light period.
- Maintain the air temperature in dark period higher than that in light period.
- Maintain the relative humidity during the dark period at 80% or lower.
- Control the CO₂ concentration during the light period at 1000 μmol mol⁻¹ with a CO₂ utilization efficiency higher than 85%.
- Provide uniform environments over and within the transplant plug trays.

Closed systems for high quality transplants

Table 2. Features of the closed system with respect to resource saving, environmental friendliness, labour saving, space saving and cost effectiveness in comparison with those of the greenhouse.

Features	Description
Resource saving	More than 95% of evapotranspired water is collected at the cooling panel (or evaporator) of air conditioner, and is reused for irrigation. Thus, net amount of water required for irrigation is 5% or less of evapotranspired water.
Environmentally friendly, Resource saving	No wastewater containing chemical fertilizer application is released to the outside. Thus, the amount of chemical fertilizers can be reduced by 30-40%, resulting in resource saving and environmental conservation.
Resource saving	Eighty to ninety percent of CO ₂ supplied to the closed system is absorbed by photosynthesis of plants when CO ₂ concentration is kept at 700-1000 $\mu\text{mol mol}^{-1}$ (ppm). It is about 50% when supplied to the greenhouse.
Environmentally friendly, Resource saving	Insect pests can rarely enter the closed system due to its structural characteristics. Thus, the amount of pesticide used in the closed system is less than 10%. The pesticide supplied to the closed system is not released to the outside due to its structural characteristics.
Resource saving	Since walls are covered with thermal insulators (thickness: 10 cm), even in winter at cold regions, room temperature during photoperiod can be kept at 25-30°C by heat generated from lamps, so that no other heating source is necessary, although heating is necessary during dark period. Even during dark period in winter at cold regions, heating load of the closed system is about 1/10 th of that of the greenhouse. Ventilation cost of the closed system is zero because of no ventilation facility in the closed system. Electricity cost for lighting and cooling is only 1-5% of the production cost.
Resource saving	Shading screen, ventilators/ventilation fans, thermal screen, heating system, and supplemental lighting system are unnecessary, which are often necessary in the greenhouse.
Space saving, Resource saving	Floor area of the closed system is about 10% of the greenhouse floor area (Table 4). Thus, the closed system needs less material and energy for construction. The closed system can be built at shaded place next to the tall buildings, waste land such as desert, on the roof of the building, etc.
Labour saving, Comfortable working space	Less labour for transportation and handling due to the 1/10 th of working floor area. Comfortable working environment regardless of the outside weather (Table 1). Automatic irrigation is easy because timing and amount of irrigation is not affected by outside weather.
Safety	Outer structure is physically rigid so that the transplants are safer with respect to strong wind and other physical disasters. It is relatively easy to keep commercial secrets of products.
Annual depreciation of initial cost per transplant	Annual rate of operation can be high in the closed system because the system can be operated throughout the year, so that depreciation per transplant can be lowered if marketing and production planning are reasonable.

7.6. EQUALITY IN INITIAL INVESTMENT

Table 3. Comparisons of initial investment for structures and equipment in the closed system and the greenhouse. Unit: JPN (Japanese Yen, 1 USD=120 JPN as of 2004).

Item	Closed system	Glass-house	Plastic house
Structure per unit floor area (JPY/m ²)	100,000	15,000	5000
Service life of the structure (year)	15	15	10
Basic environmental control units	Lamps, air conditioners, CO ₂ and nutrient solution supply units	Heating, thermal screen, ventilation, shading and alarm systems	Heating, thermal screen, ventilation, shading and alarm systems
Cost for Basic environmental control units per unit floor area (JPY/m ²)	200,000	15,000	15,000
Service life of the units	10	10	10
Optional environmental control units	Not necessary	Fog cooling, insect net, air mixing fan	None
Cost for optional environmental control units (JPY/m ²)	-	10,000	-
Floor area necessary for yearly production of 500,000 tomato transplants (m ²)	43	300	300
Cost of the whole structure	4,300,000	4,500,000	1,500,000
Cost of basic environmental control units for the whole structure	8,600,000	4,500,000	1,500,000
Cost of optional environmental control units for the whole structure	-	3,000,000	-
Total cost	12,900,000	12,000,000	6,000,000
Annual depreciation for the whole structure and equipment	1,150,000 (4,300,000/15 + 860,000/10)	1,050,000 (4,500,000/15+ 750,000/10)	600,000 (1,500,000/10 + 450,000/10)
Annual depreciation per transplant	2.3 (1,150,000/500,000)	2.1 (1,05,000/ 500,000)	1.1 (600,000/ 500,000)

An increase in yearly productivity per floor area of the closed system is about 10 times that of the greenhouse for many kinds of plant species, so that floor area of the closed system can be reduced to 10% of the greenhouse floor area to obtain the same yearly production of transplants.

It is quite possible, at least in Japan, that the initial investments of the closed system is roughly equal to or lower than that of a well-equipped greenhouse having a 10-fold floor area compared with the closed system of closed system. In facts, more than 20 closed systems have been used for commercial production of transplants in Japan as of 2005.

In Japan, the construction cost of an aluminium-structured glasshouse is currently about JPN 15,000 m⁻² (USD 125 m⁻²) and the equipment cost for heaters, thermal and shading screens, ventilators, etc. is also about USD 125 m⁻² (Table 3). Thus, a well-equipped glasshouse costs about USD 250 m⁻². On the other hand, the construction cost of the closed system having the same production capacity as the greenhouse is roughly equal to or lower than JPN 300,000 m⁻² (250 x 10 = USD 2,500 m⁻²). In many other countries, the construction costs of both the closed system and the greenhouse are less expensive than in Japan.

7.7. REDUCTION IN COSTS FOR TRANSPORTATION AND LABOUR

Labour cost can be lowered in the closed system than in the greenhouse (Table 4), because its working floor area is about 10% of the greenhouse, which reduces a daily total distance of walking by workers in the closed system to roughly 10% of that in the greenhouse.

Table 4. Estimation of percent reduction of working hours in the closed system relative to the greenhouse by labour components.

Working hour component	% reduction	Remarks on % reduction in the closed system
Substrate preparation and filling in the plug trays	30	Transplanting density is 2 times, so that the number of plug trays is half in the closed system.
Sowing	30	<i>Ibid.</i>
Nutrient solution supply/irrigation	80	It can be fully automated in the closed system.
Pesticide/insecticide application	80	Less application in the closed system is needed because no openings exist in the closed system.
Handling, transportation and shipping of plug trays with and without transplants	50	The number of plug trays is half; the floor area is 1/10; working environment is more comfortable in the closed system.
Controls of temperature, humidity and light intensity/period.	60	The controls are much easier in the closed system and season independent.
Transplant growth management	10	Percent saleable transplants and growth uniformity are 10-20% higher in the closed system.
Production supervision	40	The floor area is 1/10, and environmental and disease controls are easier in the closed system.

Initial investment and operation costs for handling and transportation of cell trays (often called ‘plug trays’) can also be lower in the closed system than in the greenhouse due to the smaller floor area of the closed system (Table 5).

Table 5. Comparison of production cost per transplant and its components between the closed system and the greenhouse in case of tomato plug transplants in Japan.

Item		Greenhouse (JPY)
Depreciation of initial investment	2.3	2.1
Seed	13.0	13.0
Substrate and plug ray	2.1	3.2
Other consumption goods	2.0	2.0
Labour	5.0	10.0
Others	5.0	5.0
Total	29.4	35.2

Note: JPN stands for Japanese Yen. 1 USD = 120 JPN as of 2004

7.8. UNIFORMITY AND PRECISE CONTROL OF MICROENVIRONMENT

A typical airflow pattern in the closed system is shown in Figure. 3. Air is sucked in at the back wall of each shelf by several micro fans (3-4W each). Thus, air temperature, relative humidity and CO₂ of outgoing air from the back wall of each shelf are the same over the trays as well as shelves. Air flows horizontally over cell trays on each shelf at a horizontal air current speed of 0.1-0.5 ms⁻¹. Generally, a higher horizontal air current speed is applied as transplants grow and/or as PPF increases.

Each shelf is 60-65 cm wide, which is about 5 cm longer than the length of cell trays. Then, the microenvironment along the airflow over the cell trays does not change significantly. Furthermore, air flow rate and PPF on each shelf can be controlled and kept, respectively, at the same levels over the shelves, so that temperature rise along with the air flow over the cell trays is less than 1°C. In short, the structure of the multi-shelves guarantees a uniform distribution of aerial environment over shelves and within the transplant canopy. This uniformity of the microenvironment is difficult to achieve in the greenhouse.

In the closed system, air temperature, CO₂ concentration and relative humidity as well as PPF can be controlled as desired even in summer. On the other hand, in the greenhouse, air temperature and PPF are often too high and CO₂ concentration is often too low on a clear day. If roof and side ventilators are opened fully to lower the air temperature in the greenhouse, pest insects may enter the greenhouse. PPF and thus air temperature and relative humidity change rapidly and frequently within a day. Therefore, accurate control of greenhouse environment is difficult to achieve.

7.9. GROWTH, DEVELOPMENT AND UNIFORMITY OF TRANSPLANTS

When air moves slowly and unevenly over the transplant canopy caused by natural convection, as often observed in the greenhouse, the microenvironment over the canopy is significantly different from that within the canopy, and air movement or diffusion of CO₂ and water vapour are restricted within the canopy, compared with above the canopy. As a result, CO₂ concentration during the photoperiod is about 50 μmol mol⁻¹ lower within the canopy than over the canopy, and relative humidity is generally 10-20% higher within the canopy than over the canopy. Under such conditions, photosynthesis and transpiration of transplants are often restricted.

Moderate and uniform horizontal airflow, caused by horizontal forced convection, over and within the transplant canopy in the closed system improves the microenvironment within the transplant canopy considerably: a) increase in CO₂ concentration and reduction in relative humidity within the canopy, b) increase in CO₂ and water vapour exchange coefficients in the canopy, c) increase in light penetration to the lower part of the canopy due to the fluttering of leaves by moving air. As a result, photosynthesis and transpiration of transplants are enhanced and their growth is promoted. In addition, uniformity of microenvironments over and within the canopy promotes uniform growth of transplants.

Also, a combination of reduced relative humidity and fluttering of leaves within the canopy makes the transplants compact in shape and vigorous. Development of plants is significantly influenced by temperature, photoperiod, and light quality. These environmental factors can be controlled precisely in the closed system, so that development of flower buds, bolting, stem elongation of transplants can be controlled easily in the closed system [12,13,14].

8. Value-added transplant production in the closed system

Using environmental control function of the closed system, value-added transplants can be produced relatively easily. The feature descriptions of the value addition are summarized below:

- Number of nodes below the first flower cluster of tomato plants can be set at about 8 in summer.
- Enhanced flower bud differentiation and growth of pansy and strawberry transplants in summer by providing relatively low temperatures.
- Retarded bolting of oriental spinach varieties in summer by providing a light period shorter than the critical photoperiod (11 hours/day)
- Increased number of runner plants obtained from strawberry mother plants by CO₂ enrichment and a photoperiod of 16 hours/d.
- Production of virus-free sweet potato transplants using single node leafy cuttings as explants.
- Uniform growth of cucumber and tomato seedlings used for grafting as scions and stock plants throughout the year.
- Enhanced nursing and acclimatization of grafted cucumber, watermelon, eggplant and tomato transplants.

- Production of vigorous Chinese cabbage, broccoli and cabbage transplants with short but thick hypocotyls.
- Enhanced or controlled flower bud differentiation and bolting of static (*Limonium latifolium*) and *Eustoma russellianum* Don. transplants.
- Year round production of herb, lettuce and chicory transplants from hydroponic culture.

Some examples of transplants produced in the closed system are also illustrated in this section. All photographs shown in this section were taken in Japan during 2000-2003.

8.1. TOMATO (*LYCOPERSICON ESCULENTUM* MILL.)

Tomato seedlings, 14 days after sowing, grown in the closed system in 128, 200 and 288-cell trays were not significantly different from each other (Figure 8). In the greenhouse, the growth of tomato transplants grown on 200 and 288-cell trays is restricted due to the high planting density. Thus, we can double the planting density in the closed system with no retarded growth compared with the greenhouse.

Development of the first flower bud and its growth were enhanced by optimal control of temperature, PPF and photoperiod in the closed system, which would result in earlier harvest of tomato fruits in the greenhouse [14].

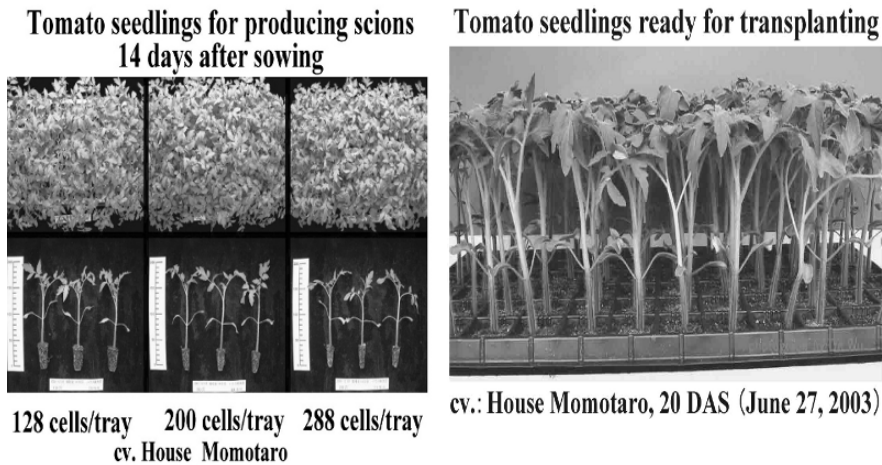


Figure 8. Tomato seedlings grown in the closed system in 128, 200 and 288- cell trays (left). There are no significant differences in growth among the treatments. The standard number of cells is 128 or 72 per tray when using the greenhouse. Thus, the transplanting density per tray can be at least 1.5 (=200/128) to 2.2 (=288/128) times higher in the closed system than in the greenhouse. Tomato seedlings grown in the closed system 20 days after sowing (DAS) (right). The growth is uniform over the tray.

8.2. SPINACH (*SPINACIA OLERACEA*)

Spinach transplants were more vigorous when grown for 14 days after sowing on 288-cell trays in the closed system than when grown on 144-cell trays in the greenhouse (Figure 9). Namely, planting density can be doubled in the closed system compared with that in the greenhouse.

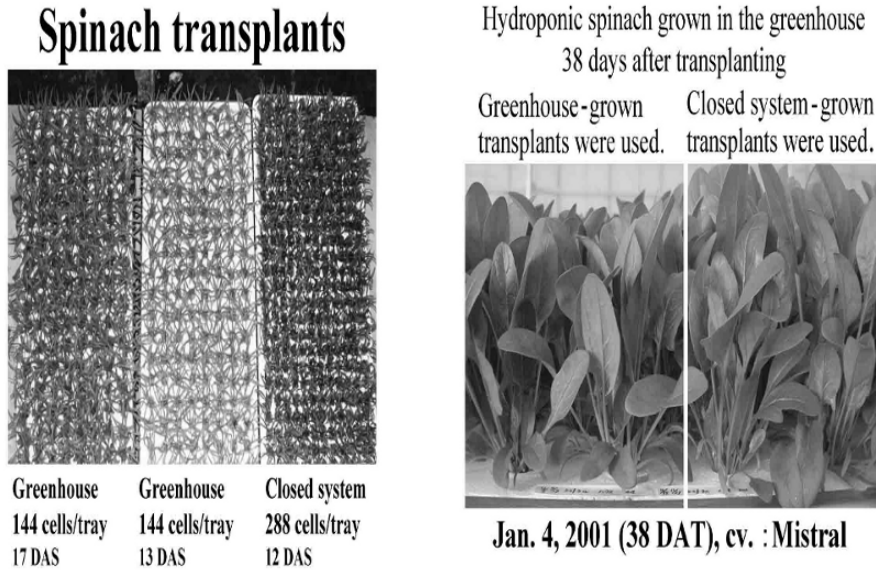


Figure 9. Spinach transplants grown for 12 days using the 288-cell trays in the closed system are greater, greener and more vigorous than those grown for 13 or 17 days using 144-cell trays in the greenhouse (left). Spinach plants at harvest, grown using a hydroponic system in the greenhouse (right). The growth of spinach plants using closed system-grown transplants was greater than that using greenhouse-grown transplants.

Bolting of spinach could be inhibited during transplant production by short photoperiod treatment in the closed system, which resulted in delayed bolting when they were subsequently grown under long photoperiod in the greenhouse [15]. It is essential that bolting in spinach plants at the time of harvest be delayed in order to keep their economic value high.

8.3. SWEET POTATO (*IPOMOEA BATATAS* L. (LAM.))

A single node cutting each with one unfolded leaf of sweet potato could be grown to a transplant within 14 days. In the greenhouse, it takes at least 20 days, and normally 25 days (Figure 10) [16]. In the closed system, virus-free transplants can be produced easily, which increases the economic values of vegetatively propagated transplants, such as sweet potato transplants.

Sweet potato Single Node Cutting (Day 0) and Transplants 14 days after Transplanting

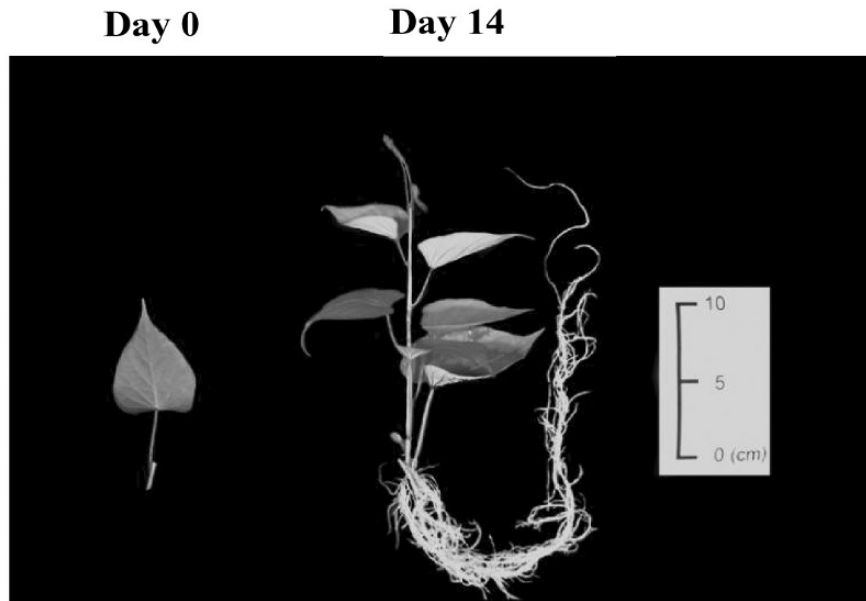


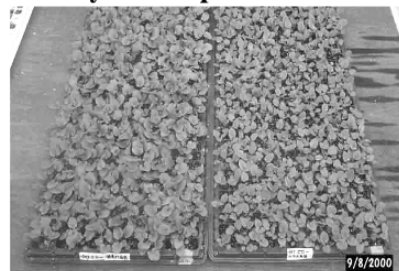
Figure 10 Sweet potato single node cutting with one leaf (Left, Day 0) and the transplant with 5 unfolded leaves 14 days after transplanting the single node cutting in the closed system (Right). The single node cutting with one leaf can be wilted easily in the greenhouse and it takes 3-4 weeks to grow to the transplant like the one shown above.

Pansy seedlings ready for potting 29 DAS (August 10, 2000)



Closed system Greenhouse
cv. Iona Yellow

Pansy Transplants 29 DAS



Closed system Greenhouse

Figure 11. Pansy transplants 29 days after sowing (DAS) in the closed system and in the greenhouse. Transplants grown in the closed system are more vigorous and uniform in growth compared with those grown in the greenhouse.

8.4. PANSY (*VIOLA X WITTROCKIANA* GAMS.)

Pansy transplants were more uniform and vigorous with higher percent of saleable transplants when grown in the closed system than in the greenhouse (Figure 11). Growth of pansy transplants was significantly greater when grown in the closed system than in the greenhouse [17]. Pansy transplants grown in the closed system and moved to a greenhouse flowered earlier than those grown from the beginning in the greenhouse (Figure 12).

Pansy Transplants at Shipping 64 DAS



Closed System

Greenhouse

Figure 12. Potted pansy plants 64 days after sowing (DAS) ready for shipping. The plants in Left were grown for the first 29 days in the closed system and then grown for 35 (= 64 - 29) days in the greenhouse. Many plants in Left are flowered due to the enhanced flower bud growth compared with those grown for 64 days in the greenhouse.

8.5. GRAFTED TRANSPLANTS

In order to produce high quality grafted transplants, it is essential to obtain rootstocks and scions in uniform size and shape (Figure 13). It is also essential to control the environment precisely for a few days after grafting to promote a successful union of grafted parts. The closed system is suitable to realize such environmental conditions. We could produce high quality grafted transplants of tomato and eggplant.

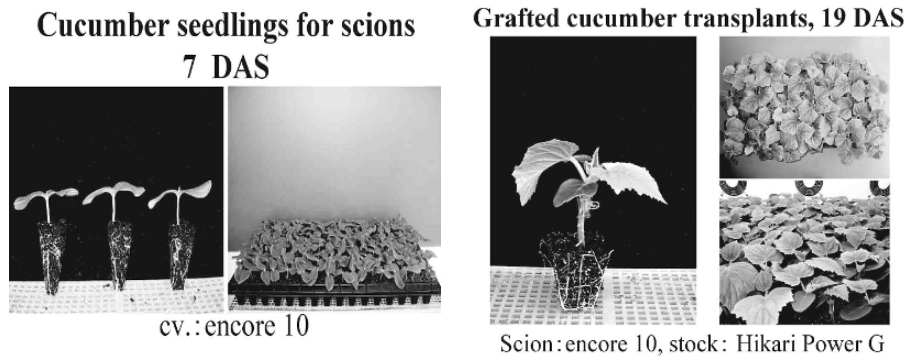


Figure 13. Uniform growth of cucumber seedlings to be used as scions for grafting (left) and grafted cucumber transplant 19 days after sowing (DAS) (Left), produced in the closed system. The grafted transplants are compact and vigorous. Seedlings to be used as scions (upper right) and those to be used as root stock plants (lower right) were grown in the closed system. Percent success of grafting is above 90%.

8.6. VEGETABLE TRANSPLANTS FOR FIELD CULTIVATION

Vigorous and compact transplants of eggplant and chinese cabbage could be produced successfully in the closed system with an electricity cost of about 1 US cent per transplant [18].

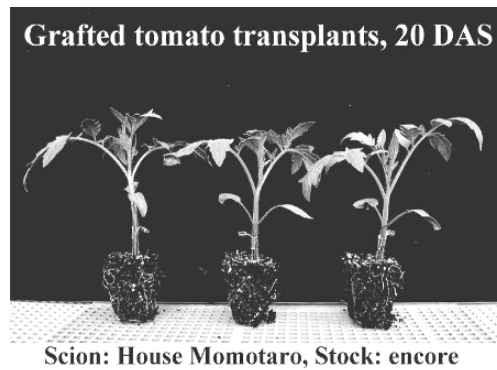


Figure 14. Grafted tomato transplants 20 days after sowing.

Transplants for field cultivations such as lettuce and cabbage plants are often transplanted by using transplanting machine. For transplanting with a high percent of success, transplants are required to be uniform in growth, vigorous and compact in shape. Transplants grown in the closed system show such characteristics to be suited for automatic transplanting machine, as shown in Figures 14-15.

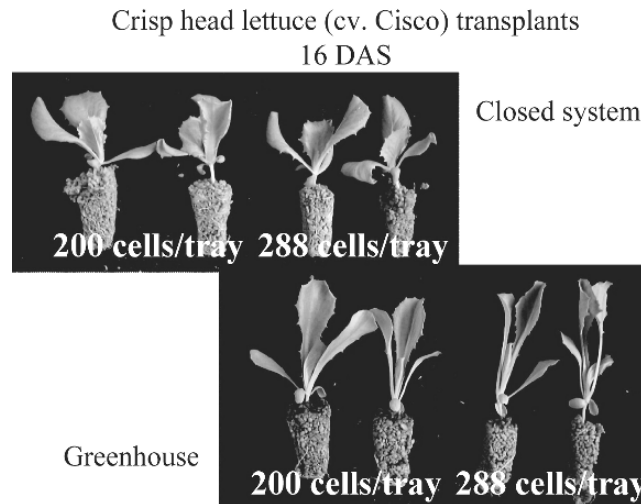


Figure 15. Crisp head lettuce transplants grown for 16 days after sowing in the closed system using 200 and 288-cell trays show wider leaves and shorter hypocotyls than those grown for 16 days after sowing in the greenhouse.

9. Increased productivity to that of the greenhouse

Increase in yearly productivity per floor area of the closed system is about 10 times than that of a standard greenhouse for various kinds of transplants (Table 6). The ratio of planting area to floor area is usually 0.8 in the greenhouse, while it is 2.0 to 3 in the closed system with use of the multi-shelves (4 or 5 shelves). Thus, planting area per floor area of the closed system is about 2-3 times that of the greenhouse. On the other hand, use of multi-shelves is not practical in the greenhouse using solar light because of obstruction of solar light by the multi-layered shelves.

The planting density per tray area can be about 2 times, as described previously. The physical and physiological reasons described in Section 7.9 allows plants to grow without stem elongation and reductions in rates of net photosynthesis and transpiration, and thus without growth retardation.

The production period can be reduced by about 30%, mainly due to the promotion of photosynthesis by CO₂ enrichment at 800-1,000 $\mu\text{mol mol}^{-1}$, and control of horizontal air current over and within the transplant canopy under an optimal combination of temperature, PPF and soil-plant water relations.

Annual operation rate of the closed system is increased by 20% due to the shortened production period even in summer and winter. Percentage of saleable plants and/or sales price can increase by about 10% due to their high quality and uniform growth. Thus, the total increase in yearly productivity per floor is higher than 7-11 fold ($=2.5 \times 2.0 \times 1.1 \times 1.3 \times 1.2 \times 1.1$), with the average of 10.

Table 6. Annual production capacity of the closed system in comparison with that of the greenhouse.

Item	Ratio to the greenhouse	Accumulated ratio	Remark
Increase in ratio of production area to floor area by use of multi-layered shelves	2-3(=1.6/0.8-2.4/0.8)	2-3	closed system: 1.6-2.4, greenhouse: 0.8
Increase in planting density by providing a higher air current speed within the transplant canopy	2	4-6 (=2x2-2x3)	
Increase in percent marketable transplants by providing the favourable environments	1.1	4.4-6.6	
Reduction in production period by providing the favourable environments	1.3	5.7-8.6	
Increase in annual operation rate	1.2	6.8-10.3	
Increase in sales price due to the high quality	1.1	7.5-11.3 (Average: 10)	

10. Costs for heating, cooling, ventilation and CO₂ enrichment

10.1. HEATING COST

Heating cost of the closed system is a few percent of that of a greenhouse during the winter even in northern countries, because all the walls/roofs of the closed system are covered with thermal insulators, such as formed polystyrene sheets, which are about 15 cm thick.

The heat transmission coefficient of 10-cm thick insulated walls ($0.28 \text{ W m}^{-2} \text{ K}^{-1}$) is about 1/15th of that of a greenhouse with a double-layer thermal screen ($4 \text{ W m}^{-2} \text{ K}^{-1}$). Furthermore, the wall and roof areas of the closed system are only about 1/7th of those of the greenhouse. Since the heating load is proportional to the heat transmission coefficient multiplied by the wall and roof areas, the heating load of the closed system is about 1/98th (=1/14 x 1/7) of the greenhouse. If the thickness of thermal insulators is 15 cm which corresponds to a heat transmission coefficient of $0.2 \text{ W m}^{-2} \text{ K}^{-1}$, the heating load is further reduced to 1/140th (=1/20 x 1/7).

When the lamps are turned on, the air in the closed system needs to be cooled by an air conditioner even when the outside temperature is below -30°C . Thus, lighting can be done at night to reduce cooling and/or heating costs when the air temperature at night is low. Also, off-peak electricity at night can be used with a reduced electricity cost.

During the dark period, heat generated by fans and other equipment in the closed system is often enough for keeping the air temperature at a set point in the closed system when

outside temperature is around -5°C or higher. Even when the outside temperature is -30°C , only a little heating is necessary during dark period, and an air conditioner driven by electricity can be used as a heater.

10.2. COOLING LOAD AND ELECTRICITY CONSUMPTION

Cooling load of the closed system is almost equal to the heat generated by lamps, fans, etc. in the closed system, because heat entering into the closed system from outside is negligibly small due to its thermally insulated structure. In other words, outside temperature does not affect the cooling load of the closed system. Then, electricity consumption for cooling the closed system is heat generated by lamps etc. divided by the C.O.P. for cooling of the air conditioner. C.O.P. for cooling is defined as the cooling capacity divided by electricity consumption of an air conditioner, both in a unit of W (Watt). The C.O.P. of a recent air conditioner for home use is 4-5 during summer (25°C inside and 35°C outside the closed system), and is 8-10 during winter (25°C inside and -5°C outside) in Tokyo area, Japan. The C.O.P. for cooling of the closed system increases as the air temperature difference increases (when outside temperature is higher than inside temperature) [19].

Then, during winter, the cooling cost of a closed system should be lower than the heating cost of a greenhouse in northern and temperate countries, because total wall area and heat transmission coefficient of the closed system are 1/7th and 1/15th, respectively, of those of the greenhouse. Since electricity consumption for lighting of the closed system is almost constant throughout the year, the electricity consumption for lighting, cooling and other equipment does not change significantly throughout the year.

10.3. COOLING COST

In the case that the C.O.P. is 4 in summer, electricity consumption for cooling accounts for about 20% of electricity consumption for lamp lighting and cooling. Lighting and cooling account for 82% and 15% respectively, of total electricity consumption of the closed system (Table 7).

Costs for fans, heating, and others account for the rest of 3%. When the percentages are significantly different from those given in Table 7, the points listed below needs to be examined.

- Are all the air conditioners turned on even during the dark period and the winter? If so, turn off some of them.
- Are the air conditioners maintained well? (Are the air filters regularly washed and dried? Are there any obstacles in front of the condenser or the evaporator, which cause the reduction in air flow rate?)
- Are the thermal insulators thick enough and well installed not to cause the excessive heat flow through the thermal insulators?
- Is the type of air distribution fans appropriately chosen and well installed to produce uniform air flow across each shelf?
- Is the type of fluorescent lamps appropriately chosen and well maintained? (No dusts on the tube surfaces and reflective sheets?)

Table 7. Percent annual electricity cost by its components in the closed system (Ohyama et al. 2002) [19].

No.	Equipment	Percentage	Remark
1	Lamps for lighting	82	40W high frequency lamps with an inverter
2	Air conditioners	15	For home-use air conditioners with annual average C.O.P. of 5 in a cooling mode
3	Others	3	For air distribution fans, pumps for nutrient solution supply, an environmental control unit, a CO ₂ supply unit, etc.

When a home-use air conditioner is used, the C.O.P is around 9 when outside air temperature is lower than 20 and room air temperature is kept at about 28°C (Figure 16).

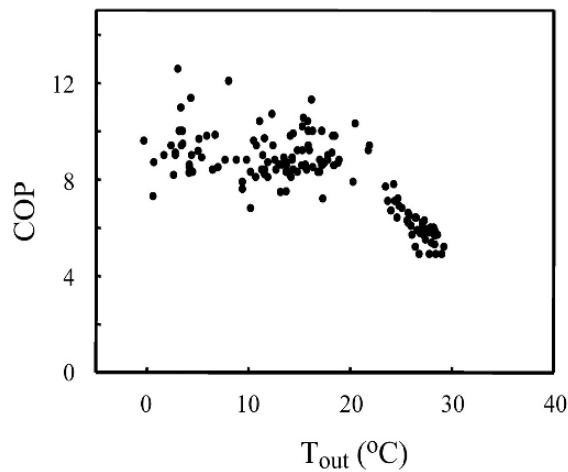


Figure 16. C.O.P. (Coefficient of performance of the closed system with a refrigerator) for cooling is as high as 8-10 when air temperatures inside and outside the closed system are 25°C and 0-20°C, respectively. Redrawn from Ohyama et al. (2002) [19].

In the case that the C.O.P. is 9 in winter, electricity consumption for cooling accounts only for about 10% of the total electricity consumption of the closed system [19].

10.4. ELECTRICITY CONSUMPTION

In northern countries such as the Netherlands, 50-100 $\mu\text{mol m}^{-2} \text{s}^{-1}$ of supplemental lighting in a greenhouse for growing crops is currently common in winter [20], because the supplemental lighting significantly promotes the growth of seedlings, leafy vegetables and other greenhouse crops.

When supplemental lighting of 70 $\mu\text{mol m}^{-2} \text{s}^{-1}$ was given during winter in New Hampshire, USA, for 11h d^{-1} using high pressure sodium lamps, daily integral of PPF in a greenhouse was increased by 45% (from 6.18 to 8.96 $\text{mol m}^{-2} \text{d}^{-1}$), resulting in an increase in daily average of PPF from 156 to 226 $\mu\text{mol m}^{-2} \text{s}^{-1}$ [21]. This means that electricity consumption for lamp lighting at PPF of 226 $\mu\text{mol m}^{-2} \text{s}^{-1}$ in the closed system is only 3.2 ($=226/70$) times that for supplemental lighting in the greenhouse during winter. The daily average PPF of 226 $\mu\text{mol m}^{-2} \text{s}^{-1}$ can be provided by six 40W fluorescent lamps easily if the lamps are placed 40 cm above the plants with photoperiod of 11h d^{-1} . The daily average PPF of 250 $\mu\text{mol m}^{-2} \text{s}^{-1}$ is achieved if the photoperiod is set at 16h d^{-1} instead of 11h d^{-1} with the same set-up of fluorescent tubes. The daily-integrated PPF over 16h is 16.4 $\text{mol m}^{-2} \text{d}^{-1}$, which is equal to the daily integral of PPF on a clear day in September in Tokyo. By doing so in the closed system, no heating cost is required and no condensation occurs on the inside surfaces of walls during winter.

Electric energy consumption for lighting is relatively small, because PPF (photosynthetic photon flux) of 200-300 $\mu\text{mol m}^{-2} \text{s}^{-1}$ is high enough for production of transplants with LAI (leaf area index) of 2-4, the transplant production period is 15-30 days, planting density is 400-1000 plants m^{-2} , and transplants are placed 20-30 cm below fluorescent lamps with reflectors, which results in a high ratio of light energy received by cell trays to light energy emitted by lamps. The short distance of 20-30 cm can be achieved because the outer surface temperature of fluorescent tubes is about 40°C when the surrounding air temperature is 25°C. Surface temperatures of high pressure sodium and metal halide lamps are about 100°C, so that they cannot to be placed close to the plants. Table 8 shows estimated electricity consumption and electricity cost in the closed system.

10.5. ELECTRICITY COST IS 1-5% OF SALES PRICE OF TRANSPLANTS

Electricity consumption per transplant is 67Wh when 200-cell plug trays are used, and is 34Wh when 400-cell plug trays are used (Table 8). It costs about 0.5 US cent per transplant when 200-cell plug trays are used and about 0.25 US cent per transplant when 400-cell plug trays are used. Then, the total electricity consumption per transplant is roughly 90Wh ($= 67 \times (100/85)$) when 200-cell trays are used, and it costs about 0.6 US cent under current conditions in Japan. The cost will be half if 400-cell plug trays are used, because the lighting cost per tray is constant. On the other hand, the sales price of transplants is typically 20 US cents to 1 US dollar per transplant. Thus, in Japan, the electricity cost currently accounts for 1 to 5% of the sales price of transplants. This percentage can be further reduced by, for example, using a co-generation system and an advanced lighting system.

Table 8. Sample calculation of electricity consumption and electricity cost for lighting in the closed system.

Item	Electricity consumption	Remarks
One span (1.4 m long) of shelf	240W	Six 40W fluorescent lamps (1.2 m long). Four plug trays each with 30 cm wide per span.
One plug tray	60W	$60 = 240/6$
One plug tray for one day	960Wh	$960 = 60 \times 16$ (16 h d-1 of photoperiod is assumed)
One plug tray for 2 weeks	1.34 kWh	$13,440 = 960 \times 14$. Transplant production period of 2 weeks is assumed.
One transplant for 2 weeks	67Wh for a plug tray with 200 cells or 34 Wh for a plug tray with 400 cells	$67.2 = 13,440/200$ $33.6 = 13,440/400$
Cost per transplant	0.67 Japanese Yen or 0.5 US cent for 67W, and 0.34 Japanese Yen or 0.25 US cent for 34Wh.	Ten Japanese Yen/kWh (8 US cents/kWh) in Tokyo as of 2004.

Notes: 1) Price of electricity in Tokyo, Japan as of 2004 was used, 2) 1 W = 1 J s⁻¹, 3) 1 Wh = 3600 J, 4) 1 US\$ = 120 Yen as of 2004

10.6. RELATIVE HUMIDITY

When lamps are turned on and an air conditioner is also turned on for cooling, dehumidification and collection of condensed water at cooling panels of air conditioner occurs. Thus, relative humidity in the closed system naturally tends to be about 70% during the photoperiod when the closed system is filled with transplants.

During the dark period, the relative humidity in the closed system tends to be about 90% or higher as it is in the greenhouse at night if air is not dehumidified by an air conditioner. This high relative humidity in the closed system during the dark period can be reduced to 70-80% at minimal electricity cost by operating the air conditioner intermittently using its dehumidification mode that requires minimum electricity.

When heat-generating equipment such as an air pump and water pump is operated during the dark period, the air conditioner is naturally operated to keep the air temperature at a set point, resulting in a reduction in relative humidity.

10.7. PAR UTILIZATION EFFICIENCY

In the closed system, PAR (photosynthetically active radiation) utilization efficiency, defined as the percent of chemical energy fixed by plant photosynthesis over PAR

energy emitted from fluorescent tubes, is about 2 times higher than that in the greenhouse, when LAI (leaf area index) of the canopy is about 2.5. The reasons for the high efficiencies of the closed system is that PPF is controlled in a range $0\text{-}300\ \mu\text{mol m}^{-2}\text{s}^{-1}$ depending upon the growth stage and CO_2 concentration is kept at $800\text{-}1100\ \mu\text{mol mol}^{-1}$ with an air horizontal current speed of $0.1\text{-}0.5\ \text{ms}^{-1}$.

Since about 25% of electric energy is converted into PAR energy by fluorescent lamps, electric energy conversion efficiency at the end of transplant production period is about 2.8% and its average efficiency over the production period is about 0.3%. For comparison, the percent conversion from electrical energy to PAR energy is about 30-35% for high-pressure sodium lamps, and about 27-32% for high-pressure metal halide lamps, and about 10-15% for LED (light emitting diode) lamps.

10.8. LOW VENTILATION COST

In the closed system, ventilation is minimized in order to minimize the release of water and CO_2 supplied into the closed system to the outside of the closed system, minimize the environmental disturbance by the weather, and protect insects and/or pathogens from entering into the closed system. In most commercialized closed systems, no ventilation unit is installed, so that its initial investment cost is zero.

In a closed system developed for research purposes, a small ventilation unit is sometimes installed to keep the air pressure inside the closed system relative to the air pressure outside the closed system slightly positive. This positive air pressure is required to prevent insects and dusts from entering through the leakage of the closed system.

Increasing the ventilation rate can reduce the cooling cost of an air conditioner in case that the actual and set point of air temperatures are higher inside than outside the closed system. However, this small decrease in cooling cost does not compensate for the advantages of minimum ventilation. The number of air exchanges per hour of the closed system, which is defined as hourly ventilation rate divided by the air volume of the closed system, needs to be kept at $0.01\text{-}0.02\ \text{h}^{-1}$. In case that the closed system is completely airtight, accumulation of ethylene gas in the closed system may cause a physiological damage to the transplants. In this case, a little ventilation is required to avoid the ethylene accumulation in the closed system.

10.9. CO_2 COST IS NEGLIGIBLY SMALL

Cost for CO_2 enrichment is negligible due to the minimum ventilation. Nearly 90% of CO_2 supplied to the closed system is fixed by plant photosynthesis (Figure 17). The remaining 10% is released to the outside of the closed system. The same applies for CO_2 produced by respiration of microorganisms, if they are present. CO_2 produced by respiration of plants and microorganisms is mostly accumulated in the system during the dark period and reaches $1500\ \mu\text{mol mol}^{-1}$ or higher at the end of dark period [22]. This accumulated CO_2 is reused as a carbon source for photosynthesis during the following photoperiod.

The price of liquid CO_2 in a container is 14-15 US cents per kg in Japan, and tens of thousands of transplants can be produced using 1kg of CO_2 in the closed system. Thus, cost of CO_2 per transplant is negligibly small compared with other operation costs.

CO₂ utilization efficiency

$$= \frac{\text{Fixed}}{\text{Supplied}} = 192/221 = 0.87$$

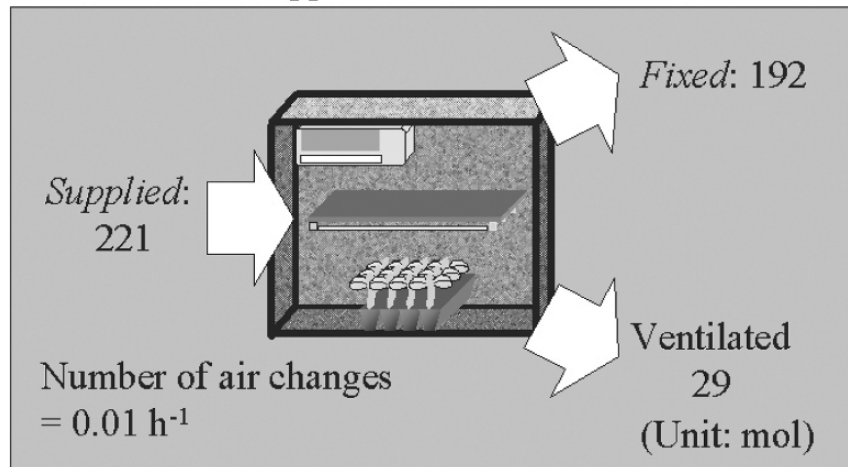


Figure 17. CO₂ utilization efficiency of the closed system, which is defined as the weight ratio of fixed CO₂ by plant photosynthesis to supplied CO₂ during the transplant production. Redrawn from Yoshinaga et al. (2000) [22].

10.10. WATER REQUIREMENT FOR IRRIGATION

In the closed system, only a few percent of irrigated water is discharged as water vapour to the outside along with the restricted infiltrated air [20]. Another few percent of irrigated water is stored in transplants as they grow and/or in substrate filled in cell trays. The rest of approximately 95-98% of evapotranspired water is condensed at the cooling panel of an air conditioner and is collected as drained water, which is reused as irrigation water in the following transplant production periods (Figure 18, Left). In other words, if evapotranspired water is not reused for irrigation, as in the greenhouse, an amount of water required for irrigation would be 20 to 50 times that of the closed system (Figure 18, Right).

Closed systems can use two kinds of irrigation systems. One is a closed water circulation system, in which water is circulated from a tank via cell trays to the tank again for collection and reuse of drained water. The other is a one-way irrigation system in which water supplied from a tank to cell trays, and all of it is evapotranspired from the cell trays with transplants, resulting in no water drainage from cell trays. The latter system is simpler and preferable compared with the former system.

Closed systems for high quality transplants

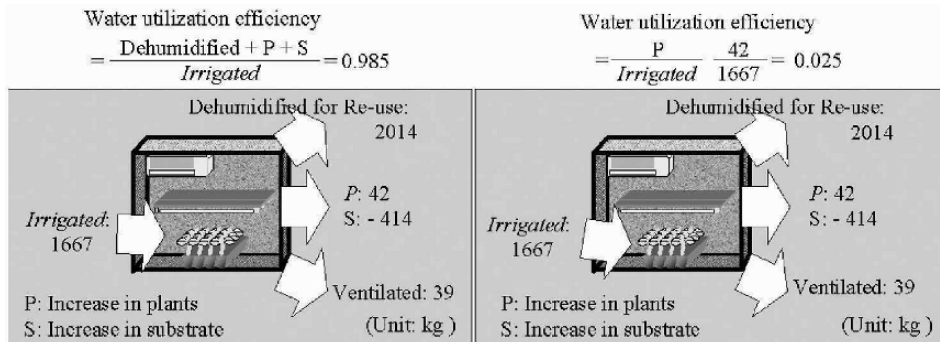


Figure 18. Water utilization efficiency of the closed system, which is defined as the weight ratio of water captured in plants or substrate to the supplied water during the transplant production. Redrawn from Ohyama et al. (2000) [14]. Left: Water collected at the cooling panel (evaporator) is reused for irrigation. Right: Water collected at the cooling panel (evaporator) is not reused for irrigation.

10.11. DISINFECTION OF THE CLOSED SYSTEM IS EASY

The evapotranspired water is basically aseptic and water collected at the cooling panels (or an evaporator) of an air conditioner is also virtually aseptic if no microorganisms exist in the water collection system and if the water collection system consists of tubes and a tank only [20].

In one of our closed systems, the substrate (either in bags or cell trays) is disinfected by submerging it in hot water (60°C in winter and 70°C in summer) in a water tank overnight, heated by a solar heater installed on the roof of the closed system. Water collected at the cooling panels is sterilized either by heating it in the hot water from a solar collector, by irradiating it with ultraviolet radiation lamps, and/or by supplying ozone gas to the water. A small hole for minimum ventilation is covered with a filter to prevent insects, dust and microorganisms from entering the closed system. Thus, disinfection of the closed system is relatively easy and inexpensive.

10.12. SIMPLER ENVIRONMENTAL CONTROL UNIT

An environmental control unit including an irrigation sub-unit is much simpler for the closed system than for the greenhouse, because the environment in the closed system is not disturbed by the weather outside the closed system. On the other hand, the greenhouse environment is considerably disturbed by the weather, especially by solar radiation. Also, the set point of each environmental factor in the closed system can be basically predetermined once the seeds are sown or cuttings are transplanted.

Furthermore, in the closed system, the amount of water required for irrigation is predictable when environmental set points are determined for each growth stage of transplants, because the air temperature, relative humidity and horizontal air current speed are controlled precisely at the set points. The same applies for CO₂ enrichment. This makes the control algorithms of an irrigation unit for the closed system much

simpler than the one for the greenhouse. On the other hand, in the greenhouse, a sophisticated control unit is necessary if irrigation is to be conducted according to the changes in solar radiation.

10.13. EASIER PRODUCTION MANAGEMENT

It is easier to predict growth and development of transplants under precisely controlled environments in the closed system than in the greenhouse. This also makes it easier to manage transplant production, i.e., to meet the customer's demand easier. Also, computer simulations using mathematical models can be practically used in production management. The costs for electricity, labour, etc. can be also predictable [21].

10.14. THE CLOSED SYSTEM IS ENVIRONMENT FRIENDLY

The closed system is an environmentally friendly system in the sense that:

- It needs only a few percent of water that is consumed for irrigation in the greenhouse and it does not release waste water containing fertilizers, pesticide and/or fungicide, etc. to the outside of the closed system,
- It also needs much less pesticides or insecticides, except for an emergency, and needs much less fertilizers than the greenhouse does, because of no drained water from the closed system.
- The main components of the closed system are mass produced for home use or industrial use, so that their recycling and reuse systems have been already established, The floor area of the closed system is only 10% of the greenhouse floor area for the same transplant production capacity, so that material resources and labour for constructing the production system can be saved significantly,
- Nearly 90% of CO₂ supplied for promoting photosynthesis of plants in the closed system is fixed by plants, so that its contribution to the increase in atmospheric CO₂ concentration is negligible. On the other hand, in the greenhouse, roughly 50% of CO₂ supplied is released to the outside due to ventilation [22],
- Heating load is negligibly small, so that oil or natural gas is not required for heating in the closed system, and
- Percentages of saleable plants are higher in the closed system than in the greenhouse, so that amount of wasted plants is less in the closed system than in the greenhouse.

In greenhouses with supplemental lighting, light pollution at night, meaning the loss of light emitted from lamps to the outside, has become a problem in northern countries where supplemental lighting are common in winter. In the near future, a 'zero emission plant production system' meaning no emission of wastes, resulting in minimum use of resources, will be realized by advancing the concept and methodology of the closed system. These advantages of the closed system can more than overcompensate for its use of electricity for lighting and cooling. Table 9 summarizes materials and energy needed in the closed system in comparison with those in the greenhouse.

Closed systems for high quality transplants

Table 9. Materials and energy needed in the closed system in comparison with those in the greenhouse.

Material and/or energy	Purpose for consumption
Electric energy consumed in the closed system only	Lighting and cooling
Electric energy consumed in the greenhouse only	Ventilation, shading, supplemental lighting, etc.
Oil, natural gas etc. consumed in the greenhouse only	Heating
Water (Its consumption in the closed system is ca 5% of that in the greenhouse in case that evapotranspired water is collected at the cooling panel of the air conditioner and the collected water is re-used in the closed system.)	Irrigation
Pesticide and insecticide (Their consumptions in the closed system are ca. 10% of those in the greenhouse.)	Prevention of disease
Substrate and plug trays (Their consumptions in the closed system are ca. 50 % of those consumed in the greenhouse because the planting density in the closed system is 2 times that in the greenhouse.)	Plug transplant production
Fertilizer (Its consumption in the closed system is ca. 70% of that consumed in the greenhouse, because no fertilizer-containing water is wasted from the closed system.)	Fertilization
Seeds (Amount of seeds consumed in the closed system is ca. 90% of that consumed in the greenhouse, because percent yield of transplants is about 10 % higher in the closed system.)	Seeding
CO ₂ (Its consumption in the closed system is about 60% of that in the greenhouse due to a considerably lower ventilation rate in the closed system.)	CO ₂ enrichment

10.15. THE CLOSED SYSTEM IS SAFER

The air temperature in the closed system does not rise significantly even in case of electric failure during the daytime on sunny and hot days, because the solar radiation does not transmit the opaque wall of the closed system. On the other hand, the air temperature in the greenhouse may rise quickly and may reach the air temperature much higher than the outside air temperature in case of electric failure especially when fan ventilation is employed or ventilators are closed. Table 10 shows the possible problems and measures in the closed system and the greenhouse in case of electric failure during the day on sunny and hot days and during the night.

Table 10. Possible problems and measures in case of electricity failure in the closed system and the greenhouse respectively.

Closed system/greenhouse	Light/Dark period	Possible problem	Possible measures against the problem
Closed system	Dark	The room air temperature reaches the outside air temperature within 1-2 hours.	No measure is needed if the transplants can survive at the outside air temperature. If they cannot survive at the outside temperature, some heat emission or absorption substances needs to be supplied.
Closed system	Light	It becomes dark in the closed system. The room air temperature reaches the outside air temperature within 1-2 hours.	No measure is needed if the transplants can survive at the outside air temperature and the electricity failure can be recovered within 24 hours.
Greenhouse	Dark (Night)	The room air temperature reaches the outside air temperature within 1 hour.	No measure is needed if the transplants can survive at the outside air temperature. If the outside temperature is too low for transplants to survive, the transplants can be covered with a plastic film to keep the temperature under cover higher than the room temperature.
Greenhouse	Light (Day)	The room air temperature can be considerably higher than the outside air temperature within half an hour on fine and hot days, especially when ventilators and/or shading screen are open.	The ventilator openings are controlled manually to decrease or increase the room air temperature, although the transplants can still be damaged considerably on clear and hot days or cloudy and cold days.

11. Conclusion

Developing a system for producing high quality transplants at low costs is an important research subjects in the 21st century for resource saving, environmental conservation and biomass production. It can be concluded that quality and productivity of transplants are definitely higher and the growth period of transplants can be shortened by 30% or over when produced in the closed system using lamps than in the greenhouse using sunlight. The closed system is energy and material efficient especially with respect to the amounts of water required for irrigation and energy required for cooling in summer and for heating in winter. In addition, the closed system is an environmentally friendly system for plant production in the sense that it does not release polluted water that

contains fertilizers to the outside and that it seldom requires pesticide and fungicide. Initial and operation costs of the closed system per annual production of transplants can be lower than or comparable to those of the greenhouse, and the closed system was first commercialized in 2002 in Japan, and has been used at 23 locations in 2004 in Japan. It is expected that the closed system is introduced in other Asian countries in 2005.

Acknowledgement

The author would like to express his special thanks to K. Ohyama for his valuable advice and to F. Afreen and H. Toida for their technical help. Special thanks are also extended to K. Okabe, Taiyo Kogyo Co. for permission to use the photographs of transplants.

References

- [1] Kozai, T.; Kubota, C.; Chun, C. and Ohyama, Y. (2000) Closed transplant production systems with artificial lighting for quality control, resource saving and environment conservation. In: Proceedings of The XIV Memorial CIGR World Congress 2000, Tsukuba, Japan; pp.103-110.
- [2] Kozai, T.; Chun, C.; Ohyama, K. and Kubota, C. (2000) Closed transplant production systems with artificial lighting for production of high quality transplants with environment conservation and minimum use of resource. In: Proceedings of The 15th Workshop on Agricultural Structures and ACESYS (Automation, Culture, Environment & System) □ Conference, Tsukuba, Japan ; pp.110-126.
- [3] Kurata, K. and Kozai T (Eds.) (1992) Transplant Production Systems. Kluwer Academic Publishers, Dordrecht, The Netherlands.
- [4] Aitken-Christie, J.; Kozai, T. and Smith, M.A.L. (1995) Automation and environmental control in plant tissue culture. Kluwer Academic Publishers, Dordrecht, The Netherlands.
- [5] Kozai, T. (2004) Closed systems with artificial lighting for high quality transplant production at low costs using minimum resources. In: Kozai,T.; Fawzia, F. and Zobayed, S.M.A. (Eds.) Photoautotrophic (Sugar-Free Medium) Micropropagation as a New Propagation and Closed Transplant System. Springer, Dordrecht, The Netherlands.
- [6] Kozai, T.; Kubota, C.; Heo, J.; Chun, C.; Ohyama, K.; Niu, G. and Mikami, H. (1998) Towards efficient vegetative propagation and transplant production of sweet potato (*Ipomoea batatas* (L.) Lam.) under artificial light in closed systems. In: Proc. of International Workshop on Sweet potato Production System toward the 21st Century, Miyazaki, Japan; pp. 201-214.
- [7] Kozai, T. (1998) Transplant production under artificial light in closed systems, In: Lu, H.Y.; Sung, J.M. and Kao, C.H. (Eds.) Asian Crop Science 1998, Taichung, Taiwan; pp. 296-308.
- [8] Kozai, T.; Ohyama, K.; Afreen, F.; Zobayed, S.; Kubota, C.; Hoshi, T. and Chun, C. (1999) Transplant production in closed systems with artificial lighting for solving global issues on environmental conservation, food, resource and energy. In: Proc. of ACESYS III Conference, Rutgers University, CCEA (Center for Controlled Environment Agriculture); pp. 31-45.
- [9] Kozai, T.; Kubota, C.; Chun, C.; Afreen, F. and Ohyama, K. (2000) Necessity and concept of the closed transplant production system. In: Kubota, C. and Chun, C. (Eds.) Transplant Production in the 21st Century, Kluwer Academic Publishers, Dordrecht, The Netherlands; pp. 3-19.
- [10] Chun, C. and Kozai, T. (2001) A closed-type transplant production system. In: Morohoshi, N. and Komamine, A. (Eds.) Molecular Breeding of Woody Plants. Elsevier Science B.V., The Netherlands; pp. 375-384.
- [11] Kozai T.; Chun, C. and Ohyama, K. (2004) Closed systems with lamps for commercial production of transplants using minimal resources. Acta Hort. 630: 239-254.
- [12] Chun, C.; Watanabe, A.; Kim, H.H.; Kozai, T. and Fuse, J. (2000) Bolting and growth of Spinach (*Spinacia oleracea* L.) can be altered by using artificial lighting to modify the photoperiod during transplant production. Hort. Sci. 35: 624-626.
- [13] Kubota, C. and Chun C. (Eds.) (2001) Transplant Production in the 21st Century, Kluwer Academic Publishers, Dordrecht, The Netherlands; pp. 290.

- [14] Ohyama, K.; Manabe, K.; Omura, Y.; Kubota, C. and Kozai, T. (2003) A comparison between closed-type and open-type transplant production systems with respect to quality of tomato plug transplants and resource consumption during summer. *Environ. Control Biol.* 41: 57-61.
- [15] Kim, H.H.; Chun, C.; Kozai, T. and Fuse, J. (2000) The potential use of photoperiod during transplant production under artificial lighting condition on floral development and bolting, using *Spinacia oleracea* L. as a model. *Hort. Sci.* 35:43-45.
- [16] Lok, Y.H.; Ohyama, K.; Kubota, C. and Kozai, T. (2002) Sweet potato propagule production rate and electric energy consumption in a closed transplant production system as affected by planting density. *J. High Technol. Agric.* 14: 10-17. (JE).
- [17] Omura, Y.; Chun, C.; Kozai, T.; Arai, K. and Okabe, K. (2000) High quality plug-transplants produced in a closed system enables pot-transplants production of pansy in the summer. In: Kubota, C. and Chun, C. (Eds.) *Transplant Production in the 21st Century*, Kluwer Academic Publishers, Dordrecht, The Netherlands; pp. 145-148.
- [18] Ohyama, K.; Fujiwara, M.; Kozai, T. and Chun, C. (2001) Consumption of electric energy and water for eggplant transplant production in a closed-type transplant production system. *J. High Technol. Agric.* 13:1-6.(JE).
- [19] Ohyama, K.; Kozai, T.; Kubota, Chun, C.; Hasegawa, T.; Yokoi, S. and Nishimura, M. (2002) Coefficient of performance for cooling of a home-use air conditioner installed in a closed-type transplant production system. *J. High Technol. Agric.* 14: 141-146.(JE).
- [20] Ohyama, K.; Yoshinaga, K. and Kozai, T. (2000) Energy and mass balance of a closed-type transplant production system (part 2) - Water balance. *J. High Technol. Agric.* 12: 217-224. (JE).
- [21] Kubota, C. and Kozai, T. (2001) Mathematical models for planning vegetative propagation under controlled environments. *Hort. Sci.* 36: 15-19.
- [22] Yoshinaga, K.; Ohyama, K.; and Kozai, T. (2000) Energy and mass balance of a closed-type transplant production system (part 3) – Carbon dioxide balance. *J. High Technol. Agric.* 12: 225-231. (JE).

Note: Literature with '(JE)' at the end denotes that the paper is written in Japanese with English abstract and figure/table captions.

AERATION IN PLANT TISSUE CULTURE

Engineering aspects of vessel design

S.M.A. ZOBAYED

*Department of Plant Agriculture, University of Guelph, Guelph, Ontario,
N1G 2W1, Canada – Fax: 519-824-4120 - Email:
szobayed@uoguelph.ca*

1. Introduction

Aeration in a plant tissue culture vessel is an important issue because the tissue culture technology is inextricably bound-up with a requirement for sterility and preventing dehydration [1]. Imposing a capping system in a tissue culture vessel to maintain the sterility and to prevent dehydration of both tissues and nutrient medium restricts gas exchange between *in vitro* and surrounding outer atmosphere and leads to poor plant development with high mortality when relocated into the greenhouse for weaning. It is long believed that the growth of *in vitro* plants depends largely on the composition of the nutrients and thus efforts are mainly made to improve the composition of the growing medium. Researchers have already revealed that the growth and development of plants or explants produced *in vitro* can be seriously affected by the composition of the gaseous atmosphere [2,3,4]. Capping systems generally used in tissue culture vessels are screw caps, aluminium foils, transparent films such as polypropylene disc, standard plastic cap (Figure 1), etc. which are currently known to restrict the air exchange between the culture vessel and the outer atmosphere. In recent times, there has been much interest on the aeration of culture vessels to minimize the difference between the gaseous environment *in vitro* and the surrounding atmosphere of the vessel. The aeration of the culture vessel has proved to have many advantages over the conventional airtight system. A tissue culture vessel can be aerated by using microporous filter membranes, capping with loosely fitted lids, using thin diffusible films such as polypropylene films or forced aeration using an air pump. The process or the mechanism of aeration of a tissue culture vessel by using these systems may be different from each other and can influence the plant growth significantly. More clear idea of the mechanism of aeration of a plant tissue culture vessel can help to design a suitable vessel and thus to improve the growth and quality of plantlets. In the current article, mechanisms of different aeration systems have been discussed with the help of mathematical equations. Aeration of a

tissue culture vessel can be influenced by different environmental factors such as temperature; light, relative humidity etc. are also evaluated in this article.

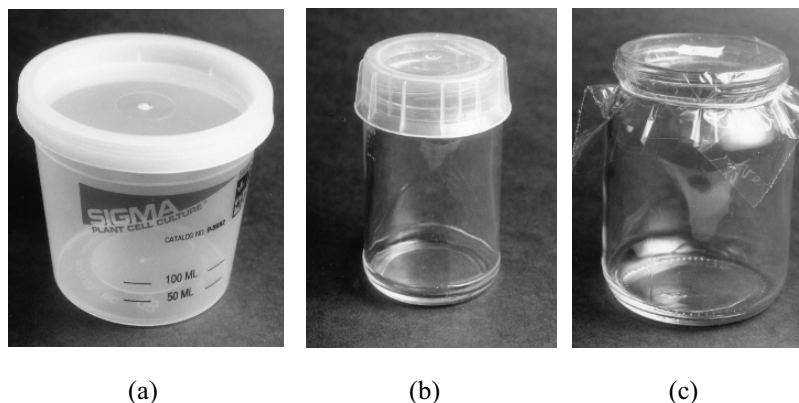


Figure 1. Tissue culture vessels designed to improve the air exchange through the leakage of the lid (a and b) or by using transparent film such as polypropylene (c).

2. Principles of aeration in tissue culture vessel

The aerial environment in a tissue culture vessel is considerably different from the surrounding outer environment. In a tissue culture vessel containing healthy chlorophyllous tissues, CO_2 concentration is generally low during the photoperiod and is high during the dark period. This difference in CO_2 concentration mainly depends on the aeration efficiency of the vessel and the photosynthetic efficiency of the tissues. In contrast, the concentrations of ethylene and water vapour (relative humidity) are high in the vessel than those of the surrounding outer environment. The water vapour concentration is high mainly due to the combined effects of continuous evaporation from the nutrient medium and the transpiration of the leaves. If the vessel contained non-chlorophyllous tissues such as callus, then the environmental condition will be very different from the above-mentioned characteristics, such as high CO_2 concentration throughout the dark or light period due to the continuous respiration and limited or no photosynthetic activity. Increased respiratory demands may also depress the O_2 concentration in the culture vessel. Ethylene and water vapour concentrations may remain high both in dark and light periods.

Aeration through the air gap between the vessel and the lid can improve the air exchange between the outer environment and the *in vitro* environment and these especially designed vessels are currently commercially available (Figure 1a, b). Such a system is the 'Vitro-vent' culture vessels (Duchefa Biochemie B.V., The Netherlands). Currently there are many specially designed tissue culture vessels commercially available to improve the air exchange.

Loosely fitted lids have been found to improve the growth and quality of micropropagated plants [5]. However, this type of aeration can increase the risk of microbial contamination especially when sucrose is used as a sole carbon source in the culture medium. Generally, the mass of medium, plant material and the air itself in the vessel is a little warmer than the surroundings and the temperature in the vessel is about 2°C higher than the ambient (Figure 2). During the dark period the temperature in the *in vitro* environment and the outer surroundings remains almost same (Figure 2). Moreover, most of the growth rooms (ambient) temperature set-point is about 3-5°C lower during the dark period than the photoperiod (Figure 2). This creates a partial vacuum, which pulls surrounding air into the vessel, and is one of the causes of exogenous contamination. Therefore, there is a need to vent the culture vessel with a reliable integral submicron membrane or the gas permeable film, which is part of a well-closed vessel.

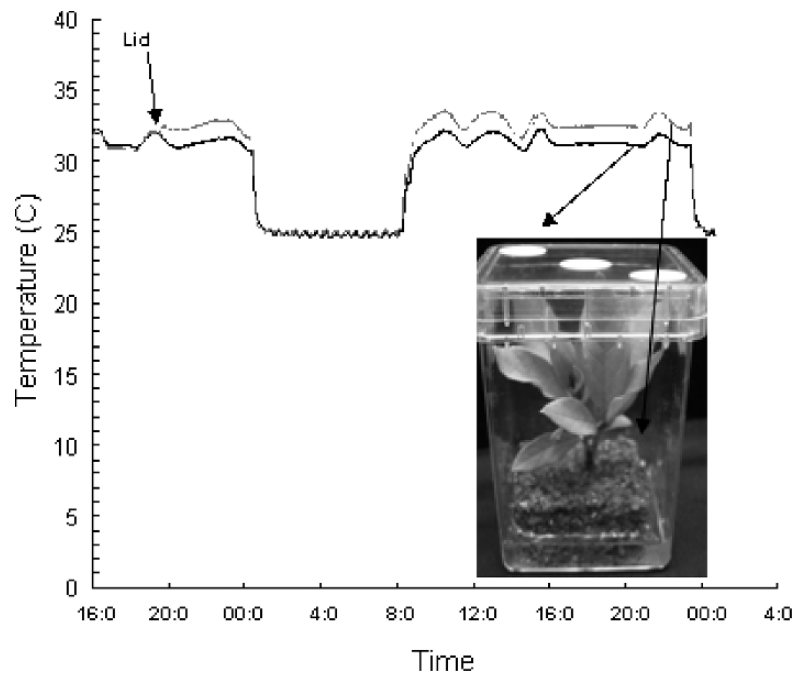


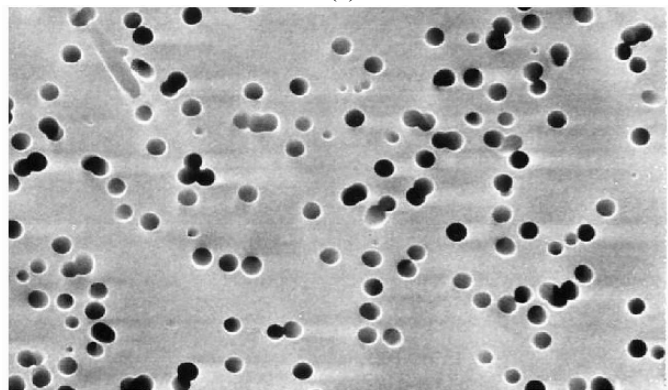
Figure 2. Temperature in a tissue culture vessel recorded during the light (8:00 to 00:00) and dark period (00:00 to 8:00).

Currently, many types of gas permeable films are commercially available, for example, MilliSeal[®] membrane (adhesive microporous filter discs, pore diameter 0.22 - 0.45 µm; MilliSeal, Nihon Millipore Ltd., Yonezawa, Japan; Figure 3), MilliWrap[®] membrane seal (Microporous sheet; pore diameter 0.45 µm; Millipore Corporation, USA), transparent polypropylene disc (thickness 25 µm; Courtaulds Films, Bridgewater, Somerset, UK), Teflon membranes (Vent Spots; pore diameter 0.5 µm; Flora

Laboratories; Australia), Suncap[®] Closer (pore diameter 0.02 μm ; Sigma, USA) (Figure 1c), TQPL[®] discs (adhesive microporous filter disc; TQPL supplies, UK). Ready-to-use vented vessels or lids attached with porous films/membranes are also currently available, such as, Culture Pack[®] (culture box made of gas permeable transparent films; 25 μm in thickness; Daikin Industries, Japan), LifeGuard[®] Sealed Vessel System (microporous filters attached to a transparent vessels; Osmotek Ltd., Israel), LifeLine[®] Vented Lids (microporous filters attached to a semi transparent lids; Osmotek Ltd., Israel) and Phytocap[®] closure (capping system for test tubes with 20 mm or 25 mm diameter; Phytotechnology Laboratories, USA).



(a)



(b)

Figure 3. a) Adhesive Millipore filter disc attached on the lids of Magenta vessels to increase natural ventilation. b) Scanning electron micrograph of a Millipore filter disc.

Generally, atmosphere of a tissue culture vessel is made of primarily two gases: nitrogen (N_2) and oxygen (O_2), which account for almost 99% of dry air (Table 1). Other gases in a culture vessel are CO_2 , ethylene and water vapour which occupy little volume but are

the most important gaseous components in a tissue culture vessel. Possible conditions for gas exchange in a tissue culture vessel under natural ventilation are:

- the pressure gradient between the inner and the outer environment
- the temperature gradient between the inner and the outer environment
- the velocity and air current pattern of the surrounding air of the vessels
- the concentration gradient of the gaseous molecule between the inner and the outer environment.

Table 1. Molecular weight (g mol^{-1}) of major gas components of dry air.

Gas	Mole Fraction	Mol. Wt. (g mol^{-1})
Nitrogen	0.78084	28.013
Oxygen	0.20948	31.998
Carbon dioxide	0.000400	44.0099

The mechanism of aeration through the microporous filter membrane in a tissue culture vessel is a complex process. The process may involve a) bulk flow of air, b) diffusion of specific gas molecules, c) convection of gases (air) induced by humidity etc. Each of these processes may not be unconnected each other and the contribution of each of these processes on total aeration of a tissue culture vessel may not be possible to separate. The contribution of each of the processes can be also varied with the types and characteristics of the venting materials, pore diameter, porosity and thickness of the venting membrane and most importantly total area of the venting membrane per vessel. Vessel size and shape, types of chlorophyllous plants in the vessel and the air velocity in the growth chamber/room are also important. Mass flow of air often enriched with CO_2 has also been used for the forced-aeration of a tissue culture vessel. The mechanism of these above mentioned aeration processes are described below.

2.1. AERATION BY BULK FLOW

When a flow occurs in between two gaseous environments in response to differences in total gaseous pressure and involves groups of atoms or molecules moving together, it is called bulk flow. Thus a spontaneous flow occurs only from a region of high pressure to a region of lower pressure. In a tissue culture vessel, the mass of growth medium, plant material and the air itself in the vessel is a little warmer than the surroundings during the photoperiod (Figure 2). This is mainly due to the warming effect of fluorescent light irradiation, and in such a case air is exchanged as bulk gas flow from the pressurized inner side to the outer atmosphere and the rate of flow is completely dependent on the pressure difference within the system. This flow, also known as laminar flow, producing a parabolic flow profile and can be determined by the Poiseuille-Hagen formula as:

$$Q = \frac{P\pi r^4}{8\eta l} \quad (1)$$

where, Q is the bulk flow ($\text{m}^3 \text{s}^{-1}$), P is pressure difference between inside and the outside of the vessel, r is the total radius of all the pores of the filter membranes, l is the thickness of the membrane (length of the pore) and η is the viscosity of air ($18.4 \times 10^{-6} \text{ kg s}^{-1} \text{ m}^{-1} = \text{N s m}^{-2}$). Therefore, flow is proportional to fourth power of radius and thus in a tissue culture vessel the characteristics of a microporous filter membrane, generally attached on the lid of a vessel, is important. The diameter of the pores in a filter membrane commonly used are $0.2 - 0.5 \mu\text{m}$ ($r = 0.1 - 0.25 \mu\text{m}$) which can prevent microbes to enter the vessel. However, the porosity (percent pore area), thickness of the microporous filter membrane (l) etc. are similarly important. Generally, a greater diffusive resistance was associated with the thicker filter membrane.

If there is no difference in the total air pressure, each gas (such as N_2 , O_2 , CO_2 , H_2O) can move due to the difference in partial pressure between inside and outside of the vessel. The partial pressure of each gas molecule is temperature dependent. The partial pressures of the gas molecules in a tissue culture vessel can be explained by using Dalton's law of partial pressures, that is, the total pressure of a mixture of gases equals the sum of the pressures that each would exert if it were present alone.

$$P_t = P_1 + P_2 + P_3 + \dots \quad (2)$$

where P_t is the total pressure of a sample which contains a mixture of gases. P_1 , P_2 , P_3 , etc. are the partial pressures of the gases in the mixture. If each of the gases behaves independently of the others then we can apply the ideal gas law to each gas component in the sample:

For the first component, n_1 = the number of moles of component 1 in the sample. The pressure due to component 1 would be:

$$P_1 V_1 = n_1 R T_1 \quad (3)$$

Therefore,

$$P_1 = \frac{n_1 R T_1}{V_1} \quad (4)$$

where P is the pressure of gas (unit kPa), V is the volume it occupies (unit liter), n is the number of moles of gas, T is temperature (unit K) and R is a universal constant (8.314 joules per Kelvin per mole), equal for all gases.

Similarly, for the second component, n_2 the number of moles of component 2 in the sample and the pressure due to component 2 would be:

$$P_2 = \frac{n_2 RT_2}{V_2} \quad (5)$$

Therefore, the total pressure P_t will be equal to:

$$P_t = P_1 + P_2 + \dots = \frac{n_1 RT_1}{V_1} + \frac{n_2 RT_2}{V_2} + \dots \quad (6)$$

If all components of the gas mixture will share the same temperature, T , and volume V , therefore, the total pressure P_t will be:

$$P_t = P_1 + P_2 + \dots = \frac{n_1 RT_1}{V_1} + \frac{n_2 RT_2}{V_2} + \dots = (n_1 + n_2) \frac{RT}{V} \quad (7)$$

Since the sum of the number of moles of each component gas equals the total number of moles of gas molecules in the tissue culture vessel:

$$P_t = n_t \frac{RT}{V} \quad (8)$$

Thus, at a constant temperature and volume, in a tissue culture vessel, the total pressure of a gas sample is proportional to the total number of moles of gas present, whether this represents a single substance, or a mixture. The temperature also directly influences the total pressure and thus increases or decreases of temperature in a tissue culture vessel can significantly influence the pressure and thus the bulk flow. However, it is very unlikely that the bulk flow is the only contributor in the total aeration process in a tissue culture vessel.

2.2. AERATION BY DIFFUSION

The spontaneous redistribution of a substance due to the random motion of the molecules, atoms or ions, of the substance from regions of an isotropic medium where their concentration is high to regions where their concentration is low is known as diffusion. The classical definition of mass transfer by diffusion refers to movement of a molecular species relative to another. If a chemical species j is present at concentration \check{C}_j at some point in an isotropic medium and is present at a lower concentration \check{C}_j other side of the medium there will be a net transfer of material towards \check{C}_j and this net transfer will continue until the two sites have attained the same uniform concentration. The velocity of the random movement or transfer process is governed by the characteristics of the medium and by the concentration of the diffusion species. This is known as diffusion coefficient quantifies the diffusivity and expressed with the units of $\text{cm}^2 \text{ s}^{-1}$; this can be varied with temperature. Diffusion can result from pressure gradients

(pressure diffusion), temperature gradients (thermal diffusion) and concentration gradients. Diffusion is described by Fick's law as:

$$J = -D \frac{\partial C}{\partial X} \quad (9)$$

where, J is the molar flux, D is the diffusion coefficient and C is the concentration of the species of interest and X is the length of diffusion pathway. In a tissue culture vessel, the principal mechanism that drives gas exchange between a) humid inner side and the drier outer side is the diffusion due to the concentration gradients of water vapor, b) low CO_2 concentration in the inner side to higher concentration in the outer side is the diffusion due to the concentration gradients of CO_2 and similarly ethylene, O_2 or any other volatile gases concentration gradients. Thus, for a tissue culture vessel, the equation of Fick's law can be expressed as:

$$\frac{J}{t} = -D * A \frac{(C_{in} - C_{out})}{X} \quad (10)$$

where, J/t is the amount of gas moved per unit time (flux density), D is the diffusion coefficient of the medium (air in case of tissue culture vessel) through which the gas is moving; A total cross sectional area of diffusion pathway; C_{in} concentration at start of pathway; C_{out} concentration at end of pathway.

The principle barrier to diffusive exchange of gases between the inner and the outer atmosphere of a tissue culture vessel is the wall of the enclosing vessel. This is invariably made of glass or plastic that is gas-impermeable and well sealed to prevent evaporative water loss and microbes to entry in the system [1]. The gases of greatest concern are O_2 , ethylene and CO_2 and among these gases, O_2 and CO_2 are principle products of aerobic respiration and photosynthesis and thus intrinsic to the most basic life sustaining metabolic pathway of plant cells. In contrast, ethylene is a plant hormone, which can strongly influence the developmental process of plants such as senescence, differentiation, leaf drop etc, at relatively small concentration. For O_2 , ethylene and CO_2 , the diffusion coefficient in air is $0.201 \text{ cm}^2 \text{ s}^{-1}$ which is almost 10,000 times smaller in water. While growing chlorophyllous plants in a tissue culture vessel, for CO_2 , it is appropriate to consider C_{out} as the atmospheric concentrations (growth room) and C_{in} usually lying between just below the ambient to near the compensation point of ($40 \mu\text{mol mol}^{-1}$ for *Brassica oleracea*; Zobayed *et al.* [6]). Oxygen concentration may not be varied significantly between the C_{out} and C_{in} . While growing non-chlorophyllous explants (such as callus) in a tissue culture vessel, C_{in} for CO_2 could be upto 100 times higher than that of the C_{out} [6]. Oxygen in such condition may be 4-5 times lower in the C_{in} compared to C_{out} [7]. For ethylene, C_{out} can be considered as zero and C_{in} upto five $\mu\text{mol mol}^{-1}$ which is known to above the physiologically active concentration. Another important gas component is the water vapour molecules; generally relative humidity inside the vessel is very high and sometimes reported nearly 100%. Thus, the C_{out} for relative humidity could be near 50% to as high as 80% (depending on the growth room

relative humidity). Therefore, for the diffusion through the capping system of a tissue culture vessel, many physiological and environmental factors describe above can influence gaseous flux density.

2.3. HUMIDITY-INDUCED CONVECTION IN A TISSUE CULTURE VESSEL

Humidity-induced convection is the mechanism commonly operates in nature to ventilate in whole plants of many wetland species [8,9,10]. In a tissue culture vessel similar types of ventilation may occur constantly if the attached filter membrane contained relatively small pores (pore diameter should be 0.2 μm or below) and within the Knudsen diffusion regime [11]. It should be mentioned that the use of filter membrane with pore diameter of 0.2 μm to ventilate a tissue culture vessel is a common practice. Most of the transparent polypropylene film use in tissue culture vessel has very small pore diameter; for example Suncap[®] (Sigma, USA) has a pore diameter of 0.02 μm . In humidity-induced convection process mass flow of gases is driven initially by diffusion of N_2 and O_2 through the small pores ($\leq 0.2 \mu\text{m}$) into the humid interior of the culture vessel. The constant humidification of the internal atmosphere through transpiration of the leaves and evaporation of the nutrient medium of the culture vessel (up to 2-3% by volume) creates and maintains high water vapour concentration, thus diluting the atmospheric gases such as N_2 and O_2 and producing a concentration gradient for their inward diffusion from the drier outer air. If pore-resistance of the microporous filters (pore diameter $\leq 0.2 \mu\text{m}$) to inward diffusion is effectively less than any Poiseuille resistance to backflow to the atmosphere, the inwardly diffusing air will cause pressurization within the culture vessel. These gases are then forced along the path of least resistance, i.e. through the leakage of the capping system. Although a more than reciprocal outward diffusion of water vapour takes place through the membrane, the water vapour is constantly replaced by evaporation and transpiration. The lower the relative humidity of the ambient air and the closer the culture medium surface is to the filter membrane (shorter the headspace), the steeper is the gradient for the inward diffusion of oxygen and nitrogen, and the faster is the flow.

The rate at which this will occur will be equal to the rate of inward diffusion across the porous partition, and will be a function of (a) the thickness of the filter membrane, (b) porosity of the membrane, (c) pore diameters, (d) the concentration difference across the membrane which is in turn a function of the water vapour concentration maintained beneath the partition, and (e) the venting path resistance. If the partition is very thin and highly porous, and provided that a high water vapour concentration can be maintained at the lower surface of the partition, high rates of flow can be realised. It should be noted that a supply of heat from the surroundings is necessary to provide the latent heat of evaporation for the water. Without this source of energy the humidity gradient could not be maintained and no flow would occur.

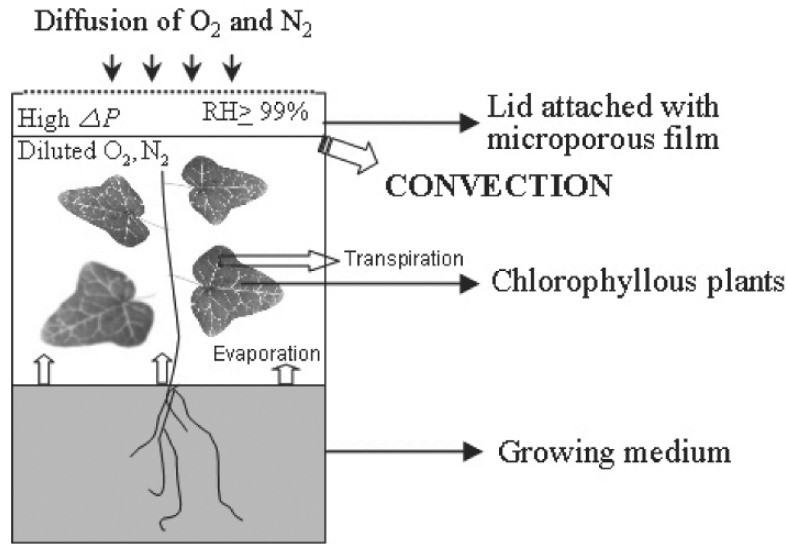


Figure 4. The mechanism of humidity induced convection in a tissue culture vessel.

Predictions of the convective flow which can be generated in such a tissue culture vessel (Figure 4) can be made using a number of relatively simple equations. For example it can be assumed that the pressure (static pressure) differential generated, although caused by the diffusive inflow of atmospheric gases as well as the replacement of any lost water vapour, will be numerically equal to that of the partial pressure of water vapour beneath the membrane. If the membrane is 'non-leaky', i.e. the pores will not allow a pressurised back flow, this pressure differential can be determined by first estimating the water vapour flux, J_{wv} , through the membrane. If R_h is the culture vessel headspace diffusive resistance, R_{md} the water vapour diffusive resistance of the membrane, and R_b , any boundary layer resistance, then:

$$J_{wv} = \frac{\left[\frac{P_{swv}}{P_a} \right]}{R_h + R_{mb} + R_b} \quad (11)$$

where, the saturated water-vapour pressure, P_{swv} , at 20°C at the water surface is 2.337 kPa, P_a is 101.3 kPa, and 2.337/101.3 is therefore a concentration difference between the water surface and the dry air above the boundary layer (in fractional volume terms $m^3 m^{-3}$), and J_{wv} has units of $m^3 s^{-1}$.

The partial pressure drop (in kPa) across the membrane itself ($\Delta P_{w(m)}$), numerically synonymous with the static pressure differential, will be:

$$\Delta P_{w(m)} = P_a (J_w * R_{md}) \quad (12)$$

Similarly, in Figure 4, the inward flow of atmospheric gases can be predicted. Since the presence of water vapour is at the expense of the other atmospheric gases, their partial pressure drop across the membrane will be equal in magnitude to that of the water vapour but in the opposite direction. This will generate an inward flow of atmospheric gases, $J_{o,n}$, into the chamber according to the equation :

$$J_{o,n} = (\Delta P_{w(m)} / P_a) \frac{1}{R'_{md}} \quad (13)$$

where, R'_{md} is the diffusive resistance of the membrane to oxygen and nitrogen. If the venting path (through the leakage of the capping system) is open and has no significant resistance, this flow will be sustained indefinitely and represents the maximum potential rate of convective gas flow. It should be noted that if pore sizes are $\leq 0.2 \mu\text{m}$, the resistances R_{md} and R'_{md} will involve Knudsen diffusion coefficients (D_k). These will always be less than the normal mutual diffusion coefficient, D_o , and are determined from the following equation:

$$D_k = \frac{d}{3} \sqrt{\frac{8RT}{\pi M_i}} \quad (14)$$

where M_i is the molecular mass of the diffusing species i . In equation 12 the Knudsen diffusion coefficient for water vapour will be used, whereas in equation 13 it will be the average Knudsen diffusion coefficient for the gases O_2 and N_2 appropriate to the pore diameters.

If pore diameters are smaller than $0.2 \mu\text{m}$ and therefore outside the Knudsen regime, R_{md} and R'_{md} , no longer depend upon pore diameter, only porosity, and they incorporate the use of the same mutual diffusion coefficient D_o , and are therefore equal. However, because the pores are outside the Knudsen regime any tendency to pressurisation in the chamber will be counteracted by a pressurised backflow ('leakiness') through the membrane.

The potential static pressure differential, $P_a(J_w * R_{md})$ (eq. 12), will not now be realised; instead, there will be some lower value attained at which a diffusive inflow will become balanced by the Poiseuille backflow. This new pressure differential, the 'effective' static pressure, ΔP_s , can be determined using the following equation where the potential static pressure differential, $P_a(J_w * R_{md})$ is represented as ΔP_{ps} :

$$\frac{\Delta P_{ps} - \Delta P_s}{P_a} * \frac{1}{R_{md}} = \frac{\Delta P_s}{R_{md}} \quad (15)$$

where, for membranes with membrane pore diameter $\geq 0.2 \mu\text{m}$, R_{mp} is the Poiseuille Flow resistance. The expressions used to determine Poiseuille Flow resistance, R_{mp} , of a porous partition (membrane) is:

$$R_{mp} = \frac{8\eta L_m}{\varepsilon A r_i^2} \quad (16)$$

where, η is the viscosity of air ($18.4 \times 10^{-6} \text{ kg s}^{-1} \text{ m}^{-1} = \text{N s m}^{-2}$), L_m is the thickness of the partition, ε its fractional porosity, A its cross-sectional area, and r_i is the radius of an individual pore. For the venting tube resistance, R_{vp} the expression would be:

$$R_{vp} = \frac{8\eta L}{\pi r^4} \quad (17)$$

The expression $\frac{\Delta P_{ps} - \Delta P_s}{P_a} * \frac{1}{R_{md}}$ will be the diffusive inflow ($\text{m}^3 \text{ s}^{-1}$) under the partial pressure gradient of atmospheric gases numerically equal to $\Delta P_{ps} - \Delta P_s$, while $\Delta P_s/R_{mp}$ will be the Poiseuille backflow ($\text{m}^3 \text{ s}^{-1}$) at the resultant effective static pressure differential ΔP_s .

To predict the convective flow rates, it is necessary to embrace the resistance, if any, to venting through the outlet tube and any attached flow-meter. If pores are within the Knudsen regime, an equation having a similar form to equation (18) may be used, but in which R_{mp} is replaced by the resistance of the venting path, R_{vp} , and in which ΔP_s falls to become the dynamic pressure, ΔP_d :

$$\frac{\Delta P_{ps} - \Delta P_d}{P_a} * \frac{1}{R'_{md}} = \frac{\Delta P_d}{R_{vp}} \quad (18)$$

The convective flow is then given by:

$$\text{Convective flow} = \frac{\Delta P_d}{R_{vp}} \quad (19)$$

If the inflow pore diameters are outside the Knudsen regime there will be two Poiseuille flow resistances acting in parallel, that of the inflow membrane - R_{mp} , and that of the venting path - R_{vp} . In a tissue culture vessel R_{vp} incorporates the outflow through the leakages of the capping system. It is necessary, therefore, to determine first the resultant resistance to pressure flow, $\sum R_p$. This can be obtained from the relationship:

$$\frac{1}{\sum R_p} = \frac{1}{R_{vp}} + \frac{1}{R_{mp}} \quad (20)$$

and $\sum R_p$ is then used in place of R_{vp} in equation 18, and R_{md} (as used in equation 15) will replace R'_{md} . It should be noted that as R_{vp} becomes very large due to a complete sealed system of the lid of a vessel, ΔP_d should approach ΔP_s .

2.4. AERATION BY VENTURI-INDUCED CONVECTION

Venturi-induced convection can occur due to wind blowing over the tops of a microporous filter membrane creating a suction which draws gases from the culture vessel, while fresh air is sucked in via leakage of the capping system or through other pores (Figure 5).

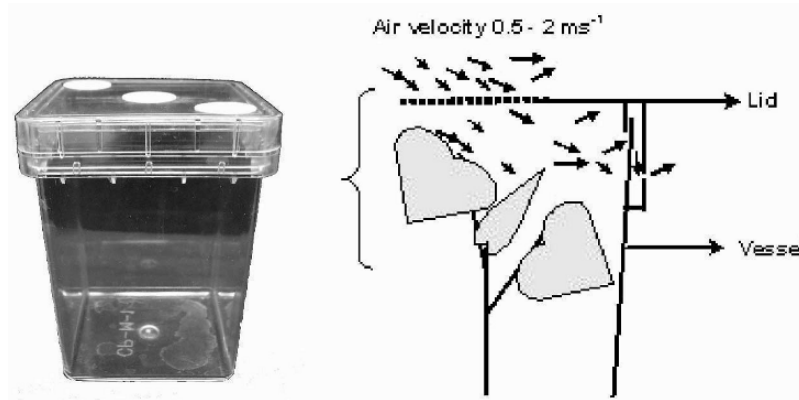


Figure 5. Aeration by venturi-induced convection in a tissue culture vessel.

The suction pressure ΔP (Pa) is developed according to the following equation:

$$\Delta P = -\left(\frac{1}{2}\right)\rho V^2 \quad (21)$$

where, ρ is the viscosity of air (approx. $1.20-1.25 \text{ kg m}^{-3}$) and V is the wind velocity (m s^{-1}). Venturi-induced flows are directly proportional to the wind-speed and will be influenced by resistances in the inflow pores and venting path that is the leakage of the capping system. Resistance to inflow will be lower with the greater numbers of large diameter inflow pores.

2.5. FORCED AERATION BY MASS FLOW

Forced aeration is the process of mechanically moving air from outside to inside of a culture vessel and vice versa. In this process a particular gas mixture is flushed directly through the culture vessel by applying pressurized force. Forced ventilation is one of the most effective methods of ventilation and the basic principle behind this method of ventilation is to create a positive pressure inside the vessel. With this system, the gaseous composition (CO_2), water vapour or any other necessary gases) of the incoming air and forced ventilation rate and/or air current speed in the culture vessel can be controlled relatively precisely by using a needle valve, mass flow controller and an air pump with an inverter [14].

For tissue cultures where large scale plant production is required, mechanised system of introducing forced aeration has been devised. In such a system comparatively large culture vessels have been used often with liquid medium where hundreds and thousands of plantlets can be grown. A setup such as this has recently been described by Zobayed *et al.* [15,16] and by Afreen *et al.* [17]. In this type of system, three new elements are introduced to improve the aeration efficiency and plant growth. Firstly, air is pumped over the cultures to carry CO_2 , water vapour and O_2 to the plants and substrate and simultaneously remove all volatile gases such as ethylene produced from the plant tissues. Secondly, the flowing air is enriched with CO_2 to further encourage photosynthesis in case the mass flow of air does not provide a CO_2 flux density for the desired rate of photosynthesis. Thirdly, the roots are grown in a porous medium to promote their aeration by diffusion. Porous substrate can improve the root quality significantly in micropropagated plantlets [18]. Moreover, unlike the conventional system, the growth medium is devoid of sucrose and thus forced the plants to grow photoautotrophically. The term photoautotrophy is defined as 'the process by which chlorophyllous organisms, such as plant, convert light energy into biologically useful energy and synthesize metabolic compounds using atmospheric carbon dioxide as a source of carbon'. A detailed account has been given and advantages of the photoautotrophic micropropagation system have recently been described by Kozai *et al.* [19]. An extended version of a commercialized photoautotrophic micropropagation system with forced ventilation has also been illustrated in the present volume.

3. Conclusions

Aeration in a tissue culture vessel can involve two different major processes. Firstly, bulk flow, humidity-induced and venturi-induced convective flows of air and diffusion of gas molecules. These processes may not be entirely unconnected and commonly can be termed as 'natural aeration' or 'natural ventilation'. Secondly, the 'forced aeration' or 'forced ventilation' where outer air are delivered to plant tissues by an external force. The demand of aeration in a tissue culture vessel can be accomplished by providing either or both of the above processes and thus tissue culture vessel should be designed more efficiently to maximize these processes.

References

- [1] Jackson, M. B. (2003) Aeration stress in plant tissue cultures. *Bulg. J. Plant Physiol.*, Special Issue :96–109.
- [2] Kozai, T.; Iwabuchi, K.; Watanabe, K. and Watanabe, I. (1991) Photoautotrophic and photomixotrophic growth of strawberry plantlets *in vitro* and changes in nutrient composition of the medium. *Plant Cell Tissue Org. Cult.* 25: 107-115.
- [3] Blazková, A. J.; Ullmann, J.; Josefusova, Z; Machackova, I. and Krekule, J. (1989) The influence of gaseous phase on the growth of plants *in vitro* : the effect of different types of stoppers. *Acta Hort.* 251: 209-214.
- [4] Jackson, M. B.; Abbott, A. J.; Belcher, A. R. and Hall, K. C. (1987) Gas exchange in plant tissue cultures. In: Jackson, M.B.; Mantell, S. and Blake, J. (Eds.) *Advances in the Chemical Manipulation of Plant Tissue Cultures*. BPGRF Monograph 16. Bristol: Plant Growth Regulators Group. 57-71.
- [5] Jackson, M. B.; Abbott, A. J.; Belcher, A. R.; Hall, K. C.; Butler, R. and Cameron, J. (1991) Ventilation in plant tissue culture and effects of poor aeration on ethylene and carbon dioxide accumulation, oxygen depletion and explant development. *Ann. Bot.* 67: 229-237.
- [6] Zobayed, S. M. A.; Armstrong, J. and Armstrong, W. (1999) Evaluation of a closed system, diffusive and humidity-induced convective throughflow ventilation on the growth and physiology of cauliflower *in vitro*. *Plant Cell Tissue Org. Cult.* 59: 113-123.
- [7] Zobayed, S. M. A.; Armstrong, J. and Armstrong, W. (2001) Micropropagation of potato: evaluation of closed diffusive and forced ventilation on growth and tuberization. *Ann. Bot.* 87: 53-59.
- [8] Dacey, J. W. H. (1981) Pressurised ventilation in the yellow water-lily. *Ecology* 62: 1137-1147.
- [9] Grosse, W. and Mevi-Schutz, J. (1987) A beneficial gas-transport system in *Nymphoides peltata*. *Am. J. Bot.* 74: 947-952.
- [10] Armstrong, J.; Armstrong, W. and Beckett, P. M. (1988) *Phragmites australis*: A critical appraisal of the ventilating pressure concept and an analysis of resistance to pressurised gas-flow and gaseous diffusion in horizontal rhizomes. *New Phytologist* 110: 383 - 390.
- [11] Leuning, R. (1983) Transport of gases into leaves. *Plant Cell Environ.* 6: 181-194.
- [12] Armstrong, W.; Armstrong, J. and Beckett, P. M. (1988) Pressurized ventilation in emergent macrophytes: the mechanism and mathematical modeling of humidity-induced convection. *Aqua. Bot.* 54: 121-135.
- [13] Armstrong, J.; Armstrong, W.; Beckett, P. M.; Halder, J. E.; Lythe, S.; Holt R. and Sinclair, A. (1996) Pathways of aeration and the mechanisms and beneficial effects of humidity- and Venturi-induced convections in *Phragmites australis* (Cav.) Trin. ex Steud. *Aqua. Bot.* 54: 177-197.
- [14] Kozai, T.; Kubota, C.; Zobayed, S.M.A.; Nguyen, Q.T.; Afreen-Zobayed, F. and Heo, J. (1999) Developing a mass-propagation system of woody plants. In: Watanabe, K. and Komamine, A. (Eds.) *Challenge of Plant and Agricultural Sciences to the Crisis of Biosphere on the Earth in the 21st Century*, Landes Company, USA; pp. 293-307.
- [15] Zobayed S. M. A, Afreen, F.; Kubota, C. and Kozai, T. (2000) Mass propagation of *Eucalyptus* in a scaled-up vessel under *in vitro* photoautotrophic condition. *Ann. Bot.* 85: 587-592.
- [16] Zobayed, S.M.A.; Afreen, F.; Xiao, Y. and Kozai, T. (2004) Recent advancement in research on photoautotrophic micropropagation using large culture vessels with forced ventilation. *In Vitro Cell. Dev. Biol.-Plant* (in press).
- [17] Afreen, F.; Zobayed, S. M. A.; Kubota, C.; Kozai, T. and Hasegawa, O. (1999) Supporting material affects the growth and development of *in vitro* sweet potato plantlets cultured photoautotrophically. *In Vitro Cell. Dev. Biol.-Plant* 35: 470-474.
- [18] Afreen, F.; Zobayed, S. M. A.; Kozai, T. (2002) Photoautotrophic culture of *Coffea arabusta* somatic embryos II: development of a bioreactor for the large-scale plantlet conversion from cotyledonary embryos. *Ann. Bot.* 9: 20-29.
- [19] Kozai, T.; Afreen, F.; Zobayed, S. M. A. (2004). Photoautotrophic (sugar-free medium) micropropagation as a new propagation and transplant production system. Springer, Dordrecht, The Netherlands (in press).

TISSUE CULTURE GEL FIRMNESS: MEASUREMENT AND EFFECTS ON GROWTH

STEWART I. CAMERON

Natural Resources Canada, Canadian Forest Service-Atlantic Forestry Centre, 1350 Regent St. South, Fredericton, New Brunswick E3B 5P7, Canada – Fax: 506-452-3525 – Email: scameron@nrcan.gc.ca

1. Introduction

The gel in a solidified tissue culture medium can influence explant or callus growth and morphology in a concentration-dependent manner. Depending on the type and stage of culture, and the plant material, different mechanisms exist: some morphogenic effects appear to be common to all gels, while others are gel-specific. Isolating and interpreting the growth effects due solely to gel concentration and/or type (agar, gellan gum or other gel) is complicated due to interactions between gel hardness, the other tissue culture medium components, and medium preparation methods. Gel strength may be modified by any or all of: pH, basal salt recipe, carbohydrate type(s) and concentration, charcoal, the dissolution/autoclaving method, storage conditions and age of the medium [1,2,3,4].

The early phases of tissue culture i.e., the initial stages—often favour proliferation over differentiation, and rapid growth tends to be best in liquid media or at moderate-to-low gel concentrations. For example, early growth of spruce apical meristems [5] and tobacco shoot organogenesis [6] both increase as the agar concentration decreases, and similarly, using a low-to-intermediate gellan gum content can improve the induction and proliferation of early-stage conifer somatic embryogenic tissue [7,8].

The later cultural stages of differentiation and plantlet development are promoted by higher gel concentrations. For instance, in several different genera and species of conifers high concentration of gellan gum enhances maturation and conversion of somatic embryogenic tissue into plantlets [4], and elevated agar levels improve organogenesis from buds [9]. In some species either gel type works [10]. In others, however, simply increasing the gel concentration may not be sufficient to solve problems like vitrification (hyperhydricity), and gel type is important [11]. For instance, gellan cannot be substituted for agar in shoot culture of some species because agar contains specific low molecular weight, sulfated polysaccharide impurities which inhibit hyperhydricity [12,13].

For the more general case, in tissue culture systems where the gel type is not critical and minor gel components do not dominate the control of morphogenic response(s), it is the density of the gel matrix itself that modulates growth. There is general agreement that, in a concentration-dependant manner, both agar and gellan gum gels limit the access of the

cultured tissue to water [10,14], nutrients [15,16], and hormones [9,17] dissolved in the medium, and may restrict the efflux into the gel of compounds from the tissue like enzymes as well [5].

In studies where both parameters have been measured, the gel water potential, Ψ , is correlated with gel concentration (more negative Ψ at higher gel concentration) [6,14,18], as is tissue Ψ and water content [4,10,19]. Several different investigators [14,20,21] have concluded that it is not the osmotic potential, Ψ_o , but the matric potential, Ψ_m , associated with gel structure and capillarity, that determines water and nutrient availability, and therefore morphogenesis, analogous to a “non-plasmolyzing” osmotic stress [4]. However, the matric potential component, Ψ_m , has been determined to be only a very small part of the total Ψ [14,21]. These observations have led to speculation that either plant tissue in culture is exquisitely sensitive to the small Ψ_m changes [19, 21], or there are additional unknown components which also contribute to the overall water potential. The suggested possibilities are vague: an explant/gel surface interaction involving mechanical pressure [14] and physical contact [17]; a “mechanical hindrance” [16]; or an undefined change “in some other gel property” [19]. Agar and gellan gum gels are structurally complex (see Section 4 below), and it is also possible that a basic water potential model simply cannot adequately describe water and/or nutrient and hormone availability to tissues cultured on a gel.

Although the physical mechanism remains unclear, the evidence is nonetheless compelling that gels limit explant or callus access to the other medium components which control growth in proportion to the gel concentration in a tissue culture medium. Therefore it is of interest to include gel firmness as yet another tissue culture parameter to be routinely monitored, and if required, manipulated by altering gel concentration. For this reason, a low-cost device designed to rapidly provide a simple empirical measure of gel firmness would be a useful tool.

2. Measurement of gel hardness

Full characterization of gels is accomplished through texture profile analysis, using instruments like an Instron[®] tester to measure hardness (rupture strength), firmness (resistance to compression), brittleness (compression distance to the gel’s rupture point) and elasticity (height recovery after compression) [22]. The instrumentation is expensive, but provides a precise and comprehensive description of gel properties for applications like quality control and product development within the food industry. Simpler instruments with more modest capabilities also are or have been commercially available (e.g., the Marine Colloids[™] gel tester).

In 2001 we described a simple, inexpensive device which can be built for laboratory use. (For construction details and operation see [23].) The prototype unit, which measures gel hardness expressed as peak force (g), is shown in Figure 1. It consists of a digital force gauge which is fixed in place but can be repositioned via a camera mount, a moveable platform, and a variable speed stepper motor. The latter was chosen so the best speed to use for measurements could be experimentally determined but, since platform speed was found to be not critical as long as it exceeds 10 mm min⁻¹, a reversible single-speed gear motor of 20-50 rpm could be substituted using the gearing specified in [23]. If a low-vibration synchronous motor is used, the tester could be

further simplified by eliminating the heavy polypropylene box and extra rubber tubing connection (used in order to damp vibrations from the stepping motor).

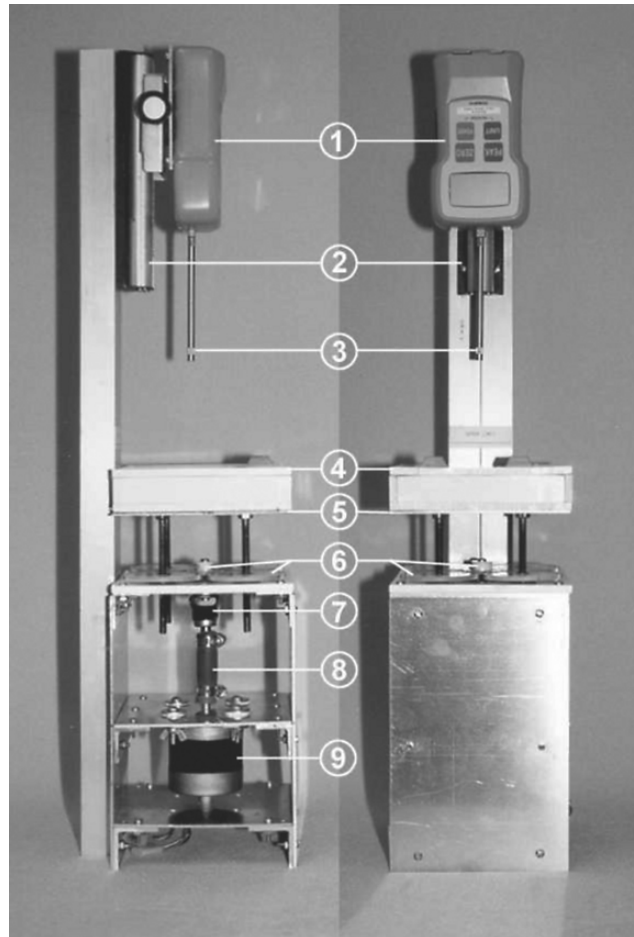


Figure 1. Prototype gel tester front and side views: (1) digital force gauge; (2) camera mount; (3) 5.4 mm diameter flat-bottomed probe; (4) polypropylene box containing lead shot; (6) movable platform; (7) flexible shaft coupler; (8) thick wall rubber tubing; (9) stepper motor. Reproduced from Cameron (2001) [23] with permission from the Society for In Vitro Biology, USA (formerly the Tissue Culture Association).

The gel rupture point readings from the force gauge (peak force in grams) are empirical, but allow comparison of gel firmness within a gel type as a function of various medium amendments and environmental conditions. The tester was designed to measure and compare gels in petri plates. For routine measurements, four plates from a batch pour (25 ml of medium per plate) are used. Four force gauge readings are made on each petri plate: one in the center and three others midway between the center and the wall of the

plate spaced equidistant (120° apart) from each other, for a total of 16 readings which are averaged. Readings may be made quite rapidly: less than 10 minutes per set of four petri plates.

The prototype gel tester was used to document the relation between firmness, gel concentration and three different media formulations commonly used in both our laboratory and elsewhere. Using both agar and gellan gum, sets of petri plates containing $\frac{1}{2}$ Litvay ($\frac{1}{2}$ LM), DCR and Murashige and Skoog (MS) media were made, and the pH was adjusted to 5.6 after autoclaving. Figure 2 demonstrates the very significant changes that result from either a change in gel concentration or medium formulation.

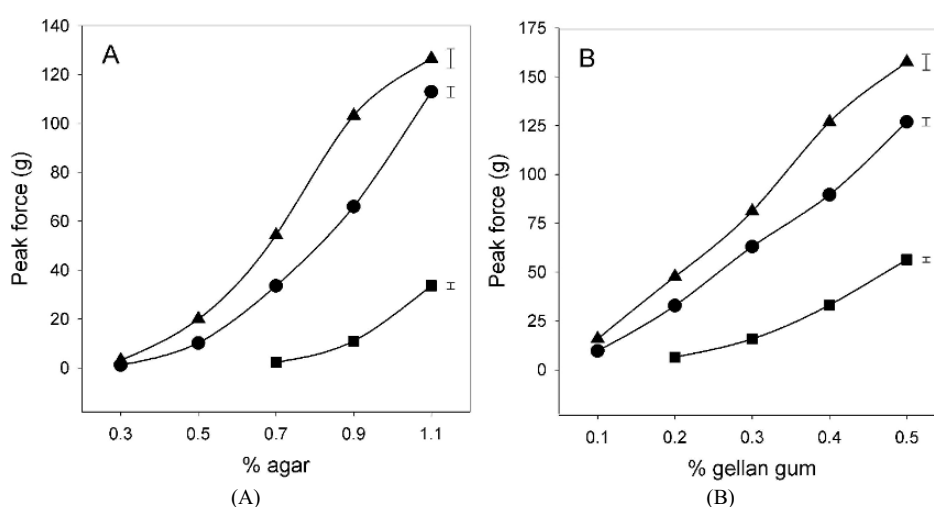


Figure 2. Hardness of three media, DCR (▲), $\frac{1}{2}$ Litvay (●), and Murashige and Skoog (■) at different concentrations of agar (A) and gellan gum (B). Bars are the maximum SE encountered for each medium over a range of gel concentrations. Reproduced from [23] with permission.

Agar is insensitive to Ca concentration, but the summed Ca + Mg molarity is 3.9, 4.4 and 4.5 mM for $\frac{1}{2}$ LM, DCR and MS medium, respectively—near the value of approximately 6 mM Ca which confers maximum hardness to gellan gum [23, 24]. Not surprisingly, however, all three media formulated with either agar or gellan gum are softer than a corresponding simple gel made to the same concentration with only Ca (see [23] and Figure 3). Indeed, MS, referred to as one of the “softer” media [2], does not even gel at either 0.3% or 0.5% agar content, or 0.1% gellan gum probably, as previously noted, because gel firmness is modified by other ions in the media [3]. For instance, agar firmness decreases with increasing NO_3 concentration, and the observed order of media hardness of $\text{DCR} > \frac{1}{2} \text{LM} > \text{MS}$ in Figure 2A is consistent with increasing NO_3 molarities of 11.7, 14.4 and 39.4 mM in MS, $\frac{1}{2}$ LM and DCR, respectively. Similarly, ions like NH_4 can decrease the gel strength of gellan gum-based media. The $\text{DCR} > \frac{1}{2} \text{LM} > \text{MS}$ order of hardness in the gellan gum media in Figure 2B is the inverse of the MS, $\frac{1}{2}$ LM and DCR NH_4 concentrations of 5.0, 15.6 and 20.6 mM, respectively.

3. Gel hardness and pH

The pH of an un-buffered gelled media, as measured prior to autoclaving, is a very dynamic variable whose value can change during most stages of medium preparation, even in the absence of a live culture on the medium. Post-autoclaving pH can vary as a function of: how the gelling agent is dissolved prior to autoclaving [25]; other media components (basal mineral salts, carbohydrate source, gelling agent and, in the case of agar, the brand, and charcoal) [26]; the length of time plates are in storage prior to use [27]; and whether storage is in the light or dark [26]. Placing live tissue on the gel accelerates pH changes as different media components are selectively taken up and metabolized, while organic exudates diffuse or are pumped back into the gel.

As described in the introductory section, gel hardness, regardless of the type, is independently affected by many of the same parameters even after adjusting post-autoclave pH values [3], so firmness might be expected to fluctuate in response to changes induced by some or all of autoclaving, pH and tissue growth.

To examine the effect of pH on gel hardness, simple gels were made consisting only of agar (agar, A-1296, Sigma) or gellan gum (Phytigel, P-8169, Sigma), with Ca and Mg gluconate (3mM and 1.5 mM, respectively), near the optimum concentration for solidifying the gellan gum [23, 24]. Hardness was measured using the gel tester shown in Figure 1 over three gel concentrations and five pH's within physiologically relevant ranges.

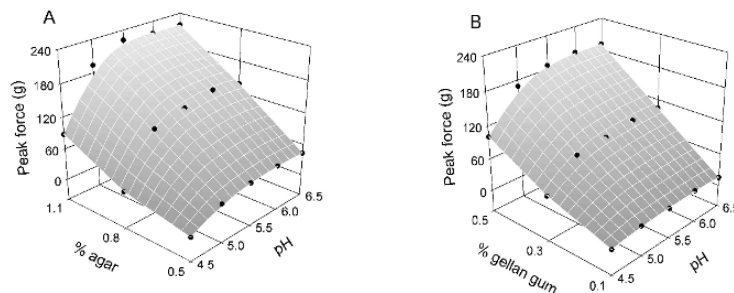


Figure 3. Hardness of agar (A) and gellan gum (B) gelled media adjusted to different pH values. Points (●) are the experimental values.

The data in Figure 3 show that gel hardness decreases at lowered pH, as has been noted previously by others [2, 3], especially between pH 4.5 and 5.0-5.5. The extent of the effect is surprising. At the highest concentrations used in this trial of gellan gum (0.5%) and agar (1.1%), an increase of just 0.5 of a pH unit from pH 4.5 to 5.0 increases hardness by 2.2- and 1.7-fold respectively. Although it is not obvious from Figure 3A and B, the increase in firmness is even sharper at the trial's lowest gel concentrations (7.2- and 2.6-fold at 0.5% agar and 0.1% gellan gum, respectively, between pH 4.5 and 5.0).

In preparing media for trials investigating the effects of pH on growth, it should be remembered that lowering the pH of a medium but retaining the same gel concentration may effectively increase the supply of water, some (but not all) nutrients [15], and

hormones [9] simply because the gel matrix is softened. Particularly at pH's of 4.5-5.5, compensatory effects of pH and gel concentration on growth have been observed where, for example, the optimum pH for adventitious bud production on spruce needles decreases as agar concentration increases [28]. The usefulness of being able to measure both pH and gel hardness, then adding sufficient gel to re-establish the medium's firmness at a lower pH is obvious. In matrix-type experiments set up to investigate the interaction between pH and concentrations of medium components whose availability is sensitive to pH, being able to maintain constant gel hardness at different pH's may minimize the risk of results being further complicated due to the secondary interaction of the opposing effects of gel texture and pH on nutrient and hormonal availability.

4. The dynamics of syneresis

Syneresis is the process of a liquid separation or "weeping" from the gel [29] due to contraction or structural changes of the gel matrix. Syneresis is often the result of events like cool or freezing temperatures and/or extended storage. All gels exhibit some degree of syneresis: agar is considered to be highly syneretic and gellan gum only slightly so [24].

Freshly poured tissue culture plates are usually "conditioned" or "dried" prior to use [30], often by leaving the petri plates either unsealed or uncovered in a laminar flow hood. Conditioning the media minimizes the formation of water on the surface of the gel and condensation on the petri plate lid.

The effect of conditioning on gel hardness is unclear, so a small trial with varied drying times was done. Petri plates were initially weighed, filled with 25 ml of 0.9% agar or 0.4% gellan gum gels, and then reweighed. As before, Ca and Mg gluconate (3 mM and 1.5 mM, respectively, adjusted to pH 5.7) were the only medium components other than the gels.

All petri plates were placed in a vertical laminar flow hood with the lids on but unsealed, and left to dry for 4-96 h. Four plates of each gel type were removed at specified intervals, reweighed, then measured for hardness (four readings per plate) using the gel tester. The time course of water loss, expressed as a percentage of the initial gel weight, and hardness changes are shown in Figure 4.

The rate of moisture loss was constant throughout the drying period. Both gel types had lost approximately 9% of their initial mass after 96 h of drying. However, during the first 8-12 hours gel hardness rapidly increased, then leveled off to relatively constant values for the remainder of the test period. The practical conclusion from such measurements is that covered petri plates should be dried for no less than 12 h or more than 24 h (with the particular style of laminar flow hood used in our laboratory). The results also suggest that water in the gel may exist in two compartments, both of which are equally accessible for diffusion into the airflow above the gel's surface. As a result of the loss of the first fraction the contraction of gel occurs. However, the second fraction does not seem to induce continued gel shrinkage.

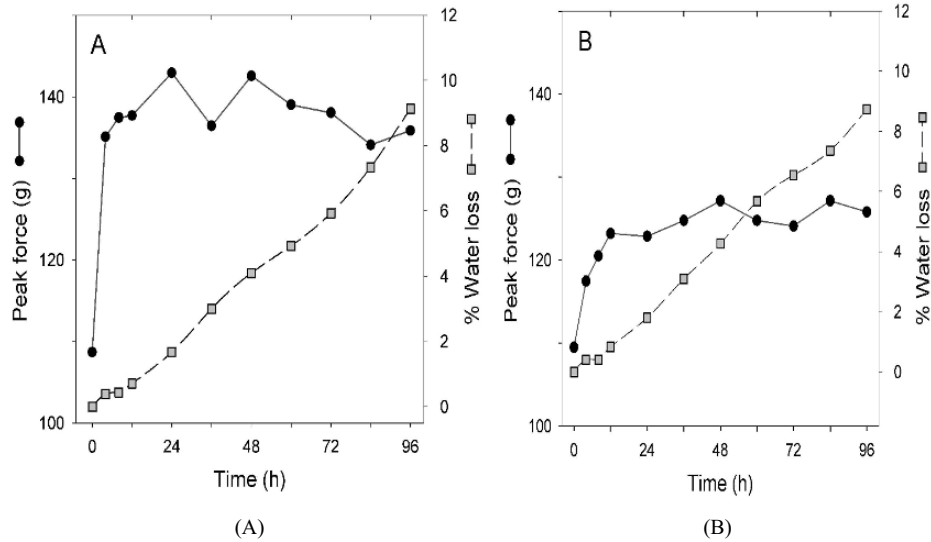


Figure 4. Water loss (B) and gel hardness (α) of agar (A) and gellan gum (B) gelled media as a function of 0, 4, 8, 12, 24, 36, 48, 60, 72, 84 or 96 h of drying time under a vertical laminar flow hood.

Though the mechanism controlling diffusional water loss is poorly defined, both water flux and hardness are likely related to pore size. Though their microstructure differs, both gellan gum and agar gels are heterogeneous. Gelled agar is reported to have “a polydispersity of bundle thickness (3 to 20 nm) and pore size (30 to 600 nm)” [16]. Similarly, gellan gum gels are observed to have two or more discrete size classes (0.1 μ and 1 μ), with thick and thin gel strands associated with the large and small pores, respectively. Maximum gel hardness, produced by using 6-8 mM Ca, corresponds to the minimum large pore size and higher water-holding capacity. [24]. The authors propose that in gellan gum the large pores formed from thick strands determine gel hardness, but with a water-holding capacity more sensitive to external forces. The thin-stranded, small pores (whose dimensions do not depend on Ca concentration) have a greater capacity to stably hold water due to their higher capillarity, so gellan gum exhibits low syneresis during long term storage.

5. Conclusion

The small tests documented above have been presented to demonstrate that simple, rapid empirical estimates of gel hardness are practical using peak force measurements from a low-cost, easily constructed device. Even though the functional mechanism remains largely unknown, agar and gellan gum gels have well-documented, concentration-dependent effects on growth and morphology in tissue culture systems. The structure and density of the gel matrix are thought to restrict access of the explant or callus to the nutrients, hormones and/or water in the gelled medium. This is independent of other

gel-concentration-dependant factors-e.g., the low molecular weight carbohydrate substances or the sulfate content of agar, or the high cation concentration in gellan gum [31]. Since gel firmness itself can modify, or be modified by, many of the cultural parameters which tissue culturists attempt to manipulate experimentally, we believe a simple assessment tool providing very basic information on gel rigidity and structure may be of value for routine use.

References

- [1] Horner, M.; McComb, J.A.; McComb, A.J. and Street, H.E. (1977) Ethylene production and plantlet formation by *Nicotiana* anthers cultured in the presence and absence of charcoal. J. Exp. Bot. 28: 1365-1372.
- [2] Wetzstein, H.Y.; Kim, C. and Sommer, H.E. (1994) Vessel volume, gelling agent, and basal salts affect pH and gel strength of autoclaved tissue culture media. Hort Sci. 29:683-685.
- [3] Huang, L.-C.; Kohashi, C.; Vangundy, R. and Murashige, T. (1995) Effects of common components on hardness of culture media prepared with Gelrite™. In Vitro Cell Dev. Biol.-Plant 31: 84-89.
- [4] Klimaszewska, K. and Smith, D.R. (1997) Maturation of somatic embryos of *Pinus strobus* is promoted by a high concentration of gellan gum. Physiol. Plant. 100: 949-957.
- [5] Romberger, J.A. and Tabor, C.A. (1971) The *Picea abies* shoot apical meristem in culture. I. Agar and autoclaving effects. Amer. J. Bot. 58: 131-140.
- [6] Brown, D.C.W.; Leung, D.W.M. and Thorpe, T.A. (1979) Osmotic requirement for shoot formation in tobacco callus. Physiol. Plant. 46: 36-41.
- [7] von Arnold, S. (1987) Improved efficiency of somatic embryogenesis in mature embryos of *Picea abies* (L.) Karst. J. Plant Physiol. 128: 233-244.
- [8] Li, X.Y.; Huang, F.H. and Gbur, E.E., Jr. (1998) Effect of basal medium, growth regulators and Phytigel concentration on initiation of embryogenic cultures from immature zygotic embryos of loblolly pine (*Pinus taeda* L.) Plant Cell Rep. 17: 298-301.
- [9] Bornmann, C.H. and Vogelmann, T.C. (1984) Effect of rigidity of gel medium on benzyladenine-induced adventitious bud formation and vitrification *in vitro* in *Picea abies*. Physiol. Plant. 61: 505-512.
- [10] Klimaszewska, K.; Bernier-Cardou, M.; Cyr, D.R. and Sutton, B.C.S. (2000) Influence of gelling agents on culture medium gel strength, water availability, tissue water potential, and maturation response in embryogenic cultures of *Pinus strobus* L. In Vitro Cell. Dev. Biol.-Plant 36: 279-286.
- [11] Pasqualetto, P.-L.; Zimmerman, R.H. and Fordham, I. (1988) The influence of cation and gelling agent concentrations on vitrification of apple cultivars *in vitro*. Plant Cell Tissue Org. Cult. 14:31-40.
- [12] Nairn, B.J.; Furneaux, R.H. and Stevenson, T.T. (1995) Identification of an agar constituent responsible for hydric control in micropropagation of radiata pine. Plant Cell Tissue Org. Cult. 43: 1-11.
- [13] Marga, F.; Vebret, L. and Morvan, H. (1997) Agar fractions could protect apple shoots cultured in liquid media against hyperhydricity. Plant Cell Tissue Org. Cult. 49: 1-5.
- [14] Owens, L.D. and Wozniak, C.A. (1991) Measurement and effects of gel matrix potential ad expressibility on production of morphogenic callus by cultured sugarbeet leaf discs. Plant Cell Tissue Org. Cult. 26: 127-133.
- [15] Singha, S.; Townsend, E.C. and Oberly, G.H. (1985) Mineral nutrient status of crabapple and pear shoots cultured *in vitro* on varying concentrations of three agars. Amer. J. Hort. Sci. 110: 407-411.
- [16] Stecchini, M.L.; Del Torre, M.; Sarais, I.; Saro, O.; Messina, M. and Maltini, E. (1998) Influence of structural properties and kinetic constraints on *Bacillus cereus* growth. Appl. Environ. Microbiol. 64: 1075-1078.
- [17] Debergh, P.C. (1982) Physical properties of culture media. In: Fujiwara, A. (Ed.) Proc. of the 5th International Congress of Plant Tissue and Cell Culture. Tokyo, Japan; pp. 135-136.
- [18] Debergh, P.C.; Harbaoui, Y. and Lemeur, R. (1981) Mass propagation of globe artichoke (*Cynara scolymus*): Evaluation of different hypotheses to overcome vitrification with special reference to water potential. Physiol. Plant. 53: 81-87.
- [19] Spomer, L.A. and Smith, M.A.L. (1996) Direct measurement of water availability in gelled plant tissue culture media. In Vitro Cell. Dev. Biol. - Plant 32: 210-215.
- [20] Debergh, P.C. (1983) Effects of agar brand and concentration on the tissue culture medium. Physiol. Plant. 59: 270-276.

Tissue culture gel firmness

- [21] Beruto, D.; Beruto, M.; Ciccarelli, C. and Debergh, P. (1995) Matric potential evaluations and measurements for gelled substrates. *Physiol. Plant.* 94: 151-157.
- [22] Whyte, J.N.C.; Englar, J.R. and Hosford, S.P.C. (1984) Factors affecting texture profile evaluation of agar gels. *Botanica Marina* 27: 63-69.
- [23] Cameron, S.I. (2001) Use of a prototype gel tester to demonstrate the effect of variable calcium concentration on gel rigidity. *In Vitro Cell. Dev. Biol.- Plant* 37: 419-424.
- [24] Mao, R.; Tang, J. and Swanson, B.G. (2001) Water holding capacity and microstructure of gellan gels. *Carbohydrate Polymers* 46: 365-371.
- [25] Sarma, K.S., Maesato, K.; Hara, T. and Sonoda, T. (1990) Effect of method of agar addition on post-autoclave pH of the tissue culture media. *Ann. Bot.* 65: 37-40.
- [26] Owen, H.R., Wengerd, D., and Miller, A.R. (1991) Culture medium is influenced by basal medium, carbohydrate source, gelling agent, activated charcoal, and medium storage method. *Plant Cell Rep.* 10: 583-586.
- [27] Skirvin, R.M.; Chu, M.C.; Mann, M.L.; Young, H.; Sullivan, J. and Fermanian, T. (1986) Stability of tissue culture medium pH as a function of autoclaving, time, and cultured plant material. *Plant Cell Rep.* 5: 292-294.
- [28] Selby, C., Lee, R., and Harvey, B.M.R. (1989) The effects of culture medium rigidity on adventitious bud production and tissue vitrification in needle cultures of Sitka spruce [*Picea sitchensis*(Bong.) Carr.] *New Phytol.* 113: 203-210.
- [29] McNaught, A.D. and Wilkinson, A. (1997) *IUPAC Compendium of Chemical Technology* 2nd ed. Blackwell Science, Oxford, UK; pp. 464. Online at: <http://www.nicmila.org/Gold/Output/S06227.xhtml>.
- [30] Krieg, N.R. and Gerhardt, P. (1981) Solid culture. In: Gerhardt, P.; Murray, R.G.E.; Costilow, R.N.; Nester, E.W.; Wood, W.A.; Krieg, N.R. and Phillips, G.B. (Eds.) *Manual of Methods for General Bacteriology*. Amer. Soc. For Microbiol., Washington DC; pp. 143-150.
- [31] Scherer, P.A.; Muller, E.; Lippert, H. and Wolff, G. (1988) Multi-element analysis of agar and gellrite impurities investigated by inductively coupled plasma emission spectrometry as well as physical properties of tissue culture media prepared with agar or the gellan gum Gelrite. *Acta Hort.* 226: 655-658.

EFFECTS OF DISSOLVED OXYGEN CONCENTRATION ON SOMATIC EMBRYOGENESIS

KENJI KURATA¹ AND TERUAKI SHIMAZU²

¹*Graduate School of Agricultural and Life Sciences, University of Tokyo, Yayoi 1-1-1, Bunkyo-ku, Tokyo 113-8657, Japan - Fax: 81-3-5841-8172 - Email: kurata@mail.ecc.u-tokyo.ac.jp*

²*Faculty of Applied Biological Science, Gifu University, 1-1 Yanagido, Gifu-city, Gifu 501-1193, Japan*

1. Introduction

Labour-reducing automation and techniques for scaling up plant micropropagation are essential for future strategies of transplant production. Somatic embryogenesis is a technique used to produce large numbers of individual embryos, and has received much interest as a means to produce artificial seeds.

The most common method of somatic embryo production for transplants or artificial seeds is inducing embryos from embryogenic cell clusters. Somatic embryos in dicotyledonous plants progress through four stages of development: globular stage, heart stage, torpedo stage, and cotyledonary stage, while they are undergoing tissue differentiation (Figure 1). The stages are based on the overall embryo shape. Cotyledonary-stage embryos have an elongated radicle and hypocotyl, which tends to exhibit hyperhydricity in liquid medium. Moreover, the elongated cotyledonary-stage embryos intertwine with each other in the bioreactor and form clumps. If somatic embryos are to be used as enclosures into the artificial seeds, it is therefore desirable to harvest somatic embryos at the torpedo stage.

The commercialization of artificial seeds or transplants using somatic embryos requires the development of a bioreactors system for large-scale production. Bioreactors enable the measurement and control of culture conditions (Dissolved oxygen, pH, temperature, electric conductivity, redox potential, mixing speed, etc.) in liquid medium.

There have been several reports on somatic embryo production systems using a bioreactor [1-8]. However, the effect of physical environmental factors such as pH [9], shear stress [10], osmotic pressure, mass transfer rate, and dissolved oxygen (Hereafter, referred to as DO) concentration on somatic embryo culture has not been investigated in detail. DO concentration is one of the most important environmental factors when growing plants in liquid systems, since oxygen is only slightly soluble in water (about 8 mg L⁻¹ at 25 °C, 1 atm in ambient air).

The relationship between DO concentration and somatic embryogenesis is not clear from the results reported in earlier studies. Kessell and Carr [11] reported that a DO concentration below a critical DO level of 1.3 mg L^{-1} was essential for the production of carrot somatic embryos in a 4-L bioreactor mechanically stirred at 90 rpm. Carman [12] concluded that a low oxygen gas level increased the number of wheat embryos. Stuart *et al.* [13] induced alfalfa somatic embryos using a 2-L bioreactor, stirred at 100 rpm by an impeller and aerated by a sparger at 1.8 L min^{-1} . They indicated that somatic embryos of alfalfa could be regenerated at high DO concentrations; at least 5.6 mg L^{-1} , in a bioreactor. Jay *et al.* [14] reported that the production of carrot somatic embryos in a 3-L mechanically stirred bioreactor operated at 50-150 rpm depended on the biomass concentration. Two cultures were produced at constant DO concentrations of 0.8 mg L^{-1} and 8.0 mg L^{-1} , using a controlled gas mixing system and a constant bubble aeration rate of 0.09 vvm (volume air per volume culture per minute). After 20 days, the yields were $170 \text{ embryos mL}^{-1}$ and $600 \text{ embryos mL}^{-1}$ in the 0.8 mg L^{-1} and 8.0 mg L^{-1} DO cultures respectively.

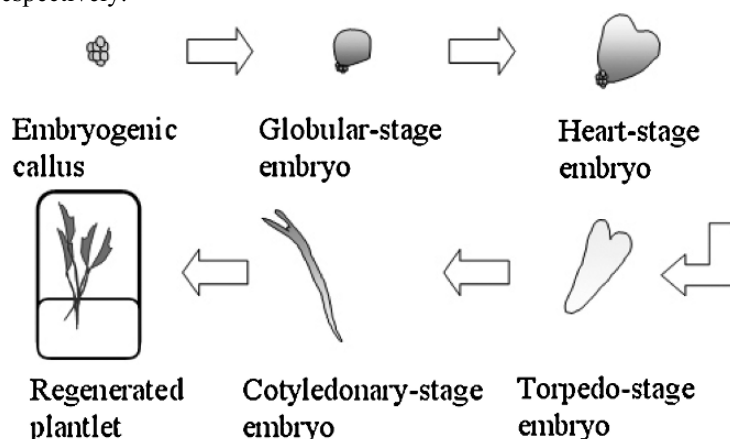


Figure 1. Developmental stages in somatic embryogenesis.

Archambault *et al.* [10] studied embryogenic cultures of a transformed *Eschscholtzia californica* cell line in an 11-L helical ribbon impeller bioreactor. They showed that the best production of somatic embryos was achieved by operating the bioreactor at 60 rpm maintaining the DO concentration at 1.6 mg L^{-1} , using surface oxygenation only (0.05 vvm , $1.4 \text{ h}^{-1} k_L a$; hereafter, it is referred to as the volumetric oxygen transfer coefficient ($k_L a$)). The high DO concentrations of 4.8 mg L^{-1} favoured undifferentiated biomass production at the expense of the slow growing somatic embryos. Okamoto *et al.* [15] reported the effect of the oxygen concentration in the aeration gas on plantlet regeneration from rice cells in bioreactor cultures. They showed that the efficiency of regeneration in cultures aerated with gas mixtures of over 40% oxygen was higher than that in a flask culture. Shigeta *et al.* [16] carried out somatic embryo production using a 250-mL Spinner flask and a 2-L jar-fermentation system. They reported that a concentration of at least 6.5 mg L^{-1} was needed for the development of globular and

heart-stage embryos during the first week of culture. However, subsequent development into torpedo-stage embryos proceeded even at low DO concentrations.

The differences in the experimental results reported could be attributed to the culture system, medium formulation, plant species, and inoculated embryogenic cell (cell density, cell cluster size, washing of residual 2,4-D and cell line used). In particular, the types of DO concentration regulation methods used differed in the mixing speed and aeration rate during the culture period. Therefore, in the reported examples the findings were also affected by the shear in the liquid medium as well as the DO concentration. To investigate only the relationship between DO concentration and somatic embryogenesis, Shimazu and Kurata [17] used a liquid culture system, which did not require either bubble aeration or changing the mixing speed to control the DO concentration. In this chapter, relationships between DO concentration and carrot somatic embryogenesis are described. The same authors developed a dynamic control method of DO concentration to enhance the ratio of torpedo-stage embryos in the suspension at the time of harvest [18]. The details of dynamic DO concentration control are also presented.

2. Relationship between DO concentration and somatic embryogenesis

2.1. CULTURE SYSTEM AND DO CONCENTRATION VARIATIONS

Figure 2 is a schematic drawing of the flask culture system in which the effect of DO concentration on carrot somatic embryogenesis was investigated. In rotary flask-culture, mild stirring occurs, but the cell or tissues are not damaged [19].

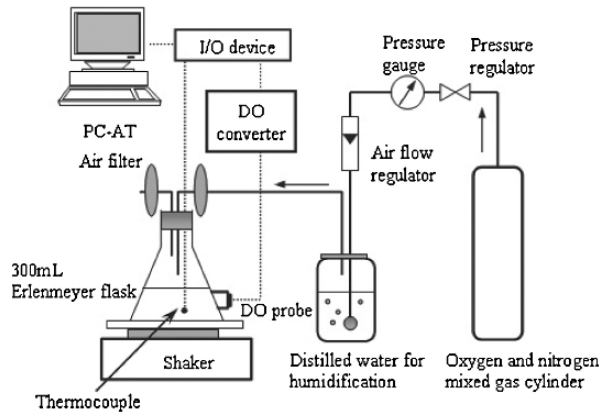


Figure 2. Schematic diagram of the culture system. Reprinted from Shimazu, T. and Kurata, K. (1999) [17] with permission from Springer Science and Business Media.

DO was regulated by adjusting the oxygen gas concentration in the headspace of the flask without changing the stirring strength. Therefore, the influence of the shear stress could be excluded from results concerning the effects of DO levels. The mixture of oxygen and nitrogen gas was humidified by bubbling through deionized water, and

supplied into each flask fitted with an air filter. During the culture period, the aeration rate into the flasks was maintained at 10 mL min^{-1} . The oxygen transfer coefficient ($k_L a$) of the flasks was 7.5 h^{-1} . Five oxygen gas concentrations levels (4%, 7%, 20%, 30% and 40%, the remainder nitrogen) aeration were tested to evaluate the effect of DO concentration level on somatic embryogenesis. The experiment duration was 23 days. Figure 3 shows the changes in DO concentration in the medium under various aeration conditions. The DO levels during the somatic embryo culture dropped somewhat from the initial saturated DO level in each treatment. However, these drops were so low that the different DO levels remained unchanged during the culture period.

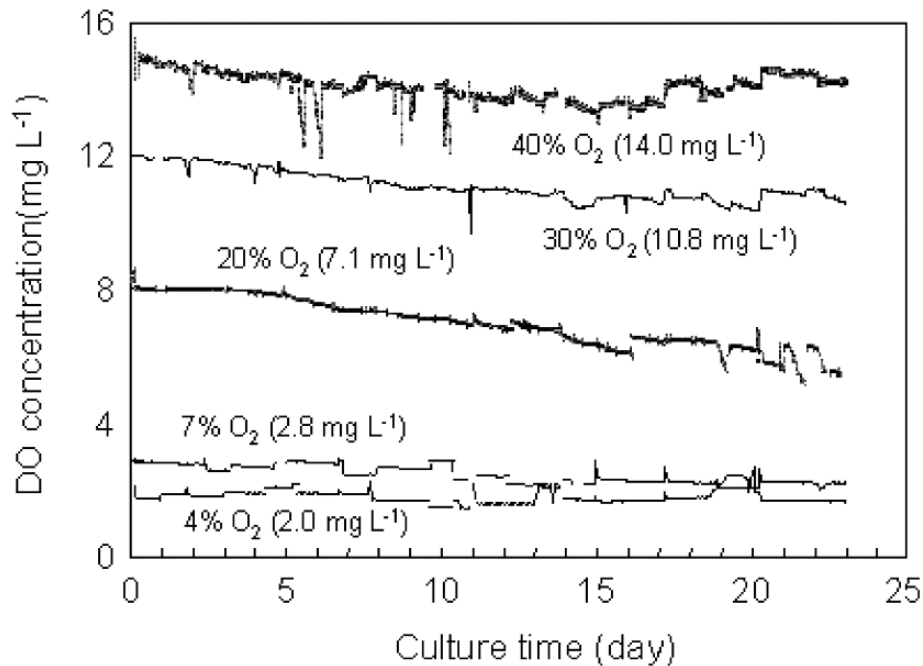


Figure 3. Changes of medium DO concentration in flask under various aeration conditions. Reprinted from Shimadzu, T. and Kurata, K. (1999) [17] with permission from Springer Science and Business Media.

Average DO concentrations of each treatment were 2.0 mg L^{-1} , 2.8 mg L^{-1} , 7.1 mg L^{-1} , 10.8 mg L^{-1} and 14.0 mg L^{-1} for 4%, 7%, 20%, 30% and 40% oxygen gas respectively. For the 40% oxygen treatment, DO level increase later in the culture period. This was attributed to the reduced oxygen uptake after the harvest of cotyledonary-stage embryos. Cotyledonary embryos were harvested everyday if present in the suspension.

2.2. TIME COURSE OF THE NUMBER OF SOMATIC EMBRYOS

Figure 4 shows the effect of DO concentration on carrot somatic embryogenesis in terms of the number of somatic embryos at each stage (globular, heart, torpedo, and cotyledonary). The rate of increase in the total number of somatic embryos (all

Effects of dissolved oxygen concentration on somatic embryogenesis

developmental stages) was not significantly affected by the DO concentration, as shown by the similarity of the curves for all treatments (Figure. 4A). The total number of somatic embryos reached a constant level after day 17 with the exception of the 4% oxygen treatment. The amount of time until somatic embryos began to appear at all developmental stages also was not affected by the DO concentration (Figure 4 B-E).

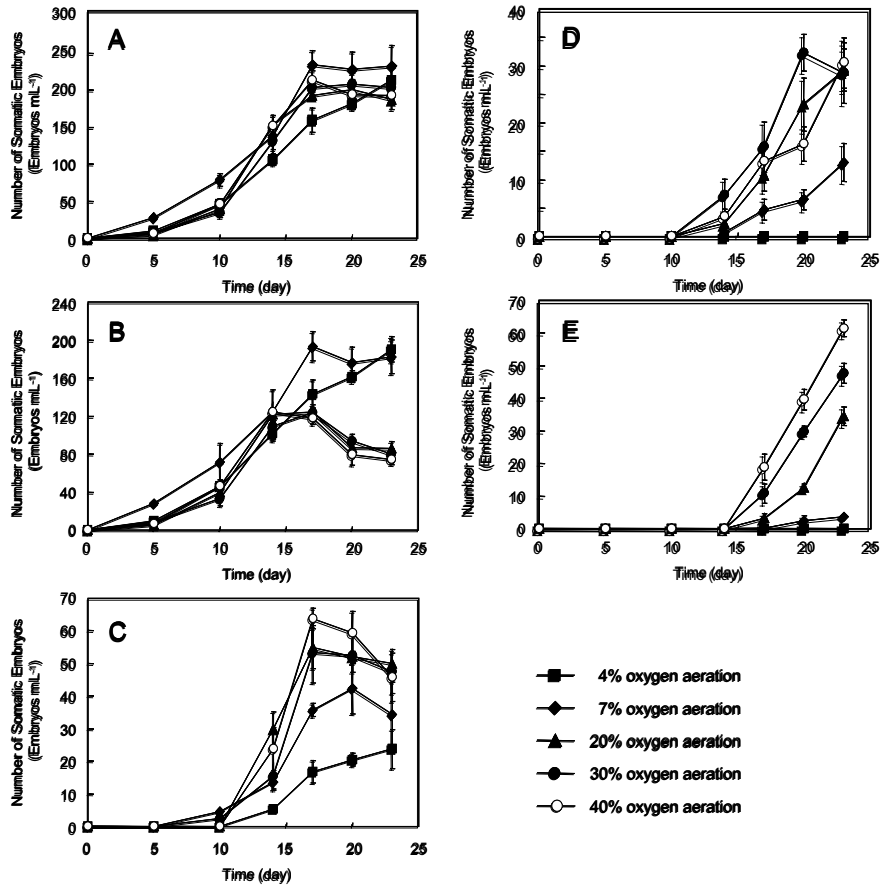


Figure 4. Time course of the mean number of carrot somatic embryos per unit volume of the culture medium. (A) Total somatic embryos, (B) Globular-stage embryos, (C) Heart-stage embryos, (D) Torpedo-stage embryos, (E) Cotyledonary-stage embryos: Cumulative number of cotyledonary-stage embryos harvested by straining through a 850- μ m steel mesh. Bars represent standard errors ($n=4$). Reprinted from Shimazu, T. and Kurata, K. (1999) [17] with permission from Springer Science and Business Media.

In the 20%, 30%, and 40% oxygen treatments, the number of globular-stage embryos increased until day 15, and decreased as the somatic embryos progressed into the heart stage (Figure 4B). However, in the 4% and 7% oxygen treatments, the number of globular-stage embryos did not decrease during the culture period (Figure 4B), and the

number of heart-stage embryos formed was lower than that in the higher oxygen treatments (Figure 4C). The number of torpedo-stage embryos increased clearly at higher oxygen treatments than 7%. Few torpedo-stage embryos were observed in the suspension aerated with 4% oxygen (Figure 4D). Figure 4E shows the cumulative number of cotyledonary-stage embryos harvested by straining through an 850- μm steel mesh. The oxygen-enriched aeration resulted in enhanced productivity of cotyledonary-stage embryos.

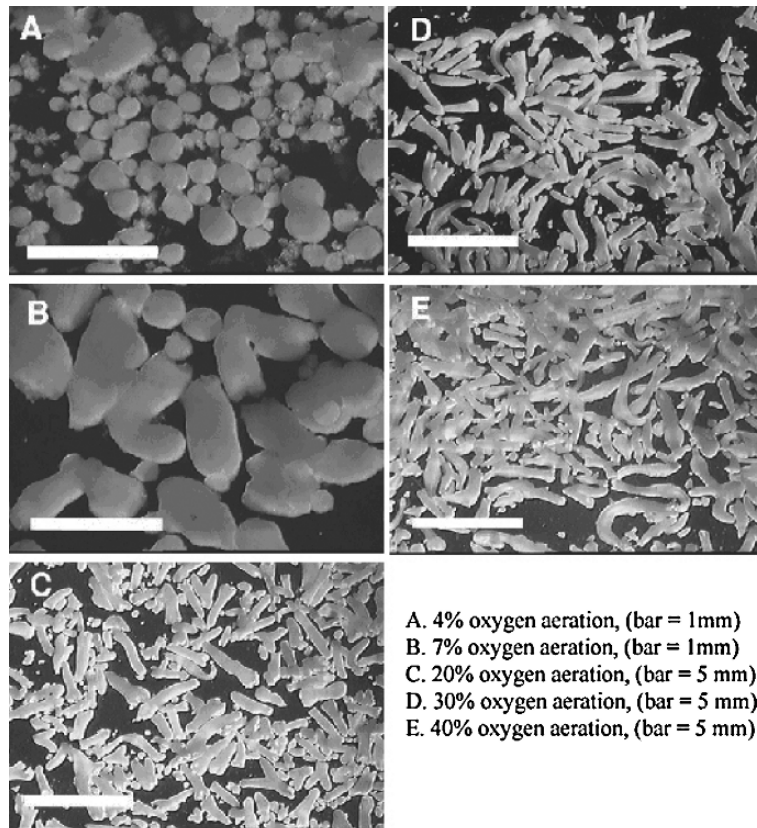


Figure 5. Somatic embryos harvested on day 23. Reprinted from Shimazu, T. and Kurata, K. (1999) [17] with permission from Springer Science and Business Media.

Somatic embryos harvested on day 23 in various DO concentrations are shown in Figure 5. In the 4% oxygen treatment, globular-stage embryos were observed, but formation of the cotyledonary part did not develop (Figure 5A). In the 7% oxygen treatment, cotyledonary part was observed, but the radicle and hypocotyl parts were not elongated (Figure 5B). Elongation of the somatic embryos was promoted by higher oxygen concentration (Figure 5C-E).

Effects of dissolved oxygen concentration on somatic embryogenesis

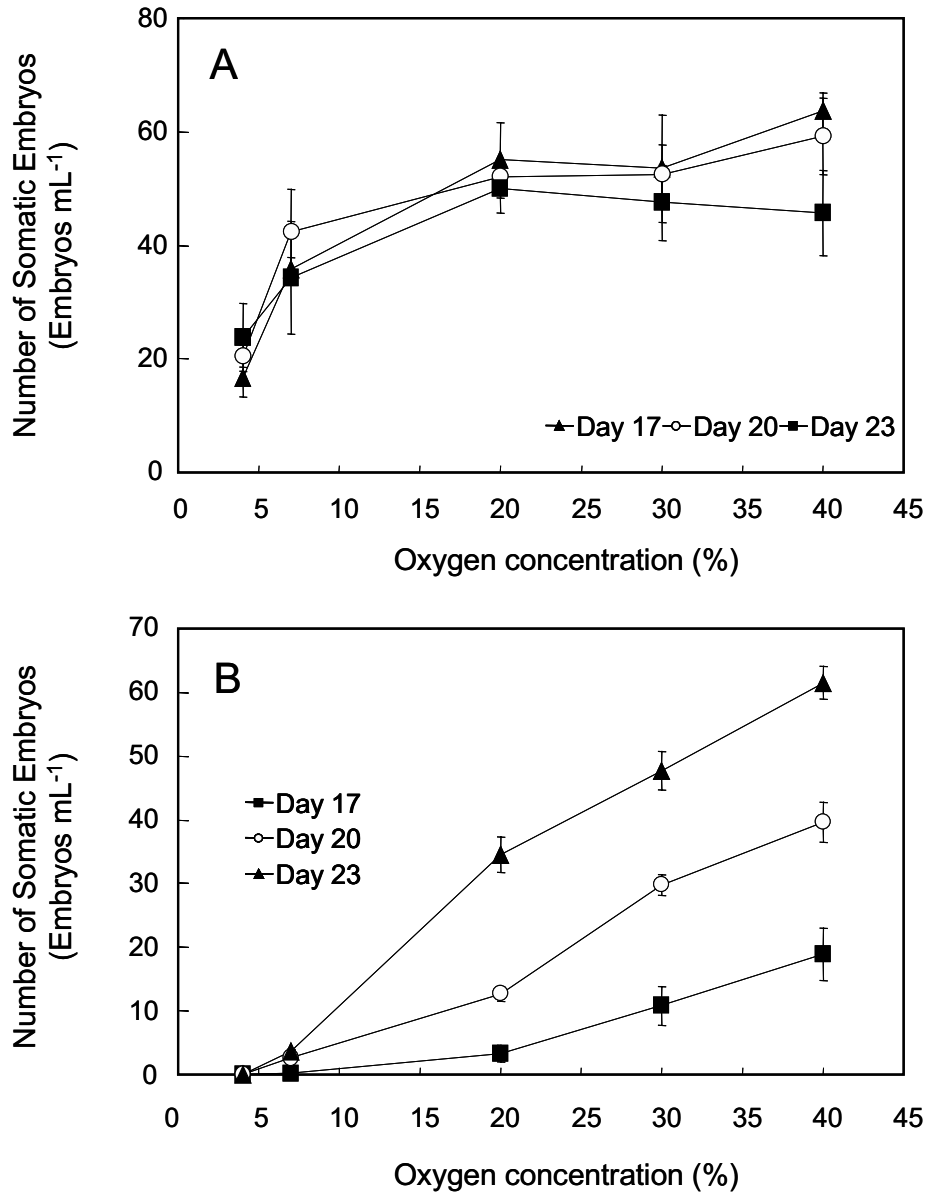


Figure 6. Relationship between headspace oxygen concentration and the number of carrot somatic embryos. Bars represent standard errors ($n=4$). (A) Heart-stage embryos, (B) Cotyledonary-stage embryos. Reprinted from Shimazu, T. and Kurata, K. (1999) [17] with permission from Springer Science and Business Media.

2.3. RELATIONSHIP BETWEEN SOMATIC EMBRYOGENESIS AND OXYGEN CONCENTRATION

Figure 6 shows the relationship between somatic embryogenesis and oxygen concentration. The number of heart-stage embryos increased sharply with increased oxygen concentration, when the range of lower oxygen concentration was raised up to 7%. However, above 20% oxygen, oxygen enrichment did not improve productivity of heart-stage embryos (Figure 6A). In contrast, the cumulative number of cotyledonary-stage embryos increased linearly with rising oxygen concentration (Figure 6B). Thus, the effect of oxygen enrichment on the somatic embryo development was remarkable at later stages. Huang *et al.* [20] suggested that the size of somatic embryos have increased and thus led to possible mass transfer limitations. Since oxygen is consumed by cell respiration during the transport through the somatic embryo, the oxygen concentration level within the somatic embryo may be lower than the bulk solution DO level.

This oxygen concentration gradient depends on the size, geometry and respiration activity of somatic embryo. The size of the later developmental stage embryos was much larger than the globular and heart-stage. Therefore, the DO concentration within somatic embryo might be below the critical level at later developmental stages if the bulk DO level is low, and the oxygen-enriched aeration promoted the production at the later stages. This hypothesis is supported by the experimental results shown in Figure 6. Similar results were reported for rice [15], and lily [21]. Figure 7 schematically illustrates this hypothesis.

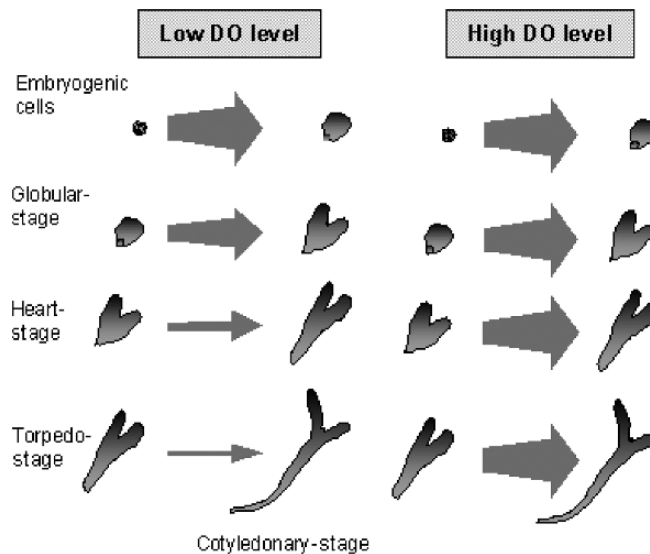


Figure 7. Schematic illustration of DO effects on somatic embryo development. The thickness of the arrow shows the frequency of development. Reprinted from Shimazu, T. and Kurata, K. (1999) [18].

3. Dynamic control of DO concentration to regulate torpedo-stage embryos

One of the main problems restricting the commercial application of somatic embryogenesis is non-uniformity of individual embryo development in a somatic embryo population during a culture period. In the case of dicotyledonous culture, embryos at various developmental stages (globular, heart, torpedo, and cotyledonary-stage) are often mixed in the suspension (Figure 5). In addition, the formation ratio of embryos in each developmental stage changes respectively during the culture period [2]. Somatic embryos are harvested at the torpedo-stage because plant conversion of embryos at this stage is better than other stages [22,23]. Therefore, attempts have been made to develop methods for obtaining a large number of torpedo-stage embryos with sufficient degree of homogeneity. These attempts can be classified into two approaches. One approach is to select torpedo-stage embryos from a heterogeneous embryo population. A few groups have reported on automated selection systems of torpedo-stage embryos combined with image analysis systems [2,7,8]. Molle *et al.* [6] developed an automated selection system that mechanically sieves torpedo-stage embryos based on filtration through a mesh. The other approach aims at improving the culture method to enhance synchronous development of embryos into torpedo-stage during the culture. Nadel *et al.* [24] showed that synchronization of celery somatic embryogenesis was promoted by addition of abscisic acid to the regeneration medium. Osuga *et al.* [25] proposed a method to improve synchronizing development into torpedo-stage embryos using the inhibitory effect of high population density on embryo development. Suehara *et al.* [26] developed an immobilized culture system in which torpedo-stage embryos of uniform size were released from gel beads. Unfortunately, these methods are not only labour intensive, but also have a high risk of contamination because of the necessity of embryo transfer out of and into the culture vessels. Jay *et al.* [9] showed that low medium pH 4.3 did not allow the development into torpedo and plantlet-stage, suggesting that the control of medium pH might be useful for synchronizing development into globular and heart-stage embryos. However, this report did not assess the development from heart-stage into plantlet-stage. Shimazu and Kurata [18] developed a dynamic DO concentration control method to enhance the ratio of torpedo-stage embryos at the time of harvest. This method does not require labour intensive operation, nor enhances the risk of contamination. Details of this method are described below.

3.1. THE METHOD OF DYNAMIC DO CONTROL

As described in the previous section, low DO concentration not only represses the development of torpedo-stage embryos into cotyledonary-stage, but also delays the development of heart-stage embryos into torpedo-stage (Figure 7), and as a result, a remarkable number of early stage embryos remains in the suspension at the time of torpedo-stage embryos harvest. This result suggested that the formation ratio of torpedo-stage embryos to total embryos of all developmental stages (FT) could be enhanced if there were a way to promote the development of globular and heart-stage embryos into the later stages, while simultaneously repressing torpedo-stage embryo development into cotyledonary-stage. It seemed that this could only be achieved by dynamically

controlling DO based on the data on the embryo development situation in the suspension.

Shimazu and Kurata [18] proposed a dynamic DO control (DyDO control) algorithm to enhance FT by promoting development of early stage embryos into torpedo-stage and simultaneously repressing development of torpedo-stage embryos into late stages. They used the same culture system as that described in the previous section (Figure 2). The algorithm they developed was based on information on the embryo population composition (formation ratio of embryos at each developmental stage to total embryos of all stages) in the suspension assessed by monitoring the culture. Since destructive sampling of somatic embryos has a risk of contamination and is labour intensive, a non-invasive monitoring method was desirable.

The simple technique of Ibaraki and Kurata [27] was adopted as noninvasive image acquisition of somatic embryo population in culture vessels. This schematic layout is shown in Figure 8. After shaking the suspension, 300-ml Erlenmeyer flasks containing the somatic embryo suspension were set on a ring stand and left for a few minutes to allow somatic embryos to settle at the bottom. The bottoms of the flasks were flat. Eight images of randomly selected parts of the flask bottom were acquired using a charge-coupled device (CCD) camera. The number of embryos at each developmental stage was estimated from the acquired images.

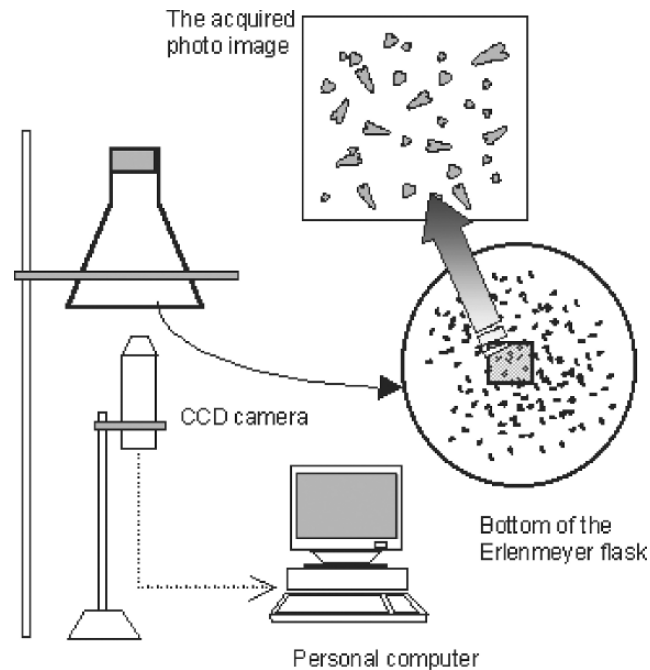


Figure 8. Schematic diagram of the apparatus for image acquisition of somatic embryos population. Reprinted from Shimazu, T. and Kurata, K. (2003) [18].

DyDO control was based on the hypothesis schematically illustrated in Figure 7. It was expected that by choosing an appropriate DO level, development of late stage embryos (large embryos) to the next stage could be repressed without retarding development of early stage embryos (small embryos), thus increasing the uniformity of the culture. Therefore, in somatic embryo culture by DyDO control, the culture period was divided into the following three phases of a different DO level to adjust the formation rate of embryos at each developmental stage to total embryos of all developmental stages (Figure 9).

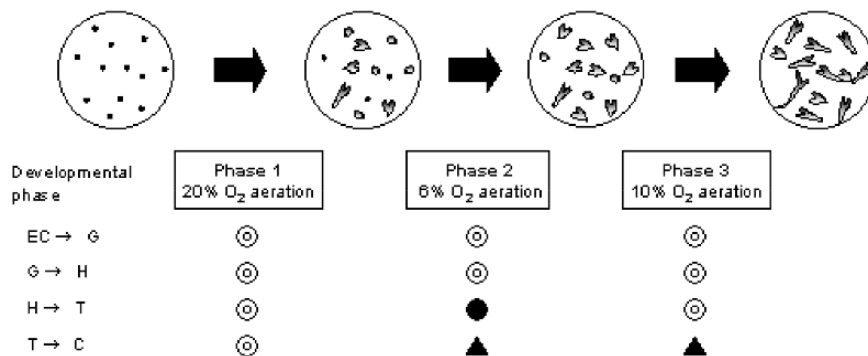


Figure 9. Synchronization process of development of embryos into torpedo-stage by dynamic DO control. Double circle: development promotion, black circle: slight development promotion, black triangle: development repression. EC, Embryogenic cells stage; G, globular-stage; H, heart-stage; T, torpedo-stage; C, cotyledonary-stage. Reprinted from Shimazu, T. and Kurata, K. (2003) [18].

In each phase a different level of oxygen gas concentration was aerated in the headspace of flasks. The timing of phase changes was decided based on the results of monitoring the culture.

- Phase 1 (20% oxygen aeration): In order to reduce the culture period, phase 1 was set as aeration with 20% oxygen gas for which the development progress of early stages (globular- and heart-stage) is not delayed. This phase promotes development of embryogenic cells into globular and heart-stage embryos, and continues until torpedo-stage embryos begin to appear in the embryo population.
- Phase 2 (6% oxygen aeration): In order to progress development of early stage embryos, and to suppress the development into cotyledonary-stage of embryos that already developed on torpedo-stage simultaneously, phase 2 was set as 6% oxygen aeration. This phase continues until the change of the formation ratio of torpedo-stage embryos plateaus.
- Phase 3 (10% oxygen aeration): In order to promote development from heart-stage embryos into torpedo-stage, while repressing formation of cotyledonary-stage embryos, phase 3 was set as 10% oxygen aeration. This oxygen concentration was determined based on Shimazu and Kurata [28] who found that the progress of development into torpedo-stage is delayed in 7% oxygen

aeration, and on the other hand, the development of torpedo-stage into cotyledonary-stage is promoted in 20% oxygen aeration. Two control experiments in which 20% and 6% oxygen gas was aerated into the headspace of the flasks respectively during the whole culture period were conducted for comparison with the DyDO control.

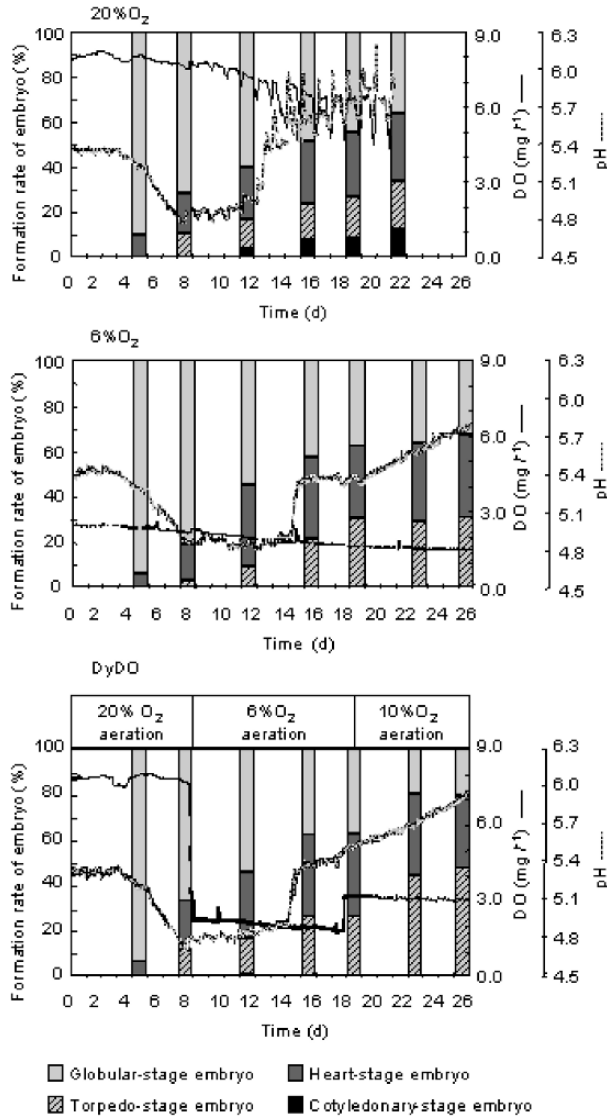


Figure 10. Time course of DO concentration, medium pH and formation rate of embryos in each developmental stage. 20% O₂, 20% oxygen aeration; 6% O₂, 6% oxygen aeration; DyDO, dynamic DO control. Reprinted from Shimazu, T. and Kurata, K. (2003) [18].

3.2. RESULTS OF DYNAMIC DO CONTROL

Figure 10 shows time course of DO levels. In the control where 20% oxygen gas (20% O₂) was aerated, DO level was maintained at approximately 8 mg L⁻¹ during the early period of the culture, and subsequently gradually lowered. The average DO level of 20% O₂ was 7.1 mg L⁻¹. On day 12, the appearance of cotyledonary-stage embryos was observed in the suspension. After that time, the DO level showed diurnal variations corresponding to the light/dark cycle in the culture room. Since the shading of the experimental system used in this study was not complete, this phenomenon might be attributed to the oxygen release of cotyledonary-stage embryos by photosynthesis. Uozumi *et al.* [22] reported that photosynthesis contributes strongly to embryo development during the cotyledonary-stage. Clear diurnal variations in DO were observed neither in the control experiment where 6% oxygen gas (6% O₂) was aerated nor in the DyDO control in the absence of cotyledonary-stage embryos. DO levels in 6% O₂ decreased from 2.5 mg L⁻¹ to 1.5 mg L⁻¹ during the culture period, and the average was 1.95 mg L⁻¹. Average DO levels in each phase of DyDO control were 7.8 mg L⁻¹ at phase 1, 2.0 mg L⁻¹ at phase 2, and 3.1 mg L⁻¹ at phase 3.

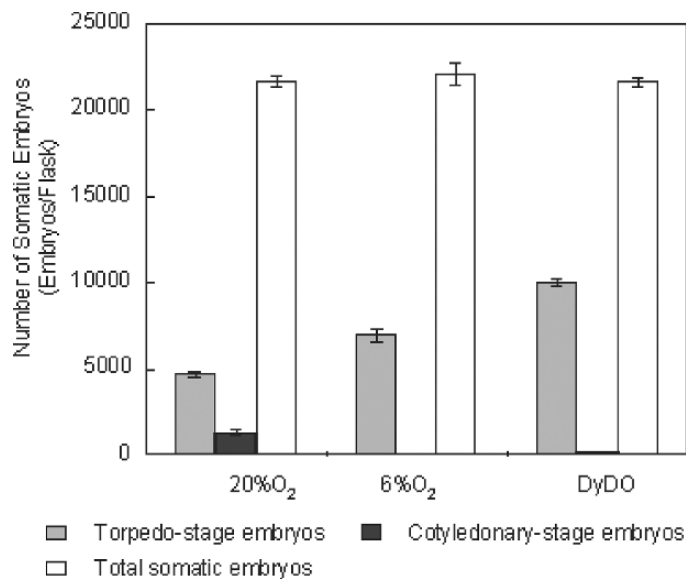


Figure 11. The number of harvested somatic embryos. Vertical bars represent standard errors of the means ($n=4$). 20% O₂, 20% oxygen aeration; 6% O₂, 6% oxygen aeration; DyDO, dynamic DO control. Reprinted from Shimazu, T. and Kurata, K. (2003) [18].

On day 8, torpedo-stage embryos began to appear in all the treatments. In 6% O₂, the FT was the lowest and the formation rate of the number of globular embryos to the number of total embryos (FG) was the highest among the three treatments on that day, suggesting that development into torpedo-stage embryos was delayed in the low DO level. In DyDO control, because torpedo-stage embryo formation was observed on day 8, the culture phase was shifted to phase 2. During days 8-16 (period of phase 2 in

DyDO control), cotyledonary-stage embryos appeared and formation ratio increased in 20% O₂, while in the other two treatments no cotyledonary-stage embryos were observed. FT in 6% O₂ increased gradually and reached 31% on day 19, but afterwards FT did not change. This result corresponds to the finding of Shimazu and Kurata [28], which showed FT increase was due to suppression of development from torpedo-stage into cotyledonary-stage by the low DO. In phase 2 of DyDO control (days 8-19), FT and formation ratio of the number of heart-stage embryos to the number of total embryos (FH) increased from 11% to 28%, and from 22% to 34%, respectively. Since FT in DyDO control hardly changed from day 16 to day 19, DyDO control was shifted to phase 3 on day 19. In phase 3 of DyDO control, FT increased remarkably to 46% in the first 3d, and in contrast, FG decreased from 37% to 20%. Cotyledonary-stage embryos did not appear in phase 3 in DyDO control.

Figure 11 shows the number of harvested somatic embryos from each treatment. The number of total somatic embryos was almost the same among the treatments. The number of torpedo-stage embryos of 20% O₂ was the fewest among the three treatments, and the total number of cotyledonary and torpedo-stage embryos was almost the same as the number of torpedo-stage embryos of 6% O₂. On the other hand, the number of torpedo-stage embryos of DyDO control was 2 and 1.4 times as many as that of 20% O₂ and 6% O₂, respectively. This result showed the effectiveness of DyDO control for torpedo-stage embryo production.

4. Conclusions

DO is one of the environmental factors that strongly affect the development of somatic embryos in the suspension. Regulating the oxygen concentrations in the headspace of flasks, DO could be controlled without changing agitation conditions. Development of late stage embryos (large embryos) to the next stage was repressed by low DO level, while development of early stage embryos (small embryos) to the next stage was little affected. Utilizing this fact, the ratio of torpedo-stage embryos to the total embryos could be remarkably enhanced by dynamically controlling DO based on the non-invasive monitoring of the suspension.

References

- [1] Preil, W. and Beck, A (1991) Somatic embryogenesis in bioreactor culture. *Acta Hort.* 289: 179-192.
- [2] Cazzulino, D.; Pedersen, H. and Chin, C.K. (1991) Bioreactors and image analysis for scale-up and plant propagation. In: Vasil, I.K. (Ed.) *Scale-up and Automation in Plant Propagation. Cell Culture and Somatic Cell Genetics of Plants, Vol.8.* Academic Press, Inc., San Diego; pp. 147-177.
- [3] Gupta, P.K.; Timmis, R.; Pullman, G.; Yancey, M.; Kreitinger, M.; Carlson, W. and Carpenter, C. (1991) Development of an embryogenic system for automated propagation of forest trees. In: Vasil, I.K. (Ed.) *Scale-up and Automation in Plant Propagation. Cell Culture and Somatic Cell Genetics of Plants, Vol.8.* Academic Press, Inc., San Diego; pp. 75-93.
- [4] Denchev, P.D.; Kuklin, A.E. and Scragg, A.H. (1992) Somatic embryo production in bioreactors. *J. Biotechnol.* 26: 99-109.
- [5] Ducos, J.P.; Bollon, H. and Pettard, V. (1993) Production of carrot somatic embryos in a bioreactor. *Appl. Microbiol. Biotechnol.* 39: 468-470.
- [6] Molle, F.; Dupuis, J.M.; Ducos, J.P.; Anselm, A.; Crolus-Savidan, I.; Petiard, V. and Freyssinet, G. (1993) Carrot somatic embryogenesis and its application to synthetic seeds. In: Redenbaugh K (Eds.) *Synseeds: Applications of synthetic seeds to crop improvement.* CRC press, Boca Raton; pp. 257-287.

- [7] Harrell, R.C.; Bieniek, M.; Hood, C.F.; Munilla, R. and Cantliffe, D.J. (1994) Automated, *in vitro* harvest of somatic embryos. *Plant Cell Tissue Org. Cult.* 39: 171-183.
- [8] Ibaraki, Y.; Fukakusa, M. and Kurata, K. (1995) SOMES2: Image-analysis-based somatic embryo sorter. *Current Plant Science and Biotechnology in Agriculture* 22: 675-680.
- [9] Jay, V.; Genestier, S. and Courduroux, J. C. (1994) Bioreactor studies of the effect of medium pH on carrot (*Daucus carota* L.) somatic embryogenesis. *Plant Cell Tissue Org. Cult.* 36: 205-209.
- [10] Archambault, J.; Williams, R.D.; Lavoie, L.; Pépin, M.F. and Chavarie, C. (1994) Production of somatic embryos in a helical ribbon impeller bioreactor. *Biotechnol. Bioeng.* 44: 930-943.
- [11] Kessell, R.H.J. and Carr, A.H. (1972) The effect of dissolved oxygen concentration on growth and differentiation of Carrot (*Daucus carota*) tissue. *J. Exp. Bot.* 23: 996-1007.
- [12] Carman, J.G. (1988) Improved somatic embryogenesis in wheat by partial simulation of the *in-ovulo* oxygen, growth regulator and desiccation environments. *Planta* 175: 417-424.
- [13] Stuart, D.A.; Strickland, S.G. and Walker, K.A. (1987) Bioreactor production of alfalfa somatic embryos. *Hort. Sci.* 22:800-803.
- [14] Jay, V.; Genestier, S. and Courduroux, J.C. (1992) Bioreactor studies on the effect of dissolved oxygen concentrations on growth differentiation of carrot (*Daucus carota* L.) cell cultures. *Plant Cell Rep.* 11: 605-608.
- [15] Okamoto, A.; Kishine, S.; Hirose, T. and Nakazono, A. (1996) Effect of oxygen-enriched aeration on regeneration of rice (*Oryza sativa* L.) cell culture. *Plant Cell Rep.* 15: 731-736.
- [16] Shigeta, J.; Sato, K. and Mii, M. (1996) Effects of initial cell density, pH and dissolved oxygen on bioreactor production of carrot somatic embryos. *Plant Sci.* 115: 109-114.
- [17] Shimazu, T. and Kurata, K. (1999) Relationship between production of carrot somatic embryos and dissolved oxygen concentration in liquid culture. *Plant Cell Tissue Org. Cult.* 57: 29-38.
- [18] Shimazu, T. and Kurata, K. (2003) Dynamic dissolved oxygen concentration control for enhancing the formation rate of torpedo-stage embryos in carrot somatic embryo culture. *J. Biosci. Bioeng.* 95: 384-390.
- [19] Nishimura, S.; Terashima, T.; Higashi, K. and Kamada, H. (1993) Bioreactor culture of somatic embryos for mass propagation of plants. In: Redenbaugh K (Ed.) *Synseeds: Applications of synthetic seeds to crop improvement*. CRC press, Boca Raton; pp. 175-181.
- [20] Huang, L. C.; Vits, H.; Staba, J. E.; Cooke, T. J. and Hu, W. S. (1992) Effect of cultivation age and embryo size on specific oxygen uptake rate in developing somatic embryos of *Daucus carota* L. *Biotech. Lett.* 14: 701-706.
- [21] Takahashi, S.; Matsubara, K.; Yamagata, H. and Morimoto, T. (1992) Micropropagation of virus free bulblets of *Lilium longiflorum* by tank culture 1. Development of liquid culture method and large-scale propagation. *Acta Hort.* 319: 83-88.
- [22] Uozumi, N.; Kohketsu, K.; Okamoto, A. and Kobayashi, T. (1993) Light dependency in celery somatic embryogenesis and plantlet development in suspension culture. *Plant Tissue Cult. Lett.* 10: 25-32.
- [23] Li, X. Q. (1993) Somatic embryogenesis and synthetic seed technology using carrot as a model system. In: Redenbaugh, K. (Ed.) *Synseeds: applications of synthetic seeds to crop improvement*. CRC press, Boca Raton; pp. 289-304.
- [24] Nadel, B. L.; Altman, A. and Ziv, M. (1990) Regulation of somatic embryogenesis in celery suspensions. 2. Early detection of embryogenic potential and the induction of synchronized cell cultures. *Plant Cell Tissue Org. Cult.* 20: 119-124.
- [25] Osuga, K.; Kamada, H.; and Komamine, A. (1993) Cell density is an important factor for synchronization of the late stage of somatic embryogenesis at high frequency. *Plant Tissue Cult. Lett.* 10: 180-183.
- [26] Suehara, K.; Kohketsu, K.; Uozumi, N. and Kobayashi, T. (1995) Efficient production of celery embryos and plantlets released in culture of immobilized gel beads. *J. Ferment. Bioeng.* 79: 585-588.
- [27] Ibaraki, Y. and Kurata, K. (1997) Image analysis based quantification of cells in suspension cultures for producing somatic embryos. *Environ. Control Biol.* 35: 63-70.
- [28] Shimazu, T. and Kurata, K. (1999) Improvement of synchronization on carrot somatic embryo culture by controlling dissolved oxygen concentration. *Environ. Control Biol.* 37: 179-184.

A COMMERCIALIZED PHOTOAUTOTROPHIC MICROPROPAGATION SYSTEM

T. KOZAI¹ AND Y. XIAO²

¹Faculty of Horticulture, Chiba University, Matsudo, Chiba 271-8510

²Institute of Environmental Science, Kunming, Yunnan 650032, China-
Fax: 81-47-308-8841-Email: kozai@faculty.chiba-u.jp

1. Introduction

A photoautotrophic micropropagation system (called a PAM hereafter) that uses a sugar-free culture medium has many advantages over the conventional, photomixotrophic micropropagation system (hereafter referred to as PMM) that utilizes a sugar-containing culture medium [1]. The advantages include the use of large culture vessels with minimum risk of microbial contamination and the enhancement of plantlet growth at a high photosynthetic photon flux (PPF) and a high CO₂ concentration inside the vessel [2,3].

In order to increase CO₂ concentration in the vessel under pathogen-free conditions, both natural and forced ventilation methods have been employed. Putting gas-permeable filter disks on the vessel lid enhances natural ventilation [4]. Forced ventilation can be conducted by supplying CO₂-enriched air with an air pump into the vessel through a gas-permeable filter disk [5]. The forced ventilation rate can be easily controlled during the production process by using an airflow controller, while the natural ventilation rate is difficult to change with passage of days [4]. In addition, it is difficult to obtain a high natural ventilation rate for a large vessel. Thus, for commercial production, forced ventilation is more convenient and practical than natural ventilation in a PAM that uses large vessels. Furthermore, many reports have shown that a PAM with forced ventilation considerably enhances the growth of plantlets compared with a PAM with natural ventilation. Fuziware *et al.* [2] developed a 20-L vessel with forced ventilation for enhancing the photoautotrophic growth of strawberry (*Fragaria x ananassa* Duch.) plantlets during the rooting and acclimatization stages. Kubota and Kozai [6] used a 2.6-L vessel containing a multi-cell tray with forced ventilation for photoautotrophic growth of potato (*Solanum tuberosum* L.) plantlets. Heo and Kozai [7] developed a similar system using a 12.8-L vessel for the photoautotrophic growth of sweet potato (*Ipomoea batatas* (L.) Lam.) plantlets. Heo *et al.* [8] developed another vessel of 11-L with air distribution pipes to improve an airflow pattern in the vessel for obtaining the uniform growth of sweet potato plantlets. Zobayed *et al.* [9] engineered a 3.5-L vessel with units of forced ventilation and sterile nutrient solution supply for uniform and enhanced growth of sweet-potato plantlets. Commercial application of the PAM may be

advantageous to additional ornamental species such as Calla lily (*Zantedeschia elliottiana*) and China fir (*Cunninghamia lanceolata* (Lamb.) Hook. However, economic analysis of the PAM has rarely been conducted [14]. The aim of this chapter is to describe the plantlet growth of Calla lily and China fir in the PAM to that of PMM and to assess the possibility of commercialisation of the PAM based on the estimation of production cost of Calla lily plantlets.

Calla lily, an herbaceous flowering plant for which there is currently a large demand, is conventionally propagated by tubers, resulting in a limited multiplication rate. The multiplication rate can be improved by a conventional micropropagation system but wide application has been limited by its high production costs, which are mainly due to poor plantlet growth, high percent of biological contamination of the medium, and labour intensive work [10]. China fir is a rapid-growing woody plant that is used in the timber, furniture, and ornamental industries. In recent years, large quantities of China fir plantlets have been produced by PMM. However, China fir, like many other woody plant species, does not easily develop roots *in vitro*. Plant growth regulators have been supplied to the medium to promote *in vitro* rooting of woody plantlets, often without success [5]. In addition, sugar-containing medium often causes callus formation at the base of shoots and a low percentage of survival for many plant species during the *ex vitro* acclimatization [11]. This paper is an extended and modified version of [12] and [13].

2. Photoautotrophic micropropagation

There are three modes of plant growth *in vitro* in terms of its carbon and energy source for plant growth:

- Photoautotrophic growth is the one that is entirely dependent on photosynthesis of plants *in vitro*.
- Heterotrophic growth is the one that is entirely dependent on sugar in the culture medium (White or yellow coloured callus grows heterotrophically).
- Photomixotrophic growth is the one that is dependent both on photosynthesis and sugar in the culture medium.

The photoautotrophic micropropagation ascribed for growing chlorophyllous, green-coloured or leafy explants *in vitro* under pathogen-free conditions on the culture medium without sugar, vitamin, amino acids, etc., and only with inorganic nutrient components, providing favourable environment for promoting photosynthesis of explants or plants *in vitro*, with special attention to CO₂ concentration, light intensity, relative humidity, etc. in the culture vessel. Photoautotrophic micropropagation is often called “sugar-free medium micropropagation”.

2.1. SUMMARY OF OUR PREVIOUS WORK

Our previous work outlined the following attributes [4]

- Slow growth of plants *in vitro* is not due to their low photosynthetic ability, but often due to low CO₂ concentration in the vessel during the photoperiod.

- Sugar in the medium is needed for plant growth *in vitro*, because CO₂ concentration in the vessel is often as low as about 100 µmol mol⁻¹, which is equivalent to CO₂ compensation point of plants *in vitro*.
- CO₂ concentration in the vessel can be increased easily by ventilation with CO₂ non-enriched or enriched air.
- Photosynthesis and growth of plants *in vitro* are promoted considerably by increasing the CO₂ concentration in the vessel.
- Microbial contamination of the medium caused by ventilation can be prevented easily by use of microporous filters at air inlets.
- Growth and quality of plants *in vitro* can be improved considerably by vessel ventilation on the sugar-free medium.
- Rooting *in vitro* is enhanced without plant growth regulators, so that the rooting stage can often be eliminated, especially when porous medium such as Florialite[®] is used. Callus formation at the shoot base is reduced in absence of sugar in the medium.
- Microorganisms do not grow significantly on the sugar-free medium, so that a large ventilated vessel can be used.
- Growth as well as multiplication rate is improved under photoautotrophic conditions due to the increase in the number of nodes or shoots available as explants. Relative humidity is reduced to 85-90%, and C₂H₄ concentration is reduced to a negligible level in a ventilated vessel, so that plant is almost acclimatized *in vitro*.
- Under such normal environmental conditions and the absence of plant growth regulators in the medium, few physiological, morphological and phenotypical abnormalities are observed.
- Thus, acclimatization *ex vitro* can be eliminated or simplified with nearly 100% *ex vitro* survival.

3. The PAM (photoautotrophic micropropagation) system and its components

The commercial production site using the PAM system was owned and operated by a research institute where the second author was working for, as a production manager.

3.1. SYSTEM CONFIGURATION

System configuration of PAM is given in Table 1, in comparison with that of PMM (photomixotrophic micropropagation) system. The PAM system consisted of a culture room (floor area: 20 m²) and culture modules. The culture room equipped with an air conditioner was thermally insulated using 10 cm thick foamed polystyrene walls to reduce the cooling and heating loads of the air conditioner. The culture room was almost airtight. To prevent insects and airborne fungi entering into the room, a small air pump continuously pumped a little amount of fresh air into the room through air filters to keep the inside room air pressure slightly higher than the outside air pressure. Ultraviolet lamps were installed on the ceiling for sterilizing the room air. Nine culture modules can be placed on the floor in the culture room. Each culture module consisted of a 5-shelf

unit with or without castors, five culture vessel units, a forced ventilation unit for supplying CO₂ enriched air, and five lighting units (Figures 1 and 2). A 20-cm-high step stool was available for reaching the uppermost vessels.

Table 1. Basic specifications of the PAM (photoautotrophic micropropagation) and the PMM (photomixotrophic micropropagation) systems.

Item (Unit)	PAM	PMM
Vessel volume (L)	120	0.37 ($\phi = 7$ cm)
Vessel bottom area (cm ²)	5980	38.5
Number of vessels per module	5	500
Ventilation type	Forced	Natural
Vessel ventilation rate (mL s ⁻¹)	0-60 (controllable)	0.05 (fixed)
Supporting material	Vermiculite	Agar (6 g L ⁻¹)
Medium sucrose conc. (g L ⁻¹)	0	30
Nutrient solution	Murashige and Skoog (1962) [14]	
Light source	Cool white fluorescent lamps	
Floor area of culture room (m ²)	20	
No. of modules per culture room	9	
No. of shelves per module	5	
Area per shelf (cm ²)	6760 (130 cm wide x 52 cm deep)	
Height of module (cm)	220	
Room air temperature (°C)	22-23 °C	
Room relative humidity	70-80%	

3.2. MULTI-SHELF UNIT

This consisted of a 220-cm high steel frame supporting five shelves (130 cm x 52 cm) each for holding one vessel. Thus, the total culture shelf area is about 3.4 (=1.3 x 0.52 x 5) m². The vertical distance between shelves was 40 cm; 2 cm for a thermally insulated panel covered with a white paper underneath for reflection of light downward, 20 cm for the culture vessel, 5 cm for airflow through the gap between the upper surface of the vessel and the insulation panel to remove the heat generated by the fluorescent lamps, 3 cm for fluorescent lamps and 10 cm for airflow through the gap between the fluorescent lamps and the bottom surface of the upper shelf.

A commercialized photoautotrophic micropropagation system

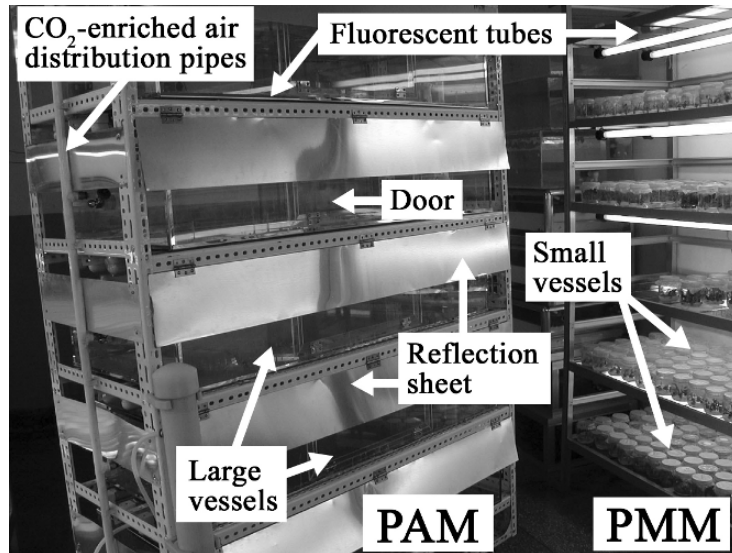


Figure 1. A culture module of the photoautotrophic micropropagation system using large culture vessels (PAM system) at the centre and a culture module of the photomixotrophic micropropagation system using small vessels with natural ventilation (PMM system) in the right.



Figure 2. A photoautotrophic micropropagation system using large vessels with forced ventilation, installed for commercialization in Kunming, Yunnan Province, China.

3.3. CULTURE VESSEL UNIT

This consisted of a Plexiglass box (115 cm wide x 52 cm deep x 20 cm high; air volume, 120 L; culture area, about 0.6 m²) with two air inlets (diameter: 5 mm) and six air outlets (diameter: 20 mm) for forced ventilation. The two inlets for providing air forcedly into the vessel were located on the sidewalls 8 cm from the bottom of vessel. Each air inlet was connected to an air-valve for controlling the number of air exchanges of the vessel, defined as the hourly ventilation rate of the vessel divided by vessel air volume. The six air outlets for discharging the vessel air naturally to the culture room were located at different points of the upper surface of the vessel (Figure 3). Locations of the air outlets are determined by trial and error to obtain a uniform air distribution in the vessel. Gas-permeable microporous filters (diameter: 20 mm, pore diameter: 0.5 μm) were attached to the air outlets to prevent dust and microbes from entering. Three trays (48×36×7 cm) were placed in each vessel. The culture vessel had a door (45 cm wide and 13 cm high) at the front side for accessing the trays.

3.4. FORCED VENTILATION UNIT FOR SUPPLYING CO₂-ENRICHED AIR

A forced ventilation unit for supplying CO₂ enriched air consisted of a CO₂ container with gas tubes, pressure gauges, airflow meters, an air pump and valves, an air disinfection and humidification tank, and a CO₂ concentration controller (Figure 4).

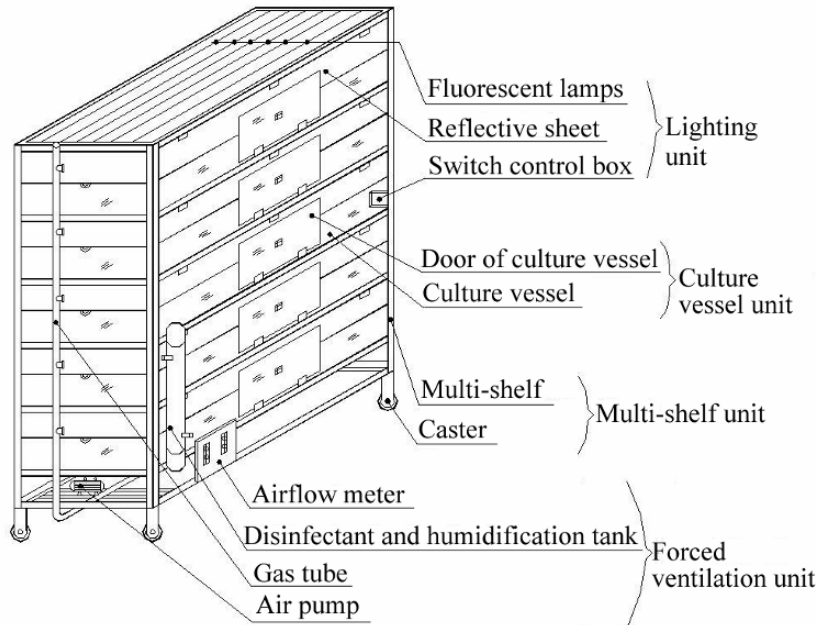


Figure 3. The culture module of photoautotrophic micropropagation system using large culture vessels with forced ventilation.

A commercialized photoautotrophic micropropagation system

This unit was used for forced ventilation of all the modules. Pure CO₂ from the CO₂ container passed through the gas tube with the CO₂ pressure gauge and airflow meter into the disinfection and humidification tank containing 2% NaClO₃ (w/v) solution. In addition, the culture room air was sent by the air pump with a microporous filter through a gas tube with an airflow meter into the disinfection and humidification tank in order to dilute pure CO₂ in the container. The pure CO₂ and culture room air were mixed in the gas tube before being sent into the disinfection and humidification tank. Finally, the disinfected CO₂- enriched air was passed through the gas tubes with the airflow meter and valves into the culture vessel through the two air inlets of the vessel. The CO₂ concentration of the mixed air was measured and adjusted by using a CO₂ concentration controller.

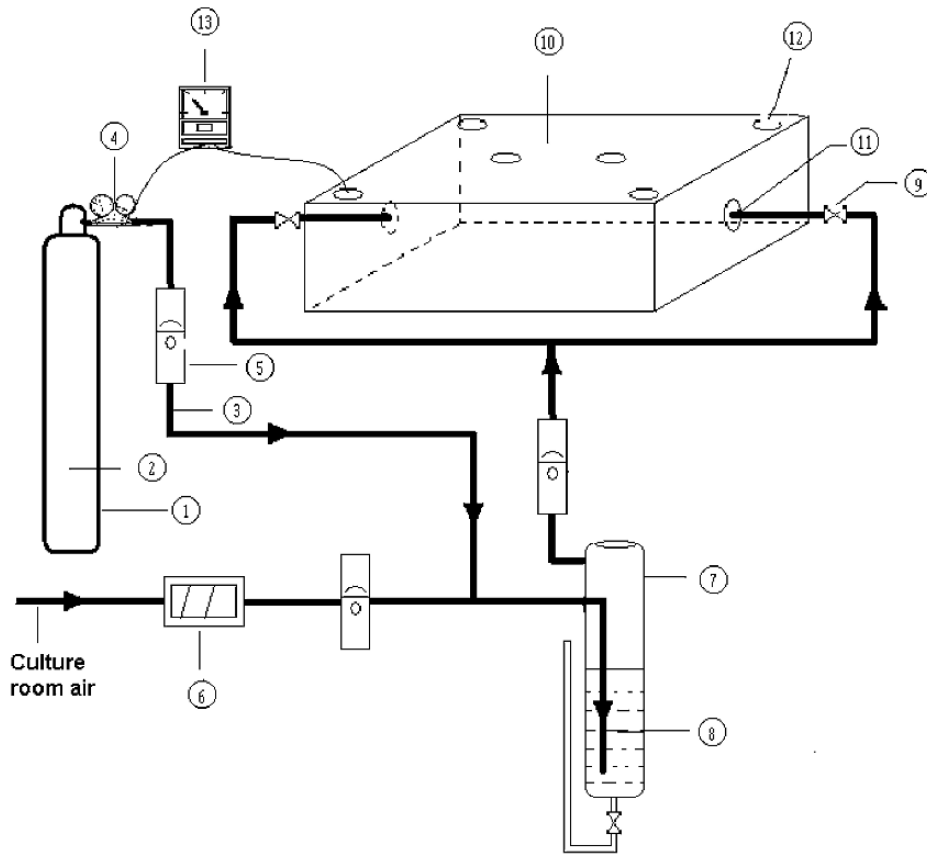


Figure 4. Schematic diagram of a forced ventilation unit for CO₂ enriched air supply. 1) CO₂ container 2) Pure CO₂ 3) Gas tube 4) CO₂ pressure gauge 5) Airflow meter 6) Air pump 7) Disinfectant and humidification tank 8) Disinfectant and humidification solution 9) Valve 10) Culture vessel 11) Air inlet of the vessel 12) Air outlet of the vessel 13) CO₂ concentration controller.

3.5. LIGHTING UNIT

White fluorescent lamps were used as a light source. Six 36-W fluorescent lamps each with one switch were installed on each shelf to adjust PPF on the shelf at a desired level in a range between 50 and 200 $\mu\text{mol m}^{-2} \text{s}^{-1}$. To increase the uniformity of PPF distribution over the shelf and the ratio of light energy received by the plantlets to the light energy emitted from the lamps, the vessel was surrounded by white reflective sheets. Two sheets (120 x 13 cm) were installed on the front and back of the vessel, and another two (50 x 13 cm) were installed on the left and right side of the vessel. The four sheets were connected with the culture shelf by hinges.

3.6. STERILIZATION

The culture vessels were sterilized as follows [15]:

- wash the culture vessel with clean water,
- wipe the culture vessel with 0.2% sodium dichloroisocyanurate ($\text{C}_3\text{O}_3\text{N}_3\text{Cl}_2\text{Na}$), a disinfectant,
- stifle the culture vessel with KMnO_4 (5 g m^{-3}), formaldehyde (10 ml m^{-3}) for 10 hours,
- spray the culture vessel with 70% ethanol before transplanting.

Trays were cleaned with water, and sterilized by dipping them into a disinfectant solution with 0.2% sodium dichloroisocyanurate for twenty minutes. Substrate (vermiculite) in 5-L cloth bags and nutrient solution in 1000-mL bottles were autoclaved at 121 to 123°C for 40 minutes. The substrate was sprayed with water to get it wet before autoclaving for increasing its thermal conductivity. Sterilized nutrient solution was supplied to the substrate. A 5-shelf unit of the PMM system was identical to the one used in the PAM, although the ventilated vessels, white reflective sheets and forced ventilation unit were not used.

4. Plantlet growth, production costs and sales price

4.1 CALLA LILY PLANTLET GROWTH

The growth of Calla lily plantlets in the PAM was compared with that of PMM. Experimental conditions are described in Table 2. Twenty plantlets were harvested at random from each of five vessels in the PAM on day 15, and two vessels each containing 10 plantlets were selected at random from each of five culture shelves and harvested on days 15 and 30 in the PMM for destructive measurements of shoot length, number of shoots, leaf area, fresh weight and dry weight. Each culture shelf was considered as a replication in both systems. *ANOVA* (Analysis of Variance) was conducted and then treatment means were compared using a least significant difference (LSD) test ($P < 0.05$). Percent loss of plantlets *in vitro* due to microbe contamination of the medium was calculated by counting dead or heavily damaged plantlets among all the plantlets.

Shoot length, leaf area, fresh and dry weight per plantlet on day 15 were 1.8, 1.8, 1.7 and 2.0 times greater in the PAM than in the PMM, respectively (Table 3 and Figure 5). The growth on day 15 in the PAM was similar to or greater than the growth on day 30 in the PMM (Table 3). Most of the plantlets on day 15 in the PAM nearly reached the inner surface of the vessel lid (about 15 cm from the medium surface), and their morphology and quality of plantlets seemed suitable for *ex vitro* acclimatization, according to visual observation.

Table 2. Conditions in *Calla lily* and *China fir* experiments using the PAM and PMM systems.

Exp. conditions common to <i>Calla lily</i> and <i>China fir</i>	PAM					PMM
	Day 0-3	Day 4-5	Day 6-9	Day 10-12	Day 13-15	Day 0-15/30
PPF ($\mu\text{mol m}^{-2} \text{s}^{-1}$)	50	50	70	100	100	50
Photoperiod (h)	12	12	14	16	16	14
CO ₂ conc. ($\mu\text{mol mol}^{-1}$)	1,500	1,500	1,500	1,500	1,500	400
Vessel ventilation (mL s^{-1})	0	5-8	13-20	25-30	50-60	0.05
RH in vessels (%)	95	95	90-95	80-90	80	95-100
<i>Calla lily</i>	PAM					PMM
Days of culture	15					30
No. of explants/vessel	1500					10
No. of explants/ treatment	7500					5000
Medium NAA (mg L^{-1})	0					1
Type of explants	Single node leafy cutting					
Leaf area, fresh and dry weights per explant	657 mm ² , 243 mg and 13 mg					
Nutrient solution supplied on day 0 per plantlet (mL)	6					6
<i>China fir</i>	PAM-0			PAM-1		PMM
Days of culture	28			28		28
No. of explants/vessel	1200			1200		8
No. of explants/treatment	2400			2400		1600
Medium NAA (mg L^{-1})	0			1		1
Type of explants	Single node leafy cuttings					
Nutrient solution supplied On day 0 per plantlet (mL)	8 (and 4 mL was added on day 18)					

RH: Relative humidity, NAA: α -naphthaleneacetic acid

Table 3. Growth and development of *Calla lily* (*Zantedeschia elliottiana*) plantlets during *in vitro* rooting stage in the PAM (photoautotrophic micropropagation) and PMM (photomixotrophic micropropagation) systems.

Treatment code	Shoot length (mm)	Number of leafy shoots	Leaf area (cm ²)	Fresh weight (mg)	Dry weight (mg)
PAM (on day 15)	91.4a	3.7a	12.8a	674a	45a
PMM (on day 15)	51.3c ^z	3.3a	7.3b	395b	23b
PMM (on day 30)	76.3b	3.4a	9.8b	579ab	36a

^zMean separation within columns by LSD test at P<0.01 (n = 100)

The PAM shortened the period of *in vitro* multiplication as well as rooting by half (from 30 to 15 days), compared with that in the PMM. The greater plantlet growth in the PAM than in the PMM was mainly due to the increased photosynthesis and transpiration under high PPF, high CO₂ concentration, enhanced air movement, and low relative humidity in the vessel [4].

Under such environmental conditions, the plantlets generally develop physiologically and morphologically normal stomata. Low relative humidity enhances transpiration, and thus nutrient uptake. The percent loss of *in vitro* plantlets due to contamination was 0% on day 15 in the PAM, and 5% on day 30 in the PMM (Table 4). Therefore, the monthly production capacity of *Calla lily* plantlets in the PAM is about 3 times (= 30/15 x 67,500/ (0.95 x 45,000) higher than that in the PMM (The factor of 0.95 in the above expression comes from the 5% loss of *in vitro* plantlets in the PMM). Percent rooting *in vitro* was 98 % in the PAM (day 15) and in the PMM (day 30).

Table 4. Production performance and sales price of the PAM (photoautotrophic micropropagation) and PMM (photomixotrophic micropropagation) systems. For culture conditions in PAM and PMM treatments see Table 1.

Calla lily	PAM (A)		PMM (B)	A/B ratio
Percent loss <i>in vitro</i>	0% on day 15		5 % on day 30	0
Percent rooting <i>in vitro</i>	98% on day 15		98% on day 30	1.0
Multiplication or rooting cycle	15 days		30 days	0.5
Percent survival <i>ex vitro</i> on day 12	95%		60%	1.6
Price per <i>in vitro</i> rooted plantlet	7.23 US cents		6.02 US cents	1.09
Price per <i>ex vitro</i> acclimatized plantlet	18.1 US cents		14.5 US cents	1.25
Yearly production capacity of <i>in vitro</i> plantlets per module	152,000		52,000	2.92
China fir	PAM-0 (A)	PAM-1	PMM (B)	A/B ratio
Percent rooting <i>in vitro</i> on day 28	91%	93%	65%	1.4
Percent survival <i>ex vitro</i> on day 12	95%	97%	16%	5.9

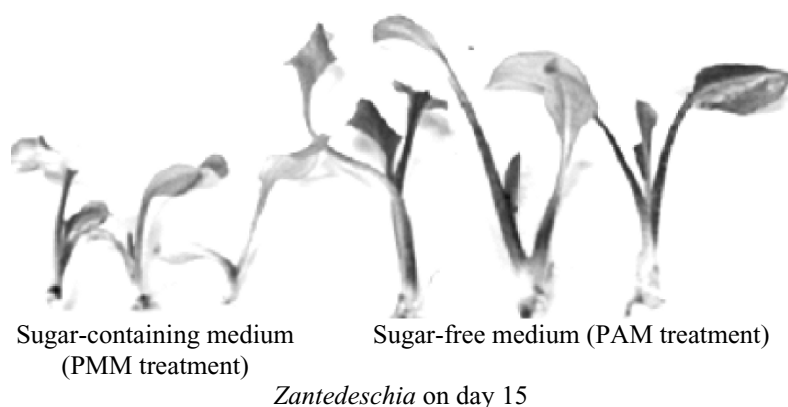


Figure 5. *Calla lily* plants grown for 15 days in the PMM and PAM systems.

4.2. CHINA FIR PLANTLET GROWTH

The growth, percent loss *in vitro* and percent *in vitro* rooting of China fir plantlets in the PAM under the presence/absence of NAA (1 mg L^{-1}) in the medium (called PAM-1 and PAM-0, respectively, hereafter) were compared with those in the PMM. Experimental conditions are described in Table 2. Forty plantlets were selected at random from each of 2 vessels in the PAM-0 and the PAM-1, respectively, and 5 vessels each containing 8 plantlets were selected at random from each of 2 culture shelves in the PMM for destructive measurements of shoot length, number of shoots, leaf area, shoot and root fresh weight, and shoot and root dry weight of plantlets. Each culture shelf was considered as a replication. The PMM treatment was considered as a control. *ANOVA* was conducted for the PAM-0 and the PAM-1, in which the presence/absence of NAA was considered as a factor. Treatment means were compared using a LSD test ($P < 0.01$).

Stem length, number of shoots, leaf area, fresh and dry weight of plantlets on day 28 were 1.7, 2.1, 5.3, 2.5 and 2.9 times greater in the PMM-0 than in the PMM (Table 5 and Figure 6). There were no significant differences in shoot growth, number of shoots or leaf area between the PAM-1 and the PAM-0. The percentages of rooted plantlets *in vitro* on day 28 in the PAM-0, PAM-1, and PMM, were 91%, 93% and 65%, respectively. In the PAM, the presence of NAA in the medium had little effect on the increase in percent *in vitro* rooting, although roots formed 2 to 3 d earlier in the PAM-1 than in the PAM-0. The higher percent of *in vitro* rooting in the PAM-0 and the PAM-1 than in the PMM was probably due to the absence of sugar in the medium, the use of porous supporting material and enhanced photosynthesis. Sugar in the medium can inhibit adventitious root development in the early stage [16]. Porous supporting materials such as vermiculite, perlite or mixtures of these materials promoted the *in vitro* rooting of plant species such as sweet potato [17], coffee [18] and sugarcane [19].

Endogenous phytohormones such as auxin necessary for rooting and carbohydrates must be more produced by plantlets in the PAM than by plantlets in the PMM.

Table 5. Growth and development of China fir (*Cunninghamia lanceolata*) plantlets on day 28 in the PAM-0, PAM-1 and PMM systems. PAM and PMM denote photoautotrophic and photomixotrophic micropropagation, respectively. PAM-0: PAM with absence of NAA in the medium, PAM-1: PAM with presence of NAA in the medium.

Treatment code	Shoot length (mm)	No. of shoots	Leaf area (cm ²)	Fresh weight (mg)		Dry weight (mg)	
				Shoot	Root	Shoot	Root
PAM-0	77.2a ^z	68a	3.88a	299a	84a	58a	4.7a
PAM-1	73.5a	56a	3.13a	272a	78a	57a	4.1a
PMM	46.1b ^z	33b	7.30b	105b	51b	19b	2.8b

^zMean separation within columns by LSD test at $P < 0.01$ ($n = 80$)

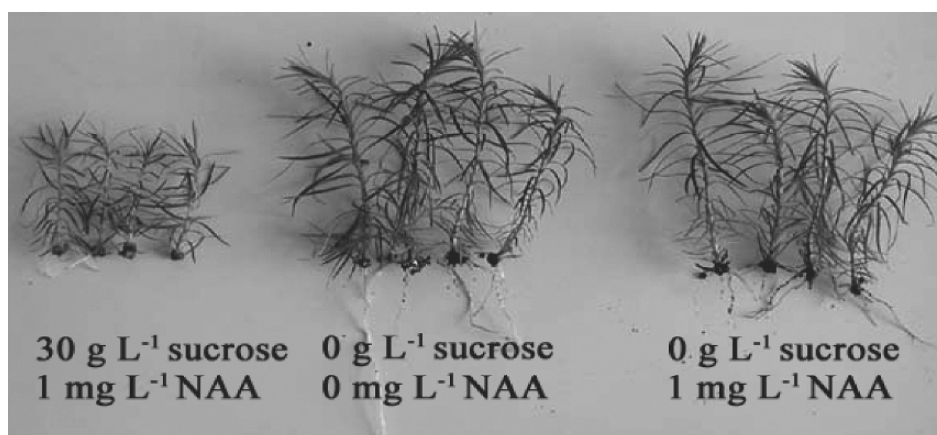


Figure 6. China fir plants grown for 28 days in the PMM and PAM systems.

4.3. PERCENT SURVIVAL DURING ACCLIMATIZATION *EX VITRO*

In vitro rooted plantlets were transplanted for acclimatization *ex vitro* in a bamboo-structured plastic greenhouse with a simple shading screen in Sept. 2001 in Kunming, China. Three thousand Calla lily plantlets and 2,000 China fir plantlets from the PAM were transplanted with substrate (vermiculite), while 3,000 Calla lily plantlets and 700 China fir plantlets from the PMM were transplanted without substrate (agar). Transplanting the plantlets with substrate reduces the amount of labour hour and root damage, and makes it possible to use automatic transplanting instead of manual transplanting. During the *ex vitro* acclimatization, average air temperature was 17°C, the

highest and lowest daily average air temperatures were 23° C and 14° C, and average relative humidity during daytime was 76%. PPF was not measured due to a technical problem. Twelve days after transplanting *ex vitro*, all the dead plantlets were counted in each treatment, and the percent survival *ex vitro* was determined. This experiment was conducted only once. In addition, 4000 *in vitro* rooted Calla lily plantlets produced in the PAM were sold without *ex vitro* acclimatization directly to a farmer, just as a trial. Then, the farmer transplanted the plantlets in a bamboo-structured plastic greenhouse without any shading screen (i.e., without *ex vitro* acclimatization). The number of dead plantlets was counted 12 days after transplanting to determine the percent survival *ex vitro*.

Percent survival of Calla lily plantlets during the *ex vitro* acclimatization was 95 % in the PAM and 60% in the PMM, and that of China fir was 95% in the PAM-0, 97% in the PAM-1, and 16% in the PMM. The percent survival was about 6 times higher in the PAM-0 and the PAM-1 than in the PMM. The lower percent survival in the PMM was probably due to the malfunction of stomata in leaves [4] and callus formation at the base of the nodal cuttings. Callus formation has been considered a cause of poor root initiation and limited uptake of nutrient and water [18]. The higher percent survival in the PAM was probably because the plantlets were already acclimatized and functionally photoautotrophic *in vitro* [11]. The percent survival of Calla lily plantlets transplanted in the farmer's greenhouse without shading (i.e., no acclimatization procedure) was 80%, compared with 95% in the greenhouse with a shading screen. Thus, by further improving the *in vitro* acclimatization method in the PAM, the *ex vitro* acclimatization process could be eliminated under moderate weather conditions [7]. This simplification is one of the advantages of the PAM.

4.4. PRODUCTION COST OF CALLA LILY PLANTLETS: A CASE STUDY

Production cost was divided into the investment (or indirect) cost and the direct production cost. The direct production cost was further divided into *in vitro* multiplication, *in vitro* rooting, and *ex vitro* acclimatization costs (The greenhouse construction cost for *ex vitro* acclimatization was included in the acclimatization cost). *In vitro* multiplication cost was divided into labour, medium, electricity and other costs. The amounts of electric energy consumed for lighting, cooling, air pumping and autoclaving during the experiments were measured separately by watt meters (DD282, Shanghai Sanxing Ammeter Co., Ltd.). Electricity cost per kWh was 8.1 US cents. The costs of labour, electricity, medium, acclimatization and initial investment for *in vitro* rooting and *ex vitro* acclimatization in the PMM and the PAM were recorded and/or calculated based upon their prices as of 2001 in Kunming, China. The number of labour hours, production costs by components, and sales prices were recorded. Costs for supervision, administration, sales and transportation of plantlets to farmers were not included in the calculation of production cost. In this experiment, the cost of *in vitro* multiplication was equal to the cost of *in vitro* rooting in both the PMM and the PAM, because these two processes differed only by the combination of plant growth regulators in the medium only.

The investment cost of the module (excluding the culture room) was US \$15,180 or CN Y126, 000 (Chinese Yuan) for the PAM (1 US\$ = 8.3 CNY as of 2003), and was 5,807 US \$ for the PMM. Since the lifetime of the PAM and PMM was considered to be

10 years, yearly depreciation was 1,518 US \$ for the PAM and 581 US \$ for the PMM. The yearly production capacity per module of the PAM was about 152,000 plantlets (= $365/18 \times 7,500$), since one multiplication cycle was 18 days; 15 days for multiplication, 1 day for harvesting and 2 days for cleaning, preparation and transplanting. On the other hand, the yearly production capacity of the PMM was about 52,000 plantlets (= $365/33 \times 5,000 \times 0.95$), since one multiplication cycle was 33 days; 30 days for multiplication, 1 day for harvesting and 2 days for cleaning, preparation and transplanting. Therefore, if the PAM and PMM were operated throughout the year, the yearly depreciation of investment cost per plantlet was 0.010 US \$ (= $1,518/152,000$) or 1.00 US cent in the PAM, and 0.0112 US \$ (= $581/52,000$) or 1.12 US cent in the PMM. In other words, the investment cost per plantlet was a little lower in the PAM than in the PMM, as shown in Table 6. The above figures indicate that the investment cost accounted for 18% of the production cost in the PAM and 12% of the production cost in the PMM.

4.4.1. Production cost per acclimatized plantlet

The production cost per *ex vitro* acclimatized plantlet from the PAM was 59% of that from the PMM (Table 6). The cost for *ex vitro* acclimatization in the PAM and the PMM accounted for 50% and 56% of the production cost, respectively. Thus, an increase in percent survival during *ex vitro* acclimatization significantly decreases the production cost. Of the total costs for *ex vitro* acclimatization in the PAM, 20% was spent on the construction of the greenhouse, 56% was spent on labour, 19% was spent on supplies such as substrate, electricity, water, fertilizer and pesticide and 5% was spent on other items. On the other hand, in the PMM, 11% was spent on the construction of the greenhouse, 38% was spent on labour, 11% was spent on supplies such as substrate, electricity, water, fertilizer and pesticide and 40% was spent on other items. The lower cost of *ex vitro* acclimatization in the PAM than in the PMM was mainly due to a higher percentage of survival *ex vitro* and less labour.

4.4.2. Cost, labour and electricity consumption for multiplication or rooting

The cost for *in vitro* multiplication, which was equal to that for *in vitro* rooting, in the PAM was 58% of that in the PMM (Table 6). Labour cost in the PAM was less than half of that in the PMM. This result is consistent with the prediction by Kozai *et al.* [5]. The reduced labour cost in the PAM significantly reduced the cost for *in vitro* multiplication and rooting. Electric energy consumption per plantlet during the *in vitro* multiplication was 27.2Wh (or 97.9 kJ = $27.2\text{Wh} \times 3600 \text{ s}$) in the PAM; 69% for lighting, 24% for cooling, 2% for air pumping and 5% for autoclaving.

A commercialized photoautotrophic micropropagation system

Table 6. A comparison of production costs, labour time and electricity consumption per plantlet of *Calla lily* in the PAM and the PMM systems.

Cost per <i>ex vitro</i> acclimatized plantlet (US cent)	PAM (A)	PMM (B)	A/B Ratio
Investment cost	1.00 (18%)	1.12 (12%)	0.89
<i>In vitro</i> multiplication	0.84 (16%)	1.44 (16%)	0.58
<i>In vitro</i> rooting	0.84 (16%)	1.44 (16%)	0.58
<i>Ex vitro</i> acclimatization	2.65 (50 %)	5.06 (56%)	0.52
Total	5.33 (100%)	9.06 (100%)	0.59
<i>In vitro</i> multiplication cost per plantlet (US cent)	PAM (A)	PMM (B)	A/B Ratio
Labour cost	0.35 (42%)	0.75 (52%)	0.47
Electricity cost	0.22 (26%)	0.36 (25%)	0.61
Medium cost	0.16 (19%)	0.22 (15%)	0.73
Others	0.11 (13%)	0.11 (8%)	1.00
Total	0.84 (100%)	1.44 (100%)	0.58
<i>Ex vitro</i> acclimatization cost per plantlet (US cent)	PAM (A)	PMM (B)	A/B ratio
Investment for greenhouse	0.53 (20%)	0.56 (11%)	0.95
Labour	1.48 (56%)	1.92 (38%)	0.77
Supplies	0.50 (19%)	0.56 (11%)	0.89
Others	0.13 (5%)	2.02 (40%)	0.06
Total	2.65 (100%)	5.06 (100%)	0.52
Labour time for <i>in vitro</i> multiplication per plantlet (s)	PAM (A)	PMM (B)	A/B Ratio
Vessel washing	0.48 (2.4%)	3.84 (9%)	0.13
Harvesting	0.48 (2.4%)	7.68 (18%)	0.06
Medium preparation	0.96 (4.8%)	3.84 (9%)	0.25
Excising/transplanting	17.28(85.6%)	25.92 (60%)	0.67
Others	0.96 (4.8%)	1.92 (4%)	0.50
Total	20.16 (100%)	43.2 (100%)	0.47
Electricity consumption for <i>in vitro</i> multiplication per plantlet (Wh)	PAM (A)	PMM (B)	A/B Ratio
Lighting	18.7 (69%)	24.1 (56%)	0.65
Cooling	6.49 (24%)	9.1 (21%)	0.71
Air pumping	0.56 (2%)	-	-
Autoclaving	1.50 (5%)	9.6 (23%)	0.20
Total	27.2 (100%)	42.8 (100%)	0.16

On the other hand, it was 42.8Wh in the PMM; 56% for lighting, 21% for cooling, 23% for autoclaving using electricity. Electric energy consumption per plantlet in the PAM, therefore, was 64% of that in the PMM. The lower electricity consumption in the PAM was mainly due to the reduction in multiplication and rooting periods by half, low electric energy consumption for autoclaving the medium and vessels, and a high percent

utilization of light energy by using white reflective sheets. A preliminary experiment showed that PPF was 1.65 times higher on a shelf with the reflective sheets ($86 \pm 8 \mu\text{mol m}^{-2} \text{s}^{-1}$) than on a shelf without the reflective sheets ($52 \pm 12 \mu\text{mol m}^{-2} \text{s}^{-1}$) when four fluorescent lamps were turned on. Average air temperature outside the culture room was 18°C during the experiment. The electricity consumption for cooling increases with increasing outside air temperature. Thus, the cooling cost would be increased by 50-60% when outside air temperature was around 35°C [4].

4.4.3. Sales price of *in vitro* and *ex vitro* acclimatized plantlets

The sales price of Calla lily plantlets *in vitro* was about 7.23 US cents when produced using the PAM, and was 6.02 US cents when produced using the PMM; i.e., the sales price was 20% higher in the PAM than in the PMM because of the higher quality produced by the PAM. The sales price of *ex vitro* acclimatized plantlets was 18.1 US cents when produced in the PAM, and was 14.5 US cents when produced in the PMM and acclimatized *ex vitro*; i.e., the sales price was 25% higher in the PAM than in the PMM. In this experiment, it was not possible to record the expenses for supervision, administration, sales, transportation of plantlets to farmers, etc., and thus to calculate the profit per plantlet. According to Chu [20], the supervision cost accounts for 13% of the total production cost in the micropropagation industry. In any case, The PAM could produce higher quality plantlets at a lower cost than the PMM, which shows that the PAM has a commercial advantage over the PMM.

5. Conclusions

In comparison with plantlets produced by the conventional micropropagation system using small vessels with sugar-containing medium, plantlets produced by the photoautotrophic micropropagation system using large vessels with sugar-free medium resulted in better growth, lower percent loss due to contamination, higher quality, higher percent survival *ex vitro*, and lower production costs. Therefore, the photoautotrophic micropropagation system has advantages over the conventional micropropagation system for commercial production of Calla lily and China fir plantlets with respect to production costs and sales price. This system should be useful for commercial production of micropropagated plantlets of other plant species.

Acknowledgement

The author would like to thank Ms. Hiromi Toida for her technical help for editing the manuscript.

References

- [1] Kozai, T. (1991) Photoautotrophic micropropagation. *In Vitro Cell. Dev. Biol.- Plant* 27: 47-51.
- [2] Fujiwara, K.; Kozai, T. and Watanabe, I. (1988) Development of a photoautotrophic tissue culture system for shoots and/or plantlets at rooting and acclimatization stages. *Acta Hort.* 230: 153-158.

- [3] Kozai, T. and Iwanami, Y. (1988) Effects of CO₂ enrichment and sucrose concentration under high photon fluxes on plantlet growth of Carnation (*Dianthus caryophyllus* L.) in tissue culture during the preparation stage. *J. Jpn. Soc. Hort. Sci.* 57: 279-288.
- [4] Kozai, T.; Kitaya, Y.; Fujiwara, K.; Smith, M.A.L. and Aitken-Christie, J. (1995) Environmental measurement and control systems. In: Aitken-Christie, J.; Kozai, T. and Smith, M.A.L. (Eds.) *Automation and Environmental Control in Plant Tissue Culture*. Kluwer Academic Publishers, Dordrecht, The Netherlands; pp. 539-574.
- [5] Kozai, T.; Kubota, C.; Zobayed, S.M.A.; Nguyen, Q.T.; Afreen-Zobayed, F. and Heo, J. (2000) Developing a mass-propagation system of woody plants. In: *Challenge of Plant and Agriculture Sciences to the Crisis of Biosphere on the Earth in the 21st Century, USA*; pp. 293-306.
- [6] Kubota, C. and Kozai, T. (1992) Growth and Net photosynthetic rate of *Solanum tuberosum* *in vitro* under forced ventilation. *Hort. Sci.* 27: 1312-1314.
- [7] Heo, J. and Kozai, T. (1999) Forced ventilation micropropagation system for enhancing photosynthesis, growth and development of sweet potato plantlets. *Environ. Contr. Biol.* 37(1): 83-92.
- [8] Heo, J.; Wilson, S. B. and Kozai, T. (2000) A forced ventilation micropropagation system for production of photoautotrophic sweet potato plug plantlets in a scaled-up culture vessel: Growth and Uniformity. *Hort. Technol.* 1: 90-94.
- [9] Zobayed, S.M.A.; Kubota, C. and Kozai, T. (1999) Development of a forced ventilation micropropagation system for large-scale photoautotrophic culture and its utilization in sweet potato. *In Vitro Cell. Dev. Biol.- Plant* 34: 350-355.
- [10] Lorenzo, J.C.; Gonzalez, B.L.; Escalona, M.; Teisson, C.; Espinosa, P.; and Borroto, C. (1998) Sugarcane shoot formation in an improved temporary immersion system. *Plant Cell Tissue Org. Cult.* 54: 197-200.
- [11] Kozai, T. and Zobayed, S.M.A. (2000) Acclimatization. In: Spier, R. (Ed.) *Encyclopaedia of Cell Technology*, John Wiley and Sons, Inc., New York; pp. 1-12.
- [12] Xiao, Y. and Kozai, T. (2004) Commercial application of a photoautotrophic micropropagation system using large vessels with forced ventilation: plantlet growth and production cost. *Hort. Sci.* 39(6): 345-356.
- [13] Kozai, T. and Xiao, Y. (2005) A commercialized photoautotrophic micropropagation system using large vessels with forced ventilation, The 5th IVCHB Symposium, Debrecen, Hungary, *Acta Hort.* (in press).
- [14] Murashige, T. and Skoog, F. (1962) A revised medium for rapid growth and bioassays with tobacco cultures. *Physiol. Plant.* 15: 473-497.
- [15] Xiao, Y.; Zhou, J. and Kozai, T. (2000) Practical sugar-free micropropagation system using large vessels with forced ventilation. In: Kubota, C. and Chun, C. (Eds.) *Transplant production in the 21st century*, Kluwer Academic Publishers, The Netherlands; pp. 266-273.
- [16] Jarvis, B.C. (1986) Endogenous control of adventitious rooting in non-woody cuttings. In: Michael, B. J. (Ed.). *New Root Formation in Plants and Cuttings*. Martinus Nijhoff Publishers, Dordrecht, The Netherlands; pp. 191-222.
- [17] Afreen-Zobayed, F.; Zobayed, S.M.A.; Kubota, C.; Kozai, T. and Hasegawa, O. (1999) Supporting material affects the growth and development of *in vitro* sweet potato plantlets cultured photoautotrophically. *In Vitro Cell. Dev. Biol.- Plant.* 35: 470-474.
- [18] Nguyen, T.Q.; Kozai, T.; Guyen, K.L. and Nguyen, U.V. (1999) Effects of sucrose concentration, supporting material and number of air exchanges of the vessel on the growth of *in vitro* coffee plantlets. *Plant Cell Tissue Org. Cult.* 58: 51-57.
- [19] Xiao, Y.; Lok, Y.H. and Kozai, T. (2003) Photoautotrophic growth of sugarcane *in vitro* as affected by photosynthetic photon flux and vessel air exchanges. *In Vitro Cell. Dev. Biol.- Plant.* 39: 186-192.
- [20] Chu, I. (1992) Perspective of micropropagation industry. In: Kurata, K. and Kozai, T. (Eds.) *Transplant Production Systems*. Dordrecht, The Netherlands; pp. 137-150.

INTELLIGENT INVERSE ANALYSIS FOR TEMPERATURE DISTRIBUTION IN A PLANT CULTURE VESSEL

H. MURASE, T. OKAYAMA, AND SUROSO

Graduate School of Agriculture and Biological Sciences, Osaka

Prefecture University, 1-1 Gakuen-cho, Sakai, Japan, 599-8531 -

Fax: 81-72-254-9918 - Email: hmurase@bics.envi.osakafu-u.ac.jp

1. Introduction

Tissue culture of a plantlet can be improved by activating the photosynthetic rate of the plantlet. This can be accomplished by environmental controls such as ventilation rate of the culture vessel, supply of CO₂ into the culture vessel and light intensity [1]. A simple method to increase light intensity is to add more light from some artificial light sources. However, air temperature in the interior of the culture vessel will be elevated when the light intensity is increased. The plantlet growth will be inhibited if air temperature inside the culture vessel becomes too high [2]. The air temperature inside the culture vessel can be reduced by blowing air to the outside surface of the culture vessel and/or by cooling down the temperature at the bottom of the culture vessel [3-5]. These treatments make it possible to increase light intensity without causing the high temperature problem. Different combinations of air velocity and bottom temperature vary temperature distributions inside the culture vessels. The temperature distribution within the culture vessel has a major influence on the development of a cultured plantlet. The optimal combination of air velocity and bottom temperature at a specific temperature distribution is important information to successfully grow the plantlet in the culture vessel. Analytical solution for finding the optimum combination of air velocity and bottom temperature is very difficult, since the culture vessel system is very complex. An exhaustive search can be used to search the optimum combination of air velocity and bottom temperature. However, the exhaustive search scheme in most cases is impractical due to time requirements. Hence, there is need to use a fast search in finding the best combination of air velocity value and bottom temperature values. In this study numerical analysis combined with artificial intelligence, are employed for this purpose.

The finite element technique can be used to analyze the problem of light intensification and the effectiveness of treatments such as blowing of air on the outside surface of the culture vessel and bottom cooling. A finite element analysis for this problem requires data regarding material properties of the culture vessel, the media it contains and coefficients of convective heat transfer over the surface of the culture vessel. Values of the material properties can be obtained from industrial standards such as ASA (American Standard Association) for material properties. Radiative heat flux

over the boundary can be calculated based on radiation of the light source and emissivity.

The coefficient of convective heat transfer, however, has to be determined experimentally for each thermal system considered. There are several experiments to determine the convective heat transfer coefficient over the surface of agricultural products. Johnson *et al.* [6] determined the coefficient of convective heat transfer on a spherically shape object. Zhang and Cavalieri [7] used the empirical equation to determine the coefficients of convective heat transfer for green beans. Brown and Otten [8] used a pseudo-random binary noise sequence (PRBNS) to determine the convective heat transfer coefficient for soybean seeds and white seeds. The PRBNS technique uses a derived thermal impulse response for the fluid (air) phase of packed bed of seed to obtain estimates for the thermal parameters of the individual particles (seeds). Those previous works for the experimental determination of coefficient of convective heat transfer were successful because these thermal systems were relatively homogeneous in structure, regular in shape, and uniform in boundary conditions.

The recent development of artificial neural networks has provided an effective and useful inverse technique. A notable feature of this inverse technique is use of the finite element technique to generate training data for the neural network. A finite element neural network inverse technique has been successfully applied in research works such as electrical engineering, electromagnetism, mechanics, etc. Alder and Guardo [9] presented a reconstruction algorithm using neural network techniques, which calculates a linear approximation of the inverse problem directly from finite element simulation of a forward problem. This inverse is adapted to the geometry of the medium and the signal to noise ratio (SNR) used during network training.

Genetic algorithms are adaptive search procedures derived from the principles of natural population genetics that provide relatively fast searching. Genetic algorithms are briefly characterized by three main concepts: Darwinian notion of fitness or strength which determines an individual's likelihood of affecting future generations through reproduction; a reproduction operation which selects individual for recombination according to their fitness or strength; and a recombination operation which creates new offspring based on the genetic structure of their parents. A genetic algorithm initially generates a finite set of solution for the problem (i.e. an initial population), each represented by a string structure, and followed by an iterative search procedure. The direction of the search is influenced only by the objective function associated with the individuals' fitness levels. Genetic algorithms are capable of searching solutions globally; however, there is always a chance to be trapped in local minimum. Many techniques have been devised to avoid the trap [10].

In this study, genetic algorithm is used to search the combination of air velocity and bottom temperature to optimize the temperature distribution inside the culture vessel based on a finite element model. The finite element analysis for this problem requires data regarding coefficients of convective heat transfer. The coefficients of convective heat transfer over the surface of the culture vessel are determined by the finite element neural network inverse technique. Specific objectives of this study are as follows:

- To develop finite element neural network inverse technique to determined parameters those identify coefficient of convective heat transfer over the surface of the culture vessel.

- To estimate constants of an empirical model that eventually gives coefficients of convective heat transfer distributed over the outside surface of the culture vessel.
- To optimize temperature distribution inside the culture vessel using genetic algorithm.

2. Theoretical backgrounds

Figure 1 illustrates how air at temperature of T_∞ and velocity of V_∞ at which air blows within the culture vessel. Convective heat transfer occurs on the outside surface of the culture vessel, the heat will flow from the surface of the culture vessel to the outside. Therefore, the temperatures of the air and gel inside the culture vessel will decrease. To get temperature distribution, thermal energy balances over the ring-shaped element as shown in Figure 1 is analyzed. Energy enters and leaves this ring by thermal conduction both in both r- and z-direction [11].

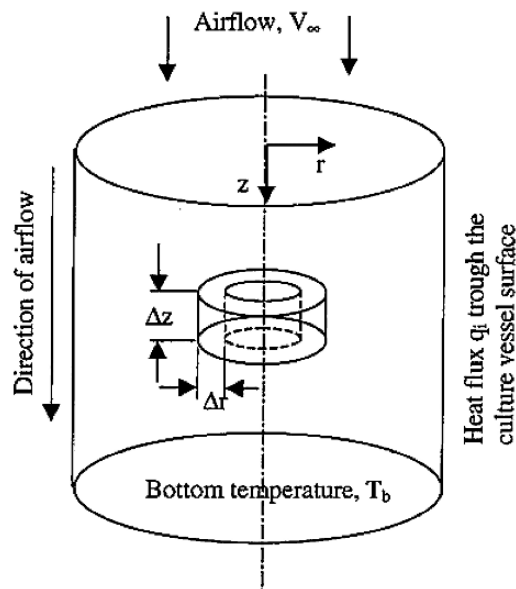


Figure 1. Illustration of heat transfer in the culture vessel due to blowing air.

Energy balances for steady state condition is

$$\begin{aligned} & \{ \text{rate of thermal energy in} \} - \{ \text{rate of thermal energy out} \} \\ & + \{ \text{rate of thermal energy production} \} = 0 \end{aligned} \quad (1)$$

Energy in by conduction at r

$$q_r|_r \cdot 2\pi r \Delta z \quad (2)$$

Energy out by conduction at $r + \Delta r$

$$q_r|_{r+\Delta r} \cdot 2\pi(r + \Delta r) \Delta z \quad (3)$$

Energy in by conduction at z

$$q_z|_z \cdot 2\pi r \Delta r \quad (4)$$

Energy out by conduction at $z + \Delta z$

$$q_z|_{z+\Delta z} \cdot 2\pi r \Delta r \quad (5)$$

It is assumed, there is no energy production inside the culture vessel. When equations (2), (3), (4) and (5) are applied into equation (1) and then divide by $2\pi \Delta r \Delta z$ this gives

$$\frac{(rq_r)|_{r+\Delta r} - (rq_r)|_r}{\Delta r} + r \frac{q_z|_{z+\Delta z} - q_z|_z}{\Delta z} = 0 \quad (6)$$

Now when Δr and Δz are allowed to approach zero gives

$$-\frac{1}{r} \frac{\partial}{\partial r} (rq_r) - \frac{\partial q_z}{\partial z} = 0 \quad (7)$$

Fourier's law for the heat conduction in both r- and z-direction;

$$q_r = -k \frac{\partial T}{\partial r} \quad q_z = -k \frac{\partial T}{\partial z}$$

Then we get the following differential partial equation:

$$k \left[\frac{1}{r} \frac{\partial}{\partial r} \left(r \frac{\partial T}{\partial r} \right) + \frac{\partial^2 T}{\partial z^2} \right] = 0 \quad (8)$$

This is a partial differential equation, which, when solved, gives the temperature as a function of both r and z in the culture vessel. The boundary conditions are

a. $T=T_b$ at $z = Z$

$$\text{b. } -k \frac{\partial T}{\partial r} = q_i \text{ at } r = R$$

Besides the two boundary conditions, convective heat transfer also occurs due to airflow on the surface of the culture vessel. Equation for the convective heat transfer on the surface of the culture vessel is

$$-k \frac{\partial T}{\partial \eta} = hA(T - T_\infty) \quad (9)$$

Coefficient convective heat transfer (h) for force convective heat transfer depends on Reynolds (Re) and Prandtl numbers (Pr) [12]. One of the empirical relationships between Nusselt number (Nu) and Re and Pr is shown in Equation (11). Prandtl number (Pr) is the parameter that relates the relative thickness of hydrodynamics and thermal boundary layers.

$$h = f(\text{Re}, \text{Pr}) \quad (10)$$

$$\text{Nu} = C\text{Re}^m \text{Pr}^n \quad (11)$$

The Reynolds number is defined by

$$\text{Re} = \frac{V \cdot L}{\nu} \quad (12)$$

V= the air velocity, m/s

ν = the kinematics viscosity of air evaluated at the fluid temperature, m²/s

The equations above show that temperature distribution inside the culture vessel is a function of air velocity and bottom temperature.

$$T(r, z) = f(V, T_b) \quad (13)$$

A specific temperature distribution can be achieved by selecting the proper air velocity and bottom temperature. Analytical solutions to select the proper air velocity and bottom temperature are very difficult. Finite element neural network inverse technique and genetic algorithm approaches are applied for selecting proper air velocity and bottom temperature.

3. Methodology

3.1. FINITE ELEMENT NEURAL NETWORK INVERSE TECHNIQUE ALGORITHM

Coefficient of convective heat transfer equation can be derived from Nusselt number equation. Constants of Nusselt number equations (C , m , and n of Equation 11) for the top and side surface of the culture vessel will be determined using a Finite Element Neural Network inverse technique. The inverse technique consisted of a finite element model and a neural network.

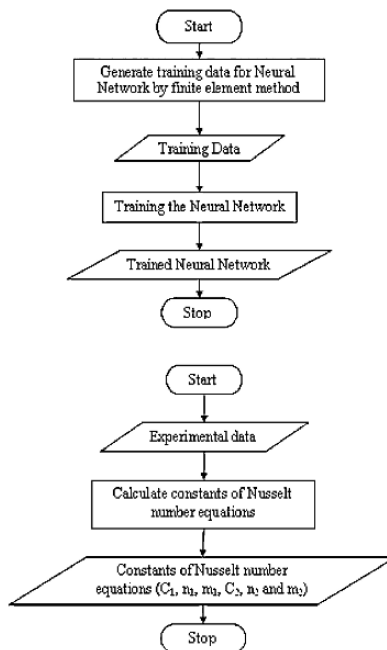


Figure 2. Flowchart of finite element neural network inverse technique.

Figure 2 shows the flowchart of finite element neural network inverse technique to determine constants of Nusselt number equations. Other similar studies are reported by Suroso *et al.* [13] and Murase *et al.* [14].

The inputs of the finite element training data generator were the constants of the Nusselt number equations (C_1 , m_1 , n_1 , C_2 and m_2 and n_2) for the top and side surface of the culture vessel, respectively. These constants were generated randomly within the proper range (Table 1). The randomized values for C , m , n were used to calculate the coefficient of convective heat transfer over the surface of the vessel. The calculated Nusselt numbers were then used to calculate the temperature distribution within the finite element model. The sets of randomly generated coefficients (C , m , n) could be

paired by corresponding finite element outputs which were temperature distributions described by nodal values of the finite element model. Considering the neural network generalization feature, those random inputs covered the entire possible combination of coefficients of convective heat transfer and temperature distribution. The finite element output was a temperature distribution inside the culture vessel. The generated input-output pair of the finite element method was used as a training data set of the neural network.

Table 1. Ranges of generated constants for Nusselts number.

	Minimum	Maximum
c	0.0	1.0
m	0.0	1.0
n	0.0	1.0

The input training data were output of the finite element and the output training data were input of the finite element. After the neural network was fully trained, measured temperatures from experiments easily determined the constants of the Nusselt equations.

3.2. FINITE ELEMENT FORMULATION

Finite element equation can be derived by integrating the differential equation for the steady state and boundary conditions. The function defined based on Equations (8) and (9) is

$$\chi = \int_V \frac{1}{2} \left[\frac{1}{r} \left[k_r \frac{\partial}{\partial r} \left(r \frac{\partial T}{\partial r} \right) \right] + k_z \frac{\partial^2 T}{\partial z^2} - 2QT \right] dV + \int_S \left[qT + \frac{1}{2} h(T - T_\infty)^2 \right] dS \quad (14)$$

and the derivative of Equation (14) is

$$\frac{\partial \chi^e}{\partial \{T\}} = [k^{(e)}] \{T\} + \{f^{(e)}\} \quad (15)$$

The minimization procedure can be obtained when the derivative equation of χ for all elements equals to zero. That is

$$\frac{\partial \chi^e}{\partial \{T\}} = \sum_{e=0}^E [[k^{(e)}] \{T\} + \{f^{(e)}\}] = 0 \quad (16)$$

or can be written in matrix equation

$$[K]\{T\} = \{F\} \tag{17}$$

where:

$$[K] = \sum_{e=1}^E [k^{(e)}] \tag{18}$$

$$\{F\} = - \sum_{e=1}^E [f^{(e)}] \tag{19}$$

where:

[K] = global stiffness matrix

{F} = global force vector

3.3. FINITE ELEMENT MODEL

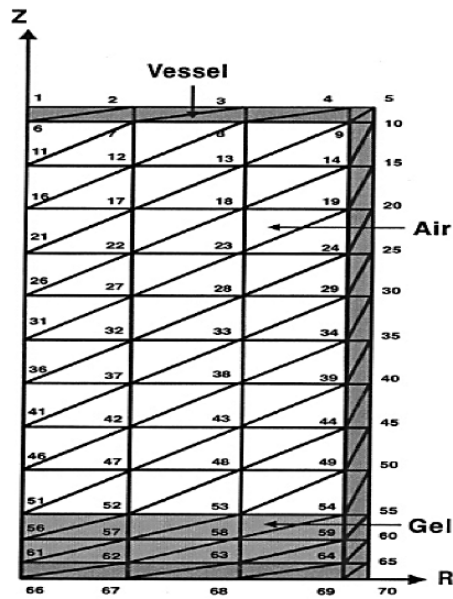


Figure 3. Finite element grid.

Figure 3 shows the finite element mesh for the culture vessel. The mesh consisted of 104 triangle elements with a total of 70 nodes. There were three boundary conditions: forced convection, heat fluxes and bottom temperature. All of the material properties and the boundary conditions were described by Suroso *et al.* [13]. Nodal temperatures within an

axsymmetric grid of the culture vessel can be approximated by a system of finite elements. Similar studies are documented by Suroso *et al.* [3] and Tani *et al.* [15].

3.4. NEURAL NETWORK STRUCTURE

Figure 4 illustrates a three-layered neural network consisting of the input layer, a hidden layer and the output layer to determine constants of Nusselt number. The input parameters of the neural network used for the inverse technique were four node temperatures defined in the finite element model. Output parameters were the constants of the Nusselt numbers for the top surface (C_1 , m_1 , and n_1) and for the side surface (C_2 , m_2 , and n_2) of the culture vessel. The values of weights (w_{ij} and v_{jk}) were adjusted during training of the neural network. The numbers of units in the hidden layer were flexible to achieve a satisfactory learning level.

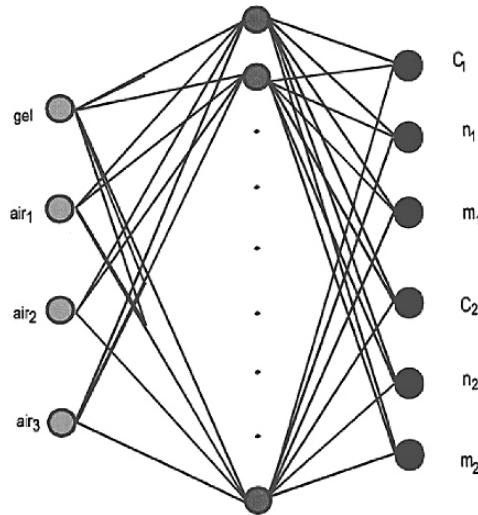


Figure 4. Neural network structure for determining constants of Nusselt number.

3.5. NEURAL NETWORK TRAINING

The input data for the neural network was generated by the finite element model at an air velocity of 3.0 m/s, ambient temperature of 23°C, bottom temperature of 15°C and light intensity PPF of 300 $\mu\text{mol}/(\text{m}^2\text{s})$. The coefficient of convective heat transfer over the surface of the culture vessel was calculated by using $h = (\text{Nu}.k)/x$, and Nusselt number was calculated by using Equation 11. The constants C , m and n of the Nusselt number for the top and side of the culture vessel were generated using a random number generator. The value of the kinematics viscosity of air at temperature of 23°C was $1.569 \times 10^{-7} \text{m}^2/\text{s}$, and the Prandtl number was 0.708 [12].

The four centre nodal temperatures were used as the input training data, i.e., gel temperature at 0.5 cm in height (T_{gel}) and three air temperatures at 3.5, 6.0 and 8.5 cm in

height (T_{air1} , T_{air2} and T_{air3}). The randomized constants of Nusselt number (C_1 , m_1 , n_1 , C_2 , m_2 , and n_2) were used as the output training data. Training of the neural network was conducted to adjust the weights. At the beginning, the weights were determined randomly and were then adjusted step by step using a neural network training method.

3.6. OPTIMIZATION OF TEMPERATURE DISTRIBUTION INSIDE THE CULTURE VESSEL

3.6.1. Genetic algorithm flowchart

Figure 5 shows the genetic algorithm flowchart to search for an optimum combination of air velocity and bottom temperature of the culture vessel.

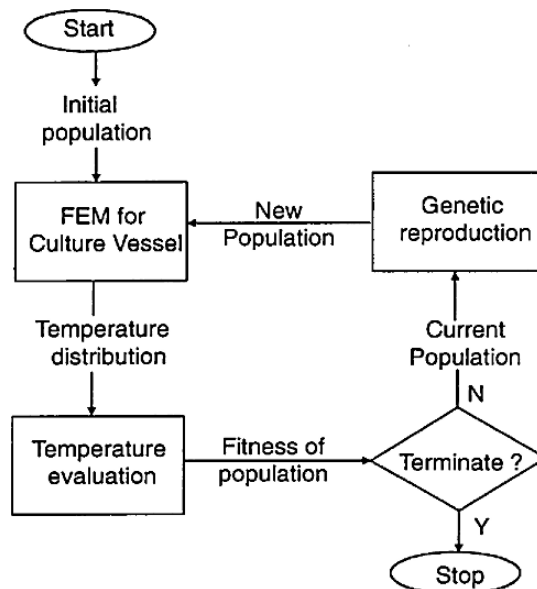


Figure 5. Genetic algorithm flowchart.

Other similar studies are documented by Suroso *et al.* [16,17]. Individual is defined as a combination of air velocity and bottom temperature. First, some individuals are generated randomly as an initial population from which the genetic process begins. At each iteration (known as a generation), each individual reproduces and recombines with others in the population on the basis of its quality or fitness. Each individual in the generated population was used to calculate temperature distribution inside the culture vessel by finite element method in order to evaluate its quality or fitness. If the calculated temperatures at the selected finite element nodes at the centre of the culture vessel are either equal to a predefined threshold of acceptance or meet other stopping criteria, the search terminates and the best fit individual among the current population is selected as the search result. If after evaluating the performance of the current

population the system has neither achieved the acceptable predefined threshold nor satisfies any other termination criteria, the genetic recombination operators are applied to the members of the current population. The crossover and mutation operators are then applied to reproduce high strength individuals, creating a new set of offspring, which theoretically yields better performance. The new population is supplied back to the finite element, and the cycle begins again until optimum combination of air velocity and bottom temperature is found.

The finite element method for calculating the temperature distribution inside the culture vessel was described in 3.2.

3.6.2. Objective function

The temperature inside the culture vessel ideally should be equal with the expected temperatures. The average value of the temperature difference between calculated temperatures and expected temperatures were used as an objective function:

$$J = \frac{\sum_i^n |T_i - T_{Ci}|}{n} \quad (20)$$

where T_i is the temperature for the i node, T_{Ci} is the expected temperature for the i node and n is the number of selected temperatures in the center of the culture vessel. The objective of this optimization is to minimize the objective function. A small value of J means that the temperature distribution inside the culture vessel are close to the expected temperatures and a large value of J means that there is a large difference in temperature distribution between computed and expected temperatures. Considering this objective function, the fitness of an individual was denoted by:

$$\text{fitness} = \frac{1}{J} \quad (21)$$

An individual with a small J has high fitness and individual with a large J has low fitness. An individual with large fitness has a high probability to be crossovered.

3.6.3. Genetic reproduction

Figure 6 shows the structure of chromosome used to search for an optimum combination of the air velocity and bottom temperature at the culture vessel system in the genetic algorithm.

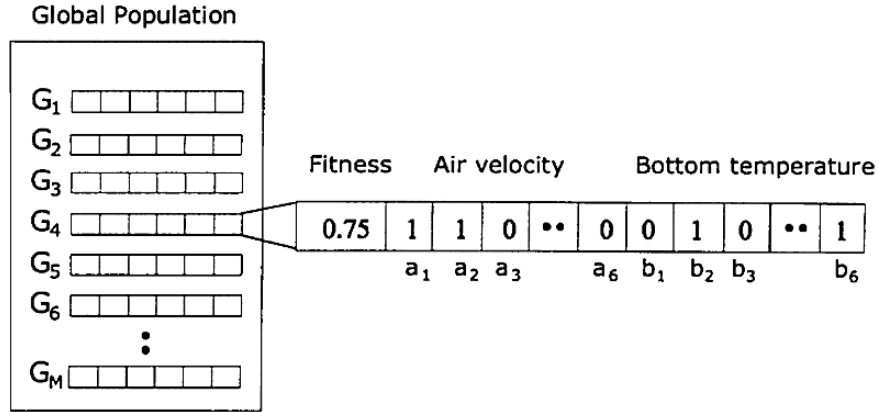


Figure 6. The structure of chromosome used in the genetic algorithm.

At each generation, there are M individuals in the population (G_1, G_2, \dots, G_M). Each individual contains air velocity and bottom temperature chromosomes and its fitness. The air velocity chromosome consists of 6 bits of binary number (a_1, a_2, \dots, a_6). The bottom temperature chromosome also consists 6 bits of binary number (b_1, b_2, \dots, b_6). To calculate the fitness, each chromosome is decoded to decimal number. The air velocity is decoded to decimal number by this equation,

$$VD = \sum_{i=1}^6 a_i \cdot 2^{(6-i)} \quad (22)$$

Because the air velocity values are between 0 and 4 m/s, the decimal number for air velocity is changed to air velocity number by this equation

$$V = \frac{4}{63} VD \quad (23)$$

The bottom temperature is decoded to decimal number by this equation

$$TD = \sum_{i=1}^6 b_i \cdot 2^{(6-i)} \quad (24)$$

The range of bottom temperature is between 5 and 20°C,

$$T_b = \frac{15}{63} TD + 5 \quad (25)$$

The air temperature and bottom temperature values are sent to the finite element method to calculate the temperature distribution. This is followed by computing objective function of some temperature nodes at the centre of the culture vessel using the Equation (20). The fitness of the individual is then calculated by Equation (21).

The individuals are arranged in an ascending order such that the top most (G_1) has the least fitness value while the bottom most (G_M) has the highest. Individuals with the highest fitness value are crossed. Crossover is a reproduction technique that takes parent chromosomes and produces child chromosomes. The crossover produces new child chromosome with higher fitness than their parents. The selected numbers of individuals to be crossed are based on crossover chances and magnification of crossover rate. Single point crossover is used:-the parent chromosomes can be split into two sub-chromosomes. The crossover point is chosen randomly for each new crossover. Each child randomly gets one sub-chromosome of one parent and other sub-chromosomes of the other parents (Figure 7). The parent chromosomes are not removed from the population. Individuals with less fitness are replaced with the new offspring from crossover.

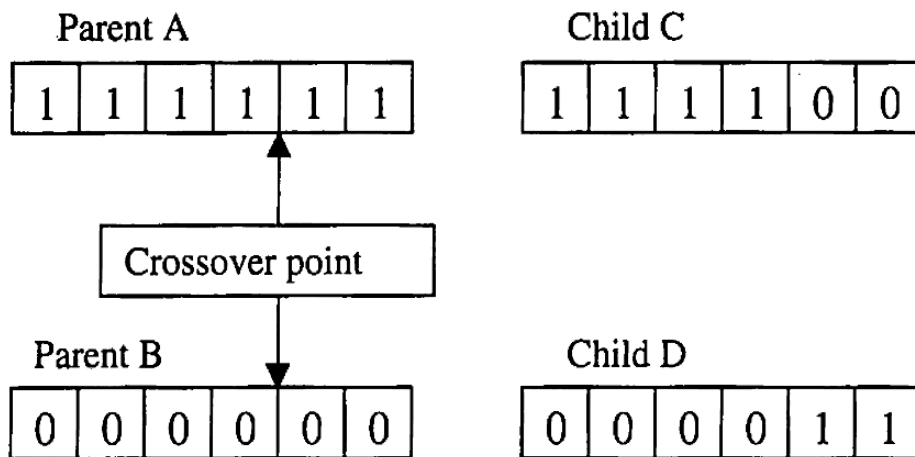


Figure 7. Illustration of gene modification in single point crossover.

Mutation is a common reproduction used for finding new points in the search space to be evaluated. When a chromosome is chosen for mutation, a random choice is made for some of the genes of the chromosome, and these genes are flipped. Figure 8 shows the illustration of gene modification in mutation, the gene number 4 is chosen to mutate, and this "1" gene is changed to "0".

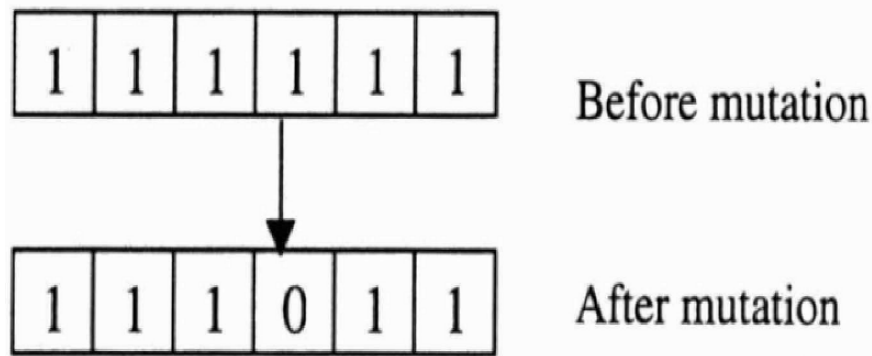


Figure 8. Illustration of gene modification in mutation.

The initial population is replaced with the newly formed reproduction. The new population is then used as the inputs of the finite element method at the next generation. In the finite element method, temperature evaluation and termination, real values of air velocity and bottom temperature are used. In the genetic reproduction, values of air velocity and bottom temperature are decoded as binary strings.

3.7. TEMPERATURE DISTRIBUTION MEASUREMENT

3.7.1. Equipment development for temperature distribution measurement

The measurement system for temperature distribution inside the plant culture vessel consisted of incubator, cooling device, fluorescent lamps, data logger and a personal computer. This equipment was also used in the research work carried out by Suroso *et al.* [3-5,13]. The culture vessel placed inside the incubator (Koiton M-201, Koito) at 23°C. To add more light, the fluorescent lamps (FMR96EX-N/A, National) were placed 20.0 cm above the culture vessel. The fan was placed above the culture vessel to generate airflow. Air velocities were measured at the top of the culture vessel. The vessel was moved vertically until the velocity-meter showed desired air velocities of 1.0, 2.0, 3.0 and 4.0 m/s. Figure 9 shows the fan used in the system measurement. The bottom temperature of the culture vessel was cooled by an electronic cooling device (Samol SL-C3, NBC). The cooling device consisted of a fan bottom cooler (SL-5F, Samol), a digital temperature controller (SL-C3, Samol) and a DC power supplier (HR-10, Samol). The cooling device is shown in Figure 10. The temperatures were measured at steady state condition using copper-constantan thermocouples and a data logger (CADAC100, Eto Denki) controlled by a Compaq Contura 4/25C computer (486 DX).

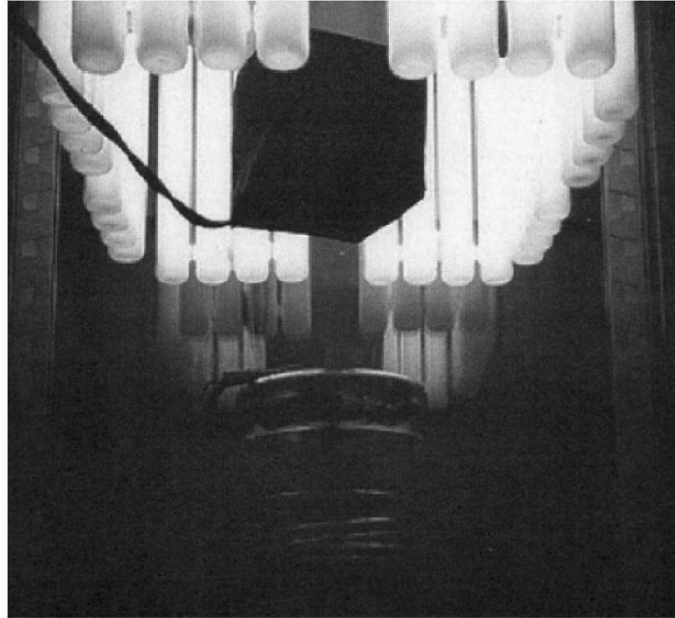


Figure 9. A fan to generate airflow in the measurement system.

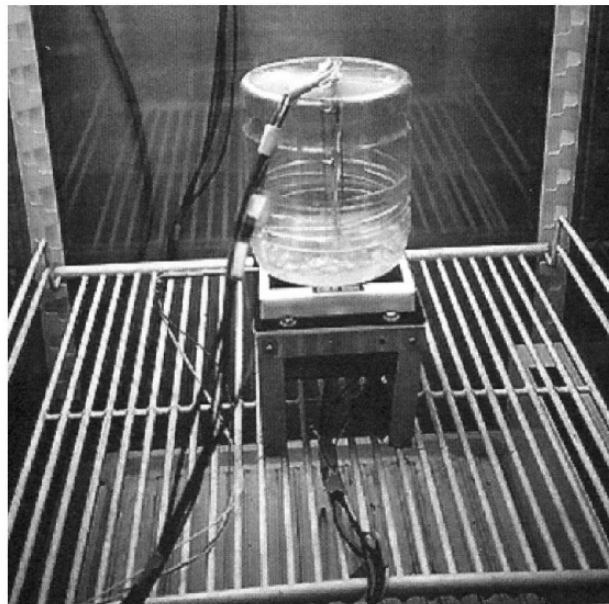


Figure 10. The bottom cooling device.

3.7.2. Temperature distribution data

Four nodal temperatures (gel temperature at 0.5 cm in height and three air temperatures at 3.5, 6.0 and 8.5 cm in height) were measured until steady state condition reached. The temperature distribution data were used for

- Determination of the Nusselt number constants
- Validation of the convective heat transfer coefficients and
- Validation of searched air velocity and bottom temperature.

The temperature distributions were conducted at combination of four levels of bottom temperature, five levels of air velocity and three levels of light intensity. The four levels of bottom temperature were 5, 10, 15 and 20°C, and five levels of air velocity were 0, 1, 2, 3 and 4 m/s. The three levels of light intensity were 75, 150 and 300 $\mu\text{mol}/(\text{m}^2\text{s})$.

4. Example of solution

4.1. COEFFICIENT OF CONVECTIVE HEAT TRANSFER

Fifty sets of training data for the neural network were generated by the finite element method. The training data were generated at PPF of 300 $\mu\text{mol}/(\text{m}^2\text{s})$, air velocity of 3.0 m/s and bottom temperature of 15°C. Constant of Nusselt number equation (C, m and n) for the top and side surface of the culture vessel were generated randomly within a range of 0-1. The input-output data pair of the finite element was selected as a set of training data when the temperature of air was not more than 35°C.

Kalman filter neural network training method was used to train the developed neural network for the inverse analysis. Output error of training was 4.2216×10^{-2} after 161 times of iteration. Input data for the trained neural network was the temperature distribution within the culture vessel. The measured values of three air temperatures and gel temperature at PPF of 300 $\mu\text{mol}/(\text{m}^2\text{s})$, air velocity of 3.0 m/s and bottom temperature of 15°C were used as inputs for the trained neural network.

Results obtained from the trained neural network were constants of the coefficient of convective heat transfer equation that were used to calculate the coefficients of convective heat at the top and side surface of the culture vessel. The values of C, m and n were 0.85, 0.55 and 0.34, for top surface of the culture vessel and 0.90, 0.61 and 0.32 for the side surface of the culture vessel, respectively. The equations for the coefficient of convective heat transfer for the top and side surfaces of the culture vessel are expressed as follows;

$$h_d = (k/d) * 0.85 \text{Re}^{0.55} \text{Pr}^{0.39} \quad (26)$$

$$h_\chi = (k/x) * 0.90 \text{Re}^{0.61} \text{Pr}^{0.32} \quad (27)$$

The value of the convective heat transfer coefficient for the top surface of the culture vessel is uniform because the Prantdl and Reynolds number for whole surface is

constant. The length parameter of Reynolds number for the surface was equal to diameter of the culture vessel. Figure 11 shows the relationship between air velocity and coefficient of convective heat transfer on top surface of the culture vessel that was calculated using Equation 26, at PPF of $300 \mu\text{mol}/(\text{m}^2\text{s})$. The coefficient of convective heat transfer increased linearly with increase in the air velocity. The calculated coefficient of convective heat transfer increased from 20.6 to $44.2 \text{ W}/(\text{m}^2\text{C})$, when the air velocity was increased from 0.0 to 4.0 m/s.

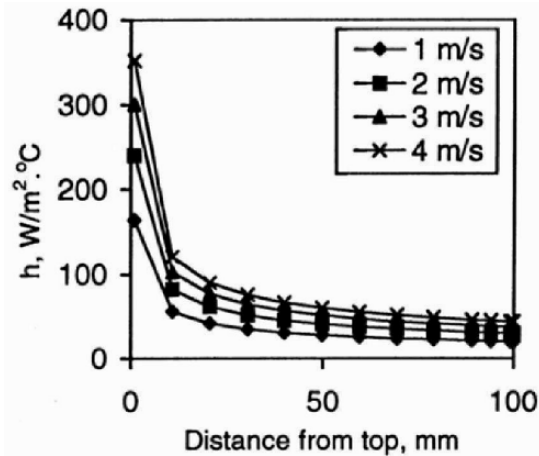


Figure 11. Relationship between coefficient of convective heat transfer over the top surface of the culture vessel and air velocity.

The coefficient of convective heat transfer on the side surface of the culture vessel decreased with increasing distance from the leading edge at all levels of air velocity. At the leading point, the distance equals zero and therefore the coefficient of convective heat transfer was not calculated. Calculation for the coefficient of convective heat transfer at side surface of the culture vessel was calculated starting at 1 mm from the leading edge. The calculated coefficient of convective heat transfer dropped dramatically within 10 mm from the leading edge. However, at distances of 10 to 100 mm, the coefficient of convective heat transfer gradually decreased. At air velocity of 1.0 m/s, the calculated coefficient of convective heat transfer dropped by $108.0 \text{ W}/(\text{m}^2\text{C})$ within 10 mm from the leading edge. In contrast, the calculated coefficient of convective heat transfer only decreased by only $35.6 \text{ W}/(\text{m}^2\text{C})$ between 10 and 100 mm distances from the leading edge.

The coefficient of convective heat transfer increased with the increase in air velocity. For example at 1 mm distance from the leading edge it increased from 164.1 to $351.0 \text{ W}/(\text{m}^2\text{C})$ when the air velocity was increased from 1.0 to 4.0 m/s. At 100 mm distance from the leading edge, the coefficient of convective heat increased from 20.6 to $44.2 \text{ W}/(\text{m}^2\text{C})$ when the air velocity was increased from 1.0 to 4.0 m/s.

4.2. VERIFICATION OF THE CALCULATED COEFFICIENT OF CONVECTIVE HEAT TRANSFER

The calculated coefficients of convective heat transfer on the surface of the culture were verified indirectly by measurement data. The coefficients of convective heat transfer for the finite element method were calculated using equation 26 and 27. The calculated coefficients of convective heat transfer were used as the inputs for the finite element method. The calculated temperatures from the finite element were then compared with the measured data.

The average coefficient of convective heat transfer from the starting point to 1 mm was calculated using Equation 26. For the subsequent edges, the coefficients of convective heat transfer were derived by an arithmetic average of the values of coefficient of convective heat transfer between starting and ending point. The values of coefficient of convective heat transfer for each edge became uniform. Table 2 shows the errors of the calculated temperatures within the culture vessel at different bottom temperatures and air velocities.

Table 2. The errors of calculated temperatures inside the culture vessel.

Bottom temperature (°C)	Air velocity (m/s)	Temperature (°C)		
		Air ₁ (3.5 cm)	Air ₂ (6.0 cm)	Air ₃ (8.5 cm)
5	1.0	3.1	3.2	3.8
	2.0	8.9	0.0	2.9
	3.0	8.0	0.4	1.8
	4.0	7.7	0.8	1.5
10	1.0	1.2	3.9	3.8
	2.0	3.6	3.3	3.6
	3.0	3.6	1.5	2.2
	4.0	2.8	1.1	0.4
15	1.0	1.1	4.6	4.1
	2.0	0.7	4.0	3.9
	3.0	1.6	2.6	2.6
	4.0	1.6	1.1	0.3
20	1.0	3.6	5.6	4.7
	2.0	1.9	5.7	5.3
	3.0	1.6	2.6	2.6
	4.0	1.6	1.1	0.3

The error, ϵ , was determined using $\epsilon = ((|T_{cal} - T_{dat}|) / T_{dat}) * 100\%$, where T_{cal} and T_{dat} represent the calculated and measured temperature, respectively. At bottom temperature of 5°C, the errors for air temperature 2 and 3 were less than 5.0 % at all levels of air velocities. However, the errors of the calculated air temperature 1 at air velocities of 2.0, 3.0 and 4.0 m/s were 8.9, 8.0 and 7.7%, respectively. At bottom temperature of 10°C and 15°C, the errors of air temperature at all levels of air velocities were less than 5.0%. At the bottom temperature of 20°C and air velocity of 1.0 m/s, the errors of all temperatures were below 5.0%, except the error of air temperature 2 is 5.6%. At the value of air velocity of 2.0 m/s, were above 5.0%, except at air temperature 1. At the value of air velocity of 3.0 and 4.0 m/s, the errors of the air temperature were below 5.0%. These results show that the finite element neural network inverse technique is capable of determining constants of the Nusselt number which can further be used to calculate the coefficients of convective heat transfer over the surface of the culture vessel. With this method, coefficients of convective heat transfer for a complicated configuration can be determined with a simple experiment.

4.3. OPTIMUM VALUES OF AIR VELOCITY AND BOTTOM TEMPERATURE

Table 3 shows searched values of air velocity and bottom temperature obtained by genetic algorithm after 15 generations and the average temperature of three nodes inside the culture vessel.

Table 3. Searched values of air velocity and bottom temperature were obtained by genetic algorithm and average temperature of three nodes inside the culture vessel.

	Air velocity (m/s)	Bottom temperature (°C)	Culture vessel temperature (°C)
PPF 75 $\mu\text{mol}/(\text{m}^2\text{s})$			
-Temperature 23 (°C)	3.8 \pm 0.1	17.9 \pm 0.3	23.7 \pm 0.5
-Temperature 25 (°C)	0.5 \pm 0.1	19.7 \pm 0.3	24.9 \pm 0.6
PPF 150 $\mu\text{mol}/(\text{m}^2\text{s})$			
-Temperature 23 (°C)	4.0 \pm 0.0	10.4 \pm 0.7	24.3 \pm 1.2
-Temperature 25 (°C)	4.0 \pm 0.0	19.8 \pm 0.3	25.3 \pm 0.5
PPF 300 $\mu\text{mol}/(\text{m}^2\text{s})$			
-Temperature 23 (°C)	4.0 \pm 0.1	5.0 \pm 0.0	26.4 \pm 1.9
-Temperature 25 (°C)	4.0 \pm 0.0	9.8 \pm 0.1	26.8 \pm 1.5

Air velocity for all the runs was around 4.0 m/s except at PPF of $75 \mu\text{mol}/(\text{m}^2\text{s})$ and temperature of 25°C was $0.5 \pm 0.1 \text{ m/s}$. Temperature on the top part of the culture vessel was higher than the expected temperatures (23°C or 25°C), when the artificial lamps increase light intensities. Therefore, the air velocity reached a maximum value (4.0 m/s) for decreasing the temperature to the expected value. The searched bottom temperatures had a negative correlation with the light intensity.

The three nodes of temperatures at the centre of the culture vessel under the searched air velocity and bottom temperature treatments are depicted in Figure 12 to 14. Almost all the figures show that the temperatures at the lower part of the culture vessel were close to the expected temperature. This indicates that cooling of the bottom-temperature effectively reduces increase in temperature in the lower part of the culture vessel. At PPF of $150 \mu\text{mol}/(\text{m}^2\text{s})$ and expected temperature of 25°C and PPF of $300 \mu\text{mol}/(\text{m}^2\text{s})$ and all expected temperatures (23 and 25°C), although the air velocity already reached the maximum value, the temperatures were still higher than the expected ones.

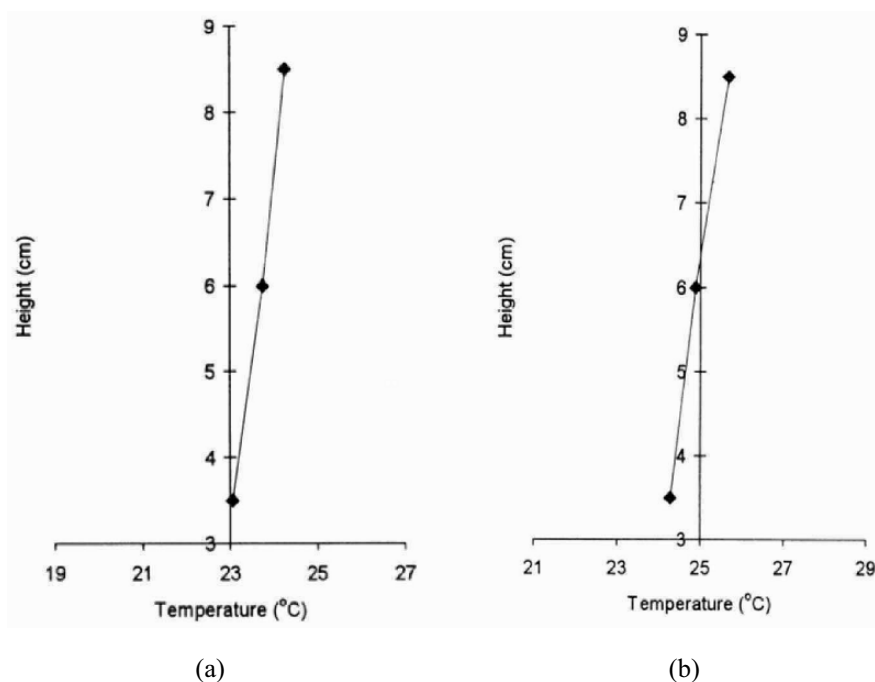


Figure 12. Temperature distribution of three nodes inside the culture vessel at searched air velocity and bottom temperature condition under PPF of $75 \mu\text{mol}/(\text{m}^2\text{s})$ and expected temperature of (a) 23°C and (b) 25°C .

Intelligent inverse analysis for temperature distribution in a plant culture vessel

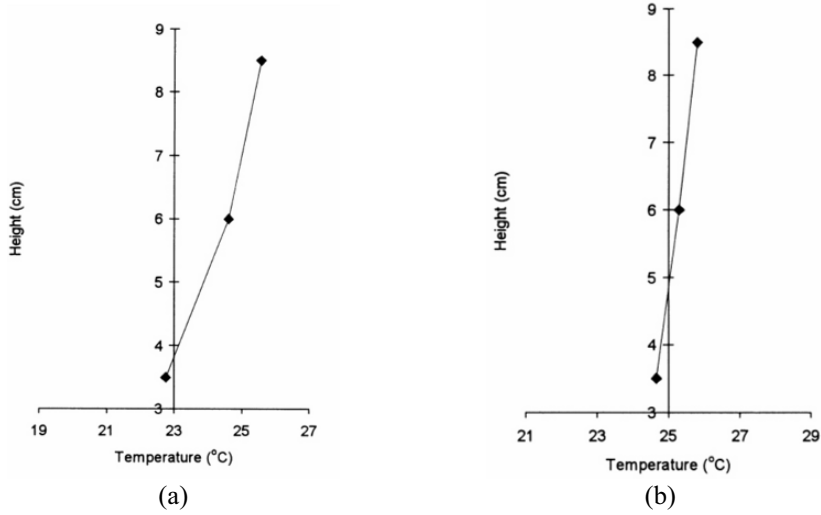


Figure 13. Temperature distribution of three nodes inside the culture vessel at searched air velocity and bottom temperature condition under PPF of $150 \mu\text{mol}/(\text{m}^2\text{s})$ and expected temperature of (a) 23°C and (b) 25°C .

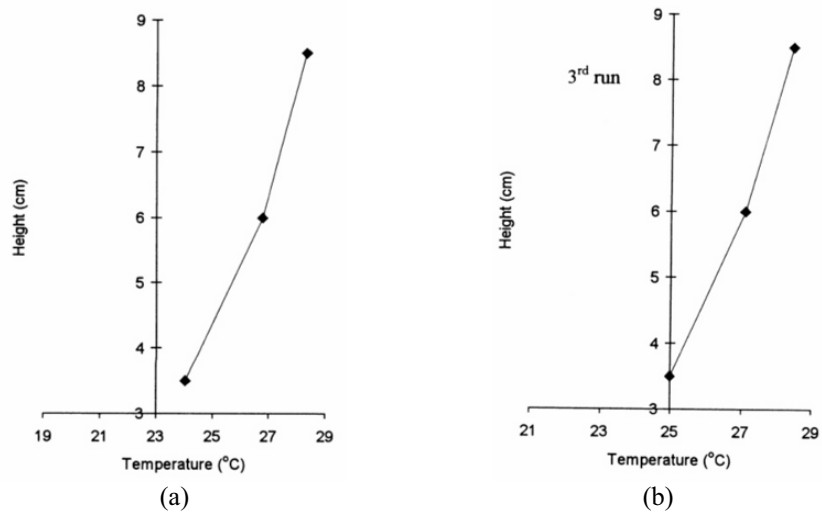


Figure 14. Temperature distribution of three nodes inside the culture vessel at searched air velocity and bottom temperature condition under PPF of $300 \mu\text{mol}/(\text{m}^2\text{s})$ and expected temperature of (a) 23°C and (b) 25°C .

This indicates that blowing air to the surface of the culture vessel with air velocity of 4.0 m/s is not enough to reduce the upper temperature. Therefore, further work should investigate with a wider range of air velocities.

References

- [1] Kozai, T.; Oki, H. and Fujiwara, K. (1990) Photosynthetic characteristics of *Cymbidium* plantlet *in vitro*. *Plant Cell Tissue Org. Cult.* 22: 205-211.
- [2] Tani, A.; Kiyota, M.; Taira, T. and Aiga, I. (1991) Effect of light intensity and aeration on temperature distribution inside plant culture vessel. *Plant Tissue Cult.* 8 (2):133-135.
- [3] Suroso; Tani, A.; Murase, H.; Honami, N.; Nishiura, Y. and Takigawa, H. (1995) Finite element analysis for temperature distribution in the interior of plant culture vessel. *Agricultural Mechanization in Asia, Africa and Latin America.* 26 (3): 19-23.
- [4] Suroso; Murase, H.; Honami, N.; Takigawa, H. and Nishiura, Y. (1995) Neural network and finite element inverse analysis for thermal behavior of plant culture vessel. *JSAM Kansai Branch Research Report* 77: 81-84.
- [5] Suroso; Murase, H.; Tani, A.; Honami, N.; Takigawa, H. and Nishiura, H. (1995) Neural network inverse analysis for convective heat transfer over the surface of plant culture vessel. In: *Proceedings of International Symposium on Automation and Robotics in Bioproduction and Processing.* Vol. 3, Kobe, Japan, 3-6 November.
- [6] Johnson, A. T.; Kirk, G. D.; Moon, S.H. and Shih, T.M. (1988) Numerical and experimental analysis of mixed forced and natural convective about a sphere. *Trans. ASAE* vol. 31(1): 293-299, 304.
- [7] Zhang, Q. and Cavalieri, R.P. (1991) Thermal model for steam blanching of green beans and determination of surface heat transfer coefficient. *Trans. Am. Soc. Agri. Engineers* 34(1): 182-186.
- [8] Brown, R.B. and Otten. L. (1992) Thermal conductivity and convective heat transfer coefficient for soybean and white bean seeds. *Can. Agri. Engineering* 34(4): 337-341.
- [9] Adler, A. and Guardo, R. (1994) A neural network image reconstruction technique for electrical impedance tomography. *IEEE Transactions on Medical Imaging* 13(4): 594-600.
- [10] Goldberg, D. E. (1989) *Genetic Algorithms in Search, Optimization and Machine Learning.* Addison Wesley, Reading, Massachusetts.
- [11] Bird, R.B.; Stewart, W. E. and Lightfoot, E. N. (1960) *Transport Phenomena.* John Wiley and Sons, New York.
- [12] Holman, J. P. (1990) *Heat Transfer.* Seventh Edition. McGraw-Hill Book Co., Singapore.
- [13] Suroso; Murase, H.; Tani, A.; Honami, N.; Takigawa, H. and Nishiura, H. (1996) Inverse technique for analysis of convective heat transfer over the surface of plant culture vessel. *Trans. Am. Soc. Agri. Engineers*, 39(6): 2277-2282.
- [14] Murase, H.; Suroso and Honami, N. (1995) Inverse analysis for convective heat transfer over the surface of plant culture vessel. *Ann. Seminar of Jap. Soc. Agri. Meteorol. and 33rd Seminar of Japanese Society of Plant Environment Control in Biology, Meijo university, Nagoya, Japan, 26-29, 1995.*
- [15] Tani, A.; Suroso; Murase, H.; Kiyota, M.; Koyama, S.; Taira, T. and Aiga, I. (1995) Development of heat balance model on plant tissue culture vessel by using finite element method. *Acta Hort.* 393: 97-102.
- [16] Suroso; Murase, H. and Honami, N. (1997) Thermal optimization of culture vessel using a genetic algorithm. In: *Proceedings of Annual Seminar of Society of High Technology in Agriculture.* Kyoto University, Kyoto, Japan, 6-8 June.
- [17] Suroso; Murase, H. and Honami, N. (1997) Micro-environmental optimization of culture vessel using a genetic algorithm. In: *Proceeding of International Symposium on Agricultural Mechanization and Automation Vol.2, Taipei, Taiwan, 17-22 November.*
- [18] Suroso; Tani, A.; Murase, H., Honami, N.; Nishiura, Y. and Takigawa, H. (1995) Finite element analysis for temperature distribution in the interior of plant culture vessel. *Agricultural Mechanization in Asia, Africa and Latin America* 26 (3): 19-23

PART 5

**PHYSICAL ASPECTS OF PLANT TISSUE
ENGINEERING**

ELECTRICAL CONTROL OF PLANT MORPHOGENESIS

COGĂLNICEANU GINA CARMEN

*Institute of Biology Splaiul Independenței 296, 060031 Bucharest
Romania-Fax: 40 -21 221-9071- Email: gina.cogalniceanu@ibiol.ro*

1. Introduction

In vitro regeneration and multiplication techniques are basic requirements for a variety of plant biotechnologies. Whatever the experimental system used (protoplasts, callus, tissue fragments), the same problem arises: how can the frequency and the speed of plant regeneration be increased. The development of plant biotechnologies and progresses in genome manipulation have encouraged researches for improving *in vitro* regeneration, both directly, through somatic embryogenesis, and indirectly, *via* callus, through organogenesis or *de novo* shoot formation.

Among the tested physical factors on these developing *in vitro* systems are electric fields. Subjecting plant cells to external electric fields proved to be a useful method for:

- the study of the electric fields (natural and/or applied) significance in the control of *in vitro* cell proliferation, differentiation and morphogenesis;
- the improvement of some biological processes by establishing correlations between the modulated electrical parameters of the field applied and some biological parameters of biotechnological concern (speed and efficiency of regeneration, viability, vigour and performance of regenerants etc.).

Electrostimulation of *in vitro* developmental processes by applying either low intensity, low frequency, long duration electric currents or short duration, high intensity electric pulses and the theoretical aspects connected with are presented in this paper.

2. Endogenous electric currents as control mechanisms in plant development

The problem of applying electric fields to developing biological systems is based on the presence of natural electric phenomena associated to all growth, differentiation and morphogenetic processes, both in animal and in plant systems. Morphogenesis, the establishment of the specific form from a single symmetric cell, the zygote, is a holistic phenomenon. It progresses according to a global plan, which specifies, in time and space, every event as if a final purpose is driving the system. Each temporal step and local configuration of cellular interactions can control the subsequent moment of the global development. In this non-local process, the DNA functions like a receiver for morphogenetic signals, the instructions for activating a particular set of genes. The

problem of cell differentiation and supracellular organization in plant development was described as depending not only on selective gene expression, but also on positional information [1,2] and on spatial and temporal patterns [3-5]. Electrical properties of the plant plasma membrane [6] and the symplasmic connections [7,8] proved to be instrumental for cell-to-cell communication and for morphogenetical signals flow. Extracellularly recorded electric currents by vibrating probe technique [9,10] have shown that changes in the intensity and pattern of small, steady endogenous ionic currents precede changes in cell polarity, causing unequal cell division and also that certain patterns of tissue growth are associated with transcellular currents flow. The possible involvement of electric currents in developmental pattern generation was investigated in different plant systems (Table 1).

Table 1. Endogenous electric patterns during developmental processes.

Developmental system	Genus	Biological process	Current density ($\mu\text{A}/\text{cm}^2$)	Electric pattern ➤ entering zone ➤ leaving zone	Reference
Zygotic embryo	<i>Elaeis</i>	Development	1-2	➤ the cotyledon ➤ the radicle	[11]
Zygotic embryo	<i>Fucus</i> , <i>Pelvetia</i>	Germination	1-2	➤ rhizoid ➤ the opposite thallus site	[12]
Somatic embryo	<i>Daucus</i>	Somatic embryogenesis	0.1-0.6 1.0-1.2	➤ the cotyledon ➤ the radicle	[13,14]
Pollen	<i>Lillium</i>	Germination	3-5	➤ the prospective germination site ➤ the opposite	[15,16]
Root	<i>Hordeum</i>	Growth and differentiation	1-2	➤ growth zone ➤ absorbing zone	[17]
Root	<i>Phaseolus</i>	Growth and differentiation	0.7	➤ root tip ➤ root growth region	[18-21]
Marine algae	<i>Acetabularia</i>	Regeneration	10-100	➤ regenerative zone	[22]

Small, endogenous ionic currents were measured at different stages in the oil palm (*Elaeis guineensis* Jacq.) zygotic embryo development [11]. Average current density values of 1–2 $\mu\text{A}/\text{cm}$ were found. Currents entered the differentiating or elongating areas and left the neighbouring regions. The currents magnitude and direction changed depending on the developmental stage. In the embryos that did not develop, the ionic currents were detected only in the radicle region and represented 10-20% of the normal values. Electric pattern association with embryo development was supported by the observed positive correlation of the current magnitude with growth and elongation rates.

The correlation between endogenous electric currents and the specific steps in plant development were described not only in zygotic, but also in somatic embryogenesis. Electric patterns have been measured and characterized for carrot (*Daucus carota* L.) somatic embryos. Very young, spherical, somatic embryos exhibit an electric gradient along the future longitudinal axis, currents entering the presumptive cotyledon and leaving the future radicle [13,14,23,24]. For a faster developing carrot cell line, a different current pattern was observed: inward current was found both at the cotyledon and radicle, while an outward current was found at the middle of the embryo [14,24]. The electrical polarity constantly manifested from the early globular stage, to the subsequent heart-, torpedo-, and plantlet-stage embryogenesis. Current density and growth were positively correlated within each stage, the current density increasing in the succession of the embryogenesis stages. Exogenous applied auxin (3 μM IAA, indole-3-acetic acid) determined a fast, but a reversible inhibition of the current density [13], suggesting a correlation of the auxin polar transport with the bioelectric currents. This hypothesis is also consistent with the ionic composition of the electric currents, as determined by Rathore *et al.* [14], who found that in the torpedo stage these currents are associated with a gradient of acidity. The extracellular pH measurements showed that the medium around the root region was more acidic than the medium around the shoot region by about 0.05 units [14].

Another model system extensively investigated for symmetry breaking and polarity establishment is represented by the *in vitro* pollen germination and the oriented tube growth. The pollen tube elongation is accomplished by a sort of cell extension restricted to a narrow apical zone (tip growth). The process is regulated by poorly-understood mechanical, electrical and chemical signals. The large steady electrical currents traverse the pollen tubes, with a current density up to 300 pAmp.cm^{-2} , the current source being the grain, and the current sink being the tube [25]. The tip was shown to always drive larger currents than the rest of the tube. A positive correlation between the tip electrical current and growth rate was shown [26], the growth being associated with a tip-focused gradient of Ca^{2+} [27]. The ionic nature of these currents was investigated [15-16], mainly by substitution experiments, being described an outward proton current in the pollen grain, an inward potassium current in the tube. Ca^{2+} was described as the major component of the pollen tube inward current at the tip [16].

Plant roots proved to be very suited for investigations concerning spontaneous spatial electric patterns. Roots display large currents, grow on minimal media and have inherent polarised growth (tip growth). Many studies of electric current patterns in roots have been made [18-20,28-30]. Stable electrochemical patterns appear around roots of higher plants, being closely related to growth. Generally, the electric current flows from the basal root part into the tip. Protons are considered to have an important role in electric current generation [21].

The causal relation between electric pattern dynamics and growth is supported by several experimental facts:

- Electric isolation of the elongation region from the mature region causes a decrease in growth speed, demonstrating the contribution of the electric currents within these regions [31];

- Electric pattern and the elongation rate significantly decrease under anoxic treatment, suggesting that the currents are produced by respiration-dependent electrogenic H⁺ pumps within the plasma membrane [32];
- Low pH into the culture medium generally induced a higher root growth speed, than a high pH [20];
- Electric potential becomes lower at the point where a lateral root will emerge. The electric current precedes the emergence of the lateral root by about 10 hours [18];
- Application of a weak electric field in the root direction from the base to the tip stimulated the root growth, whereas the reverse polarity of the applied field determined an inhibitory effect [33].

Analysing the significance of the spontaneous electric currents for the developmental phenomena in a variety of biological systems, some basic characteristics have been found:

- the endogenous electric currents always precede organogenesis and accompany local differentiation and growth;
- the electric pattern prefigures the coming morphogenetic spatio-temporal events: the electric currents enter the future site of the growth and leave through the non-morphogenetic one;
- the suppression of electric flow is always followed by the cease of growth and differentiation;
- on the basis of recorded data, no new formed structure have been observed in the absence of the self-induced electric currents;
- anoxia and electrical insulation between different tissues entail growth disorders.

In conclusion, it appears that plants are characterised by a dynamic electric pattern, which is supposed to have a connection with their growth [34] and which is maintained under a far from equilibrium condition. Glaser [35] describes an electrical structure characteristic for any living biological system, which correspond to the hierarchical morphological structure (atomic, molecular, cellular and organismic level). Growth can be therefore considered as a typical non-equilibrium phenomenon exhibiting a spatio-temporal organization, the electric membrane dynamics playing a significant role. Measurements of spatio-temporal characteristics of the self-organised electric structures can offer a new perspective for the growth mechanisms and for the interaction between biological systems and applied electric fields.

3. Electrostimulation of *in vitro* plant development

Electrostimulation, as defined by Berg [36], represents a new tool in biosciences, both for investigating and manipulating the cell functioning. Experimental data have shown that in the presence of low intensity ($E < 1$ V/cm), low frequency (< 1 kHz) electric fields [37,38], *in vitro* biological systems react in a recordable manner, changing many cell activities, depending on the electrical parameters: non-linear dependence [35,39] and on the physiological state of the cells: far from equilibrium [40,41], with consequences on proliferation, growth and differentiation. Electric influences initially affect the proper

physiological electric structure of the biological systems, and, consequently, the metabolism and/or the cell structures, at the genetic or epigenetic level. Time-dependent changes (fast transient processes, reaction during whole field application, and slow after-field effects) are caused mainly by the increased transmembrane voltage, which determines subsequent processes. The transformation of electric or electromagnetic energies to chemical reactions takes place immediately on many cellular pathways at once. The reception and transduction of the electric signals are not yet well understood, the plasma membrane being considered the primary sites of interactions with these electric fields [35,39,42]. Several theoretical models have been proposed for the transduction of the electrical signals at the plasma membrane level: “the electro-conformational coupling model” [43,44] and “the surface compartment model” [45,46] being the most frequently cited. The secondary biological effects are possible only by means of amplification processes.

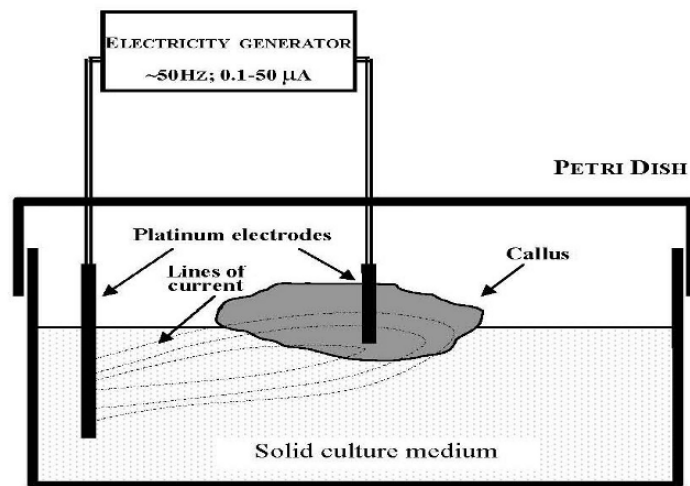


Figure 1. Experimental design for the application of low electric fields to the callus. Reproduced from Cogalniceanu et al. (1998) [52].

In the field of plant *in vitro* developmental systems, the first noticeable data about growth electrostimulation were provided by the work of Goldsworthy and Rathore [47] and Rathore and Goldsworthy [48,49]. Applying for a long period of time (22 days) a very weak, constant electric current (1-2 μA) to the undifferentiated tobacco callus cultures, *in vitro* plant cell growth rate was significantly improved [48]. The current was applied individually to each callus, through a pair of stainless-steel electrodes, one of them inserted into the callus, and the other one into the nutritive medium. This experimental system of current exposure was taken over and improved by others (Figure 1) [50-53].

The electrostimulatory effects were dependent on the polarity of the applied current, with an increase in callus growth rate up to 70%, when the callus was made negative to the culture medium, and on the nature of the exogenous auxin, only IAA, the natural auxin, mediating the stimulatory effects. In similar experiments, working on tobacco

callus cultures, Radu *et al.* [50] found that the electrostimulation of growth (up to 50%) can be obtained also by supplying the nutritive medium with NAA (naphthaleneacetic acid), an synthetic auxin, and for both current directions, in the 0.3-1 μA current intensity range. Comparable results have been found by Thavarungkul and Kanchanapoom [53], who also obtained a significant stimulation of the oil palm callus growth for both directions of the weak applied current (120 $\mu\text{A}/\text{cm}^2$, adjacent to the electrode to 1-2 $\mu\text{A}/\text{cm}^2$, at the extremity of the piece of callus) and in the presence of the auxin NAA into the culture medium. Some later experiments have shown that a weak alternating current can be extremely effective in enhancing cell division and growth in plant *in vitro* cultures [50]. Not only undifferentiated cellular mass proliferation was the subject of electrostimulation, but also *in vitro* plant regeneration. Using a prolonged electric treatment, as previously described, [47] electro-enhanced shoot differentiation was observed up to 5-fold in tobacco callus culture. The stimulation of the morphogenetic processes occurred only when the callus was made negative to the medium and only when IAA was included into the culture medium. The explanation for these stimulatory effects of the very weak continuous electric field on the cultured plant tissues involves more than one mechanism. The electrical control of physiological cell and tissues polarity is one of the most invoked mechanism [47,54]. The authors suggest that the applied current would help to align the physiological polarities of the callus cells for promoting, among others, the polar transport of auxin. An experimental confirmation for this suggested mechanism was offered by Mina and Goldsworthy [55] who demonstrated that weak electric currents applied for short periods of time (minutes to hours) were able to change the physiological electrical pattern surrounding cells from tobacco suspension culture, the cells realigning their electrical polarities (transcellular currents) in the same direction as the current that has been applied. The interference of the applied electric currents with the direction of the natural polar transport mechanisms (for growth hormones, nutrients, charged particles) and natural electric currents flow are other speculative mechanisms responsible for the improved biological parameters in the electrotreated plant *in vitro* cultures.

All these theoretical mechanisms proposed for the constant electric currents effects on the *in vitro* plant cell cultures are not operational in the case of applying sinusoidal electric currents. A significant enhancement of both cell proliferation (up to 50%) and shoot regeneration (upto 300%) was reported after the continuous (30 days) application of an alternating electric current of low level (0.1-50 μA), low frequency (50 Hz) through the tobacco callus [50,52,56]. The biological effects observed were not in a linear dependence with the electrical parameters of the external field. The dynamic nature of the electric stimulus used and the low level of its intensity and frequency raise the questions about the cellular mechanisms of the electrostimulation. The authors suggested that in the callus culture, with its asynchronous and unorganised structure, cell division and growth are not coordinated, as in the organised tissues. The commitment of the callus cells on a specific differentiation pathway is governed by the hormonal supply and is conditioned by the level of cells sensitivity. The degree of sensitivity can be indirectly assessed by measuring the strength of the cell response to a constant signal [57]. Based on these peculiarities, it was assumed that the effect of the electrical treatment was due to the individual cell perception, more cells being engaged in differentiation and organogenesis and finally producing more shoots under the action of

the external electric field. The electromodified sensitivity precedes and controls cell differentiation in the *in vitro* system [52,56]. The site of perception for the alternating current signals is considered to be the plasma membrane. Owing to its specific features (low dielectric constant and electric conductivity) compared to the adjacent media (periplasmic space and cytosol), the membrane acts like an electric field amplifier [58]. External electric field modulates the strong electric field in the membrane and consequently, all the events located there (hormonal signal transduction, transport phenomena) are modified. According to the Electroconformational Coupling Model [44], the level of external electric field needed to modulate the active transport through the membrane is of the order of V/cm or less than 1 V/cm [59], which is close to the highest stimulating condition (0.25 V/cm) experimentally observed [52].

Other hypothetical mechanisms have been proposed for explaining the influences of the weak external electric fields on the morphogenesis and growth in plants development. Growth-promoting effect of a dynamic electric field of low strength and low frequency (10^{-4} - 10^{-1} V/cm, 10 Hz) was emphasized when applied to roots of garden cress (*Lepidium sativum* L.) [60]. An increase in root cells growth and endoplasmic reticulum cisternae abundance in the root cap cells was mediated by the stimulation of the plasma membrane H⁺-ATP-ase of the root cells, in accordance with the theoretical model of Tsong and Astumian [61]. In other experiment, increase with 20% of the growth speed for an adzuki bean (*Phaseolus angularis*) root was obtained when a current of 1-10 $\mu\text{A}/\text{cm}^2$ was applied from the root base to the tip for 15-60 minutes [33]. The amplitude of the physiological electric pattern and the acidification around the root increased as a consequence of the action of the applied electric field. When an electric field of 500 mV/cm was applied in the transverse direction across the root, the root bent to the side of the positive electrode and the acidification around the root became asymmetrical [32]. These results suggest that the induced perturbation of the H⁺ flow around the root has affected the growth. Toko *et al.* [20] advanced the idea that the electric pattern of the roots are in accordance with the principle of minimum energy dissipation or minimum entropy production [62]. Based on these experimental data, the biological electric patterns are considered as “electric dissipative-like structures”, with a significant causal role in growth processes [20]. Thus, electrical non-equilibrium theories may provide an useful tool for analyzing the interaction between biological systems and electric fields, and much more, for controlling the developmental phenomena through an adequate electric treatment.

4. High-voltage, short-duration electric pulses interaction with *in vitro* systems

High-voltage, short-duration (micro- or milli-seconds) pulses are used in most plant biotechnological research and applications for facilitating electroporation, electrofusion, electrotransformation of protoplasts [63], or electropermeabilization of tissue samples [64-70].

Under the strong external electric field, plasma membrane is temporarily disrupted, the distribution, size and number of the hydrophilic transient pores leading to an increase in transmembrane conductivity and diffusive permeability [71,72]. The electropores allow molecules, ions and water to pass from one side of the membrane to the other. If the electric field pulse has the proper parameters, the electro-

permeabilization is reversible and the electric treated cells can recover (the physiological plasma membrane structure is spontaneously restored in minutes). The number and the diameter of the pores increase mainly with the pulse amplitude and duration, but over an upper limit threshold of these electrical parameters, the plasma membrane can not recover and the cells viability is drastically affected. Based on these experimental findings, the technique of electroporation was developed in the 1980s as a method to deliver molecules (drugs, DNA) into living cells safely and reliably, to insert proteins into the cell membrane or to fuse cells [73]. Experimental evidences indicated that plant protoplasts react in a complex manner to the exogenous pulsed field, long time after the treatment, and their cellular off-springs express some electro-induced modifications.

4.1. EFFECTS OF ELECTRIC PULSES TREATMENT ON PLANT PROTOPLASTS

Fundamental knowledge on the detailed mechanisms of applied pulsed electric field effects on the plant protoplasts evolution in culture are still poor and hypothetical. After the pioneering researches, excellent analysed and reviewed by Davey *et al.* [74], experiments on growth and morphogenesis stimulation in plant cell systems by electroporation methods have diminished.

The protocols for a particular application of the electric pulses treatment in plant protoplasts have usually been developed empirically, by testing pulse parameters (number, amplitude, duration, waveform and pulse repetition frequency) that allowed a good permeabilization and transformation efficiency and, at the same time, preserving protoplasts viability. Only in certain experimental conditions and for certain values of the electric field, pulses were capable of causing additional benefits, such as stimulation of plating-efficiency, regeneration phenomena, DNA and protein synthesis [74]. The design of experiments was extremely variable, in concordance with the aim of the experiments (Table 2).

In most cases, the equipments used for generating electric pulses were commercially available devices (electroporators), and there are detailed reviews about the techniques of signal generation and about the performances and limitations of these electro-permeabilization devices [84,85].

Electrical control of plant morphogenesis

Table 2. Variability of experimental conditions for stimulating different biological processes in protoplasts by electric pulses treatment.

Biological processes	Plant species and tissue sources	Pulsed electric field parameters	Reference
Cell wall regeneration	<i>Glycine canescens</i> L. – seedling cotyledons <i>Prunus avium</i> x <i>pseudocerasus</i> – cell suspension <i>Pyrus communis</i> L. - callus <i>Solanum dulcamara</i> L. – cell suspension <i>Solanum viarum</i> Dunal – seedling cotyledons	3 exponential pulses of 10-50 μ s duration, at 10 s intervals, with voltage ranging from 250 to 2000 V, at 10-50 nF capacitance	[75]
Plating efficiency	<i>Glycine canescens</i> L. – seedling cotyledons <i>Prunus avium</i> x <i>pseudocerasus</i> – cell suspension <i>Pyrus communis</i> L. - callus <i>Solanum dulcamara</i> L. – cell suspension <i>Solanum viarum</i> Dunal – seedling cotyledons	3 exponential pulses of 10-50 μ s duration, at 10 s intervals, with voltage ranging from 250 to 2000 V, at 10-50 nF capacitance	[75]
	<i>Pennisetum squamulatum</i> – cell suspension	6 exponential pulses of 100, 250 and 500 V, 40 nF capacitance, at 10 s intervals	[76]
Regenerative capacity	<i>Hordeum vulgare</i> L.cv. Dissa – callus initiated from immature embryos scutelum	2 rectangular (20 μ s) or 2 exponential pulses (0.25 μ F), field strength between 0-700 V/cm	[77]
	<i>Prunus avium</i> x <i>pseudocerasus</i> – cell suspension	3 exponential pulses of 10-50 μ s duration, at 10 s intervals, with voltage ranging from 250 to 2000 V	[78,79]
	<i>Solanum dulcamara</i> – cell suspension	3 exponential pulses of 10-50 μ s duration, at 10 s intervals, with voltage ranging from 250 to 1250 V/cm,	[80]
	<i>Helianthus annuus</i> L. cv. Cerflor and Euroflor – seedling hypocotyl tissue	2-3 pulses of 10 μ s at 1500V/cm or 2-3 pulses of 50 μ s at 1200 V/cm	[81]
DNA synthesis	<i>Prunus avium</i> x <i>pseudocerasus</i> – cell suspension <i>Solanum dulcamara</i> – cell suspension	Pulses of 87 μ s at 250 V/cm and pulses of 29 μ s at 750 V/cm	[82]
Protein synthesis	<i>Daucus carota</i> L. cv. Nobo – cell suspension <i>Nicotiana tabacum</i> L. cv. TxD – cell suspension <i>Beta vulgaris</i> L. cv. M1 – cell suspension	Single rectangular electric pulse of 100, 400 or 999 μ s duration at 0-250 V/mm	[83]
Growth and vigour of regenerated shoots	<i>Prunus avium</i> x <i>pseudocerasus</i> – cell suspension	3 exponential pulses of 10-50 μ s duration, at 10 s intervals, with voltage from 250 to 2000 V	[79]

Numerous researches devoted during mid and late 1980s to study the effects of the short-duration, high-voltage electrical pulses on protoplasts evolution in culture have revealed several aspects:

- For obtaining good electrostimulative effects, a large range of parameters have to be tested: electric pulses number, duration, amplitude, frequency, waveshape. The protoplasts sources (cell suspensions, calluses, young embryos, plantlets or seedlings, any meristematic or differentiated tissues), genotype and size, the density of the inoculum, the electroporation buffer osmolarity, all have been found to be important for achieving the maximum expected results [74].
- Several biological parameters and processes appeared to be influenced by the pulsed electric field treatments: cell wall regeneration, plating efficiency, regenerative capacity [75-78,80,86,87], DNA synthesis [82], protein synthesis [83].
- Evidence of the long-lasting effects of the pulsed electric field treatment on protoplasts, such as: (i) enhanced biomass production rate [80]; (ii) improved competence for plant regeneration of the protoplast-derived tissues [75,76,78,80]; (iii) a stable modification of the regenerated plants vigour, phenotype and availability to subsequent *in vitro* manipulation [79], all these may indicate that the electroporation influences are expressed long time after the electric treatment moment, being transferred to the protoplasts descendants.
- The applied electric pulsed field seems to promote the differentiation of organised structures (shoots/embryos) by modifying cell polarity through changes in the intracellular distribution and networking of microtubules [88,89]. Other suggested mechanisms, such as the modification of expression of the genes involved in developmental processes control, require further investigations.

These experimental findings recommend the electroporation as a useful method for improving the regenerative capacity for any species which generally are difficult to regenerate and to multiply *in vitro*.

4.2. EFFECTS OF ELECTRIC PULSES TREATMENT ON TISSUE FRAGMENTS OR ENTIRE PLANTLETS

The confirmation of stimulating effects of the short-term electric pulses of high or moderate intensity on the protoplasts regenerative processes has motivated the extension of this methodology to more complex and stable systems, such as tissue fragments and even entire plants, to facilitate a high frequency of totipotency in recalcitrant plant systems. Gill *et al.* [90] exposed whole plants or hypocotyl segments of *Vigna aconitifolia* to unique pulses of 2 or 15 μ s length and with voltages between 0.5-3 kV/cm, using the basal nutrient medium as liquid of immersion in the discharge chamber. The electric treatment generated different responses on hypocotyl segments and plantlets. Application of the electric pulses significantly stimulated shoot bud formation on hypocotyl fragments, in a direct correlation with the field intensity, and negatively correlated with the pulse length. The maximum stimulating effects were obtained at a voltage of 2 kV/cm, and at 2 μ s pulse duration. At the same electrical

parameters used, after the growth period, the whole plants were stunted compared to the controls, with decreased internodal length. Necrosis of plantlets apical meristem was observed at 15 μ s pulses of 0.5-2.5 kV/cm. These data showed the same characteristics of the electric field–organised tissues or whole plants interaction: the stimulating effects were obtained at windows of field intensity and pulse duration. The positive effects of electroporation on the efficiency of *in vitro* regeneration was also revealed by De Padua *et al.* [69], who demonstrated that peanut intact embryonic leaflets subjected to field strengths between 500 and 625 V/cm displayed a significantly higher number of shoots and initiated faster growing calluses relative to control explants. The higher regeneration frequencies of the electric pulses treated tissues opened a new direction of investigations. In a series of experiments, Cogălniceanu *et al.* [91-93] subjected intact tobacco seedlings, with two leaves fully developed, to short duration (78 ms), moderate-voltage rectangular electric pulses (field strength between 0-400 V/cm, below the values reported in literature as assuring electroporation) using an electroporation protocol. The aim of these experiments was to assess the advantages of using intact plantlets for electromanipulation procedures.

Some of the hypotheses tested were (a) if an early phase in the postembryonic development is opened to external influences, thus enabling control of morphogenetic processes based on a disturbed homeostasis; (b) what is the mechanism of action of low intensity and extremely short duration applied electric field.

After the electric treatment, seedlings were cultivated on specific media, with controlled hormonal formulae, for providing different experimental seedlings evolution. The effects of the applied electrical field differed significantly depending on the subsequent seedlings evolution induced by the hormonal manipulation of the culture medium. When the electric pulses represented the only external influence applied and the seedlings were allowed to grow normally, a “dwarf effect” was observed, with fresh mass and stem length gradually diminishing with increased field intensity. This response was similar with those observed by Gill *et al.* [90] using intact plantlets of *Vigna aconitifolia* subjected to higher voltages (0.5-3 kV/cm pulses of 2 or 15 μ s duration). Cogălniceanu *et al.* [91] have found that a relatively constant number of leaves differentiated, both on sample and control seedlings, but the leaves from the electrotreated seedlings were much smaller. The dry mass was not influenced in a similar manner, suggesting that the aqueous equilibrium was strongly affected. The total protein concentration determined 24 hours after the electric treatment showed a slight decrease for electric treated seedlings, probably due either to a loss of cytosolic proteins, or a reduction of the protein biosynthesis rate, as a consequence of the effects entailed by the field action onto the plasma membrane and/or cell wall.

The authors suggested that the decreased water content of the electropulsed seedlings could be explained by the perturbations in plasma membrane permeability and/or in biosynthesis or functioning of water channel proteins. At the end of the growth period (30 days) more electrophoretic bands were observed in the electric treated seedlings, appreciated as stress proteins by the authors. This fact, correlated with the “dwarf effect”, indicated that the electric field acted as a stress factor, the newly synthesised stress proteins interacting with the developmental program.

In the experiments in which the electric treatment was followed by a hormonal manipulation of the nutritive medium [92,93], both callusing and adventitious shoots

regeneration were significantly enhanced by the electric treatment, showing a “window response”, that was dependent on the field strength and had a maximum at 100 V/cm, for callus proliferation (almost 100% increase) and at 300 V/cm, for *de novo* shoots differentiation (almost five fold more regenerated shoots as the control). The successive application of the two external signals (electrical followed by hormonal) at a certain stage in the postembryony development induced alterations in the normal developmental programme, indicating that already differentiated cells were reprogrammed and evolved in a different direction under the external hormonal command. Although intact seedlings are ongoing developing systems, with a complex and hierarchical endogenous control of the morphogenetic programme, the postcotyledon phase proved to be open to environmental influences. Developmental homeostasis was overwhelmed by hormonal manipulation of the culture medium, dedifferentiated cells or *de novo* shoots appearing all over the seedlings, in the absence of a “pattern” or without any preferred area for these abnormal cellular processes. These responses were synergistically enhanced by the application of the electric pulses [93]. The seedlings response to the electric field action varied largely, the higher average value being obtained not as a result of a homogenous response by all seedlings within an experimental variant, but a relatively large response by some more sensitive seedlings. The cytological analysis of the callus indicated a direct correlation between the intensity of the applied electric current and both the size of the callus cells and the load of the cells with amyloplasts, the callus generated by the seedlings subjected to 100 V/cm rectangular pulses being smallest, with a higher load of amyloplasts compared to the control and the other electric variants. When induced by the exogenous hormonal supply, adventitious shoots were differentiated both directly and indirectly (*via* callus), and recurrent shoot regeneration was observed. The dynamics of shoots regeneration were also significantly influenced by the electric treatment, regenerated shoots being apparent 2-3 days earlier in the electric treated seedlings, and for the 300 V/cm variant the morphogenetic process being twice as fast as in the control. As a conclusion, after the action of the external electric treatment, more cells escaped from the integrative developmental mechanisms (postembryonic developmental pattern) and engaged in a distinct path of differentiation, commanded by the hormonal balance in the nutritive culture medium. Applied as a pre-treatment, the exposure to the electric field can cause a wakening of the control hierarchical intercellular interactions. The physiological state of the cells also influences the interaction with the applied electric field, the non-equilibrium state (far from equilibrium) allowing for optimal receptivity towards the electrical stimulus applied [41]. The effects of the applied electric field proved to be more efficient if the biological system was in a state of physiological stress, in which the integrative control was absent [40]. Biological systems *in vitro* respond to this requirement, showing a cultivation stress, even under “optimal” growth conditions. Compared with other types of biological systems currently used in plant electromanipulation experiments, especially protoplasts, which express stress of isolation, poor viability, regeneration difficulty and genetic instability, intact seedlings used as inoculum in such experiments have several advantages: the absence of wounding or cutting stress, high percentage of viability, significant yield of adventitious shoots or callus mass, a shortened and simplified experimental protocol. All these

results have revealed that short high-voltage pulses can stimulate *in vitro* morphogenetic and proliferative processes in plant systems more complex than protoplasts.

Searching for an explanatory mechanism which mediates the interaction: electric field–intact seedlings, Cogălniceanu *et al.* [94] recorded the variations of plasmalemma conductivity and diffusive permeability induced by the action of short duration high-voltage pulses applied to very young intact tobacco seedlings. The protocol of electrical treatments was identical as in the experiments previously described. After the electric treatment, each lot of 35 seedlings electroporated with 100,200,300,400 and 500 V/cm rectangular pulses was sterile collected and 24 hours kept in a glass vessel with 10 ml deionized water (including the water in which the seedlings were electroporated). Two sets of measurements were done: (a) At 24 hours after the electroporation, the effluxes through the plasma membranes were characterized by measuring in the stocking deionized water: the pH, the electric conductivity, Ca^{2+} concentration and the spectrophotometric absorbance at 259 nm (characteristic for DNA fragments); (b) The seedlings were boiled for 30 minutes into the stocking water, when the plasma membranes were broken, and the total cellular ionic content was estimated. The cellular effluxes induced by the electric treatment were estimated as the percentage from the whole cellular ionic content. Electric conductivity of the storing deionised water, calcium efflux and 259 nm absorbance had increased depending on the intensity of the applied electric field, compared to the control, but the differences were statistically significant only at values higher than 300 V/cm. At 500 V/cm the efflux of total charged particle, including calcium ions, had doubled compared to the control, while the absorbance values at 259 had increased 2.5 times. These results are indicative of the poor efficiency of the electroporation (the puncture of the plasmalemma and the formation of the transient pores) at field values smaller than 300 V/cm. Because the morphogenetic stimulative effects of the extremely short electric pulses were obtained at an intensity window between 100-300 V/cm, the authors concluded that the electrostimulation of *in vitro* cytodifferentiation and morphogenesis is a process mediated by other mechanisms than the induction of transient pores into the plasmalemma.

Strong external electric fields are leading to an increase in transmembrane conductivity and diffusive permeability, as a result of formation of aqueous pores in the membrane, which also alter the electrical potential across the membrane. Thus, electroporation of cell membranes is used as a tool for delivering large molecules (especially DNA) into the cell [71] and is also the basic mechanism of tissue injury in high-voltage electric shock [72].

Plant cells have a relatively neutral cytosol, with high potassium and low calcium concentrations. The presence of a cell wall and of an osmotic active vacuole implies the existence of sophisticated ion movement mechanisms and exchanges. The asymmetric distribution of ions across membranes generates electrical potentials [95], associated with: apical growth and cell elongation [95], somatic embryos differentiation [14], leaves morphogenesis [96], root growth [97] and pollen germination [16]. The asymmetric distribution of ions appears also to be involved in cellular signalling, in positional information specification and in codification of the cellular identities [1,5,98]. Under the action of very short duration and moderate intensity electric pulses, the distribution of plasma membrane ionic fluxes are modified, generating electrical

potentials across membranes. The cells in seedlings subjected to moderate electric pulses and their electric connections with neighbouring cells (as a part of intercellular communication pathways) were strongly perturbed [91,92,94]. Owing to the disturbed integrative supracellular control, many cells became more sensitive to the external influences and were induced to redifferentiate, long time after the pulse action.

5. Potential applications of the electric manipulation in plant biotechnology

During the last years the problem of reproducible and measurable effects of the external electric fields on plant *in vitro* cultures has raised considerable interest [99]. A broad range of responses induced by electric treatments on various *in vitro* plant systems were reported. Even if the experimental findings are sometimes difficult to compare because of the numerous and different electrical and biological parameters, it became evident that plant cells can react sensitively by various metabolic responses. Although the mechanisms that mediate the interaction between the artificial electric fields and the biological systems are still unknown, the considerable interest in such procedures is due to their potential biotechnological applications. Whatever type and level of external electric field is used in stimulating experiments, interference between exogenous and endogenous electric fields occurs, with consequences on the simultaneous or subsequent developmental processes.

Electrostimulation of plant *in vitro* developmental systems using low intensity, low frequency, long duration electric fields has several potential biotechnological applications:

- Enhancing the proliferation rate of plant biomass [48,50];
- Enhancing the expression of totipotency in recalcitrant plant species [90];
- Increasing the rate and efficiency of plant regeneration [49,51,52,56];
- Increasing the viability and biological performances of the plant regenerants [81];
- Intensification of the secondary metabolites biosynthetic rate in *in vitro* systems [100,101];
- Influencing the timing and the performance of some physiological processes in plants [102];
- Improving the speed and success of seed germination [103-105];
- Enhancing the efficiency of *in vitro* stress-selection by using low intensity, low frequency electric field as co-stressing factor [106,107].

High-voltage, short-duration pulses applied to plant protoplasts, tissues or even to intact seeds, plantlets or seedlings can also promote:

- Stimulation of protoplasts division [75,76,78];
- Enhancement of shoot regeneration from protoplast-derived tissues [78,81] or from intact tissues or plants [90-92];
- Enhancement of regenerants viability [79];
- Stimulation of protein synthesis [83];
- Enhancement of DNA synthesis in cultured plant protoplasts [82,108].
- Improving the speed and rate of seed germination (Cogălniceanu *et al.* unpublished).

References

- [1] Wolpert, L. (1971) Positional information and pattern formation. *Curr. Opin. Dev. Biol.* 6: 183-224.
- [2] Wolpert, L. (1981) Positional information and pattern formation. *Philos. Trans. R. Soc. London B.* 295: 441-450.
- [3] Meinhardt, H. (1982) *Models of Biological Pattern Formation*. Academic Press, London.
- [4] Meinhardt, H. (1994). Biological pattern-formation new observations provide support for theoretical predictions. *Bioessays* 16: 627-632.
- [5] Meinhardt, H.; Koch, A.J. and Bernasconi, G. (1998) Models of pattern formation applied to plant development. In: Barabe, D. and Jean, R.V. (Eds.) *Symmetry in Plants*. World Scientific Publishing, Singapore; pp. 723-758.
- [6] Hedrich, R.; Stoeckel, H. and Takeda, K. (1990) Electrophysiology of the plasma membrane of higher plant cells: new insights from patch-clamp studies. In: Larsson, C. and Moller, I.M. (Eds.) *The Plant Plasma Membrane*. Springer-Verlag Berlin, Heidelberg; pp. 182-202.
- [7] Rinne, P.L.H. and van der Schoot, C. (1998) Symplasmic fields in the tunica of the shoot apical meristem coordinate morphogenetic events. *Development* 125: 1477-1485.
- [8] Scheres, B. and Berleth, T. (1998) Root development: new meanings for root canals? *Curr. Opin. Plant Biol.* 1: 32-36.
- [9] Jaffe, L.F. and Nuccitelli, R. (1977) Electrical controls of development. *Ann. Rev. Biophys. Bioeng.* 6: 445-476.
- [10] Shipley, A.M.; Feijó, J.A. (1999) The use of vibrating probe technique to study steady extracellular currents during pollen germination tube growth. In: Hayst, W. and Feinleib, M.E. (Eds.) *Fertilization in Higher Plants*. Springer-Verlag, Berlin Heidelberg, New York; pp. 235-252.
- [11] Thavarungkul, P. (1997) Vibrating probe measurement of ionic currents around developing embryo of oil palm (*Elaeis guineensis* Jacq.). *J. Exp. Bot.* 48: 1647-1653.
- [12] Nuccitelli, R. and Jaffe, L.F. (1974) Spontaneous current pulses through developing fucoid eggs. *Proc. Nat. Acad. Sci. USA* 71: 4855-4859.
- [13] Brawley, S.H.; Wetherell, D.F. and Robinson, K.R. (1984) Electrical polarity in embryos of wild carrot precedes cotyledon differentiation. *Proc. Natl. Acad. Sci. USA* 81: 6064-6067.
- [14] Rathore, K.S.; Hodges, T.K. and Robinson, K.R. (1988) Ionic basis of currents in somatic embryos of *Daucus carota*. *Planta* 175: 280-289.
- [15] Weisenseel, M.H. and Jaffe, L.F. (1976) The major growth current through pollen tubes enters as K^+ and leaves H^+ . *Planta* 133: 1-7.
- [16] Feijó, J.A.; Malho, R. and Obermeyer, G. (1995) Ion dynamics and its possible role during *in vitro* pollen germination and tube growth. *Protoplasma* 187: 155-167.
- [17] Weisenseel, M.H. (1979) Induction of polarity. In: Hayst, W. and Feinleib, M.E. (Eds.) *Encyclopedia of Plant Physiology*. Springer, Berlin; pp. 485-505.
- [18] Hamada, S.; Ezaki, S.; Hayashi, K.; Toko, K. and Yamafuji, K. (1992) Electric current precedes emergence of a lateral root in higher plants. *Plant Physiol.* 100: 614-619.
- [19] Toko, K.; Hayashi, K. and Yamafuji, K. (1986) Spatio-temporal organization of electricity in biological growth. *Trans. IEICE of Japan.* 4: 485-487.
- [20] Toko, K.; Iiyama, S.; Tanaka, C.; Hayashi, K.; Yamafuji, K. and Yamafuji, K. (1987) Relation of growth process to spatial patterns of electric potential and enzyme activity in bean roots. *Biophysical Chem.* 27: 39-58.
- [21] Toko, K. and Yamafuji, K. (1988) Spontaneous formation of the spatial pattern of electric potential in biological systems. *Ferroelectrics* 86: 269-279.
- [22] Novak, B. and Bentrup, F.W. (1972) An electrophysiological study of regeneration in *Acetabularia mediterranea*. *Planta* 103: 227-244.
- [23] Gorst, J.; Overall, R.L. and Wernicke, W. (1987) Ionic currents traversing cell clusters from carrot suspension culture reveal perpetuation of morphogenetic potential as distinct from induction of embryogenesis. *Cell Differentiation* 21: 101-109.
- [24] Rathore, K.S. and Robinson, K.R. (1989) Ionic currents around developing embryos of higher plants in culture. *Biological Bulletin* 176: 46-48.
- [25] Weisenseel, M.H.; Nuccitelli, R. and Jaffe, L.F. (1975) Large electrical currents traverse growing pollen tubes. *J. Cell Biol.* 66: 556-567.

- [26] Feijó, J.A.; Shipley, A.M. and Jaffe, L.M. (1994) Spatial and temporal patterns of electric and ionic currents around *in vitro* germinating pollen. In: Spanswick, R.; Lucas, W.J. and Dainty, J. (Eds.) XIII International Congress on Sexual Plant Reproduction. Abstract book, Vienna; pp. 40.
- [27] Pierson, E.; Miller, D.D.; Callahan, D.A.; Shipley, A.M.; Rivers, B.A.; Cresti, M. and Hepler, P.R. (1994) Pollen tube growth is coupled to the extracellular calcium ion flux and the intracellular calcium gradient: effect of BAPTA-type buffers and hypertonic media. *Plant Cell* 6: 1815-1828.
- [28] Weisenseel, M.H.; Dorn, A. and Jaffe, L.F. (1979) Natural H⁺ currents traverse growing roots and root hairs of barley (*Hordeum vulgare* L.). *Plant Physiol.* 64: 512-518.
- [29] Miller, A.L.; Shand, E. and Gow, N.A.R. (1988) Ion currents associated with root tips, emerging laterals and induced wound sites in *Nicotiana tabacum*: spatial relationship proposed between resulting electrical fields and phytophthora zoospore infection. *Plant Cell Environ.* 11: 21-25.
- [30] Rathore, K.S.; Hotanry, K.B. and Robinson, K.R. (1990) A two-dimensional vibrating probe study of currents around lateral roots of *Raphanus sativus* developing in culture. *Plant Physiol.* 92: 543-546.
- [31] Iiama, S.; Toko, K. and Yamafuji, K. (1985) Band structure of surface electric potential in growing roots. *Biophys. Chem.* 21: 285-295.
- [32] Ezaki, S.; Toko, K.; Yamafuji, K. and Tanaka, C. (1990) Electrical control of growth of the higher plant. *Memoirs of the Faculty of Engineering Kyushu University.* 50: 377-393.
- [33] Ezaki, S.; Toko, K. and Yamafuji, K. (1990b) Electrical stimulation on the growth of a root of the higher plant. *Trans. IEICE of Japan.* 73: 922-927.
- [34] Jaffe, L.F. (1980) Control of plant development by steady ionic currents. In: Spanswick, R.; Lucas, W.J. and Dainty, J. (Eds.) *Plant Membrane Transport: Current Conceptual Issues.* Elsevier, New York; pp. 381-388.
- [35] Glaser, R. (1992) Current concepts of the interaction of weak electromagnetic fields with cells. *Bioelectrochem. Bioenerg.* 27: 255-268.
- [36] Berg, H. (1993) Electrostimulation of cell metabolism by low frequency electric and electromagnetic fields. *Bioelectrochem. Bioenerg.* 31: 1-25.
- [37] Weaver, J.C. and Astumian, R.D. (1990) The response of living cells to very weak electric fields: the thermal noise limit. *Science* 247: 459-462.
- [38] Weaver, J.C. and Astumian, R.D. (1992) Estimates for ELF effects: noise-based thresholds and the number of experimental conditions required for empirical searches. *Bioelectromagnetics Suppl.* 1: 113-138.
- [39] Adey, W.R. (1990) Electromagnetic fields and the essence of living systems. In: Back, J. and Anderson, J. (Eds.) *Modern Radio Science.* Oxford University Press, UK; pp. 1-36.
- [40] Findl, E. (1987) Membrane transduction of low energy level fields and the Ca²⁺ hypothesis. In: Blank, M. and Findl, E. (Eds.) *Mechanistic Approaches to Interactions of Electric and Electromagnetic Fields with Living Systems.* Plenum Publishing, New York; pp. 15-38.
- [41] McLeod, B.; Liboff, A.R. and Smith, S.D. (1992) Biological systems in transition: sensitivity to extremely low-frequency fields. *Electro- and Magneto-Biology* 11: 29-42.
- [42] Tenforde, T.S. (1993) Cellular and molecular pathways of extremely low frequency electromagnetic field interactions with living systems. In: Blank, M. (Ed.) *Electricity and Magnetism in Biology and Medicine.* San Francisco Press, San Francisco; pp. 1-8.
- [43] Tsong, T.; Chauvin, F. and Astumian, R.D. (1987) Interaction of membrane proteins with static and dynamic electric fields via electroconformational coupling. In: Blank, M. and Findl, E. (Eds.) *Mechanistic Approaches to Interactions of Electric and Electromagnetic Fields with Living Systems.* Plenum Publishing, New York; pp. 187-201.
- [44] Tsong, T. (1992) Molecular recognition and processing of periodic signals in cells: study of activation of membrane ATPases by alternating electric fields. *Biochimica Biophysica Acta.* 1113: 53-70.
- [45] Blank, M. (1987) The surface compartment model: a theory of ion transport focused on ionic processes in the electrical double layers at membrane protein surfaces. *Biochimica Biophysica Acta.* 906: 277-294.
- [46] Blank, M. and Goodman, R. (1988) An electrochemical model for the stimulation of biosynthesis by external electric fields. *Bioelectrochem. Bioenerg.* 19: 569-580.
- [47] Goldsworthy, A. and Rathore, K.S. (1985) The electrical control of growth in plant tissue cultures: the polar transport of auxin. *J. Exp. Bot.* 36: 1134-1141.
- [48] Rathore, K.S. and Goldsworthy, A. (1985) Electrical control of growth in plant tissue cultures. *Bio/Technol.* 3: 253-254.
- [49] Rathore, K.S. and Goldsworthy, A. (1985) Electrical control of shoot regeneration in plant tissue cultures. *Bio/Technol.* 3: 1107-1109.

- [50] Radu, M.; Cogălniceanu, G. and Brezeanu, A. (1994) Control of *Nicotiana tabacum* L. callus growth by weak alternating and pulsed electric field. *Electro- Magneto-Biol.* 13: 195-201.
- [51] Cogălniceanu, G.; Radu, M.; Fologea, D.; Moiso, N. and Brezeanu, A. (1996) Electroenhancement of differentiation and morphogenesis in tobacco callus culture, In: Crăciun, C. and Ardelean (Eds.) *A Current Problems and Techniques in Cellular and Molecular Biology*. Edit. Mirton. Timișoara 1: 567-570.
- [52] Cogălniceanu, G.; Radu, M.; Fologea, D.; Moiso, N. and Brezeanu, A. (1998) Stimulation of tobacco shoot regeneration by alternating weak electric field. *Bioelectrochem. Bioenerg.* 44: 257-260.
- [53] Thavarungkul, P. and Kanchanapoom, K. (2002) Effect of applied currents to growth in oil palm (*Elaeis guineensis* Jacq.) tissue cultures. *Songklanakarin J. Sci Technol.* 24: 283-291.
- [54] Goldsworthy, A. (1996) Electrostimulation of cells by weak electric currents. In: Lynch, P.T. and Davey, M.R. (Eds.) *Electrical Manipulation of Cells*. Chapman and Hall, New York; pp. 249-272.
- [55] Mina, M.G. and Goldsworthy, A. (1991) Changes in the electrical polarity of tobacco cells following the application of weak external currents. *Planta* 186: 104-108.
- [56] Cogălniceanu, G.; Radu, M.; Fologea, D. and Brezeanu, A. (1998) Are the electric field effects coupled with the hormonal reception of cells in plant callus culture? *Roum. Biotechnol. Lett.* 3: 201-206.
- [57] Trewavas, A. (1991) How do plant growth substances work? *Plant Cell Environ.* 14: 1-12.
- [58] Neumann, E. (1986) Digression on biochemical membrane reactivity in weak electromagnetic fields. *Bioelectrochem. Bioenerg.* 16: 565-567.
- [59] Berg, H. and Zhang, L. (1993) Electrostimulation in cell biology by low-frequency electromagnetic fields. *Electro-and Magneto-Biol.* 12: 147-163.
- [60] Stenz, H.G.; Wohlwend, B. and Weisenseel, M.H. (1998) Weak AC-electric fields promote root growth and ER abundance of root cap cells. *Bioelectrochem. Bioenerg.* 44: 261-269.
- [61] Tsong, T. and Astumian, R.D. (1986) Absorbtion and conversion of electric field energy by membrane bound ATP-ases. *Bioelectrochem. Bioenerg.* 15: 457-476.
- [62] Gransdorff, P. and Prigogine, I. (1971) *Thermodynamic Theory of Structure, Stability and Fluctuations*. Wiley – Interscience, Gordon.
- [63] Lowe, K.C.; Davey, M.R. and Power, J.B. (1996) *Plant tissue culture: past, present and future*. *Plant Tissue Cult. Biotechnol.* 2: 175-186.
- [64] Teissié, J. (2002) Membrane destabilizations supporting electroporation. *Cell. Mol. Biol. Lett.* 7: 96-100.
- [65] Xinping, X. and Baojian, L. (1988) Fertile transgenic indica rice plants obtained by electroporation of the seed embryo cells. *Plant Cell Rep.* 13: 237-242.
- [66] Kloti, A.; Iglesias, V.A.; Wunn, J.; Burkhardt, P.K.; Datta, S.K. and Potrykus, I. (1993) Gene transfer by electroporation into intact scutellum cells of wheat embryos. *Plant Cell Rep.* 12: 671-675.
- [67] Arencibia, A.; Molina, P.R.; De la Riva, G. and Selman, H. (1995) Production of transgenic sugarcane (*Saccharum officinarum* L.) plants by intact cell electroporation. *Plant Cell Rep.* 14: 305-309.
- [68] Chowrira, G.M.; Akella, V. and Lurquin, P.F. (1995) Electroporation-mediated gene transfer into intact nodal meristems in plants. *Generating transgenic plants without in vitro tissue culture*. *Mol. Biotechnol.* 3: 7-23.
- [69] Fologea, D.; Brezeanu, A.; Radu, M.; Cornea, P. and Vătafu, I. (1999) Gene transfer by electroporation into intact tobacco petiole tissue. *Electro-and Magneto-Biology* 18: 1-6.
- [70] De Padua, V.L.M.; Pestana, M.C.; Margis-Pinheiro, M. and Mansur, E. (2000) Electroporation of intact embryonic leaflets of peanut: gene transfer and stimulation of regeneration capacity. *In Vitro Cell. Dev. Biol.- Plant* 36: 374-378.
- [71] Tsong, T. (1991) Electroporation of cell membranes. *Biophys. J.* 60: 297-306.
- [72] Lee, R.C. (1994) Characterization of non-linear electrical behaviour of lipid bilayer of cell membranes. In: Lin, J. C. (Ed.) *Advances in Electromagnetic Fields in Living Systems*. Vol.1, Plenum Press, New York; pp. 81-127.
- [73] Potter, H. (1988) Electroporation in biology: methods, applications and instrumentation. *Anal. Biochem. Bioenerg.* 174: 361-373.
- [74] Davey, M.R.; Blackhall, N.W.; Lowe, K.C. and Power, J.B. (1996) Stimulation of plant cell division and organogenesis by short-term, high-voltage electrical pulses. In: Lynch, P.T. and Davey, M.R. (Eds.) *Electrical Manipulation of Cells*. Chapman and Hall, New York; pp. 273-286.
- [75] Rech, E.L.; Ochatt, S.J.; Chand, P.K.; Power, J.B. and Davey, M.R. (1987) Electroenhancement of division of plant protoplast-derived cells. *Protoplasma* 141: 169-176.
- [76] Gupta, H.S.; Rech, E.L.; Cocking, E.C. and Davey, M.R. (1988) Electroporation and heat shock stimulate division of protoplasts of *Penisetum squamulatum*. *J. Plant Physiol.* 133: 457-459.

- [77] Mordhorst, A.P. and Lörz, H. (1992) Electrostimulated regeneration of plantlets from protoplasts derived cell suspensions of barley (*Hordeum vulgare*). *Physiol. Plant.* 85: 289-294.
- [78] Ochatt, S.J.; Chand, P.K.; Rech, E.L.; Davey, M. and Power, J.B. (1988a) Electroporation-mediated improvement of plant regeneration from colt cherry (*Prunus avium* x *Pseudocerasus*) protoplasts. *Plant Sci.* 54: 165-169.
- [79] Ochatt, S.J.; Rech, E.L.; Davey, M. and Power, J.B. (1988b) Long-term effect of electroporation on enhancement of growth and plant regeneration of Colt cherry (*Prunus avium* x *pseudocerasus*) protoplasts. *Plant Cell Rep.* 7: 393-395.
- [80] Chand, P.K.; Ochatt, S.J.; Rech, E.L.; Power, J.B. and Davey, M.R. (1988) Electroporation stimulates plant regeneration from protoplasts of the woody medicinal species *Solanum dulcamara* L. *J. Exp. Bot.* 206: 1267-1274.
- [81] Barth, S.; Voeste, D.; Wingender, R. and Schnabl, H. (1993) Plantlet regeneration from electrostimulated protoplasts of sunflower (*Helianthus annuus* L.). *Bot. Acta.* 106: 220-222.
- [82] Rech, E.L.; Ochatt, S.J.; Chand, P.K.; Davey, M.R.; Mulligan, B.J. and Power, J.B. (1988) Electroporation increases DNA synthesis in cultured plant protoplasts. *Bio/Technol.* 6: 1091-1093.
- [83] Joersbo, M. and Brunstedt, J. (1990) Stimulation of protein synthesis in electroporated plant protoplasts. *J. Plant Physiol.* 136: 464-467.
- [84] Jones, B.; Lynch, P.T.; Power, J.B. and Davey, M.R. (1996) Electrofusion and electroporation equipment. In: Lynch, P.T. and Davey, M.R. (Eds.) *Electrical Manipulations of Cells*. Chapman and Hall, New York; pp. 1-14.
- [85] Puc, M.; Čorović, S.; FliStar, K.; Petrošek, M.; Nastran, J. and Miklavčič, D. (2004) Techniques of signal generation required for electroporation. *Survey of electroporation devices. Bioelectrochemistry.* 64: 113-124.
- [86] Dijak, M.; Smith, D.L.; Wilson, T.J. and Brown, D.C.W. (1986) Stimulation of direct embryogenesis from mesophyll protoplasts of *Medicago sativa*. *Plant Cell Rep.* 5: 468-470.
- [87] Montane, M.H. and Teissié, J. (1992) Electrostimulation of plant protoplast division. Part 1. Experimental results. *Bioelectrochem. Bioenerg.* 29: 59-70.
- [88] Dijak, M. and Simmonds, D.H. (1988) Microtubule organization during early direct embryogenesis from mesophyll protoplasts of *Medicago sativa* L. *Plant Sci.* 58: 183-191.
- [89] De Jong, A.J.; Schmidt, E.D.L. and De Vries, S.C. (1993) Early events in higher-plant embryogenesis. *Plant Mol. Biol.* 22: 367-377.
- [90] Gill, R.; Mishra, K.P. and Rao, P.S. (1987) Stimulation of shoot regeneration of *Vigna aconitifolia* by electrical control. *Ann. Bot.* 60: 399-403.
- [91] Cogălniceanu, G.; Carasan, M.; Radu, M.; Fologea, D. and Brezeanu, A. (2000) The influence of external electric field on the *in vitro* postcotyledonary development of *Nicotiana tabacum* L. cv. Xanthi seedlings. *Roum. Biotechnol. Lett.* 5: 45-54.
- [92] Cogălniceanu, G.; Radu, M.; Brezeanu, A. and Fologea, D. (2000) High voltage short duration pulses promote adventive shoot differentiation from intact tobacco seedlings. *Electro-and Magneto-Biology* 19: 177-187.
- [93] Cogălniceanu, G.; Radu, M.; Carasan, M.E. and Brezeanu, A. (2003) Interactions between exogenous applied signals (electrical, hormonal) and the *in vitro* developmental control mechanisms, *Proceedings of the Institute of Biology.* 5: 465-471.
- [94] Cogălniceanu, G.; Radu, M.; Câmpeanu, C. and Brezeanu, A. (2002) Variations of plasmalemma conductivity and diffusive permeability induced by external electric field. *In vitro* developmental significance, *Proceedings of the Institute of Biology* 4: 413-420.
- [95] Harold, F.M. and Caldwell, J.H. (1990) Tips and currents: electrobiology of apical growth. In: Heath, T.H. (Ed.) *Tip Growth in Plant and Fungal Cells*. Academic Press, New York; p.59-89.
- [96] Hush, J.M.; Newman, I.A. and Overall, R.L. (1991) A calcium influx precedes organogenesis in *Graptopetalum*. *Plant Cell Environ.* 14: 657-665.
- [97] Allen, N.S.; Bennet, M.N.; Cox, D.N.; Shipley, A.; Erhardt, D.W. and Long, S.R. (1994) Effects of nod factors on alfalfa root hair Ca^{++} and H^{+} currents on cytoskeletal behaviour. In: Daniels, M. J. (Ed.) *Advances in Molecular Genetics of Plant-Microbe Interactions*, Vol. 3. Kluwer Academic Publishers, The Netherlands; pp. 107-113.
- [98] Weisenseel, M.H. and Kicherer, M.R. (1981) Ionic currents as control mechanism in cytomorphogenesis. In: Kiermayer, M. (Ed.) *Cytomorphogenesis in Plants*. Springer, Wien; pp. 379-399.
- [99] Teissié, J. (1988) Effects of electric fields and currents on living cells and their potential use in biotechnology: a survey. *Bioelectrochem. Bioenerg.* 20: 133-142.

Electrical control of plant morphogenesis

- [100] Takeda, J.; Senda, M.; Ozeki, Y. and Komamine, A. (1988) Membrane potential of cultured carrot cells in relation to the synthesis of anthocyanin and embryogenesis. *Plant Cell Physiol.* 29: 817-824.
- [101] Cogălniceanu, G.; Brezeanu, A.; Lupsea, S.; Matienco, B. (1999) Factors that enhance cell proliferation and secondary metabolism (anthocyanin biosynthesis) in pericarp long-term callus culture of *Vitis vinifera* cv. Isabell. *Acta Hort. Bot. Buc.* 28: 303-317.
- [102] Machackova, J. and Krekule, J. (1991) The interaction of direct current with endogenous rhythms of flowering in *Chenopodium rubrum*. *J. Plant Physiol.* 138: 365-369.
- [103] Kasanova, Z.M. (1972) After-sowing processing of spring wheat seeds in electrical constant current. *Electr. Process. Mat.* 4: 71-72.
- [104] Davies, M.S. (1996) Effects of electromagnetic fields on early growth in three plant species and replication of previous results. *Bioelectromagnetic.* 17: 154-164.
- [105] Staselis, A. and Optazas, R. (1996) Influence of electromagnetic fields to sprout of seeds tomato and cucumber and morphogenesis of seedlings. *Research papers LIAg. Eng and LA of Ag.* 28: 121-130.
- [106] Mittenzwei, R.; Süßmuth, R.; Mei, W. (1996) Effects of extremely low-frequency electromagnetic fields on bacteria – the question of co-stressing factor. *Bioelectrochem. Bioenerg.* 40: 21-27.
- [107] Gutzeit, H.O. (2001) Biological effects of ELF-EMF enhanced stress-response: new insights and new questions. *Electro-Magneto-Biol.* 20: 15-26.
- [108] Blank, M. and Goodman, R. (1999) Electromagnetic fields may act directly on DNA. *J. Cell Biochem.* 75: 369-374.

THE USES OF ULTRASOUND IN PLANT TISSUE CULTURE

VICTOR GABA¹, K. KATHIRAVAN², S. AMUTHA¹, SIMA SINGER¹, XIA XIAODI³ AND G. ANANTHAKRISHNAN⁴

¹*Dept. of Virology, ARO Volcani Center, POB 6 Bet Dagan 50250, Israel
- Fax: 972-3-9604180 - Email: vpgaba@volcani.agri.gov.il*

²*Department of Biotechnology, Jamal Mohamed College, Tiruchirapalli
620 020, India*

³*Plant Industry Division, CSIRO, Canberra City, Canberra ACT 2600,
Australia*

⁴*University of Florida, Citrus Research and Education Center, 700
Experiment Station Rd., Lake Alfred, FL 33850-2299, USA*

1. Introduction

Ultrasound is the field of science dealing with the application of sound frequencies in the inaudible range, generally from 20-100 kHz, although special applications occur outside that range. The application of ultrasound at high power for the disruption of biological material has been used for many years. In the period of the 1950-1970s many experiments were conducted on the effect of low levels of ultrasound radiation on a wide range of biological materials including plants. Recently more subtle uses have been found for ultrasound in plant tissue culture. These applications include transformation of several plant species in tissue culture by direct DNA transfer or sonication-assisted *Agrobacterium*-mediated transformation (SAAT). Additionally, ultrasound has been used to stimulate growth of recalcitrant explants, and to sort somatic embryos.

At the organism (plant) level ultrasound enhances the germination of various seeds and the subsequent growth of the seedling [1-5]. The growth of some species is inhibited by the same frequency and exposure time that stimulated the growth of other species [4]. The frequency and amount of energy required for the effect of ultrasonic treatment appear to vary widely between species and cultivars.

Mild ultrasonic irradiation can stimulate protein synthesis in plant cells and protoplasts significantly [6], and affected plasmamembrane permeability [7,8]. Ultrasonic treatment was reported to cause reversible inhibition of DNA, RNA and protein synthesis in *Pisum sativum* root meristem cells [9]. Ultrasound caused changes in the less stable, extended form of nucleolar chromatin [10]. Low doses of ultrasound caused reversible callose deposition on sieve plates in cotton (*Gossypium hirsutum*) cotyledon petioles [11]. A low dose of ultrasound damaged the testa of *Orchis*

papilionacea seeds, permitting *in vitro* germination and subsequent protocorm and minituber production [12].

2. The generation of ultrasound

Ultrasound is generated in most of the applications for plant tissue culture by water bath sonicators. Ultrasound is nowadays generally produced by a piezoelectric crystal (currently the most popular and versatile type of transducer), which converts an alternating electric current into mechanical vibrations (high frequency sound). The transducer is designed as a thin ceramic disk, from which the ultrasound wave is directed away from the transducer. The transducer crystal can be shaped to give a desired wave shape; a concave ceramic face will produce an ultrasound wave focused to a particular point. Often ultrasonic baths are supplied with several transducers to produce sufficient power. Ultrasonic transducers should operate at their optimum resonance frequency or the operation will be less effective. The transducers on a piece of equipment must be matched in operating frequency to within 200 Hz, or efficiency again will be reduced. (<http://www.healthsonics.com>).

Many ultrasonic instruments used in biology are general-purpose laboratory machines designed and mainly used for cleaning small pieces of apparatus, not particularly well maintained, and therefore of doubtful calibration. Notably, the ultrasonic output of water bath sonicators is difficult to measure. Although "Ultrasonic Cavitation Energy Meters" are now commercially available, the power uniformity and pattern in an ultrasonic water bath can be recorded by noting the effect of 20s exposure of aluminium foil in the tank. Normally such a test would give uniform "pebbling" effect—holes or empty areas would indicate lack of uniformity (www.healthsonics.com).

The power of an ultrasonic bath can be rated in different ways, and this makes it difficult to compare the power of different instruments. The best rating method is probably RMS power consumption (in watts) by the transducers. Additionally, the frequency used affects the cavitation force of the bubbles: doubling the frequency reduces the power by a factor of 10. However, the higher the frequency the smaller the bubbles, and therefore are able to enter smaller locations. It is unclear that the nominal rated output is actually what is produced, and it is rare to find a report concerning plant biology (or plant tissue culture) where the output factors have been measured. Additionally, different locations within the instrument may very well have different power values, and damage, aging or failure of the transducers might affect the power distribution.

It is notably difficult to compare ultrasonic treatments by different authors. There is a wide range of instrument types used with different geometries and nominal power outputs, and additionally a wide range of ultrasound frequencies are used (Table 1). However, different instruments producing a wide range of frequencies and output power can produce similar results in SAAT [16]. Ultrasound can be produced by other means e.g. powerful tunable instruments emitting via "horns" (e.g. [14]), commonly used for tissue disruption, or by laboratory-produced equipment [23].

The uses of ultrasound in plant tissue culture

Table 1. Tissue culture responses to ultrasound treatment. All reports in this Table used ultrasonic baths of various makes, with the exception of a probe sonicator [14]. NA = information not available. * = transgenic plants produced.

Plant material	Response	Frequency/time/power/quantity and volume	Reference
Tobacco leaf explants	naked DNA transformation*	freq NA/ 30 min/ 0.5Wcm ² / quantity NA in 3 ml	[13]
Sugar beet and tobacco protoplasts	naked DNA transformation	20 kHz/200-1000ms/ 30-105W/ 0.38 ml	[14]
Soyabean, cowpea, maize, wheat, Ohio buckeye - various tissues	SAAT*	55 kHz/ 0.2-100s/50W/10-20 × 2-4 mm clumps in 1 ml in 13×100 mm glass tube	[15]
Soyabean embryogenic callus	SAAT*	55 kHz/ 0-300s/50W/10-20 × 2-4 mm clumps in 1 ml in 13×100 mm glass tube	[16]
Soyabean immature embryos	SAAT*	55 kHz/ 0.1-10s/50W /10 cots in 0.5 ml in 1.5 ml microfuge tube	[17]
Soyabean cotyledonary nodes	SAAT*	55 kHz/6-600s/50W/10 explants covered in <i>Agrobacterium</i> solution in 16×125 mm glass tube	[18]
Ohio buckeye	SAAT*	55 kHz/ 0-60s/50W /10 embryogenic clumps in 1 ml in 13×100 mm glass tube	[19]
<i>Robina pseudoacacia</i> cotyledon	SAAT*	30 kHz/ 60s/ 60 W /10 explants in 20 ml in 50 ml Falcon tube	[20]
Squash cotyledon explant	multiple shoot regeneration	47 kHz/ 30-120s/ 35W/ 20 explants (420 mg) in 10 ml in 25×150 mm glass tube	[21,22]

Ultrasound can be supplied as a continuous waveform, or as pulses, propagating wave or standing wave, a fact little discussed in the literature of plant tissue culture. The waveform was of importance for survival of *Petunia hybrida* cell suspensions, as propagating waves reduce cell viability compared to standing wave fields of equal energy density [24]. The biophysics of ultrasound effects has been reviewed [25,26].

3. Mechanisms of action of ultrasound

Different mechanisms have been proposed for the biological action of ultrasound (see reviews [25-27]). The major effects of ultrasound are generally believed to be through acoustic cavitation (transient or collapse cavitation). In this process minute gas bubbles (of micron diameter) are formed because the local static liquid pressure is below the vapour pressure of the liquid at the given temperature. The microbubbles produced by ultrasound grow rapidly until they implode, causing microcavitation. Cavitation causes localized heating, and eventually heating of the liquid medium. The implosions generate

very high pressures and temperatures under extraordinary conditions during the final stages, along with free radical formation causing many damaging chemical reactions [28]. Reactions with the radicals occur within the collapsing bubbles and in the surrounding medium. The pressure shock waves that emanate from the collapse of the bubble cause mechanical effects (i.e. damage) to the surrounding material. Another mode of ultrasonic action is microstreaming (stable cavitation) where large and rapid oscillations in bubble size cause a violent flow of the fluid medium surrounding the bubble, causing microstreaming [27].

4. Sonication-assisted DNA transformation

To cause genetic transformation tobacco, (*Nicotiana tabacum* L.) leaf explants were sonicated in a solution of plasmid and carrier (salmon sperm) DNA [13]. Sonication at higher power (1-2Wcm⁻²) raised the temperature of the solution significantly, and the explants were morphologically damaged. Under the regime used (Table 1) large areas of the leaf tissue expressed transgenic β -glucuronidase (GUS) activity, and numerous transgenic plants regenerated. Notably, there was an absolute requirement for a large dilution of the transformation plasmid with salmon sperm carrier DNA.

Transient expression of transgenes in sonicated protoplasts of sugar beet (*Beta vulgaris* L.) and tobacco (Table 1) was demonstrated [14]. Protoplast viability (and subsequent microcalli formation) declined with time (to 1000 ms) or power dose (either at fixed power and varied time, or by varying power output) of application of the probe sonicator used, whereas maximum transgene expression occurred in the midrange of sonicator power output (ca. 60W) [14]. Additionally, sugar beet cells and protoplasts could be inoculated with beet necrotic yellow vein virus following ultrasound treatment. Mild sonication permits transitory solubilization of cell membranes, permitting the passage of large virus particles without killing the cells. Interestingly, even an hour after sonication the protoplast membrane was still permeable enough to permit some virus inoculation [7].

5. Sonication-assisted *Agrobacterium*-mediated transformation

SAAT is currently the most important use of ultrasound in plant tissue culture. SAAT was first reported by Trick and Finer [15], who used this technique for the production of transgenic soyabean (*Glycine max*) and Ohio buckeye (*Aesculus glabra*) plants, and transient expression of a foreign gene in different tissues of maize (*Zea mays*), cowpea (*Vigna unguiculata*), spruce (*Picea glauca*) and wheat (*Triticum aestivum*). In SAAT plant tissue is damaged by sonication, permitting the tissue to be much more easily transformed by *Agrobacterium tumefaciens* (Table 1). Surface damage was observed by scanning electron microscopy (SEM) [15-17]. Microwounding probably accounts for the increase in the rate of transformation, as energy released from the cavitation of microbubbles causes minute visible wounds within and on the tissue [15-17]. The microwounds permitted *Agrobacterium tumefaciens* cells to enter and colonize surface and interior cells [15,16], which did not occur in controls. SAAT enabled transient and permanent transformation of plant cells, leading to the recovery of transgenic plants

[15-18,20] (Table 1). Control (untreated) explants showed very low levels of transient or permanent transformation [15]. Transient GUS-expression increased with sonication treatment time (dose) to 30s, and then decreased [15]. Brief treatments which enhanced transient GUS enzyme expression caused observable surface damage and slowed growth of soyabean callus for several days [16]. Increasing times (doses) of exposure to ultrasound caused damage as the micro-wounds produced by the ultrasound became larger [15,17]. Indeed, longer treatments with ultrasound could be lethal to explants [17,18], and SAAT repeatedly reduced shoot proliferation in some soyabean cultivars [18]. Technical aspects of SAAT are discussed further (<http://www.oardc.ohio-state.edu/plantranslab/sonicate.htm>).

The use of SAAT has developed in recent years, in attempts to transform many different crops, with variable results. Sonication of sunflower (*Helianthus annuus*) shoot tips for a brief period combined with the use of macerating enzymes increased transient expression of green fluorescent protein, but only slightly increased the number of regenerated shoots expressing the transgene [29]. However, maceration alone was more successful in the production of transgenic shoots than when used with SAAT [29]. Sonication prior to application of *Agrobacterium* was most effective for the transformation of *Eucalyptus*, and a longer period of sonication (120s) enabled the production of transgenic shoots [30]. The use of SAAT was attempted in the transformation of precultured wheat inflorescence tissue, and although the number of explants showing transient GUS expression doubled with a brief sonication treatment, the number of expressing areas per explant was reduced, leaving no great benefit [31]. Transient gene expression in *Pinus pinea* cotyledons was greatly increased by SAAT, but none of the tissues survived to the end of the bud initiation period, due to a hypersensitive response to *Agrobacterium* [32]. Only at very low *Agrobacterium* concentrations were *Pinus* cotyledons able to survive SAAT and produce transgenic buds [32]. Transformation of kenaf (*Hibiscus cannabinus*) was stimulated by SAAT [33]. Brief ultrasound treatment (5s) produced more transient expression than 10s and caused less tissue damage (callus production), and was adopted for the production of transgenic plants [33]. Brief sonication enhanced *Agrobacterium*-mediated transient and permanent genetic transformation of loblolly pine (*Pinus taeda*), being improved further by use of *Agrobacterium* with additional virulence genes [34].

6. Stimulation of regeneration by sonication

A brief sonication treatment can stimulate shoot regeneration from recalcitrant accessions of squash (*Cucurbita pepo* L.). We recently reported direct regeneration from *in vitro* seedling-derived cotyledons of squash *in vitro* [35]. During attempts to transform squash cotyledons by SAAT, explants derived from some batches of squash seed were found to be unable to regenerate multiple shoots without a brief sonication treatment. A 30-120s ultrasonic treatment (Table 1) stimulated multiple shoot production to levels observed in non-recalcitrant batches, giving shoot production five times that of the control, coupled with massive growth of the explant. Without sonication explants regenerated a very small shoot, which produced a single fasciated shoot on transfer to elongation medium. Ultrasonic treatments for 5-10 minutes also promoted regeneration and growth, accompanied, however, by massive hyperhydration

[21]. Ultrasound has not previously been reported to cause hyperhydration. SEM observations showed that 120s ultrasound treatment changed the joint area between epidermal cells, and removed some of the waxy cotyledon surface. The 10 minutes hyperhydrating ultrasound treatment caused further removal of the waxy surface, from between epidermal cells, and even more from the cell surface. Notably, both the 120s and 10 minutes treatments did not cause gross surface injury to the explants, with the exception of damaging stomatal complexes. However, a non-physiological treatment of 30 minutes ultrasound produced significant surface damage: areas of the external cell wall from the outside of the explant peeled off, and isolated exploded cells and cracks in the explant surface were observed. It seems probable that ablation of the surface of the explant by cavitation effected ultrasound-stimulated regeneration. This has been confirmed by the use of other treatments (without ultrasound) that degraded the surface of the explant (Amutha and Gaba, unpublished results). This is the first report of stimulation of *in vitro* regeneration by ultrasound treatment [21,22].

Different accessions of *Cucurbita* species respond differently to 60s or 120s of ultrasound treatment: the short treatment stimulates regeneration greatly of some accessions, while the longer treatment inhibits (Kathiravan and Gaba, unpublished results). Alternatively, some accessions are very sensitive to ultrasound, and both treatments reduce the regeneration to near zero (Kathiravan and Gaba, unpublished results).

7. Summary of transformation and morphogenic responses to ultrasound

We have listed important ultrasound application parameters in Table 1. It is difficult to draw overall conclusions for the engineering of the morphogenetic and transformation responses described in Table 1 and sections 4-6 above. Experimenters have generally used whatever ultrasonic bath was available, and have varied the ultrasound dose by changing the exposure time (0.2s to 30 minutes; Table 1) to obtain a practical result. For the transformation and morphogenetic responses described the ultrasound frequencies vary from 20-55 kHz (Table 1). Power dose is difficult to evaluate (Table 1), as information on the factor that really matters (power density in the sample zone) is not easily available: most of the power values given in Table 1 are the nominal power consumption of the ultrasound units, or at best the transducers. Probably a vital piece of information would be the power density per unit of plant material per volume of bathing solution. However, the quantity (mass) of plant material being treated and the volume of the bathing solutions are quite variable (Table 1). Increasing the density of plant material (number of explants per unit volume) reduces the effect of the ultrasound treatment (Gaba *et al.* unpublished data). Additionally, the tube in which the plant material is sonicated varies (Table 1): plastic has greater absorption of ultrasound frequencies than glass. Probably the best conclusion one can draw from Table 1 and the other references is that under a diverse range of conditions, ultrasound can effect plant transformation and affect morphogenesis: these applications will expand in the future.

8. Fractionation of somatic embryos

Ultrasound was used to breakup embryo clusters and then to fractionate effectively somatic embryos of carrot (*Daucus carota*), cork oak (*Quercus suber*), grapevine (*Vitis berlandieri* × *rupestris*), and cherry (*Prunus incisa* × *serrula*) [23]. Mature embryos of different species were sorted using purpose-built equipment operating at a higher frequency than reported in Table 1 (carrot embryos at 190 kHz in pulses at 0.5-1.5W; the larger tree embryos at 175 kHz in pulses at 0.7W). The embryos were sorted by size, using an ultrasound standing wave to trap cells in a flow-through system, as the particles are much smaller than the acoustic wavelength used [23]. As the embryos were about 1 mm in size, an acoustic wavelength of about 7 mm was used to trap the embryos at the antinodes of the sound velocity field, where there is less acoustic energy, and they are not damaged by acoustic forces [23]. In this flow-through system, smaller embryos and cells which had not differentiated sufficiently were not trapped, and passed through for resorting [23]. This method can replace sieving of embryos as a method of sizing, and has been used in fermentation of animal cells, but not previously with somatic embryos or particles this size [23].

9. Secondary product synthesis

Secondary product synthesis in suspension cultures of *Lithospermum erythrorhizon* was increased by low doses of ultrasound. Part of the increase was due to an amplified release of shikonin into the medium due to increased solubilization of cell membranes. Additionally, activities of two key enzymes for secondary metabolite biosynthesis, phenylalanine ammonia lyase and p-hydroxybenzoic acid geranyltransferase, were stimulated by the ultrasound [8]. Taxol production by *Taxus chinensis* cell suspension cultures was increased following a brief low-power ultrasound treatment [36]. The taxol production increase followed a transient burst in production of reactive oxygen species and jasmonic acid [36]. A sonication treatment of 30s or more at 1.02 MHz permitted the release of vacuole-located pigment from cells of *Beta vulgaris* L. (red beet root), which were undamaged, and could be subsequently subcultured and continue growth [37].

10. Ultrasound and control of micro-organisms

Surface sterilization by mild ultrasound treatment has been reported [38]. Sonication of the root meristem of onion bulb in the presence of detergent removed external bacteria when the use of antibiotics and/or cleaning failed [38]. Increased lethal uptake of antibiotic by a plant pathogen (*Pseudomonas aeruginosa*) in response to ultrasound, by stressing or perturbing the cell membrane, was reported whereas ultrasound had no effect on fungal growth [39].

11. Conclusions

Ultrasound treatment is unique among existing methods, being simple, cheap and multifunctional. It is an ideal method for use in plant tissue culture, as tissues in culture can be manipulated without being physically touched. For instance, sonication permits reversible solubilization of different cellular membrane, a process that must be useful in many future biotechnology procedures. We shall probably see an expansion in the use of sonication, considering the success of the applications (especially SAAT) listed here. However, it is clear that the most interesting applications will require collaboration between plant tissue culture experts and engineers/physicists to obtain elegant solutions as described by Maitz *et al.* [23]. The use of fermentation-based systems [40] with purpose-built flow-through ultrasonic transducers which produce different frequencies and powers for particle separation, “sieving”, and release of secondary products will doubtless increase, and enable new economically viable industries of the future.

Acknowledgements

Contribution from the Agricultural Research Organization, The Volcani Center, Bet Dagan, Israel, No. 517/04. This work was partially supported by Research Grant No. US2541-95R from BARD, The United States-Israel Binational Agricultural Research and Development Fund to V.G. G.A. and S.A. were supported by the MASHAV program of the Ministry of Foreign Affairs, Government of Israel. K. Kathiravan received a BOYSCAST Fellowship from the Ministry of Science and Technology, Government of India. The authors thank colleagues for sending unpublished information on their methods. The authors thank Dr. B. Steinitz for critical comments on the manuscript.

References

- [1] Weinberger, P.; Anderson, P. and Donovan, L.S. (1979) Change in production, yield, and chemical composition of corn (*Zea mays*) after ultrasound treatment of seeds. *Radiat. Environ. Biophys.* 16: 81-88.
- [2] Miyoshi, K. and Mii, M. (1988) Ultrasonic treatment for enhancing seed germination of terrestrial orchid, *Calanthe discolor*, in asymbiotic culture. *Sci. Hort.* 35: 127-130.
- [3] Mukhamedkhanov, O. and Shermukhamedor, K. (1971) Effect of ultrasound on development and yield of cotton cv.108-F. *Nauchn. Tr. Trashk. skh. Ins.* 22: 45-71 (*Field Crop Abstr.* 1972, 25: 4165).
- [4] Timonin, M.I. (1966) Effect of ultrasound on the germination of white spruce and jack pine seeds. *Can. J. Bot.* 44: 113-115.
- [5] Weinberger, P. and Burton, C. (1981) The effect of sonication on the growth of some tree seeds. *Can. J. For. Res.* 11: 840-844.
- [6] Joersbo, M. and Brunstedt, J. (1990) Protein synthesis stimulated in sugar beet cells and protoplasts. *Ultrasound Med. Biol.* 16: 719-724.
- [7] Joersbo, M. and Brunstedt, J. (1990) Inoculation of sugar beet protoplasts with beet necrotic yellow vein virus particles by mild sonication. *J. Virol. Methods* 29: 63-9.
- [8] Dong, L.L.; Yong, W.J.; Lin, L.D. and Wu, J.Y. (2002) Enhancement of shikonin production in single- and two-phase suspension cultures of *Lithospermum erythrorhizon* cells using low-energy ultrasound. *Biotechnol. Bioeng.* 78: 81-88.
- [9] Millar, M.V.; Ciaravino, V.; Allen, D. and Jensen, S. (1976) Effect of 2 MHz ultrasound on DNA, RNA and protein synthesis in *Pisum sativum* root meristem cells. *Int. J. Radiat. Biol.* 30: 217-222.

- [10] Higashi, K.; Hanasaki, N.; Nakanishi, A.; Shimomura, E.; Hirano, H.; Gotoh, S. and Sakamoto, Y. (1978) Difference in susceptibility to sonication of chromatins containing transcriptionally active and inactive ribosomal genes. *Biochim. Biophys. Acta.* 520: 612-622.
- [11] Currier, H. B. and Webster, D.H. (1964) Callose formation and subsequent disappearance: studies in ultrasound stimulation. *Plant Physiol.* 39: 843-847.
- [12] Pedroso, M.C. and Pais, M.S. (1992) Minituber production from immature seed suspension culture of *Orchis papilionacea*. *In Vitro Cell. Dev. Biol.- Plant* 28P:183-186.
- [13] Zhang, L.J.; Cheng, L.M.; Xu, N.; Zhao, N.M.; Li, C.G.; Jing, Y. and Jia, S.R. (1991) Efficient transformation of tobacco by ultrasonication. *Bio/Technol.* 9: 996-997.
- [14] Joersbo, M. and Brunstedt, J. (1990) Direct gene transfer to plant protoplasts by mild sonication. *Plant Cell Rep.* 9: 207-210.
- [15] Trick, H.N. and Finer, J.J. (1997) SAAT: Sonication-assisted *Agrobacterium*-mediated transformation. *Transgenic Res.* 6: 329-336.
- [16] Trick, H.N. and Finer, J.J. (1998) Sonication-assisted *Agrobacterium*-mediated transformation of soybean (*Glycine max* L.) Merrill embryogenic suspension culture tissue. *Plant Cell Rep.* 17: 482-488.
- [17] Santarem, E.R.; Trick, H.N.; Essig, J.S. and Finer, J.J. (1998) Sonication-assisted *Agrobacterium*-mediated transformation of soybean immature cotyledons: optimization of transient expression. *Plant Cell Rep.* 17: 752-759.
- [18] Meurer, C.A.; Dinkins, R.D. and Collins, G.B. (1998) Factors affecting soybean cotyledonary node transformation. *Plant Cell Rep.* 18: 180-186.
- [19] Trick, H.N. and Finer, J.J. (1999) Induction of somatic embryogenesis and genetic transformation of Ohio buckeye (*Aesculus glabra* Willd.) *In Vitro Cell. Dev. Biol. – Plant* 35: 57-60.
- [20] Zaragoza, C.; Munoz-Bertomeu, J. and Arrillaga, I. (2004) Regeneration of herbicide-tolerant black locust transgenic plants by SAAT. *Plant Cell Rep.* 22: 832-838.
- [21] Gaba, V.; Xia X.; Singer S.; Elman C.; Gal-On, A. and Ananthakrishnan, G. (2001) Ultrasonic treatment induces shoot regeneration in squash cotyledon explants *in vitro*. *In Vitro Cell. Dev. Biol.–Plant* 37: 859-860. Abstract no. P3022.
- [22] Gaba, V.; Xia, X.; Singer, S.; Fischer, I.; Gal-On, A. and Ananthakrishnan, G. (2002) Ultrasonic treatment damages the surface layer of explants and induces shoot regeneration in squash cotyledon explants. Abstract P-1385, p. 130. Book of Abstracts, IAPTC&B Congress, Florida, USA, June 2002.
- [23] Maitz, M.; Trampler, F.; Gröschel, M.; da Camarar Machado, A. and Laimer da Camara Machado, M. (2000) Use of ultrasound cell retention system for the size fractionation of somatic embryos of woody species. *Plant Cell Rep.* 19: 1057-1063.
- [24] Bohm, H.; Antony, P.; Davey, M.R.; Briarty, L.R.; Power, J.B.; Lowe, K.C.; Benes, E. and Groschl, M. (2000) Viability of plant cell suspensions exposed to homogeneous ultrasonic fields of different energy density and wave type. *Ultrasonics* 38: 629-32.
- [25] Nyborg, W.L. (1968) Mechanisms for nonthermal effects of sound. *J. Acoust. Soc. Am.* 44: 1302-1309.
- [26] Peacock, A.R. and Pritchard, N.R. (1968) Some biophysical aspects of ultrasound. *Prog. Biophys. Mol. Biol.* 18: 187-208.
- [27] Joersbo, M. and Brunstedt, J. (1992) Sonication: a new method for gene transfer to plants. *Physiol. Plant.* 85: 230-234.
- [29] Weber, S.; Friedt, W.; Landes, N.; Molinier, J.; Himber, C.; Rousselin, P.; Hahne, G. and Horn, R. (2002) Improved *Agrobacterium*-mediated transformation of sunflower (*Helianthus annuus* L.): assessment of macerating enzymes and sonication. *Plant Cell Rep.* 21: 475-482.
- [30] Gonzalez, E.R.; de Andrade, A.; Bertolo, A.L.; Lacerda, G.C.; Carneiro, R.T.; Prado, D.V.A.; Labate, M.T.V. and Carlos, A. (2002) Production of transgenic *Eucalyptus grandis* × *E. urophylla* using the sonication-assisted *Agrobacterium* transformation (SAAT) system. *Functional Plant Biol.* 29: 97-102.
- [31] Amoah, B.K.; Wu, H.; Sparks, C. and Jones, H.D. (2001) Factors influencing *Agrobacterium*-mediated transient expression of uidA in wheat inflorescence tissue. *J. Exp. Bot.* 52: 1135-1142.
- [32] Humara, J. M.; Lopez, M. and Ordas, R. J. (1999) *Agrobacterium tumefaciens*-mediated transformation of *Pinus pinea* L. cotyledons: An assessment of factors influencing the efficiency of uidA gene transfer. *Plant Cell Rep.* 19: 51-58.
- [33] Srivatanakul, M.; Park, S.H.; Sung H.; Salas, M.G. and Smith, R. H. (2001) Transformation parameters enhancing T-DNA expression in kenaf (*Hibiscus cannabinus*) *J. Plant Physiol.* 158: 255-260.
- [34] Tang, W. (2003) Additional virulence genes and sonication enhance *Agrobacterium tumefaciens*-mediated loblolly pine transformation. *Plant Cell Rep.* 21:555-562.
- [35] Ananthakrishnan, G.; Xia, X.; Elman, C.; Singer, S.; Paris, H.; Gal-On, A. and Gaba, V. (2003) Shoot production in squash (*Cucurbita pepo*) by *in vitro* organogenesis. *Plant Cell Rep.* 21: 739-746.

- [36] Yong, W.J.; Chun, G.X.; Wu, J.Y. and Ge, X.C. (2004) Oxidative burst, jasmonic acid biosynthesis, and taxol production induced by low-energy ultrasound in *Taxus chinensis* cell suspension cultures. *Biotechnol. Bioeng.* 85: 714-721.
- [37] Kilby, N.J. and Hunter, C.S. (1990) Repeated harvest of vacuole-located secondary product from *in vitro* grown plant cells using 1.02 MHz ultrasound. *Appl. Microbiol. Biotech.* 33: 448-451.
- [38] Aller, P.; Fernandez-Gomez, M.E. and Diez, J.L. (1978) RNA synthesis in root meristems of *Allium cepa* bulbs. I. Sonication as a method to eliminate contaminating bacteria. *Zeitschrift fur Pflanzenphysiologie* 89: 29-40.
- [39] Rediske, A.M.; Rapoport, N. and Pitt, W.G. (1999) Reducing bacterial resistance to antibiotics with ultrasound. *Lett. Appl. Microbiol.* 28: 81-84.
- [40] Levin, R.; Gaba, V.; Tal, B.; Hirsch, S.; DeNola, D. and Vasil, I.K. (1988) Automated plant tissue culture for mass propagation. *Bio/Technol.* 6: 1035-1040.

ACOUSTIC CHARACTERISTICS OF PLANT LEAVES USING ULTRASONIC TRANSMISSION WAVES

MIKIO FUKUHARA¹, S. DUTTA GUPTA² AND LIMI OKUSHIMA³

¹*Materials and Components Div., Tungaloy, Kokusai-Shinkawasaki Bld., 50, 2-1, Kitakase, Saiwai, Kawasaki, Japan 212-0057 -Fax: 81-44-587-2670 - E-mail: a80010@tungaloy.co.jp*

²*Department of Agricultural and Food Engineering, Indian Institute of Technology, Kharagpur 721302, India*

³*National Institute of Rural Engineering, Tsukuba, Japan*

1. Introduction

For decades, ultrasonic techniques have been used for non-destructive testing and imaging of industrial materials. Physical characteristics such as velocity, damping and elasticity have been examined with ultrasonic techniques in industrial materials [1-4]. They also have many medical applications. The use of ultrasound as an in-line and non-destructive method is proposed due to the dependence of ultrasonic waves on the physical properties of a medium through which they are propagated. However, limited applications of these techniques have been made in agricultural fields.

Leaves are the principal organs in which photosynthesis, transpiration and food manufacturing occur. They also provide important and useful information about the morphological and physiological status of growing plants. Leaf characteristics vary greatly in size, shape, venation, surface-nature, water content, photosynthetic and anatomical behaviour.

In general, it is very difficult to measure the acoustic characteristics of thin biological specimens. In recent years, attempt has been made in a non-destructive manner to evaluate the acoustic characteristics of leaves in terms of their viscoelasticity as associated with the imaginary parts of complex waves [5,6]. A relation between ultrasonic propagation time and hardness has been shown to exist for some kinds of plant leaves, using longitudinal ultrasonic waves passing through the leaves suspended in water [6]. The idea is to use a particular broadband spectroscopy to effectively penetrate even soft and acoustically absorbent materials such as leaves. This non-destructive technique is named as Vibrating Resonance Penetration (VRP) method.

In the VRP method, acoustic energy is transmitted from the transmitter to the receiver through the medium of water. Using this technique, the phase shift caused by moving leaves into and out of the acoustic pathway between the transmitting and receiving transducers can be measured accurately. The VRP method is capable of

providing a bio-physical evaluation of the fundamental characteristics of living leaves, which are thought to be dispersive media.

For the ultrasonic nondestructive measurement of rigid thin specimens, the frequency domain [7], time domain [8] and variable trigger and strobe (VTS) [9] methods have been developed. However, these measurements are limited to the evaluation of the real parts of the complex acoustic properties of transmitted waves. Fukuhara *et al.* [5,6] for the first time emphasized on the imaginary parts of complex waves for the acoustic evaluation of acoustically absorbent materials such as leaves. It has been suggested to use the phase velocity method in place of conventional group velocity for materials that are more acoustically absorbent and softer than polymers. The VRP method is found to be useful in evaluating acoustic characteristics of leaves and appears to have significant potential in the study of sap physiology and fluid pathology.

The purpose of this chapter is to introduce the diagnostic aspects of ultrasonics to plant scientists both working under *in vivo* and *in vitro* conditions. The first part of this chapter will describe the theoretical considerations of acoustic parameters, followed by the description of system design used for ultrasonic measurement. The second part will discuss the application of ultrasonic techniques to acoustic evaluation of tea and rice leaves grown *in vivo* for detection of plant maturity and diagnosis of disease respectively. Finally, the third one will document a case study of acoustic evaluation of gladiolus leaves regenerated *in vitro* highlighting the significant potential of VRP method in detecting the hyperhydric status of regenerated plants for successful *ex vitro* transfer.

2. Theoretical considerations and system description

Important factors to be considered in ultrasonic include phase velocity, frequency, propagation time and attenuation coefficient. These parameters were determined from through sample and reference (water path-only) signals; and was done by comparing the magnitudes and phases of their Fourier coefficients using a diagnosis and analysis apparatus (USH-B, Toshiba Tungaloy) fitted with a transmitter/receiver set at 298 K as described previously [6]. The apparatus and block diagram for measurement are presented schematically in Figure 1. The electric power of 200 V applied to the pulsar. Using synchronized PCI boards the time course fluctuation error in the circuit signal between the pulsar and the receiver was minimized, and flight time accuracy obtained was ± 50 ps (pico seconds). Amplifier gain was adjusted from -5.5 to + 65 dB, to compensate for impedance differences between the specimens and the water medium. Facing broad-bandwidth longitudinal wave transducers of 3.3 MHz frequency and 4 mm in diameter were used as the transmitter and the receiver. Planar PZT transducers were used to suppress the phase modulation, which occurred at the boundary between the leaf surface and the water. The leaf was suspended between the two facing transducers, which were separated by 9 mm of water. The wave transmission was measured from the right side of the leaf blade half way between the midrib and the outer edge. The software control was used to remove noisy wavelength signals and to receive waves between 1 to 2 MHz.

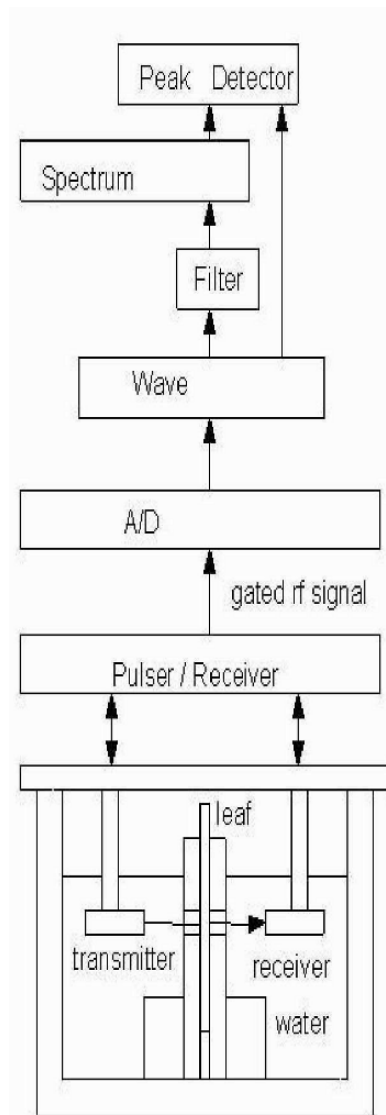


Figure 1. The apparatus and block diagram for measurement. Reprinted from Fukuhara, M.; Degawa, T.; Okushima, L. and Homma, T. (2000) [5].

To accurately measure the acoustic velocity of uneven leaves with soft tissue, phase velocity, V_p , was calculated using the following formula [10,11]:

$$V_p = \frac{V_w}{1 - \frac{V_w \Delta\phi(\omega)}{d\omega}} \quad (1)$$

where, time shift $\Delta t = t_w - t$ and phase shift $\Delta\phi = \phi_w - \phi$ were the differences of the starting point and of the phase angle in power spectra of the transmitted waves generated by the specimen in the acoustic path respectively. The V_w is the sound velocity (1497.0 m/s at 298 K) of water [12]. The ω is angular frequency ($\omega = 2\pi f$). The time shift Δt can be either positive or negative depending on whether group velocity [9] is faster or slower than V_w . However, since the group velocity is remarkably affected by measurement errors of thickness, as compared with the phase velocity [6], phase velocity was used throughout the study.

Fourier transformation of the digitized receiving waveform from the dispersive media was carried out to determine the main frequencies f and phases ϕ at f . To match the frequency of the test and the reference signals, we used the frequency (f_w) of 1.6 MHz for water and phase (ϕ_w) of 0.0019 rad. at f_w . The phase shift $\Delta\phi$ is defined as

$$\Delta\phi = \arctan[Im(\omega)/Re(\omega)] - \arctan[Im(\omega)/Re(\omega)], (0 < \phi < \pi/2) \quad (2)$$

where, $Re(\omega)$ and $Im(\omega)$ are respectively the real and imaginary parts of complex waves passing through the sample and water. Since all the phases were observed at f lay in between 0 and $\pi/2$, the unfolding problem was avoided. The attenuation coefficient α and the damping ratio δ of the samples were determined by the expression:

$$\alpha = \frac{\delta}{d} = \frac{\ln(A_1/A_2)}{d} \quad (3)$$

where, A_1 and A_2 are amplitudes of the first and the second wavelets for receiving wave patterns, respectively.

The Nyquist diagram was plotted in the complex plane of the open-loop transfer (propagation) wave function for all the complex frequencies, using a vector locus [13]. The correlation coefficients between the two random parameters were calculated by the method of least squares.

3. Case studies on possible ultrasonic diagnosis of plant leaves

3.1. ULTRASONIC TESTING OF TEA LEAVES FOR PLANT MATURITY

Tea is a popular and medicinal drink enjoyed by many people all over the world. Physical properties of tea leaves may have great influence on harvest timing, the process operation and quality of the products. Thus, the physical parameters may be used to set

minimum quality standards. Especially, leaf thickness, one of the physical parameters, reflects many characteristics such as hardness, density, water potential [14] and photosynthetic capacity [15]. Fukuhara *et al.* [16], investigated the leaf behaviour employing leaf thickness analogous to polymers properties.

3.1.1. Wave velocity and dynamic modulus for leaf tissue development

The thickness dependence of tea leaves is shown in Figure 2. The phase velocity increases with increasing thickness. As ultrasonic wave propagates more easily through the hard surfaces, the finding indicates the development of fibrous tissues in the leaves. The wavelengths are almost equivalent to their thickness up to 0.5 mm, and then increase with a slope of 0.4 in thickness between 0.5 mm and 1.0 mm. As can be seen from the internal structure of a dicotyledonous leaf, the standing wave with the second harmonic mode occurs in leaves of thickness d fixed at three points on the surfaces and the vein up to thickness of 0.5 mm, and over 0.5 mm the wave with higher order mode proceeds due to development of an extensive network throughout the leaf. Similar trend exists in tea leaves and relates to growth of leaves. The velocity of the leaves was less (1497 ms^{-1} at 298 K) [12] than that of pure water, even though the texture of the tea leaf is not like fine foamy bulk such as found in leaves of a water hyacinth. One possible explanation for such behaviour is that the internal structure of the leaves is occupied by loosely packed parenchyma cells separated by intercellular air spaces. The other possibility is that the mechanical contact required in making the thickness measurement causes sample deformation, making it difficult to determine the sound speed in leaves with high accuracy.

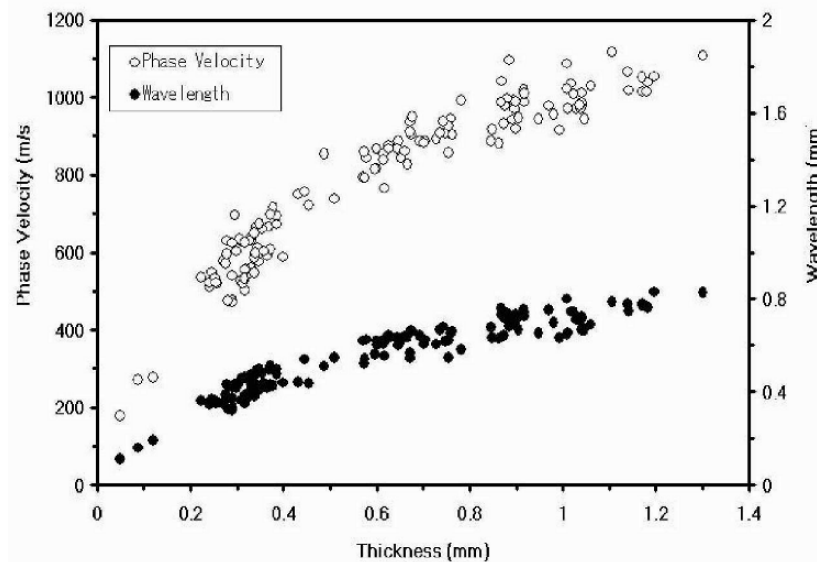


Figure 2. The thickness dependence of phase velocity and wavelength for tea leaves. Reproduced from Fukuhara, M.; Okushima, L.; Matsuo, K. and Honma, T. (2004) [16].

From Eq. (1), the phase velocity (Figure 2) indicates more delayed phase with higher phase velocity. Here, it should be noted that the viscoelastic properties of polymers [17,18], naphthenic hydrocarbon oils with high viscosity [19] and high damping alloy, $Mn_{73}Cu_{20}Ni_5Fe_2$ [20] could be evaluated from their phase modulation in complex waves. The phase modulation of living tea leaves, like soft polymers (e.g. rubber), must involve a Newtonian viscous component to the elastic response: such a situation is denoted as viscoelasticity, associated with complex waves [21]. The phase dependence of viscoelasticity and dynamic modulus are shown in Figure 3. As the phase angle increases, the viscoelasticity exponentially increases and the dynamic modulus gradually decreases with wide dispersion ($r = 0.561$). In other words, decrease in viscoelasticity with subsequent increase in dynamic modulus, suggests differentiation of tissues in the leaves toward plant maturity.

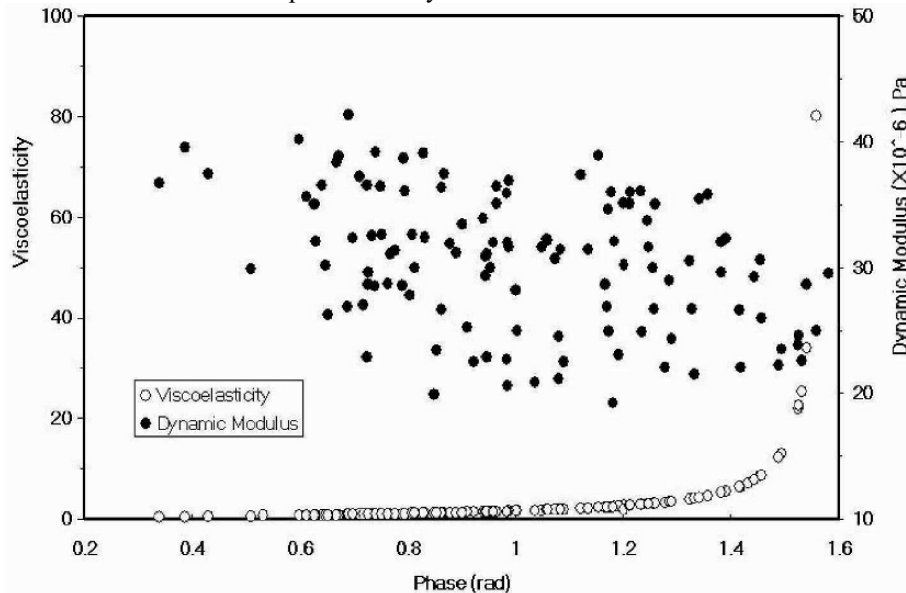


Figure 3. The phase dependence of viscoelasticity and dynamic modulus for tea leaves. The correlation coefficient between phase and dynamic modulus is 0.561. Reproduced from Fukuhara, M.; Okushima, L.; Matsuo, K. and Honma, T. (2004) [16].

3.1.2. Dynamic viscosity and imaginary parts in complex waves

To determine the modulation of the propagated wave patterns for tea leaves, attention was paid to Nyquist diagrams for the propagated waves. The Nyquist diagrams for four representative tea leaves with different thickness are presented in Figure 4. With increasing thickness, the diagram changes from hexagon shape ($d = 0.048$ mm) to pentagon ($d = 0.224$ mm), square ($d = 0.646$ mm) and triangle ($d = 1.182$ mm) ones in turn, and the area of the third and fourth quadrants in the loop decreases. The decrease of the apex number means frequency convergence in the power spectrum, showing development of the fibrous tissues, which also increases the rigidity. This tendency

persists even with more counting run. The decrease in the area suggests restoration of relay in phase, that is, decrement of imaginary parts in complex waves.

To distinguish development of external appearance and internal tissues in botanical perspective, the thickness dependence of the attenuation coefficient and dynamic viscosity are presented in Figure 5. As thickness increases, the damping ratio decreases linearly and the viscosity also decreases but with wide dispersion ($r = 0.769$). The decrease in the viscosity reversibly correlates with the increase in dynamic modulus as shown in Figure 3. In other words, this is a viscoelastic manifestation of tissue differentiation in the leaves. We can actually see the fibrous effect in the fibre-reinforced materials. Thus, the degree of maturity of tea leaves could be estimated by the attenuation coefficient.

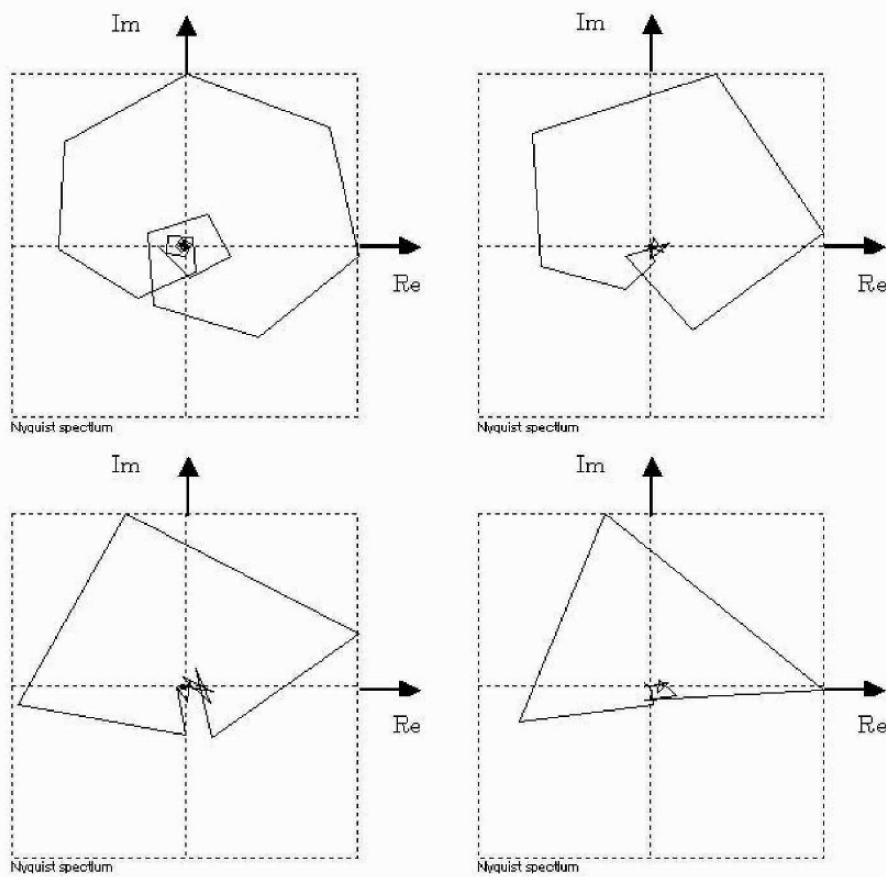


Figure 4. Nyquist diagram of the propagated waves for representative four tea leaves; (a) $d = 0.048$ mm, (b) $d = 0.224$ mm, (c) $d = 0.646$ mm and (d) $d = 1.182$ mm. Reproduced from Fukuhara, M.; Okushima, L.; Matsuo, K. and Honma, T. (2004) [16].

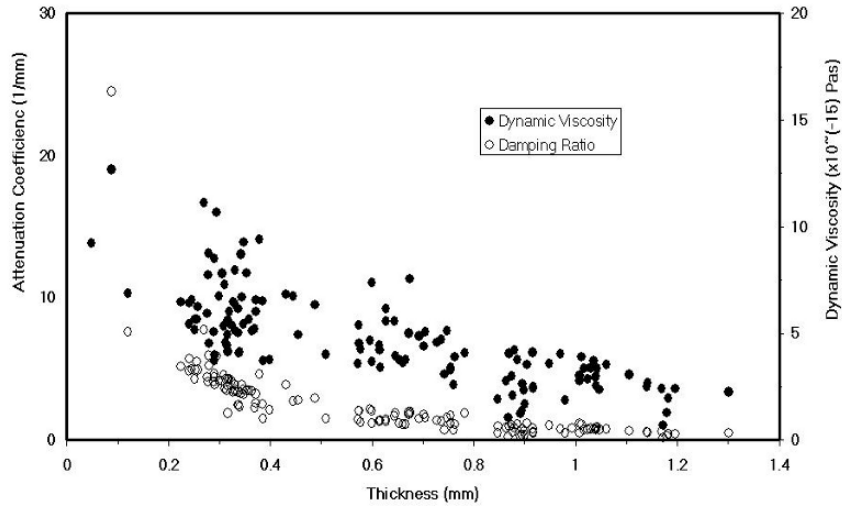


Figure 5. The thickness dependence of attenuation coefficient and dynamic viscosity for tea leaves. The correlation coefficient between thickness and dynamic viscosity is 0.769. Reproduced from Fukuhara, M.; Okushima, L.; Matsuo, K. and Honma, T. (2004) [16].

3.2. ULTRASONIC DIAGNOSIS OF RICE LEAVES

The VRP method was employed to test the hypothesis that whether ultrasonic wave characteristics can be used to detect rice blast disease and harvest yield. Traditionally, this evaluation uses human senses. It is very important to develop non-destructive and effective sensing methods for leaves. Evaluation of physical properties of leaves using ultrasonic techniques would be of help in pre-symptomatic detection of diseases and for attainment of heavy crop yield. For the diagnosis purposes of leaves, we investigated the propagation time and phase.

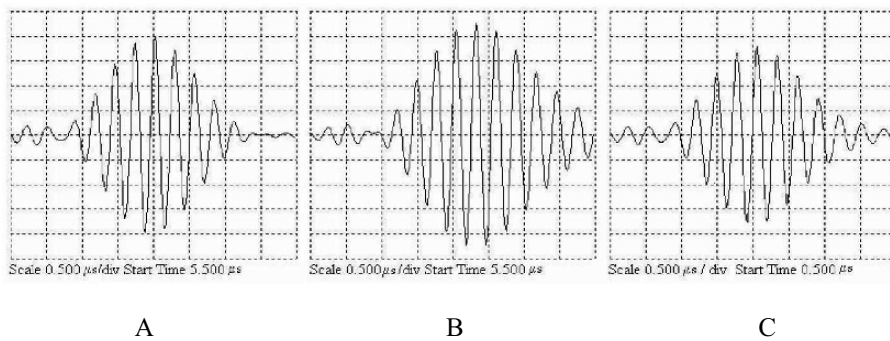


Figure 6. Wave patterns of rice leaves; (A) young, (B) mature and (C) infected leaves.

Wave patterns of representative young, mature and infected leaves are shown in Figure 6. We can read acoustic information of rice leaves from Figure 6. The acoustic properties of these leaves are presented in Table 1. The propagation time decreases, *i.e.*, velocity increases with further tissue differentiation, suggesting development of fibrous tissues. However, phase at main frequency delayed in infected leaves, suggesting decrease in water content. This phenomenon bears resemblance to thermal degradation of polymers by thermal chain scission [22,23]. Although, damping coefficient is not suitable for diagnosis of diseases, because of surface roughness of rice leaves.

Table 1. Acoustic properties of young, mature and infected leaves of rice plants.

Leaf	Thickness (mm)	Propagation time (μ s)	Frequency (MHz)	Damping coefficient (neper/cm)	Phase (rad)
Young	0.177	7.5154	3.6	27.88	2.453
Mature	0.166	7.5558	3.6	3.927	1.897
Infected	0.598	7.8399	3.6	22.22	0.230

3.3. ACOUSTIC CHARACTERISTICS OF *IN VITRO* REGENERATED LEAVES OF GLADIOLUS

The receiving wave pattern of *in vitro* grown leaves of gladiolus is presented in Figure 7 along with the pattern of water as medium in the same time scale. Compared to water, wave pattern of leaves are characterized by higher damping and lower frequency with fewer number of wavelets. Similar to previous findings [5,6], it suggests that during wave passage regenerated leaves can absorb waves with high frequency and thus behave like a quasi-polymer. It is worthy to mention that waves with frequency higher than 2 MHz are absorbed during propagation of ultrasonic waves through polymers and soft metals. [6]. Presumably, the internal structures of leaves with types and arrangement of parenchyma cells along with intercellular air spaces may account for such acoustic behaviour.

Since regenerated leaves also exhibit polymer like features for transmission of ultrasound, wave transmission characteristics of *in vitro* grown leaves may predict the variation of leaf characters during the culture period, in a non-destructive manner which in turn would be of help in detecting hyperhydric status of the regenerated plants. Compared to plants growing *in vivo*, *in vitro* regenerated plants can have abnormal morphological, anatomical and physiological characteristics. Such atypical shoots or plantlets are difficult to propagate: their capacity for *in vitro* survival may be severely reduced and many of them may perish even in multiplication stage. The aforesaid abnormalities found in plants cultured *in vitro*, collectively are described as hyperhydricity.

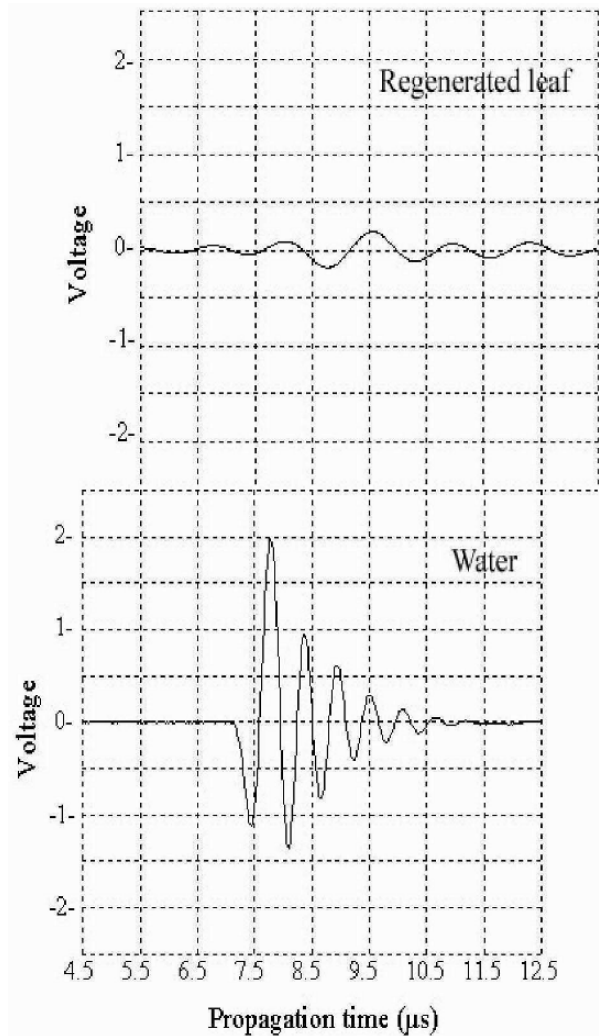


Figure 7. Wave pattern of regenerated leaves of gladiolus.

For ultrasonic behaviour of regenerated leaves, we investigated the relation between thickness, propagation time, frequency, attenuation coefficient and phase (Figure 8). The effective transmitted frequency of regenerated leaves lies in between 0.8-1.2 MHz. Compared to *in vivo* grown leaves of tea and rice, *in vitro* leaves transmit waves at lower frequencies. The lower frequency range is indicative of loose arrangement of parenchyma cells with large intercellular space during leaf differentiation under *in vitro* conditions. Increase in frequency with development of rigid reticular tissues in *in vivo* condition has already been suggested [5,6]. In artificial materials also increment of frequency results from atomic lattice shrinkage [24].

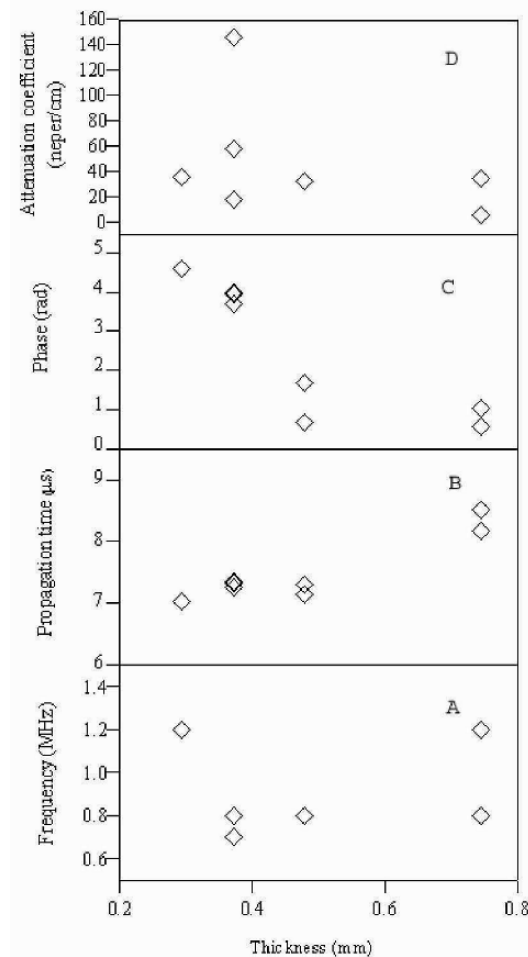


Figure 8. The thickness dependence of frequency (A), propagation time (B), phase (C) and attenuation coefficient (D) for regenerated leaves of gladiolus.

The thickness dependency of frequency and propagation time is presented in Figure 8a. There is no correlation between thickness and frequency. With increasing thickness frequency remains unchanged. However, propagation time increases with increasing thickness (Figure 8b). Ultrasonic waves seem to propagate more easily through the hard surface than through the softer parts. The present findings on thickness dependence of propagation time and frequency do not correlate well with the development of fibrous tissue. Similar kind of relationship with thickness and propagation time was observed in gum tree, which has been placed under thick-juicy-succulent category [6].

The thickness dependences of phase and attenuation coefficient are presented in Figures 8c and 8d. Phase and attenuation coefficient decreases with increasing thickness.

Since phase ϕ is defined as $\arctan (Im/Re)$ in Eq. (2), the phase variation indicates changes in tissue differentiation similar to what has been observed in tea leaves [5]. Interestingly, delay in phase at main frequency was also noted in infected rice leaves. There is a similarity between the infected rice leaves and regenerated leaves with respect to phase delay, as both are in stressed condition.

Ultrasonic behaviour of *in vitro* regenerated leaves of gladiolus along with the findings of Fukuhara [6] suggests succulent nature of regenerated plants. In other words, *in vitro* regenerated plants manifest hyperhydric symptom probably with loose parenchyma, large air space and higher water content in the leaves. Indeed, the degree of hyperhydricity could be measured by shift in frequency and delay in phase. However, it remains to be seen to what extent the ultrasonic behaviour in *in vitro* differ from *in vivo* grown gladiolus plants.

4. Conclusions

The present study successfully describes the acoustic characteristics of botanical leaves for various possible diagnosis purposes. The acoustic behaviour was measured using longitudinal ultrasonic waves passing through the leaves suspended in water. The phase velocity of the leaves correlated with their thickness. The wavelengths were almost equal to leaf thickness, producing the second harmonic wave fixed at three points on both surfaces of the leaves, and on the midrib. A delay in the phase of the transmitted wave, with higher phase velocity was found to be associated with increment in viscosity. The positive frequency dependence of phase velocity correlates with the development of the rigid reticular tissues of the leaves. The attenuation coefficients decrease parabolically with an increase in thickness and phase velocity, showing intrinsic characters of leaves, which are associated with changes in tissue morphology. The phase velocities of the leaves were smaller than that of pure water (1497 m/s), because of their loosely packed parenchyma cells. This may be due to the internal structure of leaves with loosely packed parenchyma cells. Therefore, botanical leaves acoustically can be regarded as natural quasi-polymers with high viscoelasticity.

Interestingly, acoustic properties of leaves can be extrapolated to various detection and diagnosis purposes such as detection of plant maturity, pre-symptomatic diagnosis of diseases and evaluation of hyperhydric status of regenerated plants. However, plant biotechnologists need to see more published examples of ultrasonic applications in agriculture with the developed VRP method before they feel confident with it.

Acknowledgement

S. Dutta Gupta acknowledges the financial support given by the JSPS, Japan.

References

- [1] Fukuhara, M. and Yamauchi, I. (1993) Temperature dependence of the elastic moduli, internal friction and acoustic wave velocity for alumina, (Y) PSZ and β' -sialon ceramics. J. Mater. Sci. 28: 4681-4688.

- [2] Fukuhara, M. and Sampei, A. (1993) Elastic moduli and internal frictions of carbon and stainless steels as a function of temperature. *Iron and Steel Inst. J. Int.* 33: 508-512.
- [3] Fukuhara, M. and Sampei, A. (1994) Low-temperature elastic moduli and dilational and shear internal frictions of superconducting ceramic $GdBa_2Cu_3O_{7-\delta}$. *Phys. Rev.* B49: 13099-13105.
- [4] Numata, H. and Fukuhara, M. (1997) Low-temperature elastic anomalies and heat generation of deuterated palladium. *Fus. Tech.* 31: 300-310.
- [5] Fukuhara, M.; Degawa, T.; Okushima, L. and Homma, T. (2000) Propagation characteristics of leaves using ultrasonic transmission waves. *Acoust. Lett.* 24:70-74.
- [6] Fukuhara, M. (2002) Acoustic characteristics of botanical leaves using ultrasonic transmission waves. *Plant Sci.* 162: 521-528.
- [7] Kinra, V. K. and Dayal, V. (1988) A new technique for ultrasonic non-destructive evaluation of thin specimen. *J. Exp. Mech.* 28: 288-297.
- [8] Kinra, V. K. and Zhu, C. (1993) Time-domain ultrasonic NDE of the wave velocity of a subhalf-wavelength elastic layer. *J. Test. Eval.* 21: 29-35.
- [9] Wan, M.; Jiang, B. and Cao, W. (1997) Direct measurement of ultrasonic velocity of thin elastic layers. *J. Acoust. Soc. Am.* 101:626-628.
- [10] Sachse, W. and Pao, Y. H. (1978) On the determination of phase and group velocities of dispersive waves in solids. *J. Appl. Phys.* 49: 4320-4.
- [11] Mobley, J.; Waters, K. R.; Hall, C. S.; Marsh, J. N.; Hughes, M. S.; Brandenburger G.H. and Miller, J. G. (1999) Measurements and predictions of the phase velocity and attenuation coefficient in suspensions of elastic microspheres. *J. Acoust. Soc. Am.* 106: 652.-659.
- [12] Del Gross, V. A. and Mader, C.W. (1972) Speed of sound in pure water. *J. Acoust. Soc. Am.* 52: 1442-1446.
- [13] Nyquist, H. (1932) Regeneration theory. *Bell System Tech. J.* 11: 126-147.
- [14] McBumey, T. (1992) The relationship between leaf thickness and plant water Potential. *J. Exp. Bot.* 43:327-332.
- [15] Nakamoto, K.; Oku, T.; Hayakawa, S. (1996) Photosynthetic characteristics of tea leaves growth under field conditions. *Environ. Control Biol.* (in Japanese) 34: 277-283.
- [16] Fukuhara, M.; Okushima, L.; Matsuo, K. and Honma, T. (2005) *Jpn. Agri. Res. Quart.* (in press).
- [17] Fukuhara, M. and Sampei, A. (1996) Low-temperature elastic moduli and dilational and shear internal friction of polycarbonate. *Jpn. J. Appl. Phys.*35: 3218- 3221.
- [18] Fukuhara, M.; Kuwano, Y.; Tsugane, A.; Yoshida, M. (1999) Determination of thermal degradation of vulcanized rubbers using diffracted SH ultrasonic waves. *J. Polym. Sci. Pt. B: Polym. Phys.* 37: 497-503.
- [19] Fukuhara, M. and Tsubouchi, T. (2003) Naphthenic hydrocarbon oils transmissible for transverse waves. *Chem. Phys. Lett.* 371:184-188.
- [20] Fukuhara, M.; Yin, F.; Kawahara, K.(2004) Acoustic characteristics of high damping $Mn_{73}Cu_{20}Ni_5Fe_2$ alloy. *Phys. Stat. Sol.(a)* 201: 454-458.
- [21] Maeda, Y. (1957) Dynamic Viscoelasticity, Polymers, In: *Lecture on Experimental Chemistry* (in Japanese), Vol.8, Maruzen, Tokyo; pp. 155.
- [22] Fukuhara, M.; Kuwano, Y. and Oguri, M. (1996) Determination of thermal degradation of heated polyvinyl chloride using diffracted SH ultrasonic waves. *Jpn. J. Appl. Phys.* 35: 3088-3092.
- [23] Kuwano, Y.; Fukuhara, M.; Omura, H.; Takayama, S.(1996) Determination of thermal degradation of polypropylene using diffracted SH ultrasonic waves. *The First Symposium for Polymer Analysis*, Jpn. Soc. Chem. Analysis (in Japanese), Inst. Nagoya Tech.,Tokyo; pp. 155-156.
- [24] Fukuhara, M. and Sampei, A. (2000) Ultrasonic elastic properties of steel under tensile stress. *Jpn. J. Appl. Phys.* 39: 2916-2921.

PHYSICAL AND ENGINEERING PERSPECTIVES OF *IN VITRO* PLANT CRYOPRESERVATION

ERICA E. BENSON¹, JASON JOHNSTON¹, JAYANTHI MUTHUSAMY² AND KEITH HARDING¹

¹*Plant Conservation Group, School of Contemporary Science, University of Abertay Dundee, Bell Street, Dundee, DD1 1HG, Scotland, UK- Fax: 00 44 (0) 1382 308261-Email: e.e.benson@abertay.ac.uk*

²*Forest Research Institute of Malaysia, Kepong, 52109, Kuala Lumpur, Malaysia*

1. Introduction

Cryopreservation is the conservation of living cells and organisms at ultra low temperatures usually at -196°C in liquid nitrogen, it is a safe, long-term means of securing *in vitro* germplasm in culture collections. Cryogenic storage is used extensively in medical, horticultural, agricultural, aquaculture and forestry sectors and assists environmental research by preserving test organisms used in environmental monitoring. Designing and operating instruments and analytical equipment required to study and conserve biological samples at cryogenic temperatures poses a challenge dictated by the physical and safety constraints of operating at very low temperatures. This chapter overviews the physical and engineering aspects of *in vitro* plant cryopreservation including an introduction to the safe use of cryogenic systems. It concludes with a comparative case study of how thermal instrumentation may be applied to develop cryopreservation methods for temperate and tropical plant germplasm maintained in tissue culture.

Cryobiology is a broad discipline and includes the preservation of a broad spectrum of biodiversity, as well as medical, polar and environmental low temperature research [1]. Plant cell cryopreservation requires the input of theoretical and practical expertise from diverse disciplines, including: engineering, computing and physics; chemistry, biology and biotechnology and, increasingly environmental knowledge. Cryobiologists network across multidisciplinary sectors, (www.cobra.ac.uk; <http://www.sltb.info>; <http://www.societyforcryobiology.org/>; <http://www.agr.kuleuven.ac.be/dtp/tro/CRYMC EPT>) which historically has led to the development of generic analytical cryogenic instrumentation and storage technologies [1]. Cryogenic engineering is highly specialist, encompassing the design, construction and utilization of equipment capable of effective and safe operations at ultra low temperatures. In many situations this involves withstanding the physical constraints of operating, often rapidly, through different thermal cycles, under elevated pressures and in contact with liquid nitrogen vapour and

liquid. Operator and sample safety is an essential component of cryogenic engineering and the provision of specialist protective wear, safety-monitoring instrumentation and procedures must underpin all aspects of its application.

2. The properties of liquid nitrogen and cryosafety

Nitrogen (N_2) makes up ca. 80% of the atmosphere; it is odourless, colourless, tasteless, and not detectable by human senses. When cooled to its boiling point (-196°C) N_2 can be condensed to form Liquid Nitrogen (LN), remaining in this state provided that it is at or below this temperature. On warming, N_2 is released and a concomitant white vapour frequently and briefly forms containing frozen water. Whilst LN is not toxic it has two life-threatening hazards: (a) on evaporation N_2 displaces air, creating an atmosphere that cannot support life because of asphyxiation; (b) the severe and extreme cold of LN and its vapours causes serious frostbite and cryogenic burns. The safety information provided here is intended as a basic alert for the reader of the potential dangers of handling cryogenic equipment and LN. It is the ultimate responsibility of the reader to ensure that full safety assessments are performed and that appropriate protective and safety procedures (including oxygen monitors) are used before handling cryogenic equipment, liquids and facilities. As a guide, see the UK's Health and Safety Executive website (www.hse.gov.uk) and the suppliers of cryogenic equipment (*e.g.* www.WessingtonCryogenics.co.uk).

Together with the other cryogenic gases (helium and argon) very small amounts of LN can evaporate into large quantities of gas in a ratio of about 700:1; in enclosed and limited spaces oxygen becomes depleted and asphyxiation ensues. Entry of personnel into atmospheres <20% oxygen is not recommended, atmospheres containing < 18% oxygen are potentially dangerous and at < 10% oxygen, brain damage and death occurs. Oxygen monitors and alarm systems should be located in laboratories that carry LN and appropriate safety procedures, including strict protocols for the safe exit from and entry into cryogenic laboratories should be in place. LN-containment in vacuum-insulated vessels (termed cryogenic dewars) and/or specialised delivery and storage dewars cause "leakage" of N_2 to the atmosphere, over time causing N_2 enrichment. Rupture of vacuum insulated cryogenic vessels is a rare, but real possibility and as such an event may cause the rapid and potentially lethal enrichment of N_2 in the atmosphere, it is important that all cryogenic storage vessels are regularly checked and certified as safe by suitably trained personnel. Vacuum insulated dewars and pressurised vessels are under the control of legal legislation that requires regular inspection and decommissioning after an appropriate lifetime of use.

Cryogenic cold burns arise from contact with either liquid or vapour phase LN and from instruments and equipment cooled by LN, eyes are particularly vulnerable when exposed to LN vapour. Unprotected skin can "stick" to cold surfaces because skin moisture forms ice and tearing occurs if the operator attempts to disengage from the surface. Inhalation of LN vapours damages lungs and may bring on asthma attacks in susceptible operators. Specialist cryosafety wear comprising protective gloves, aprons, visors (full face shields) glasses and goggles resistant to LN should be used.

Handling instruments and equipment used in cryobiology poses special hazards and these are assigned to static, pressurised and/or accessory (*e.g.* cryovials) handling

categories. It is extremely important to use certified equipment labelled with proven manufacturer's tolerance of cryogenic temperatures, such that providers have certified LN safety compliancy. LN should only be placed under pressure in vessels designed for this purpose as many materials become brittle on exposure to LN and fracture causes more hazards. Over-pressurisation of storage dewars can cause explosions and ice can form in dewars that are left open blocking outlets and safety valves. When releasing pressure from pressurized dewars (e.g. programmable freezing units) care must be taken to ensure operators do not stand in the vicinity of the vent. Exposing sealed samples and containers to LN (e.g. cryovials and Eppendorf tubes) can cause a build up of internal pressures. Return to ambient room temperatures or water baths, can lead to tubes exploding and eye protection must be worn. Transfer and retrieval of samples from LN vessels should be performed using LN-resistant tongs and forceps and transferring and pouring LN should be undertaken carefully to avoid spills, the generation of excess vapour and splashing onto operators. For these reasons open-toed footwear must not be worn, lab coats must be fastened and sleeves and trousers should be worn over gloves and boots, preventing the catchments of LN in a close proximity to the skin. Transport of LN is potentially extremely hazardous and operators should never travel in the lift at the same time as the transport vessel or in a closed transport vehicle.

3. Physics of ice

"Ice Physics" is a term borrowed from Hobbs (1974) [2], which appraises the unusual properties of water at low temperatures. For a low molecular weight compound, water has extraordinary properties, particularly related to its thermal behaviour. Water exists as a liquid over a wide temperature range (defining the Celsius temperature scale, previously Centigrade); at normal pressure it freezes at 0°C and boils at 100°C. Water's anomalous properties are due to its molecular structure (Figure 1).

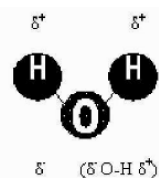


Figure 1. Polar H₂O.

H₂O's central oxygen forms covalent bonds with two hydrogen atoms. This leaves oxygen with two unpaired electrons resulting in an approximate tetrahedron geometry. This makes water a dipolar molecule with different parts having positive and negative charges (designated as δ^+ δ^-). Water contains two lone electron pairs on the oxygen atom and two polarized hydrogen atoms, these can form hydrogen bonds. The H-bond is very important to biological systems, forming wherever a covalent bond, involving H, resides in close proximity to electronegative groups (the acceptor). Neighbouring water molecules have a tendency to orientate such that each partially positive (δ^+) hydrogen is aligned with a partially (δ^-) oxygen. Each H₂O can potentially participate in 4 H-bonds,

because it has 2H to act as an electron donor and two pairs of unshared electrons that can accept an H donor. Molecules possessing hydrogen bond donating and accepting properties tend to display physical properties more characteristic of larger molecular weights. This explains the wider ranging melting and boiling points of water as compared to other molecules of similar size, this is because H₂O has a substantial dipole moment and strong hydrogen bonding capabilities. The attractive forces of H-bonds play a major role in how water molecules associate, the preference being to arrange into a tetrahedron with each oxygen atom positioned at the apex. Water is thus less disordered than most liquids and more like a crystal.

3.1. WATER'S LIQUID AND ICE MORPHOLOGIES

The unusual molecular characteristics of liquid water determine how it behaves on freezing and thawing [2-4] and controlling water phase transitions [5] is essential for developing successful cryoprotection strategies. The structure of liquid water has been extensively debated [5], two main models have been proposed, *mixture* and *continuum*. The latter proposing that discrete sub-types of liquid water do not occur, rather it comprises a distorted H-bond structure. The preferred mixture models propose that liquid water is made up of molecules forming 1-4 H-bonds as well as monomeric water that has no H-bonds. Mixture models [5] encompass the interstitial model hypothesizing that monomeric water molecules inhabit ice-like "clathrate" cages formed by tetrahedrally H-bonded water. A second mixture model described as a "flickering cluster" or "iceberg" (a more appropriate term for cryobiologists!) contains islands of tetrahedrally bonded H-water interspersed in a "sea" of unbounded molecules. Mazur [5] explains that the iceberg clusters only form transiently and have lifetimes of 10⁻¹¹ or 10⁻¹⁰ seconds. Their associations are dependent upon thermal and energetic fluctuations; most importantly this has important cryobiological implications with respect to providing a theory for ice nucleation (also known as "seeding"). Thus, local changes in the thermal energy of the system cause two molecules of water to come together and form H-bonds, making it more energetically favourable for them to form third and fourth H-bonds. Mazur [5] explains that this is consistent with the mechanism of ice nucleation in water supercooled to -40°C, the temperature of homogenous ice formation. Water rarely freezes as is popularly thought at 0°C, it can be supercooled to far lower temperatures and manipulated to freeze by ice nucleating agents. At the point of homogenous ice nucleation critically sized "ice embryos" are formed or are "seeded" and the number of water molecules that come together to form a critical size occurs at or around -40°C, after which ice crystals are formed. The theory of homogenous ice nucleation is complex and it has been proposed [2] that in supercooled water there are fluctuations in microscopic structure, which cause the continual formation and breakdown of ice embryos within the liquid matrix. Once an ice embryo has reached a critical size which is thermodynamically favourable for it to grow it will become an ice crystal. The crystalline structure, ice, normally consists of a matrix arranged with each oxygen atom surrounded tetrahedrally by four other oxygen atoms and hydrogen atoms in between. This creates a very ordered structure, comprising an open network with a lot of space between the molecules. If the ice were manipulated (e.g. under pressure) to pack more molecules together the hydrogen bonds would not be able to form in the

same way, as they would not be aligned in the correct position. Thus the “spaces” in ice cause it to have an unusually low density even though H-bonding makes it rigid.

When ice forms there is an energetic change “*disorder becomes order*” causing a release of energy as thermal heat, this is substantial and is called the “*Latent Heat of Fusion*”. When water is supercooled there is a heat deficit caused by cooling water below its nominal freezing (e.g. 0°C) point and this absorbs some of the heat of fusion so that when ice is eventually seeded it propagates very rapidly and the temperature will rise to the nominal melting temperature. However, this also influences any solutes present which become more concentrated as the water “freezes out” and as solute concentration increases the freezing point of the remaining water becomes depressed. Ice continues to form as the temperature is reduced until it reaches the eutectic point, which is the moment at which the whole sample solidifies without further change in composition. Heterogeneous ice nucleation also occurs as a direct deposition of ice from the vapour phase or freezing in a supercooled or cooled liquid. This generally occurs above the temperature of homogeneous ice nucleation and is affected by purity, droplet size, nucleating agents and cooling rate.

3.1.1. Making snowflakes: a multiplicity of ice families

Most compounds exist only in a few different states; this is not the case for water, which exists in liquid, vapour, vitrified and solid states. A vitrified or “glassy” state is a solid that lacks organised crystalline structure; it is amorphous and meta-stable as molecules can revert to a crystalline structure if energetic conditions allow nucleation. The temperature at which a substance forms a glass is called the glass transition temperature (T_g). Snowflakes comprise the most diverse of water’s crystal families; they form in the upper atmosphere when tiny droplets of water vapour freeze, behaving very differently to those encountered in cryopreservation [6]. In the latter, ice forms and grows in bulk solutions, branch like fingers or needles; termed dendrites (many branched crystals) often grow following a six-point symmetry that looks like the arms of snowflakes.

In addition to snowflakes, H_2O has a large family of 11-13 different types of ice [2], [4]; differing in how the tetrahedrons are packed together and the pressures exerted on the ice mainly influence this. Under normal conditions as experienced in nature, pressures are not extreme enough and the main form of ice that naturally occurs is hexagonal ice or Ih ($I_{\text{hexagonal}}$) also called Ice I. So named because it has a hexagonal symmetry, the best manifestation of this is seen in snowflakes, which have six corners [5,6]. Ice forms in two main phases in the liquid phase (the phase of most interest to cryobiologists) as demonstrated in supercooled water, and in the atmosphere. Snowflakes form in the upper atmosphere as water vapour freezes out into micro seeds; under these conditions water molecules associate to give symmetrical structures of great variety and beauty and their form is hexagonal [6]. However, it is also possible to deposit water vapour onto a surface that is already at a low temperature (-80 to -130°C) leading to the formation of a crystalline solid phase of water that is cubic in structure and hence called cubic ice or Ic ($I_{\text{cubic ice}}$). If water vapour is deposited as micro-droplets [2] onto surfaces <-140°C or at liquid nitrogen temperatures the drops become amorphous ice and as it is most likely vitrified [2] is not really ice at all [4]. The dynamics of forming an amorphous solid at low temperatures and crystalline structures at higher low temperatures is due to differentials in energy dissipation [2]. If the

temperature of the receiving surface is very low (e.g. liquid nitrogen vapour) a water molecule alighting on it from the vapour phase will rapidly dissipate energy and remain near to its landing point. At higher temperatures water molecules have more energy and are able to move across surfaces to positions of minimum potential energy, which are favourable for crystal formation. If pressure is exerted on ice then the crystals can change their structure and a number of high-pressure ice polymorphs are formed (ices ii-ix or more). This phenomenon involves a phase transition in which the same compound can exist in different phases. The “higher ices” are not of direct relevance in cryopreservation and for those forms that do occur in nature they are largely considered in polar and glacier ice dynamics.

Ih has an open structure and as it is less dense than liquid water, on freezing it floats on liquid water. For these reasons ponds, lakes and oceans do not freeze from the bottom up but from the top down. Most liquids reach their maximum density at their freezing point but this is not so for water which reaches its maximum density at 4°C. This means that freezing to great depths in natural water bodies will be suppressed by water cooled below 4°C, which floats to the surface. This has important consequences for life located in the depths of water bodies, which is able to survive in an unfrozen state due to the anomalous density of water.

How ice grows in liquids has important implications for cryobiologists working on both the preservation and destruction of cells. If water is frozen in liquid systems by either induced seeding or spontaneously, needle (dendrites) crystals often form and as they grow small branches of crystals develop, creating the “feather” patterns observed on frosted windows. As ice grows any solutes in the original liquid will be excluded from the growing ice front and if crystal growth is rapid the solutes do not have sufficient time to diffuse from the ice front and a concentration gradient is established in the liquid encompassing the growing crystal [7]. This lowers the freezing point in the advancing region and continued planar ice growth will be limited by the diffusion of solutes away from the region, which becomes supercooled. Ice formed in bulk liquids is different to planar ice and nucleated ice produces circular or semi circular disks, in regions where nucleation agents are present. Crystal growth in this state is impacted by the latent heat of fusion created at its surface dissipated by conduction from the crystal or surrounding supercooled liquid. How this occurs dictates the shape of the crystals, if latent heat is conducted away through the ice then the crystal will grow smoothly as heat is rapidly lost on either side of the ice crystal rather than on one planar front. If conduction occurs via the liquid there will be a rise in the liquid temperature surrounding the crystal and when these molecules become energised they are less likely to join a planar surface where H-bonding involves a single molecule. The H₂O molecule has the energy to orientate such that it preferentially joins with more neighbours, using kinetic energy for H-bonding [7]; ice thus grows as a symmetrical, hexagonal disk. However, the whole system is extremely dynamic and where domains of solutes are excluded to the sides as well as to the front of planar ice growth then small regions of solutes will be formed, these will form hexagonal dendrites with side branches. These form encapsulated channels of solute-concentrated areas interspersed between advancing dendrites; importantly for cryobiologists, cells can become entrapped in these regions.

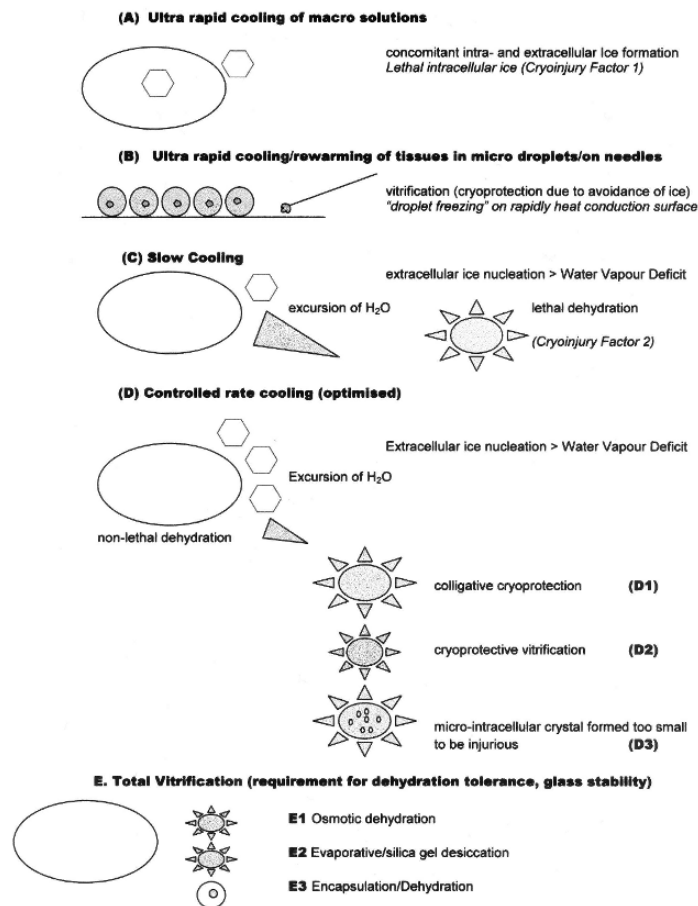


Figure 2. Cryogenic modalities involved in cryoprotection, cryopreservation and cryodestruction.

4. Cryoprotection, cryodestruction and cryopreservation

How ice nucleates and grows is important, as freezing rate is a major determinant of cell survival. Mazur's two-factor theory of cryoinjury [5] caused by ice and dehydration has been related to cryogenic injury in plant cells [8]. In nature this is best demonstrated by the tree line of alpine ecosystems correlating with an annual minimum temperature of ca. -40°C , the point of homogeneous ice nucleation. Cells of hardy trees remain supercooled even when extracellular ice has formed, thereby avoiding intracellular ice formation however, nature's cryoprotective mechanisms do not confer complete tolerance at liquid nitrogen temperatures. The interplay of freezing rate with cryoprotective and cryodestructive modalities is summarised in Figure 2. If cells are

rapidly cooled (at a critical rate defined by the biological systems) in the absence of an optimised cryoprotective strategy there is a simultaneous formation of intra cellular and extracellular ice, which causes lethal cryoinjury (Figure 2A). Ultra rapid cooling normally results in cell death due to intracellular ice, however under certain conditions it may be possible to create a system that, in energetic terms, impairs ice nucleation. If such a strategy is applied to highly cytoplasmic cells then further inhibition of ice nucleation results as water forms “amorphous ice” and cells are cryoprotected by vitrification.

4.1. PHYSICAL PERSPECTIVES OF ULTRA RAPID AND DROPLET FREEZING

If micro-sized water droplets are deposited on a very cold surface that rapidly conducts heat, H₂O molecules do not have a sufficient critical mass or energy to nucleate [2,4] and become vitrified. Hobbs [2] reviews the early X-ray diffraction studies of Burton and Oliver [9] that examine water deposited onto surfaces cooled to -80°C . Ih formed as confirmed by X-ray diffraction patterns, but at temperatures around -110°C , patterns similar to those observed in liquid water formed, it was deduced that a vitreous or amorphous solid occurred at or below this critical temperature.

Hobbs [2] explains that the formation of Ih at higher sub-zero temperatures and amorphous “ice” at ultra low temperatures is due to water vapour droplets being deposited onto highly conductive surfaces that are at a critically ultra low temperature resulting in the very rapid dissipation of heat energy away from the point of initial contact. The water molecules do not have sufficient energy to migrate across the surface to positions of alignment that have the minimum potential energy favourable for crystal formation. Dowell *et al.* [10] demonstrated vitreous ice condensed onto surfaces of -160°C to a thickness of 60 μm . This was meta-stable forming a mixture of vitrified and Ic water at $160\text{-}130^{\circ}\text{C}$; crystalline transformation was dependent upon increasing temperature. It was concluded using X-ray diffraction cameras [10] that vitrified ice contained large spatial open domains with configurations similar to solid ice but dispersed in a random pattern. At temperatures $>-160^{\circ}\text{C}$, water spontaneously formed unstable sites that supported the rapid growth of ice embryos.

Whilst the aforementioned studies were undertaken on pure water it may be interesting to speculate their relevance to understanding cryoprotective modalities involved in ultra rapid and droplet freezing of plant germplasm. Specifically, those cryopreservation protocols that expose very small, highly cytoplasmic meristems and embryos contained in μl droplets on needles or thin aluminium foils. These parameters have marked similarities to those conditions used to produce amorphous ice in physical studies [2]. Figure 2B demonstrates the significance of amorphous ice formed on ultra rapid cooling in the cryopreservation of plant germplasm. Three other cryoprotective factors must also be examined: (a) rapid rewarming, see [2,9,10] required to ensure that devitrification does not occur on return to biological temperatures; (b) cryoprotective additive and (c) germplasm status. Note that densely cytoplasmic cells with high viscosities promote vitrification. The ultra rapid freezing of plant germplasm (Figure 2B) suspended in cryoprotectant droplets on aluminium foils or hypodermic needles was first and respectively devised for the cryopreservation of cassava shoot-tips by Kartha and Kartha *et al.* [11,12] and potato shoot-tips by Grout and Henshaw [13]. Initially droplet freezing, involved cryoprotecting 0.4-0.5 mm meristems in dimethyl

sulphoxide (15% v/v) which were then delivered in 2-3 μl microdroplets of cryoprotectant onto the surface of aluminium foil of 18 μm thickness. These are cooled using slow controlled rate freezing ($0.5^\circ\text{C min}^{-1}$) to an intermediate terminal temperature (with greatest survival achieved $\geq 40^\circ\text{C}$) before rapidly cooling in LN and rewarming at 37°C . Kartha [11] noted ice formation in this initial study and a high degree of variation in recovery responses, despite this, the method greatly improved upon the application of conventional methods of cryopreservation. Benson *et al.* [14] explored Kartha's original [12] droplet method, but this time by ultra rapidly, cooling naked cassava shoot-tips suspended in 15% (v/v) DMSO droplets of 5 μl , 50 μl and 80 μl sizes. Ice nucleation characteristics of the droplets were investigated using visual observations, a temperature probe, and comparisons of ultra rapid and slow cooling (at a rate of $-0.5^\circ\text{C min}^{-1}$) followed by direct exposure to LN. Ice nucleation of 5 μl and 50 μl droplets was not consistently achieved and direct exposure to LN on aluminium foils frequently did not result in the visualization of ice formation (opaque droplets). Suggesting that the droplets on occasions may have formed amorphous ice, whereas the larger 80 μl droplets consistently and spontaneously nucleated at ca. -22°C . This modification [14] of the original Kartha method [12] using the naked freezing of very small cryoprotectant droplets containing meristems was further refined for cryopreserving potato [15]. Apices were contained in 2.5 μl droplets placed on 0.03mm thick-aluminium foils suspended in cryovials filled with LN. However, no details as to the ice nucleation characteristics of the droplet were presented in this study, but as observed in the initial study [14] of cassava it is highly likely that vitrification occurs. Grout and Henshaw [13] used hypodermic needles to deliver "naked" potato shoot meristems (in μl -sized droplets of 10% (v/v) DMSO) into LN and postulated the formation of vitreous ice as described by Luyet [16]. The "flash-frozen" meristems were only 2-4mm size, so the rapidly conducting needle surfaces may also contribute to the formation of glasses. This approach was later successfully applied to cryopreserve shoots of a wider genotype range of potato [17].

Wesley-Smith *et al.* [18] developed ultra rapid cooling to cryopreserve recalcitrant plant embryos that cannot tolerate desiccation. This explores the possibility that higher cooling rates minimise ice crystallisation, size and growth (Figure 2B and 2D, D3) and thus increases the tolerable water content of cells such that hydrated tissues can withstand cryopreservation. This is because at ultra rapid rates of cooling, water molecules cannot energetically arrange themselves into a crystal form. Wesley-Smith *et al.* [18] cautions that water mobility is restricted below -134°C and no further ice growth occurs below this temperature. However, if hydrated cryopreserved samples are warmed to higher than this critical point, small and unstable ice crystals coalesce, growing larger structures. In pure water the critical temperature range for ice formation and growth is 0 to -134°C . Cryoprotectants depress the freezing point (generally -30 to -40°C) and increase the temperature of re-crystallization above -134°C , reducing therefore the range of temperatures supportive of ice crystal growth [18]. Wesley-Smith *et al.* [19] used the ultra rapid freezing to obtain survival of cryopreserved *Camellia sinensis* embryos cooled at $200^\circ\text{C min}^{-1}$ at a water content of 0.7 to 0.4g $\text{H}_2\text{O g}^{-1}$ dry mass, increasing the cooling rate to $500^\circ\text{C min}^{-1}$ and 100% survival was reported for higher water contents (1.1 to 1.6 $\text{H}_2\text{O g}^{-1}$). Technologically this method [18,19] comprises two parts, first, drying germplasm over activated silica gel at $25-28^\circ\text{C}$ to a

critically determined moisture content based on species-desiccation tolerance limits. Secondly, cooling ultra rapidly with a specially constructed spring-loaded, rapid plunge-cooling apparatus [18] devised using cryo-electron microscopy principles. The tension and speed of travel of the spring-loaded delivery mechanism into a cryogen (LN/isopentane) delivered cooling rates of 5000-7000°C min⁻¹. Ultra rapid cooling was one of the first approaches used to cryopreserve plants [13,20,21]; its application being superseded, to some extent, by the arrival of controlled rate cooling methods followed by vitrification. The potential of using ultra rapid freezing is still however compelling for recalcitrant germplasm as dehydration beyond critical points of desiccation tolerance is not necessary.

4.2. CONTROLLED RATE OR SLOW COOLING

Mazur's two-factor hypothesis (Figure 2) explains that the rate of change of temperature at which cells are exposed to freezing controls the rate at which water moves across cell compartments and that this influences cell solute concentration [5]. The dynamics of freeze-induced water movement determines survival as water moving from intracellular to extracellular spaces causes a colligative effect as solutes become increasingly concentrated (Figure 2D). During controlled rate freezing ice will initially nucleate extra-cellularly, forming a water vapour deficit that initiates the movement of intra-cellular water to the outside of the cell whereupon it freezes. The process is, in fact cryodehydration and as it progresses the concentration of cellular solutes increase, as a consequence freezing point is depressed and the cells supercool. Successful cryopreservation is dependent upon achieving a cooling rate that allows cryodehydration to occur to such an extent that little or no intra-cellular water is available to form ice crystals on exposure to liquid nitrogen (Figure 2D,D1). In the case of cryoprotected cells undergoing slow cooling, water can be supercooled to a temperature of -40°C, the point of homogeneous ice nucleation. Applying penetrating "colligative" cryoprotectants to the cell before freezing reduces damaging solution effects of cryodehydration. Colligative protection requires cryoprotectants to penetrate the cell (e.g. DMSO) and remain in solution at sufficiently low temperatures that allow freezing point depression (supercooling) to a point at which the cell can survive colligative stress. Penetrating cryoprotectants act as "cellular solvents", reducing the concentration of damaging solutes and increasing the unfrozen fraction, thereby limiting the deleterious volume changes. Cells cryopreserved by controlled rate cooling are taken to a "terminal transfer temperature" at, or around, the temperature of homogeneous ice nucleation (-40°C). In some cases ice is manually or electronically initiated ("seeded") at a higher heterogeneous transfer temperature so evoking cryodehydration. To ensure that sufficient water has left the cell a holding time is usually incorporated (30-40 minutes) at the terminal transfer temperature, giving the opportunity for more water to be withdrawn. After reaching and holding at the terminal transfer temperature cells and cryoprotectants are then immersed in LN. Survival ultimately depends on preventing or limiting ice formation in any remaining intra-cellular water, such that: (a) there is not sufficient water to form large ice crystals, those that are formed are so small that they are not injurious or (b) cellular viscosity is so high that any remaining intra-cellular water becomes vitrified.

4.3. VITRIFICATION

Vitrification is the “solidification” of liquids in the absence of crystallization, a state with a random molecular structure but possessing physical and mechanical properties similar to a solid. Glasses are metastable as de-vitrification can occur on re-warming, the glass returning to either a liquid or crystalline state. Achieving a stable vitreous state during cryopreservation is important and involves controlling molecular mobility by enhancing cellular viscosity through osmotic, evaporative and cryodehydration and/or by the loading of penetrating cryoprotectants (Figure 2E). High viscosity solutions restrict the ability of H₂O molecules to re-arrange into crystals and ice nucleation becomes more difficult as temperature decreases. Moreover, the viscosity of highly concentrated solutes rises further during cooling and the molecular mobility of water is virtually arrested. At this stage the liquid becomes a glass; the glass transition temperature (T_g) is used to characterize that point at which the physical properties of the system change. Glasses; unlike ice crystals do not significantly change the structure or composition of solutions and their effects in cryopreservation are less damaging than ice. But, cells have to be dehydration and desiccation tolerant because practically the vitrification (Figure 2E) of plant germplasm requires and increase in cell viscosity. This is achieved by: evaporative desiccation using still or laminar flow air; chemical desiccants such as silica gel; osmotic dehydration, (sugars and polyols); alginate encapsulation/dehydration and the loading of chemical cryoprotectant cocktails (penetrating and non-penetrating). Vitrification is advantageous as samples are plunged directly into liquid nitrogen but rapid re-warming is critical ensuring movement through the T_g before ice crystallization occurs. Vitrification protocols do not require controlled rate-cooling apparatus and are “low tech”, whereas programmable freezers are preferred in genebanks so that large accessions can be processed more efficiently. Thus, vitrification is best applied to recalcitrant germplasm and laboratories without access to controlled rate freezers.

5. Cryoengineering: technology and equipment

Cryoengineering is a wide field, mainly developed in medical faculties [22]. Plant cryopreservation requires equipment for controlled rate cooling, cryogenic storage and cryogenic shipment this review will also focus on cryomicroscopy and Differential Scanning Calorimetry (DSC).

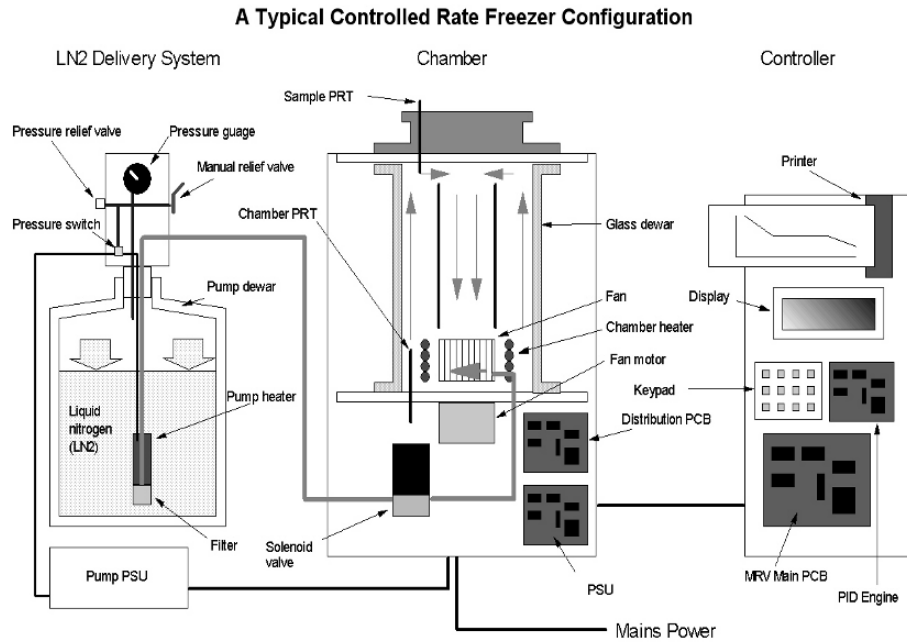
5.1. CRYOENGINEERING FOR CRYOGENIC STORAGE

Mazur presents “*The Inverted U*” as one of the basic principles of cryopreservation related to the two causal factors intra-cellular and dehydration of cryoinjury [5]. These are determined by the rate at which cells are cooled, the “U” describes the graphics of survival versus cooling rate. Maximum survival occurs when the dynamics of the excursion of H₂O in controlled rate cooling is optimised (Figure 2D) and colligative cryoprotection obviates the damaging effects of excessive solute concentration. In plant cryopreservation optimum cooling rates are within the range 0.2 to 1.0°C min⁻¹ for the majority of cell types. The precise control of cooling rates, and for many systems, the

temperature at which ice nucleation is initiated is critical to survival and best achieved using specialist apparatus.

5.1.1. Controlled rate freezers

Withers and King [23] developed one of the first widely applicable, higher plant cell cryopreservation methods using a simple, custom-built controlled rate freezer unit regulated by a solvent coolant. The system comprised an insulated plastic bin with a 5 L capacity glass beaker housing a dip cooler capable of chilling to -40°C (temperature of homogeneous ice nucleation) and a heating coil connected to a thermostated bath with a pump to circulate the coolant, 30% (v/v) methanol. A temperature probe was inserted for regulation and the samples placed in cryovials and suspended over the coolant in polystyrene rafts. Thermocouples were inserted to monitor sample and coolant temperatures. The cooling capacity of the freezing unit was calibrated for different volumes of solvent coolant and cooling rates for different volumes determined by thermostatic control of the dip cooler. Using this approach the Withers and King [23] devised a slow freezing protocol utilising a 3-component cryoprotectant mixture containing sucrose, glycerol and DMSO and a cooling rate of $-1^{\circ}\text{C min}^{-1}$ to an intermediate temperature of -35°C at which the cells are placed on hold for 30 minutes before transferring to liquid nitrogen. Specifically engineered programmable controlled rate freezers using liquid nitrogen as the coolant were first developed in the 1970s by medical cryobiologist, David Pegg, (now Professor of Cryobiology, University of York, UK) in association with Planer plc, the London-based company who manufactured the equipment (Planer, G. personal communications). This system, known as stepwise cooling, was a major breakthrough in human and animal cell cryopreservation and soon became widely applied in medical and animal husbandry sectors. Early Planer freezers used a cam controller to produce multi-component cooling regimes and then went on to manufacture full digital computer controllers from the 1980s onwards. Today's Planer units (Figure 3) are based on the principle of a pulse-width modulated solenoid valve to admit liquid nitrogen into the freezing chamber. The solenoid pulses on and off at a time varied by the control unit in response to the difference between the actual and desired temperature. Planer freezing chambers are typically 16 L capacity and large or smaller units can be manufactured in accordance to fitness of purpose.

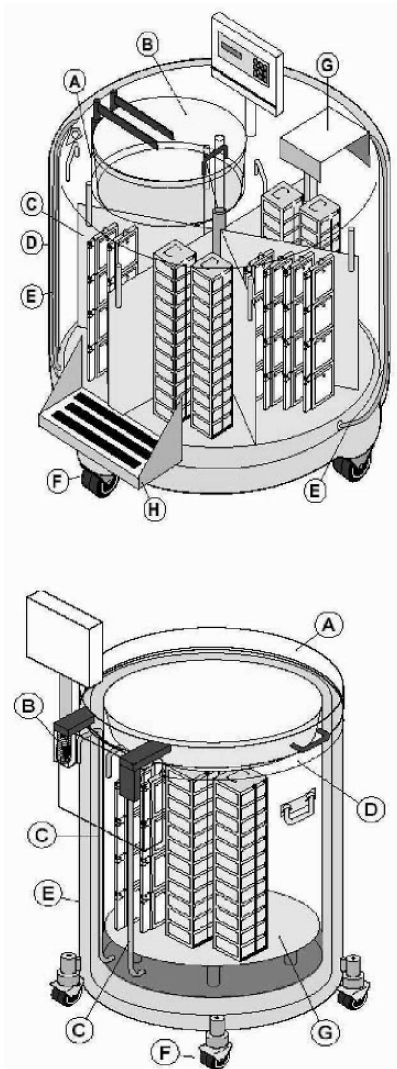


Courtesy of Planer plc

Figure 3. Controlled rate freezer design.

Freezer units comprise three basic parts: a coolant (LN) delivered by a pressurised dewar system, the freezing chamber that houses the samples and a control unit (Figure 3). Today many companies (Biotronics, Cryomed, Cryologic, L’Air Liquide) have developed controlled rate freezers most of which are based on the original Planer/Pegg design, (Planer, G. personal communications).

Operations of cryogenic equipment in plant conservation laboratories must take into account functionality in potential extremes of temperature and humidity, particularly in humid, tropical locations. Contemporary-designed controlled rate freezers have advantages, as they are robust instruments with respect to environmental parameters. They hold reserved liquid nitrogen capacities such that external environmental control is not a limiting factor as they function at relatively low ambient temperature conditions and up to 40°C. The main problem however is humidity, which causes door frosting especially in front-loading machines and at delivery port of tubing, an RH limit of 65% is recommended. If frosting does occur this causes an accumulation of water so it is important to thoroughly dry the machine as re-cooling causes potential ice damage and the immobilization of samples, moving parts and doors.

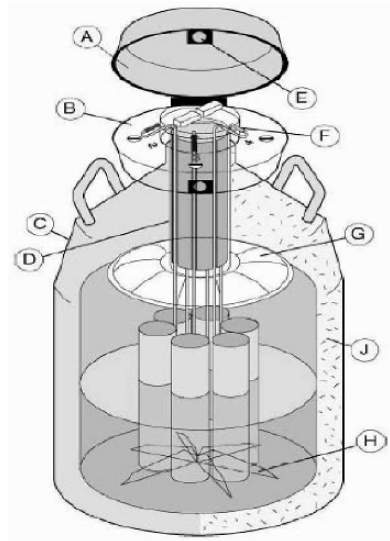


- I. High performance storage dewar
- A. Offset neck designed to maintain at -150°C in vapour storage and low liquid nitrogen consumption with standard racks.
- B. Durable metal lid for longer life.
- C. Rotating interior tray providing easy access to samples.
- D. Low maintenance, all stainless steel construction.
- E. Annular filling lines designed to reduce frost and ice formation at the lid.
- F. Rack stand.
- G. Step up platform (specified by model).

- II. Storage dewar, non-cabinet type
- A. Metal lid designed for longer-life.
- B. Tough durable hinges.
- C. Annular filling lines designed to reduce frost and ice formation at the lid.
- D. High performance under lid temperature.
- E. Low maintenance, all stainless steel construction.
- F. Tough, durable casters.
- G. Vapour platform (optional).

Figure 4. Exemplars of high performance and non-cabinet type cryogenic storage dewars (MVE Design), by courtesy of Planer, G. and Pattenden, N. [Planer Select].

Adequate ventilation of LN vapour is required for the venting of waste/exit points from the machine and if the size of the room restricts this then an oxygen monitor with outside repeater alarms and external venting should be in place. Programmable freezers are frequently operated with an external dewar (30-40 L), which delivers the coolant LN, via a solenoid valve under pressure to the chamber.



- Dry shipper
- A. Durable, tamper proof lid design.
 - B. Low-maintenance lid design.
 - C. Superior strength, lightweight aluminium construction.
 - D. High strength neck tube to reduce liquid nitrogen loss.
 - E. Locking tab.
 - F. Colour-coded canister/lid numbering system.
 - G. Chemical retention system designed for superior vacuum performance over life.
 - H. Spider design for easy retrieval and insertion of product canisters.
 - I. Insulation, engineered for maximum thermal performance.

Figure 5. Exemplar of Dry shipper by courtesy of Planer, G. and Pattenden, N. [Planer Select].

5.1.2. Cryogenic storage and shipment

Following a controlled rate freezing run (Figures 2 and 3), samples are transferred to specialist liquid nitrogen tanks (dewars), which are vacuum insulated (Figures 4 and 5). Storage in liquid nitrogen has the advantage that all biological activity ceases and germplasm can be held indefinitely so long as the LN supply is maintained. MVE tanks from Chart Inc. were the first to be produced for vapour shipment and liquid storage (Planer, G. pers. com.). An absorbent is placed in the base of the storage tank and once charged with nitrogen they become “dry shippers” and have holding times of up to 30 days (Figure 5). This allows for the safe transport of frozen germplasm. Vessels can range in size from holding 6000 to almost 1000,00, larger scale cryogenic systems contain up to 90,000 vials in a relatively small space. Inventory systems that utilise colour codes and computerized software help to identify sample location. The efficiency of dewars is dependent upon insulation specifications, high efficiency systems have over 90% of their surface covered by insulated vacuum, this reduces evaporative dispersal giving liquid nitrogen cost savings of up to 70% as compared with standard dewars.

International exchange of cryopreserved germplasm is an important component of global gene banking and requires engineering specifications that comply with international safety codes. The MVE dry shipper is designated for safe transport of biological samples at -150°C and is IATA approved and certificated (Figure 5). These vessels are made from durable lightweight aluminium and contain a hydrophobic

absorbent that holds liquid nitrogen, allowing spill free shipment and safety in transit. A ShipsLog[®] datalogger keeps an accurate, downloadable temperature history of the samples, providing safeguards during transport. The logger can be connected to an alarm in transit and a visual warning is given if tripped.

5.1.3. Sample safety, security and identification

Failure of a freezing run is an important safety consideration, particularly when working with precious, valuable (e.g. patented) or endangered plant germplasm. Considerable variations occur between different cryogenic protocols due to the broad genetic diversity of plant species so the transfer of cryopreservation technologies from one laboratory to the other must take into account differences in programmable freezer instrumentation. Studies on the exchange of *Ribes* germplasm for cryopreservation have highlighted this [24] and it prudent to test-run cryopreservation protocols developed for one type of programmable freezer before applying it to another. Protocol adjustments may be required to accommodate different freezer performances, particularly when operating instruments that have different “seeding” devices for the initiation of ice nucleation [24]. Containment of germplasm in ampoules certified for cryogenic use ensures their capacity to withstand storage in liquid and vapour phases. Glass vials risk explosion and the transfer of vials from LN to heated water baths for rewarming can cause less robust plastic vials to explode. Alarm systems that alert operators to a fall in liquid nitrogen levels in cryogenic tanks are an important safeguard and can be integrated with automatic fill devices and level sensors for smaller dewars. Cryogenic storage inevitably requires the removal and insertion of samples to and from storage dewars and during this operations it is essential not to allow samples not required for retrieval to warm up. An effective and efficient inventory system is therefore very important to enable the operator to easily locate specific samples. Effective ergonomic access (Figure 3) ensures efficient and rapid retrieval, as do dividers, colour, and alphanumeric identity coding systems.

6. Cryomicroscopy

Cryomicroscopy allows that real time visualisation of ice nucleation and melting events during the cryoprotection, cooling and rewarming of cells. Diller [25] reviews the contributions that engineers have made in this area. Sachs was one of the first to develop a low temperature stage for a light microscope and visualise extracellular ice formation and the concentration of solutes within cells. Molish (cited in [25]), invented a low temperature microscope, which was independently controlled. Both these early microscopic studies provide support for Mazur’s hypothesis for the two-factor basis of cryoinjury [5]. Diller and Cravalho [26] built the first quantitatively controlled cryomicroscope, based on balancing the capacity of concomitant heating and cooling inputs delivered to the specimen positioned on a mounting platform and responsive to feedback from a thermocouple. Specimens viewed by cryomicroscopy are placed on a transparent viewing platform heated using one of two technologies:

- Convection stages: cells are mounted on a surface cooled by a flow of gas (LN) through the chamber from below the sample; the gas removes heat vertically over the whole platform.
- Conduction stages: cells are mounted on a slide on a stage across a hole in a chilled metal block; heat is passed horizontally across the viewing area to the edges of the hole creating a horizontal temperature gradient. Changing the temperature of the metal block by a LN coolant regulates the temperature in the middle of the slide.

The thermal gradients of the conduction system may provide a more stable temperature than the convection system [25]. The Diller and Cravalho [26] cryomicroscope was cooled by a constant stream of refrigerant vapour flowing below the sample holder and heating was controlled electrically using a transparent resistive film adhered onto the bottom of the surface mounting. Specialist laboratories have also devised custom-built cryomicroscope stages, [27-29]. Hayes and Stein [29] describe a simple microscope based on the original design of Diller and Cravalho [26]. This uses convection heating and an electrical current passed via a thin resistive film overlaying the sample platform controls temperature and heat is balanced against heat extracted. A thermocouple attached to the upper surface of the sample unit connects to an electronic thermometer and feedback control system. One of the advantages of the model is that it may be built using basic workshop skills and commonly available components. McGrath [27] developed a conduction microscope in which heat was displaced from the sample by radial conduction through a metal plate to a refrigerant stream. Fleck *et al.* [30] summarises the historical development of commercial cryomicroscopes, the Planer CM3[®] Cryostage (Planer, UK), was one of the first to be built, followed by the Linkam BCS[®] 196 (Linkam, UK). Both instruments use LN as the coolant, the delivery of which is electronically controlled. Samples are mounted on a transparent heater on the stage and the cooling rate regulated by a thermal gradient. Cooling is controlled by programming ramps regulated by rate of temperature change, terminal temperature and holding at the terminal temperature. Fleck *et al.* [30] undertook a comparative study of two different cryomicroscopes to assess cryoinjury in the coenocyte alga *Vaucheria sessilis*. A Planer CM3[®] and a Linkam BCS[®] 196 were compared and used to study the impacts of two-step freezing. The cryomicroscopes differed in their manifestations of extracellular ice nucleation, which for the Planer CM3[®] cryostage occurred at high sub-zero temperatures (0-2°C), and did not parallel that expected. This may be due to seeding of the extracellular solution caused by a temperature gradient generated across the stage. By comparison, the Linkam instrument provided a uniform temperature across a conduction block allowing supercooling and homogeneous ice nucleation of the extracellular solution to be observed within expected parameters.

In addition to the visualisation of freezing and thawing, cryomicroscopy can be used to study the dynamics of water loss in cells exposed to cryoprotection and cryodehydration (Figure 2). Diller [25] describes studies of osmotic behaviour, specifically using convection microscopes, which can supercool prior to extracellular ice formation because there is a uniform distribution of temperature across the stage. By programming the thermal controller to maintain a constant preset temperature and by applying a small jet of LN onto part of the slide outside the field of view it is possible to control the formation of extracellular ice during an experiment. By taking this approach

it is potentially possible to visualise the dynamics of temperature, solute and osmotic effects and ice formation when cells are exposed to controlled freezing. Experiments of this type may be used to monitor the sensitivities of cell membranes to cryoprotectants and freezing.

Confocal Laser Scanning Microscopy [26,31] can also be used in conjunction with conduction cryomicroscopy to monitor dynamic changes in ice formation. Placing a conduction heat transfer stage onto a Bio-Rad MRC600 cryoconfocal laser scanning microscope system and connecting the apparatus to a temperature controller operating CM3 Planer Products Plc software provides a means of marrying the two instruments. A conducting slide is constructed by embedding a 5 μ m-thick copper/constantan thermocouple cooled by LN. Rate of cooling was used to measure ice crystal formation and the main advantage of the system is that opaque and solid samples could be observed during the freezing process. This permitted observations of ice growth dynamics and crystal size could be determined in autofluorescent or fluorescence labelled biological samples. Visualising the effects of cryoprotective additives is very important (Figure 2) and the perfusion cryomicroscope engineered by Walcerz and Diller [32] simultaneously and continuously monitors the impacts of cryoprotectants administered during controlled freezing.

6.1. NUCLEAR IMAGING IN CRYOGENIC SYSTEMS

Nuclear Magnetic Resonance (NMR) spectroscopy and powerful non-invasive NMR microscopy has been used to visualize the location of unfrozen water in plant cells and tissues at subzero temperatures [33]. NMR spectroscopy utilizes the magnetic properties of chemical nuclei. When a chemical nucleus is placed in a magnetic field it produces resonance absorption energy from a beam of radiation, the resonance frequency of which is characteristic of the field strength and the nucleus. NMR technologies detect specific nuclei and the strength of the resonating signal can be quantified to be directly proportional to the number of nuclei resonating. Water is one of the most important chemicals to study in cryobiology and conveniently physical chemists developing and studying NMR techniques have focused a lot of their interest on hydrogen atoms. This is because H is found in a vast majority of molecules and its nucleus has one of the strongest resonance signals found. NMR imaging is similar to MRI (magnetic resonance imaging) used in medical diagnostics, but has a much higher resolution permitting visualisation at the tissue and cell level. Ishikawa *et al.* [34] initially visualised freezing in flower buds of Full-Moon Maple and ¹H-density images revealed the fine scale localization of unfrozen water in the samples. By comparing NMR images at a range of freezing temperatures it was possible to visualize contrasting behaviours of freezing in plant tissues. The analytical advantages of NMR microscopy in studying cryogenic systems are considerable as it is non-invasive and allows the dynamic investigation of freezing and thawing. It is highly sensitive to both chemical and physical contrast mechanisms [34] and can produce image contrasts that are concomitant with water relaxation times associated with the decrease in motion of water molecules as they undergo crystalline transitions. Light areas of an image contain liquid water and dark areas represent frozen areas, or areas of low proton density. Using NMR imaging it has been possible [34] to profile extra cellular freezing in scales and bark tissues of *Rhododendron japonicum*, and supercooling and lethal ice nucleation in flower

primordial of *Acer japonicum*. Ishikawa *et al.* [34] suggest a range of applications for NMR imaging in plant cryopreservation. These visualise changes in the spectroscopic characteristics of protons and include chemical shift imaging of: sucrose distribution, cryoprotectant penetration, vitrification, glass stability, and water transitions.

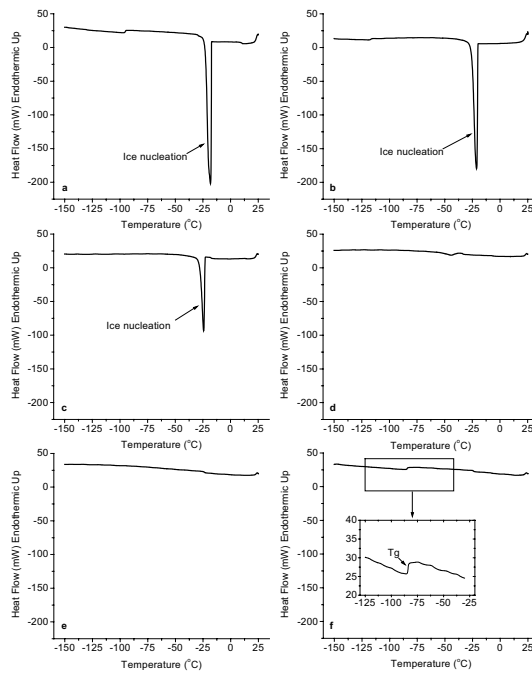


Figure 6. DSC cooling thermograms for meristems from *Ribes sanguineum*, cv King Edward VII, at different stages of the encapsulation-dehydration protocol. The stages analysed were a) immediately after encapsulation; after 20h of dehydration in liquid medium supplemented with 0.75M sucrose and air-flow desiccation for b) 0h c) 1h, d) 2h, e) 3h and f) 4h. Samples were held at 25°C for 1 min and cooled to -150°C at a rate of 10°C per min. Tg = glass transition.

7. Thermal analysis

Differential scanning calorimetry (DSC) is a powerful tool used to measure physical thermal parameters (freezing, melting and glass transitions) critical for the survival of cryopreserved tissues. Its application, together with recent advancements in thermal engineering will be explored using a comparative study of cryoconservation applied to tropical and temperate plant germplasm.

7.1. PRINCIPLES AND APPLICATIONS

DSC measures heat flow and water state transitions in samples as a function of time and temperature. Tissue of known mass is sealed in an airtight aluminium alloy pan and placed inside a chamber alongside an unloaded reference pan, both are cooled or warmed in parallel at a programmable rate to a selectable final temperature. Differences in heat flow between the two pans is measured during cooling and heating and plotted against temperature or time to produce a heat differential thermogram. Thermal events alter the amount of heat required to maintain both pans at the same temperature causing a change in differential heat flow and a deflection in the thermogram associated with thermal transitions. The main cryobiological application of DSC is to analyse the physical state of water during cooling and heating. Transitions between liquid, amorphous glassy and ice states can be detected by heat flow data manifested as an exothermic peak during cooling (Figure 6a) and an endothermic peak during re-warming (Figure 7a).

The point of change from a liquid to a glass is the glass transition (T_g) temperature detected as a deflection in heat flow (Figure 6f). Thermal profiles provide critically important information about the cryoprotective treatments required to obviate lethal ice formation and stabilize glasses. There is debate as to the terminology used to describe the water component that does not form ice in the supercooled state [35,36].

Unfreezable water, unfrozen water, bound water and osmotically inactive water are terms used to explain the phenomenon [35-37]. In this review, water content will be referred to, as either osmotically inactive or osmotically active, defining in part, its ability to participate in colligative processes. The content of osmotically active water is estimated using the enthalpy melt constant for water and the area of the melt endotherm peak [36]. The content of osmotically inactive water is calculated as the difference between total water and osmotically active water contents. Examples of its use in plant cryopreservation include: coffee seed and shoot-tips from *Humulus lupulus*, *Olea europaea*, and *Ribes*, for which ice formation is a lethal event [37-40].

Santos and Stushnoff [41] found limited intracellular ice formation was not lethal in embryonic axes from *Citrus sinensis*, although survival was improved by further desiccation to eliminate ice formation. In highly recalcitrant, homeohydrous germplasm the complete removal of osmotically active water is detrimental to survival [42]. For these systems the possibility that limited intracellular ice nucleation may be tolerated is contentious and intriguing as tissues may potentially survive limited intracellular ice formation if the crystals formed are too small to cause significant damage (see Figure 2). One may speculate that highly meristematic cells survive cryopreservation, whilst more differentiated and vacuolated cells undergo ice formation and do not survive. Achieving optimum water status for cryoprotection is species and tissue specific, reflecting complex differentials in desiccation tolerance [43,44], but clearly excessive loss of osmotically inactive water reduces cell viability. The formation of a stable glassy state (defined by the T_g , demonstrated in Figure 6f) during cooling and warming is a prerequisite for vitrification based cryoprotection. As confirmed in different plant culture systems [38,45,46].

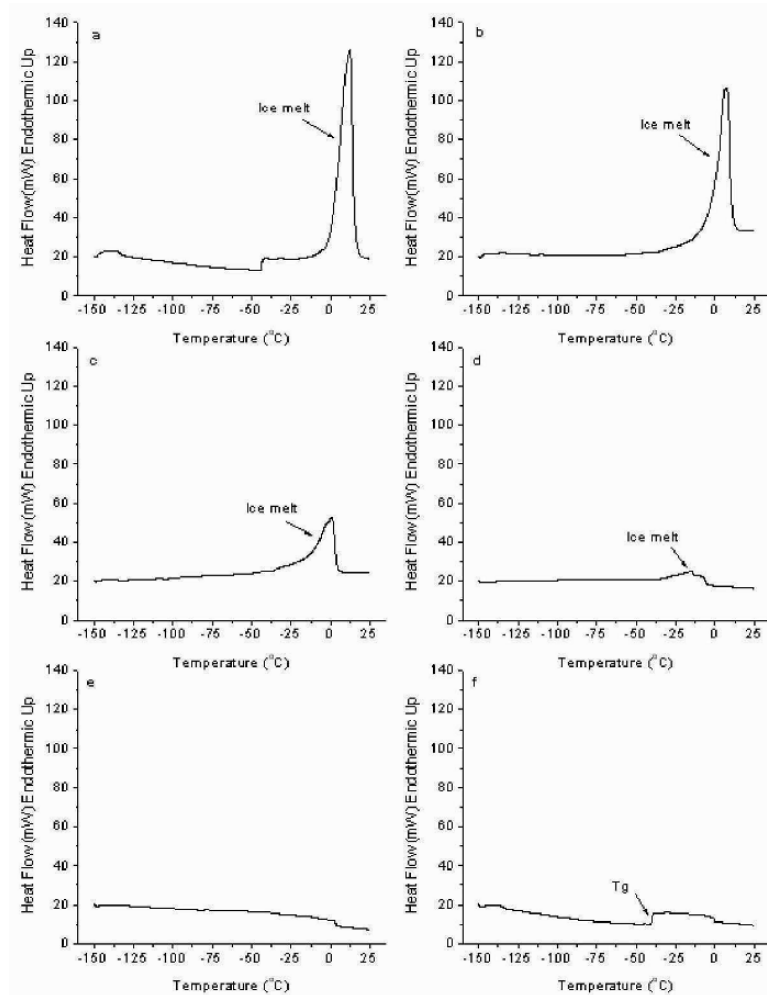


Figure 7. DSC heating thermograms for meristems from *Ribes sanguineum*, cv King Edward VII, at different stages of the encapsulation-dehydration protocol. The stages analysed were: a) immediately after encapsulation; after 20 h of dehydration in liquid medium supplemented with 0.75M sucrose and air-flow desiccation for b) 0h c) 1h, d) 2h, e) 3h and f) 4h. Samples were held at -150°C for 1 min and cooled to 25°C at a rate of 10°C per min. Tg = glass transition.

Glasses are metastable as devitrification can occur on rewarming, resulting in ice formation. The physical causes of devitrification and glass relaxation are complex [47] and can be related, in part, to tissue water content and warming rates. Thermal profiles of glass transitions and devitrification are often difficult to interpret, as exemplified by studies of *Phaseolus vulgaris* seeds [47] that show glass thermal behaviour is influenced by water content, thermal history prior to glass formation, and the

complexity and heterogeneity of glassy matrixes and their cellular components. The biochemical properties of plant germplasm also influence thermal stability [48,49] and lipid and sugar composition may be particularly important. Lipid-rich coffee seeds demonstrated an endothermic peak during re-warming occurring at a slightly higher temperature than the ice melt endotherm; analysis of a purified lipid extracts from coffee seed confirmed the second endotherm is lipid-associated [37]. Seeds with a low lipid content contained more osmotically inactive water than those with higher contents, suggesting that lipids interact with water and affect thermodynamic properties during cryopreservation. DSC can assess fatty acid composition [48] and the extent of peroxidation [49]. As lipid peroxidation contributes to cryoinjury [50] thermal analysis may allow the concomitant profiling of water and lipid thermodynamic properties associated with cryogenic changes in fatty acid composition and oxidative status. Sugars are important cryoprotectants and help maintain molecular stability and cell function [20,51]. The thermodynamic properties of different sugars have been analysed by DSC to explain differences in cryoprotective capabilities [52] and osmotic changes in cell volume and water transport may also be profiled [52-55]. Solutions containing trehalose have more osmotically inactive water and a higher glass transition temperature during cooling than sucrose, fructose and glucose; similarly, sucrose solutions contain a higher T_g and component of osmotically inactive water than fructose and glucose. The thermodynamic properties of trehalose and sucrose may thus explain their enhanced cryoprotective properties as compared to fructose and glucose.

7.1.1. DSC and the optimisation of cryopreservation protocols

The optimisation of vitrification-based plant protocols, particularly for storage-recalcitrant germplasm is an important application of DSC [56,57]. Studies of the effects of pre-treatments on *C. sinensis* embryonic axes revealed sucrose improves cryogenic survival by increasing the osmotically inactive water content and altering tissue dehydration rates [41]. In *A. thaliana* cell suspensions [55], enhanced survival following sucrose pre-treatment was associated with an increased rate of the removal of osmotically active water during desiccation and a higher glass transition temperature.

Encapsulation-dehydration consists of a number of steps and DSC has been used to optimise protocol as demonstrated for a number of diverse species [38,40,41,46]. The way in which beads are prepared may also impact their thermal properties as studies of empty alginate beads showed that their osmotically inactive water content is influenced by bead polymerisation times and total water content [36]. The retention of osmotically inactive water during desiccation may improve survival through stabilising cellular structures. Comparisons of the thermodynamic properties of empty beads, beads containing tissue, and tissues indicate that different components may desiccate at a different rates [36,46], creating differential moisture gradients that cause glass destabilisation on warming. In the case of cryoprotective additives, DSC can help optimise chemical cryoprotectant loading, thereby minimising toxicity [38,55,58]. One of the most important applications of DSC is in the study of seed storage behaviour, which is extremely complex with respect to the formation, and stabilization of different physical states of water [59]. Ice formation is lethal to coffee seeds and complete removal of osmotically active water is required to achieve successful cryopreservation [37], in contrast, this may not be the case for *Landolphia kirkii* embryonic axes [42].

DSC analysis helped to determine the optimal desiccation rates and water content required to cryopreserve seed-derived germplasm of *Quercus robur* and *Araucaria hunsteinii*; elucidating the relationship between osmotically inactive water and desiccation injury [43,60].

7.1.2. A DSC study comparing cryopreserved tropical and temperate plant germplasm

This chapter concludes with a novel, comparative demonstration of the use of thermal instrumentation in cryopreservation protocol development using *in vitro* germplasm derived from temperate [46] and tropical species [61] and an update on new thermal technologies [62]. Cryopreservation is becoming increasingly important [63] for tropical tree conservation and thermal analysis provides a fundamental approach to improve the current understanding of recalcitrant species. Comparing the physical and thermal characteristics of recalcitrant tropical tissues with those from tolerant temperate species may provide insights into the physical basis of cryo-tolerance and sensitivity. This study compares thermal behaviours of encapsulated/dehydrated somatic embryos from the tropical, medicinal tree, neem (*Azadirachta indica* A. Juss) with similarly cryoprotected shoot-tip germplasm from a temperate woody species (*Ribes sanguineum* cv King Edward VII); DSC was also applied to optimise critical points of the cryoprotective strategies.

In the case of neem, the aim is to determine which parts of a cryoprotective protocol requires moderating to ensure stable glass formation. This exemplifies how DSC may be applied as an investigative tool to help formulate new cryoprotection strategies for limited-access, rare and at risk tropical germplasm that has never been cryo-conserved before. For *Ribes*, the study demonstrates how thermal analysis may be used to improve on already established protocols thereby producing more robust cryo-conservation methods that may be utilised in large-scale germplasm repositories.

Somatic embryos were induced from *A. indica* species on Murashige and Skoog (MS) medium supplemented with 10 μ M Thidiazuron; 1-phenyl-3-(1,2,3-thiodiazol-5-yl)urea (TDZ), [61]; encapsulated in 3% (w/v) sodium alginate beads and pre-cultured on MS medium supplemented with 0.3, 0.5 and 0.7M sucrose for 24 hours. After which they were desiccated using in laminar airflow for 1,2, 3 and 4 hours before DSC. *Ribes* shoot-tip meristems were cryopreserved using the encapsulation-dehydration protocol described by Dumet *et al.* [46], except 20 g.l^{-1} glucose was maintained at all stages of the protocol. Meristems were encapsulated with 3% (w/v) alginate \pm 0.75M sucrose to determine the thermal effects of sucrose bead loading. DSC was performed after encapsulation, 20h dehydration in 0.75M sucrose, and following airflow desiccation for 0, 1, 2, 3 and 4h. Rewarming and survival were monitored according to Dumet *et al.* [46] for encapsulation and 4h desiccation controls, and after direct plunging in liquid nitrogen. DSC was undertaken as described by Benson *et al.* [38] using a Perkin Elmer DSC 7, with Pyris (c) software, calibrated using zinc and indium and pure water as a standard for cryogenic operations.

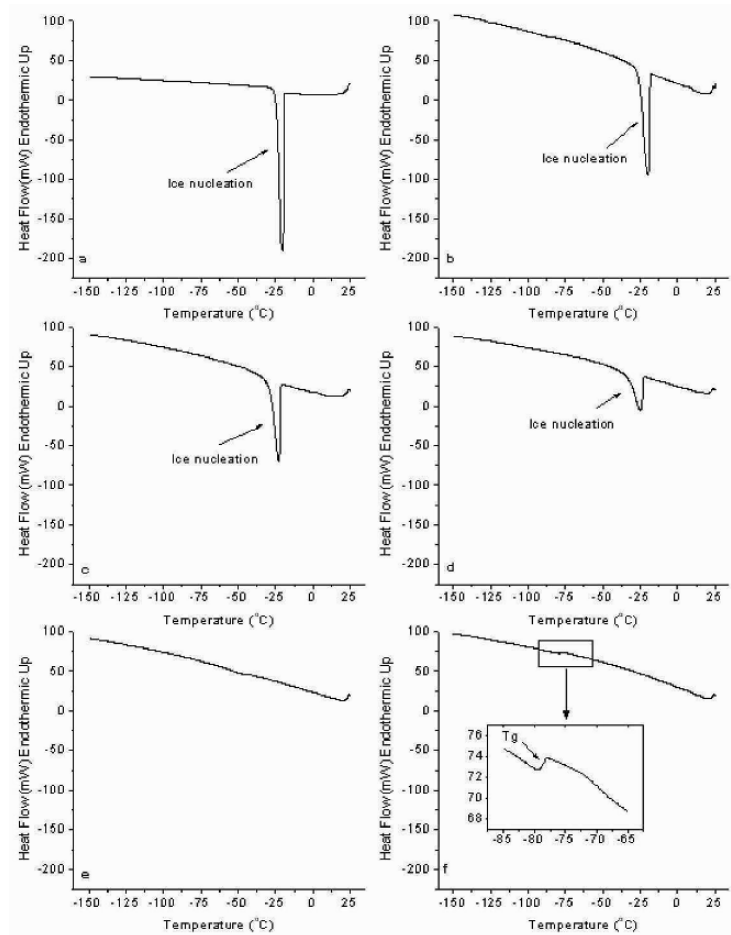


Figure 8. DSC cooling thermograms for alginate-encapsulated *Azadirachta indica* A. Juss. somatic embryos following sucrose pre-treatment and air-flow desiccation. Treatments were: a) no pretreatment and 0h desiccation; pre-treatment with 0.75M sucrose for 24h and desiccation for b) 0h, c) 1h, d) 2h, e) 3h and f) 4h. Samples were held at 25°C for 1 min and cooled to -150°C at a rate of 10°C per min. Tg = glass transition.

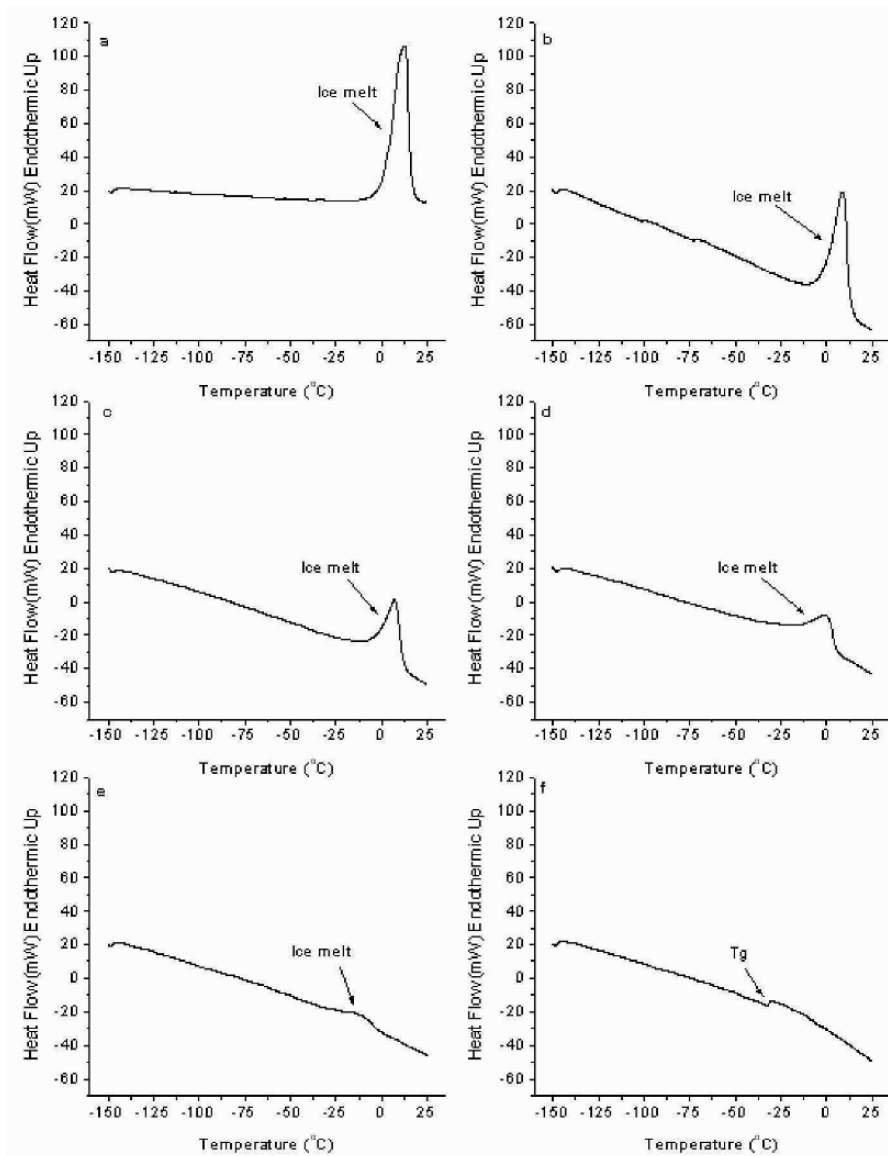


Figure 9. DSC heating thermograms for alginate-encapsulated *Azadirachta indica* A. Juss. somatic embryos following sucrose pre-treatment and air-flow desiccation. Treatments were: a) no pretreatment and 0h desiccation; pre-treatment with 0.75M sucrose for 24h and desiccation for b) 0h, c) 1h, d) 2h, e) 3h and f) 4h. Samples were held at -150°C for 1 min and cooled to 25°C at a rate of 10°C per min. Tg= glass transition.

Table 1. Water content of meristems from *Ribes sanguineum*, cv King Edward VII, following encapsulation with alginate \pm 0.75M sucrose, 20h dehydration with 0.75M sucrose and air-flow desiccation. Means and standard errors of the mean are displayed (n=2-3 meristems).

Cryopreservation step	Alginate \pm 0.75M sucrose	Water content (%FW)	Water content (g.g ⁻¹ DW)	Osmotically active water content ¹ (g.g ⁻¹ DW)	Osmotically inactive water content ² (g.g ⁻¹ DW)
Encapsulation	+	83.5 \pm 0.8	5.066 \pm 0.300	3.993 \pm 0.112	1.073 \pm 0.188
20h dehydration with 0.75M sucrose	+	67.9 \pm 1.6	2.126 \pm 0.162	1.578 \pm 0.056	0.548 \pm 0.106
1h desiccation	+	46.1 \pm 0.1	0.855 \pm 0.001	0.366 \pm 0.021	0.489 \pm 0.022
2h desiccation	+	34.4 \pm 4.2	0.531 \pm 0.099	0.028 \pm 0.028	0.503 \pm 0.127
3h desiccation	+	32.3 \pm 0.2	0.477 \pm 0.004	Not detected	0.477 \pm 0.004
4h desiccation	+	24.6 \pm 4.9	0.332 \pm 0.086	Not detected	0.332 \pm 0.086
Encapsulation	-	87.3 \pm 0.1	6.876 \pm 0.053	6.266 \pm 0.032	0.610 \pm 0.085
20h dehydration with 0.75 M sucrose	-	63.9 \pm 3.2	1.810 \pm 0.303	1.411 \pm 0.149	0.399 \pm 0.157
1h desiccation	-	55.1 \pm 5.1	1.295 \pm 0.357	0.507 \pm 0.162	0.788 \pm 0.496
2h desiccation	-	23.4 \pm 0.1	0.306 \pm 0.001	Not detected	0.306 \pm 0.001
3h desiccation	-	22.4 \pm 5.4	0.296 \pm 0.091	Not detected	0.296 \pm 0.091
4h desiccation	-	25.7 \pm 0.1	0.347 \pm 0.002	Not detected	0.347 \pm 0.002

¹Calculated by dividing the melt endotherm peak area (J) by 334.5 J.g⁻¹; 1g of water releases/absorbs 334.5 J of energy during the transition between liquid and ice [36,46].

²Calculated as the difference between total and osmotically active water contents.

Comparing tropical and temperate germplasm thermal profiles, *R. sanguineum* and *A. indica* share some common thermal characteristics as both had comparable ice nucleation exotherms (Figures 6a and 8a), and ice melting endotherms (Figures 7a and 9a) after dehydrating pre-treatments. As each germplasm type was progressed through subsequent evaporative desiccation steps, exotherm size diminished to a point at a critical time (3h) at which nucleation was inhibited and a vitrified state formed (Figures 6 and 8). Similarly, the magnitude of the endotherm melt decreased with increasing desiccation time in both tissues (Figures 7 and 9). A minor melt was detected in neem after 3h of desiccation indicating glass destabilisation on rewarming and that further desiccation (to 4h) was required to achieve complete stabilization. Stable Tgs for both

tissues only occurred after 4h of desiccation for cooling (Figures 6f and 8f) and rewarming (Figures 7f and 9f).

Table 2. Water content of alginate-encapsulated somatic embryos from *Azadirachta indica* A. Juss, following sucrose pretreatment and air-flow desiccation. Means and standard errors of the mean are displayed ($n=2$ somatic embryos).

Pretreatment	Desiccation time (h)	Water content (%FW)	Water content ($\text{g}\cdot\text{g}^{-1}$ DW)	Osmotically active water content ¹ ($\text{g}\cdot\text{g}^{-1}$ DW)	Osmotically inactive water content ² ($\text{g}\cdot\text{g}^{-1}$ DW)
No pretreatment	0	78.1 ± 0.1	4.158 ± 0.502	4.151 ± 0.504	0.007 ± 0.002
0.3M sucrose	0	49.5 ± 0.2	1.817 ± 0.072	1.774 ± 0.104	0.042 ± 0.032
0.5M sucrose	0	44.8 ± 0.5	1.606 ± 0.443	1.558 ± 0.437	0.048 ± 0.006
0.7M sucrose	0	40.3 ± 0.2	1.018 ± 0.352	0.964 ± 0.347	0.054 ± 0.004
0.7M sucrose	1	28.3 ± 0.2	0.484 ± 0.098	0.402 ± 0.128	0.082 ± 0.030
0.7M sucrose	2	22.5 ± 0.1	0.284 ± 0.001	0.171 ± 0.014	0.011 ± 0.014
0.7M sucrose	3	16.2 ± 0.1	0.191 ± 0.001	0.035 ± 0.007	0.156 ± 0.008
0.7M sucrose	4	13.1 ± 0.1	0.015 ± 0.002	Not detected	0.015 ± 0.002

¹Calculated by dividing the melt endotherm peak area (J) by $334.5 \text{ J}\cdot\text{g}^{-1}$; 1g of water releases/absorbs 334.5 J of energy during the transition between liquid and ice [36,46].

²Calculated as the difference between total and osmotically active water contents.

The total water content in *Ribes* germplasm was reduced during osmotic dehydration by 15-25% on a fresh weight basis, and 55-75% on a dry weight basis (Table 1). Air-flow desiccation for 4h reduced it by a further 35-45% to a final content of ca. 25% on a fresh weight basis, and by 20-35% to a final content of ca. $0.3 \text{ g}\cdot\text{g}^{-1}$ on a dry weight basis. For neem, total water content was reduced during sucrose pretreatment by 20-30% on a fresh weight basis, and by 55-75% on a dry weight basis (Table 2). Air-flow desiccation for 4h reduced water content by a further 27% to final content of 13% on a fresh weight basis, and by 25% to a final content of $0.015 \text{ g}\cdot\text{g}^{-1}$ on a dry weight basis.

Thus, the water content after 4h of desiccation is considerably less in neem than in *Ribes* demonstrating that the water content required to form a stable vitrified state during cooling and rewarming is tissue dependent. The water contents required to achieve vitrification in *R. sanguineum* is similar to that of other *in vitro* *Ribes* species [38]. Compared to neem, *Ribes* germplasm contained ca. 10x more osmotically inactive water (Tables 1 and 2). This may be attributed to morphogenetic, physiological (somatic embryos, shoot meristems, temperate, tropical) as well as genotype differences. Thus, comparative studies of thermal behaviour in tropical and temperate germplasm suggest that cryopreservation protocols for tropical species may particularly benefit from the use of DSC to help optimise osmotically inactive water content.

Table 3. Thermodynamic cooling properties of alginate-encapsulated somatic embryos from *Azadirachta indica* A. Juss, following sucrose pretreatment and air-flow desiccation. Means and standard errors of the mean are displayed (n=2 somatic embryos).

Pretreatment	Desiccation time (h)	Thermal event ¹	Onset (°C)	Midpoint (°C)	Endpoint (°C)	Enthalpy (J.g ⁻¹)	Heat capacity (J.g*°C ⁻¹)
No pretreatment	0	Ice nucleation (2/2)	-19.1 ± 0.0	-20.4 ± 367.0	-24.4 ± 0.2	-216.8 ± 0.8	NA
0.3M sucrose	0	Ice nucleation (2/2)	-17.6 ± 0.9	-19.8 ± 0.1	-25.7 ± 0.2	-192.0 ± 7.0	NA
0.5M sucrose	0	Ice nucleation (2/2)	-18.6 ± 1.4	-20.4 ± 1.7	-26.5 ± 3.1	-176.0 ± 9.4	NA
0.7M sucrose	0	Ice nucleation (2/2)	-17.8 ± 0.6	-19.3 ± 0.4	-25.9 ± 0.5	171.4 ± 13.6	NA
0.7M sucrose	1	Ice nucleation (2/2)	-20.8 ± 0.7	-22.2 ± 0.9	-27.4 ± 0.9	-129.1 ± 12.9	NA
0.7M sucrose	2	Ice nucleation (2/2)	-26.7 ± 3.8	-28.9 ± 3.8	-36.2 ± 3.6	-59.9 ± 13.9	NA
0.7M sucrose	3	Ice nucleation (2/2)	-31.0 ± 12.2	-35.0 ± 14.5	-37.8 ± 15.9	-1.1 ± 1.6	NA
0.7M sucrose	4	Tg (2/2)	-53.9 ± 24.1	-54.5 ± 24.1	-55.1 ± 24.1	NA	0.9 ± 0.2

¹ Number of replicates the thermal event occurred in.

7.1.2.1. Using thermal analysis to optimise cryoprotective strategies

The success of the encapsulation/dehydration method is critically dependent upon achieving a cellular viscosity that stabilises the glassy state. For neem, thermal analysis was used to ascertain the optima for sucrose concentration pretreatment and airflow desiccation times by profiling for thermal stabilities during cooling and re-warming (Figures 8 and 9). Increasing the sucrose concentration during pretreatment and evaporative desiccation times reduced the onset and midpoint temperatures for ice nucleation (Table 3) and melting (Table 4). Depression in onset temperature for the Tg is characteristic of solutions with a greater osmotic potential as is a reduction in the enthalpies associated with ice nucleation (Table 3) and melting (Table 4), in this study this was achieved by manipulating water status using osmotic and evaporative treatments thereby reducing ice formation. Increasing sucrose concentrations during pretreatment also increased osmotically inactive water contents in neem (Table 2), a phenomenon also found in aqueous sugar solutions by Wang and Haymet [52]. Airflow desiccation removed both osmotically active and inactive water from neem, with the osmotically inactive component being reduced to 30-40% of that present after sucrose pretreatment (Table 2). Thermal analysis revealed that 0.7M sucrose pretreatment followed by 4h airflow desiccation is optimal for producing a stable vitrified state in neem.

In the case of the *Ribes* protocol, inclusion of 0.75M sucrose in alginate medium during encapsulation reduced the enthalpy associated with ice nucleation (Table 5) and melting (Table 6). Inclusion of sucrose also lowered total water and osmotically active water, and increased osmotically inactive water after encapsulation (Table 1). This treatment also lowered the total water content after 1h of desiccation and the desiccation rate thereafter was slower than in alginate beads without sucrose. A slower desiccation rate may be partially attributed to improved retention of osmotically inactive water during 1-3h. The more rapid initial removal of water followed by a slower desiccation in beads encapsulated with sucrose resulted in a Tg occurring in all replicates after 3h of desiccation, while beads encapsulated without sucrose only had a Tg in all replicates after 4h of desiccation (Tables 5 and 6). The Tg occurred at water content of ca. 25% when encapsulated without sucrose, but occurred at higher water content (ca. 32%) when encapsulated with sucrose. Sucrose loading of beads was not important for survival (Figure 10) however; a Tg after 3h desiccation of meristems encapsulated with sucrose suggests this may be an optimum. Other factors may also be involved as post-storage vigour improved after 4h desiccation for other *Ribes* genotypes [38].

Table 4. Thermodynamic heating properties of alginate-encapsulated somatic embryos from *Azadirachta indica* A. Juss, following sucrose pretreatment and air-flow desiccation. Means and standard errors of the mean are displayed (n=2 somatic embryos).

Pretreatment	Desiccation time (h)	Thermal event ¹	Onset (°C)	Midpoint (°C)	Endpoint (°C)	Enthalpy (J.g ⁻¹)	Heat capacity (J.g ⁻¹ °C ⁻¹)
No pre-treatment	0	Ice melt (2/2)	1.6 ± 0.1	12.5 ± 0.0	16.2 ± 0.0	268.6 ± 6.6	NA
0.3M sucrose	0	Ice melt (2/2)	1.3 ± 1.2	13.2 ± 1.5	17.2 ± 1.0	210.6 ± 7.1	NA
0.5M sucrose	0	Ice melt (2/2)	0.2 ± 2.0	11.7 ± 2.7	15.5 ± 3.1	193.6 ± 20.2	NA
0.7M sucrose	0	Ice melt (2/2)	-0.8 ± 1.1	9.4 ± 0.4	13.5 ± 1.0	153.7 ± 29.9	NA
0.7M sucrose	1	Ice melt (2/2)	-1.9 ± 1.1	6.0 ± 1.3	10.2 ± 1.1	89.0 ± 22.9	NA
0.7M sucrose	2	Ice melt (2/2)	-18.6 ± 7.2	-5.1 ± 5.3	1.0 ± 3.7	44.6 ± 3.5	NA
0.7M sucrose	3	Ice melt (2/2)	-23.9 ± 3.3	-14.2 ± 3.0	-5.7 ± 2.7	10.0 ± 2.1	NA
0.7M sucrose	4	Tg (2/2)	-17.8 ± 14.5	-17.2 ± 14.5	-17.7 ± 14.8	NA	1.6 ± 0.0

¹Number of replicates the thermal event occurred in.

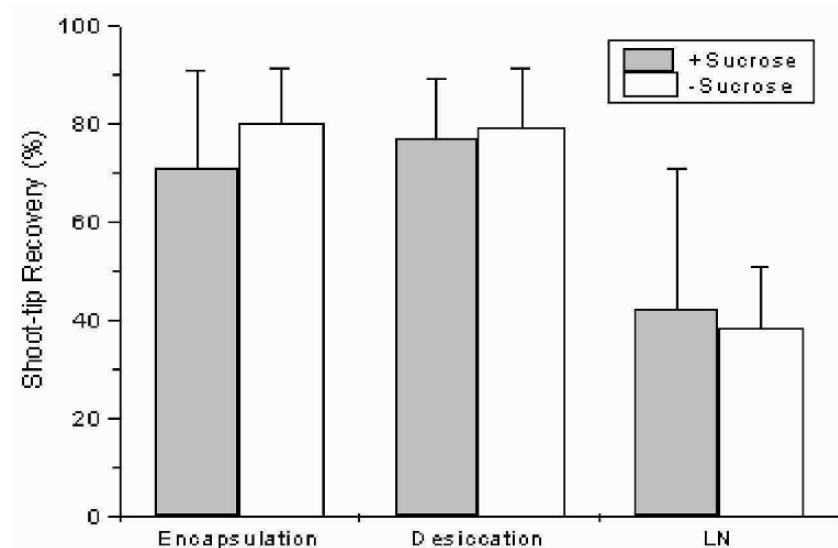


Figure 10. Percentage of *Ribes sanguineum*, cv King Edward VII, meristems that developed healthy shoots after 6 weeks of recovery following encapsulation, 4h air-flow desiccation, and direct plunging in liquid nitrogen (LN). Means and standard errors of the mean are displayed ($n=3$ replicates, 5 meristems per replicate for encapsulation and desiccation controls and 25-28 meristems per replicate plunged in liquid nitrogen).

8. Cryoengineering futures

Presently, new thermal analysis techniques offer exciting approaches to studying plant cryoprotection. HyperDSC[®], (Paul Gabbott, personal communications) incorporating power compensation DSC has cooling and warming scan rate capabilities of up to $500^{\circ}\text{C min}^{-1}$. These instruments use platinum resistance thermometers, have a low mass furnace design (<1g) operate isothermally and have a rapid response equilibration time. This thermal instrumentation more closely approximates the direct plunging and rapid rewarming techniques used in some cryopreservation protocols. However, it is in the detection, characterisation and stability profiling of Tg's that HyperDSC[®] offers the greatest potential, particularly in characterising glassy states in complex and heterogeneous mixtures that contain desiccated and dehydrated plant germplasm in association with cryoprotective mixtures and embedded in alginate-sugar matrices. HyperDSC[®] can measure very small glass transitions and overlapping thermal events are separated based on their differential kinetics. The detection of small Tg's and the profiling of glass relaxations and melting phenomena on germplasm rewarming may be elucidated with greater precision.

Physical and engineering perspectives of *in vitro* plant cryopreservation

Table 5. Thermodynamic cooling properties of meristems from *Ribes sanguineum*, cv King Edward VII, following encapsulation with alginate \pm 0.75M sucrose, 20 h dehydration with 0.75M sucrose and air-flow desiccation. Means and standard errors of the mean are displayed ($n=2-3$ meristems).

Cryopreservation step	Alginate \pm 0.75M sucrose	Thermal event ¹	Onset (°C)	Midpoint (°C)	Endpoint (°C)	Enthalpy (J.g ⁻¹)	Heat capacity (J.g ⁻¹ °C ⁻¹)
Encapsulation	+	Ice nucleation (2/2)	-18.7 \pm 0.9	-19.8 \pm 0.8	-24.0 \pm 0.9	-176.0 \pm 0.6	NA
20h dehydration in 0.75M sucrose	+	Ice nucleation (2/2)	-19.3 \pm 0.7	-20.6 \pm 0.9	-24.6 \pm 2.0	-157.3 \pm 8.0	NA
1h desiccation	+	Ice nucleation (2/2)	-25.2 \pm 0.1	-26.6 \pm 0.1	-29.7 \pm 0.2	-86.7 \pm 11.3	NA
2h desiccation	+	Tg (2/2)	-74.9 \pm 26.3	-75.6 \pm 26.3	-76.2 \pm 26.3	NA	1.5 \pm 0.5
3h desiccation	+	Tg (2/2)	-84.6 \pm 23.8	-85.2 \pm 23.7	-85.9 \pm 23.6	NA	1.3 \pm 0.4
4h desiccation	+	Tg (2/2)	-41.4 \pm 26.8	-42.3 \pm 26.5	-43.1 \pm 26.2	NA	1.4 \pm 0.3
Encapsulation	-	Ice nucleation (2/2)	-17.6 \pm 0.4	-18.9 \pm 0.7	-23.3 \pm 0.6	-214.8 \pm 7.5	NA
20h dehydration in 0.75 M sucrose	-	Ice nucleation (3/3)	-17.9 \pm 1.4	-19.4 \pm 1.1	-24.0 \pm 0.7	-172.0 \pm 2.1	NA
1h desiccation	-	Ice nucleation (3/3)	-26.4 \pm 3.0	-28.0 \pm 3.4	-32.1 \pm 4.7	-99.0 \pm 21.9	NA
2h desiccation	-	Ice nucleation (1/2)	-39.6	-44.4	-52.0	-11.8	NA
3h desiccation	-	Tg (1/2)	-77.7	-78.3	-78.8	NA	1.6
4h desiccation	-	Tg (2/2)	-98.3 \pm 14.9	-98.9 \pm 14.9	-99.4 \pm 14.9	NA	1.4 \pm 0.2

¹Number of replicates the thermal event occurred in.

Table 6. Thermodynamic heating properties of meristems from *Ribes sanguineum*, cv King Edward VII, following encapsulation with alginate \pm 0.75M sucrose, 20 h dehydration with 0.75M sucrose and air-flow desiccation. Means and standard errors of the mean are displayed ($n=2-3$ meristems).

Cryopreservation step	Alginate \pm 0.75M sucrose	Thermal event ¹	Onset (°C)	Midpoint (°C)	Endpoint (°C)	Enthalpy (J.g ⁻¹)	Heat capacity (J.g*°C ⁻¹)
Encapsulation	+	Ice melt (2/2)	-1.5 \pm 0.1	8.7 \pm 0.5	12.0 \pm 0.5	220.4 \pm 4.7	NA
20h dehydration in 0.75M sucrose	+	Ice melt (2/2)	-2.9 \pm 0.9	7.5 \pm 1.3	11.0 \pm 1.5	169.0 \pm 2.7	NA
1h desiccation	+	Ice melt (2/2)	-13.9 \pm 0.5	-2.5 \pm 0.7	1.1 \pm 0.4	65.9 \pm 3.9	NA
2h desiccation	+	Ice melt (1/2)	-16.8	-14.5	-8.4	13.0	NA
3h desiccation	+	Tg (2/2)	-43.5 \pm 5.9	-43.0 \pm 6.0	-42.5 \pm 6.0	NA	2.9 \pm 0.4
4h desiccation	+	Tg (2/2)	-15.8 \pm 13.6	-14.9 \pm 14.1	-13.9 \pm 14.6	NA	2.0 \pm 0.7
Encapsulation	-	Ice melt (2/2)	1.2 \pm 0.1	13.0 \pm 0.6	16.7 \pm 1.5	266.1 \pm 3.2	NA
20h dehydration in 0.75M sucrose	-	Ice melt (3/3)	-1.8 \pm 0.8	7.5 \pm 0.7	10.9 \pm 0.8	168.0 \pm 2.4	NA
1h desiccation	-	Ice melt (3/3)	-12.1 \pm 1.4	-1.8 \pm 2.4	1.8 \pm 2.0	-99.0 \pm 21.9	NA
2h desiccation	-	No event detected	NA	NA	NA	NA	NA
3h desiccation	-	Tg (1/2)	-43.6	-43.0	-42.5	NA	2.1
4h desiccation	-	Tg (2/2)	-42.9 \pm 2.2	-42.4 \pm 2.2	-41.9 \pm 2.2	NA	3.1 \pm 0.4

¹Number of replicates the thermal event occurred in.

Modulated-DSC also offers some potential for cryopreservation experiments, traditional DSC uses a constant heating or cooling rate, whilst modulating DSC uses a modulating (or saw-tooth) heating or cooling profile [62]. In comparison to conventional DSC, modulating DSC may improve detection sensitivity and help resolve over-lapping thermal events in heterogeneous samples [62]. Modulated DSC or HyperDSC[®] may be applied to simultaneously analyse the thermodynamic behaviour of a several cellular components during cryopreservation of complex biological systems. This may also assist studies of the relative rewarming stabilities of vitrification solutions containing germplasm with respect to glass cracking phenomena [64]. Combining thermal analysis with other types of instrumentation offers a powerful approach to studying the different impacts of cryogenic treatments. A two-dimensional X-ray diffraction (XRD) study of ice crystallisation in dextran Sephadex G25 polymeric gel [65] was undertaken in simultaneous conjunction with DSC. The procedure detected exothermic events assigned to the nucleation of ice crystals < 10 µm in diameter and discovered that endotherms formed prior to exotherms were not due to a glass transition but to the melting of very small ice crystals. The XRD patterns observed in the frozen gels were dependent upon the cross-linking density of the gels and that ice crystals of different size and dimension are formed in the gel matrix. This finding may have significant extrapolations for the study of stability in cryopreserved, alginate encapsulated in plant germplasm. Optical DSC simultaneously acquires optical and thermal data from cryopreserved cells [66] and greatly assists the understanding of water transport, ice nucleation of cryogenic dehydration. This system consists of an optical DSC stage connected to a thermal control unit and images and thermograms can be delivered at the same time. The future of DSC applications research will particularly benefit from the improvement of engineering technologies that allow definitive characterizations of the glassy state, particularly for storage recalcitrant species. The wider use of cryopreservation for difficult to conserve plant germplasm; the implementation of fast throughput robust storage regimens in genebanks and enhancing our understanding of the vitrified state present some of the most important future research directives for plant cryoconservationists. Advances in cryogenic and analytical engineering will most certainly play a role in meeting these challenges.

Acknowledgements

The authors acknowledge the EU Framework 5 cryopreservation programmes COBRA QLRI-CT-2001-01645 and CRYMCEPT QLK5-CT-2002-01297, the European Social Fund and The Forest Research Institute of Malaysia and the technical assistance of Isobel Pimbley and Mike Black. Thanks to Paul Gabbot of PETA Solutions (www.thermal-instruments.com); Geoffrey Planer, Paul Lakra and Jamie Bennet of Planer Select, (www.planer.co.uk) and Roland Fleck (National Institute of Biological Standards and Control) for provision of information pertaining to cryogenic equipment, safety, thermal analysis and cryomicroscopy.

References

- [1] Fuller, B.J.; Lane N. and Benson E.E. (2004) (Eds.) Life in the Frozen State. CRC Press, London, UK.
- [2] Hobbs, P.V. (1974) Ice Physics. Clarendon Press, Oxford. UK.
- [3] Ball, P. (1999) H₂O a Biography of Water. Phoenix Press, London, UK.
- [4] Franks, F. (1972) Water: A Comprehensive Treatise Volume I. The Physical and Physical Chemistry of Water. Plenum Press, London, UK.
- [5] Mazur, P. (2004) Principles of cryobiology. In: Fuller, B.; Lane, N. and Benson, E.E. (Eds.) Life in the Frozen State. CRC Press, London, UK; pp. 4-65.
- [6] Price, W. (2003) Snow crystals- A History of their Study and Microscopy. *Quekett J. Microscopy* 39: 483-490.
- [7] Muldrew, K.; Acker, J.; Elliott, A.W. and McGann, L.E. (2004) The water to ice transition. In: Fuller, B.; Lane, N. and Benson, E.E. (Eds.) Life in the Frozen State. CRC Press, London, UK; pp. 67-108.
- [8] Meryman, H.T. and Williams, R.J. (1984) Basic principles of freezing injury to plant cells; natural tolerance and approaches to cryopreservation. In: Kartha, K.K. (Ed.) Cryopreservation of Plant Cells and Organs. CRC Press, Florida, USA; pp.14-48.
- [9] Burton, E.F. and Oliver, W.F. (1935) The crystal structure of ice at low temperature. *Proc. Roy. Soc.A153*: 166-172.
- [10] Dowell, L.G.; Molne, S.W. and Rinfret, A.P. (1962) A low-temperature x-ray diffraction study of ice structures formed on aqueous gelatin gels. *Biochem. Biophys. Acta.* 59: 158-167.
- [11] Kartha, K.K. (1984) Meristem culture and germplasm preservation, In: Kartha, K.K. (Ed.) Cryopreservation of Plant Cells and Organs. CRC Press, Florida, USA; pp. 115-133.
- [12] Kartha, K.K.; Leung, N.L. and Moroginski, L.A. (1982) *In vitro* growth and plant regeneration from cryopreserved meristems of cassava (*Manihot esculenta* Crantz.) *Zeitschrift Pflanzenphysiol.* 107: 133-140.
- [13] Groot, B.W.W. and Henshaw, G.G. (1978) Freeze preservation of potato shoot-tips. *Ann. Bot.* 42: 1227-1229.
- [14] Benson, E.E.; Chabrilange, N. and Engelmann, F. (1992) Mise au point de méthodes de cryoconservation de méristèmes pour la conservation a long terme des ressources génétiques du manioc (*Manihot spp.*) Rapport de fin d'étude, Laboratoire de Ressources Génétiques et Amélioration des Plantes Tropicale, ORSTOM, Montpellier, France.
- [15] Mix-Wagner, G.; Schumacher, H.M. and Cross, R.J. (2002) Recovery of potato apices after several years of storage in liquid nitrogen. *CryoLetters* 24: 33-41.
- [16] Luyet, B.J. (1937) The vitrification of organic colloids of protoplasts. *Biodynamica* 1: 1-14.
- [17] Benson, E.E.; Harding, K. and Smith, H. (1989) The effects of pre-and post-freeze light on the recovery of cryopreserved shoot-tips of *Solanum tuberosum*. *CryoLetters* 10: 323-344.
- [18] Wesley-Smith, J.; Vertucci, C.W.; Berjak, P. and Pammenter, N.W. (1999) A method for the cryopreservation of embryonic axes at ultra-rapid cooling rates. In: Marzalina, M; Khoo, KC; Jayanthi, N; Tsan, F.Y. and Krishnapillay, B. (Eds.) IUFRO Symposium 1998 Recalcitrant Seeds. FRIM, Kuala Lumpur, Malaysia; pp.132-139.
- [19] Wesley-Smith, J.; Vertucci, C.W.; Berjak, P.; Pammenter, N.W. and Crane, J. (1992) Cryopreservation of desiccation-sensitive axes of *Camelia sinensis* in relation to dehydration, freezing rate and the thermal properties of tissue water. *J.Plant Physiol.*140: 596-604.
- [20] Benson, E.E. (2004) Cryoconserving algal and plant diversity: historical perspectives and future challenges. In: Fuller, B; Lane, N. and Benson E.E. (Eds.) Life in the Frozen State. CRC Press, London, UK; pp. 299-328.
- [21] Sakai, A. (2004) Plant cryopreservation. In: Fuller, B; Lane, N. and Benson E.E. (Eds.) Life in the Frozen State. CRC Press, London, UK; pp. 329-346.
- [22] Benson, E.E. (1997) Analytical techniques in low temperature biology: Symposium summaries (Society for Low Temperature Biology) *CryoLetters* 18: 65-76.
- [23] Withers, L.A. and King, P.J (1980) A simple freezing unit and routine cryopreservation method for plant cell cultures. *CryoLetters* 1: 213-220.
- [24] Reed, B.M.; Dumet, D.; J.M. DeNoma, and E.E. Benson. (2001) Validation of cryopreservation protocols for plant germplasm conservation: a pilot study using *Ribes* L. *Biodiversity and Conservation* 10: 1-11.
- [25] Diller, K.R., (1997) Engineering-based contributions in cryobiology. *Cryobiology* 34: 304-314.

- [26] Diller, K.R. and Cravalho, E.G. (1970) A cryomicroscope for the study of freezing and thawing processes in biological cells. *Cryobiology* 7: 191-199.
- [27] McGrath, J.J. (1987) Temperature-controlled cryogenic light microscopy and introduction to cryomicroscopy. In: Grout, B.W.W. and Morris, G.J. (Eds.) *The Effects of Low Temperatures on Biological Systems*. Arnold, London, UK; pp. 234-267.
- [28] Fleck, R.A. (1998) Mechanisms of cell damage and recovery in cryopreserved freshwater protists. Ph.D Thesis, University of Abertay Dundee, Scotland.
- [29] Hayes, A.R. and Stein, A. (1989) A cryomicroscope. *CryoLetters* 10: 257-268.
- [30] Fleck, R.A.; Day, J.G.; Rana, K.J. and Benson, E.E. (1997) Visualisation of cryoinjury and freeze events in the coenocytic alga *Vaucheria sessilis* using cryomicroscopy. *CryoLetters* 18: 343-354.
- [31] Evans, J.; Adlers, J.; Mitchell, J.; Blanshard, J. and Rodger, G. (1996) Use of a confocal laser scanning microscope with a conduction transfer stage in order to observe dynamically the freeze-thaw cycle of an autofluorescent substance and to measure ice crystal size *in situ*. *Cryobiology* 33: 27-33.
- [32] Walcerz, D.B. and Diller, K.R. (1991) Quantitative light microscopy of combined perfusion and freezing processes. *J. Micros.* 161: 297-311.
- [33] Ishikawa, M.; Ide, H.; Price, W.S.; Arata, Y. and Kitashima, T. (2000) Freezing behaviours in plant tissues visualized by NMR microscopy and their regulatory mechanisms. In: Engelmann, F. and Takagi, H. (Eds.) *Cryopreservation of Tropical Plant Germplasm: Current Research Progress and Application*. IPGRI, Rome, Italy; pp. 22-35.
- [34] Ishikawa, M.; Price, W.S.; Ide, H. and Arata, Y. (1997) Visualization of freezing behaviour in leaf and flower buds of Full-Moon Maple by nuclear magnetic resonance microscopy. *Plant Physiol.* 115: 1515-1524.
- [35] Wolfe, J.; Bryant, G. and Koster, K.L. (2002) What is 'unfreezable water', how unfreezable is it and how much is there? *CryoLetters* 23: 157-166.
- [36] Block, W. (2003) Water status and thermal analysis of alginate beads used in cryopreservation of plant germplasm. *Cryobiology* 47: 59-72.
- [37] Dussert, S.; Chabrilange, N.; Rocquelin, G.; Engelmann, F.; Lopez, M. and Hamon, S. (2001) Tolerance of coffee (*Coffea* spp.) seeds to ultra-low temperature exposure in relation to calorimetric properties of tissue water, lipid composition, and cooling procedure. *Physiol. Plantarum* 12: 495-504.
- [38] Benson, E.E.; Reed, B.M.; Brennan, R.M.; Clacher, K.A. and Ross, D.A. (1996) Use of thermal analysis in the evaluation of cryopreservation protocols for *Ribes nigrum* L. germplasm. *CryoLetters* 17: 347-362.
- [39] Martínez, D. and Revilla, M.A. (1998) Cold acclimation and thermal transitions in the cryopreservation of hop shoot tips. *CryoLetters* 19: 333-342.
- [40] Martínez, D.; Arroyo-García, R. and Revilla, M.A. (1999) Cryopreservation of *in vitro* shoot-tips of *Olea europaea* L. var. Arbequina. *CryoLetters* 20: 29-36.
- [41] Santos, I.R.I. and Stushnoff, C. (2003) Desiccation and freezing tolerance of embryonic axes from *Citrus sinensis* [L.] Osb. pretreated with sucrose. *CryoLetters* 24: 281-292.
- [42] Vertucci, C.W.; Berjak, P.; Pammenter, N.W. and Crane, J. (1991) Cryopreservation of embryonic axes of an homeohydrous (recalcitrant) seed in relation to calorimetric properties of tissue water. *CryoLetters* 12: 339-350.
- [43] Pritchard, H.W. and Manger, K.R. (1998) A calorimetric perspective on desiccation stress during preservation procedures with recalcitrant seeds of *Quercus robur* L. *CryoLetters* 19: 23-30.
- [44] Crowe, J.H.; Carpenter, J.F.; Crowe, L.M. and Anchordoguy, T.J. (1990) Are freezing and dehydration similar stress vectors? A comparison of modes of interaction of stabilizing solutes with biomolecules. *Cryobiology* 27: 219-231.
- [45] Dereuddre, J.; Hassen, N.; Bland, S. and Kaminski, M. (1991) Resistance of alginate-coated somatic embryos of carrot (*Daucus carota* L.) to desiccation and freezing in liquid nitrogen. *Cryoletters* 12: 135-148.
- [46] Dumet, D.; Block, W.; Worland, R.; Reed, B.M. and Benson, E.E. (2000) Profiling cryopreservation protocols for *Ribes ciliatum* using differential scanning calorimetry. *CryoLetters* 21: 367-378.
- [47] Leprince, O. and Walters-Vertucci, C. (1995) A calorimetric study of the glass transition behaviours in axes of bean seeds with relevance to storage stability. *Plant Physiol.* 109: 1471-1481.
- [48] Huang, C-H. (2001) Mixed-chain phospholipids: structures and chain-melting behaviour. *Lipids* 36: 1077-1097.
- [49] Tan, C.P. and Che Man, Y.B. (2002) Recent developments in differential scanning calorimetry for assessing oxidative deterioration of vegetable oils. *Trends Food Sci. Technol.* 13: 312-318.

- [50] Benson, E.E. and Bremner, D.H. (2004) Oxidative stress in the frozen plant: a free radical point of view. In: Fuller, B; Lane, N. and Benson E.E. (Eds.) Life in the Frozen State Fuller. CRC Press, London, UK; pp. 299-328.
- [51] Turner, S.; Senaratna, T.; Touchell, D.; Bunn, E.; Dixon, K. and Tan, B. (2001) Stereochemical arrangement of hydroxyl groups in sugar and polyalcohol molecules as an important factor in effective cryopreservation. *Plant Sci.* 160: 489-497.
- [52] Wang, G.M. and Haymet, A.D.J. (1998) Trehalose and other sugar solutions at low temperature: modulated differential scanning calorimetry (MDSC). *J. Physical Chem. B* 102: 5341-5347.
- [53] Devireddy, R.V. and Bischof, J.C. (1998) Measurement of water transport during freezing in mammalian liver tissue: part II – the use of differential scanning calorimetry, *J. Biomechanical Eng.* 120: 559-569.
- [54] Luo, D.L.; Han, X.; He, L.; Cui, X.; Cheng, S.; Lu, C.; Liu, J. and Gao, D. (2002) A modified differential scanning calorimetry for determination of cell volumetric change during the freezing process. *CryoLetters* 23: 229-236.
- [55] Bachiri, Y.; Bajon, C.; Sauvanet, A.; Gazeau, C. and Morisset, C. (2000) Effect of osmotic stress on tolerance of air-drying and cryopreservation of *Arabidopsis thaliana* suspension cells. *Protoplasma* 214: 227-243.
- [56] Bachiri, Y.; Song, G.Q.; Plessis, P.; Shoar-Ghaffari, A.; Rekab, T. and Morisset, C. (2001) Routine cryopreservation of kiwifruit (*Actinidia* spp) Germplasm by encapsulation-dehydration: importance of plant growth regulators. *CryoLetters* 22: 61-74.
- [57] Dumet, D.; Grapin, A.; Bailly, C. and Dorion, N. (2002) Revisiting crucial steps of an encapsulation/desiccation based cryopreservation process: importance of thawing method in the case of *Pelargonium* meristems. *Plant Sci.* 163: 1121-1127.
- [58] Markarian, S.A.; Bonora, S.; Bagramyan, K.A. and Arakelyan, V.B. (2004) Glass-forming property of the system diethyl sulphoxide/water and its cryoprotective action on *Escherichia coli* survival. *Cryobiology* 49: 1-9.
- [59] Vertucci, C.W. (1990) Calorimetric studies of the state of water in seed tissues. *Biophysical J.* 58: 1463-1471.
- [60] Pritchard, H.W.; Tompsett, P.B.; Manger, K. and Smidt, W.J. (1995) The effect of moisture content on the low temperature responses of *Araucaria hunsteinii* seed and embryos. *Ann. Bot.* 76: 79-88.
- [61] Akula, C.; Akula, A. and Drew, R. (2003) Somatic embryogenesis in clonal neem, *Azadirachta indica* A. Juss and analysis for *in vitro* azadirachtin production. *In Vitro Cell. Dev. Biol.-Plant* 39: 304-310.
- [62] Simon, S.L. (2001) Temperature-modulated differential scanning calorimetry: theory and application. *Thermochimica Acta* 374: 55-71.
- [63] Krishnapillay, B. (2000) Towards the use of cryopreservation as a technique for the conservation of tropical recalcitrant seeded species. In: Razdaan, M.K. and Cocking, E.C. (Eds.) Conservation of Plant Genetic Resources *In Vitro*, Volume II. Applications and Limitations. Science Publishers, Inc, New Hampshire, USA; pp.137-163.
- [64] Towill, L.E and Bonnart, R. (2003) Cracking in a vitrification solution during cooling and warming does not affect growth of cryopreserved mint shoot tips. *CryoLetters* 24: 341-346.
- [65] Murase, N.; Abe, S.L Takahashi, H.; Katagiri, C; and Kikegawa, T. (2004) Two-dimensional diffraction study of ice crystallisation in polymer gels. *CryoLetters* 25: 227-234.
- [66] Yuan, Y. and Diller, K.R. (2001) Study of freezing biological systems using optical differential scanning calorimeter. Bioengineering Conference, American Society for Mechanical Engineers, (ASME) 2001, Biomedical Engineering Division (BED) Proceedings 50: 117-118.

INDEX

acclimatization.....	18, 26, 85, 98, 109, 116, 117, 122, 124, 125, 131, 132, 198, 287, 293, 355, 356, 357, 363, 366, 367, 368, 369, 370
acoustic cavitation.....	419
acoustic characteristics.....	427, 428, 438
<i>Aequorea victoria</i>	34
aeration.....	85, 86, 87, 88, 89, 90, 92, 93, 139, 140, 142, 151, 162, 164, 187, 188, 191, 193, 206, 208, 217, 218, 313, 314, 317, 319, 326, 327, 340, 341, 342, 344, 346, 349, 350, 351, 353, 394
aeroponics.....	119, 120
airlift bioreactor.....	90, 91, 92, 93, 164, 165, 171, 172, 188, 225, 227
<i>Ajuga reptans</i>	70
<i>Allium sativum</i>	220, 223
<i>Alocasia</i>	107, 108, 109, 110
<i>Anchusa officinalis</i>	137, 156
ancymidol.....	107, 108, 109, 113, 116, 117, 232, 234
<i>Antirrhinum majus</i>	145, 157
apoplastic water.....	187
applied electric field.....	403, 407, 408, 409
artificial intelligence.....	47, 66, 108, 373
artificial light.....	275, 279, 282, 311, 373
artificial neural network.....	48, 57, 73, 154
<i>Atropa belladonna</i>	143, 156, 169, 170
attenuation coefficient.....	428, 430, 433, 434, 436, 437, 439
<i>Azadirachta indica</i>	463, 464, 465, 467, 468, 469, 476
balloon type bioreactor.....	166, 168
<i>Beta vulgaris</i>	127, 130, 166, 172, 405, 420, 423
biofermentation.....	231, 234, 238, 239, 247
Biomass estimation.....	57, 66, 67, 159
bioreactor technology.....	84, 98, 99, 101, 131
blob analysis.....	35, 43
<i>Brassica oleracea</i>	320
Calla lily.....	356, 362, 363, 364, 365, 366, 367, 369, 370
<i>Camellia sinensis</i>	449
Cartesian coordinates.....	261, 262
<i>Carthamus tinctorius</i>	127, 130
<i>Catharanthus roseus</i>	132, 137, 154, 156, 158, 159, 163, 170, 225
cell suspension cultures.....	69, 70, 73, 74, 77, 78, 125, 133, 135, 136, 139, 148, 153, 155, 156, 157, 159, 186, 197, 226, 227, 423
China fir.....	356, 363, 364, 365, 366, 367, 370
closed production system.....	278, 279
CO ₂ enrichment.....	124, 127, 132, 193, 286, 287, 293, 299, 300, 305, 307, 309, 371
<i>Coffea arabica</i>	193
<i>Colocasia</i>	87, 88, 93, 95, 104, 107, 108, 109, 110

Index

cost accounting	238
cryopreservation .. 441, 445, 446, 447, 448, 449, 450, 451, 452, 456, 459, 460, 462, 463, 467, 470, 473, 474, 475, 476	
<i>Dianthus caryophyllus</i>	95, 123, 131, 371
Differential scanning calorimetry	459
<i>Digitalis lanata</i>	206, 224
disposable bioreactor	203, 204, 205, 206, 225
dissolved oxygen	145, 164, 168, 174, 179, 180, 183, 184, 188, 206, 210, 339, 353
<i>Drosera muscipula</i>	105, 106
DyDO control	348, 349, 350, 351, 352
dynamic modulus	431, 432, 433
electroporation	403, 404, 406, 407, 409, 413, 414
electrostimulation	401, 402, 409
environment control	285
expansin	138
Fick's law	103, 319, 320
finite element method	379, 382, 383, 385, 386, 388, 390, 394
Florialite	357
forced ventilation	192, 193, 199, 286, 326, 327, 355, 358, 359, 360, 361, 362, 371
gas phase	127, 128, 132, 175, 177, 179, 183, 185, 188
gel tester	330, 331, 332, 333, 334, 337
gellan gum	329, 330, 332, 333, 334, 335, 336, 337
genetic algorithm	374, 375, 377, 382, 383, 384, 391, 394
<i>geranium</i>	254
germplasm ... 185, 237, 243, 441, 448, 449, 451, 455, 456, 459, 460, 462, 463, 466, 467, 470, 473, 474, 475	
ginsenosides	166, 219, 222, 226
gladiolus	62, 66, 99, 428, 435, 436, 437, 438
glass transition temperature	445, 451, 462
glucuronidase	145, 420
<i>Gossypium hirsutum</i>	417
hairy roots 125, 126, 127, 128, 129, 130, 131, 133, 134, 146, 157, 162, 163, 164, 165, 166, 167, 169, 170, 171, 172, 180, 185, 203, 205, 209, 210, 222, 223, 224, 225, 226	
<i>Hemerocallis</i>	102, 107, 108, 117, 249
heterotrophic growth	101, 103
<i>Hosta</i>	104, 106, 107, 108, 109, 116, 117
Hough transform	254, 259, 261, 263, 265, 269
hydrodynamic shear	141, 142, 143, 144, 156, 217
<i>Hyoscyamus muticus</i>	127, 133, 165, 170, 186, 219, 222, 223, 227
hyperhydration	122, 123, 124, 131, 235, 421
hyperhydricity	53, 85, 106, 117, 187, 191, 198, 199, 234, 329, 336, 339, 435, 438
Ice nucleation	449, 468, 471
impeller designs	142, 152
<i>Ipomoea batatas</i>	70, 74, 295, 311, 355

Index

Kalman filter.....	56, 57, 59, 60, 154, 159, 388
kinematics viscosity	377, 381
Knudsen diffusion coefficients.....	323
Knudsen diffusion regime	320
Liquid Lab Vessel®	111, 112, 113
liquid nitrogen	441, 442, 445, 447, 450, 451, 452, 453, 454, 455, 456, 463, 470, 474, 475
<i>Lithospermum erythrorhizon</i>	161, 169, 226, 423, 424
machine vision.....	25, 62, 65, 72, 78, 108, 198, 253, 254, 255, 265, 270, 272
mass transfer.....	92, 119, 128, 130, 139, 148, 152, 157, 158, 165, 174, 175, 176, 177, 178, 179, 180, 181, 182, 183, 184, 185, 186, 188, 221, 319, 339, 346
membrane bioreactor.....	204
Microarrays	32
microenvironment	16, 27, 29, 59, 101, 115, 117, 149, 292, 293
micropropagation.....	v, vii, 3, 4, 5, 6, 8, 15, 18, 21, 26, 28, 61, 65, 84, 99, 101, 105, 106, 108, 109, 110, 111, 112, 115, 116, 117, 119, 120, 121, 122, 123, 124, 125, 130, 131, 132, 133, 185, 187, 189, 191, 193, 200, 201, 206, 224, 225, 231, 233, 234, 235, 237, 238, 241, 242, 243, 244, 245, 246, 247, 248, 249, 250, 253, 254, 255, 257, 271, 275, 326, 327, 336, 339, 355, 356, 357, 358, 359, 360, 364, 366, 370, 371
<i>Morinda elliptica</i>	140, 156
<i>Narcissus</i>	109, 117
Newtonian fluids	213
<i>Nicotiana tabacum</i>	95, 137, 156, 159, 219, 220, 405, 412, 413, 414, 420
NMR spectroscopy	458
Nyquist diagram	430, 433
<i>Oryza sativa</i> L	353
oxygen demand.....	137, 145, 146, 151, 178, 181, 182, 183, 184, 189
oxygen transfer.....	92, 93, 139, 140, 151, 165, 170, 173, 174, 175, 176, 177, 178, 180, 181, 182, 184, 185, 186, 188, 217, 221, 340, 342
packed cell volume.....	138, 149
paclitaxel	219, 221, 227
paclobutrazol	99, 108, 109, 116
<i>Panax ginseng</i>	133, 137, 164, 166, 168, 171, 172, 219, 222, 224
particle bombardment.....	32, 33, 34, 35, 45
<i>Petunia hybrida</i>	95, 419
phase velocity.....	428, 429, 430, 431, 432, 438, 439
<i>Phaseolus angularis</i>	403
photoautotrophic.....	15, 19, 28, 83, 100, 132, 191, 193, 195, 196, 197, 198, 199, 201, 249, 275, 326, 327, 355, 356, 357, 358, 359, 360, 364, 366, 367, 370, 371
photomixotrophic micropropagation.....	355, 358, 359, 364
photosynthetic photon flux.....	26, 282, 303, 355, 371
<i>Pisum sativum</i>	417, 424
plant propagation.....	83, 84, 86, 87, 88, 89, 95, 96, 98, 99, 100, 115, 187, 189, 199, 200, 272, 275, 352

Index

plant transformation	35, 45, 422
Poiseuille-Hagen formula.....	317
pro-embryogenic mass	74
quantitative image analysis	46
recombinant protein.....	135, 136, 137, 145, 146, 148, 150, 151, 153, 155
Reynolds number.....	128, 181, 210, 377, 388
rheological property	138
<i>Ribes sanguineum</i>	459, 461, 463, 466, 470, 471, 472
RITA bioreactor	189, 196
seed germination.....	181, 184, 410, 424
shoot organogenesis	103, 116, 329
shoot separation.....	264, 265, 266, 268, 269, 270, 271
somatic embryogenesis	78, 79, 99, 193, 198, 199, 200, 231, 336, 339, 340, 341, 342, 346, 347, 352, 353, 397, 399, 425
somatic embryos.....	56, 57, 58, 66, 70, 73, 74, 75, 77, 78, 84, 87, 99, 123, 124, 190, 193, 195, 198, 200, 206, 224, 232, 234, 235, 237, 239, 248, 327, 336, 339, 340, 342, 343, 344, 345, 346, 348, 351, 352, 353, 399, 409, 411, 417, 423, 425, 463, 464, 465, 467, 468, 469, 475
sonication.....	417, 420, 421, 423, 424, 425
<i>Spathiphyllum</i>	84, 87, 91, 93, 94, 95, 244, 249
<i>Stevia</i>	84, 94, 95, 96, 97, 100
stirred tank bioreactor.....	162, 166, 187
<i>Swertia chirata</i>	164, 171
syneresis	334, 335
Taxol.....	169, 227, 423
<i>Taxus baccata</i>	161, 169, 219, 221, 224, 227
<i>Taxus cuspidata</i>	157, 166, 172, 225
temperature distribution	57, 59, 60, 373, 374, 375, 377, 378, 382, 383, 385, 386, 388, 394
texture analysis	69, 70, 71, 72, 73, 74, 75, 77, 78
thin films.....	102
TRI-bioreactor	192, 193, 194, 195, 196, 197, 198, 199
ultrasonic treatment	417, 421
ultrasonics.....	123, 126, 428
<i>Vigna aconitifolia</i>	406, 407, 414
viscoelasticity	427, 432, 438
vitrification ..	187, 200, 329, 336, 337, 448, 450, 451, 459, 460, 462, 467, 473, 474, 476
VRP method	427, 428, 434, 438
Wave Bags.....	209, 210, 212, 214, 218, 221, 223
X-ray diffraction.....	448, 473